ASD TECHNICAL REPORT 61-119
PART I

RADIATION HEAT TRANSFER ANALYSIS FOR SPACE VEHICLES

J. A. STEVENSON
J. C. GRAFTON

SPACE AND INFORMATION SYSTEMS DIVISION
NORTH AMERICAN AVIATION, INC.

SID 61-91

DECEMBER 1961

FLIGHT ACCESSORIES LABORATORY
CONTRACT AF 33(616)-7635
PROJECT No. 6146
TASK No. 61118

AERONAUTICAL SYSTEMS DIVISION
AIR FORCE SYSTEMS COMMAND
UNITED STATES AIR FORCE
WRIGHT-PATTERSON AIR FORCE BASE, OHIO

NOTICES

When Government drawings, specifications, or other data are used for any purpose other than in connection with a definitely related Government procurement operation, the United States Government thereby incurs no responsibility nor any obligation whatsoever; and the fact that the Government may have formulated, furnished, or in any way supplied the said drawings, specifications, or other data, is not to be regarded by implication or otherwise as in any manner licensing the holder or any other person or corporation, or conveying any rights or permission to manufacture, use, or sell any patented invention that may in any way be related thereto.

Qualified requesters may obtain copies of this report from the Armed Services Technical Information Agency, (ASTIA), Arlington Hall Station, Arlington 12, Virginia.

This report has been released to the Office of Technical Services, U. S. Department of Commerce, Washington 25, D. C., for sale to the general public.

Copies of ASD Technical Reports and Technical Notes should not be returned to the Aeronautical Systems Division unless return is required by security considerations, contractual obligations, or notice on a specific document.

FOREWORD

This is one of a series of reports which summarizes the first 6-month phase of a planned 3-year study of thermal and atmospheric control systems of manned and unmanned space vehicles. The study was conducted by the Space and Information Systems Division of North American Aviation, Inc., under contract AF 33(616)-7635, and was sponsored by the Flight Accessories Laboratory of Aeronautical Systems Division (formerly Wright Air Development Division). The Los Angeles Division of North American Aviation, Inc., and AiResearch Manufacturing Company were subcontractors in the study effort.

The reports covering the results of the first 6-month period of this study are listed below. Because of the intention to revise, amplify, and extend the material presented, each report has been designated as Part I. Additional parts of these reports will be published as the program progresses. In addition to publishing these subsequent parts, new phases of the study will result in additional reports.

ASD TR 61-164 (Part I)	Environmental Control Systems Selection for Unmanned Space Vehicles (secret)
ASD TR 61-240 (Part I)	Environmental Control Systems Selection for Manned Space Vehicles, Volume I (unclassified) and Volume II (secret)
ASD TR 61-161 (Part I)	Space Vehicle Environmental Control Requirements Based on Equipment and Physiological Criteria
ASD TR 61-119 (Part I)	Radiation Heat Transfer Analysis for Space Vehicles
ASD TR 61-30 (Part I)	Space Radiator Analysis and Design
ASD TR 61-176 (Part I)	Integration and Optimization of Space Vehicle Environmental Control Systems
ASD TR 61-162 (Part I)	Analytical Methods for Space Vehicle Atmospheric Control Processes

The thermal and atmospheric control program was under the direction of A. L. Ingelfinger and Lieutenant N. P. Jeffries of the Environmental Control Section, Flight Accessories Laboratory. E. A. Zara of the Environmental Control Section acted as monitor of this report. A. C. Martin served as project engineer at S&ID. The radiation heat transfer studies were conducted by J. A. Stevenson and J. C. Grafton.

Appreciation is expressed to the Astronautics and Fort Worth Divisions of Convair (General Dynamics Corporation) and, in particular, John C. Ballinger of the Astronautics Division. Much of the data included in this report was obtained from Convair.

The authors also wish to express their appreciation to G. A. McCue of the Aero-Space Laboratories of S&ID who contributed a major part to the orbiting space vehicle studies at S&ID.

ABSTRACT

This document covers problems associated with one part of the thermal and atmospheric control study—the analysis of radiation heat transfer in space. The basic theory of radiation heat transfer and the thermal radiation environment in space are described. Analysis techniques are included for calculating space vehicle surface temperatures and for solving radiation heat transfer problems in general. Tabulated configuration factor data and emittance data are presented.

(pp) (fig.) (tbls..) (ref.)

PUBLICATION REVIEW

This report has been reviewed and is approved.

FOR THE COMMANDER:

William C. Savage

WILLIAM C. SAVAGE
Chief, Environmental Branch
Flight Accessories Laboratory

CONTENTS

APPENDIXES

ILLUSTRATIONS

TABLES

Section I

INTRODUCTION

STUDY PROGRAM

The Thermal and Atmospheric Control Study conducted for Aeronautical Systems Division (formerly Wright Air Development Division) is an analytical and experimental program concerned with the problems of environmental control of future space vehicles. Three broadly defined tasks were designated for this study. They are:

1. Improved analysis methods for predicting the requirements for and the performance of space environmental control systems
2. Improved methods, techniques, systems, and equipment required for environmental control
3. Development of criteria and techniques for the optimization of environmental control systems and the integration of these systems with other vehicle systems

To accomplish these tasks, industrial organizations and military establishments were surveyed to obtain data concerned with current and future thermal and atmospheric control technology. Other endeavors include evaluating existing and newly created methods of analysis, selection, integration, and optimization of control systems and components. The refurbishment and development of existing and new analog or digital computer programs, applicable to this study, are included. In addition, laboratory verification of analyses and new design concepts form a part of the effort associated with these tasks.

To guide all of the endeavors along lines which will find immediate and practical application, components and systems associated with specific vehicles were studied. The vehicles selected were representative of a number of earth-orbital and cislunar missions. These hypothetical vehicles were carried through preliminary design and used as thermal and atmospheric control models.

ROLE OF RADIANT HEAT TRANSFER ANALYSIS

Although transfer of heat within a space vehicle or satellite can occur by radiation, conduction, or convection, the only means by which the vehicle

---

Manuscript released by the authors May 1961 for publication as an ASD Technical Report.

can exchange heat with its environment is by radiation. Temperature control systems, either active or passive, must eliminate heat by radiation to space. An accurate method of radiation heat transfer analysis is therefore of prime importance for the prediction of vehicle and component temperatures and the performance of temperature control systems.

This report documents a study of available methods of radiation heat transfer analysis and reviews the basic principles of thermal radiation. Included in the appendix sections are tables of emissivity and reflectivity for certain surface coatings which can be applied to space vehicles. This area is also of prime importance because even the most refined analysis techniques are only as accurate as the values of emittance and reflectance which are used.

Section II

GLOSSARY OF RADIATION TRANSFER TERMS

The following terms conform in terminology and symbolic representation to those most widely used in radiation heat transfer literature.

Absorptance or absorptivity α

Ratio of absorbed radiant energy to incident radiation. Related to reflectance and transmittance by

$$\alpha + \rho + \tau = 1$$

Albedo, a

Ratio of radiant energy reflected by planet or satellite to that received by it. A dimensionless decimal equal to or less than 1. Care must be taken to avoid confusion between the albedos of total and visible radiant energy.

Angstrom, $\mathring{A}$

Unit of measurement of wavelength of electromagnetic waves.

$$1 \text{ cm} = 10^8 \mathring{A} = 10^4 \mu$$

Black body

Hypothetical body having the characteristic of absorbing all radiant energy striking it and reflecting and/or transmitting none.

$$\alpha = 1.0, \rho = \tau = 0$$

Diffuse reflection

Reflection that follows Lambert's cosine law (i.e., intensity I is constant regardless of angle). Nonmetallic surfaces are often nearly perfect diffusive reflectors.

Emittance, ϵ

Ratio of emissive power E of a body to emissive power E_b of a black body at the same temperature. A dimensionless decimal equal to or less than 1. Distinctions are made between difference types of emittance.

Total emittance

Emittance of the whole range of wavelengths.

Monochromatic emittance	Emittance radiating at a particular wavelength.
Hemispherical emittance	Emittance radiating in all directions from the surface.
Normal emittance	Emittance radiating in a direction normal to the surface.
Directional emittance	Emittance radiating in a direction at an angle ϕ to the normal to the surface.
Emissive power E	Radiant energy emitted at a given temperature per unit time and unit area of radiating surface. Also called flux density. Expressed as Btu/(hour) (square foot).
Monochromatic emissive power, E_λ	Emissive power emitted at a single wavelength for a given temperature.
Total emissive power	Emissive power emitted over the whole spectrum of wavelengths. $$E = \sum_{\lambda=0}^{\lambda=\infty} E_\lambda d_\lambda$$
Emissivity, ϵ	See emittance. Characterizes a certain material in pure polished and opaque form, while emittance pertains to a particular specimen. In this report, however, no distinction is made between emissivity and emittance.
Equilibrium	Condition in which the interchange of radiant energy between bodies becomes and remains constant.
Flux density	See emissive power and incident radiation.
Gray body	A body or surface for which $$\alpha_\lambda = \epsilon_\lambda = \alpha = \epsilon$$ at all wavelengths and temperatures. Its emission distribution curve therefore parallels that of a black body or surface but is of lesser magnitude.

Hemispherical	Refers to the boundary condition of a specular measurement in which the solid angle being considered is equal to 2π steradians.
Incident radiation	Radiant energy impinging on a surface per unit time and per unit area. Also called irradiation or flux density.
Infrared	Region of the electromagnetic spectrum extending approximately from 0.75 to about 300 microns.
Intensity of radiation, I	Rate of emission in a direction at an angle ϕ to the normal to the surface. Expressed as energy/(area)(time)(solid angle)(cos ϕ) or energy/(time)(solid angle)(projected area)
Irradiation	See incident radiation.
Isotropic radiation	Radiation impinging on a surface having the same characteristics regardless of the location and direction of the surface.
Monochromatic	Having a single wavelength and single frequency of electromagnetic vibration.
Radiance	See emissive power.
Radiancy	See emissive power.
Radiant energy	Energy emitted from a surface in the form of electromagnetic waves.
Radiant heat	Radiant energy emitted in consequence of the temperature of a body. Usually considered to be that part of the electromagnetic or radiant energy spectrum between 2,000 and 50,000 angstroms.
Radiosity, J	Sum of emitted, reflected, and transmitted radiation flux per unit area. Usually expressed in Btu/(hour)(square foot).

Reflectance, ρ	Ratio of reflected to incident radiant energy. Related to absorptance and transmittance by $$\rho + \alpha + \tau = 1$$
Spectral energy distribution	Monochromatic emissive power over the range of the spectrum of an emitting surface.
Specular reflection	Refers to reflection which occurs in such a way that the angle between the reflected beam of radiation and the normal to the surface equals the angle made by the impinging beam with the same normal.
Stefan-Boltzmann constant, σ	Constant which is independent of surface and temperature and relates heat radiated q_r to absolute temperature, area, and emissivity. The relationship is $$q_r = \sigma \epsilon A T^4$$
Thermal radiation	See radiant heat.
Transmittance, τ	Ratio of radiant energy transmitted through the body to the incident radiation. Related to absorptance, and reflectance by $$\tau + \alpha + \rho = 1$$
Total radiation	Sum of all radiation over the entire spectrum of emitted wavelengths.
Ultraviolet	Region of the electromagnetic spectrum extending approximately from 0.01 to 0.4 micron.
Visible	Region of the electromagnetic spectrum extending approximately from 0.4 to 0.75 micron.
Wavelength, λ	Distance measured along line of propagation between two points which are in phase on adjacent waves.

Section III

THEORY OF RADIATION HEAT TRANSFER*

BASIC CONCEPTS OF THERMAL RADIATION

The process of emission of radiant energy by a body, which depends on its temperature, is called thermal radiation. Each body, by virtue of its temperature, is constantly emitting electromagnetic radiation from its surface into the surrounding space and is absorbing radiant energy originating elsewhere and incident upon it. Electromagnetic radiation is composed of all wavelengths, including extremely short-wave secondary gamma rays and the longest radio waves. Theoretically, all bodies emit radiation over the entire electromagnetic spectrum (Figure 1).

The amount of energy emitted generally varies with wavelength in a manner similar to that shown in Figure 2. The curves give the spectral distribution of radiation from a black body at temperatures of 2700, 1980, and 1260 R. The maximum energy emitted by a body increases as the temperature increases, and the wavelength at which the maximum energy is radiated becomes shorter as the temperature increases.

The rate of radiation from a black, or ideal, body is proportional to the fourth power of its absolute temperature. For other bodies, the rate of radiation is also proportional to the fourth power of their absolute temperature, but the magnitude varies depending on material, surface condition, and temperature. The rate of emission of energy per unit area for non-black-body materials is never greater than the rate of energy emission per unit area from a black body. For this reason, the black body is used as a standard or reference, and emission from other bodies is compared with it.

RADIATION LAWS

Kirchhoff's Law

Kirchhoff, in 1860, proposed a system consisting of a completely enclosed hollow space into which a thin plate is placed, the enclosure and plate being at the same temperature.

---

*The material in this section of the report was gathered from References 1 through 5.

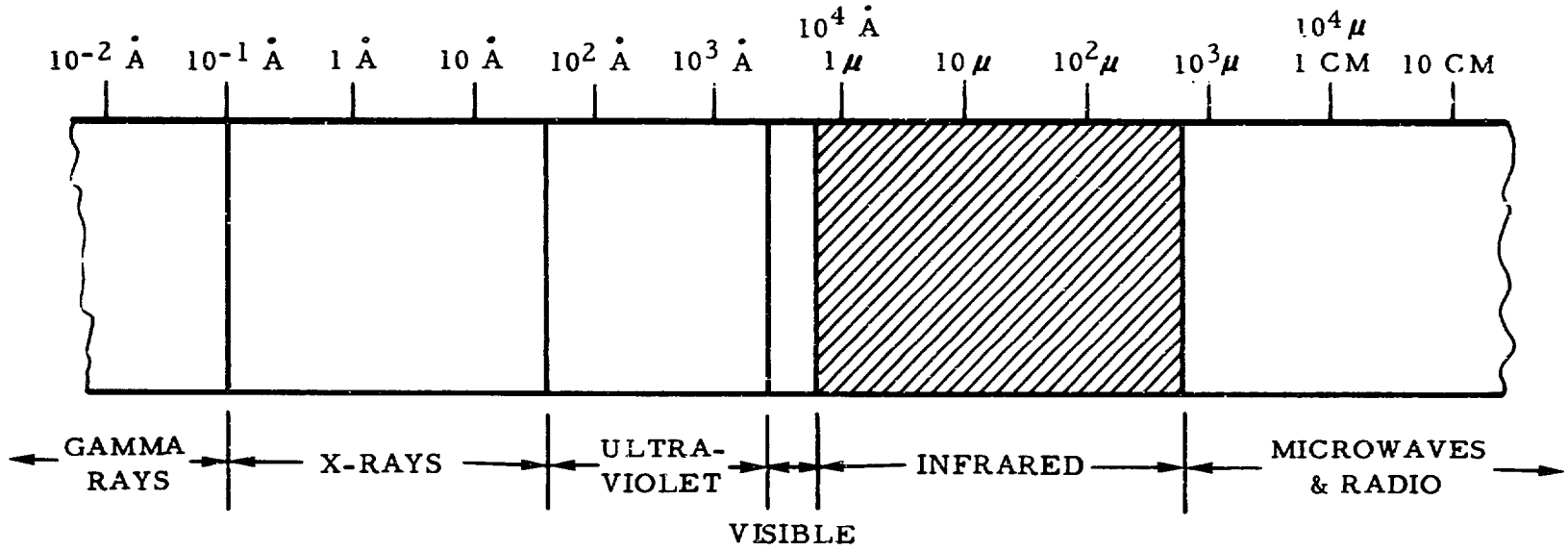

μ OR MICRON = 10^{4} Å = 10^{-4} CM

Figure 1. Electromagnetic Spectrum

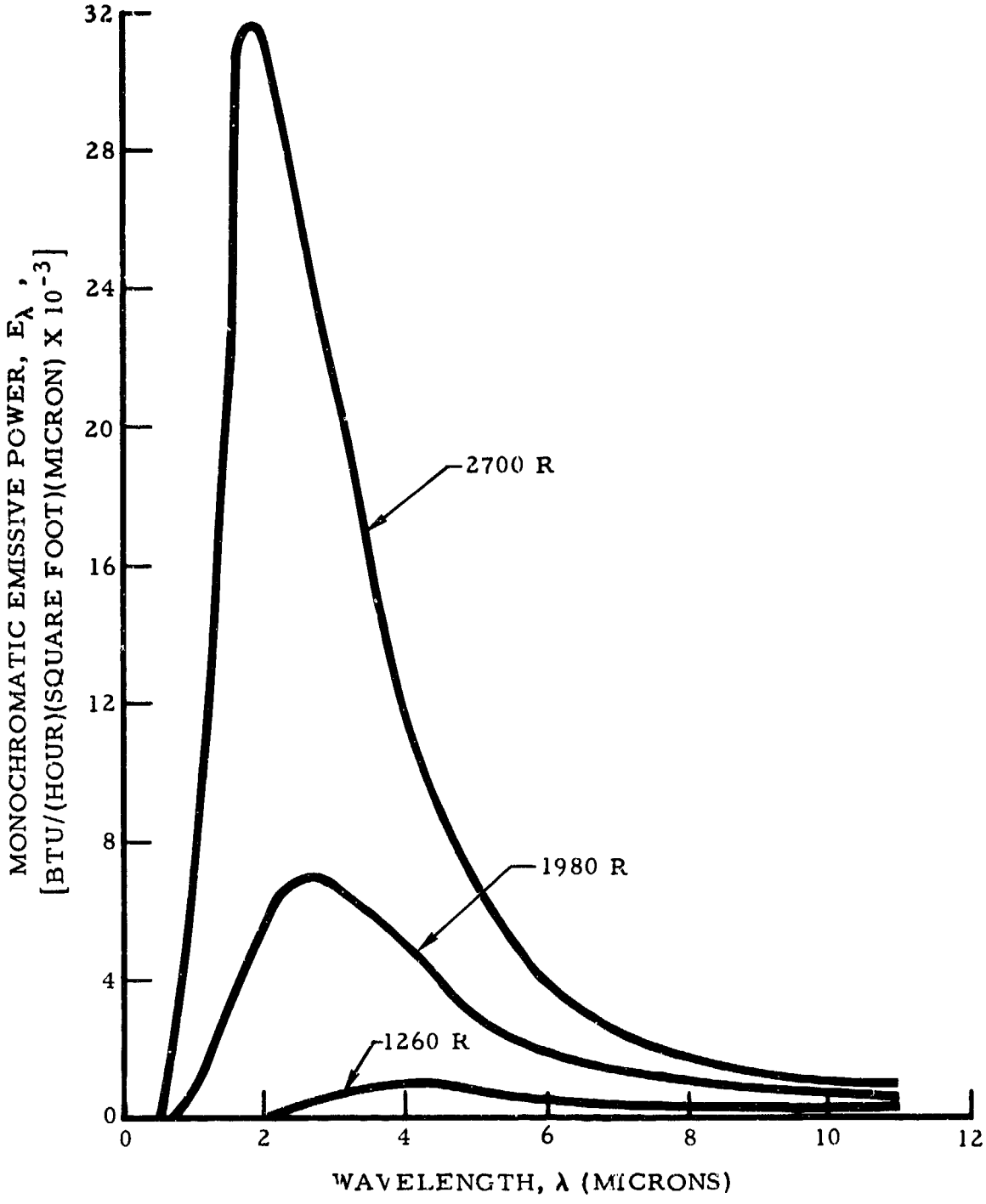

Figure 2. Energy Distribution of Black Body

By using the electromagnetic theory, which holds that radiation falling upon a surface exerts a pressure upon that surface, and the concept of mechanical equilibrium of radiation, it can be shown that the radiant energy incident upon the plate must equal the energy radiated from the plate, or work will be done upon the plate by moving it. The entire system is at the same temperature, however, and the second law of thermodynamics denies the possibility of transforming heat into external work unless a temperature difference exists. Because the second law of thermodynamics has thus far proven inviolate, the assumption of equal amounts of energy incident upon the plate and radiated from the plate must be accepted.

Kirchhoff also suggested that a nearly perfect black surface can be produced by employing a hollow enclosure into which a small aperture is available. Radiation passing into the enclosure through the aperture, which itself acts as a black surface, can be made to suffer such a large number of reflections around the walls of the enclosure that almost none of the entering radiation can escape out of the enclosure through the aperture, and the absorptance of the aperture approaches the limiting value of unity.

From the assumption of equilibrium of radiation, it is apparent that a constant-temperature enclosure which receives radiant energy from a source at the same temperature must emit an equal amount of radiant energy. Such a system is now considered with the stipulation that the source is emitting the maximum amount of energy that can be emitted from any source of like size at this temperature. The enclosure absorbs all of the incoming energy ($\alpha = 1$). The enclosure, also, must emit back to the source, through the aperture, an equal amount of energy. Then, if the Kirchhoff black surface is acceptable, a black surface has the additional characteristic of emittance equal to unity ($\epsilon = 1$). That is, a black surface must emit the maximum amount of energy (per unit area and unit time) that can be radiated from any surface at the same temperature.

It becomes obvious that Kirchhoff's black surface can be used as either a black surface source or a black surface receiver with the stipulation that the temperature of the entire enclosure must be constant and equal to that for which the black surface characteristics are required.

Lambert's Cosine Law

Lambert's cosine law states that the radiant heat flux from a plane source of radiation varies as the cosine of the angle measured from the normal to the surface. This assumes diffuse radiation as opposed to specular radiation, that is, in diffuse radiation, intensity I, expressed in Btu/(hour)(solid angle)(projected area), is a constant regardless of the angle from the normal to the surface.

Consider Figure 3, letting the elemental area dA_1 represent Lambert's diffusely reflecting surface. When a constant density of radiation in space is assumed and only radiation in the visible range is considered, the area $dA_1 \cos\phi$ viewed from M appears equally as bright as the area dA_1 viewed from N, and the quantity of light falling upon any area dA_2 is directly proportional to the area $dA_1 \cos\phi$. These same concepts apply equally as well to radiation of longer wavelength as they do to radiation of the visible range. The amount of radiant energy reaching a surface dA_2 from a black surface dA_1 is directly proportional to the area $dA_1 \cos\phi$.

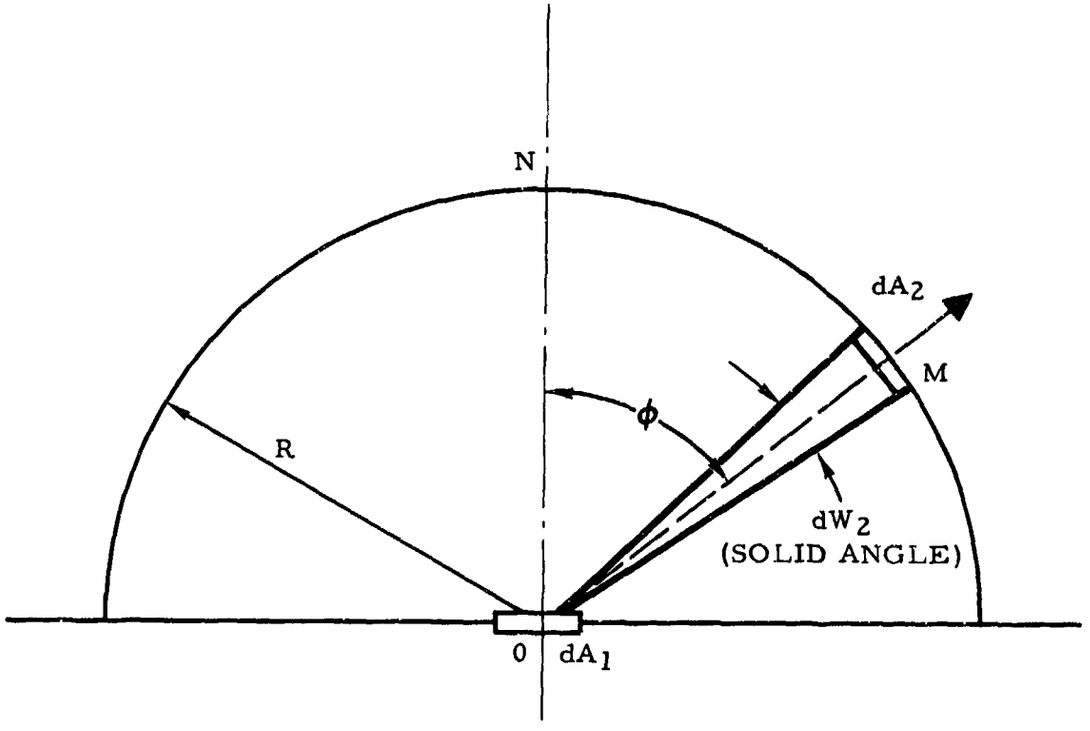

Figure 3. Representation of Lambert's Cosine Law

True surfaces vary from this law depending upon the material. When the radiation intensity of a surface follows the cosine law, the directional emittance is independent of the angle of emission and is identical with the hemispherical emittance. Actually, the emittance of all true surfaces is dependent to a certain degree on the angle of emission.

Stefan-Boltzmann's Law

Stefan empirically found the relationship between the intensity of radiation from a black surface source and the absolute temperature of the surface. Later, Boltzmann theoretically reduced this same relationship, stating that the heat radiated by a black body is proportional to the fourth power of its absolute temperature, or

$$q = \sigma A T^4 \tag{1}$$

where

q = Total heat emitted, Btu/hr

σ = Stefan-Boltzmann constant = 0.1713×10^{-8} Btu/(hr)(sq ft)($^\circ R^4$)

A = Emissive area, sq ft

T = Absolute temperature, °R

For non-black bodies, the heat emitted equals the black body heat emitted multiplied by the emittance, or

$$q = \epsilon(\sigma A T^4) \tag{2}$$

where

ϵ = Emittance of non-black body

Wien's Displacement Law

For black body radiation, if the wave of length λ_2 at T_2 is displaced from that of length λ_1 at T_1, such that $\lambda_2 T_2 = \lambda_1 T_1$, the monochromatic emissive powers at these two wavelengths are directly proportional to the fifth powers of the absolute temperatures, or

$$\frac{E\lambda_1}{E\lambda_2} = \frac{T_1^5}{T_2^5} \tag{3}$$

Wien also determined that when the temperature of a radiating black body increases, the wavelength corresponding to the maximum energy decreases in such a way that the product of the absolute temperature and wavelength is a constant. (See Figure 2.) This is expressed as

$$\lambda_{max} T = 5216.2\ \mu(^\circ R) \tag{4}$$

Planck's Distribution Law

The present understanding of radiation and the spectrum began to develop in 1900 when Max Planck formulated his theory of the "granular" nature of energy and developed a new kind of statistics, the quantum theory, to handle his concept mathematically. Radiant energy leaving a surface is distributed over the entire wavelength range, and the distribution of the energy with wavelength is a function of the temperature and nature of the surface. The emissive power distribution at a given temperature for a black body is given as

$$E_\lambda = \frac{C_1 \lambda^{-5}}{e^{C_2/\lambda T} - 1} \tag{5}$$

where

$C_1 = 1.1870 \times 10^8$ Btu μ^4/(hr)(sq ft)

$C_2 = 25,896\ \mu(°R)$

e = Base of natural logarithm

Absorption and Emission of Radiant Energy

The efficacy of the surface to emit or absorb radiation is presented in terms of emissivity and absorptivity factors. These factors are defined as the ratio of energy emitted or absorbed at each wavelength to the energy emitted or absorbed by a black body at the same temperature. These factors are usually presented as the total or average values over all wavelengths for a particular surface.

In addition to being functions of wavelength, emissivity and absorptivity are functions of the angle the light ray makes with the surface. Values are reported usually in terms of the normal (perpendicular to the surface) or hemispherical (average overall angles). The variation between normal and hemispherical emissivity is shown in Figure 4, as taken from Reference 3. Emissivities or absorptivities are often presented as total hemispherical or total normal, or they are given as a function of wavelength for normal or hemispherical radiation. Reflectance, or transmittance for transparent materials, is sometimes given rather than absorptivity. This, of course, is simply $1 - \alpha$.

Absorption or emission of energy up to about 2- microns wavelength is due primarily to raising the energy levels of the orbital electrons. These excited electrons then give up their energy usually in the form of molecular vibrational energy or fluorescence. Most electronic transitions involve

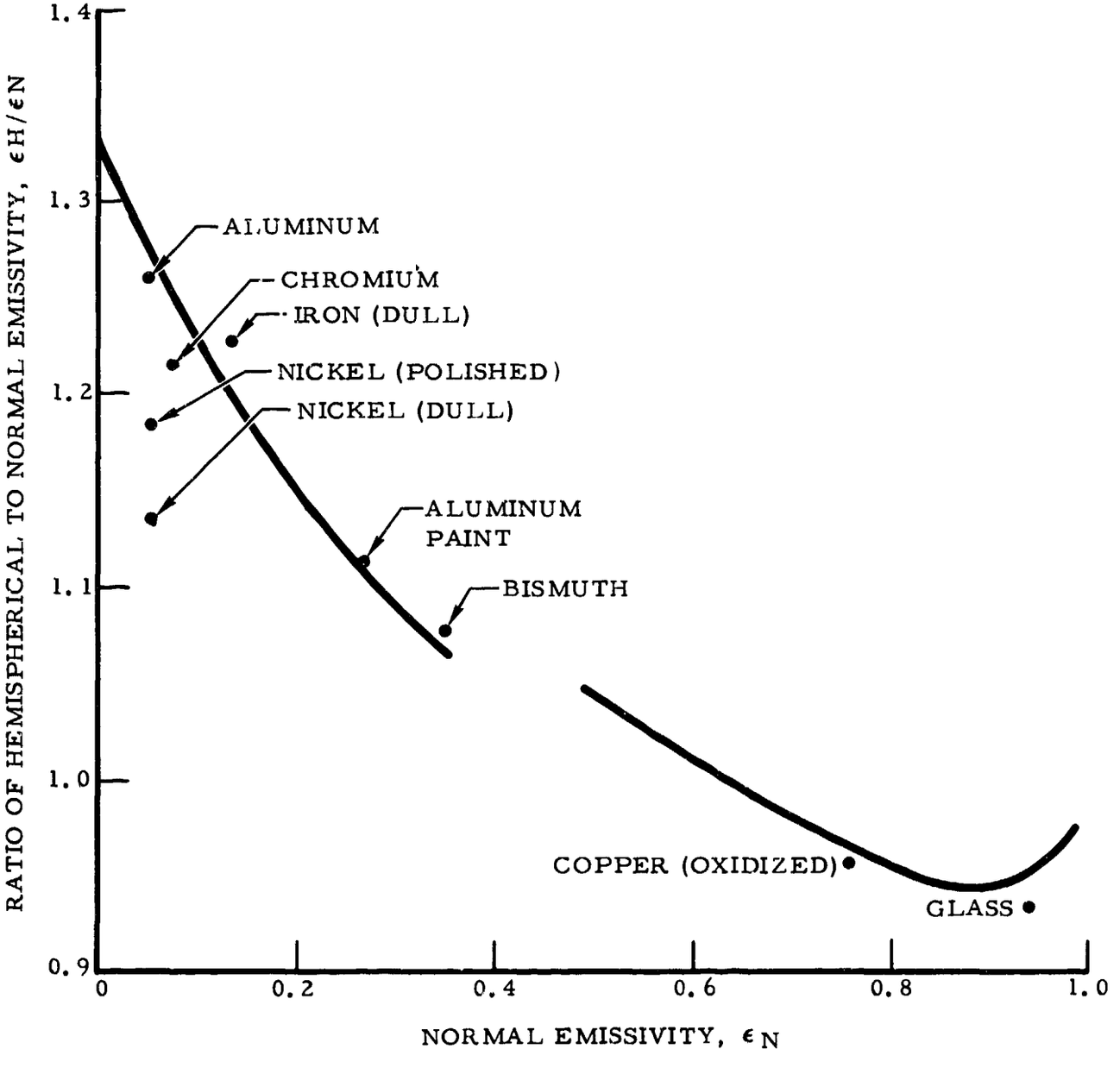

Figure 4. Theoretical and Experimental Values for Ratio of Hemispherical to Normal Emissivity

relatively large energy steps, and the temperature of the surface therefore has little effect on absorption in this range. Because almost all the solar energy lies in the wavelength below 2 microns, solar absorptivity α_s should be nearly constant with surface temperature. Some minor effects are noted with temperature, caused by such factors as crystal structure changes.

Absorption or emission beyond 2 microns is due to raising the vibrational and kinetic energy levels of the molecules themselves. Organic materials are more sensitive to vibrational absorption than electrically conductive materials. Semiconductor materials are generally transparent to a large portion of the infrared region. The absorptivity or emissivity of any material varies with wavelength, and this variation is not the same for different materials.

Absorption can also occur by optical interference, where light is reflected 90 degrees out of phase from successive layers of a multilayer coating. This interference results in absorption of the energy rather than reflection. The coatings are usually alternate thin layers of metal and a dielectric, as shown schematically in Figure 5. For maximum absorption, the coating should be applied in thicknesses of one-quarter wavelength. If the thickness is one-half wavelength, the rays reinforce rather than cancel each other. By proper choice of materials and thicknesses, narrow or broad bands of light can be absorbed.

Another technique for achieving high absorption is to allow multiple reflections to take place before the radiant energy leaves the surface. This can be accomplished by placing cavities on the surfaces, either by sandblasting or by using wire mesh, honeycomb, or similar techniques. This effect is shown schematically in Figure 6. If the holes are small, only short wavelength radiation is absorbed and the surface appears flat to long wavelength radiation. The effect of sandblasting is to increase emissivity by about 10 percent, as shown in Figure 7 for oxidized 310 stainless steel.

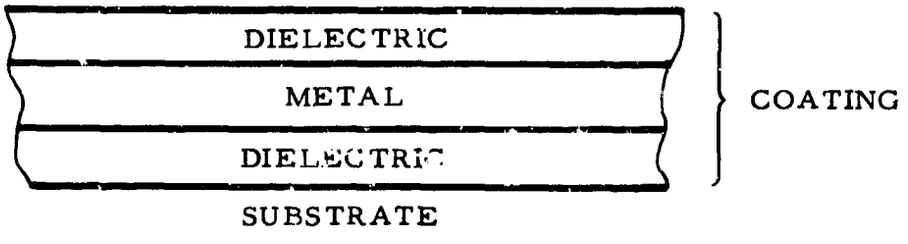

Figure 5. Absorption by Optical Interference

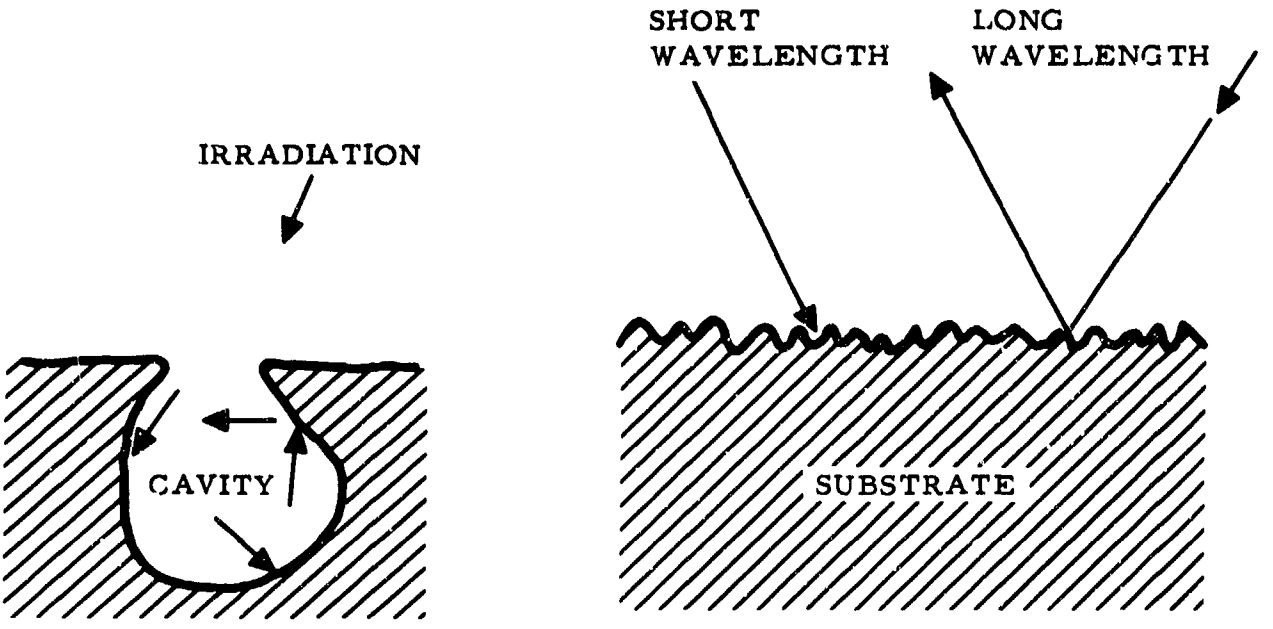

Figure 6. Cavity Absorption

Diffuse and Specular Radiation

Reflection from a surface can be either specular, where the angle of reflection is equal to the angle of incidence, or diffuse, where the reflection follows Lambert's cosine law regardless of incident angle; or it can be various combinations of diffuse and specular. Some of the combinations are indicated in Figure 8. A highly polished surface generally yields specular reflection, while roughened surfaces cause diffuse reflection.

Reflection of infrared energy by metals is caused by the interaction with the conduction electrons. If the unbound electrons remain free during the radiation period, the surface is a perfect reflector; if electrons intercept with other electrons, energy is transferred to the atoms. The reflectivity can be expressed mathematically as (Reference 6)

$$\rho_\lambda = 1 - 0.365\sqrt{\frac{P}{\lambda}} \qquad (6)$$

where

ρ_λ = Reflectivity at wavelength

P = Resistivity, ohm-mm

λ = Wavelength, μ

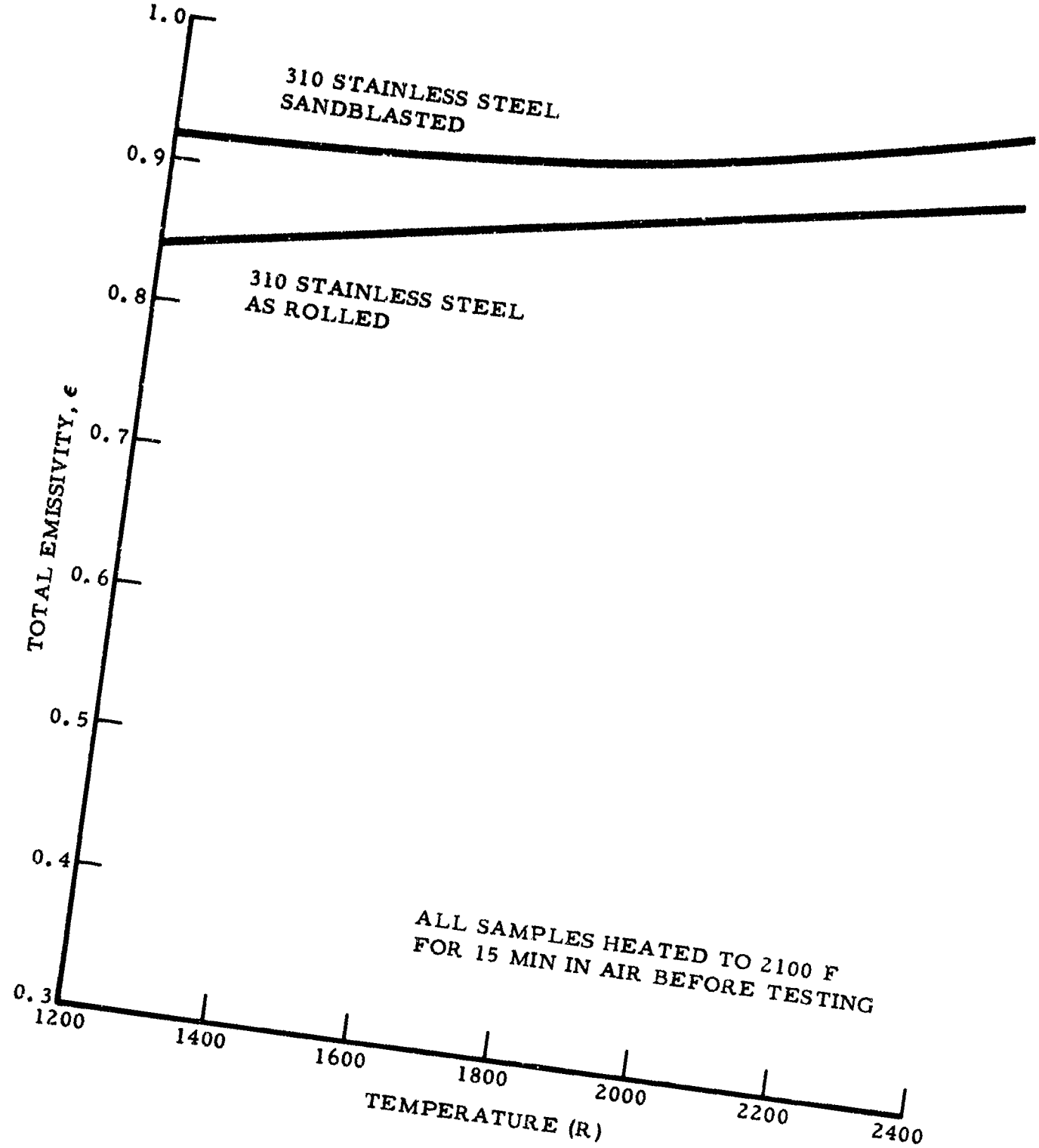

Figure 7. Effect of Sandblasting on Total Emissivity

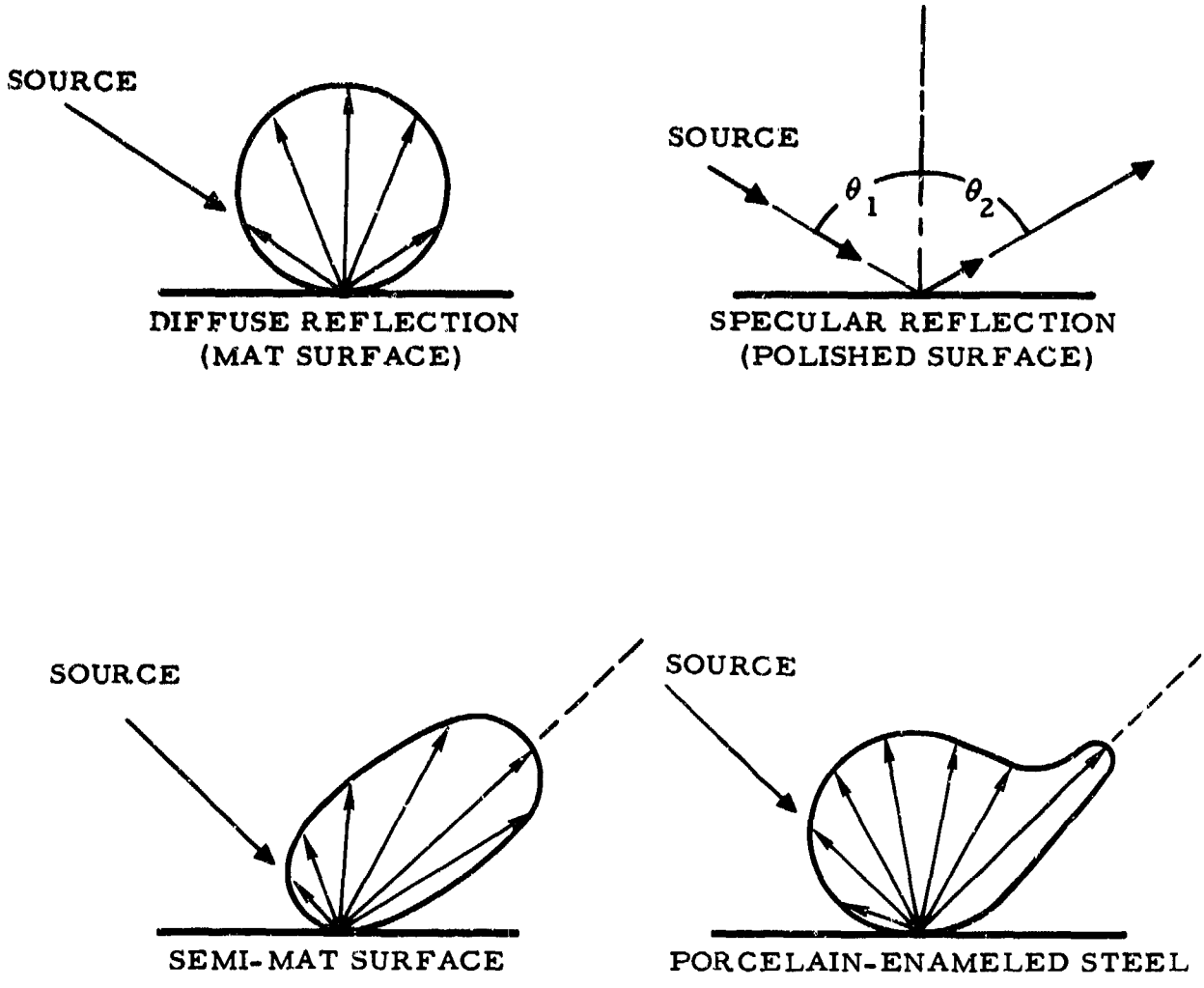

Figure 8. Reflective Surfaces

Equation 6 holds reasonably well for clean metallic surfaces for wavelengths greater than approximately 2 microns.

Fresnel reflections can occur from the surface of a dielectric material. By the use of alternate layers of materials of low and high index of refraction, highly reflective surfaces can be achieved. For minimum absorption, these coatings are applied with a thickness of one-half wavelength. White paints reflect light due to Fresnel reflection, although the reflecting layers are randomly distributed. The nature of Fresnel reflection is indicated in Figure 9.

RADIANT HEAT EXCHANGE BETWEEN SURFACES

The Stefan-Boltzmann equation for the net radiant exchange of energy between two black body radiators, one completely enclosing the other, is

$$q_{net} = \sigma A_1 T_1^4 - \sigma A_2 T_2^4 \qquad (7)$$

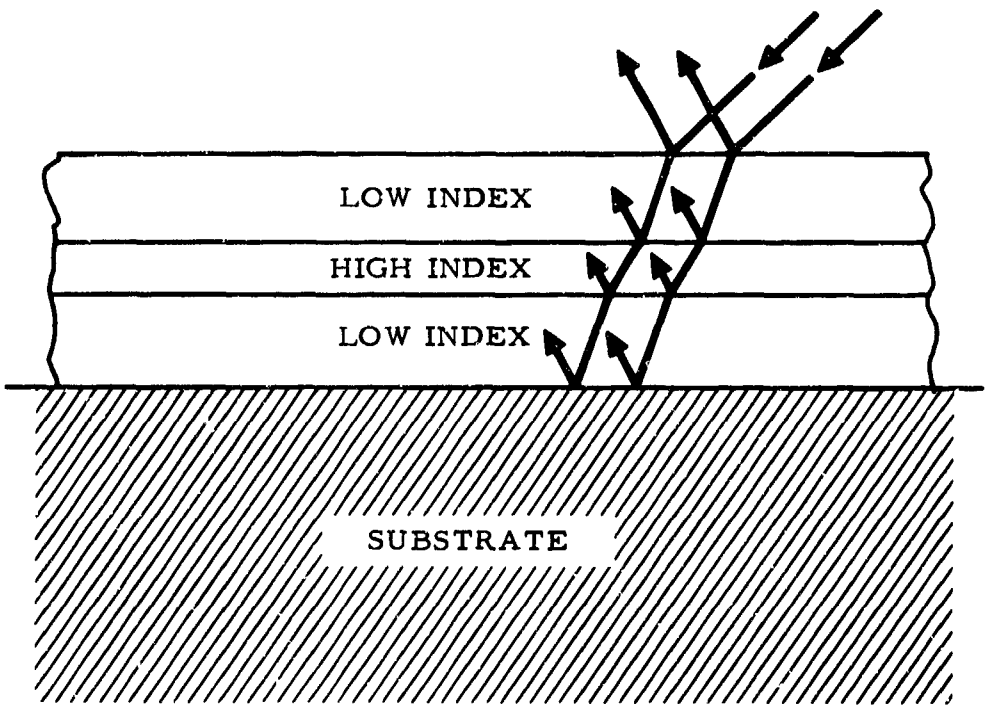

Figure 9. Fresnel Reflection

Most cases of radiant energy transfer, however, do not consist of one body completely enclosing the other. The interchange between the two surfaces depends upon the view the surfaces have of each other. Usually, only a small fraction of the energy leaving one surface is incident upon the other. To account for this, a configuration factor is introduced into the Stefan-Boltzmann equation, as

$$q_{net} = \sigma A_1 F_{12} (T_1^4 - T_2^4) \tag{8}$$

The configuration factor F_{12} is defined as that fraction of the total energy originating at A_1 which is intercepted by A_2. Although the concept of the configuration factor is widely used in both thermal radiation problems and illuminating engineering, no standard designation or symbol for this quantity is currently used in the literature. Names often used include "configuration factor," "shape factor," "shape modulus," "view factor," "sky factor," "form factor," "P factor," and "flux factor."

The mathematical expression for the configuration factor is derived as follows.

Suppose it is desired to determine the radiant heat exchange between the horizontal and vertical black surfaces of Figure 10. The amount of energy which leaves dA_1 and impinges on dA_2 is

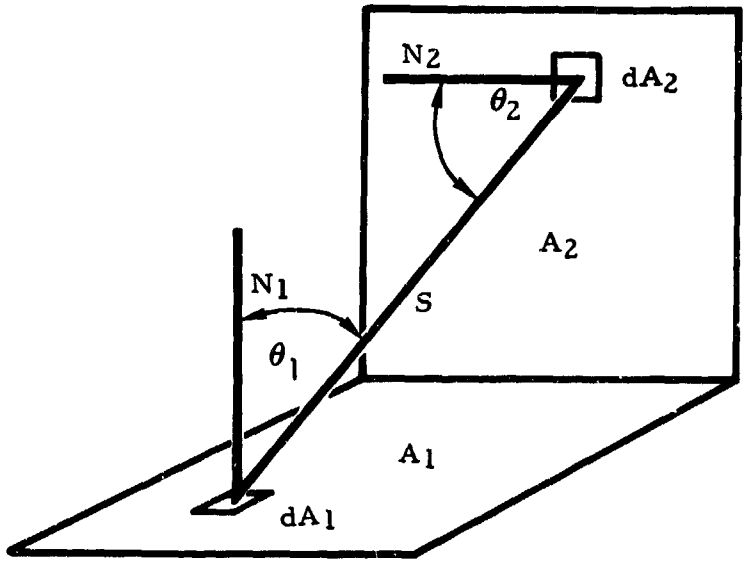

Figure 10. Heat Exchange Between Two Surfaces

$$dq_{12} = I_1 \, dA_1 \cos \theta_1 \left(\frac{dA_2 \cos \theta_2}{S^2} \right) \tag{9}$$

where

I = Intensity of radiation, Btu/(hr)(projected area)(solid angle)

Because the radiation is assumed to be of diffuse form, I is constant in all directions. Therefore, the expression $I_1 \, dA_1 \cos \phi_1$ in Equation 9 determines the rate at which radiant energy leaves dA_1 in the direction of dA_2. The amount of this energy which is intercepted by dA_2 depends on the solid angle which dA_2 subtends with center at dA_1. This solid angle is given in Equation 9 by the expression in parentheses.

In a like manner, the amount of energy which flows from dA_2 to dA_1 is given by

$$dq_{21} = I_2 \, dA_2 \cos \theta_2 \left(\frac{dA_1 \cos \theta_1}{S^2} \right) \tag{10}$$

Therefore,

$$dq_{net} = (I_1 - I_2) \frac{\cos \theta_1 \cos \theta_2 \, dA_1 \, dA_2}{S^2} \tag{11}$$

For diffuse radiation,

$$I = \frac{E}{\pi} = \frac{\sigma T^4}{\pi}$$

Therefore,

$$dq_{net} = \sigma (T_1^4 - T_2^4) \left(\frac{1}{\pi} \right) \frac{\cos \theta_1 \cos \theta_2 \, dA_1 \, dA_2}{S^2} \tag{12}$$

and

$$q_{net} = \sigma (T_1^4 - T_2^4) \left(\frac{1}{\pi} \right) \int_{A_1} \int_{A_2} \frac{\cos \theta_1 \cos \theta_2 \, dA_1 \, dA_2}{S^2} \tag{13}$$

It follows from Equations 8 and 13 that

$$A_1 F_{12} = \frac{1}{\pi} \int_{A_1} \int_{A_2} \frac{\cos \theta_1 \cos \theta_2 \, dA_1 \, dA_2}{S^2} \tag{14}$$

and

$$F_{12} = \frac{1}{A_1 \pi} \int_{A_1} \int_{A_2} \frac{\cos \theta_1 \cos \theta_2 \, dA_1 \, dA_2}{S^2} \tag{15}$$

Equation 15 is the integral expression for the configuration factor and is dependent on the geometry of the system only. Although this discussion has been limited to black surfaces, it is evident that for a non-black surface the configuration factor F_{12} also represents the fraction of radiation from A_1 intercepted by A_2 (but not necessarily absorbed). It should also be evident that

$$F_{12} + F_{13} + F_{14} + \ldots = 1 \tag{16}$$

where F_{13}, F_{14}, ... are the configuration factors for other surfaces which are seen by A_1. If A_1 is not flat, it may see portions of itself and have a finite F_{11}.

It should also be pointed out that

$$F_{12} A_1 = F_{21} A_2 \tag{17}$$

Equation 17 is often called the reciprocity theorem. Thus, for the net exchange between two black surfaces,

$$q_{net} = A_1 F_{12} \sigma T_1^4 - A_2 F_{21} \sigma T_2^4 \tag{18}$$

and

$$q_{net} = \sigma A_1 F_{12} (T_1^4 - T_2^4)$$

$$= \sigma A_2 F_{21} (T_1^4 - T_2^4) \tag{19}$$

In most cases, radiant heat exchange between two surfaces is influenced by the absorption, reflection, and emission from connecting surfaces. If the surfaces are non-black (i. e., gray or real), a complete accounting of

all the interreflections is quite difficult to accomplish analytically. Fortunately, methods are available for the more complicated radiation problems. These are discussed in Section VI.

Section IV

THERMAL RADIATION ENVIRONMENT IN SPACE

Incident radiation consists of the direct radiation from the sun, scattered and reflected sun radiation from a nearby planetary body, and radiation directly emitted by the planetary body. The value of irradiance varies over the surface of a vehicle and depends on the relative position of the surface with respect to the sun and other planetary bodies.

DIRECT SOLAR RADIATION

The release of energy from the sun produces radiation in many forms. Most of the radiation is thermal, concentrated in the visible and infrared spectrum. The total energy radiated in X-ray and ultraviolet bands is only a very small portion, measured in thousandths of a percent, of the total energy output of the sun.

Radiation intensity is inversely proportional to the square of the distance from the sun. At 1 astronomical unit (the distance from the sun to the earth), the total value of the solar constant is 443 Btu/(hour)(square foot) (Reference 7). The variation of irradiance for the solar system is shown in Figure 11. The solar constant is influenced by sunspot and other activity, but variations are small (less than 0.4 percent).

Many calculations are based on the assumption that the sun radiates as a 10,340 F black body. The black body radiant temperature, however, varies for each wavelength, and these variations should be analyzed for more exact calculations. Examples of approximate temperatures at which the sun radiates are given in Table 1 for several wavelengths (Reference 8). The deviation in spectral energy distribution from black body radiation is probably caused by variations in absorption by the solar atmospheric gases. The spectral energy curve of the sun is shown in Figure 12 (Reference 7).

The minimum temperature for any wavelength is approximately 6750 F. For the production of very short ultraviolet wavelengths and X-rays, the temperature in the corona is in the range of 1×10^6 F. Sunspot temperatures are approximately 3600 F less than the photosphere; they emit only about 10 percent as much energy as equal areas of the solar surface.

Curves of intensity and wavelength of the solar spectrum show that most of the energy from the sun is carried in wavelengths between 2000 and

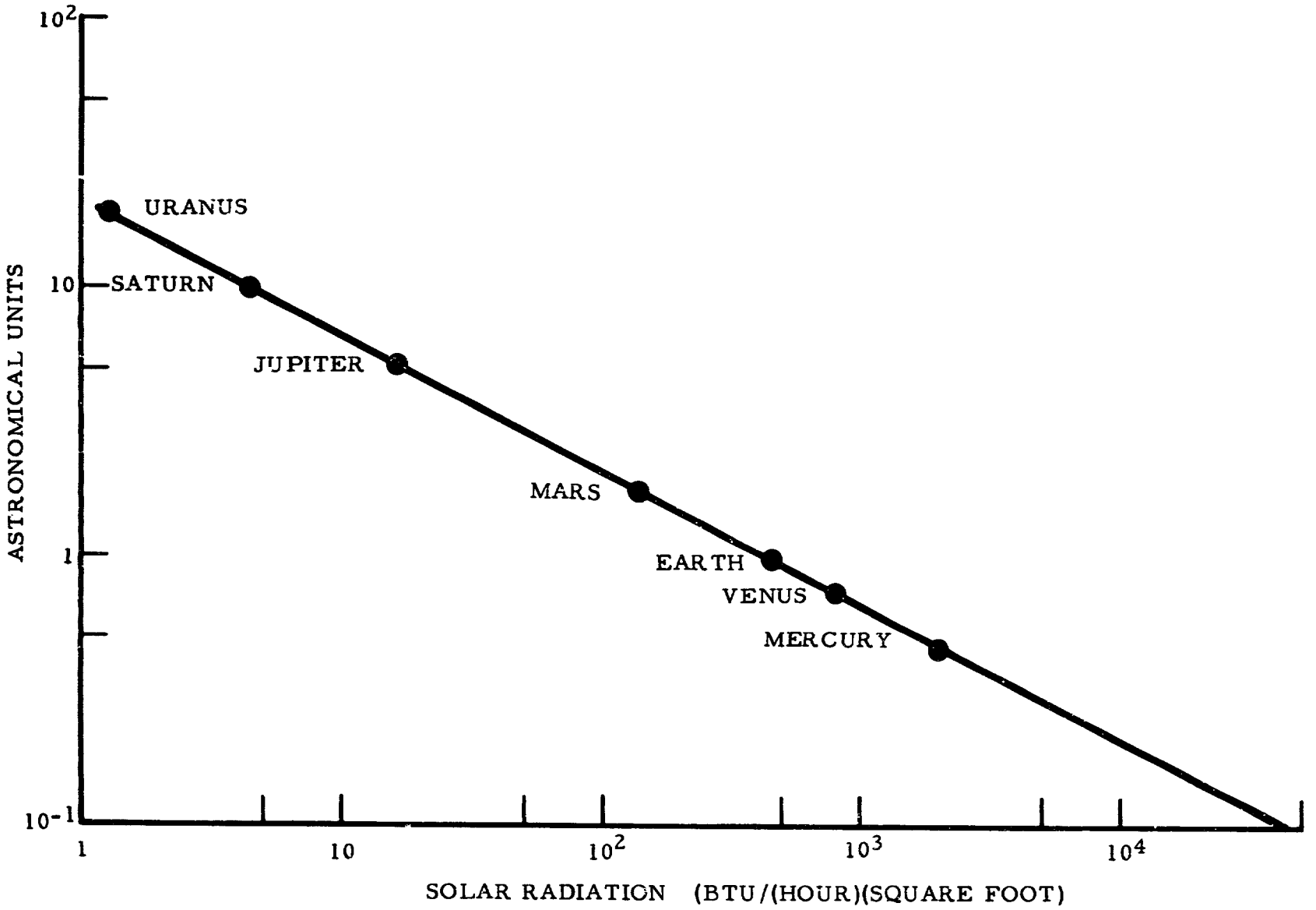

Figure 11. Solar Radiation at Various Distances From Sun

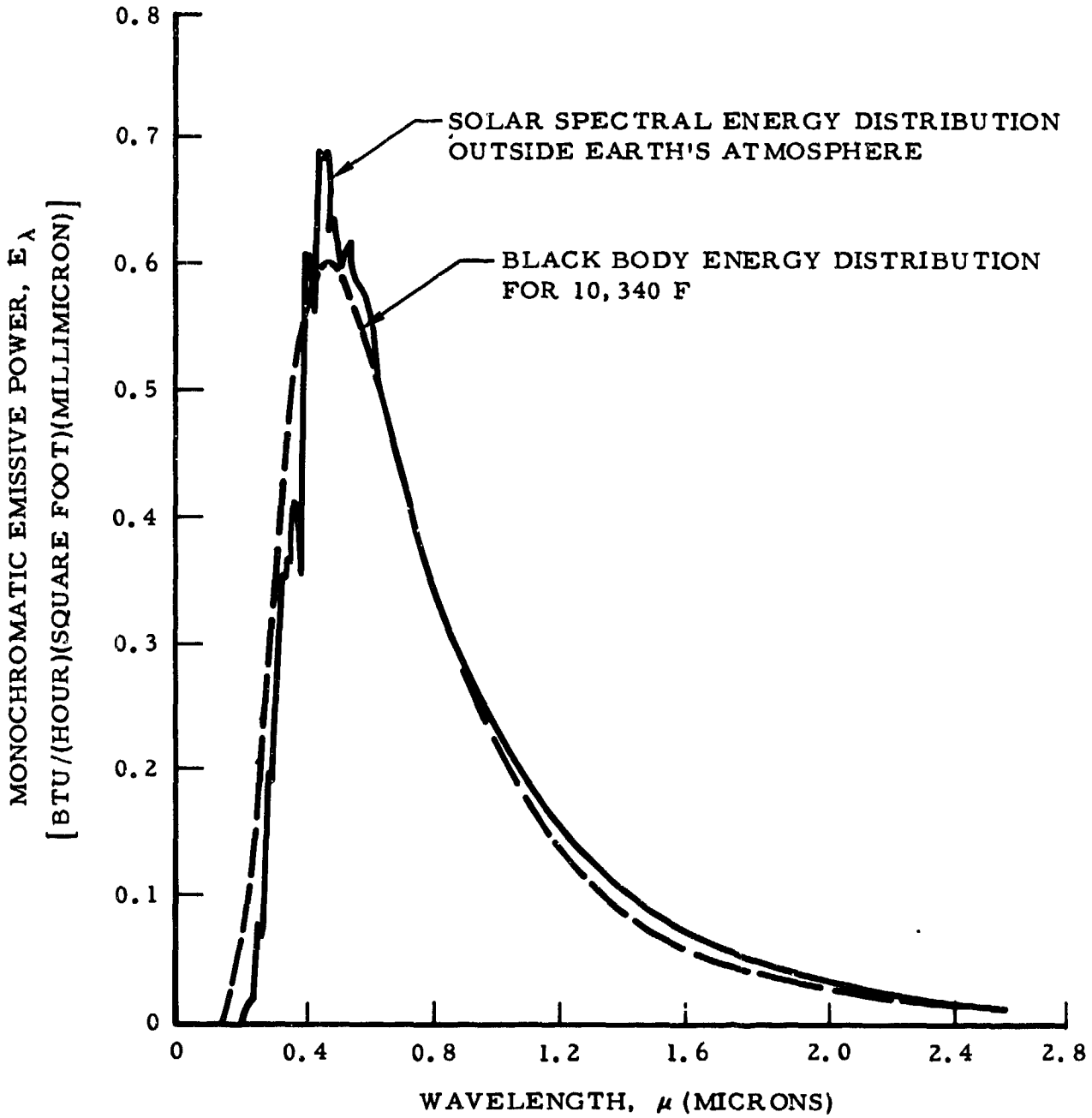

Figure 12. Spectral Energy Curve of Sun

Table 1. Solar Radiation Temperatures

Wavelength (Å)	Temperature (F)
3500	9430
2900	9430
2600	8530
2200	8360
2000	7650
1500	7650
1200	10, 500

20, 000 angstroms, with the maximum energy centered about 4700 angstroms. The approximate energy distribution of solar radiance by percent of the total is given in Table 2 for several wavelength intervals (Reference 8).

Table 2. Energy Distribution of Solar Electromagnetic Radiation

Type	Wavelength Interval (Å)	Approximate Radiant Energy (percent)
X-ray and ultraviolet	1 to 2000	0. 2
Ultraviolet	2000 to 3800	7. 8
Visible	3800 to 7000	41
Infrared	7000 to 10, 000	22
Infrared	10, 000 to 20, 000	23
Infrared	20, 000 to 100, 000	6

The normal sun produces X-rays with power density on the order of 0. 316 Btu/(hour)(square foot). These are probably produced in the corona. During a quiet sun, X-rays reaching the earth are neither very intense nor energetic. Wavelengths as short as 20 angstroms are present and penetrate the atmosphere to within 60 miles of the earth's surface when the sun is overhead. During maximum coronal activity the total output of X-rays may increase by a factor of 2 or 3 and, at the same time, tend to become harder with wavelengths as short as 6 or 7 angstroms. Flares are a still more important factor in producing hard X-rays, but their intensity near the earth is still low.

In the ultraviolet portion of the spectrum below 2000 angstroms, the greatest portion of the energy is found at the wavelength (1216 angstroms) of the resonance emission line of hydrogen atoms. In spectroscopy, this is

known as the Lyman alpha line. Below the wavelength of Lyman alpha are many other emission lines. One which appears to have more energy than the rest combined, but still much less than Lyman alpha, is found at 304 angstroms, which is the wavelength emitted by ionized helium. These emissions are detected only above the earth's atmosphere.

The small amount of ozone present in the atmosphere absorbs all wavelengths of ultraviolet radiation below about 2900 angstroms and attenuates those up to 3500 angstroms. Consequently, ultraviolet is much more penetrating and intense above approximately 19 miles (100,000 feet). Above about 47 miles the ultraviolet light is practically unfiltered.

At the infrared end of the spectrum, a number of bands are absorbed in the atmosphere by water vapor and carbon dioxide, but the cutoff wavelength does not occur until in the far infrared. The effect of the absorption, then, is to diminish the intensity but not to eliminate completely the near infrared even at the surface.

A thorough discussion of visible and infrared thermal radiation can be found in Reference 8.

REFLECTED SOLAR RADIATION

The ratio of solar radiation scattered back into space without absorption to that incident upon the planet is termed "albedo". The albedo of an object is the fraction of the incident energy which is reflected by the object in the entire band from ultraviolet to the far infrared. The spectral reflectance of an object ideally is the fraction of monochromatic incident energy of wavelength λ reflected by the object, but in practice it always refers to a finite narrow band. The visual albedo of an object refers only to the visible part of the spectrum. The luminous reflectance of various objects is shown in Table 3 (Reference 9).

The planetary albedo is caused by scattering at the planet's surface, scattering by clouds and dust in its atmosphere, and molecular scattering by atmospheric gases. The characteristics of the radiation emerging from the top of a planetary atmosphere are complex as they are functions of terrain, cloud covers, optical thickness of the atmospheric gases, the sun's elevation angle, nadir angle, azimuth angle with respect to sun, and radiation wavelength. The albedo of the various planets is shown in Table 4 (References 10 and 11).

The visual albedo of the earth as determined from earth shine varies with the seasons from 0.52 in October to 0.32 in July, with an average value of 0.35. Variations in cloudiness may account for most of the seasonable variations. Reference 11 reports that albedo of clouds alone is about 0.5, which is in keeping with maximum seasonal values stated. Taking the measured visual albedo of the whole earth as 0.39 (Reference 11), the albedo

Table 3. Luminous Reflectance of Various Earth Objects

Object	Luminous Reflectance (percent)		
	Smithsonian Tables	Sewing Handbook	Krinov
Water surfaces			
Bay	3 to 4		
Bay and river	6 to 10		
Inland water	5 to 10		5
Ocean	3 to 7		
Ocean, deep	3 to 5		
Bare areas and sand			
Snow, fresh	70 to 86		77
Snow, with ice			75
Limestone, clay			63
Calcareous rocks		30	
Granite		12	
Mountain tops, bare			24
Sand, dry		31	24
Sand, wet		18	
Clay soil, any		15	
Clay soil, wet		7.5	9
Ground, bare, dry	10 to 20	7.2	9
Ground, bare, wet		5.5	
Ground, black earth			3
Field, plowed	20 to 25		
Vegetative formations			
Coniferous forest, winter			3
Coniferous forest, summer	3 to 10		8
Deciduous forest, fall			15
Deciduous forest, summer			10
Coniferous forest, summer, from airplane			3
Dark hedges		1	
Meadow, dry, grass	3 to 6		8
Grass, lush	15 to 25		10
Meadow, low grass			8
Field crops, ripe	7		15
Roads and buildings			
Earth roads			3
Black top roads		8	
Concrete road, smooth, dry		35	
Concrete road, smooth, wet		15	
Concrete road, rough, dry		35	
Concrete road, rough, wet		25	
Buildings			9
Limestone tiles		25	

Table 4. Planetary Albedos

Planet	Albedo
Mercury	0.07
Venus	0.76
Earth	0.35
Mars	0.15
Jupiter	0.51
Saturn	0.50
Uranus	0.66
Neptune	0.62
Pluto	0.16

of the earth in total sunlight is computed to be 0.35. The albedos of the earth's surface, clouds, and atmosphere are computed separately in ultraviolet, visible, and infrared. After 2 percent is allowed for absorption by ozone, the albedo of the whole earth is 0.5 in ultraviolet, 0.39 in visible, and 0.28 in infrared wavelengths. Of the total incident light on the earth, the percentage reflected is 2.3 percent by the earth's surface, 23 percent by clouds and 9 percent by the atmosphere, making a total of 35 percent.

Because of the complexity of the problem and because variations in terrain affect the albedo greatly, the planetary albedo is assumed to be constant over the surface of a planet; and the planet is considered to be a diffuse reflector. It should be kept in mind, however, that the average value is open to question and that local variations could be large.

PLANETARY EMITTED RADIATION

A planet radiates thermal energy into space due to its temperature. The nature of this radiation is a function of latitude, surface characteristics of the planet, composition and optical thickness of atmospheric gases, clouds, and the wavelength region of the radiation under consideration. The temperatures of the various planets are shown in Table 5 (Reference 2).

Difficulties are encountered with the earth-atmosphere model used to determine earth emission. If the usual assumption is made that the earth system is in a state of thermal equilibrium, the magnitude of the average earth emission becomes a function of the average albedo. However, the effective temperature at which the earth-atmosphere system radiates and the spectral distribution of the energy are not well defined. Some sources estimate effective temperatures near -6 F. Such temperatures are effective black body temperatures based on an average albedo and an equilibrium earth system. With only 25 percent of the earth emission

Table 5. Planetary Temperatures

Planet	Probable Temperature (F)
Mercury	339
Venus	-46
Earth	-6
Mars	-68
Jupiter	-276
Saturn	-323
Uranus	-372
Neptune	-400
Pluto	

coming from the earth and 75 percent coming from the atmosphere, it might be expected that the spectral energy distribution would be different from that for a black body.

The effective temperature of the earth-atmosphere system is low enough to cause the bulk of the earth emission to fall in the infrared, where the spectral characteristics of many materials are not very sensitive to wavelength. Also, the local heat balance of the earth system is too complex to yield useful values for local variations.

Section V

SPACE VEHICLE SURFACE TEMPERATURE ANALYSIS

INTRODUCTION

This section of the report presents some available analytical techniques and solutions for space vehicle thermal problems. These satellite studies include the following:

1. A simplified steady-state analysis for near-earth orbits based on a cylindrical satellite configuration with its axis on a line passing through the center of the earth

2. An IBM 7090 program for the transient heat transfer analysis of a multi-sided space vehicle in any elliptical or circular orbit

3. A space thermal environment study, including spherical, cylindrical, hemispherical, and flat-sided satellites

Regardless of the type of temperature control system used aboard a space vehicle, system requirements are a function of the vehicle's outer surface temperature. These surface temperatures, in turn, are dependent on the following parameters:

Orbital characteristics
Optical properties of surfaces and components, such as emittance and absorptance
Vehicle orientation to sun and planet
Heat capacity of vehicle walls and equipment
Conductive, radiative, and possibly convective heat transfer between surfaces and equipment
Internal heat generation
Aerodynamic heating for near-earth orbits below 200 miles
Solar constant
Planetary albedo
Planetary emission
Vehicle configuration

It is also true that, by proper selection of optical properties, the surface temperatures can be controlled to different levels anywhere within a very large range. In optimizing a vehicle design, however, the selection of the proper control system is made complex because of the many variations that can exist in the parameters listed. Variations caused by errors in orbital characteristics, unknowns in the nature of the radiation environment, vehicle stabilization errors which affect orientation, instability of surface coatings, and other uncertainties all influence the heat balance on the vehicle that determines the surface temperature.

Determination of aerodynamic heating in the free-molecular flow regime will not be considered in this report. For low-altitude orbits below 200 miles, however, it may be significant in comparison with the magnitude of the other energy inputs.

The analytical techniques presented in this section illustrate the complexity of the problem. They point out ways of determining the form factor between the space vehicle and the planet and sun, and the manner in which each of the factors enters into the heat balance.

SIMPLIFIED SPACE RADIATION ANALYSIS

The discussion here is of a simplified space radiation analysis which takes into account the contributions of solar and terrestrial radiation and assumes steady-state heat transfer. The material was prepared by AiResearch Manufacturing Division for incorporation in this report.

NOMENCLATURE

a	Earth albedo
D	Diameter of radiator cylinder, ft
L	Length of radiator cylinder, ft
q_{CY}	Internal heat input to element, Btu/hr
$q_{E(SR)}$	Solar radiation reflected from earth and absorbed by element, Btu/hr
$q_{E(TR)}$	Thermal radiation from earth absorbed by element, Btu/hr
q_S	Total solar energy absorbed by radiator, Btu/hr
q_{SR}	Direct solar radiation absorbed by element, Btu/hr
q_{TR}	Heat radiated from element, Btu/hr
S	Solar constant = 443 Btu/(sq ft)(hr)
T	Radiator surface temperature, °R
T_E	Effective radiating temperature of earth, °R
α_S	Solar absorptivity of radiator surface
α_T	Absorptivity of radiator surface to earth emission
ϵ_E	Emissivity of earth for thermal radiation
σ	Stefan-Boltzmann radiation constant = 0.1713×10^{-8} Btu/(sq ft)(hr)$(°R)^4$
Ω	Solar elevation angle measured from vertical, deg

HEAT BALANCE

The thermodynamic aspects of the heat transfer problem are illustrated by considering the steady-state heat flow balance equation (heat outflow equals heat inflow) for an element of surface area

$$dq_{TR} = dq_{CY} + dq_{SR} + dq_{E(TR)} + dq_{E(SR)} \qquad (20)$$

To determine the radiator surface area required per unit of internal heat flow, it is necessary to determine what physical orientation of the surface maximizes the sum of q_{SR}, $q_{E(TR)}$, and $q_{E(SR)}$, because this situation imposes the most severe requirement on the radiator surface. The radiator is assumed to be a cylindrical surface with its axis on a line passing through the center of the earth, located at a known distance h above the earth's surface. For this geometry (shown in Figure 13), $q_{E(TR)}$ is essentially independent of the sun's position, whereas dq_{SR} and $dq_{E(SR)}$ are both functions of the sun's position relative to earth and vehicle, and $dq_{E(SR)}$ is also a function of the earth's albedo. When an appropriate assumption is made regarding the earth's albedo, the radiator design considers the solar position relative to earth and vehicle for which the sum of q_{SR} and $q_{E(SR)}$ is a maximum.

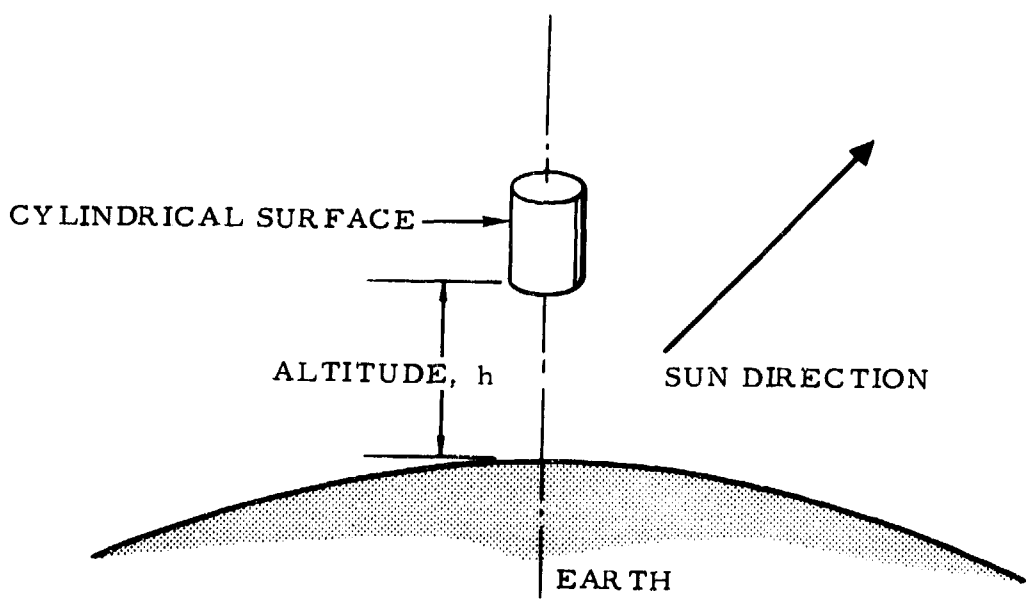

Figure 13. Space Vehicle Orientation

ANALYSIS DESCRIPTION

In the analysis which follows, the radiator surface required per unit heat flow rate is determined as a function of the radiator surface temperature and a parameter which includes the effects of the values chosen for the various emissivities and absorptivities involved and for the earth's albedo.

The analysis was performed in two parts: (1) consideration of a simplified geometry in which the earth is assumed to be an infinite plane, and (2) refinement of the simplified geometric model to take into account the spherical shape of the earth. This approach has an advantage in that the first part illustrates the essential physical phenomena, unobscured by the procedural complications of the second part.

Simplified Geometry Analysis

To determine the solar elevation angle ω, at which the sum of q_{SR} and $q_{E(SR)}$ is maximized, the definition is made that

$$q_S = q_{SR} + q_{E(SR)} \tag{21}$$

The term q_S is thus the total solar energy absorbed by the radiator. Defining further,

$$q_{SR} = \alpha_S \, DLS \sin \Omega \tag{22}$$

$$q_{E(SR)} = \frac{1}{2} \alpha_S \, DLaS \cos \Omega \tag{23}$$

The factor 1/2 is used in Equation 23 for $q_{E(SR)}$ because the infinite plane is 50 percent effective in enclosing the radiator.

To determine the maximum value of q_S and the value of Ω at which this maximum occurs, $dq_S/d\Omega$ is set equal to zero. It follows that

$$\frac{dq_S}{d\Omega} = \frac{d}{d\Omega} \left[\alpha_S \, DLS \left(\sin \Omega + \frac{\pi a}{2} \cos \Omega \right) \right] \tag{24}$$

$$0 = \alpha_S \, DLS \left(\cos \Omega - \frac{\pi a}{2} \sin \Omega \right) \tag{25}$$

To define the angle Ω_{max} at which the total solar radiation absorbed by the radiator is maximized,

$$\Omega_{max} = \tan^{-1}\left(\frac{2}{\pi a}\right) \tag{26}$$

From which

$$\sin \Omega_{max} = \frac{2}{\pi a\sqrt{1 + \frac{4}{\pi^2 a^2}}} \tag{27}$$

and

$$\cos \Omega_{max} = \frac{1}{\sqrt{1 + \frac{4}{\pi^2 a^2}}}, \tag{28}$$

The maximum solar radiation absorbed by the radiator is

$$q_{S(max)} = \alpha_S \, DLS \left(\frac{\frac{2}{\pi a} + \frac{\pi a}{2}}{\sqrt{1 + \frac{4}{\pi^2 a^2}}}\right) \tag{29}$$

$$= \alpha_S \, DLS \sqrt{1 + \frac{\pi^2 a^2}{4}}$$

The effect of earth albedo a on Ω_{max} and $q_{S(max)}$ is shown in the following table:

Earth Albedo a	Solar Elevation Angle Ω_{max} (deg)	$\frac{q_{S(max)}}{\alpha_S \, DLS}$
0	90	1.00
0.2	72.5	1.05
0.4	57.9	1.18
0.6	46.7	1.37
0.8	38.5	1.61
1.0	28.3	1.86

For a small element of radiator surface, dA, the heat balance equation is

$$dq_{TR} = dq_{CY} + dq_{E(TR)} + dq_{S(max)} \tag{30}$$

From which can be obtained

$$\sigma T^4 A = q_{CY} + \sigma \epsilon_E \alpha_T T_E^4 \left(\frac{A}{2}\right) + \alpha_S \left(\frac{SA}{\pi}\right)\sqrt{1 + \frac{\pi^2 a^2}{4}} \tag{31}$$

Refined Geometry Analysis

Refinement of the previous analysis, to account for a spherical earth rather than an infinite plane, is desirable because the simplified analysis may be conservative to an unrealistic degree.

The analytical process to be followed is similar in principle to that discussed previously. In the present analysis, expressions for $q_{E(SR)}$ and $q_{E(TR)}$ contain shape factors in the form of integrals which must be evaluated numerically. Because the mechanics of the derivations are quite cumbersome, only the results of each analysis are reported in the following discussion.

Evaluation of $q_{E(TR)}$

Evaluation of $q_{E(TR)}$, assuming a spherical earth of 3960-mile radius and a radiator altitude of approximately 300 miles above the earth's surface, leads to the result

$$q_{E(TR)_2} = 0.2722 \sigma \epsilon_E \alpha_T A T_E^4 \tag{32}$$

which compares with the previous result given by Equation 31

$$q_{E(TR)_1} = \sigma \epsilon_E \alpha_T T_E^4 \left(\frac{A}{2}\right) \tag{33}$$

Equation 33 was calculated assuming the earth to be an infinite plane. This result indicates that the radiator surface absorbs only 54.4 percent of the thermal radiation from the earth as estimated previously.

Evaluation of $q_{E(SR)}$

Evaluation of $q_{E(SR)}$, again assuming a spherical of 3960-mile radius and a radiator altitude of 300 miles, yields

$$q_{E(SR)} = 0.2696\ \alpha_S\ DLS\ \pi\ a \cos \Omega \tag{34}$$

which is, again, about 54 percent of that calculated assuming the earth to be an infinite plane.

Evaluation of Ω_{max}

Using the relation given in Equation 34 for $q_{E(SR)}$,

$$q_S = q_{E(SR)} + q_{SR}$$

is written

$$q_S = \alpha_S DLS \sin \Omega + 0.2696\ \alpha_S DLS\ \pi\ a \cos \Omega \tag{35}$$

By differentiating Equation 35 and equating the result to zero, Ω_{max} is found to be

$$\Omega_{max} = \tan^{-1} \left(\frac{1}{0.2696 \pi a} \right) \tag{36}$$

Evaluation of $q_{S(max)}$

Using the result for Ω_{max} (Equation 36),

$$q_{S(max)} = \alpha_S\ DLS \sqrt{1 + (0.2696)^2 \pi^2 a^2} \tag{37}$$

This relation is valid only for values of Ω_{max} where the entire portion of the earth visible from the radiator is illuminated by the sun. For the assumed radiator elevation of 300 miles, this implies $0 \leq \Omega_{max} \leq 67.6$ degrees.

IBM 7090 PROGRAM FOR TRANSIENT HEAT TRANSFER ANALYSIS OF ORBITING SPACE VEHICLES

An IBM 7090 program has been developed at S&ID which will simulate the thermal environment of a multisided space vehicle in any earth orbit. This program will determine the transient temperature history of the satellite shell; and, if desired, will also provide the complete history of the radiant energy incident upon the vehicle surfaces due to direct solar radiation, earth emission, and earth reflected solar radiation. These heat loads can be used as input data in a general heat transfer program if it is desired to obtain a detailed thermal analysis of the interior of the vehicle.

The evaluation studies presented in Section VIII were obtained through the use of this program. They demonstrate the flexibility of the program when a parametric study is conducted.

A description of the analysis techniques utilized by the program is presented in this discussion. The areas covered are orbital mechanics, earth shadow intersection points, vehicle configuration and orientation, temperature determination, and vehicle-to-earth geometric configuration factors. A complete presentation of these subjects, as well as programing techniques and program philosophy, can be found in report SID 61-105, "Program for Determining Temperatures of Orbiting Space Vehicles," by G. A. McCue (Reference 33). Data entry, data output, sample problems, the program listing, and program flow diagram are also contained in report SID 61-105.

NOMENCLATURE

A	Surface area of satellite, sq ft
a	Semimajor axis of orbit ellipse
a_s	Semimajor axis of shadow ellipse
A_1	Angle defined in Figures 27 and 28
b	Semiminor axis of orbit ellipse
c	Construction defined in Figure 25

c_p	Specific heat, Btu/(lb_m) (°R)
d	Construction defined in Figure 25
E	Eccentric anomaly
E_E	Planetary emission, Btu/(hr) (sq ft)
e	Eccentricity of orbit ellipse
F_E	Geometric form factor for planetary emission
F_R	Geometric form factor for reflected solar radiation
F_s	Geometric form factor for direct solar radiation
h	Height above earth's surface
i	Inclination of orbit ellipse
M	Mean anomaly
m	Subscript indicating mass
P	Semilatus rectum of orbit ellipse
$\overline{P}$	Perigee vector
q	Internal heat load, Btu/hr
q_o	Construction defined in Figure 25
r	Radius of spherical vehicle
r_E	Planetary albedo
r_o	Radius from geocenter (orbit ellipse)
r_s	Radius from geocenter (shadow ellipse)
R	Earth's radius
R_E	Reflected solar energy from planet, Btu/(hr) (ft^2)
S	Solar constant, Btu/(hr) (ft^2)
$\overline{S\ell_o}$	Sun's projection upon the orbit plane
s	Construction defined in Figures 27 and 28
t	Time, hr
T	Temperature, °R
T_o	Epoch time

T_m	Maximum expected temperature, °R
T_s	Fraction of orbit time in earth's shadow
V	Velocity
W	Mass of satellite or surface, lb_m
x, y, z	Rectangular coordinates of equatorial coordinate system
α	Construction defined in Figures 26 through 28
α_s	Solar absorptivity of satellite or surface
α_E	Infrared absorptivity of satellite or surface
α_R	Absorptivity to reflected solar
β	Angle between $\overline{S\ell_o}$ and $\overline{P}$ vectors
γ	Construction defined in Figures 26 through 28
δ	Construction defined in Figures 27 and 28
ϵ	Construction defined in Figures 27 and 28
ϵ_s	Emissivity of satellite surface
η	Construction defined in Figures 27 and 28
θ	True anomaly increment between satellite's position and the line of nodes
$\theta - \omega$	True anomaly
θ_s	Angle between earth-sun line and the vertical between the earth and satellite
θ_N	Angle between the normal to a satellite surface and the line between the sun and satellite
θ_1	Angle between the normal to a satellite surface and the line between the earth and satellite
θ_2	Half of the angle subtended by the earth as viewed from the satellite
μ	Gravitation constant
σ	Stefan-Boltzmann constant = 0.1713×10^{-8} Btu/(hr) (sq ft) ($^oR^4$)
σ_o	Mean anomaly at epoch

ϕ Angle between the satellite and the sun's projection upon the orbit plane

ϕ_c Angle defined in Figures 27 and 28

ω Argument of perigee

Ω Right ascension of the ascending node

ORBITAL MECHANICS

The physical model of orbital motion to be utilized in this analysis is an isolated dynamic system consisting of an earth, an earth satellite, and a sun which revolves in the ecliptic in the astronomical place of the apparent sun, but is infinitely distant from earth. It is assumed that the earth has no atmosphere, and is represented gravitationally by the zero-order and second-order spherical harmonics of its potential. It is further assumed that such a trajectory can be described as a function of time by considering a set of six varying orbital elements. The elements which will be used for this analysis are semimajor axis, eccentricity, argument of perigee, right ascension of the ascending node, inclination, and the mean anomaly at epoch (a, e, ω, Ω, i, σ_o). These elements, along with pertinent equations of elliptical motion, are indicated in Figure 14. The position of the satellite in the ellipse is described by the angular advance from perigee, $\theta - \omega$ (true anomaly). The presence of harmonics in the earth's gravitational potential will cause periodic and secular variations in several of the orbital elements. Only the secular perturbations which result in regression of the nodes and advance of the perigee position are considered in this analysis. Other periodic changes nave negligible effect upon the shadow intersection problem. First-order perturbation theory as developed by Cunningham (Reference 4) has been applied to determine these variations.

The angles Ω and ω are then described as a function of time by the linearized expressions

$$\Omega = \Omega_o + \dot{\Omega}\,(t - T_o) \tag{38}$$

$$\omega = \omega_o + \dot{\omega}\,(t - T_o) \tag{39}$$

where $\dot{\Omega}$ and $\dot{\omega}$ are obtained from Cunningham's equations, and $t - T_o$ is the time since epoch.

The geocentric position of the sun is computed by the program from linearized expressions involving the earth's mean motion and the equation of time as a function of date. A simple transformation of coordinates can then

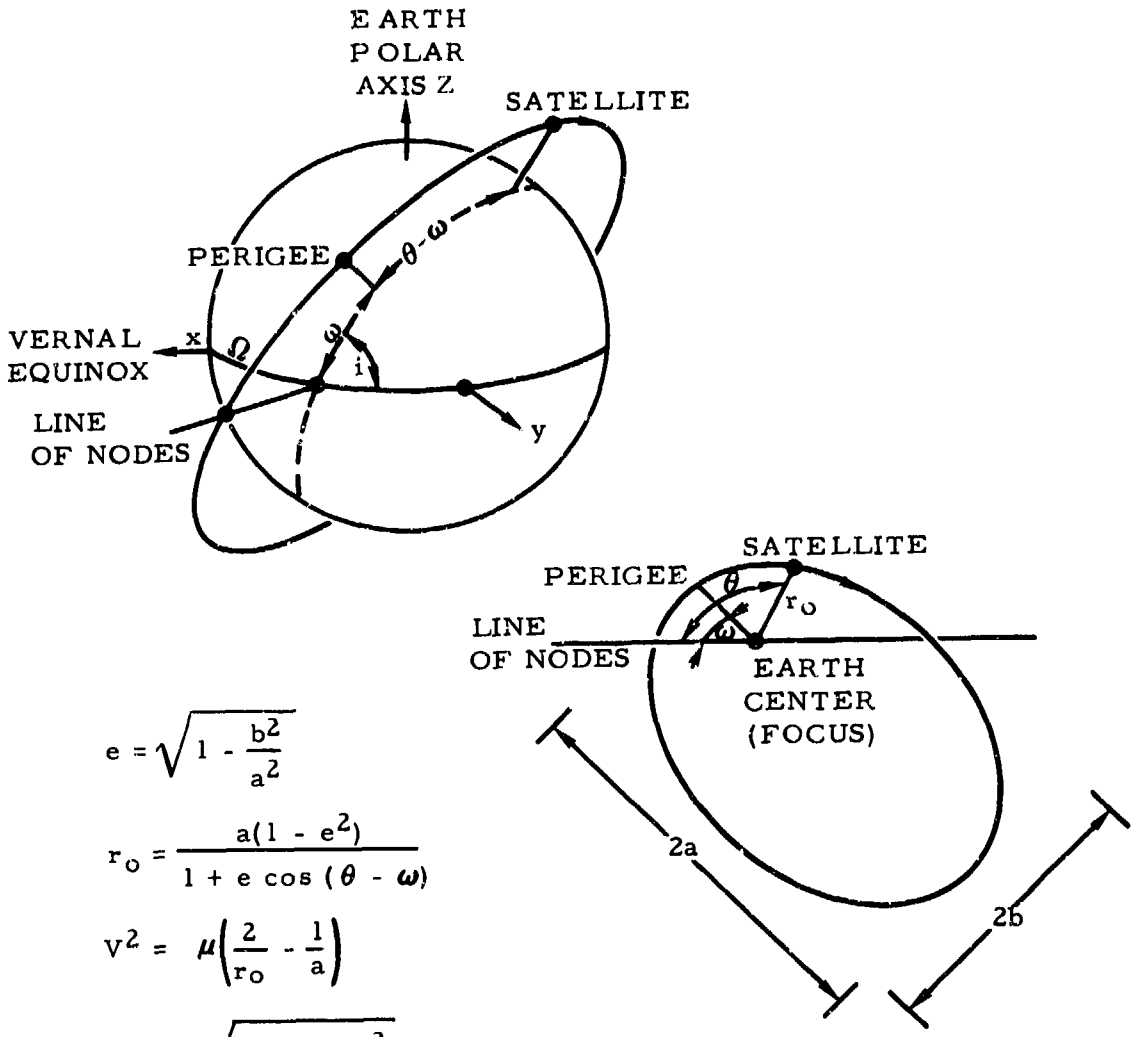

$$e = \sqrt{1 - \frac{b^2}{a^2}}$$

$$r_o = \frac{a(1 - e^2)}{1 + e \cos(\theta - \omega)}$$

$$V^2 = \mu\left(\frac{2}{r_o} - \frac{1}{a}\right)$$

$$r^2\dot{\theta} = \sqrt{\mu a (1 - e^2)}$$

$$P = \frac{2\pi a^{3/2}}{\mu^{1/2}}$$

$$M = \frac{\mu^{1/2}}{a^{3/2}} t + \sigma_o$$

$$M = E - e \sin E$$

$$\tan\frac{E}{2} = \sqrt{\frac{1 - e}{1 + e}} \tan\frac{(\theta - \omega)}{2}$$

Figure 14. Elements of Elliptic Orbits

be employed to yield the sun's position relative to an orbit plane coordinate system. (It should be noted that a more detailed description of the orbital mechanics and associated vector algebra can be found in Reference 33.)

SOLUTION FOR SHADOW INTERSECTION POINTS

Perhaps the most important factor that contributes to temperature variations during any orbital revolution is the satellite's being eclipsed by the earth's shadow. For this reason it is important to accurately incorporate this effect into any temperature prediction program.

A method for determining the shadow entrance and exit true anomalies from the coordinates of the sun relative to the orbit plane system was devised and packaged as a Fortran subroutine for the IBM 7090. Further information about this subroutine and its use in computing the percent of eclipse time as a function of various orbit parameters may be found in Reference 13. A brief description of the calculation scheme employed by this subroutine appears below.

The relative orientation of the orbit, earth, and sun having been specified, it is seen that the earth casts a shadow which will at times eclipse the satellite. In reality the sun is not at infinity, and casts a converging conical umbral shadow. However, a rigorous specification of the position at which the satellite enters and exits from earth's true shadow leads to needlessly complicated expressions. For this reason, the following simplifying assumptions concerning shadow geometry were made:

1. The earth was assumed spherical with its radius R equal to 3960 statute miles.

2. The earth's shadow was assumed cylindrical and umbral (sun at infinity).

3. Atmospheric refraction and penumbral effects were neglected.

The soundness of these assumptions was verified through telescopic observation of satellites as they entered the earth's shadow. Actual entrance times observed during several transits of 1959 Alpha II and 1960 Iota I usually differed from predictions by only a few seconds.

The points of intersection of an elliptical orbit and a cylinder axially oriented toward the sun are the required solution to the stated problem. Describing these positions in three-dimensional notation results in rather complicated expressions. Considerable simplification can be achieved by considering the projection of the cylindrical shadow upon the orbit plane. (See Figure 15.)

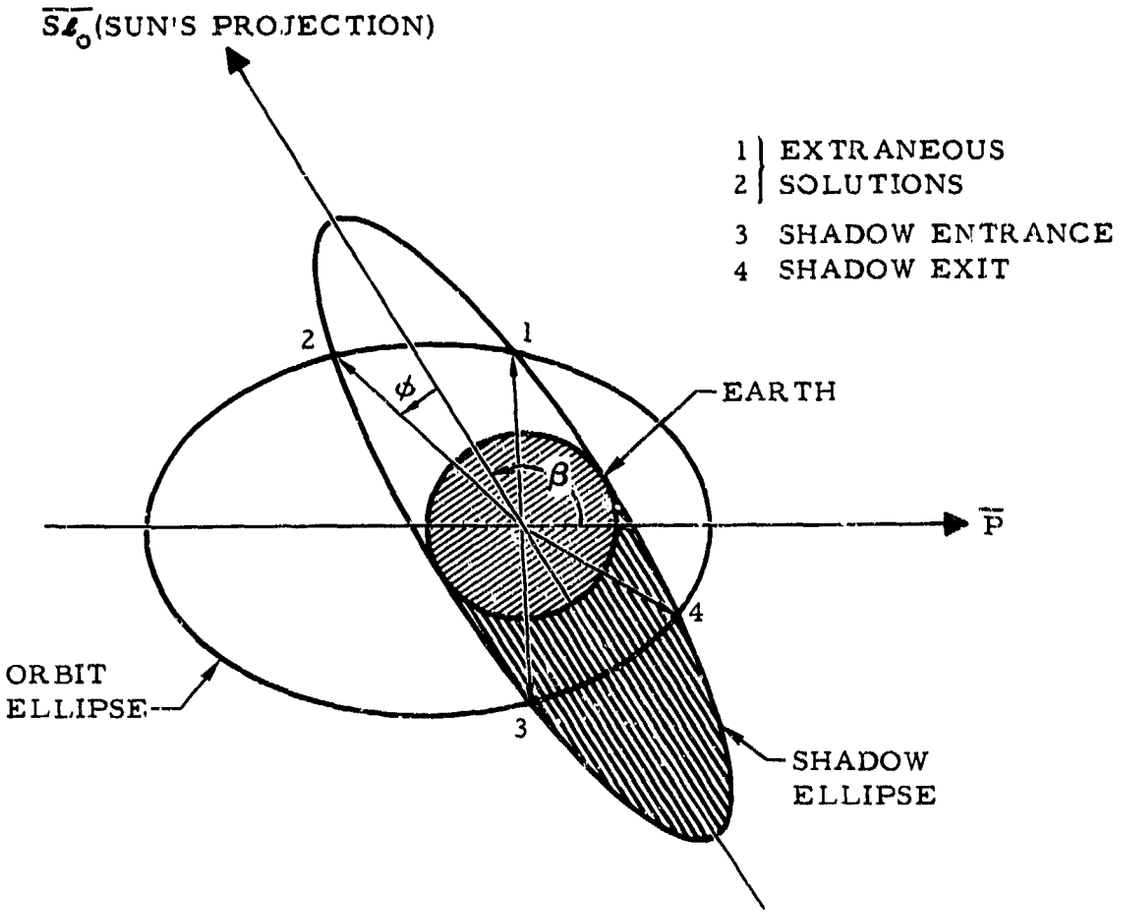

Figure 15. Shadow Geometry (Projection Upon Orbital Plane)

A geocentric ellipse results from the shadow cylinder's cutting the orbit plane, and is described in polar coordinates by

$$r_s = \frac{a_s}{\sqrt{(1 - a_s^2)\cos^2\phi + a_s^2}} \tag{40}$$

where r_s and a_s are in earth radii.

The elliptical orbit can be represented in polar coordinates by

$$r_o = \frac{a(1 - e^2)}{1 + e\cos(\phi + \beta)} \tag{41}$$

where r_o and a are in earth radii.

It is apparent from the geometry of Figure 15 that the two ellipses need not intersect; they may be tangent or may intersect in as many as four points. Of course, no more than two of these intersections can represent the required sunlight-shadow transitions, and the remaining solutions must be eliminated.

The required solutions must satisfy the condition

$$\Delta r = r_o - r_s = 0 \tag{42}$$

A similar expression,

$$(\Delta r)^2 = r_o^2 - r_s^2 = 0 \tag{43}$$

was incorporated into the subroutine since it yielded less complex equations. A functional iteration scheme was employed to seek the necessary solutions to the problem.

The fraction of orbit time T_s spent in the earth's shadow can be computed by the equations of Figure 14 through introduction of the eccentric anomaly E and the use of Kepler's equation. Thus,

$$T_s = \frac{1}{2\pi}\left[(E_4 - e\sin E_4) - (E_3 - e\sin E_3)\right] \tag{44}$$

As an illustration of the use of this program, the fraction of each day spent in the shadow was calculated as a function of date for several parameters including inclination, semimajor axis, eccentricity, and launch time.

The percent of eclipse time for various orbit classes was computed from Equation 44. and is presented in Figures 16 through 23 as a function of date. Except as otherwise noted, the initial conditions were as follows:

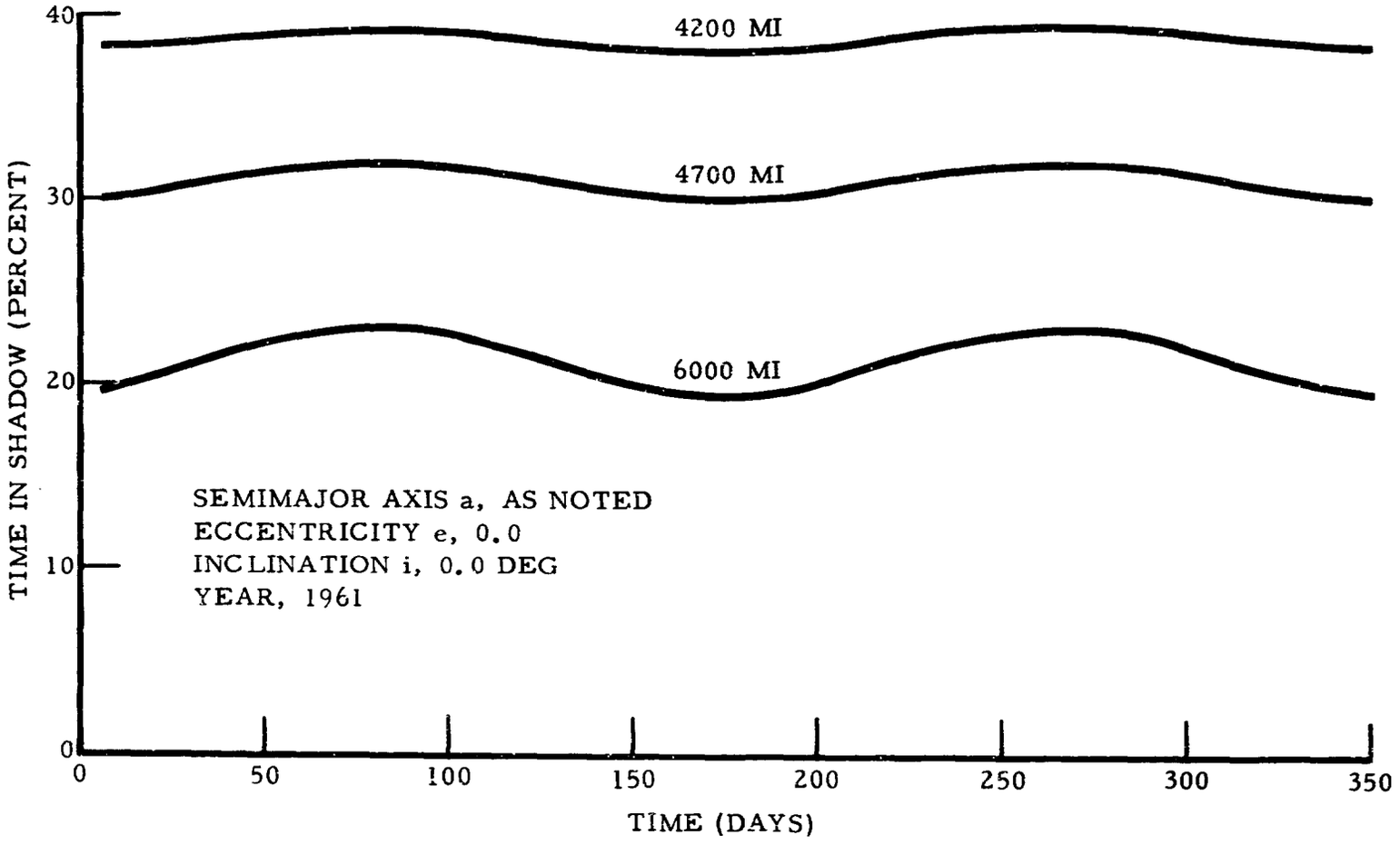

Figure 16. Eclipse Time as Function of Date
(Zero Eccentricity, 0-Degree Inclination)

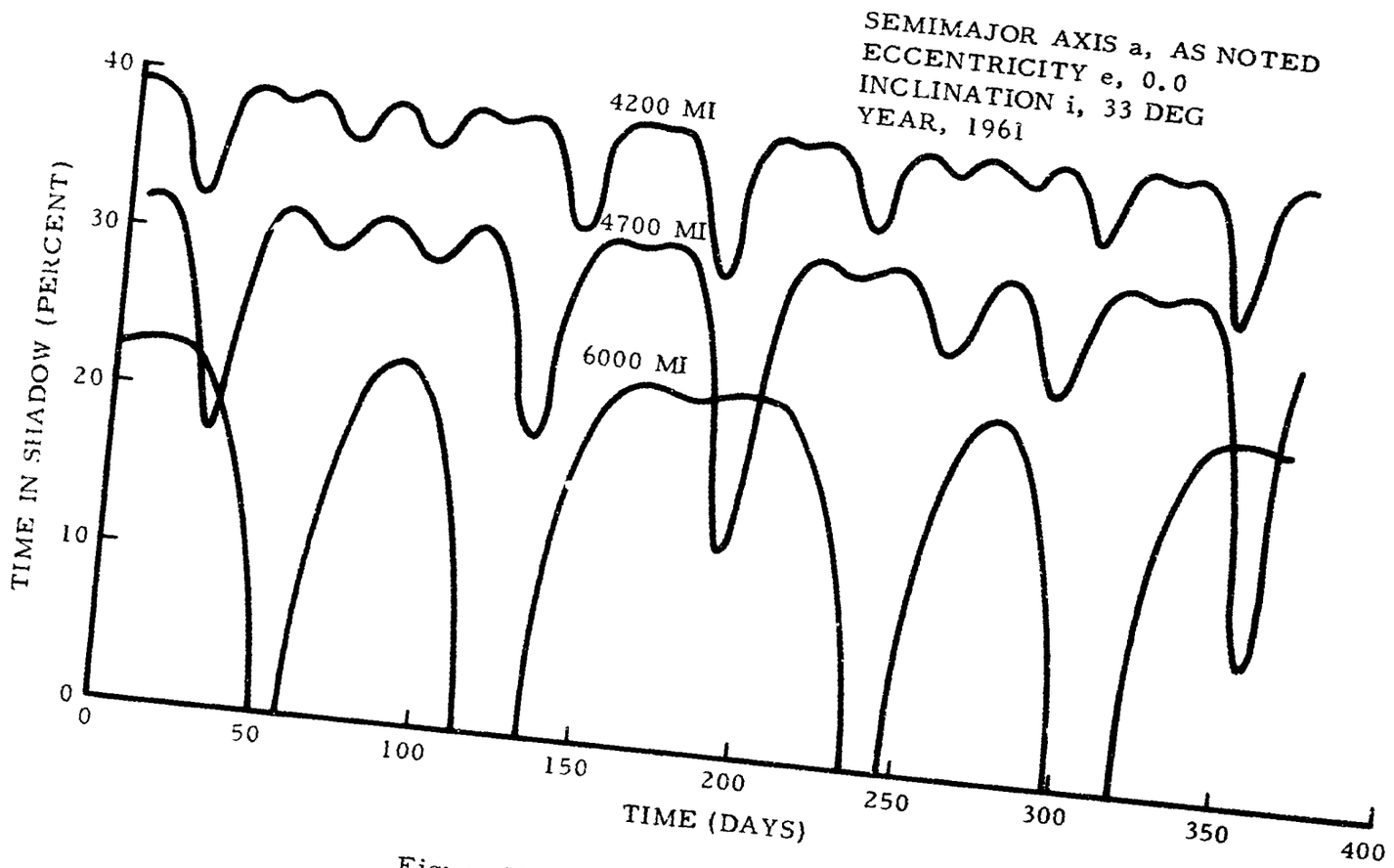

Figure 17. Eclipse Time as Function of Date
(Zero Eccentricity, 33-Degree Inclination)

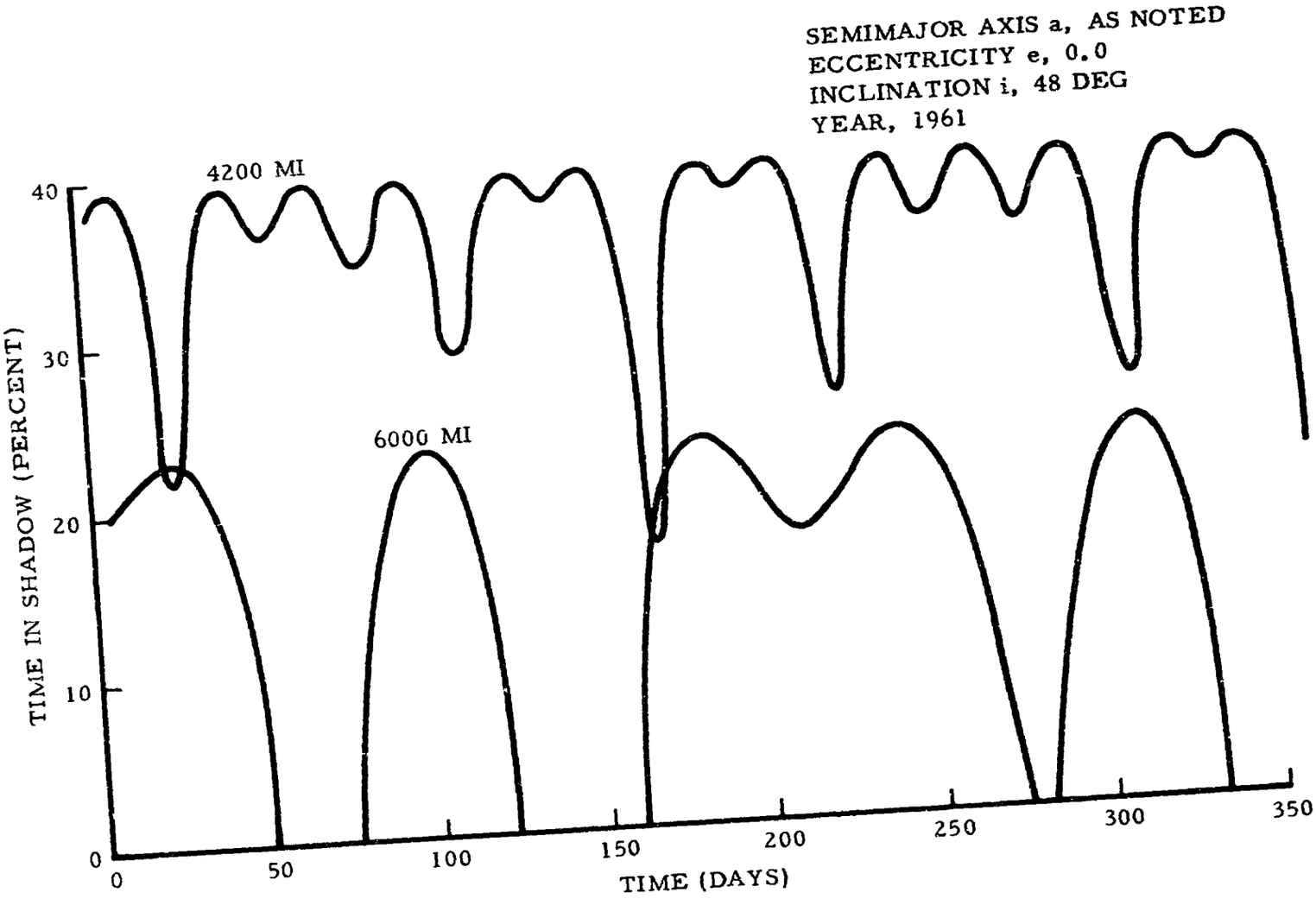

Figure 18. Eclipse Time as Function of Date
(Zero Eccentricity, 48-Degree Inclination)

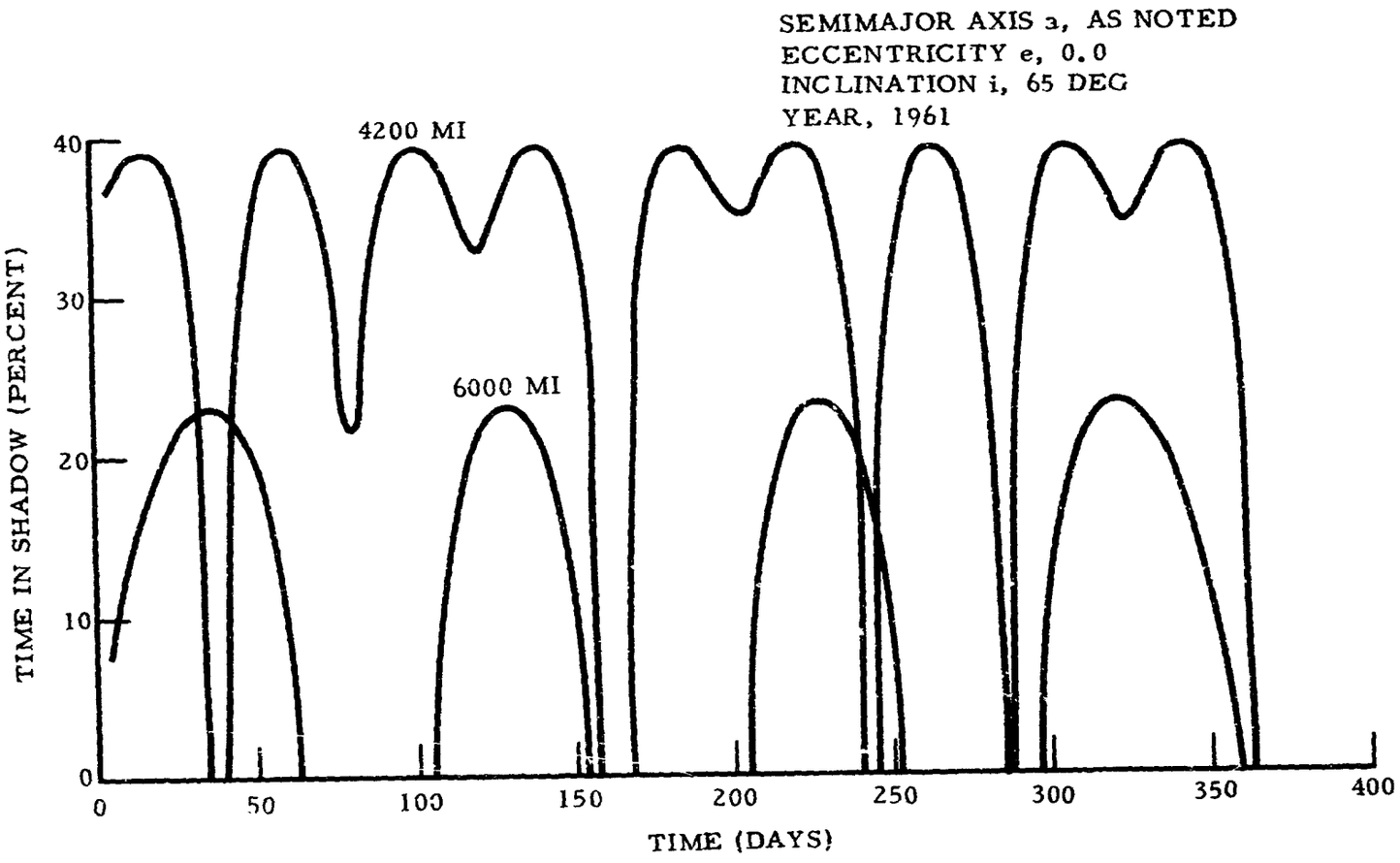

Figure 19. Eclipse Time as Function of Date
(Zero Eccentricity, 65-Degree Inclination)

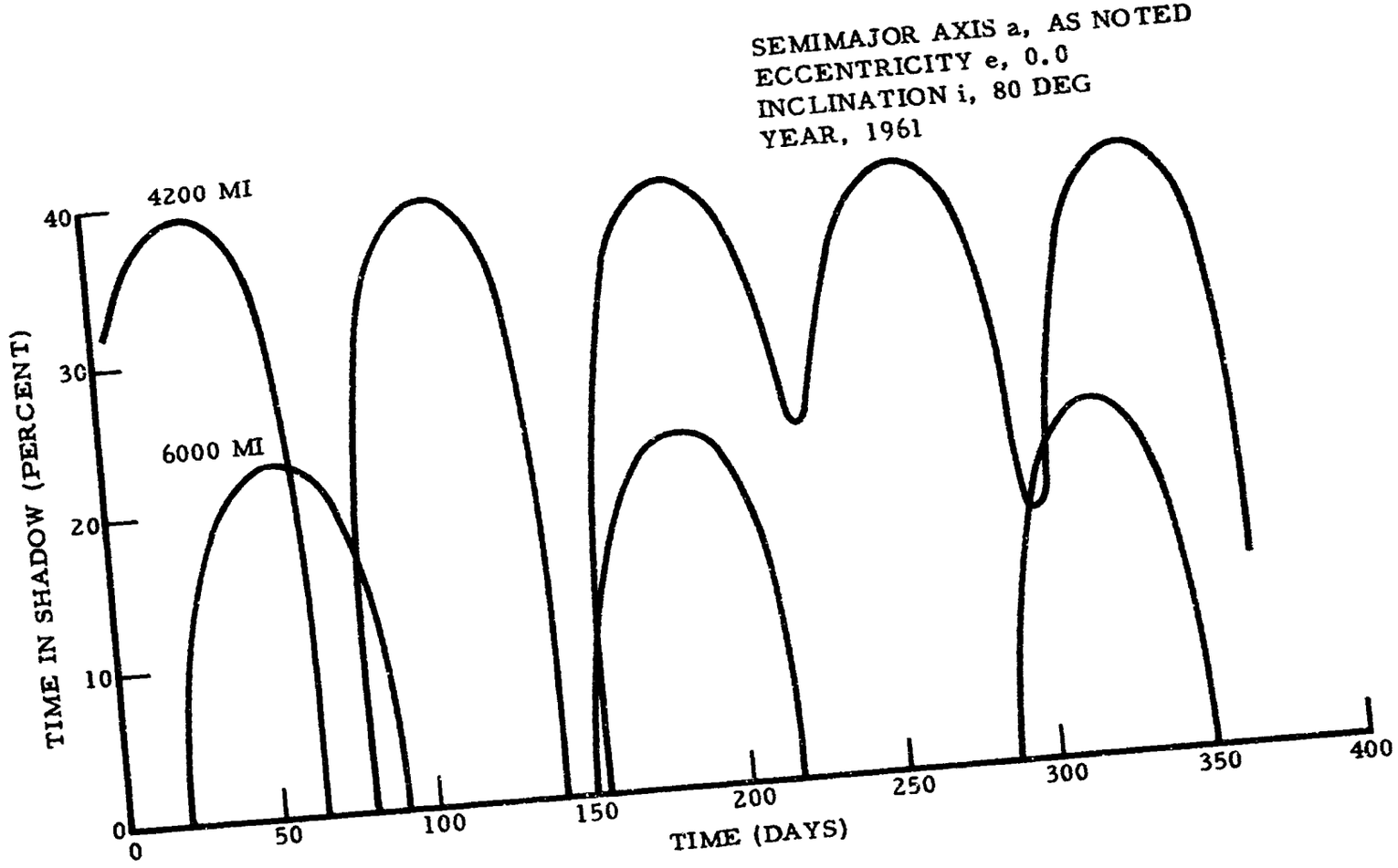

Figure 20. Eclipse Time as Function of Date
(Zero Eccentricity, 80-Degree Inclination)

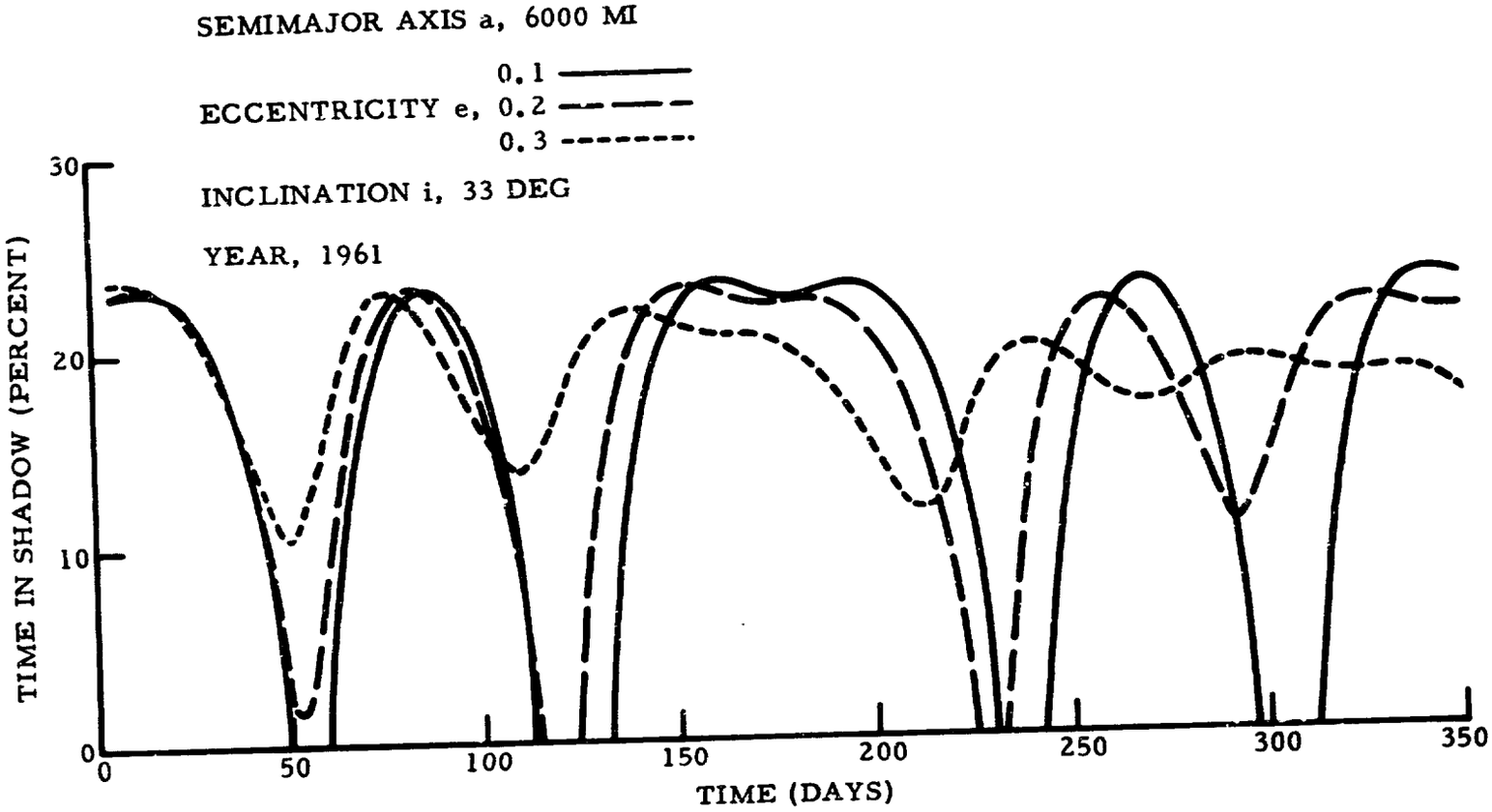

Figure 21. Effect of Variation in Eccentricity on Eclipse Time as Function of Date

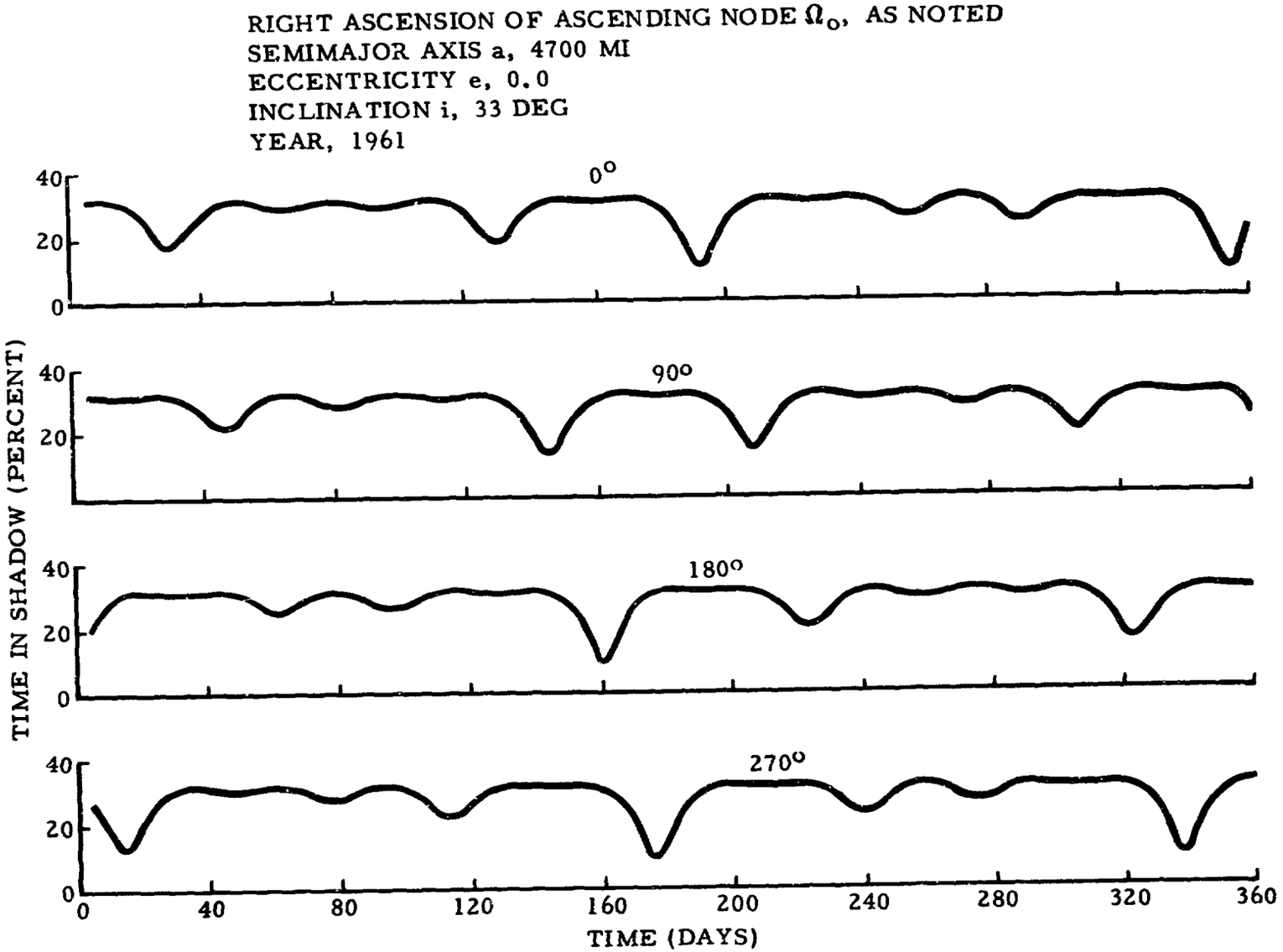

Figure 22. Effect of Variation in Launch Time on Eclipse Time as Function of Date

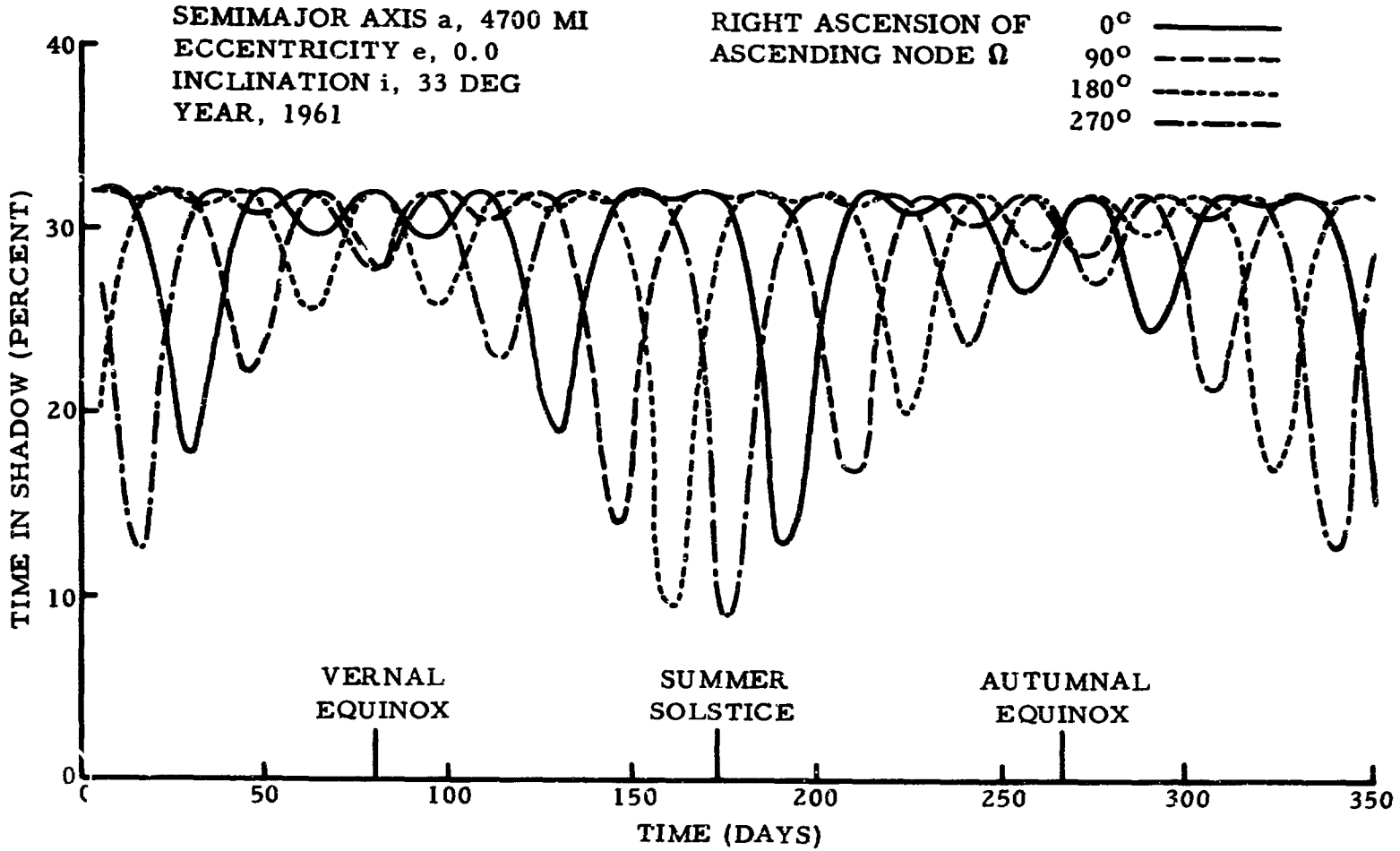

Figure 23. Seasonal Boundaries of Shadow Intersection Characteristics

$$e = 0.0$$
$$\omega = 0.0$$
$$\Omega = 0.0$$
$$T_o = 1 \text{ January } 1961$$

The results are generally self-explanatory and, therefore, only a few of the more interesting points are mentioned here.

Figures 16 through 20 illustrate the effects of varying the semimajor axis and/or inclination. With zero inclination (Figure 16), eclipse time is seen to vary seasonally as the sun moves between the northern and southern hemisphere. Increasing the semimajor axis results in increased seasonal variations, although maximum eclipse time is decreased. Changes in precession rates that arise from variations in semimajor axis and inclination are illustrated by Figures 17 through 20. It is to be noted that increasing the inclination and/or the semimajor axis generally yields less eclipse time.

Figure 21 is concerned with variations in eccentricity. The maxima, which occur each time the sun is in the orbit plane, are not always equal as was the case for circular orbits. Also, increasing the eccentricity tends to decrease the probability of obtaining total sunlight because the perigee remains nearer the earth.

Initial right ascension of the ascending node was assigned four different values to produce the curves of Figure 22. This variable, which is a function of launch time and date, is seen to cause a phase shift in the occurrence of maxima and minima. Thus, within limits, the launch time can be chosen to produce the most desirable eclipse conditions.

Figure 23 superimposes the curves of Figure 22 to illustrate seasonal effects upon eclipse characteristics. It will be noted that at the equinoxes, when the sun is near the earth's equatorial plane, there is only a slight day-to-day variation in eclipse time. Conversely, at the solstices, the minima become quite pronounced.

VEHICLE CONFIGURATION AND ORIENTATION

No attempt was made to write a completely general program with respect to satellite shape. Thus it was decided that the problem of specifying vehicle configuration and subsequently orienting the vehicle in space would be handled by a separate subroutine within the program. This requires a new subroutine for each vehicle configuration, but the extra cost for their writing can be amortized through less complex programs, increased reliability, and better problem understanding.

At the present time, subroutines are available for handling the satellite shapes shown in Figure 24; these are explained in detail in the sample problem section of Reference 33. It is felt that an experienced Fortran programer should be able to devise subroutines for different configurations as the need arises.

The information determined by the orientation subroutine is utilized in turn by the geometric form factor subroutine which calculates the geometric form factors necessary in the temperature analysis. The geometric form factor subroutine is described in the next discussion.

GEOMETRIC CONFIGURATION FACTORS

In order to calculate the temperature of an orbiting space vehicle, it is necessary to determine the geometric form factors, which always constitute a basic problem with radiation heat transfer analysis. As explained in the previous discussion, an orientation subroutine supplies information relative to the position of the vehicle with respect to space, the earth, and the sun. This information, in turn, is used by a geometric form factor subroutine which calculates the form factors needed in the analysis.

Since the form factor subroutine is a separate closed subroutine within the main program, it may easily be replaced or changed to incorporate whatever method of form factor computation is desired. Several routines that have been devised to compute the form factors for rotating spheres, plane surfaces, and rotating cylindrical surfaces are described here. Listings of the three subroutines for these cases appear in Reference 33.

Rotating Sphere

The direct solar form factor for a uniformly rotating sphere is derived thusly

$$F_s = \frac{\text{Projected area}}{\text{Total surface area}}$$

$$= \frac{\pi r^2}{4 \pi r^2} = 0.25 \qquad (45)$$

The geometric form factor for earth emission F_E may be derived by considering the satellite to be a point source in space viewing the earth. This assumption is correct if the satellite is rotating or has a uniform surface temperature. Referring to Figure 25, it is seen that F_E is therefore equal to the shaded percentage of the sphere with radius c.

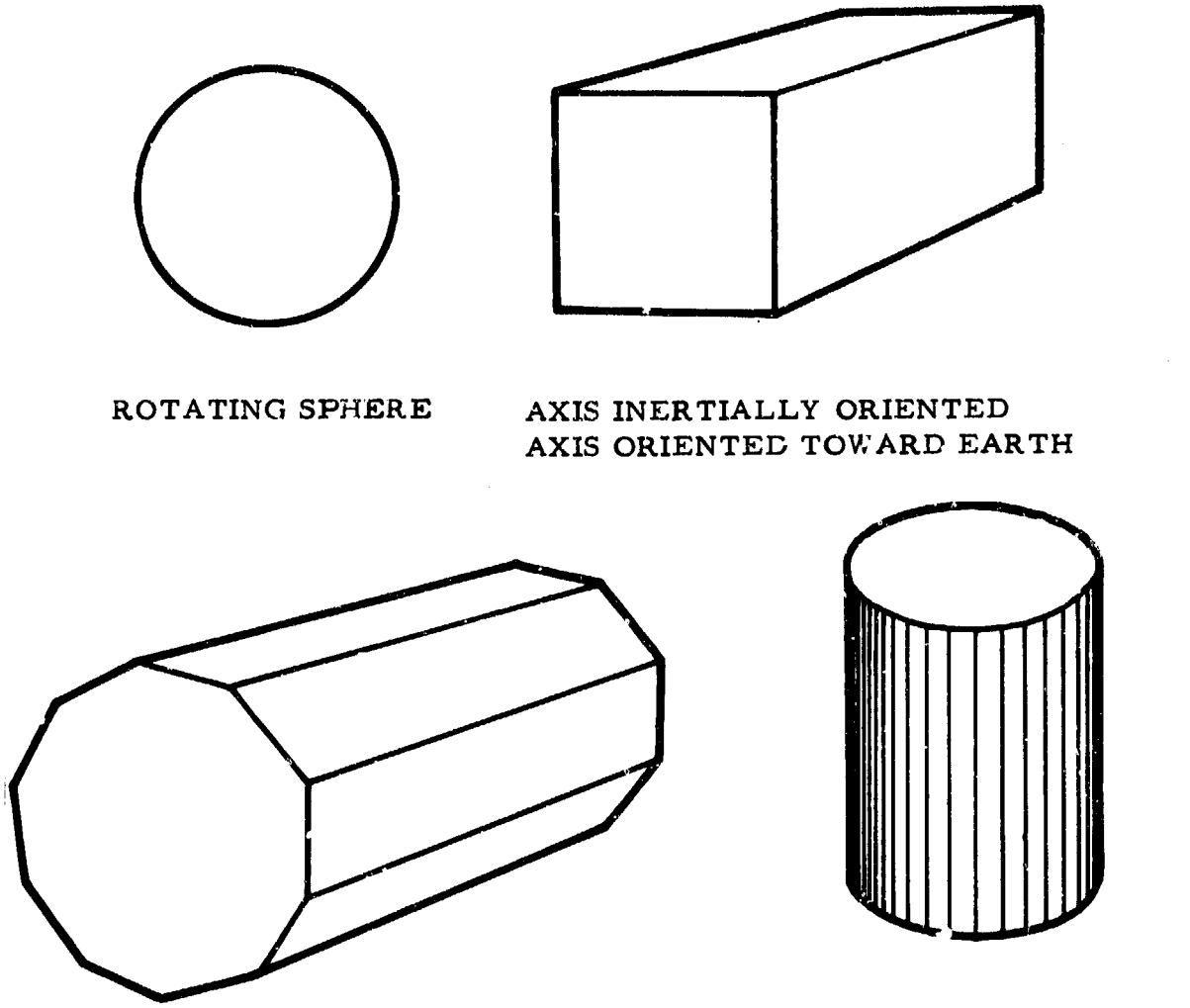

Figure 24. Satellite Configurations Used in Transient Temperature Analysis

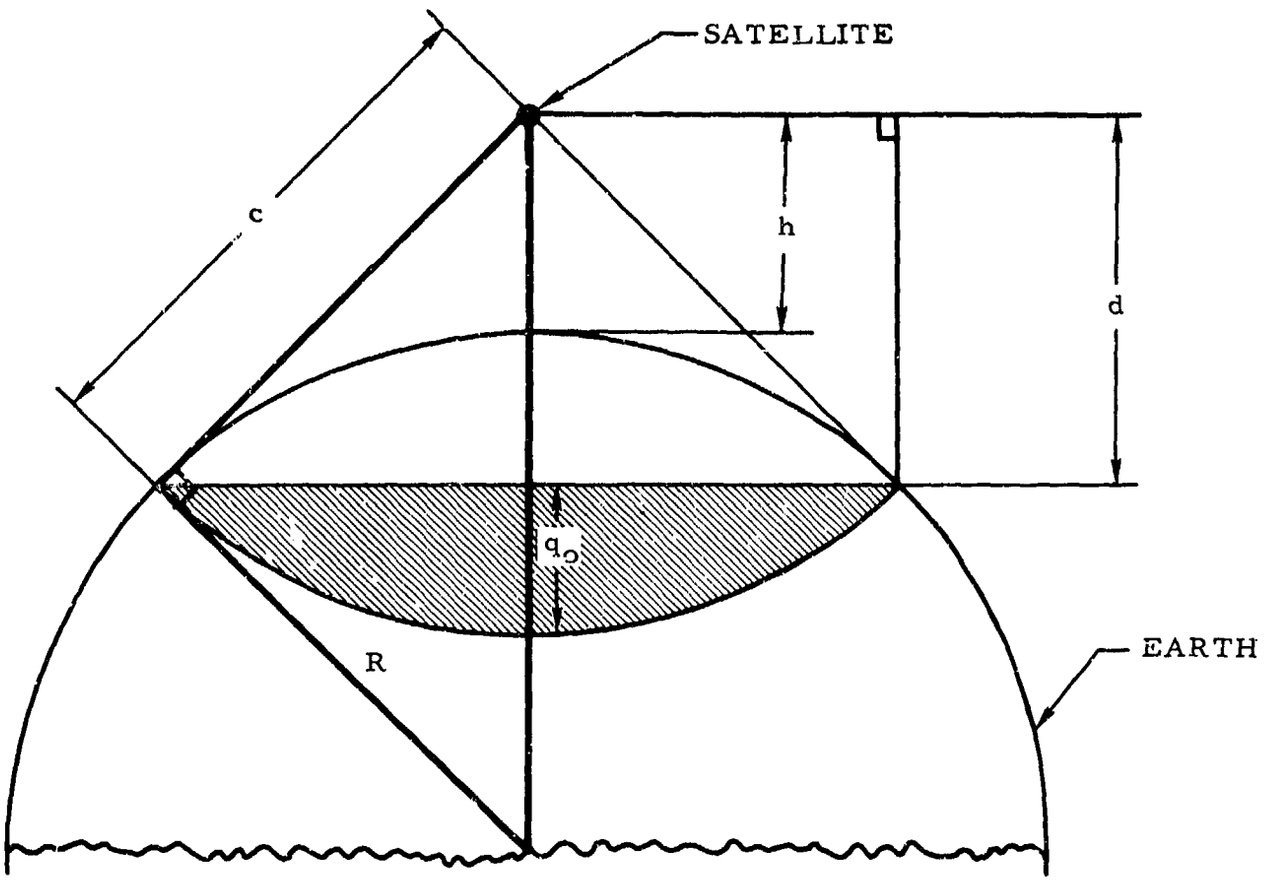

Figure 25. Planetary Emission Form Factor (Rotating Sphere)

Considering the right triangle formed by R, c, and (R + h), one may write

$$c^2 = (h + R)^2 - R^2$$

$$c = \sqrt{h\,(h + 2R)} \tag{46}$$

Considering the auxiliary constructions which yield d and q, and comparing the similar right triangles, it is seen that

$$\frac{d}{c} = \frac{c}{R + h}$$

and therefore,

$$d = \frac{c^2}{R + h}$$

and

$$q_o = c - d = c\left(1 - \frac{c}{R + h}\right) \tag{47}$$

F_E is computed by comparing the area of spherical segment with height q_o to the sphere's total surface area. Thus,

$$F_E = \frac{2\pi c q_o}{4\pi c^2} = c\left(\frac{1 - \frac{c}{R + h}}{2c}\right)$$

or

$$F_E = \frac{1}{2}\left(1 - \frac{\sqrt{h\,(h + 2R)}}{R + h}\right) \tag{48}$$

Form factors for reflected solar were approximated by the equation

$$F_R = F_E \cos \theta_s \tag{49}$$

This simplification results in an error due to the reflected solar being set equal to zero at the terminator. Actually, the vehicle can still receive some reflected solar radiation when beyond the terminator. However, the error introduced by this assumption is felt to be negligible.

Form Factors for Plane Surfaces

The direct solar form factor for a plane surface is simply the ratio of the projected area exposed to the sun to the total surface area, or

$$F_s = \cos \theta_N \tag{50}$$

Computation of the earth emission form factor F_E is considerably more complicated. It is accomplished by one of three methods, depending upon the geometry. The unit sphere method is employed to derive the form factor equations.

Case I

The first case occurs when the surface can "view" the entire earth. Referring to the geometry of Figure 26, it is seen that θ_1 is the angle between the surface normal and the radius vector to earth, and θ_2 is half the angle subtended by the earth. θ_2 may be found from the expression

$$\sin \theta_2 = \frac{R}{R + h} \tag{51}$$

Let a be the radius of the earth's projection upon a unit sphere constructed upon the surface (note auxiliary constructions). Then,

$$a = \sin \theta_2 = \frac{R}{R + h} \tag{52}$$

The circle of radius a may then be projected upon the plane representing the vehicle surface to form an ellipse with semimajor axis a and semiminor axis γ (plan view). γ equals the projected length of a, or

$$\gamma = a \cos \theta_1 \tag{53}$$

The earth emission form factor for this case is therefore given by

$$F_E = \frac{\text{Area of ellipse}}{\text{Area of unit circle}}$$

$$= \frac{\pi a \gamma}{\pi} = a \gamma$$

or

$$F_E = a^2 \cos \theta_1 \tag{54}$$

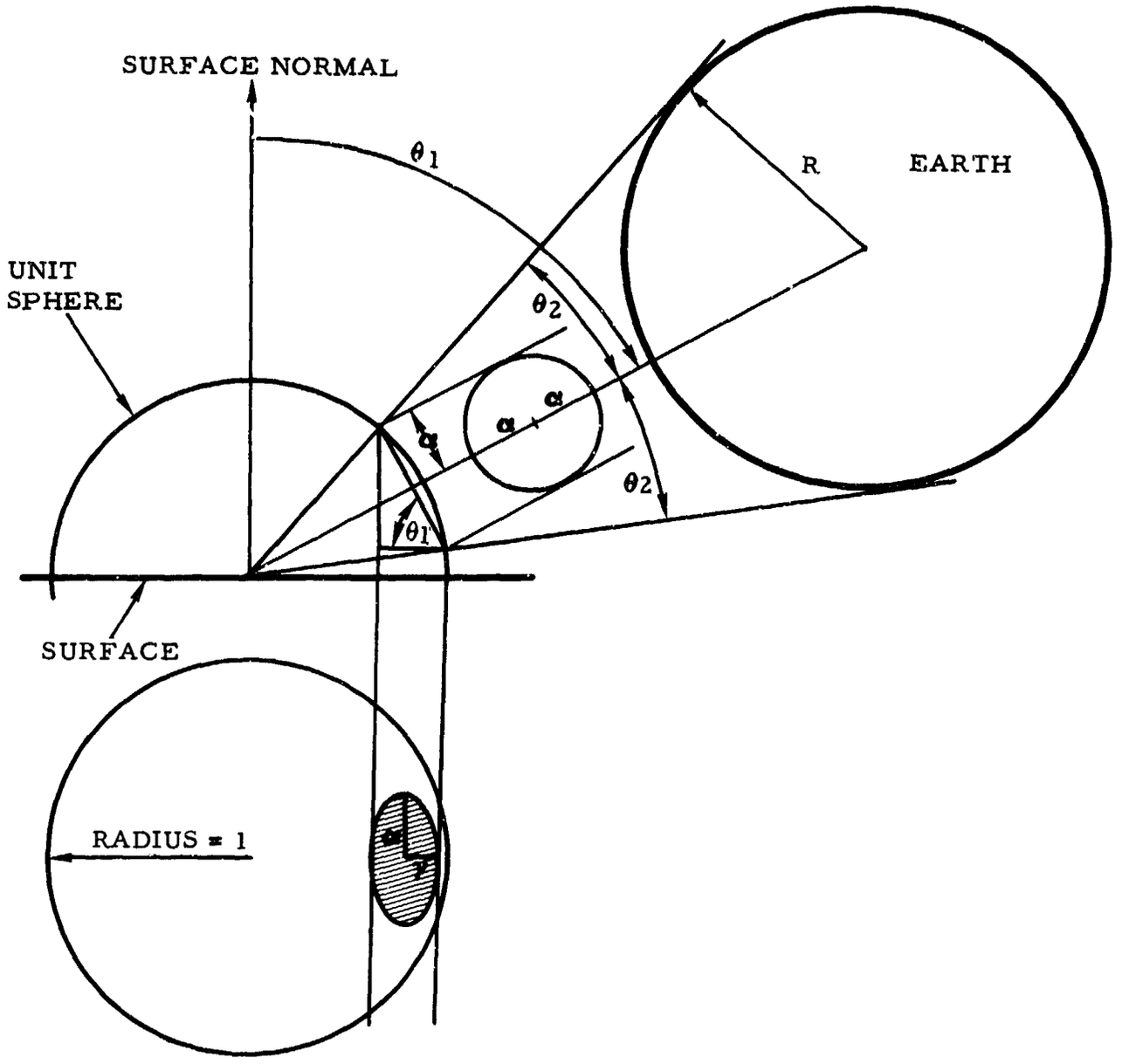

Figure 26. Form Factor Determination (Case I)

Case II

When the sum of θ_1 and θ_2 exceeds 90 degrees (Figure 27), part of the earth is not visible to the surface. The projection upon the surface of the earth's projection upon a unit sphere forms an ellipse with dimensions α and γ. The areas of interest are the shaded half-ellipse and the similarly shaded segments of the ellipse and circle. The dimensions δ and η must be found in order to evaluate the area of the ellipse segment. Referring to the auxiliary constructions of Figure 27, the derivation proceeds as follows:

$$\epsilon = \cos \theta_2$$

and therefore,

$$s = \epsilon \tan (90 - \theta_1) = \cos \theta_2 \tan (90 - \theta_1)$$

Noting that

$$\tan (90 - \theta_1) = \frac{\cos \theta_1}{\sin \theta_1}$$

and

$$\cos \theta_2 = \sqrt{1 - \sin^2 \theta_2} = \sqrt{1 - \alpha^2}$$

it follows that

$$s = \sqrt{1 - \alpha^2} \frac{\cos \theta_1}{\sin \theta_1}$$

Therefore,

$$\eta = s \cos \theta_1 = \sqrt{1 - \alpha^2} \frac{\cos^2 \theta_1}{\sin \theta_1} \tag{55}$$

The derivation of δ proceeds as follows:

$$\delta = \alpha \cos \phi_c = \alpha \sqrt{1 - \sin^2 \phi_c}$$

where

$$\sin \phi_c = \frac{s}{\alpha} = \frac{1}{\alpha} \sqrt{1 - \alpha^2} \frac{\cos \theta_1}{\sin \theta_1}$$

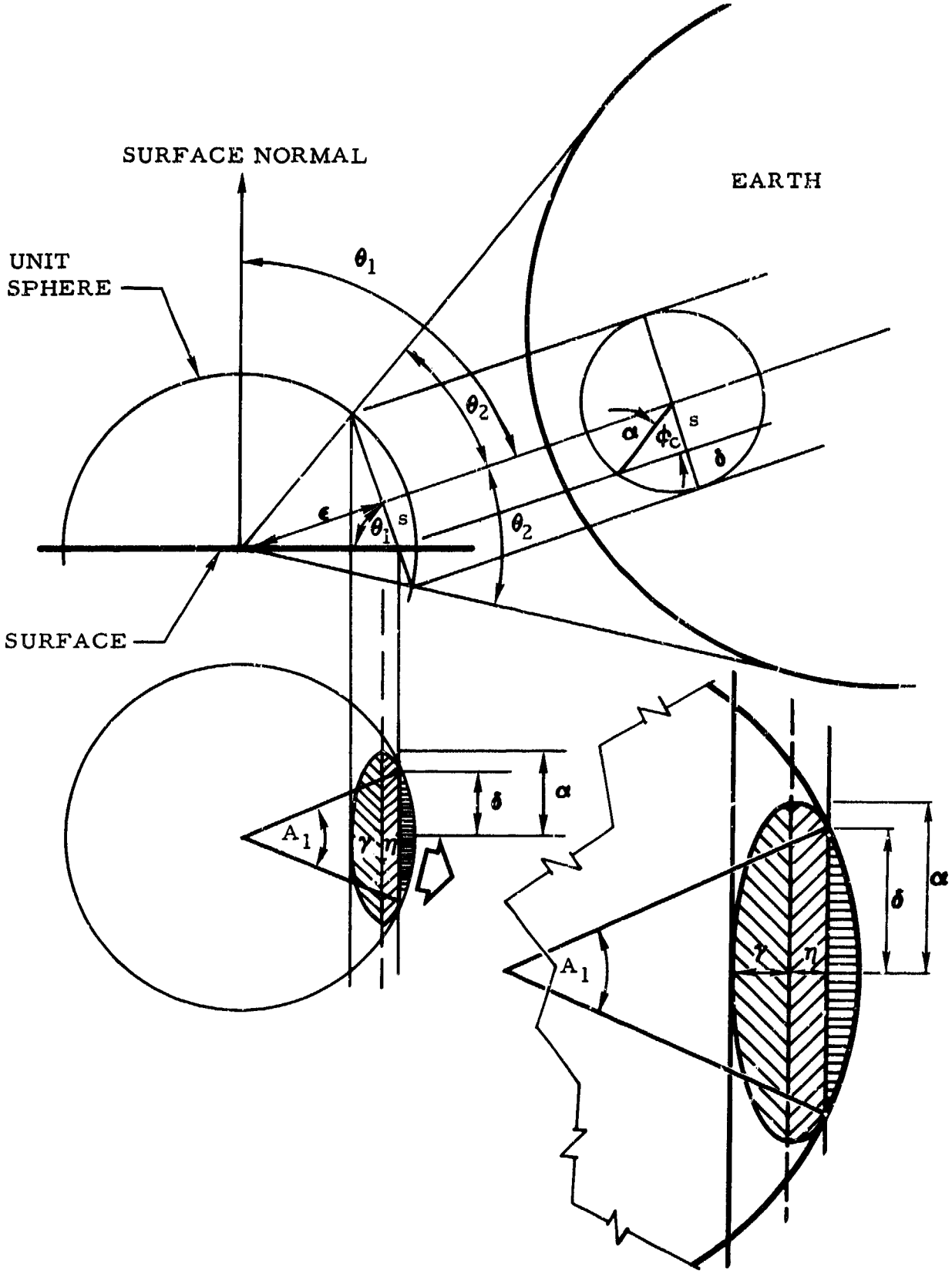

Figure 27. Form Factor Determination (Case II)

Substitution and trigonometric manipulation yields

$$\delta = \frac{1}{\sin \theta_1} \sqrt{a^2 - \cos^2 \theta_1} \tag{56}$$

The required form factor is given by the equation

$$F_E = \frac{1/2 \text{ (Area of ellipse)} + \text{Segment of ellipse} + \text{Segment of circle}}{\text{Area of circle}}$$

which becomes

$$F_E = \frac{1}{\pi} \left[\frac{\pi}{2} a\gamma + \delta\eta + a\gamma \sin^{-1} \frac{\eta}{\gamma} + \frac{1}{2} (A_1 - \sin A_1) \right] \tag{57}$$

where A_1 is found from

$$\sin \frac{A_1}{2} = \delta \tag{58}$$

Case III

A third case occurs when θ_1 is greater than 90 degrees as seen in Figure 28. Again, the projection upon the surface of earth's projection upon the unit sphere is an ellipse with dimensions a and γ. The area required for form factor determination is the shaded portion of the circle excluded from the ellipse. Utilizing auxiliary constructions once more, it is seen that

$$\epsilon = \cos \theta_2$$

and

$$s = \epsilon \tan (\theta_1 - 90) = \cos \theta_2 \tan (\theta_1 - 90)$$

Noting that

$$\cos \theta_2 = \sqrt{1 - \sin^2 \theta_2} = \sqrt{1 - a^2}$$

and

$$s = \sqrt{1 - a^2} \tan (\theta_1 - 90)$$

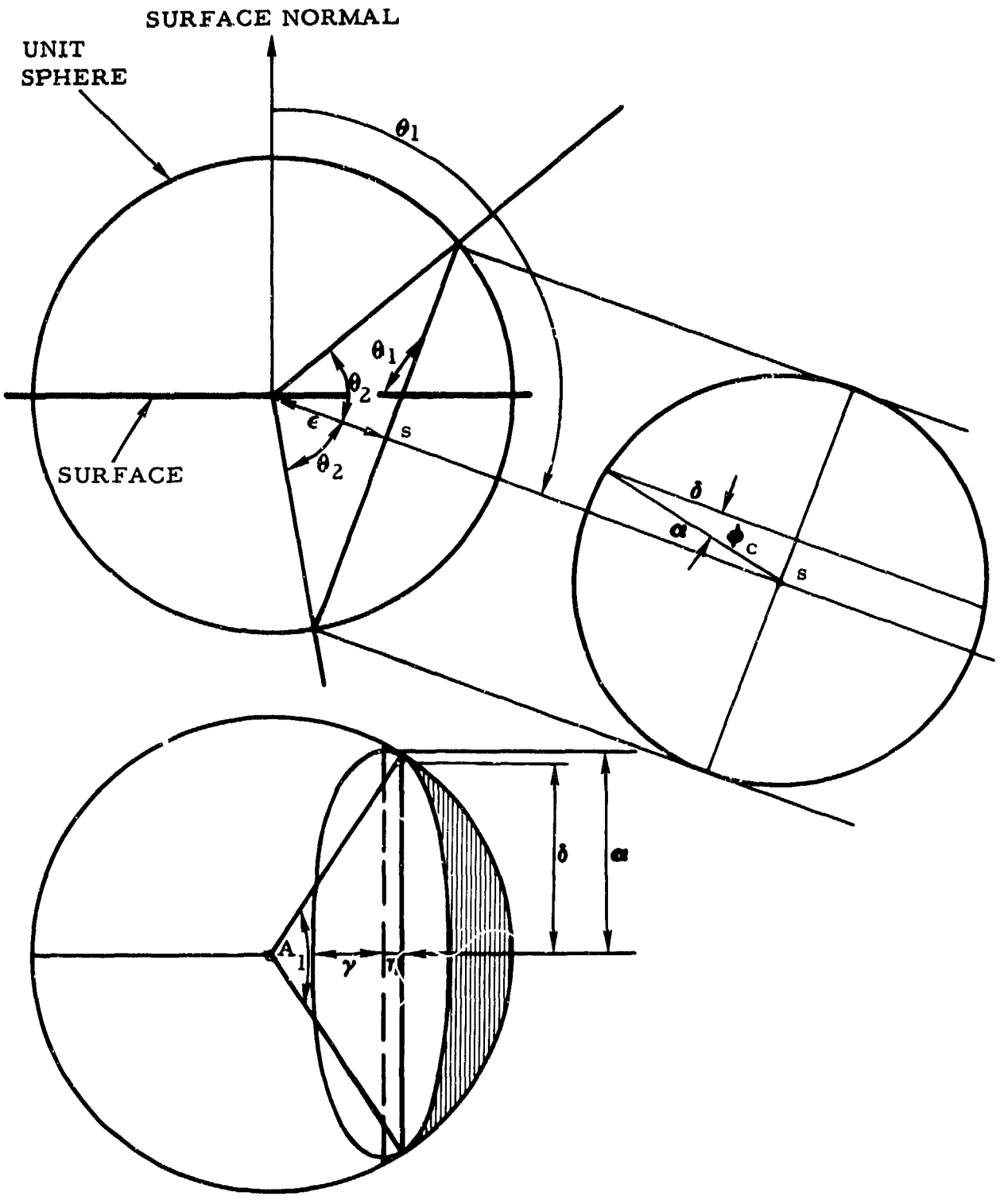

Figure 28. Form Factor Determination (Case III)

it follows that

$$\eta = -s \cos \theta_1 = -\sqrt{1 - a^2} \cos \theta_1 \tan (\theta_1 - 90) \tag{59}$$

δ may be derived from the auxiliary construction by first noting that

$$\delta = a \cos \phi_c = a \sqrt{1 - \sin^2 \phi_c}$$

where

$$\sin \phi_c = \frac{s}{a} = \frac{1}{a} \sqrt{1 - a^2} \tan (\theta_1 - 90)$$

Substitution and trigonometric manipulation yields

$$\delta = \frac{1}{\cos (\theta_1 - 90)} \sqrt{a^2 - \sin^2 (\theta_1 - 90)} \tag{60}$$

The earth emission form factor is found from the expression

$$F_E = \frac{\text{Segment of circle + Segment of ellipse - 1/2 (Area of ellipse)}}{\text{Area of circle}}$$

which becomes

$$F_E = \frac{1}{\pi} \left[\frac{1}{2} (A_1 - \sin A_1) + \delta \eta + a\gamma \sin \frac{\eta}{\gamma} - \frac{\pi}{2} a\gamma \right] \tag{61}$$

where A_1 is found from

$$\sin \frac{A_1}{2} = \delta$$

By inspection of the geometry of Figure 28, it is apparent that F_E becomes zero when $\theta_1 - \theta_2 > 90$ degrees.

It was assumed that the reflected solar form factor could be approximated by the expression

$$F_R = F_E \cos \theta_s \tag{62}$$

The formulas just developed were incorporated into the form factor routine for plane surfaces which appears in Reference 33.

Form Factors for Curved Surfaces

A good approximation to a curved surface may be obtained by dividing it into an adequate number of plane surfaces. This procedure was utilized to simulate the rotating cylindrical vehicle of sample problem 4 of Reference 33. In this example, the cylindrical surface was approximated by 24 plane surfaces equally spaced around the principal axis. The contributions of each plane were then averaged to obtain a single form factor for the rotating cylindrical surface. (The assumption of rapid rotation results in a uniform surface temperature.)

TEMPERATURE DETERMINATION

The surface temperature of a space vehicle in orbit about the earth is determined by the heat balance between the vehicle surface and its environment, which includes the sun, the earth and its atmosphere, and space which acts as a heat sink (Figure 29). The vehicle receives solar energy directly from the sun or indirectly (reflected) from the earth and its atmosphere. Energy emitted by the earth and its atmosphere also contributes measurably to this heat balance. (The largely geometrical problem of determining what radiation the vehicle receives from each source at successive positions around the orbit was presented in the previous discussion, which described the procedures used in calculating the geometric form factors.)

Other factors which influence this heat balance are the value of the solar constant, the planetary albedo, and assumptions concerning planetary emission. The planetary emitted energy was assumed to be uniform over the earth's surface and approximately equivalent to that of a black body for the temperatures shown in Table 5. The vehicle's surface absorptivity for this energy was assumed equivalent to the total hemispherical emissivity of the surface at approximately the same temperature.

The rate of change of the temperature of a surface of an orbiting satellite may be obtained from

$$Wc_p \frac{dT}{dt} = \alpha_s A F_s S + \alpha_E F_E A E_E + \alpha_R F_R A R_E + q - \epsilon_s \sigma A T^4 \qquad (63)$$

where

T = Temperature of shell, °R

t = Time, hr

W = Mass of satellite or surface, lb_m

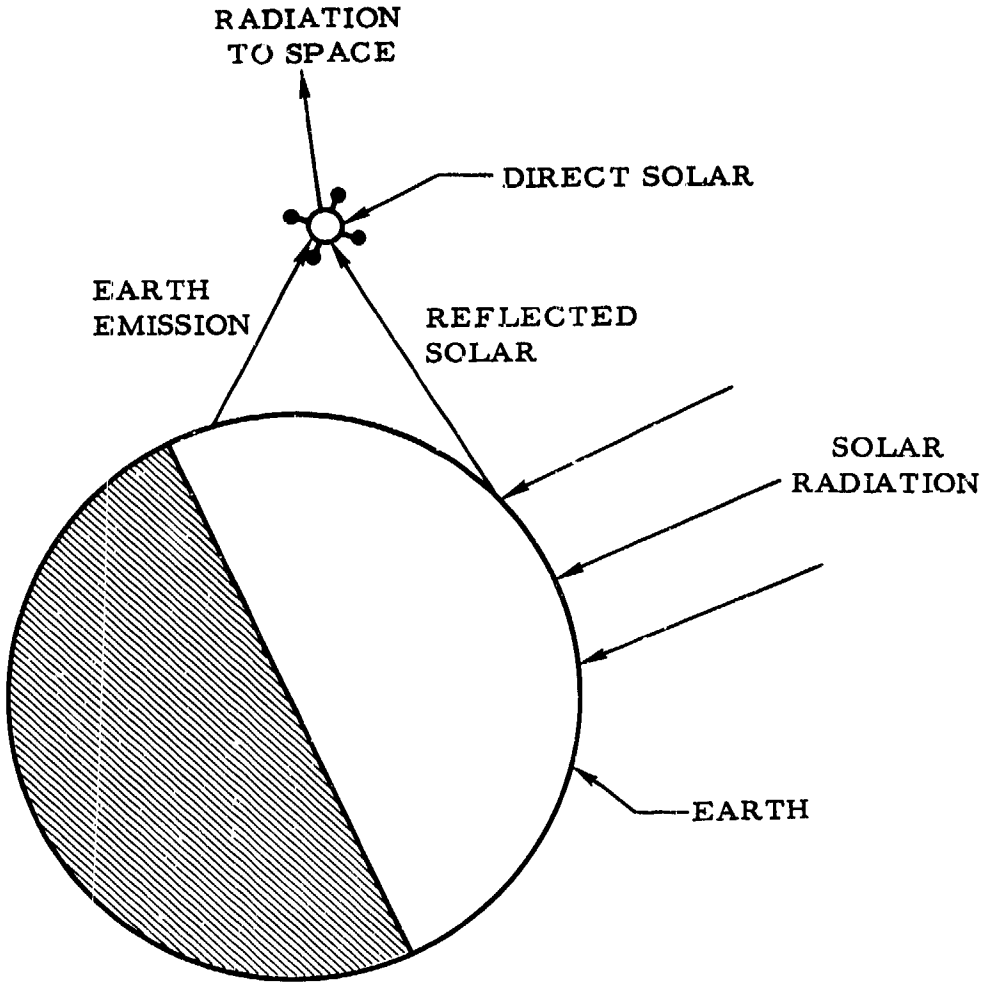

Figure 29. Space Vehicle Heat Balance

c_p = Specific heat, Btu/(lb_m) (°R)

A = Surface area of satellite, sq ft

q = Internal heat load, Btu/hr

σ = Stefan-Boltzmann constant = 0.1713×10^{-8} Btu/(hr)(sq ft)($°R^4$)

α_s = Solar absorptivity of satellite

α_E = Infrared absorptivity of satellite

α_R = Absorptivity to reflected solar

F_s = Geometric form factor for direct solar radiation

F_E = Geometric form factor for planetary emission

F_R = Geometric form factor for reflected solar radiation

S = Solar constant, Btu/(hr)(sq ft)

E_E = Planetary emission, Btu/(hr)(sq ft)

R_E = Reflected solar energy from planet, Btu/(hr)(sq ft)

ϵ_s = Emissivity of satellite surface

The temperature prediction program incorporates a finite difference version of the Equation 63. The following assumptions are made:

$$\alpha_s = \alpha_R$$

$$\alpha_E = \epsilon_s$$

$$R_E = S r_E \tag{64}$$

$$E_E = \frac{1 - r_E}{4} S$$

$$F_R = F_E \cos \theta_s$$

where

r_E = Planetary albedo

θ_s = Angle between earth-sun line and vertical from planet to satellite

The program utilizes several tolerances to ensure that the finite difference method will yield valid results. Steps are taken to ensure that the maximum time interval used during any step in true anomaly will not exceed a time tolerance entered as data or one computed from the equation

$$TOL = \frac{1}{16}\left(\frac{W c_p}{\sigma T_m^3 \epsilon_s A}\right) \tag{65}$$

Computation is begun by providing approximate values of the various surface temperatures at perigee. The program will then compute temperatures at successive intervals around the orbit until it has returned to perigee. Chances are that the approximate value and the newly computed temperature at perigee will not agree. The program then repeats the computation, utilizing the new temperature as an initial value. This iteration process is repeated until initial and final temperatures converge to within an acceptable tolerance.

Thus, the program obtains a transient temperature history during a particular revolution of the satellite. Figure 30 shows the described convergence effect for a case involving a rotating sphere. Computation was begun with an initial temperature guess of 100 F. The lower curve shows the temperature history computed during the first iteration, while the upper curve represents the results of the third iteration. After three iterations, the initial and final temperatures coincide. This curve therefore represents the transient temperature history during the revolution in question.

That the lower curve would represent the temperature history during the first orbital revolution of a satellite injected into orbit with an initial temperature of 100 F is noteworthy. By the third revolution, the temperature curve would become rather stable. Thereafter, it would experience slight day-to-day changes brought about by orbital precession and other factors.

Although the foregoing discussion was confined to temperature determination, it should be noted that the amount of radiant energy that is absorbed by each satellite surface from the space environment is also available from the program. This information may be utilized as input data in a general heat transfer program if it is desired to obtain a detailed thermal analysis of the interior of the vehicle. This capability of the program may prove to be more important than its capability to compute satellite shell temperature histories.

PROGRAM LISTING AND DECK SETUP

Figures 31 and 32 illustrate the general approach used in the program by showing the main program flow diagram and deck setup. It is beyond the scope of this report to go into detail with respect to these diagrams, since they are primarily of interest to program writers. It is recommended that Reference 33 be consulted for a complete explanation of these areas of interest.

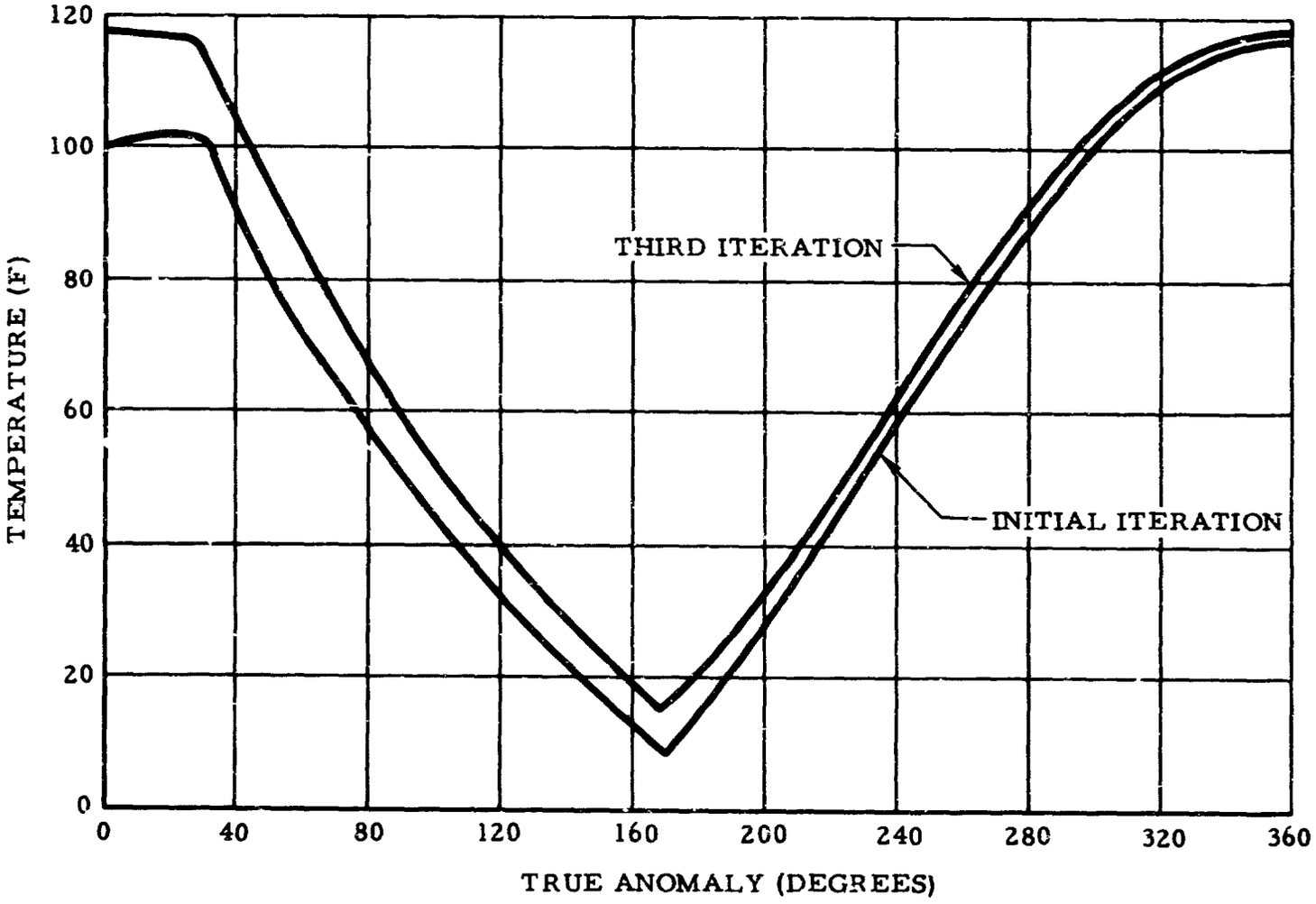

Figure 30. Satellite Temperature Determination

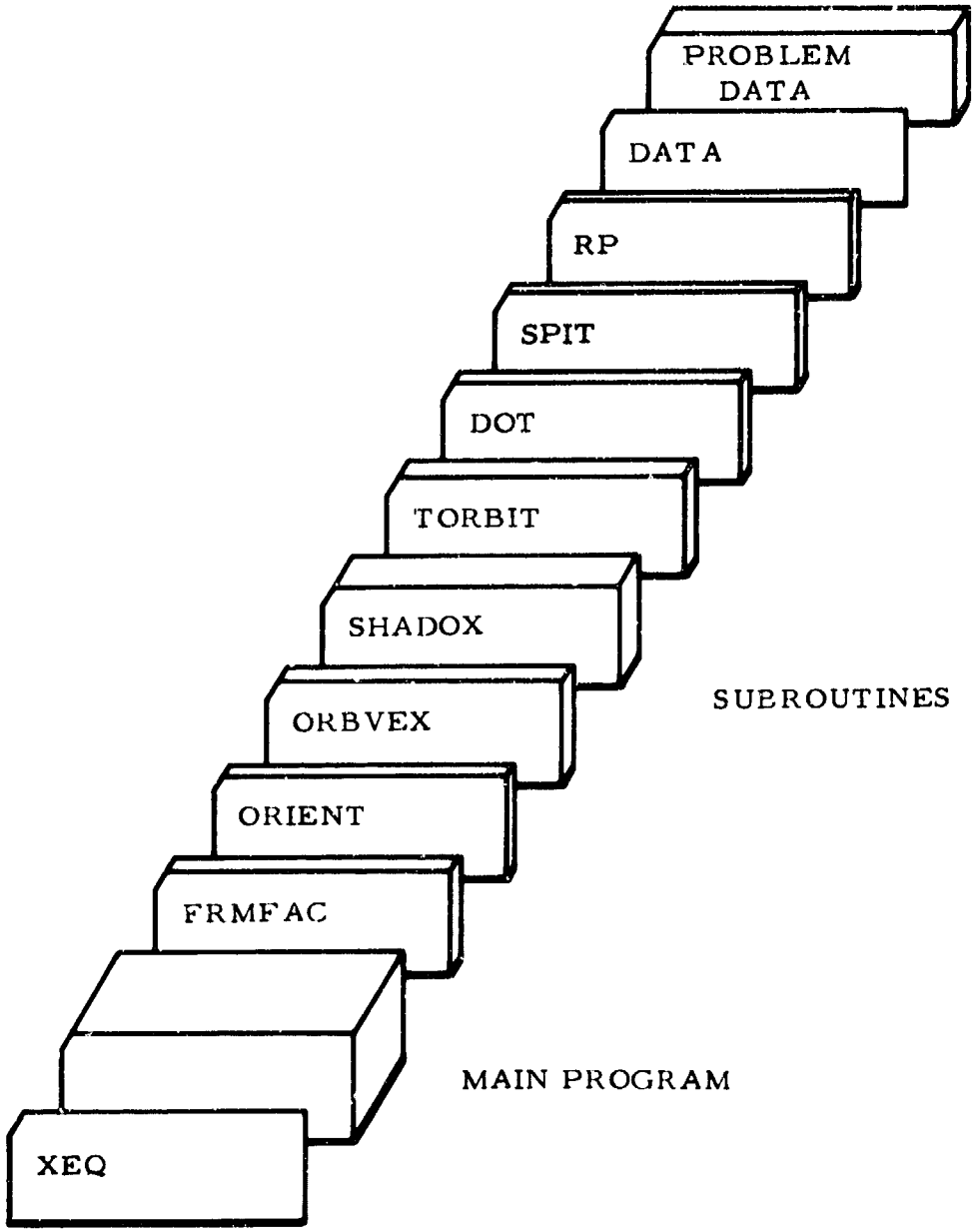

Figure 31. Deck Setup

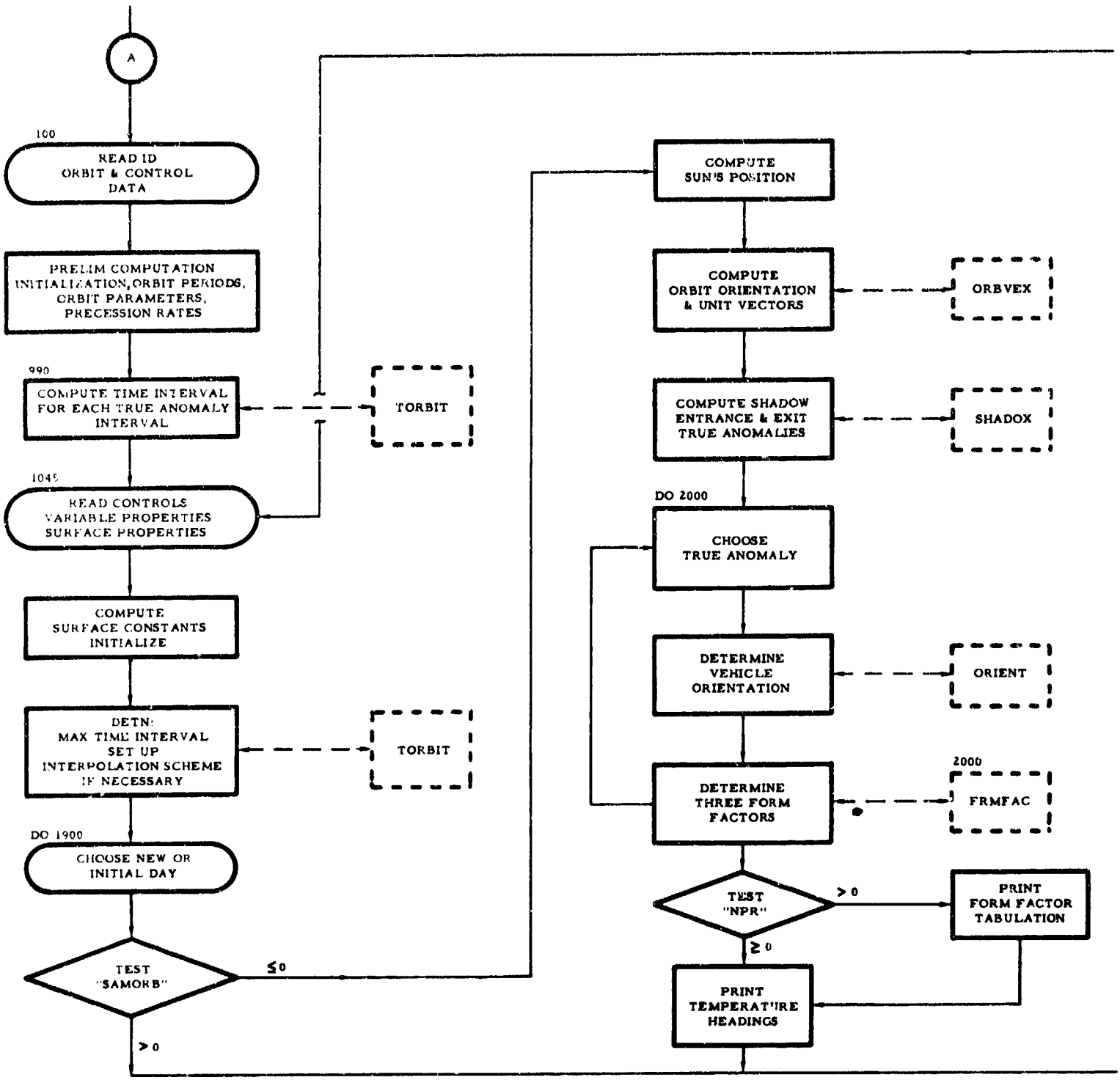
A
100
READ ID
ORBIT & CONTROL
DATA
PRELIM COMPUTATION
INITIALIZATION, ORBIT PERIODS,
ORBIT PARAMETERS,
PRECESSION RATES
990
COMPUTE TIME INTERVAL
FOR EACH TRUE ANOMALY
INTERVAL
TORBIT
1045
READ CONTROLS
VARIABLE PROPERTIES
SURFACE PROPERTIES
COMPUTE
SURFACE CONSTANTS
INITIALIZE
DETN:
MAX TIME INTERVAL
SET UP
INTERPOLATION SCHEME
IF NECESSARY
TORBIT
DO 1900
CHOOSE NEW OR
INITIAL DAY
TEST
"SAMORB"
≤0
>0
COMPUTE
SUN'S POSITION
COMPUTE
ORBIT ORIENTATION
& UNIT VECTORS
ORBVEX
COMPUTE SHADOW
ENTRANCE & EXIT
TRUE ANOMALIES
SHADOX
DO 2000
CHOOSE
TRUE ANOMALY
DETERMINE
VEHICLE
ORIENTATION
ORIENT
2000
DETERMINE
THREE FORM
FACTORS
FRMFAC
TEST
"NPR"
>0
≥0
PRINT
FORM FACTOR
TABULATION
PRINT
TEMPERATURE
HEADINGS

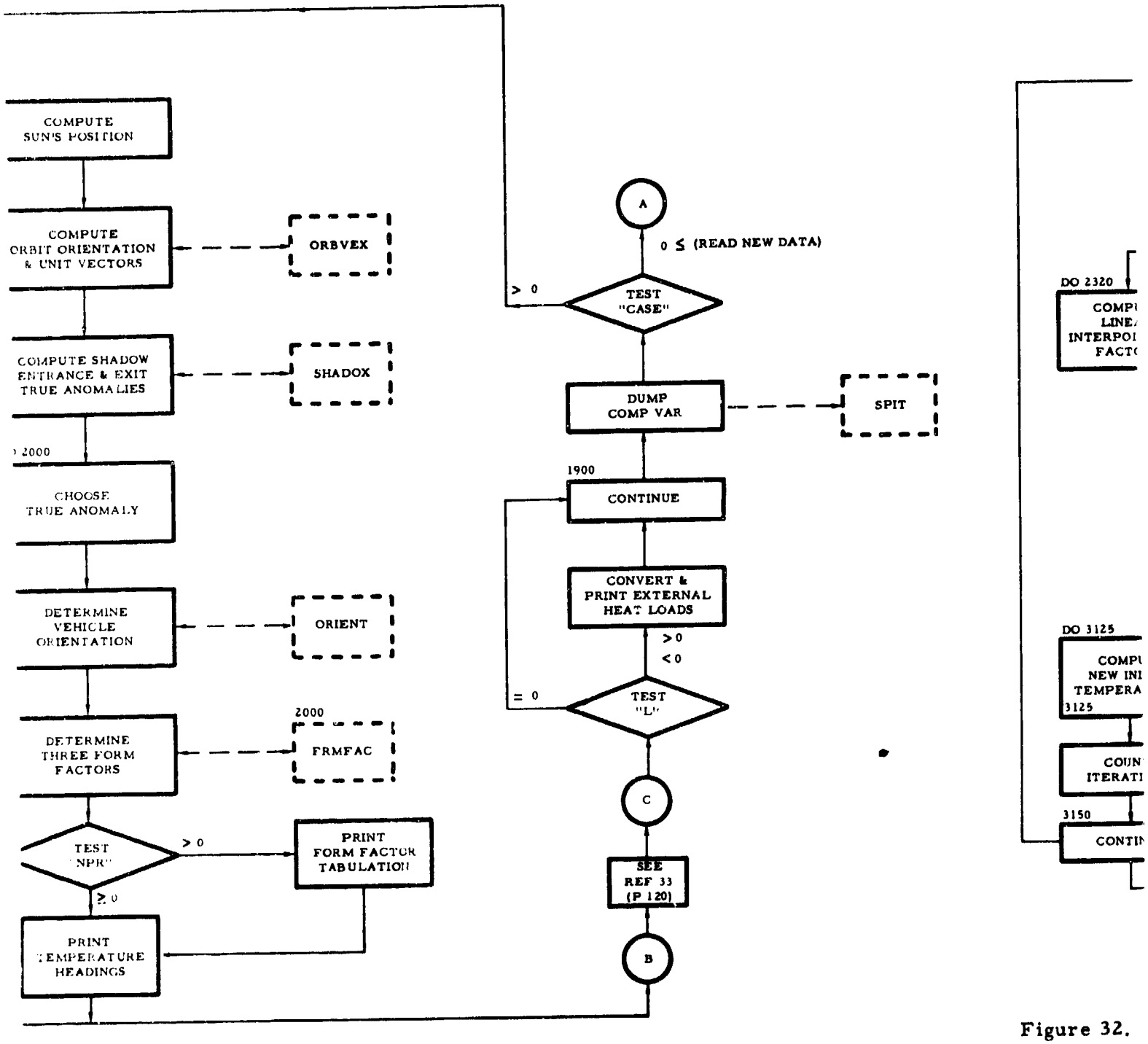
COMPUTE SUN'S POSITION
COMPUTE ORBIT ORIENTATION & UNIT VECTORS
ORBVEX
COMPUTE SHADOW ENTRANCE & EXIT TRUE ANOMALIES
SHADOX
2000
CHOOSE TRUE ANOMALY
DETERMINE VEHICLE ORIENTATION
ORIENT
DETERMINE THREE FORM FACTORS
2000
FRMFAC
TEST "NPR"
> 0
PRINT FORM FACTOR TABULATION
≥ 0
PRINT TEMPERATURE HEADINGS
A
0 ≤ (READ NEW DATA)
> 0
TEST "CASE"
DUMP COMP VAR
SPIT
1900
CONTINUE
CONVERT & PRINT EXTERNAL HEAT LOADS
> 0
< 0
= 0
TEST "L"
C
SEE REF 33 (P 120)
B
DO 2320
COMPU
LINE
INTERPOL
FACT
DO 3125
COMPU
NEW INI
TEMPERA
3125
COUN
ITERATI
3150
CONTIN

Figure 32.

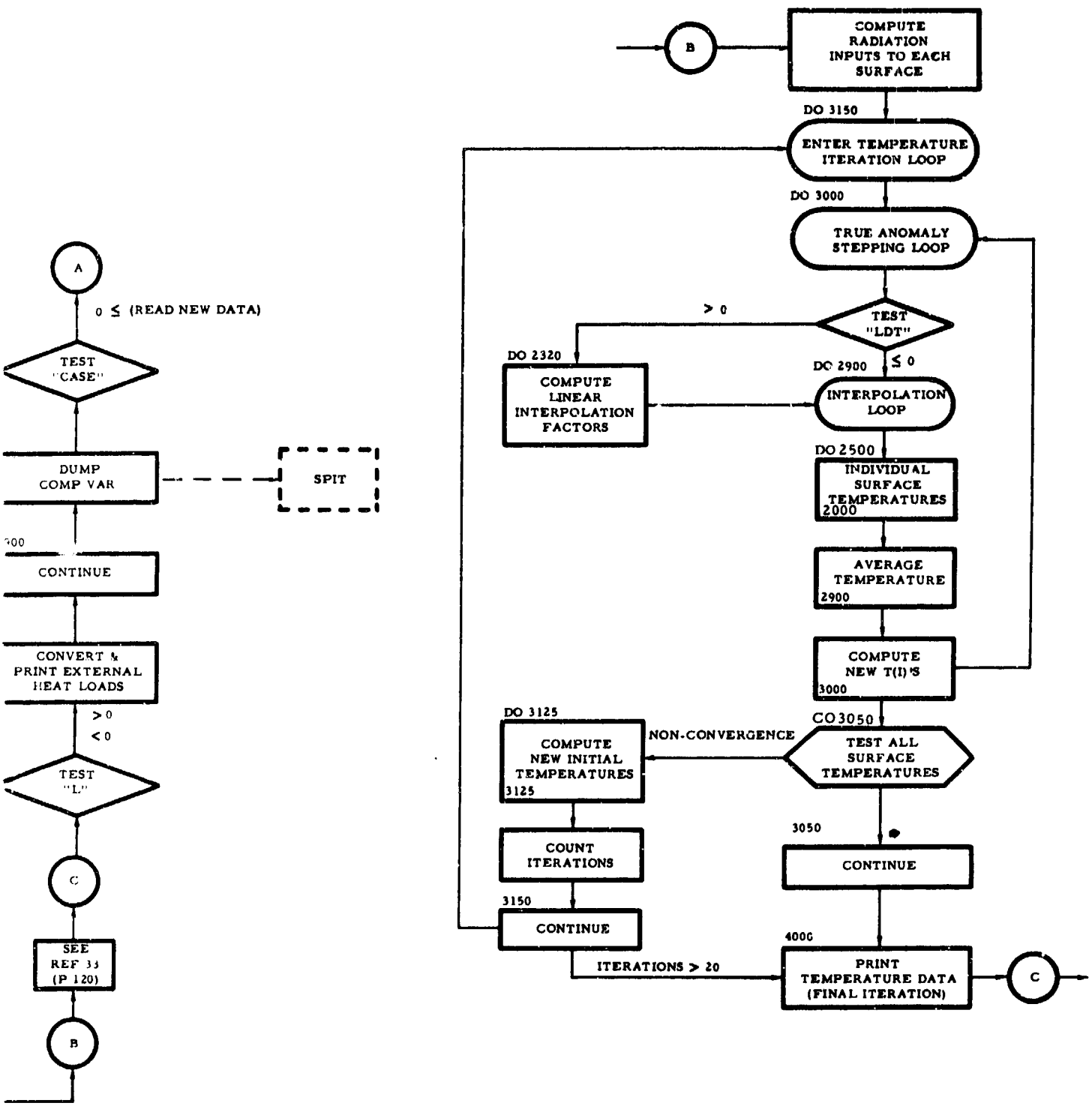

Figure 32. Main Program Flow Diagram

SPACE THERMAL ENVIRONMENT STUDY

The results of parametric analyses conducted by the Astronautics Division of Convair (General Dynamics Corporation) are presented here (Reference 15). Elemental vehicle shapes, including a sphere, cylinder, hemisphere, and plane surfaces, are considered with attitudes and altitudes as parameters. The development of the analysis for the planetary reflected solar takes into account the incident radiation as the vehicle crosses the terminator, thus representing a more detailed solution of the form factor than previously discussed.

NOMENCLATURE

A	Area, sq ft
a	Albedo
b	Distance defined in Figure 39
D	Cylinder diameter, ft
d	Radius defined in Figure 39
ds	Element of planet surface area, sq ft
E_r	Solar energy rate reflected per planet unit area, Btu/(hr)(sq ft)
E_t	Total energy rate emitted per planet unit area, Btu/(hr)(sq ft)
E_a	Energy rate emitted or reflected per planet unit area in the direction a, Btu/(hr) (sq ft)
F	View factor for flat plate
h	Altitude above planet surface, nautical miles
L	Length of cylinder, ft
P	Area of flat plate, sq ft
p	Radius of integrating hemisphere (Figure 39)
q	Radiant energy rate received by vehicle, Btu/hr

R	Radius of planet, nautical miles
r	Radius of sphere or hemisphere, ft
S	Solar constant, Btu/(hr)(sq ft)
x	Distance defined in Figure 39 or Figure 42
α	Angle between normal to planetary element and vector to vehicle, deg
β	Angle between earth-sun vector and extended normal to planetary elemental area, deg
γ	Angle between vertical to vehicle and cylinder or hemisphere axis or normal to flat plate, deg
Δ	Angle between axis of cylinder or hemisphere or normal to flat plate and vector from vehicle to planetary elemental area, deg
δ	Angle between vehicle-earth vector and vector from vehicle to planetary elemental area, deg
θ	Spherical ordinate, deg
θ_o	Spherical ordinate of horizon as seen from vehicle, deg
λ	Angle defined in Figure 39, deg
ρ	Distance between planet surface element and vehicle, naut mi
ϕ	Spherical abscissa, deg
ϕ_c	Angle of rotation of axis of cylinder or hemisphere or normal to flat plate about vertical to the vehicle, measured from plane of the earth-vehicle and earth-sun vectors, deg
ψ	Angle defined in Figure 39, deg
ω	Angle defined in Figure 39, deg

Subscripts

0, 1, 2, ...	Refer to various intersections on planetary sphere

PLANETARY THERMAL EMISSION

Analysis Method

Thermal energy is radiated by planets in the same manner as by any heated body. The magnitude of this radiation depends on the surface temperature and its emission characteristics. The latter involves the properties of any atmosphere which may exist, as well as the emissivity of the surface itself. Consequently, changes of atmospheric conditions, topography, season, and time of day introduce variations in the planetary thermal radiation. Neglecting details of the planet surface, however, it is possible to compute the average energy radiated by a planet using a thermal balance based on the solar radiation absorbed by the planet. As the temperatures of most planets do not vary appreciably over extended periods, it can be concluded that the thermally radiated energy is equivalent to the absorbed solar energy. Therefore, since the incident solar energy and average albedo are well known for most planets, the average thermal radiation can be readily calculated.

The energy balance is

$$(1 - a)\, S \pi R^2 = 4 \pi R^2 E_t \tag{66}$$

or

$$E_t = \left(\frac{1 - a}{4} \right) S \tag{67}$$

where

S = Solar heat flux per unit projected area of planet (as seen from sun)

Since the magnitudes of the thermal radiation from the various planets are established, there remains only the calculation of this energy in space as it will be intercepted by a space vehicle. To make this analysis possible parametrically, it is assumed that the planet surface is radiating uniformly so that the average value applies to any region of the surface. Because of the expected spacecraft velocities and trajectories, this appears to be a reasonable assumption. In addition, since thermal radiation is only significant for altitudes less than about three planet diameters, the radiation is far from being parallel and, consequently, the vehicle external configuration must be specified for a heat flux value in space to be meaningful. The shapes considered here include the sphere, hemisphere, cylinder, and flat plate. In general, any space vehicle shape could be analyzed, for practical purposes, as an assembly of flat plates, making it unnecessary to study, in

parametric detail, specific configurations whose analytical treatments are appreciably more complex than that of the flat plate. Configurations other than those mentioned will generally be in this area of higher complexity.

For convenience, thermal radiation heating data calculated for the stated configurations are plotted in reference to the earth. To use the curves for a vehicle in the proximity of another planet, it is only necessary to correct the altitude being considered to an equivalent earth altitude by multiplying it by the ratio of the earth radius to the planet radius, and using the appropriate planetary thermal radiation value (E_t) in the ordinate term.

Emission to Sphere

The geometrical relationship for a spherical body is shown in Figure 33. The radiant heat flux, incident to a sphere of radius r from the element of planet surface ds is

$$dq = \frac{\pi r^2 E_\alpha}{\rho^2} ds \tag{68}$$

where the energy radiated in the direction determined by α is

$$E_\alpha = \frac{E_t \cos \alpha}{\pi} \tag{69}$$

Then

$$dq = \frac{r^2 E_t \cos \alpha \, ds}{\rho^2} \tag{70}$$

Making the substitutions,

$$H = h + R \tag{71}$$

$$\cos \alpha = \frac{H \cos \theta - R}{\rho} \tag{72}$$

$$ds = R^2 \sin \theta \, d\theta \, d\phi \tag{73}$$

$$\rho^2 = R^2 + H^2 - 2RH \cos \theta \tag{74}$$

The total incident heating rate from the planet to the sphere is

$$q = 2r^2 R^2 E_t \int_0^{\pi} \int_0^{\theta_o} \frac{(H \cos \theta - R) \sin \theta}{(R^2 + H^2 - 2RH \cos \theta)^{3/2}} \, d\theta \, d\phi \tag{75}$$

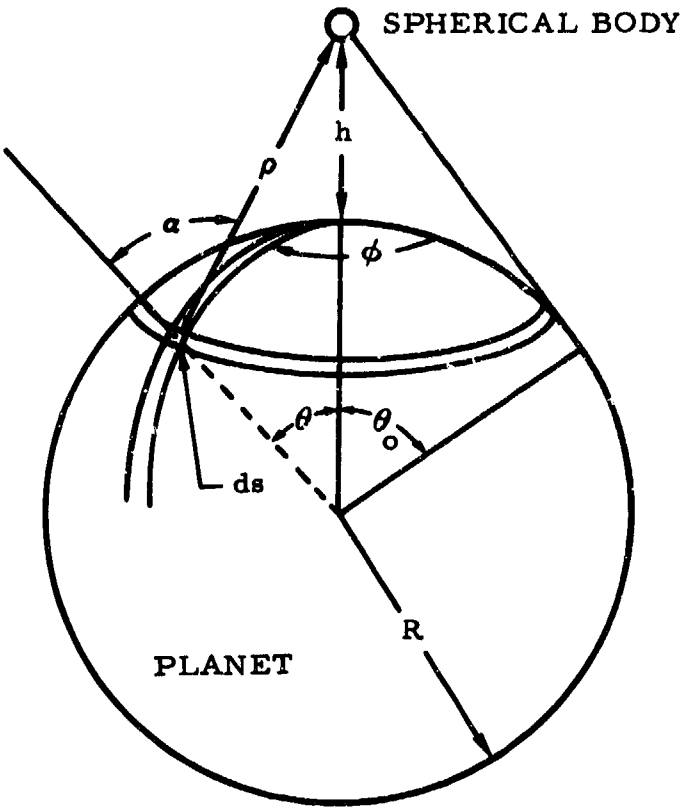

Figure 33. Geometry of Planetary Thermal Emission to Sphere

which, after integration and substitution of $\cos \theta_o = R/H$, yields

$$q = 2\pi r^2 E_t \left(1 - \frac{\sqrt{2Rh + h^2}}{H}\right) \qquad (76)$$

Figure 34 shows the value $q/\pi\ r^2 E_t$, the planetary thermal radiation to a sphere per unit of great circle (or projected) area and per unit of surface thermal radiation, as a function of the altitude above the earth surface. The term E_t is included in the ordinate scale definition rather than in the curve plot itself to preclude obsolescence of the curves in the event a more accurate value for earth albedo is determined in the future.

Emission to Cylinder

The configuration for a cylindrical body is shown in Figure 35. A new variable, the attitude of the cylinder with respect to the planet, defined by the angle γ, has to be considered.

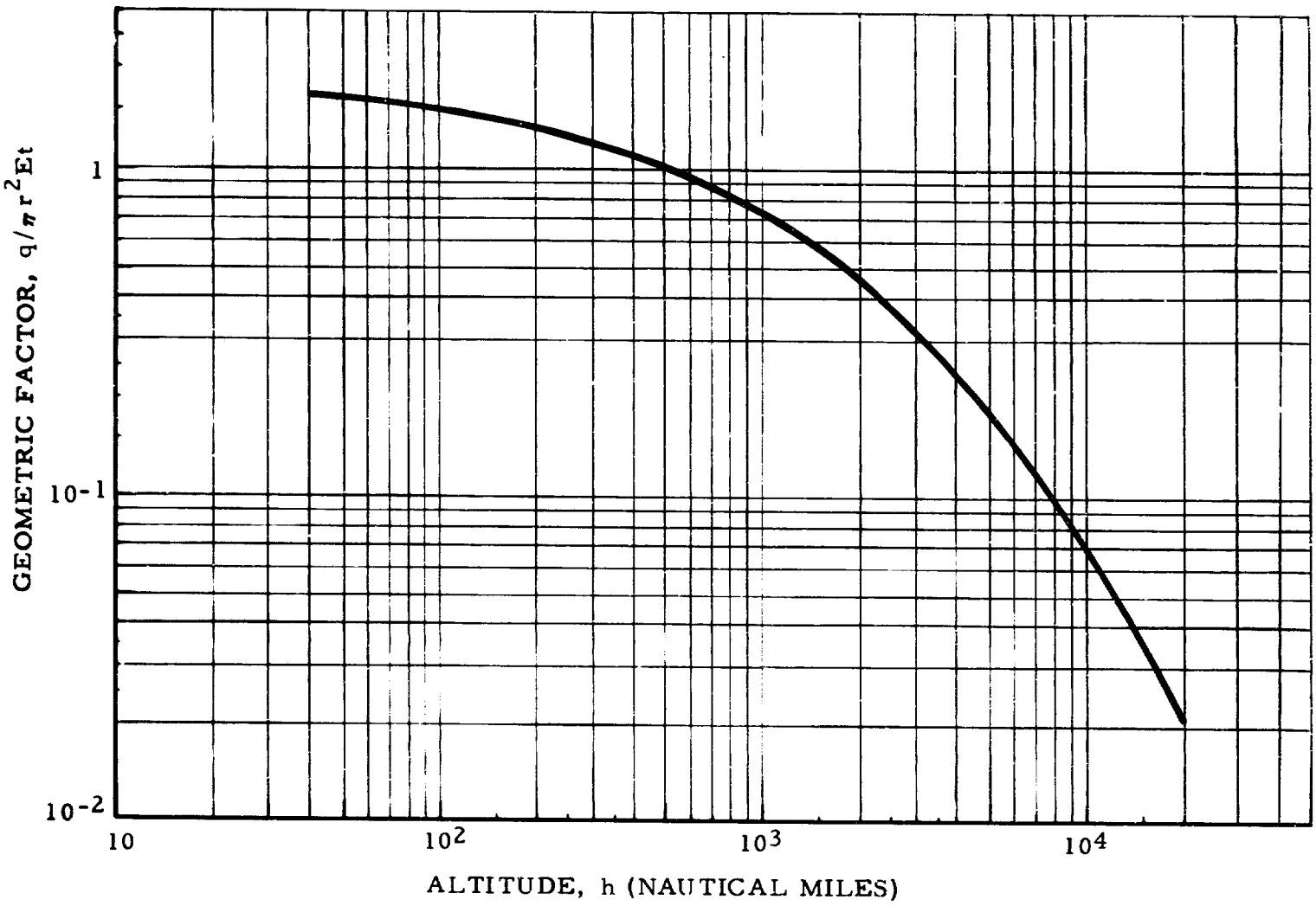

Figure 34. Geometric Factor for Earth Thermal Emission Incident to Sphere Versus Altitude

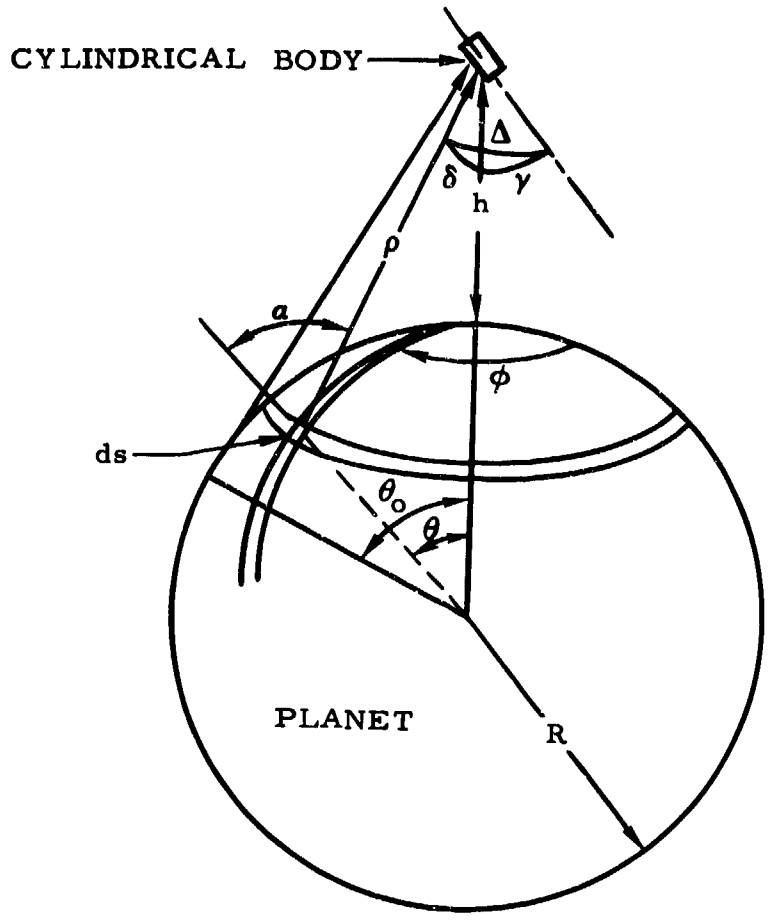

Figure 35. Geometry of Planetary Thermal Emission to Cylinder

The radiant heat flux incident to the lateral surface of a cylinder of dimeter D and length L from the element of planet surface ds is

$$dq = \frac{DL \sin \Delta E_t \cos a \, ds}{\pi \rho^2} \qquad (77)$$

where DL sin Δ is the projection of the cylinder surface as seen from ds, and $E_t \cos a/\pi$ is the energy radiated in the direction a. The values of H, cos a, ds, and ρ^2 are given again by Equations 71 through 74.

The value of sin Δ is

$$\sin \Delta = \sqrt{1 - (\cos \delta \cos \gamma + \sin \delta \sin \gamma \cos \phi)^2} \qquad (78)$$

where

$$\cos \delta = \frac{H - R \cos \theta}{\rho} \tag{79}$$

$$\sin \delta = \frac{R \sin \theta}{\rho} \tag{80}$$

After substitutions and some algebraic manipulation, the total incident heat flux from the planet to the cylinder can be written as

$$q = \frac{2DLE_t R^2}{\pi} \int_0^{\pi} \int_0^{\theta_o} \frac{(H \cos \theta - R) \sin \theta}{(H^2 + R^2 - 2RH \cos \theta)^2} \; X \tag{81}$$

$$\left(\sqrt{A + B \cos \phi - C \cos^2 \phi} \; d\theta d\phi \right)$$

where

$$A = R^2 + H^2 - H^2 \cos^2 \gamma - 2RH \cos \theta \sin^2 \gamma - R^2 \cos^2 \theta \cos^2 \gamma \tag{82}$$

$$B = 2R^2 \sin \theta \cos \theta \sin \gamma \cos \gamma - 2RH \sin \theta \sin \gamma \cos \gamma \tag{83}$$

$$C = R^2 \sin^2 \theta \sin^2 \gamma \tag{84}$$

Equation 81 cannot be integrated analytically; a numerical integration is required. To perform this, and other numerical integrations mentioned later, the solutions were programed on an automatic digital computer. The results are plotted in Figure 36, where the values of q/DLE_t are given as a function of the altitude above the earth surface h, with the attitude angle γ as a parameter.

To apply the curves of Figure 36 to a vehicle in the proximity of a planet other than earth, the same procedure and correction term as given for the case of the sphere may be used.

Emission to Hemisphere

The configuration for a hemispherical body is shown in Figure 37. The orientation parameter γ for the hemisphere, although similar to that for a cylinder, must assume values throughout 180 degrees because the hemisphere is only symmetrical about one orthogonal axis.

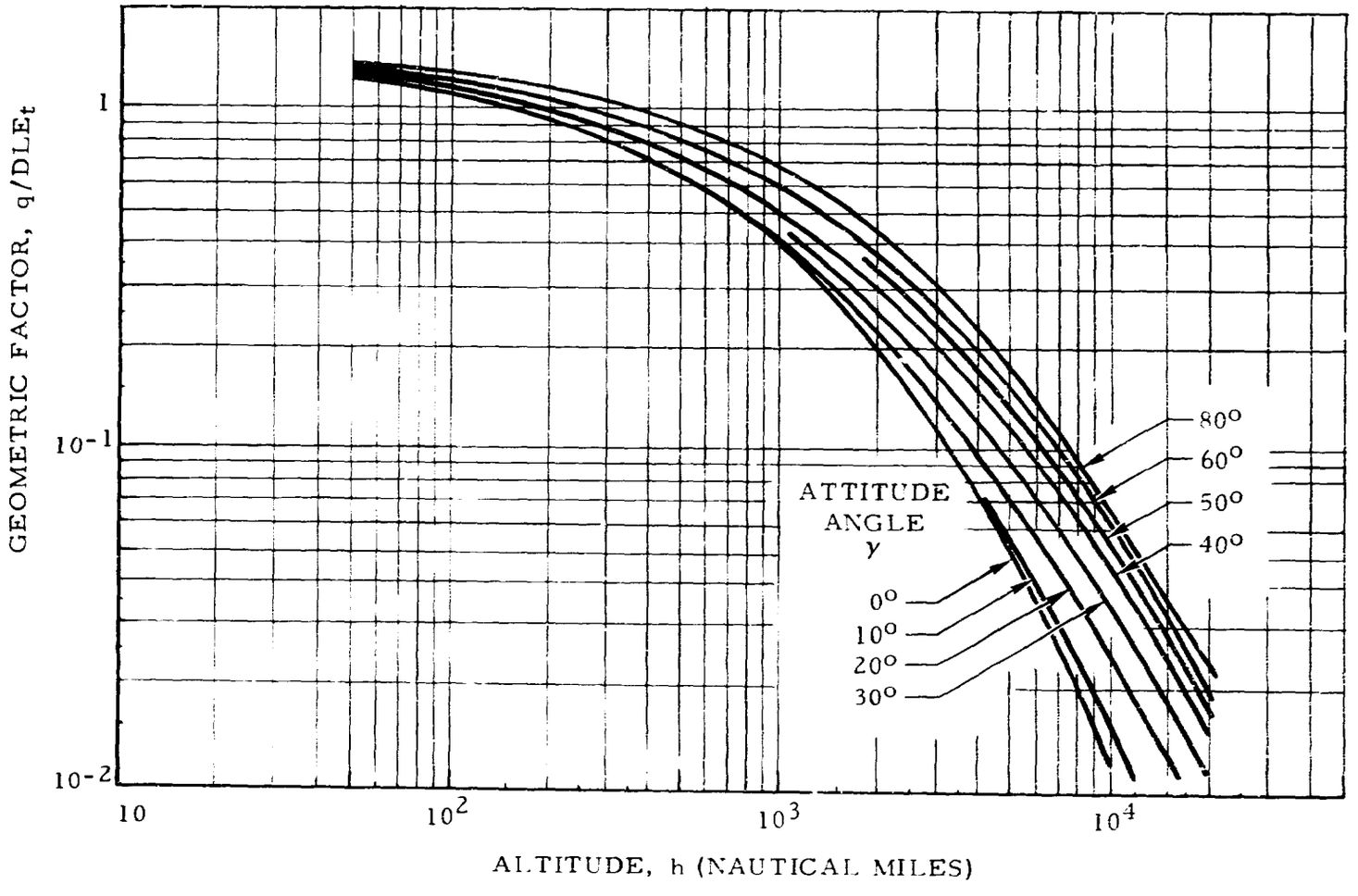

Figure 36. Geometric Factor for Earth Thermal Emission Incident to Cylinder Versus Altitude as Function of Attitude Angle

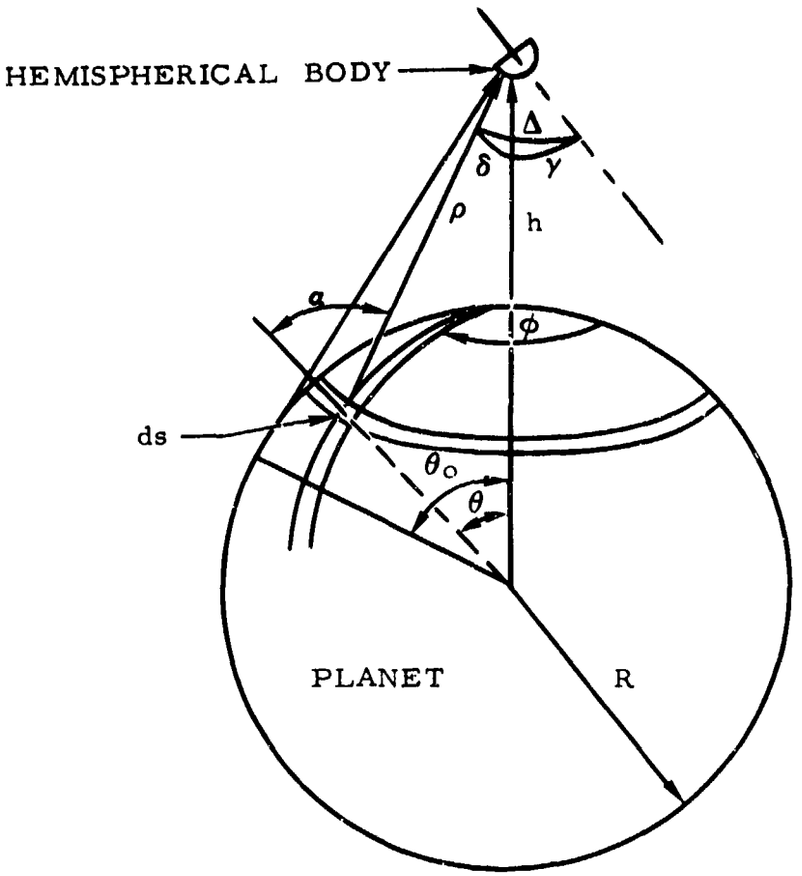

Figure 37. Geometry of Planetary Thermal Emission to Hemisphere

The radiant heat flux incident to the hemispherical surface of radius r from the element of planet surface ds is

$$dq = \frac{\frac{1}{2}\pi r^2(\cos \Delta + 1)\, E_t \cos \alpha \, ds}{\pi \rho^2} \tag{85}$$

where $1/2\ \pi r^2(\cos \Delta + 1)$ is the projection of the hemispherical surface as seen from ds, and $E_t \cos \alpha / \pi$ is the energy radiated in the direction α. The values of H, $\cos \alpha$, ds, and ρ^2 are given again by Equations 71 through 74.

The value of $\cos \Delta$ is

$$\cos \Delta = \cos \delta \cos \gamma + \sin \delta \sin \gamma \cos \phi \tag{86}$$

where $\cos \delta$ and $\sin \delta$ are as defined in Equations 79 and 80.

After substitutions and algebraic manipulation, the total incident heat flux from the planet to the hemispherical surface can be written as

$$q = E_t r^2 R^2 \int_0^{\pi} \int_0^{\theta_o} \frac{(H \cos\theta - R) \sin\theta}{(H^2 + R^2 - 2RH \cos\theta)^{3/2}} \, d\theta d\phi$$

$$+ \int_0^{\pi} \int_0^{\theta_o} \frac{(H \cos\theta - R) \sin\theta \, (A + B \cos\phi)}{(H^2 + R^2 - 2RH \cos\theta)^2} \, d\theta d\phi \qquad (87)$$

where

$$A = H \cos\gamma - R \cos\theta \cos\gamma$$

$$B = R \sin\theta \sin\gamma$$

The first term of the integration may be performed analytically to give the heat flux as

$$q = E_t r^2 \left[\pi \left(1 - \frac{\sqrt{2Rh + h^2}}{H} \right) \right.$$

$$\left. + R^2 \int_0^{\pi} \int_0^{\theta_o} \frac{(H \cos\theta - R) \sin\theta}{(H^2 + R^2 - 2RH \cos\theta)^2} (A + B \cos\phi) d\theta d\phi \right] \qquad (88)$$

The second term was integrated numerically. The results are plotted in Figure 38, where the geometric factor $q/\pi r^2 E_t$ is given as a function of altitude h above the earth's surface with the attitude angle γ as a parameter. These curves may be used for other planets as explained for the case of the sphere.

Emission to Flat Plate

For a flat plate, an integration method similar to that explained for spheres may be used. However, a similar solution can be found by resorting to a geometrical method of obtaining the view factor.

It can be proved that the view factor of a surface from a small flat plate can be geometrically determined. The surface is projected from the viewing point onto a sphere having its center at the viewing point. The image on the

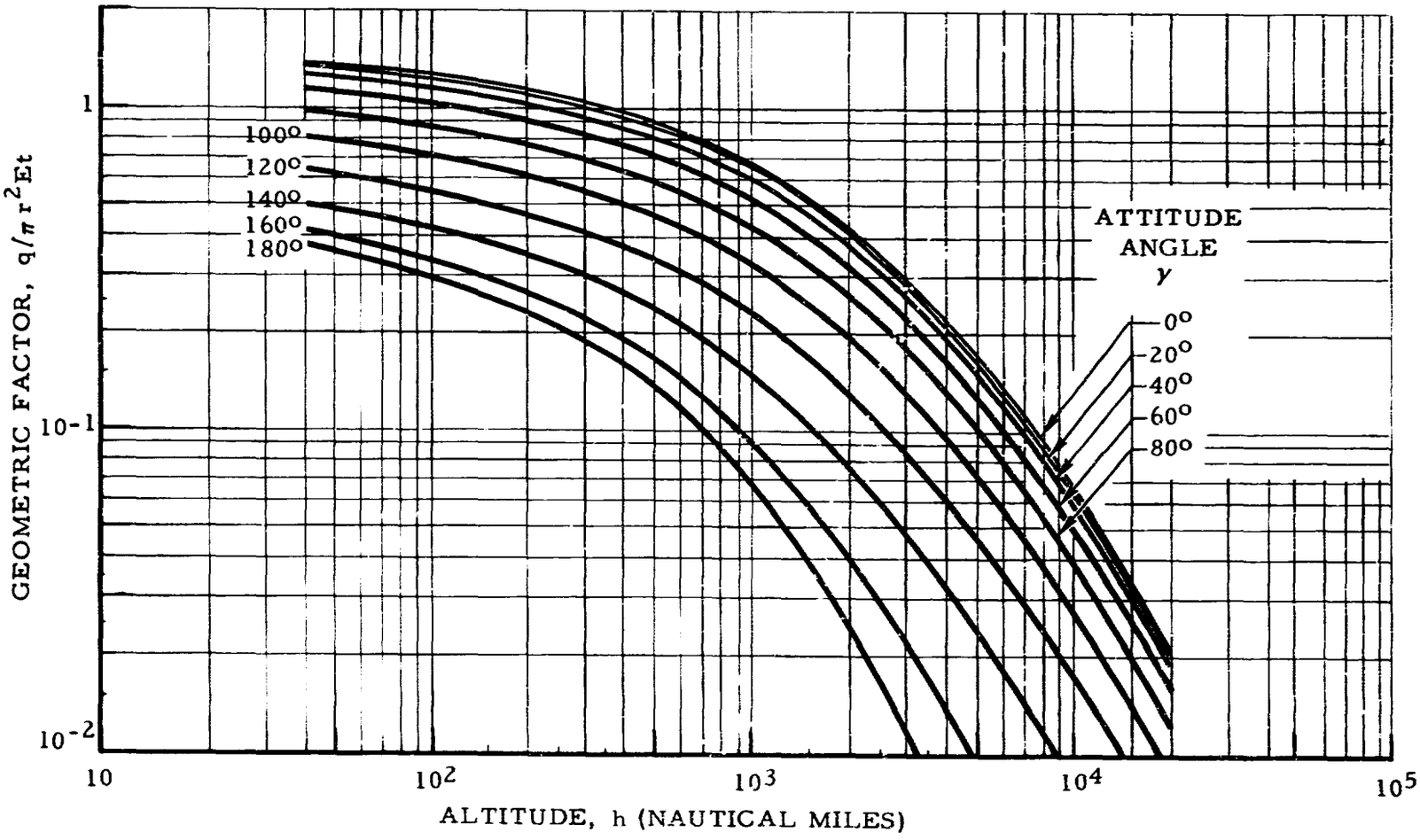

Figure 38. Geometric Factor for Earth Thermal Emission Incident to Hemisphere Versus Altitude as Function of Attitude Angle

sphere is then projected onto the plane of the small flat surface. The view factor is then determined from

$$F = \frac{\text{area projected on plane}}{\pi \rho^2} \tag{89}$$

For this case, the surface is the region of the planet which the flat plate can see, and the radius of the sphere is taken as the distance between the plate and the tangency point T, as shown in Figure 39. The general case, in which the plane of the plate intersects the planet, will be analyzed first.

The area of the circular segment A_1 is

$$A_1 = \frac{\pi d^2 \omega_1}{360} - \frac{d^2 \sin \omega_1}{2} \tag{90}$$

To obtain the value of ω_1,

$$\omega_1 = 180 - 2\psi \tag{91}$$

$$\psi = \sin^{-1} \frac{b}{d} \tag{92}$$

$$b = \frac{h + x}{\tan \gamma} \tag{93}$$

$$h + x = p \sin \theta_0 \tag{94}$$

$$\sin \theta_o = \frac{p}{H} \tag{95}$$

$$h + x = \frac{p^2}{H} \tag{96}$$

$$b = \frac{p^2}{H \tan \gamma} \tag{97}$$

$$d = p \cos \theta_o = p \frac{R}{H} \tag{98}$$

$$\omega_1 = 180 - 2 \sin^{-1} \frac{p}{R \tan \gamma} \tag{99}$$

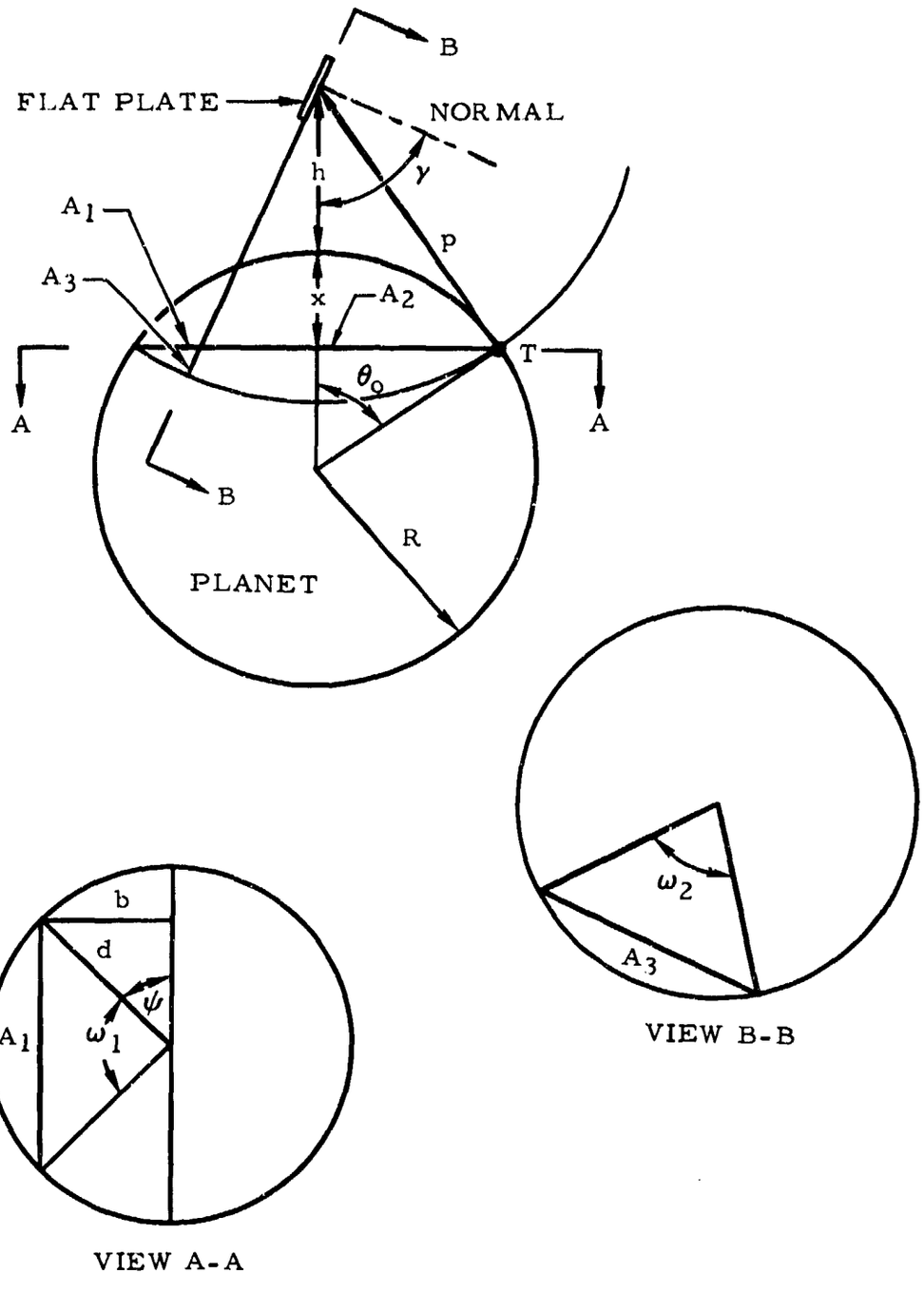

Figure 39. Geometry of Planetary Thermal Emission to Flat Plate

and since

$$p = \sqrt{H^2 - R^2}$$

$$\omega_1 = 180 - 2 \sin^{-1} \frac{\sqrt{H^2 - R^2}}{R \tan \gamma} \tag{100}$$

The area A_1 is subtracted from πd^2 to give A_2. The area of the circular segment A_3 is

$$A_3 = \frac{\pi p^2 \omega_2}{360} - \frac{p^2 \sin \omega_2}{2} \tag{101}$$

As for ω_2, it can be found that

$$\omega_2 = 180 - 2 \sin^{-1}\left(\frac{\sqrt{H^2 - R^2}}{H \sin \gamma}\right) \tag{102}$$

The view factor is obtained, then, by projecting the areas A_2 and A_3 on the plane of the flat plate, and dividing the sum of their projections by πp^2. The resulting expression is

$$\begin{aligned} F = {} & \frac{1}{360}\left[180 - 2 \sin^{-1}\left(\frac{\sqrt{H^2 - R^2}}{H \sin \gamma}\right)\right] - \frac{1}{2\pi} \sin\left[2 \sin^{-1}\left(\frac{H^2 - R^2}{H \sin \gamma}\right)\right] \\ & + \left\{\frac{R^2}{H^2} - \frac{1}{360}\left(\frac{R^2}{H^2}\right)\left[180 - 2 \sin^{-1}\left(\frac{\sqrt{H^2 - R^2}}{R \tan \gamma}\right)\right]\right. \\ & \left. + \frac{1}{2\pi}\left(\frac{R^2}{H^2}\right) \sin\left[2 \sin^{-1}\left(\frac{\sqrt{H^2 - R^2}}{R \tan \gamma}\right)\right]\right\} \cos \gamma \end{aligned} \tag{103}$$

A much simpler expression is obtained when the plane of the plate does not intersect the planet. In that case $A_1 = A_3 = 0$ and $A_2 = \pi d^2$. Then

$$F = \frac{A_2 \cos \gamma}{\pi p^2} = \frac{R^2}{H^2} \cos \gamma \tag{104}$$

In either case, the total heat flux from the planet to the flat plate is given by

$$q = E_t F P \tag{105}$$

where P is the area of the plate. Figure 40 is a plot of the thermal radiation to a flat plate as a function of altitude with the attitude angle γ as a parameter. Again, to apply these curves to planets other than the earth, the procedure given for the sphere may be used.

PLANETARY REFLECTED SOLAR RADIATION

As mentioned earlier, planetary albedo is the ratio of reflected to total incident solar radiation. As such, the units of the term albedo are dimensionless; however, the expression has been used more and more frequently in recent years to mean the reflected energy itself. Whatever the final, precise definition of the term, it clearly differentiates the portion of the incident solar energy which is reflected by the planet from that which is absorbed and reradiated.

The average albedo for planets located up to 10 astronomical units from the sun is known with reasonable accuracy, the value for the earth being the least accurate. At distances greater than about 10 astronomical units from the sun, the accuracy of the planetary albedo falls off significantly because of the very small magnitude of the reflected energy.

To permit a parametric analysis of the solar energy reflected from a planet, the same assumption which was made for thermal radiation (i.e., a uniform planet surface with regard to radiation characteristics) will be made. It is further assumed that the planet surface reflects diffusely (i.e., it obeys Lambert's law). While these assumptions may not be entirely accurate, particularly for the earth where large bodies of water exist, they can be justified by consideration of vehicle trajectories, orbits, and velocities used in the analysis.

Based upon these assumptions, it is clear that the reflected energy has a cosine distribution, not only with respect to the angular radiation from a given area but over the sunlit surface of the planet as well. This considerably complicates the problem over the case of thermal radiation, with the result that a direct analytical solution is not available even for the case of a spherical vehicle; for the cases of vehicles other than a sphere, the number of computations is greatly increased by the increased number of variables. The result is that some 97 pages of curves are necessary to adequately describe reflected heating to the sphere, hemisphere, cylinder, and flat plate which were used in the thermal radiation analyses. As a consequence of the bulk involved, these albedo heating data are included as Appendix B of this report.

As in the case of the thermal radiation analysis, the heating data is plotted in reference to the earth. Also, the data may be used for vehicles in the proximity of other planets by applying the same radius ratio correction terms to obtain an equivalent earth altitude and then using the appropriate

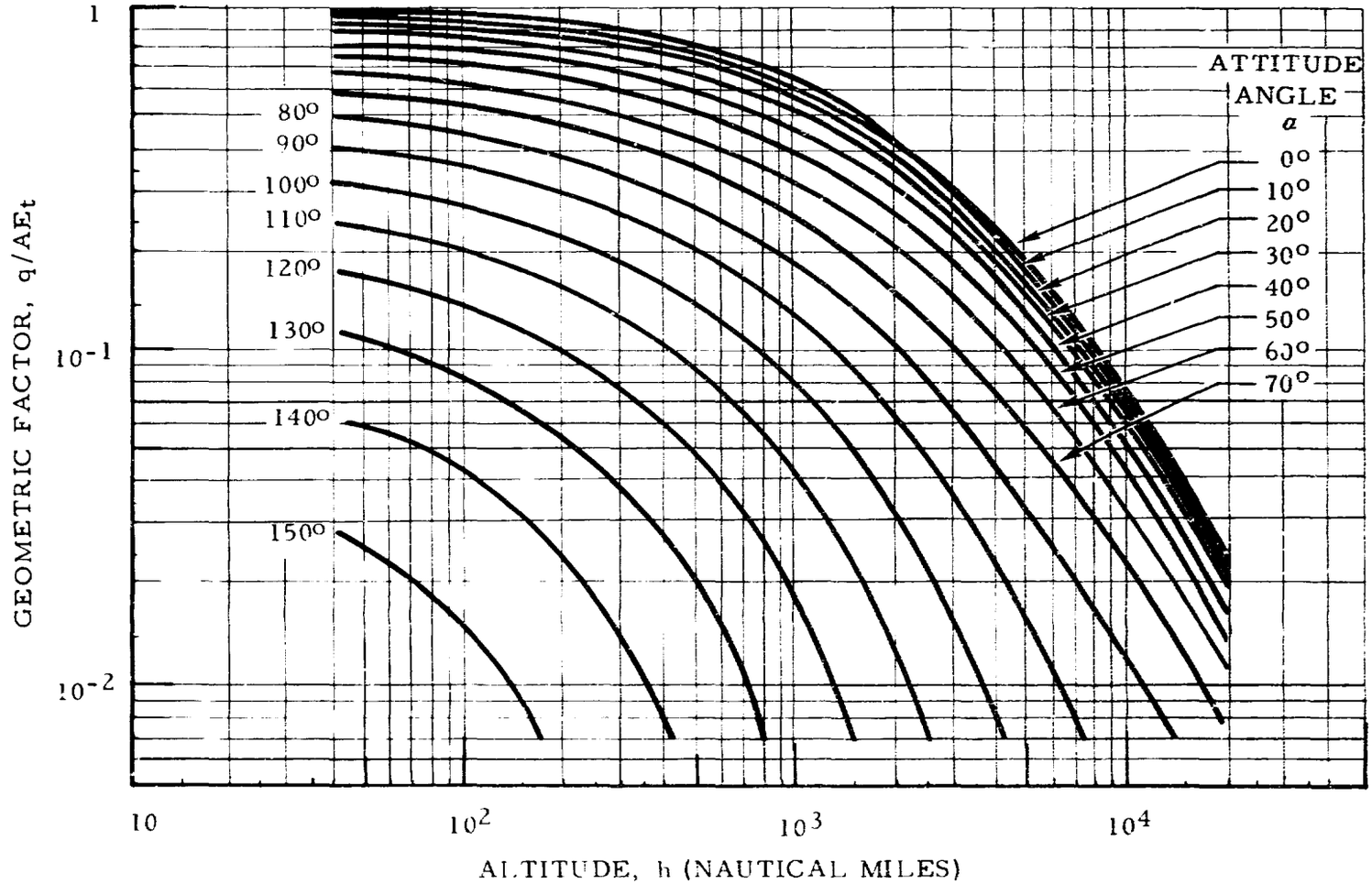

Figure 40. Geometric Factor for Earth Thermal Emission Incident to Flat Plate Versus Altitude as Function of Attitude Angle

ordinate multiplying factor. This factor takes into account the albedo and solar heat input to the planet considered.

Reflected Solar to Sphere

Considering the reflected (or albedo) heat flux incident to a sphere in space, the most general configuration is given in Figure 41. As in the case of thermal radiation, this heat flux to a sphere of radius r from the element of planet surface ds is

$$dq = \frac{\pi r^2 E_a \, ds}{\rho^2} \tag{106}$$

where

$$E_a = \frac{E_r \cos a}{\pi}$$

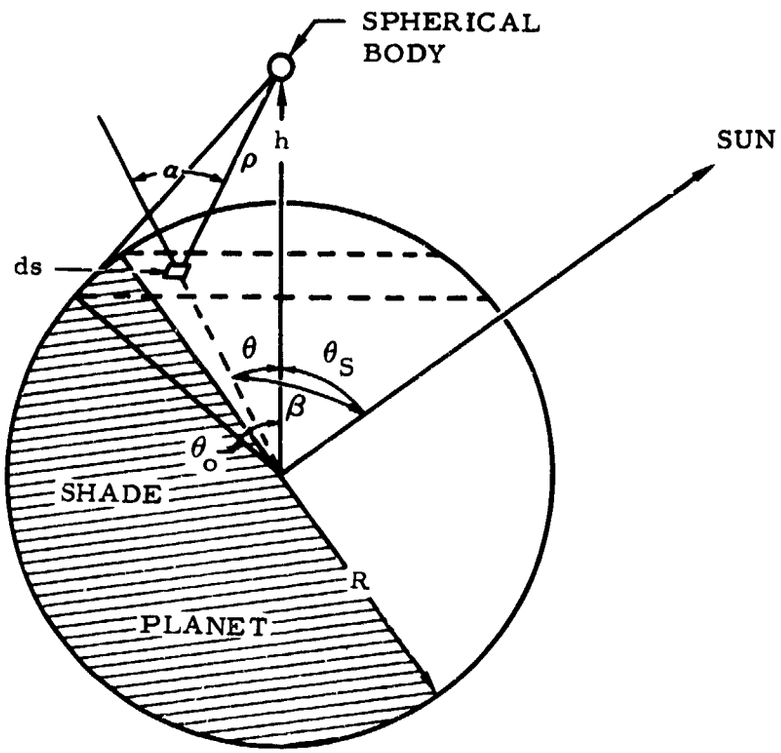

Figure 41. Geometry of Planetary Reflected Solar Radiation to Sphere

is the fraction of reflected solar radiation in the direction determined by α. E_r is the total reflected energy per unit of planet surface, and is given by

$$E_r = Sa \cos \beta \tag{107}$$

where S (the direct solar heat flux normal to the sun direction), a, and β are as shown in Figure 41. Then

$$dq = \frac{r^2}{\rho^2} Sa \cos \alpha \cos \beta \, ds \tag{108}$$

The values of $\cos \alpha$, ds and ρ^2 are given by Equations 72 through 74. The value of $\cos \beta$ is

$$\cos \beta = \cos \theta \cos \theta_S + \sin \theta \sin \theta_S \cos \phi \tag{109}$$

By substituting these expressions in Equation 108 and integrating for θ and ϕ, q can be obtained. Careful consideration, however, has to be given to the limits of integration. Two cases should be considered, as illustrated in Figure 42.

The first occurs when the region of the planet seen from the satellite is completely sunlit. This condition can be expressed as

$$\theta_o \leq \frac{\pi}{2} - \theta_S$$

wherein the limits of integration for θ are 0 and θ_o and for ϕ are 0 and π (the integral with respect to ϕ is multiplied by 2).

When the region of the planet seen from the satellite is only partially sunlit,

$$\theta_o > \frac{\pi}{2} - \theta_S$$

wherein a variable upper limit for ϕ has to be introduced. It is convenient to perform the integration for two regions, as shown in Figure 42. Region 1 is totally sunlit, and the limits are 0 to $\pi/2 - \theta_S$ for θ and 0 to π for ϕ. The limits for region 2 are $\pi/2 - \theta_S$ to θ_0 for θ and 0 to $\pi/2 + \sin^{-1}(\text{ctg } \theta_S \text{ ctg } \theta)$ for ϕ. This variable limit can be obtained as follows. From Figure 42 it is evident that

$$\phi = \frac{\pi}{2} + \lambda \tag{110}$$

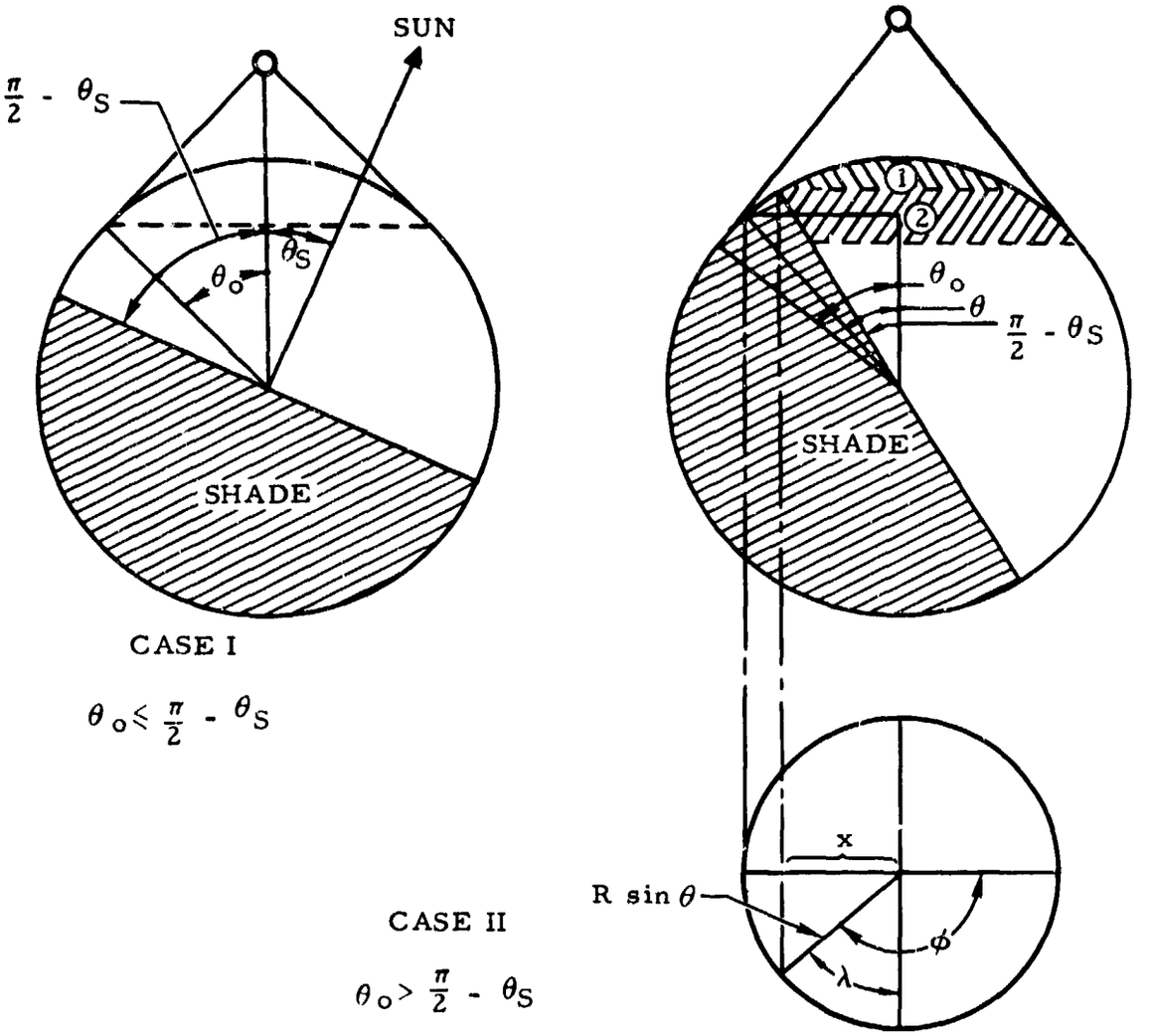

Figure 42. Cases for Limits of Integration in Reflected Solar Radiation to Sphere

Also

$$x = R \cos\theta \operatorname{ctg} \theta_S \tag{111}$$

and

$$\sin\lambda = \frac{x}{R \sin\theta} = \operatorname{ctg} \theta_S \operatorname{ctg} \theta \tag{112}$$

Therefore

$$\phi = \frac{\pi}{2} + \sin^{-1}(\operatorname{ctg} \theta_S \operatorname{ctg} \theta) \tag{113}$$

Finally, by adding the integrals over regions 1 and 2 in Figure 42, the total solar radiation reflected by the planet incident upon the sphere is

$$q = 2r^2 Sa\, R^2 \int_0^{\frac{\pi}{2}-\theta_S} \int_0^{\pi} \frac{(H\cos\theta - R)(\cos\theta \cos\theta_S + \sin\theta \sin\theta_S \cos\phi)\sin\theta d\theta d\phi}{(R^2 + H^2 - 2RH\cos\theta)^{3/2}}$$

$$+ 2r^2 SaR^2 \int_{\frac{\pi}{2}-\theta_S}^{\theta_o} \int_0^{\frac{\pi}{2} + \sin^{-1}(\operatorname{ctg}\theta_S \operatorname{ctg}\theta)} \frac{(H\cos\theta - R)(\cos\theta \cos\theta_S + \sin\theta \sin\theta_S \cos\phi)\sin\theta d\theta d\phi}{(R^2 + H^2 - 2RH\cos\theta)^{3/2}} \tag{114}$$

Equation 114 holds for $\theta_S < \pi/2$. For $\theta_S \geq \pi/2$, the first term disappears and the lower lower limit on θ of the second term becomes $\theta_S - \pi/2$.

Integration with respect to ϕ is immediate, but not so with respect to θ which requires a numerical method. Figure 43 shows the value of $q/\pi r^2 Sa$, which is the heat flux to a sphere per unit of great circle (projected) area per unit of reflected solar radiation, as a function of altitude above the earth surface, with θ_S as a parameter.

Reflected Solar to Cylinder

The albedo to a cylinder is computed by a numerical method similar to that used for a sphere; however, the integrand is more complex because two additional parameters defining the attitude of the cylinder must be included. The general configuration is shown in Figure 44.

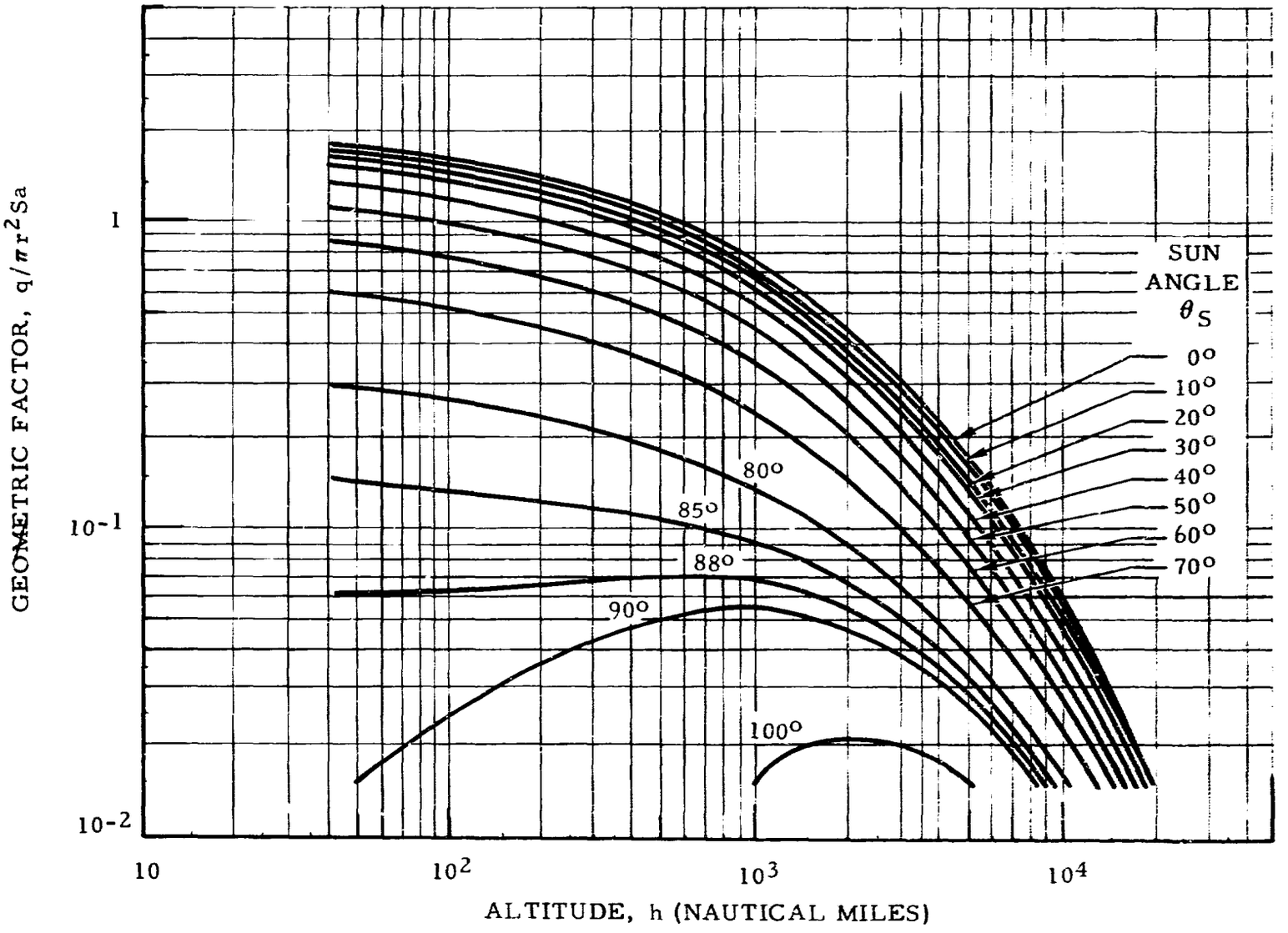

Figure 43. Geometric Factor for Earth Reflected Solar Radiation Incident to Sphere Versus Altitude as Function of Sun Angle

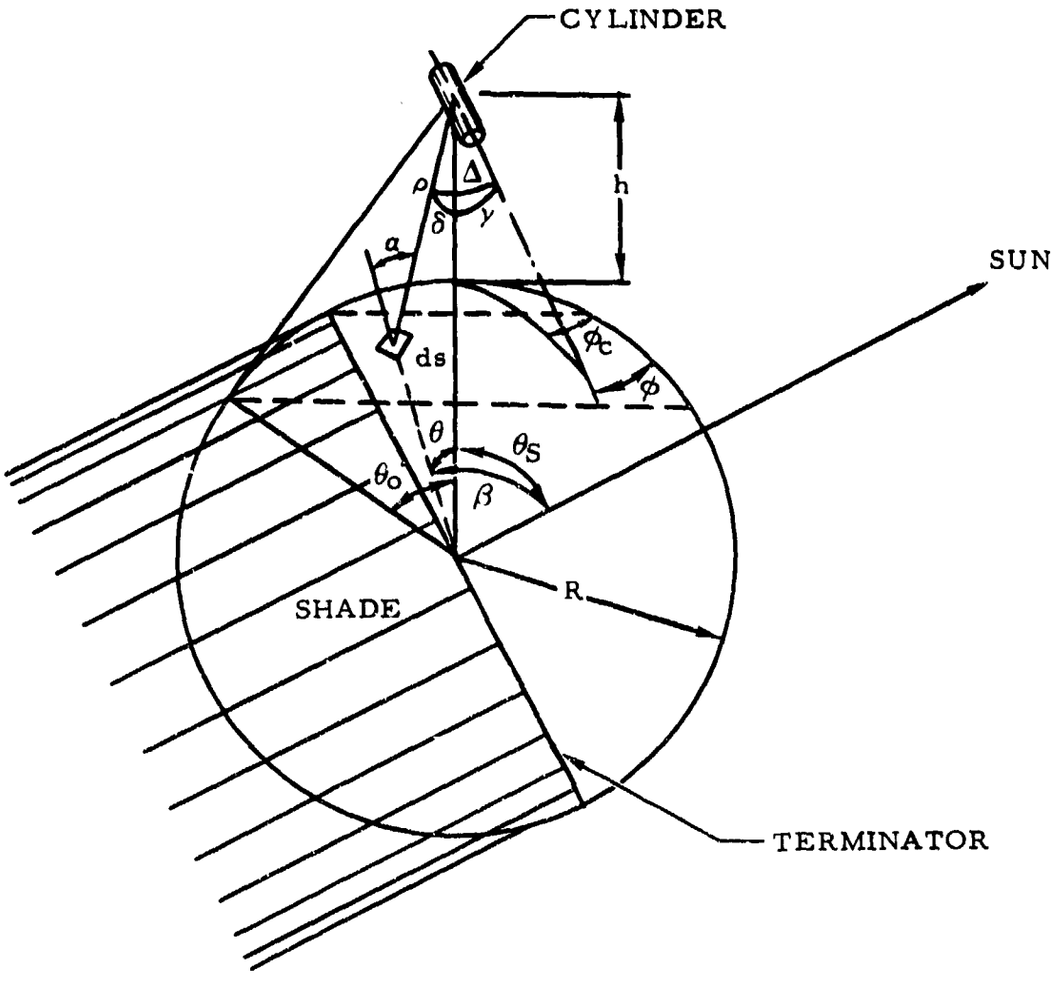

Figure 44. Geometry of Planetary Reflected Solar Radiation to Cylinder

The radiant heat flux incident to the cylinder lateral surface of diameter D and length L due to reflected solar energy from the element of planet surface ds is

$$dq = \frac{DLE_a \sin \Delta \, ds}{\rho^2} \tag{115}$$

where

$$E_a = \frac{E_r \cos a}{\pi}$$

is the fraction of reflected solar radiation in the direction determined by α. E_r is the total reflected energy per unit of planet surface, and is given by Equation 107.

DL sin Δ is the projection of the lateral surface of the cylinder as seen from ds. With the symbols defined, the elemental incident flux to the cylinder may be written as

$$dq = \frac{DLSa \cos\beta \cos\alpha \sin\Delta \, ds}{\pi\rho^2} \tag{116}$$

The terms cos α, ds, and ρ^2 are given by Equations 72 through 74, and sin Δ is given by

$$\sin\Lambda = \left\{ 1 - \left[\cos\delta \cos\gamma + \sin\delta \sin\gamma \cos(\phi - \phi_c) \right]^2 \right\}^{1/2} \tag{117}$$

where cos δ and sin δ are as defined in Equations 79 and 80.

The angle ϕ_c is one of the attitude parameters, the angle of rotation of the cylinder axis about a vertical to the cylinler. ϕ_c is 0 when the axis lies in the plane containing the earth-cylinder vector and the earth-sun vector. The angle γ is the other attitude parameter, the angle between the vertical to the cylinder and the axis of the cylinder.

The value of cos β may be expressed as given in Equation 110, where θ_S is as defined for albedo to a sphere and may be referred to as the zenith distance from the vehicle to the sun, and θ and ϕ are the variables of integration. After substitution and integration with respect to θ and ϕ, q can be obtained.

Again as in the case of a sphere, two cases should be considered: when the entire area of the planet seen from the cylinder is sunlit, and when the area is only partially sunlit, that is, when the satellite can see a portion of the terminator, in which case a variable limit for ϕ is required and is again given by Equation 114. If symmetry about the plane containing the earth-vehicle vector and the earth sun vector is recognized, total reflected solar heat flux from the planet incident on the cylindrical surface can be written for $\theta_S < \pi/2$ as

$$q = \frac{2DLSaR^2}{\pi}\left[\int_0^{\frac{\pi}{2}-\theta_S} \int_0^{\pi} \frac{A \cdot B \cdot C \cdot D}{E^2} \, d\theta d\phi + \int_{\frac{\pi}{2}-\theta_S}^{\theta_o} \int_0^{\frac{\pi}{2}+\sin^{-1}(\mathrm{ctg}\,\theta_S \,\mathrm{ctg}\,\theta)} \frac{A \cdot B \cdot C \cdot D}{E^2} \, d\theta d\phi \right] \tag{118}$$

where

$$A = H\cos\theta - R$$

$$B = \cos\theta_S \cos\theta + \sin\theta_S \sin\theta \cos\phi$$

$$C = \sin\theta$$

$$D = \sqrt{R^2 + H^2 - 2RH\sin^2\gamma\cos\theta - H^2\cos^2\gamma - R^2\cos^2\gamma\cos\theta - 2RH\cos\gamma\sin\gamma\sin\theta\cos(\phi - \phi_c) + 2R^2\cos\gamma\sin\gamma\sin\theta\cos\theta\cos(\phi - \phi_c) - R^2\sin^2\gamma\sin^2\theta\cos^2(\phi - \phi_c)}$$

$$E = R^2 + H^2 - 2RH\cos\theta$$

When

$$\frac{\pi}{2} \leq \theta_S \leq \frac{\pi}{2} + \theta_o$$

the integration limits change and integration occurs over only one zone with limits given as

$$q = \frac{2DLSaR^2}{\pi} \int_{\theta_o - \frac{\pi}{2}}^{\theta_o} \int_{o}^{\frac{\pi}{2} + \sin^{-1}(\mathrm{ctg}\,\theta_S \,\mathrm{ctg}\,\theta)} \frac{A \cdot B \cdot C \cdot D}{E^2}\, d\theta\, d\phi \qquad (119)$$

The heat flux integrals (Equations 118 and 119) have been integrated numerically on an IBM 704 computer. The results are tabulated in Appendix B as the geometric factor (q/DLSa) as a function of altitude with zenith distance θ_S, angle between the vertical to the cylinder and the cylinder axis γ and angle of rotation ϕ_c of the axis of the cylinder about the vertical to the cylinder referenced to the plane containing the vertical and the earth-sun vector (Figure 44). The values considered for the attitude parameters were γ = 0, 30, 60, and 90 degrees and simultaneously ϕ_c = 0, 30, 60, 90, 120, 150, and 180 degrees. The parameter γ need only be considered to 90 degrees as the cylinder has end-for-end symmetry.

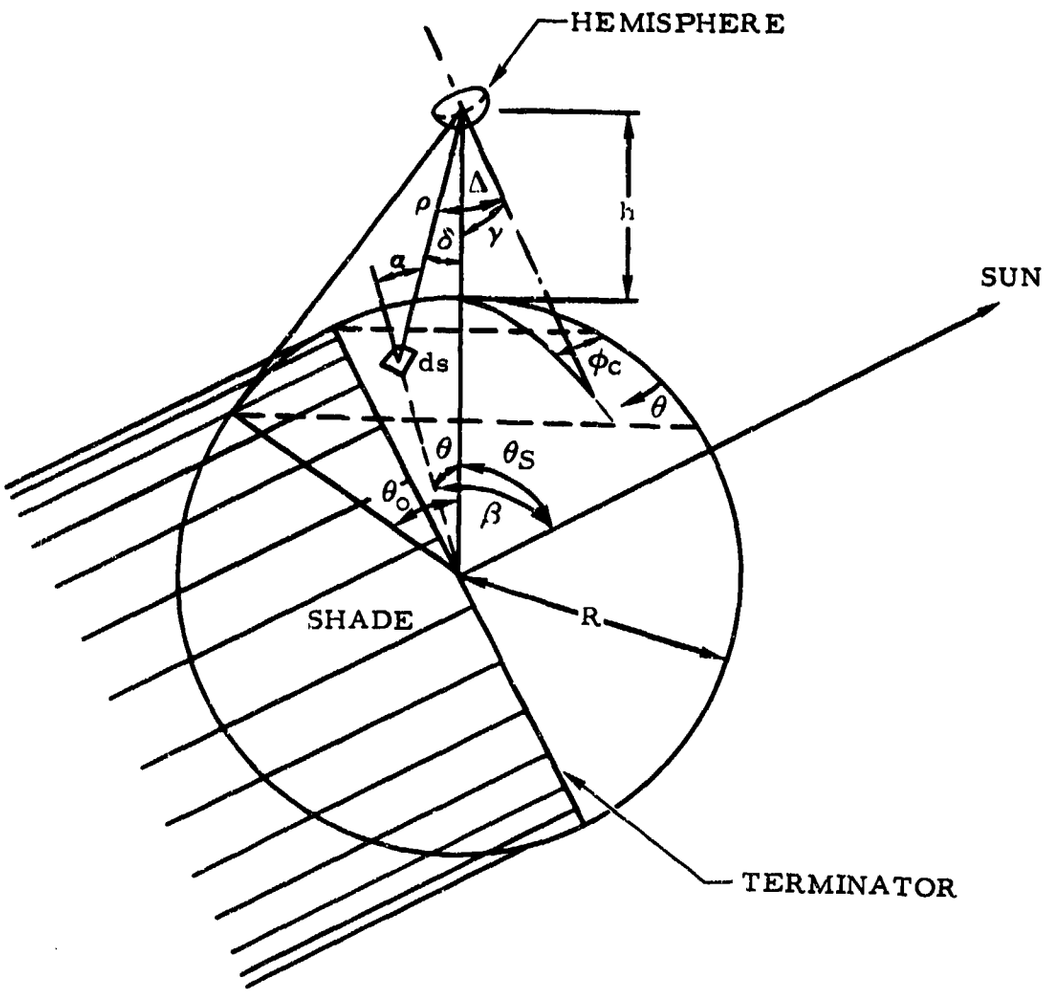

Figure 45. Geometry of Planetary Reflected Solar Radiation to Hemisphere

Reflected Solar to Hemisphere

The solution for albedo to a hemisphere is very similar to that for a cylinder, the two major differences being that the expression for the projected area of the hemisphere with respect to ds is somewhat different and that values of γ from 0 to 180 degrees must be considered because end-for-end symmetry is not present. The general configuration for albedo to a hemisphere is shown in Figure 45.

The radiant heat flux incident to the hemispherical surface of radius r due to reflected solar energy from the planet surface ds is

$$dq = \frac{\frac{1}{2}\,\pi^2\,(1+\cos\Delta)\,E_\alpha\,ds}{\rho^2} \tag{120}$$

where $1/2\,\pi r^2(1+\cos\Delta)$ is the projected area of the hemispherical surface as seen from ds and the remaining symbols are as defined for a cylinder. Thus, the elemental incident heat flux to a hemisphere may be written as

$$dq = \frac{\frac{1}{2}\pi r^2\,Sa\cos\beta\cos\alpha(1+\cos\Delta)\,ds}{\pi\rho^2} \tag{121}$$

The term $\cos\Delta$ is given by

$$\cos\Delta = \cos\gamma\cos\delta + \sin\gamma\sin\delta\cos(\phi - \phi_c) \tag{122}$$

with the terms defined as for the cylinder solution. Again, $\cos\beta$ is given by Equation 109, and $\cos\alpha$, ds, and ρ^2 are given by Equations 72 through 74.

The integration techniques and limits are as defined for albedo to a cylinder. The total reflected solar heat flux from the planet incident on the hemispherical surface can be written for $\theta_S < \pi/2$ as

$$q = r^2\,Sa\,R^2\left[\int_0^{\frac{\pi}{2}-\theta_S}\int_0^{\pi}\frac{A\cdot B\cdot C\,(\sqrt{E}+F)}{E^2}\,d\theta\,d\phi\right. \tag{123}$$

$$\left. + \int_{\frac{\pi}{2}-\theta_S}^{\theta_o}\int_0^{\frac{\pi}{2}+\sin^{-1}(\mathrm{ctg}\,\theta_S\,\mathrm{ctg}\,\theta)}\frac{A\cdot B\cdot C\,(\sqrt{E}+F)}{E^2}\,d\theta\,d\phi\right]$$

where

$$A = H\cos\theta - R$$

$$B = \cos\theta_S\cos\theta + \sin\theta_S\sin\theta\cos\phi$$

$$C = \sin\theta$$

$$E = R^2 + H^2 - 2RH\cos\theta$$

$$F = H\cos\gamma - R\cos\gamma\cos\theta + R\sin\gamma\sin\theta\cos(\phi - \phi_c)$$

When

$$\frac{\pi}{2} \leq \theta_S \leq \frac{\pi}{2} + \theta_o$$

the heat flux to the hemisphere is

$$q = r^2 Sa R^2 \int_{\theta_S - \frac{\pi}{2}}^{\theta_o} \int_o^{\frac{\pi}{2} + \sin^{-1}(\text{ctg}\,\theta_S\ \text{ctg}\,\theta)} \frac{A \cdot B \cdot C\ (\sqrt{E} + F)}{E^2}\, d\theta\, d\phi \qquad (124)$$

The heat flux integrals (Equations 123 and 124) have been integrated numerically on an IBM 7090 computer. The results are displayed as the geometric factor $q/\pi r^2$ Sa as a function of altitude with the three angles θ_S, γ, and ϕ_c as parameters. This tabular presentation is given in Appendix B. The values considered for the attitude parameters were 0, 30, 60, 90, 120, 150, and 180 degrees for γ and simultaneously 0, 30, 60, 90, 120, 150, and 180 degrees for ϕ_c.

Reflected Solar to Flat Plate

The most general configuration used in considering the albedo heat flux incident on one side of a flat plate in space is given in Figure 46. Development of the integral takes the same form as that for a cylinder or a hemisphere. The heat flux incident to a flat plate of area P from the element of planet surface ds is

$$dq = \frac{P \cos\Delta E_\alpha\, ds}{\rho^2} \qquad (125)$$

where P cos Δ is the projected area of the plate as seen from ds. Since the remaining symbols to be defined are identical to those for a cylinder, Equation 125 may be written as

$$dq = \frac{P Sa \cos\beta \cos\alpha \cos\Delta\, ds}{\pi\rho^2} \qquad (126)$$

wherein cos γ, ds, and ρ^2 are given by Equations 72 through 74, and cos β is given by Equation 109.

The term cos Δ is given by Equation 122, with the terms defined as for the cylinder solution. The total reflected solar heat flux from the planet incident on the flat plate can be written as an indefinite integral.

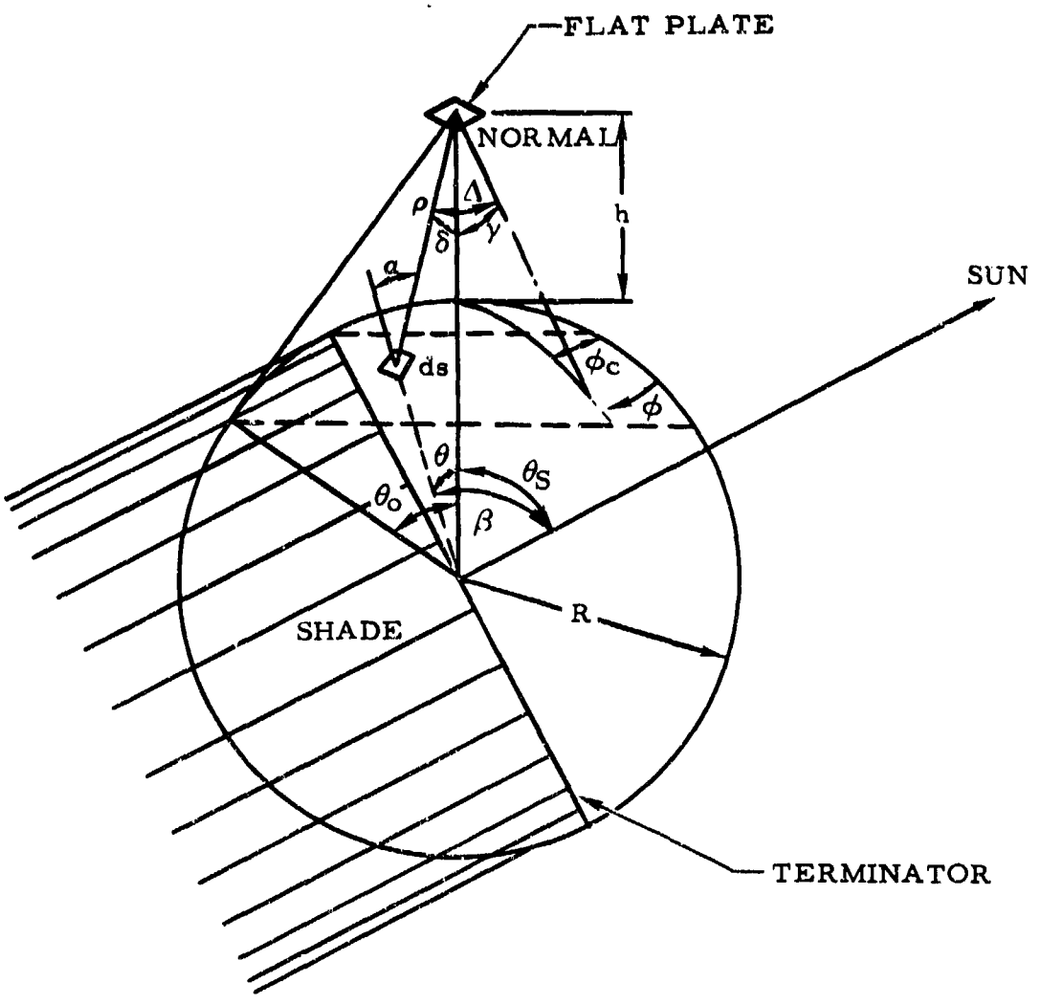

Figure 46. Geometry of Planetary Reflected Solar Radiation to Flat Plate

$$q = \frac{P S a R^2}{\pi} \int_{\theta} \int_{\phi} \frac{A \cdot B \cdot C\,(G + F)}{E^2}\, d\theta\, d\phi \qquad (127)$$

where A, B, C, and E are as defined for a cylinder, and

$$F = R \sin\gamma \sin\theta \cos(\phi - \phi_c)$$

$$G = \cos\gamma\,(H - R\cos\theta)$$

The problem of limits for the integration of Equation 127 is severely complicated in that the plane of the flat plate may cut off portions of the sunlit area of the planet.

The limits considered are discussed with respect to the computer solution of Equation 127. Two major conditions are considered: (1) if the flat plate sees the sunlit surface of the planet with the plane in which it lies not cutting any portion of the sunlet area, and (2) if the plane of the flat plate cuts the sunlit area. If the plane does not cut the sunlit area, two conditions may be involved. Either the plane sees a full sunlit zone (i. e., does not see the terminator), in which case Equation 127 becomes

$$q = \frac{2PSaR^2}{\pi} \int_0^{\theta_o} \int_0^{\pi} \frac{A \cdot B \cdot C\,(G + F)}{E^2}\, d\theta\, d\phi \qquad (128)$$

or the plane sees part of the terminator, in which case, when $\theta_s < \pi/2$, Equation 128 becomes

$$q = \frac{2PSaR^2}{\pi} \left[\int_0^{\frac{\pi}{2} - \theta_S} \int_0^{\pi} \frac{A \cdot B \cdot C\,(G + F)}{E^2}\, d\theta\, d\phi \right]$$

$$+ \frac{2PSaR^2}{\pi} \left[\int_{\frac{\pi}{2} - \theta_S}^{\theta_o} \int_0^{\frac{\pi}{2} + \sin^{-1}(\operatorname{ctg}\theta_S \operatorname{ctg}\theta)} \frac{A \cdot B \cdot C\,(G + F)}{E^2}\, d\theta\, d\phi \right] \qquad (129)$$

when

$$\frac{\pi}{2} \leq \theta_S \leq \frac{\pi}{2} + \theta_o$$

then

$$q = \frac{2PSaR^2}{\pi} \left[\int_{\theta_S - \frac{\pi}{2}}^{\theta_o} \int_0^{\frac{\pi}{2} + \sin^{-1}(\operatorname{ctg}\theta_S \operatorname{ctg}\theta)} \frac{A \cdot B \cdot C\,(G + F)}{E^2}\, d\theta\, d\phi \right] \qquad (130)$$

The problem becomes more complex when the plane cuts the sunlit area because the limits of θ and ϕ are determined by more complex equations. If the plane cuts the sunlit area but the plane does not see the terminator, Equation 127 becomes for $\theta_S < \pi/2$ and $\gamma < \pi/2$,

$$q = \frac{PSaR^2}{\pi}\left[\int_0^{\theta_1}\int_{-\pi}^{\pi}\frac{A\cdot B\cdot C\,(G+F)}{E^2}\,d\theta\,d\phi\right] \tag{131}$$

$$+\frac{PSaR^2}{\pi}\left[\int_{\theta_1}^{\theta_o}\int_{-\left[\frac{\pi}{2}-\phi_c+\sin^{-1}\left\{\frac{\tan\left[\cos^{-1}\left(\frac{R\sin\theta}{\sqrt{R^2+H^2-2RH\cos\theta}}\right)\right]}{\tan\gamma}\right\}\right]}^{\frac{\pi}{2}+\phi_c+\sin^{-1}\left\{\frac{\tan\left[\cos^{-1}\left(\frac{R\sin\theta}{\sqrt{R^2+H^2-2RH\cos\theta}}\right)\right]}{\tan\gamma}\right\}}\frac{A\cdot B\cdot C\,(G+F)}{E^2}\,d\theta\,d\phi\right]$$

where θ_1 was determined by the Newton-Raphson iteration procedure for determining roots from

$$\frac{\pi}{2} = \sin^{-1}\left\{\frac{\tan\left[\cos^{-1}\left(\frac{R\sin\theta_1}{\sqrt{R^2+H^2-2RH\cos\theta_1}}\right)\right]}{\tan\gamma}\right\} \tag{132}$$

For $\pi/2 < \gamma < \pi/2 + \theta_o$, q is given by Equation 131 with the first integral term eliminated. It should be noted that for $\gamma > \pi/2 + \theta_o$, q is equal to 0, (i. e., the plane surface does not see the earth).

A number of forms of Equation 127 are possible if the plane of the flat plate cuts the sunlit area and also sees a portion of the terminator. For the case where the plane of the flat plate for $\gamma < \pi/2$ intersects the terminator in two points, (ϕ_3, θ_3) and (ϕ_4, θ_4), and θ_3 and $\theta_4 > \theta_o$, $\phi_3 > \phi_4$, and $\phi_4 < \pi$, Equation 127 becomes

$$q = \frac{PSaR^2}{\pi}\left[\int_0^{\theta_1}\int_{-\pi}^{\pi}\frac{A\cdot B\cdot C\,(G+F)}{E^2}\,d\theta\,d\phi\right. \tag{133}$$

$$\left. + \int_{\theta_1}^{\theta_4}\int_{-\left[\frac{\pi}{2}-\phi_c+\sin^{-1}\left\{\frac{\tan\left[\cos^{-1}\left(\frac{R\sin\theta}{\sqrt{R^2+H^2-2RH\cos\theta}}\right)\right]}{\tan\gamma}\right\}\right]}^{\frac{\pi}{2}+\phi_c+\sin^{-1}\left\{\frac{\tan\left[\cos^{-1}\left(\frac{R\sin\theta}{\sqrt{R^2+H^2-2RH\cos\theta}}\right)\right]}{\tan\gamma}\right\}}\frac{A\cdot B\cdot C\,(G+F)}{E^2}\,d\theta\,d\phi\right]$$

$$+\frac{PSaR^2}{\pi}\left[\int_{\theta_4}^{\theta_3}\int_{-\left[\frac{\pi}{2}-\phi_c+\sin^{-1}\left\{\frac{\tan\left[\cos^{-1}\left(\frac{R\sin\theta}{\sqrt{R^2+H^2-2RH\cos\theta}}\right)\right]}{\tan\gamma}\right\}\right]}^{\frac{\pi}{2}+\sin^{-1}(\mathrm{ctg}\,\theta_S\,\mathrm{ctg}\,\theta)}\frac{A\cdot B\cdot C\,(G+F)}{E^2}\,d\theta\,d\phi\right.$$

$$\left. + \int_{\theta_3}^{\theta_o}\int_{-\left[\frac{\pi}{2}+\sin^{-1}(\mathrm{ctg}\,\theta_S\,\mathrm{ctg}\,\theta)\right]}^{\frac{\pi}{2}+\sin^{-1}(\mathrm{ctg}\,\theta_S\,\mathrm{ctg}\,\theta)}\frac{A\cdot B\cdot C\,(G+F)}{E^2}\,d\theta\,d\phi\right]$$

where θ_4 and θ_3 were determined by the Newton-Raphson method from Equations 134 and 135, respectively.

$$\sin^{-1}(\mathrm{ctg}\,\theta_S\,\mathrm{ctg}\,\theta_4) = \phi_c + \sin^{-1}\left\{\frac{\tan\left[\cos^{-1}\left(\frac{R\sin\theta_4}{\sqrt{R^2+H^2-2RH\cos\theta_4}}\right)\right]}{\tan\gamma}\right\} \tag{134}$$

$$-\sin^{-1}(\operatorname{ctg}\theta_S \operatorname{ctg}\theta_3) = \phi_c - \sin^{-1}\left\{\frac{\tan\left[\cos^{-1}\left(\frac{R\sin\theta_3}{\sqrt{R^2+H^2-2RH\cos\theta_3}}\right)\right]}{\tan\gamma}\right\} \tag{135}$$

For $\phi_4 > \pi$, two conditions may be considered. If $\pi/2 - \theta_S < \theta_1$, Equation 127 becomes

$$q = \frac{PSaR^2}{\pi}\left[\int_0^{\frac{\pi}{2}-\theta_S}\int_{-\pi}^{\pi}\frac{A\cdot B\cdot C\,(G+F)}{E^2}\,d\theta\,d\phi\right. \tag{136}$$

$$\left. + \int_{\frac{\pi}{2}-\theta_S}^{\theta_1}\int_{-\left[\frac{\pi}{2}+\sin^{-1}(\operatorname{ctg}\theta_S\operatorname{ctg}\theta)\right]}^{\frac{\pi}{2}+\sin^{-1}(\operatorname{ctg}\theta_S\operatorname{ctg}\theta)}\frac{A\cdot B\cdot C\,(G+F)}{E^2}\,d\theta\,d\phi\right]$$

$$+ \frac{PSaR^2}{\pi}\left[\int_{\theta_1}^{\theta_4}\int_{-\left[\frac{\pi}{2}+\sin^{-1}(\operatorname{ctg}\theta_S\operatorname{ctg}\theta)\right]}^{\frac{\pi}{2}+\phi_c+\sin^{-1}\left\{\frac{\tan\left[\cos^{-1}\left(\frac{R\sin\theta}{\sqrt{R^2+H^2-2RH\cos\theta}}\right)\right]}{\tan\gamma}\right\}}\frac{A\cdot B\cdot C\,(G+F)}{E^2}\,d\theta\,d\phi\right.$$

$$\left. + \int_{\theta_1}^{\theta_3}\int_{-\left[\frac{\pi}{2}-\phi_c+\sin^{-1}\left\{\frac{\tan\left[\cos^{-1}\left(\frac{R\sin\theta}{\sqrt{R^2+H^2-2RH\cos\theta}}\right)\right]}{\tan\gamma}\right\}\right]}^{\frac{\pi}{2}+\sin^{-1}(\operatorname{ctg}\theta_S\operatorname{ctg}\theta)}\frac{A\cdot B\cdot C\,(G+F)}{E^2}\,d\theta\,d\phi\right]$$

$$+ \quad \frac{PsaR^2}{\pi} \left[\int_{\theta_3}^{\theta_o} \int_{-\left[\frac{\pi}{2} + \sin^{-1}(\operatorname{ctg}\theta_S \operatorname{ctg}\theta)\right]^1}^{\frac{\pi}{2} + \sin^{-1}(\operatorname{ctg}\theta_S \operatorname{ctg}\theta)} \frac{A \cdot B \cdot C\,(G+F)}{E^2}\, d\theta\, d\phi \right]$$

θ_3 is determined by Equation 135, and θ_4 is determined by

$$\pi + \sin^{-1}\left(\operatorname{ctg}\theta_S \operatorname{ctg}\theta_4\right) = \phi_c + \sin^{-1}\left\{\frac{\tan\left[\cos^{-1}\left(\frac{R\sin\theta_4}{\sqrt{R^2+H^2-2RH\cos\theta_4}}\right)\right]}{\tan\gamma}\right\} \tag{137}$$

If $\pi/2 - \theta_S > \theta_1$, the limits change somewhat.

$$q = \frac{PSaR^2}{\pi} \left[\int_o^{\theta_1} \int_{-\pi}^{\pi} \frac{A \cdot B \cdot C\,(G+F)}{E^2}\, d\theta\, d\phi \right. \tag{138}$$

$$\left. + \int_{\theta_1}^{\frac{\pi}{2} - \theta_S} \int_{-\left[\frac{\pi}{2} - \phi_c + \sin^{-1}\left\{\frac{\tan\left[\cos^{-1}\left(\frac{R\sin\theta}{\sqrt{R^2+H^2-2RH\cos\theta}}\right)\right]}{\tan\gamma}\right\}\right]}^{\frac{\pi}{2} + \phi_c + \sin^{-1}\left\{\frac{\tan\left[\cos^{-1}\left(\frac{R\sin\theta}{\sqrt{R^2+H^2-2RH\cos\theta}}\right)\right]}{\tan\gamma}\right\}} \frac{A \cdot B \cdot C\,(G+F)}{E^2}\, d\theta\, d\phi \right]$$

$$+ \quad \frac{PSaR^2}{\pi} \left[\int_{\frac{\pi}{2} - \theta_S}^{\theta_4} \int_{-\left[\frac{\pi}{2} + \sin^{-1}(\operatorname{ctg}\theta_S \operatorname{ctg}\theta)\right]}^{\frac{\pi}{2} + \phi_c + \sin^{-1}\left\{\frac{\tan\left[\cos^{-1}\left(\frac{R\sin\theta}{\sqrt{R^2+H^2-2RH\cos\theta}}\right)\right]}{\tan\gamma}\right\}} \frac{A \cdot B \cdot C\,(G+F)}{E^2}\, d\theta\, d\phi + \right.$$

$$\int_{\frac{\pi}{2}-\theta_S}^{\theta_3} \int_{-\left[\frac{\pi}{2}-\phi_c+\sin^{-1}\left\{\frac{\tan\left[\cos^{-1}\left(\frac{R\sin\theta}{\sqrt{R^2+H^2-2RH\cos\theta}}\right)\right]}{\tan\gamma}\right\}\right]}^{\frac{\pi}{2}+\sin^{-1}(\operatorname{ctg}\theta_S\operatorname{ctg}\theta)} \frac{A\cdot B\cdot C\,(G+F)}{E^2}\,d\theta\,d\phi$$

$$+\frac{PSaR^2}{\pi}\left[\int_{\theta_3}^{\theta_o} \int_{-\left[\frac{\pi}{2}+\sin^{-1}(\operatorname{ctg}\theta_S\operatorname{ctg}\theta)\right]}^{\frac{\pi}{2}+\sin^{-1}(\operatorname{ctg}\theta_S\operatorname{ctg}\theta)} \frac{A\cdot B\cdot C\,(G+F)}{E^2}\,d\theta\,d\phi\right]$$

For the case where the plane of the flat plate intersects the terminator in one point, (ϕ_4, θ_4), and the circle defined by $\theta = \theta_o$ in one point, (ϕ_3, θ_o), and $\phi_4 < \pi$, Equation 127 becomes

$$q = \frac{PSaR^2}{\pi}\left[\int_{o}^{\theta_1} \int_{-\pi}^{\pi} \frac{A\cdot B\cdot C\,(G+F)}{E^2}\,d\theta\,d\phi\right. \tag{139}$$

$$\left. +\int_{\theta_1}^{\theta_4} \int_{-\left[\frac{\pi}{2}-\phi_c+\sin^{-1}\left\{\frac{\tan\left[\cos^{-1}\left(\frac{R\sin\theta}{\sqrt{R^2+H^2-2RH\cos\theta}}\right)\right]}{\tan\gamma}\right\}\right]}^{\frac{\pi}{2}+\phi_c+\sin^{-1}\left\{\frac{\tan\left[\cos^{-1}\left(\frac{R\sin\theta}{\sqrt{R^2+H^2-2RH\cos\theta}}\right)\right]}{\tan\gamma}\right\}} \frac{A\cdot B\cdot C\,(G+F)}{E^2}\,d\theta\,d\phi\right]$$

$$+ \frac{PSaR^2}{\pi}\left[\int_{\theta_4}^{\theta_o}\int_{-\left[\frac{\pi}{2} - \phi_c + \sin^{-1}\left\{\frac{\tan\left[\cos^{-1}\left(\frac{R\sin\theta}{\sqrt{R^2+H^2-2RH\cos\theta}}\right)\right]}{\tan\gamma}\right\}\right]}^{\frac{\pi}{2} + \sin^{-1}(\mathrm{ctg}\,\theta_S\,\mathrm{ctg}\,\theta)} \frac{A\cdot B\cdot C\,(G+F)}{E^2}\,d\theta\,d\phi\right]$$

where θ_4 is again determined by Equation 134.

For $\phi_4 > \pi$, two conditions are again considered. If $\pi/2 - \theta_S < \theta_1$, Equation 127 becomes the same as Equation 136 except that the last term is eliminated and the upper limit, θ_3, for the fourth term is replaced by θ_o. If $\pi/2 - \theta_S > \theta_1$, Equation 127 becomes the same as Equation 138 except that the last term is eliminated and the upper limit, θ_3, for the fourth term is replaced by θ_o.

For the case where the plane of the flat plate intersects the circle defined by $\theta = \theta_o$ in two points, (ϕ_4, θ_o) and (ϕ_3, θ_o), for $\pi/2 - \theta_S < \theta_1$, Equation 127 becomes the same as Equation 136 with the last term eliminated and the upper limits of the third and fourth terms replaced by θ_o. For $\pi/2 - \theta_S > \theta_1$, Equation 127 becomes the same as Equation 138 with the last term eliminated and the upper limits of the third and fourth terms replaced by θ_o.

For $\gamma > \pi/2$, a similar step procedure in the integration of Equation 127 must be used which follows the same method set forth for $\gamma < \pi/2$. This will not be done here, however.

Some difficulty is encountered in determining when the plane of the flat plate cuts the sunlit region in the vicinity of the terminator. To determine whether intersection of the plane and terminator occurs for a given ϕ_c and h, the γ_2 for the plane with $\phi_c = o$ to be tangent to the terminator was calculated as

$$\gamma_2 = \cos^{-1}\left(\frac{R\sin\theta_2}{\sqrt{R^2+H^2-2RH\cos\theta_2}}\right) \qquad (140)$$

where

$$\theta_2 = \frac{\pi}{2} - \theta_S$$

The maximum possible γ_o without intersection with the sunlit area was then calculated as

$$\gamma_o = \theta_o \tag{141}$$

Corresponding to this point is an angle, ϕ_{co}, calculated from

$$\phi_{co} = \frac{\pi}{2} - \sin^{-1} (\text{ctg}\,\theta_S \text{ ctg}\,\theta_o) \tag{142}$$

For a given ϕ_c, the limiting γ_{lim} for intersection of the plane of the flat plate with the terminator was calculated from

$$\gamma_{lim} = \gamma_2 - \left(\frac{\gamma_2 - \gamma_o}{\phi_{co}}\right)\phi_c \tag{143}$$

This is not an exact determination of the γ for tangency of the plane of the plate with the terminator circle; however, the error introduced is small.

The heat flux integrals were integrated numerically on an IBM 7090 computer. The results are presented in Appendix B as the geometric factor (q/PSa) as a function of altitude with the three angles, θ_S, γ, and ϕ_c, as parameters. Each table is for a constant γ and ϕ_c.

The albedo data for a flat plate is also useful in determining albedo to an irregular surface. The irregular surface may be approximated by a series of flat plates and the albedo input is obtained by summing the individual values for each of the flat plates.

DISCUSSION OF ASSUMPTIONS

SIMPLIFIED SPACE RADIATION ANALYSIS

1. It is assumed that all thermal radiation considered in the analysis is in diffuse form except direct solar radiation. Fortunately, most thermal radiation is in diffuse form, which is relatively simple to analyze when compared with specular radiation.

2. It is assumed that direct solar radiation impinges upon the earth and upon the satellite with parallel rays, due to the great distance between the sun and its planets. Almost zero error is introduced into the analysis by this assumption.

3. In all cases, it is assumed that the earth emits as a black body and is in a state of thermal equilibrium (i. e., the planetary emitted energy is equal to the absorbed solar energy). It is also assumed that the earth emission is a constant at any point on its surface and does not vary from day to night. These are reasonable assumptions because little is known of the actual spectral and local variations in the planetary emitted radiation.

4. The earth reflected solar radiation is assumed to follow the cosine law (i. e., it is a maximum at the subsolar point and decreases to zero at the terminator). This assumption greatly simplifies the analysis and is quite accurate except in the region of the terminator, where a slight error is introduced.

5. In all cases, the planetary albedo is assumed to be constant over the surface of the planet, and the planet is assumed to be a diffuse reflector. This is done because of the complications of the problem and because local variations are almost impossible to define.

6. In all cases, conduction and convection between the satellite and its surroundings were neglected. This is reasonable because orbital heights are usually too far above the atmosphere for thermal effects to appear.

7. It is assumed that the absorptivity to direct solar radiation of the vehicle surface is equal to the absorptivity to the earth reflected solar radiation. This is correct if the spectral quality of the

reflected solar energy is the same as for the direct solar energy. It is felt that only a very small error is introduced by this assumption.

8. No transient heat transfer effects are considered in this analysis. Steady-state conditions are assumed for purposes of simplification.

9. An earth-oriented vertical cylinder is the assumed configuration in all cases for purposes of simplification. The ends of the cylinder are ignored in the analysis. The cylinder wall is assumed to be at a uniform temperature, which is correct for a vertical cylinder spinning on its axis or for a cylinder with a shell of very high thermal conductivity.

10. In the discussion on simplified geometry analysis the earth is assumed to be a flat plate. This, in effect, results in the satellite-to-space configuration factor and the satellite-to-earth configuration factor both being equal to 0. 5.

11. In the refined geometry analysis discussion, the earth is assumed to be a sphere. As a result, this analysis is considerably more accurate than the simplified geometry analysis.

IBM 7090 PROGRAM FOR TRANSIENT HEAT TRANSFER ANALYSIS OF ORBITING SPACE VEHICLES

1. It is assumed in this analysis that the earth can be represented gravitationally by the zero-order and second-order spherical harmonics of its potential. The presence of harmonics in the earth's gravitational potential causes periodic and secular variations in several of the orbital elements. Only the secular perturbations which result in regression of the nodes and advance of the perigee position are considered in the analysis. Other periodic changes have negligible effect upon the shadow intersection problem.

2. A rigorous specification of the position at which the satellite enters and exits the earth's true shadow leads to needlessly complicated expressions. For this reason, the following simplifications concerning shadow geometry were assumed:

   a. The earth was assumed spherical with its radius equal to 3960 statute miles.
   b. The earth's shadow was assumed cylindrical and umbral (sun at infinity).
   c. Penumbral effects were ignored.

The error involved is extremely small even when large orbits are considered. For instance, a satellite in a circular orbit with an altitude of 10,000 miles has an orbit period of approximately 560 minutes, with perhaps 50 minutes spent in earth shadow (depending on orbit orientation). By assuming a cylindrical earth shadow and ignoring penumbral effects, the analysis uses an umbral shadow time that is about 50 seconds longer than the true umbral shadow time. This is a negligible error. For a 1000-mile-altitude circular orbit, the negligible error is approximately 18 seconds in an orbit period of 118 minutes. Additionally, it should be mentioned that the assumption of no penumbral effects tends to lessen these errors introduced by the assumption of cylindrical umbral shadow, so that there is almost zero error from a thermal analysis standpoint.

3. It is assumed that all thermal radiation considered in the analysis, except direct solar radiation, is in diffuse form. Fortunately, most thermal radiation is in diffuse form, which is relatively simple to analyze when compared with specular radiation.

4. It is assumed that direct solar radiation impinges upon the earth and upon the satellite with parallel rays, due to the great distance between the sun and its planets. Almost zero error is introduced into the analysis by this assumption.

5. In all cases, it is assumed that the earth emits as a black body and is in a state of thermal equilibrium (i.e., the planetary-emitted energy is equal to the absorbed solar energy). It is also assumed that the earth emission is a constant at any point on its surface and does not vary from day to night. These are reasonable assumptions because little is known of the actual spectral and local variations in the planetary emitted radiation.

6. The earth reflected solar radiation is assumed to follow the cosine law (i.e., it is a maximum at the subsolar point and decreases to zero at the terminator). This assumption greatly simplifies the analysis and is quite accurate except in the region of the terminator, where a slight error is introduced.

7. In all cases, the planetary albedo is assumed to be constant over the surface of the planet, and the planet is assumed to be a diffuse reflector. This is done because of the complications of the problem and because local variations are almost impossible to define.

8. In all cases, conduction and convection between the satellite and its surroundings are neglected. This is reasonable because orbital heights are usually too far above the atmosphere for thermal effects to appear.

9. It is assumed that the absorptivity of the vehicle surface to planetary thermal emission is equal to the emissivity of the vehicle surface. Since the effective temperature of the earth and the temperatures of most vehicle surfaces are nearly the same, this assumption is validated by Kirchhoff's law.

10. Any scattering effects of direct solar radiation upon the satellite due to the earth's atmosphere are ignored. It is felt that this will introduce a negligible error into the analysis.

11. The geometrical configuration factor from the spherical satellite to earth was calculated with the assumption that the satellite is a point source in space. The assumption is valid if the satellite is uniform in temperature; it would be if spinning or if its shell had a very high thermal conductivity.

12. It is assumed that any internally generated heat load is uniformly distributed over the particular vehicle surface specified. Internal heat transfer paths are neglected. This was done in order to simplify the analysis.

SPACE THERMAL ENVIRONMENT STUDY

1. It is assumed that all thermal radiation considered in the analysis, except direct solar radiation, is in diffuse form. Fortunately, most thermal radiation is in diffuse form, which is relatively simple to analyze when compared with specular radiation.

2. It is assumed that direct solar radiation impinges upon the earth and upon the satellite with parallel rays, due to the great distance between the sun and its planets. Almost zero error is introduced into the analysis by this assumption.

3. In all cases, it is assumed that the earth emits as a black body and is in a state of thermal equilibrium (i. e., the planetary emitted energy is equal to the absorbed solar energy). It is also assumed that the earth emission is a constant at any point on its surface and does not vary from day to night. These are reasonable assumptions because little is known of the actual spectral and local variations in the planetary emitted radiation.

4. In all cases, the planetary albedo is assumed to be constant over the surface of the planet, and the planet is assumed to be a diffuse reflector. This is done because of the complications of the problem and because local variations are almost impossible to define.

5. In all cases, conduction and convection between the satellite and its surroundings were neglected. This is reasonable because orbital heights are usually too far above the atmosphere for thermal effects to appear.

Section VI

TECHNIQUES FOR RADIATION HEAT TRANSFER PROBLEM SOLUTION

GENERAL ANALOG HEAT TRANSFER ANALYSIS METHODS

NOMENCLATURE

A	Area, sq ft
C_E	Electrical capacitance
C_T	Thermal conductance, Btu/(hr)(°F)
c_p	Specific heat, Btu/(lb)(°F)
F	Configuration factor
f	Interchange factor
h_c	Convection heat transfer coefficient, Btu/(hr)(sq ft)(°F)
h_r	Radiation heat transfer coefficient, Btu/(hr)(sq ft)(°F)
I	Current flow, amp
k	Thermal conductivity, Btu/(hr)(sq ft)(°F/ft)
L	length, ft
q	Heat flow, Btu/hr
R_E	Electrical resistance, ohms
R_T	Thermal resistance, hr(°F)/Btu
t	Temperature, °F
Δt	Temperature difference at time θ
Δt_o	Temperature difference at time 0
V	Voltage potential
V_o	Voltage potential at time 0
θ	Time, hr
σ	Stefan-Boltzmann constant = 0.1713×10^{-8} Btu/(hr)(sq ft)($°R^4$)
ω	Mass, lb

ELECTRIC CIRCUIT ANALOGY

The basic equations governing the flow of electricity are similar to those governing heat flow; therefore, a close analogy exists between the concepts of an electrical circuit and a "thermal circuit." In complicated heat transfer problems it is often necessary to rely upon this analogy to arrive at the solution.

In the thermal circuit, temperature difference is considered analogous to voltage potential and heat flow is considered analogous to current flow. Thus, the analogous equations

$$I = \frac{\Delta V}{R_E} \quad \text{(amp)} \tag{144}$$

$$q = \frac{\Delta t}{R_T} \quad \text{(Btu/hr)} \tag{145}$$

Thermal resistance R_T is evaluated with respect to the mode of heat transfer

$$R_T = \frac{L}{kA} \quad \text{for conduction} \tag{146}$$

$$R_T = \frac{1}{h_c A} \quad \text{for convection} \tag{147}$$

$$R_T = \frac{1}{h_r A} \quad \text{for radiation} \tag{148}$$

where

$$h_r = \sigma f(T_1^2 + T_2^2)(T_1 + T_2)$$

It is often convenient to use the concept of thermal conductance instead of thermal resistance. Conductance is merely the reciprocal of resistance. Thus

$$C_T = \frac{kA}{L} \quad \text{for conduction} \tag{149}$$

$$C_T = h_c A \quad \text{for convection} \tag{150}$$

$$C_T = h_r A \quad \text{for radiation} \tag{151}$$

STEADY-STATE AND TRANSIENT PROBLEM SOLUTION

An example of a simple steady-state heat transfer problem utilizing the network method of solution is an insulated round wire carrying an electrical current. The heat generated inside the wire is i^2R watts, which must be dissipated by conduction through the insulation and by

convection and radiation to the environment. The temperature of the wire t_w and the ambient temperature t_a are known. The problem is to determine the amount of heat dissipated and the temperature of the surface of the insulation t_s (Figure 47). It is convenient to combine R_C and R_R into a single resistance as shown in Figure 48.

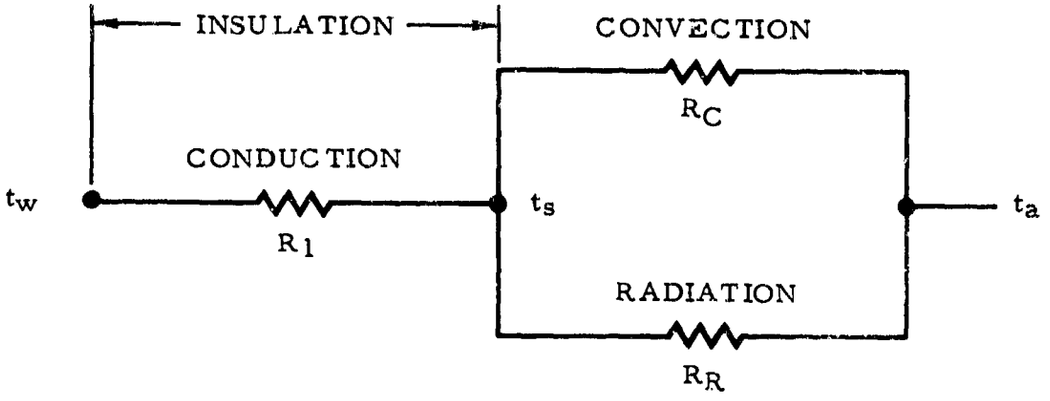

Figure 47. Thermal Network for Insulated Wire

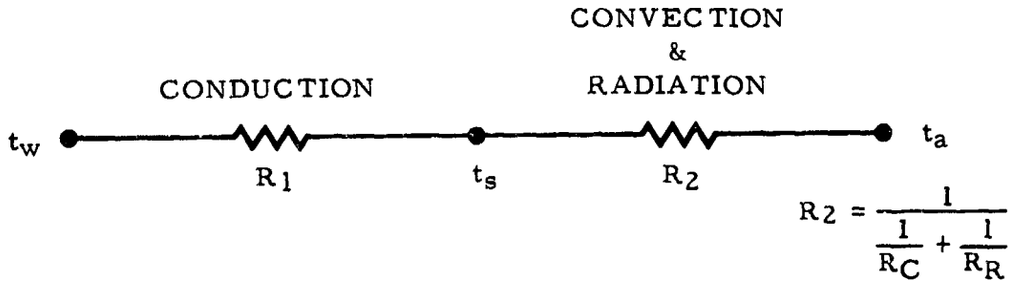

Figure 48. Simplified Thermal Network for Insulated Wire

The total heat loss is given by

$$q = \frac{t_w - t_a}{R_1 + R_2} \tag{152}$$

and the surface temperature of the insulation is given by

$$t_s = \frac{C_1 t_w + C_2 t_a}{C_1 + C_2} \tag{153}$$

It will be noted that the discussion has been limited to steady-state conditions. However, it is often required to analyze heat transfer problems on a transient basis (i.e., temperature versus time). In this case, the effect of heat capacity must be included. The analogous equations for transient conditions are

$$V = V_o e^{-\theta/R_E C_E} \tag{154}$$

$$\Delta t = \Delta t_o e^{-\theta/R_T(\omega c_p)} \tag{155}$$

where

Δt_o = Temperature difference at time 0 = $t_a - t_o$

Δt = Temperature difference at time θ = $t_a - t_\theta$

It is evident that the term ωc_p is the thermal capacitance. The thermal circuit for a single node, single resistor transient problem (represented in Equation 155) is shown in Figure 49.

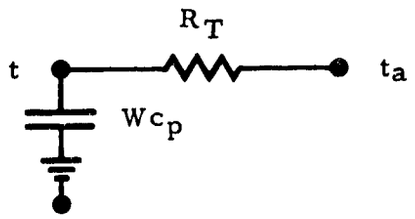

Figure 49. Thermal Network for Single Node, Single Resistor Transient Problem

Multiple node transient heat transfer problems are handled by connecting a thermal capacitance between each node (temperature) and ground. This type of circuit is difficult to solve by hand, and usually requires the use of an analog or digital computer. The network for the temperature distribution versus time in a slab might appear as shown in Figure 50.

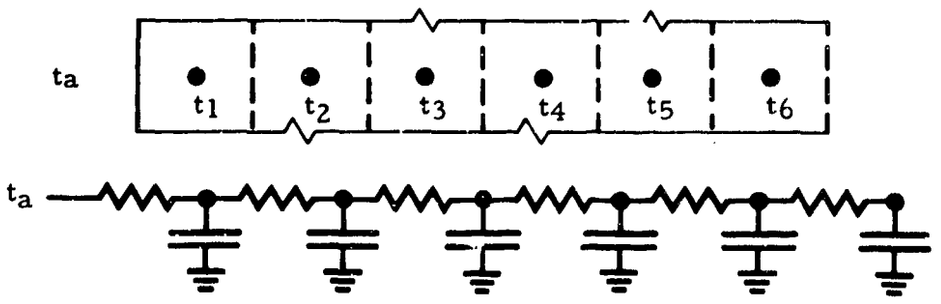

Figure 50. Thermal Network for Temperature Distribution Versus Time in Slab

RADIATION HEAT TRANSFER ANALYSIS METHODS

NOMENCLATURE

A	Area, sq ft
E	Black body emissivity power, Btu/(hr)(sq ft)
F	Configuration factor
f	Interchange factor
G	Sum of all incident radiation, Btu/(hr)(sq ft)
h_r	Radiation heat transfer coefficient, Btu/(hr)(sq ft)(° F)
J	Radiosity of surface, Btu/(hr)(sq ft)
q	Heat flow, Btu/hr
r	Reflectivity
ϵ	Emissivity

RADIOSITY ANALOG METHOD

Problems concerning radiation heat transfer involve proper accounting of all interreflections between the various objects, shields, and surfaces being investigated. This can be achieved very satisfactorily by utilizing the radiosity analog network method as developed by A. K. Oppenheim of the University of California (Reference 16). The significance of this technique becomes apparent when interreflections with multiple surfaces are considered. Other methods of analysis, at best, can only approximate interreflections for most cases. The radiosity method presents an analytically exact solution, without need for such items as "modified" configuration factors.

The radiosity method is normally restricted to problems concerning gray bodies; however, problems concerning real bodies can be analyzed if the additional effort is warranted. It should be noted, however, that the analysis is limited to diffuse emission and reflection, but radiation from most surfaces is fortunately in diffuse form.

In describing this technique, it is important to define the radiosity of a surface J. Radiosity is the sum of all the emitted, reflected, and transmitted radiant energy streaming away from a surface. For a gray opaque surface, radiosity is the sum of the emitted and reflected radiation and is given by

$$J = rG + \epsilon E \tag{156}$$

where

$$E = \sigma T^4$$

Therefore

$$G = \frac{J - \epsilon E}{r} \tag{157}$$

Also

$$q_{net} = A(J - G) \tag{158}$$

Substituting

$$\frac{q_{net}}{A} = J - \frac{J - \epsilon E}{r} = J - \frac{J}{r} + \frac{\epsilon}{r} E$$

$$= \frac{rJ - J}{r} + \frac{\epsilon}{r} E$$

$$= \frac{(r - 1) J}{r} + \frac{\epsilon}{r} E$$

$$= \frac{\epsilon (E - J)}{r}$$

$$= \left(\frac{\epsilon}{1 - \epsilon}\right) (E - J)$$

Therefore

$$q_{net} = \left(\frac{\epsilon A}{1 - \epsilon}\right)(E - J) \tag{159}$$

Thus, the net radiation leaving or entering a surface is analogous to the current flow when a potential of E - J is applied across a conductance of $\epsilon A/(1 - \epsilon)$.

Furthermore, the direct radiation exchange between any two surfaces A_1 and A_2 can be expressed as

$$q_{12} = (FA)_{12} J_1 - (FA)_{21} J_2 = (FA)_{12} (J_1 - J_2) \tag{160}$$

It follows, then, that the net radiation exchange between a surface A_i and its surroundings, consisting of n surfaces, is the total energy impinging on A_i minus the total energy leaving A_i, or

$$q_{i(net)} = \sum_{k=1}^{n} (FA)_{ik} (J_k - J_i) \tag{161}$$

Equations 159 and 161 form the basis for a network completely describing radiation exchange between any number of surfaces. Figure 51 is an example for a four-sided enclosure.

It is often convenient, especially with transient radiation problems and combination radiation-convection-conduction problems, to use a conventional analog network, thus eliminating the floating potential nodes J. With this approach it is still possible to account for all the interreflections by using an equivalent conductance (fA) which is readily obtained from the radiosity network (Reference 16).

Briefly, it can be stated that the equivalent conductance $f_{1i}A_1$ between any two potential nodes 1 and i is equal to the current flowing into node i when it is grounded and short-circuited with all the remaining potential nodes, with the exception of node 1 on which a potential of unity is imposed. As an example, suppose it is desired to represent the four-sided enclosure of Figure 51 with a conventional network. Note that

$$h_{r12} A_1 = \sigma (fA)_{12} (T_1^2 + T_2^2)(T_1 + T_2) \tag{162}$$

To determine $(fA)_{12}$, for instance, it would be necessary to use the radiosity network of Figure 51, setting E_1 equal to 1.0 and E_2, E_3, and E_4 equal to 0. Solving for q_{12} would then give the desired answer as

$$q_{12} = (fA)_{12} = J_2 \left(\frac{A_2 \epsilon_2}{1 - \epsilon_2} \right) \tag{163}$$

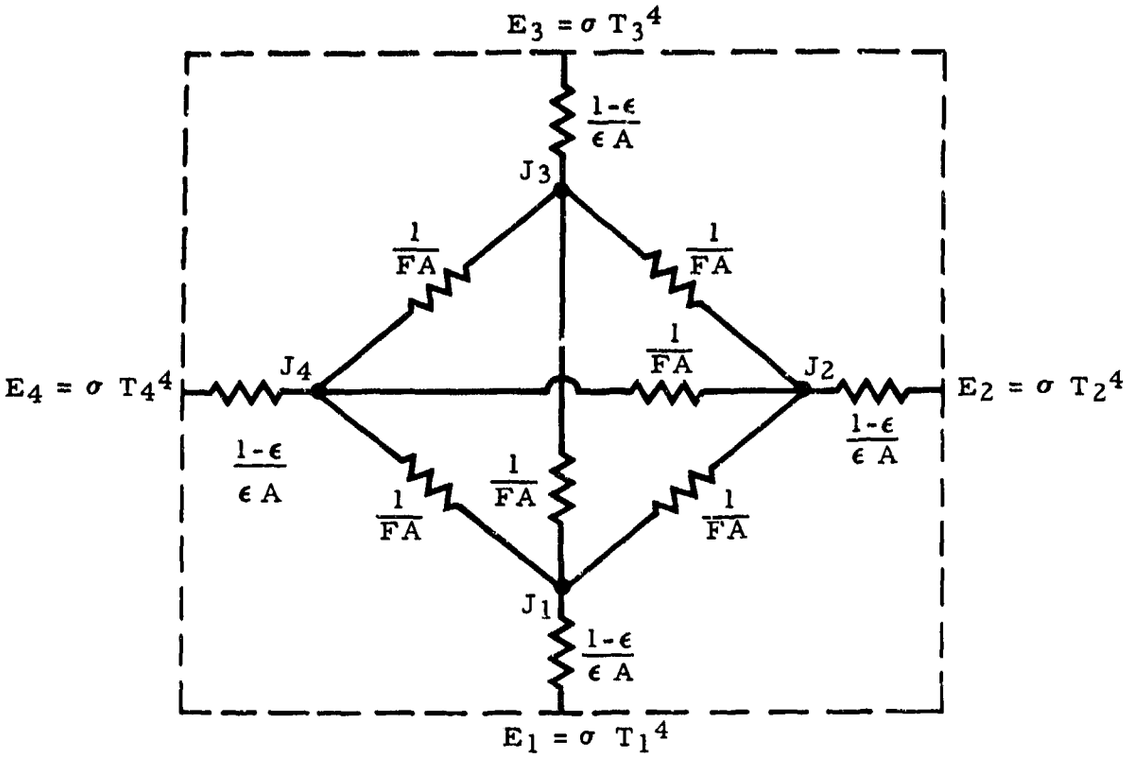

Figure 51. Radiosity Analog Network for Four-Sided Enclosure

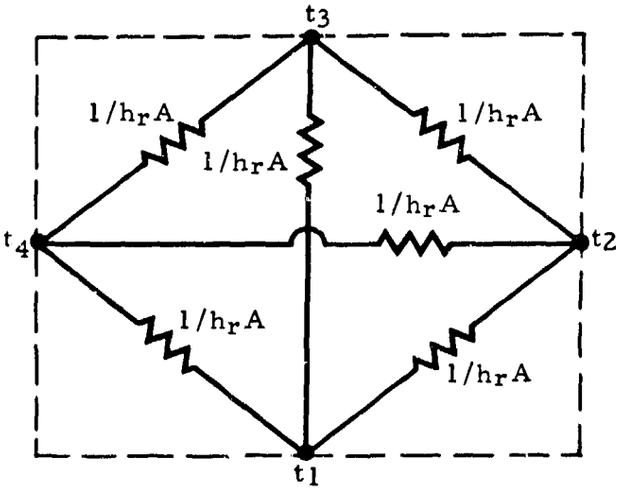

Figure 52. Conventional Analog Network for Four-Sided Enclosure

In a like manner, the equivalent conductances $(fA)_{13}$, $(fA)_{14}$, $(fA)_{24}$, $(fA)_{23}$, and $(fA)_{34}$ can be obtained and then used in the network of Figure 52 for the general solution to the problem.

COMMONLY USED METHODS

One of the earliest relationships for the net heat transfer between two bodies is the simplified equation from Hottel (Reference 17).

$$q_{12} = \sigma F_e F_a A_1 (T_1^4 - T_2^4) \tag{164}$$

where

F_a = Configuration factor

F_e = Factor which includes emissivities allowing for departure of source and receiver from complete blackness and which depends upon ϵ_1, ϵ_2, and configuration of surfaces.

A second method developed by Hottel (Reference 18) to evaluate the net exchange between two surfaces is expressed by

$$q_{12} = \sigma f_{12} A_1 (T_1^4 - T_2^4) \tag{165}$$

where

$$f_{12} = \frac{1}{\frac{1}{F_{12}} + \frac{1}{\epsilon_1} - 1 + \frac{A_1}{A_2}\left(\frac{1}{\epsilon_2} - 1\right)}$$

and

F_{12} = Configuration factor from surface 1 to surface 2

Equations 164 and 165 are limited in application with respect to multiple interreflecting surfaces. An attempt has been made to account for reflecting (refractory) surfaces by replacing the geometric configuration factor F with a modified configuration factor $\overline{F}$, which includes both direct and reflected radiation effects. Values of $\overline{F}$ are usually obtained from charts or graphs and are rather limited in application because these graphs are available for certain specific configurations only.

COMPARISON OF ANALYTICAL METHODS

At the present time, a variety of techniques is used to analyze radiation heat transfer problems. The radiosity analog network method is an extremely useful technique for obtaining an exact solution for any type of gray body, multiple-surface configuration. The ray tracing method, to be discussed in the following section, also gives quite accurate results. Extreme care must be exercised, however, in choosing the proper technique for a particular problem. Large errors can occur if the proper technique is not used, particularly in problems where there are multiple reflecting surfaces.

The illustrative examples given here show the variation in results obtained by the different techniques.

Problem 1

Two parallel and equal disks of diameter d are separated by distance ℓ. (See Figure 53.) There are no refractory walls. Calculate the net radiant interchange between the disks.

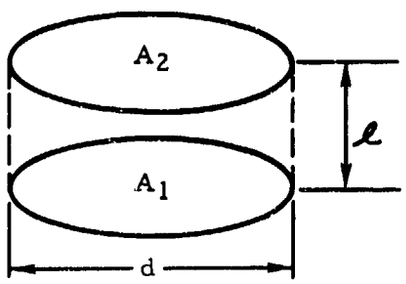

Figure 53. Parallel Disks

Given

$$d = 1.0 \text{ ft}$$

$$\ell = 0.5 \text{ ft}$$

$$\epsilon_1 = 0.7$$

$$\epsilon_2 = 0.3$$

$$t_1 = 500 \text{ F}$$

$$t_2 = 100\ F$$

$$F_{12} = F_{21} = 0.37 \text{ (p 57, Reference 17)}$$

Solution 1A

From Reference 17 (Equation 164),

$$q_{12} = \sigma F_e F_a A_1 (T_1^4 - T_2^4)$$

where

$F_e = \epsilon_1\ \epsilon_2 = 0.21$ (p 56, case 10, Reference 17)

$F_a = 0.37$

$A_1 = \pi r^2 = \pi (0.5)^2 = 0.786$ sq ft

$T_1 = 500 + 460 = 960\ ^\circ R$

$T_2 = 100 + 460 = 560\ ^\circ R$

$\sigma = 0.1713 \times 10^{-8}$ Btu/(hr)(sq ft)($^\circ R^4$)

Therefore

$$q_{12} = 0.1713\ (0.21)(0.37)(0.786)(9.6^4 - 5.6^4)$$

$$= 0.1713\ (0.21)(0.37)(0.786)(8500 - 983)$$

$$= 0.1713\ (0.21)(0.37)(0.786)(7517) = 78.6 \text{ Btu/hr}$$

Solution 1B

From Reference 18 (Equation 165),

$$q_{12} = \sigma f_{12} A_1 (T_1^4 - T_2^4)$$

where

$$f = \frac{1}{\frac{1}{F_{12}} + \frac{1}{\epsilon_1} - 1 + \frac{A_1}{A_2}\left(\frac{1}{\epsilon_2} - 1\right)}$$

$$\epsilon_1 = 0.7$$

$$\epsilon_2 = 0.3$$

$$F_{12} = 0.37$$

and where

$$F = \frac{1}{\frac{1}{0.37} + \frac{1}{0.7} - 1 + 1\left(\frac{1}{0.3} - 1\right)}$$

$$= \frac{1}{2.7 + 1.429 - 1 + 3.33 - 1}$$

$$= \frac{1}{5.462} = 0.183$$

Therefore

$$q_{12} = 0.1713\ (0.183)(0.786)(9.6^4 - 5.6^4)$$

$$= 0.1713\ (0.183)(0.786)(7517) = 185.1 \text{ Btu/hr}$$

Solution 1C (Radiosity Network)

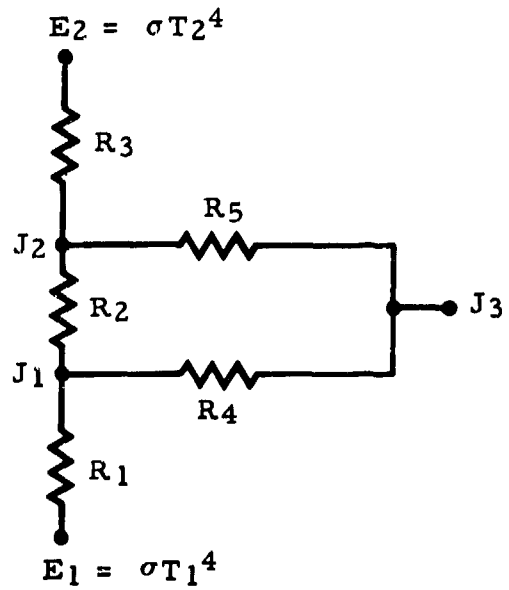

Figure 54. Radiosity Network for Problem 1

As shown in Figure 54,

$$E_1 = \sigma T_1^4 = 0.1713\,(9.6^4) = 1456$$

$$E_2 = \sigma T_2^4 = 0.1713\,(5.6^4) = 168.4$$

$$C_1 = \frac{1}{R_1} = \frac{\epsilon_1 A_1}{1 - \epsilon_1} = \frac{0.7\,(0.786)}{1 - 0.7} = 1.833$$

$$C_2 = \frac{1}{R_2} = F_{12} A_1 = 0.37\,(0.786) = 0.2908$$

$$C_3 = \frac{1}{R_3} = \frac{\epsilon_2 A_2}{1 - \epsilon_2} = \frac{0.3\,(0.786)}{1 - 0.3} = 0.3372$$

$$C_4 = \frac{1}{R_4} = F_{13} A_1 = 0.63\,(0.786) = 0.495$$

$$C_5 = \frac{1}{R_5} = F_{23} A_2 = 0.63\,(0.786) = 0.495$$

Since there are no refractory walls, the irradiation from the surroundings is zero and $J_3 = 0$ To calculate q_{12}, it is necessary to determine the equivalent conductance $(fA)_{12}$. Let $E_1 = 1.0$, $E_2 = 0$, $J_3 = 0$ (Figure 55).

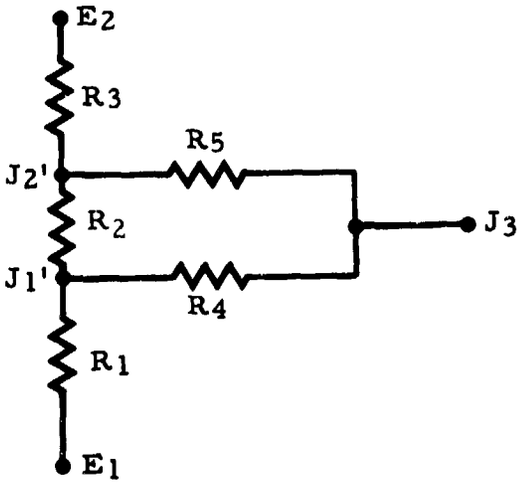

Figure 55. Radiosity Network for Determining Equivalent Conductance

Solving for J_1' and J_2'

$$C_1(E_1 - J_1') + C_4(J_3 - J_1') + C_2(J_2' - J_1') = 0$$

$$C_3(E_2 - J_2') + C_5(J_3 - J_1') + C_2(J_1' - J_2') = 0$$

$$1.833(1 - J_1') + 0.495(0 - J_1') + 0.2908(J_2' - J_1') = 0$$

$$0.3372(0 - J_2') + 0.495(0 - J_2') + 0.2908(J_1' - J_2') = 0$$

$$1.833 + 0.2908 J_2' - 2.6188 J_1' = 0$$

$$0.2908 J_1' - 1.1230 J_2' = 0$$

$$J_1' = 3.86 J_2'$$

$$J_2' = 0.1868$$

Therefore

$$(fA)_{12} = C_3(J_2 - 0) = 0.3372(0.1868) = 0.063$$

and

$$q_{12} = \sigma(fA)_{12}(T_1^4 - T_2^4)$$

$$= 0.1713(0.063)(9.6^4 - 5.6^4) = 81.2 \text{ Btu/hr}$$

Discussion of Problem 1

If Problem 1 were recalculated for the case where F_{12} was 0.9 instead of 0.37, the following comparison could be made:

Method	$F_{12} = 0.37$	$F_{12} = 0.9$
Equation 164	78.6 Btu/hr	191 Btu/hr
Equation 165	185.1 Btu/hr	262 Btu/hr
Radiosity network	81.2 Btu/hr	231 Btu/hr

As Oppenheim has pointed out in his paper (Reference 16), the radiosity network gives the exact solution to radiant interchange problems, with the basic stipulation that the radiant energy be in diffuse form. Thus it can be stated that the answers obtained by use of the radiosity network for both cases of problem 1 are the correct results. These are presented in the table above as 81.2 and 231 Btu/hour, respectively. Equation 164 is correct for the first case but is about 20 percent in error in the second case. Equation 165 is over 100 percent in error in the first case and about 15 percent in error in the second.

Problem 2

Given

To show the effect of reflecting surfaces, let the configuration of Problem 2 be enclosed with a single reflecting (refractory) surface. It is assumed that the reflecting wall reflects all the incident radiation.

Solution 2A

From Reference 17 (Equation 164),

$$q_{12} = \sigma F_e F_a A_1 (T_1^4 - T_2^4)$$

where

$$F_e = \epsilon_1 \epsilon_2 = 0.21 \text{ (p 56, case 10, Reference 17)}$$

$$F_a = \overline{F}_a = 0.64 \text{ (Figure 4-7, p 57, Reference 17)}$$

Therefore

$$q_{12} = 0.1713\,(0.21)\,(0.64)\,(0.786)\,(9.6^4 - 5.6^4)$$

$$= 0.1713\,(0.21)\,(0.64)\,(0.786)\,(7517) = 136 \text{ Btu/hr}$$

Solution 2B

From Reference 18 (Equation 165),

$$q_{12} = \sigma f_{12} A_1 (T_1^4 - T_2^4)$$

where

$$f_{12} = \frac{1}{\frac{1}{\overline{F}_{12}} + \frac{1}{\epsilon_1} - 1 + \frac{A_1}{A_2}\left(\frac{1}{\epsilon_2} - 1\right)}$$

$$\epsilon_1 = 0.7$$

$$\epsilon_2 = 0.3$$

$$\overline{F}_{12} = 0.64$$

Therefore

$$f_{12} = \frac{1}{\frac{1}{0.64} + \frac{1}{0.7} - 1 + \frac{1}{1}\left(\frac{1}{0.3} - 1\right)}$$

$$= \frac{1}{1.563 + 1.429 - 1 + 3.333 - 1} = 0.231$$

and

$$q_{12} = 0.1713\ (0.231)\ (0.786)\ (7517) = 234 \text{ Btu/hr}$$

Solution 2C (Radiosity Network)

As shown in Figure 56,

$$E_1 = \sigma T_1^4 = 1456$$

$$E_2 = \sigma T_2^4 = 168.4$$

and

$$C_1 = 1.833$$

$$C_2 = 0.2908$$

$$C_3 = 0.3372$$

$$C_4 = 0.495$$

$$C_5 = 0.495$$

Since there is no current in R_6, the radiosity of the reflecting surface J_R must equal E_R. This shows that the reflectivity of a perfectly insulated reflecting surface is completely ineffective because the addition of a surface resistor such as R_6 has no effect on the network.

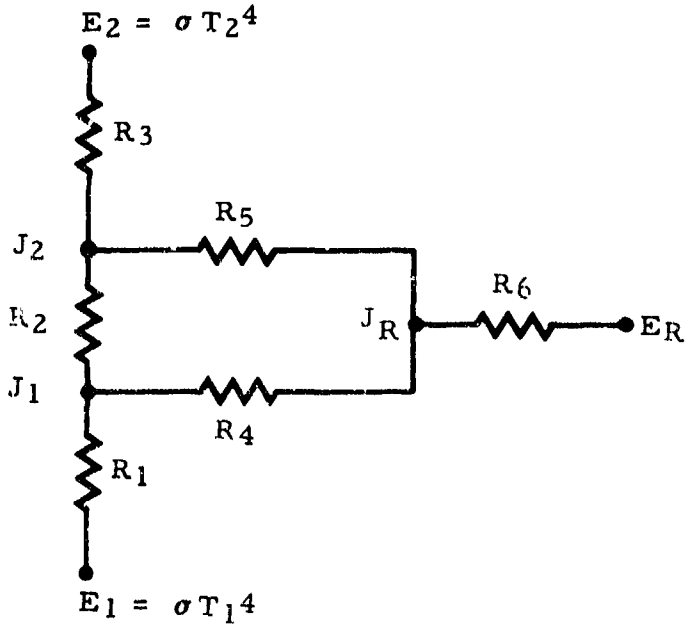

Figure 56. Radiosity Network for Problem 2

$$R_4 = \frac{1}{C_4} = \frac{1}{0.495} = 2.02$$

$$R_5 = \frac{1}{C_5} = \frac{1}{0.495} = 2.02$$

$$R_{4,5} = R_4 + R_5 = 4.04$$

$$C_{4,5} = \frac{1}{R_{4,5}} = \frac{1}{4.04} = 0.2475$$

$$C_{2,4,5} = C_2 + C_{4,5} = 0.2908 + 0.2475 = 0.5383$$

$$R_{2,4,5} = \frac{1}{C_{2,4,5}} = \frac{1}{0.5383} = 1.858$$

$$R_1 = \frac{1}{C_1} = \frac{1}{1.833} = 0.546$$

$$R_3 = \frac{1}{C_3} = \frac{1}{0.3372} = 2.97$$

$$R_{total} = R_1 + R_{2,4,5} + R_3 = 0.546 + 1.858 + 2.97 = 5.374$$

Therefore

$$q_{12} = \frac{1}{R_{total}} (E_1 - E_2)$$

$$= \frac{1}{5.374} (1456 - 168.4)$$

$$= \frac{1287.6}{5.374} = 240 \text{ Btu/hr}$$

Discussion of Problem 2

Problem 2 is summarized as follows:

Equation 164	136 Btu/hr
Equation 165	234 Btu/hr
Radiosity network	240 Btu/hr

In the case where interreflecting surfaces are present, it can be seen that Equation 164 is in considerable error even with the use of a modified F_a. In this case, however, Equation 165 is close to the correct answer of 240 Btu/hour.

In reviewing the results of Problems 1 and 2, it is concluded that Equations 164 and 165 are correct only if they are chosen with care to suit the problem at hand. The radiosity network method of analysis, however, is always correct for cases involving diffuse radiation.

RAY TRACING ANALYSIS METHOD

Very accurate results may be obtained from the ray tracing method of heat transfer analysis. Unfortunately, however, the method is difficult to use without a high-speed digital computer because of the lengthy and tedious calculations involved. A method has been developed whereby this technique can be programed for an IBM 704 or 709 computer (Reference 19), although the programing has not yet been done. The material for this discussion was supplied by the Los Angeles division of North American Aviation.

NOMENCLATURE

a	Area of surface
e	Monochromatic emissivity power of black surface at particular surface temperature and wavelength
f	Configuration form factor
q	Heat flow
u	Energy emitted by surface
v	Energy received by surface
W	Energy absorbed by surface
ϵ	Emissivity
λ	Wavelength
ρ	Reflectance

RADIANT INTERCHANGE ANALYSIS

This discussion is concerned with an enclosure made up of a finite number of finite surfaces. The enclosure contains a nonabsorbing media. Each of the surfaces of this enclosure is considered to be opaque, homogeneous, diffusely reflecting, uniformly irradiated, and at a uniform temperature. The i^{th} surface of this n surface enclosure emits radiant energy in the amount

$$u_i = a_i(1-\rho_{i,j})e_{i,j}(\Delta\lambda)_j \qquad (j = 1, 2 \ldots p) \qquad (166)$$

where

a_i = Area of i^{th} surface

$\rho_{i,j}$ = Reflectance of i^{th} surface for radiation of average wavelength λ_j in narrow wavelength band of $(\Delta\lambda)_j$

$e_{i,j}$ = Monochromatic emissive power of black surface at temperature of i^{th} surface and at wavelength λ_j

The term reflectance describes the behavior of a particular specimen, while reflectivity is reserved to describe the behavior of the material itself (i.e., the reflectance of a highly polished specimen of a material is numerically equal to the reflectivity of that material).

The right-hand side of Equation 166 actually represents p terms where p is the number of wavelength bands into which the important part of the electromagnetic spectrum has been divided. This notation convention will be used throughout this discussion. That is, whenever a subscript appears two or more times in any product on the right-hand side of an equation and does not appear on the left-hand side of that equation, it is to be understood that the product in question is to be summed on the subscript, as the subscript takes on all of its possible identities.

The i^{th} surface receives from the n surfaces directly emitted radiation which has suffered no reflections in passing from the originating surface to the i^{th} surface. This energy is in the amount

$$ {}_{o}v_{i,j} = u_{k,j} f_{ki} \qquad (k = 1, 2 \ldots n) \tag{167} $$

where

f_{ki} = Configuration factor from k^{th} to i^{th} surface

In Equation 167, the subscript o denotes the fact that no reflections have taken place in the transfer of the energy.

Of the energy ${}_{o}v_{i,j}$, the i^{th} surface absorbs

$$ {}_{o}w_{i,j} = (1-\rho_{i,j}) u_{k,j} f_{ki} \tag{168} $$

where, in the general case,

$$ {}_{o}w_{i} = \sum_{j=1}^{p} {}_{o}w_{i,j} \tag{169} $$

Energy which has suffered β reflections before reaching the i^{th} surface is

$$\beta^{v}_{i,j} = u_{k,j} f_{k\ell} \rho_{\ell,j} f_{\ell m} \rho_{m,j} f_{mn} \rho_{n,j} \cdots f_{si} \tag{170}$$

The amount of this energy absorbed by the i^{th} surface is

$$\beta^{w}_{i,j} = (u_{k,j} f_{k\ell} \rho_{\ell,j} f_{\ell m} \rho_{m,j} f_{mn} \rho_{n,j} \cdots f_{si})(1-\rho_{i,j}) \tag{171}$$

An energy balance on the i^{th} surface for radiation of average wavelength λ_j is

$$q_{i,j} = u_{i,j} - \sum_{\beta=0}^{\infty} \beta^{w}_{i,j} \tag{172}$$

That is,

$$q_{i,j} = u_{i,j} - (1-\rho_{i,j})(u_{k,j} f_{ki} + u_{k,j} f_{k\ell} \rho_{\ell,j} f_{\ell i} + u_{k,j} f_{k\ell} \rho_{\ell,j} f_{\ell m} \rho_{m,j} f_{mi} + \cdots) \tag{173}$$

where the energy q_i, which must be added to or removed from the i^{th} surface to take into account the differences between the radiant energy leaving and entering the surface, is

$$q_i = \sum_{j=0}^{\infty} q_{i,j} \tag{174}$$

The form of Equation 173 is not suited to computations. Therefore, the procedures are directed toward obtaining forms of the energy balance equation that are more suitable for computation. The terms can be written as a product of certain matrices. For example,

$$o^{v}_{i,j} = u_{k,j} f_{ki} = \begin{bmatrix} u_{1,j} u_{2,j} \cdots u_{n,j} \end{bmatrix} \begin{bmatrix} f_{1i} \\ f_{2i} \\ \vdots \\ f_{ni} \end{bmatrix} = U_j F(i) \tag{175}$$

and

$$
\begin{aligned}
{}^{1}v_{i,j} &= u_{k,j} f_{k\ell}\, \rho_{\ell,j} f_{\ell i} \\
&= \begin{bmatrix} u_{i,j} u_{2,j} \cdots u_{n,j} \end{bmatrix}
\begin{bmatrix} f_{11} f_{12} \cdots f_{1n} \\ f_{21} f_{22} \cdots f_{2n} \\ \cdot \quad \cdot \quad \cdot \\ \cdot \quad \cdot \quad \cdot \\ \cdot \quad \cdot \quad \cdot \\ f_{n1} f_{n2} \cdots f_{nn} \end{bmatrix}
\begin{bmatrix} \rho_{1,j} & 0 & \cdots & 0 \\ 0 & \rho_{2,j} & \cdots & 0 \\ \cdot & \cdot & & \cdot \\ \cdot & \cdot & & \cdot \\ \cdot & \cdot & & \cdot \\ 0 & 0 & \cdots & \rho_{n,j} \end{bmatrix}
\begin{bmatrix} f_{1i} \\ f_{2i} \\ \cdot \\ \cdot \\ \cdot \\ f_{ni} \end{bmatrix} \\
&= U_j F R_j F(i)
\end{aligned}
\tag{176}
$$

The capital letters are reserved for matrix quantities unless otherwise stated. That is

$$U_j = \begin{bmatrix} u_{1,j} u_{2,j} \cdots u_{n,j} \end{bmatrix} \tag{177}$$

$$F = \begin{bmatrix} f_{11} f_{12} \cdots f_{1n} \\ f_{21} f_{22} \cdots f_{2n} \\ \cdot \quad \cdot \quad \cdot \\ \cdot \quad \cdot \quad \cdot \\ \cdot \quad \cdot \quad \cdot \\ f_{n1} f_{n2} \cdots f_{nn} \end{bmatrix} \tag{178}$$

$$R_j = \begin{bmatrix} \rho_{1,j} & 0 & \cdots & 0 \\ 0 & \rho_{2,j} & \cdots & 0 \\ \cdot & \cdot & & \cdot \\ \cdot & \cdot & & \cdot \\ \cdot & \cdot & & \cdot \\ 0 & 0 & \cdots & \rho_{n,n} \end{bmatrix} \tag{179}$$

$$F(i) = \begin{bmatrix} f_{1i} \\ f_{2i} \\ \cdot \\ \cdot \\ \cdot \\ f_{ni} \end{bmatrix} \tag{180}$$

Equation 173 can be written in the form

$$q_{i,j} = u_{i,j} - (1 - \rho_{i,j}) \left[U_j F(i) + U_j F R_j F(i) + U_j F R_j F R_j F(i) + \ldots \right] \tag{181}$$

or

$$q_{i,j} = u_{i,j} - (1 - \rho_{i,j})U_j \left[I + (FR_j) + (FR_j)^2 + (FR_j)^3 + \ldots \right] F(i) \qquad (182)$$

where

$$I = \begin{bmatrix} 1 & 0 & \ldots & 0 \\ 0 & 1 & \ldots & 0 \\ \vdots & \vdots & & \vdots \\ \vdots & \vdots & & \vdots \\ \vdots & \vdots & & \vdots \\ 0 & 0 & \ldots & 1 \end{bmatrix} \qquad (183)$$

It can be shown that

$$\left[I + (FR_j) + (FR_j)^2 + (FR_j)^3 + \ldots \right] = \left[I - FR_j \right]^{-1} \qquad (184)$$

where

$\left[I - FR_j \right]^{-1}$ is the inverse of the matrix $\left[I - FR_j \right]$

Finally, Equation 173 may be written in the form

$$q_{i,j} = u_{i,j} - (1 - \rho_{i,j})U_j \left[I - FR_j \right]^{-1} F(i) \qquad (185)$$

The total net energy leaving or entering surface i is

$$q_i = u_i - (1 - \rho_{i,j})U_j \left[I - FR_j \right]^{-1} F(i) \qquad (186)$$

The matrix equation for the entire system of n equations is

$$Q = U - (I - R_j)U_j \left[I - FR_j \right]^{-1} F \qquad (187)$$

where

$$Q = \left[q_1 q_2 \ldots q_n \right] \qquad (188)$$

and

$$U = \left[U_1 U_2 \ldots U_n \right] \qquad (189)$$

DIGITAL COMPUTATION

For the purpose of digital computations of heat transfer and temperatures of n surfaces, equations in the form of Equation 186 will be used. Let

$$C_j = \left[I - FR_j\right]^{-1} \begin{bmatrix} C_{11,j} & C_{12,j} & \cdots & C_{1n,j} \\ C_{21,j} & C_{22,j} & \cdots & C_{2n,j} \\ \vdots & \vdots & & \vdots \\ C_{n1,j} & C_{n2,j} & \cdots & C_{nn,j} \end{bmatrix} \tag{190}$$

The matrix product in Equation 186 can be shown to be

$$\begin{aligned} U_j \left[I - FR_j\right]^{-1} F(i) = {} & u_{1,j}(c_{11,j}f_{1i} + c_{12,j}f_{2i} + \cdots + c_{1n,j}f_{ni}) \\ & + u_{2,j}(c_{21,j}f_{1i} + c_{22,j}f_{2i} + \cdots + c_{2n,j}f_{ni}) \\ & \vdots \\ & + u_{n,j}(c_{n1,j}f_{1i} + c_{n2,j}f_{2i} + \cdots + c_{nn,j}f_{ni}) \end{aligned} \tag{191}$$

Planck's equation gives the relationship for monochromatic emissive power of an ideal radiator at temperature T_i.

$$e_{i,j} = \frac{C_1 \lambda_j^{-5}}{\exp \dfrac{C_2}{\lambda_j T_i} - 1} \tag{192}$$

where C_1 is 1.18070×10^8 Btu (microns)^4/(hour)(square foot) and C_2 is 25896 microns (°R), where microns is the measure of wavelength.

Let

$$y_{i,j} = \frac{C_1 \lambda_j^{-5} (\Delta\lambda)_j}{\exp \dfrac{C_2}{\lambda_j T_i} - 1} \quad \text{Btu/(hr)(sq ft)} \tag{193}$$

Then

$$U_j \left[I - FR_j \right]^{-1} F(i) = a_1(1-\rho_{1,j})y_{1,j}(C_{11,j}f_{1i}+C_{12,j}f_{2i}+\ldots+C_{1n,j}f_{ni})$$
$$+a_2(1-\rho_{2,j})y_{2,j}(C_{21,j}f_{2i}+C_{22,j}f_{2i}+\ldots+C_{2n,j}f_{ni})$$
$$\vdots \qquad \vdots \qquad \vdots \qquad \vdots \qquad (194)$$
$$+a_n(1-\rho_{n,j})y_{n,j}(C_{n1,j}f_{ni}+C_{n2,j}f_{2i}+\ldots+C_{nn,j}f_{ni})$$

Let

$$C_{\ell k,j}f_{ki} = \left[C_{\ell 1,j}f_{1i}+C_{\ell 2,j}f_{2i}+\ldots+C_{\ell n,j}f_{ni}\right] \qquad (195)$$

so that

$$U_j \left[I - FR_j \right]^{-1} F(i) = a_\ell \epsilon_{\ell,j} y_{\ell,j} C_{\ell k,j} f_{ki} \quad \left(\begin{matrix} \ell \\ k \end{matrix} \right| = 1, 2 \ldots n \Big) \qquad (196)$$

where

$$\epsilon_{i,j} = 1-\rho_{i,j} \qquad (197)$$

From Equation 186,

$$q_i = a_i \epsilon_{i,j} y_{i,j} - a_\ell \epsilon_{i,j} \epsilon_{\ell,j} y_{\ell,j} C_{\ell k,j} f_{ki} \qquad (198)$$

or

$$q_i + a_1 \epsilon_{i,j} \epsilon_{1,j} y_{1,j} C_{1k,j} f_{ki} + \ldots + a_i \epsilon_{i,j} y_{i,j} (\epsilon_{i,j} C_{ik,j} f_{ki} - 1) \qquad (199)$$
$$+ \ldots + a_n \epsilon_{i,j} \epsilon_{n,j} y_{n,j} C_{nk,j} f_{ni} = 0$$

The system of n equations may be written in the form

$$\left.\begin{array}{l} q_1 + d_{11,j}y_{1,j} + \ldots + d_{1n,j}y_{n,j} = 0 \\ \vdots \qquad \vdots \qquad \vdots \\ q_i + d_{i1,j}y_{1,j} + \ldots + d_{ii,j}y_{i,j} + \ldots + d_{in,j}y_{n,j} = 0 \\ \vdots \qquad \vdots \qquad \vdots \\ q_n + d_{n1,j}y_{1,j} + \ldots + d_{nn,j}y_{n,j} = 0 \end{array}\right\} \qquad (200)$$

where

$$d_{\alpha\beta} = a_{\beta}\epsilon_{\alpha,j}(\epsilon_{\beta,j}C_{\beta k,j}f_{k\alpha} - \delta_{\alpha\beta}) \tag{201}$$

where $\delta_{\alpha\beta}$ is the Kronecker delta and

$$\delta_{\alpha\beta} = \begin{cases} 1 \text{ if } \alpha = \beta \\ 0 \text{ if } \alpha \neq \beta \end{cases}$$

The quantity q_i may be heat that is conducted or convected to the surface i or it may be that generated internally in the material of surface i. Therefore, in general, the system of equations to be solved for the unknown temperatures $T_1, T_2 \ldots T_i, \ldots T_n, T_a, T_b \ldots$ is

$$\left.\begin{aligned}
&d_{11,j}y_{1,j} + \ldots + d_{1n,j}y_{n,j} + d'_{11}T_1 + \ldots + d'_{1n}T_n + d''_{1a}T_a + d''_{1b}T_b + \ldots + \eta_1 = 0 \\
&\quad\vdots \\
&d_{i1,j}y_{1,j} + \ldots + d_{in,j}y_{n,j} + d'_{i1}T_1 + \ldots + d'_{in}T_n + d''_{ia}T_a + d''_{ib}T_b + \ldots + \eta_i = 0 \\
&\quad\vdots \\
&d_{n1,j}y_{1,j} + \ldots + d_{nn,j}y_{n,j} + d'_{n1}T_1 + \ldots + d'_{nn}T_n + d''_{na}T_a + d''_{nb}T_b + \ldots + \eta_n = 0
\end{aligned}\right\}$$

Other equations containing only T_s to the first power equal zero. (202)

where T_a, T_b, and so forth, are temperatures of elements of the system which are not involved in the radiant energy interchange. All terms having the primed coefficients are reserved, of course, for conduction and convection. This assumes that the conduction and convection of energy can be written in such a manner that only the first powers of the temperatures are involved. The η terms are reserved for internal energy generation within elements of the system.

It should be noted that this analysis has been set up using the assumption that Lambert's cosine law adequately defines the space density of emitted and reflected radiation. Obviously, this is not the physical case. A more exact analysis would include the variation of space density of reflected and emitted radiation. However, because no such data are now available and because such a numerical analysis would be complex for even the most advanced computing machines, it has not appeared necessary that these more accurate descriptions of the actual physical system be included at this time.

The preceding analysis is general for the case of varying values of reflectance with wavelength. Here, again, it would be a major task to actually sum across the spectrum and at the same time solve the required set of nonlinear equations. Therefore, as a first step in probing such solutions, it has been decided that a gray body analysis should be used. This simply means that the quantity y will be replaced by σT^4. This assumption, of course, has been used many times in the past even though it often leads to inaccurate solutions. It is not, then, necessary to sum on j in the expression for $d_{\alpha\beta}$ in Equation 201.

DISCUSSION OF ASSUMPTIONS

1. The methods of analysis discussed in this section have the common restriction that radiant energy is emitted or reflected in diffuse form, as opposed to specular form. A satisfactory method of handling partly diffuse, partly specular radiation has not yet been devised. Fortunately, most thermal radiation encountered in engineering applications can be considered to be in diffuse form.

2. The radiosity network method is usually applied only to gray body radiation and is so used in this report. Methods have been developed whereby non-gray radiation can be treated, but this is considered beyond the scope of this report.

Section VII

CONFIGURATION FACTOR STUDIES AND DATA

CONFIGURATION FACTOR EVALUATION

One of the most difficult areas in the analysis of radiation heat transfer is proper calculation of the geometric configuration factor. Basically, the configuration factor F_{12} from A_1 to A_2 is defined as the fraction of the total radiant flux leaving A_1 that is incident upon A_2. The configuration factor from a plane point source to a finite surface (commonly known as a differential-finite configuration factor) is obtained by integration over A2, and the mean configuration factor from a finite source (finite-finite configuration factor) is the average of the point configuration factors over the finite source. The integral expression for the differential-finite configuration factor from dA_1 to A_2 is given by

$$F_{(dA_1 - A_2)} = \frac{1}{\pi} \int_{A_2} \frac{\cos\theta_1 \cos\theta_2 \, dA_2}{S^2} \tag{203}$$

The integral expression for the finite-finite configuration factor from A_1 to A_2 is given in the Section III discussion on radiant heat exchange between surfaces.

$$F_{12} = \frac{1}{A_1 \pi} \int_{A_1} \int_{A_2} \frac{\cos\theta_1 \cos\theta_2}{S^2} \, dA_1 dA_2 \tag{204}$$

As an example (from Reference 20) consider the two mutually perpendicular surfaces shown in Figure 57. The left-hand corner of the horizontal surface is assumed to be the origin, with the x, y, and z axes as shown. The horizontal surface has overall dimensions of D and W while those of the vertical are H and W. Thus

$$F_{12} = \frac{1}{WD\pi} \int_{A_1} \int_{A_2} \frac{\cos\theta_1 \cos\theta_2}{S^2} \, dA_1 dA_2 \tag{205}$$

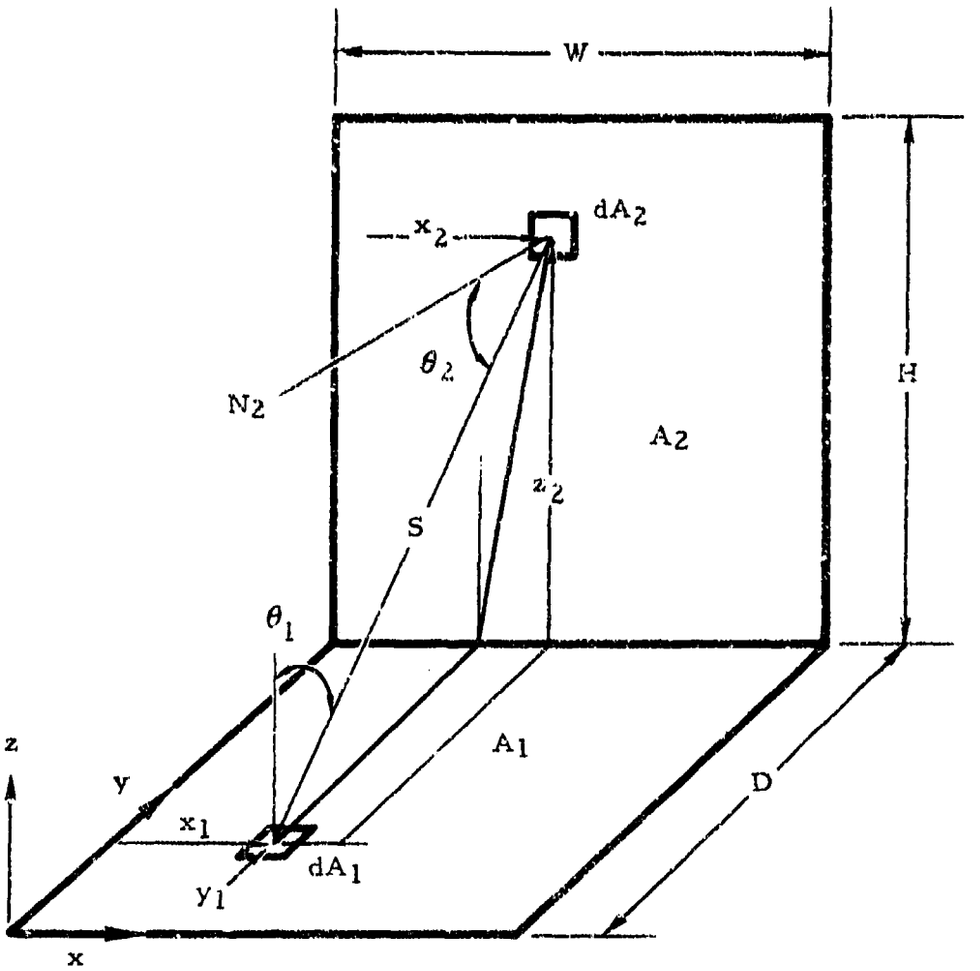

Figure 57. Geometry for Calculation of Configuration Factor for Two Mutually Perpendicular Surfaces

where $\cos\theta_1 = \frac{z}{s}$

$\cos\theta_2 = \frac{D-y}{s}$

$s = \sqrt{(x_2 - x_1)^2 + (D - y)^2 + z^2}$

and

$dA_1 = dx_1\, dy$

$dA_2 = dx_2\, dz$

therefore

$$F_{12} = \frac{1}{WD\pi} \int_0^H \int_0^D \int_0^W \int_0^W \frac{z\,(D - y)}{\left[(x_2 - x_1)^2 + (D - y)^2 + z^2\right]^2} dx_1 dx_2 dy dz \qquad (206)$$

Integrating Equation 206 yields

$$F_{12} = \frac{1}{WD\pi} \left\{ \frac{1}{4} \left[(D^2 - W^2 + H^2) \ln (D^2 + H^2 + W^2) \right.\right.$$

$$\left.\left. - (D^2 + H^2) \ln (D^2 + H^2) - (D^2 - W^2) \ln (D^2 + W^2) \right] \right\} \qquad (207)$$

$$- \frac{1}{WD\pi} \left\{ \frac{1}{4} \left[(H^2 - W^2) \ln (H^2 + W^2) - D^2 \ln D^2 - H^2 \ln H^2 + W^2 \ln W^2) \right] \right.$$

$$+ \frac{1}{WD\pi} \left[HW \tan^{-1} \frac{W}{H} + DW \tan^{-1} \frac{W}{D} - W \sqrt{D^2 + H^2} \tan^{-1} \frac{W}{\sqrt{D^2 + H^2}} \right]$$

It can be seen that the integration process is often tedious, even for simple shapes such as in the example. In fact, for most cases the integration cannot be solved analytically and other means must be used to obtain the answer. Under these circumstances the following approach can be utilized:

1. If the areas in question can be assumed infinite in one direction, there are several very simple and rapid methods available with which to obtain the configuration factor.

2. If step 1 does not fit the problem, the next step is to use tables and charts which are available for specific configurations. These are discussed in this section and provide solutions to a number of different configurations, with the help of form factor algebra.

3. If the previous steps are not adequate, there is available an IBM program which calculates the configuration factor between any two plane areas if they are in the form of parallelograms.

4. The method that can be used where all other methods prove to be inadequate is called the unit sphere method. This is a highly accurate technique, although unfortunately it is rather tedious. Most mechanical integrators are based on the unit sphere principle.

A most useful method for evaluating the configuration factor between surfaces infinite in one direction is called the "string" method and is presented in Reference 21 (p 66-68).

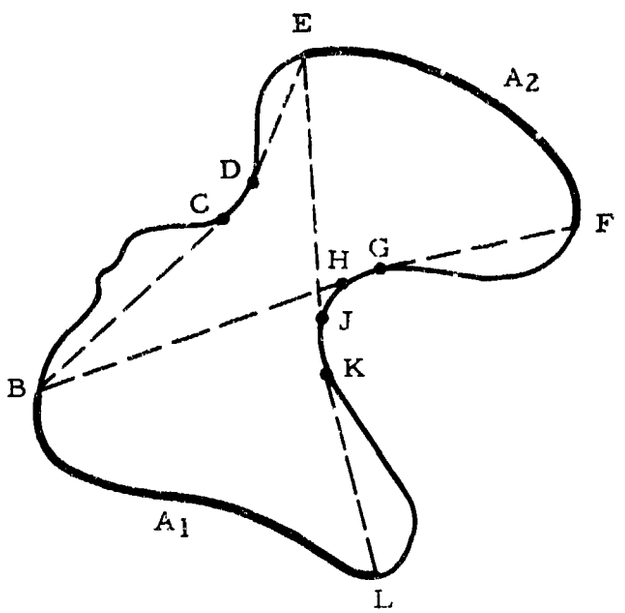

Figure 58. Diagram of Infinite Enclosure

Consider the enclosure of Figure 58. It is desired to compute the configuration factor from surface A_1 to surface A_2. A minimum-length line is stretched over the surface connecting edge B of A_1 to edge E of A_2 (dotted line BCDE) as well as a minimum-length line from edge L of A_1 to edge F of A_2 (line LKJHGF). A minimum-length line is now stretched from B to F (line BHGF) a second line from L to E (line LKJE). The configuration factor F_{12} can then be obtained from the expression

$$A_1F_{12} = A_2F_{21} = \frac{(LKJE + BHGF) - (BCDE + LKJHGF)}{2} \qquad (208)$$

Equation 208 states that the AF product between two surfaces, per unit of length normal to the sketch of Figure 58, is the sum of the lengths of crossed strings stretched between the ends of the lines representing the two surfaces, less the sum of the lengths of uncrossed strings similarly stretched between the surfaces, all divided by 2.

Another useful method is that which calculates the configuration factor from a differential area to an infinitely long surface (Figure 59). Surface A_2 is any surface generated by an infinitely long line moving parallel to itself and to the plane dA_1.

$$F_{(dA_1-A_2)} = \frac{1}{2}(\cos\phi - \cos\theta) \tag{209}$$

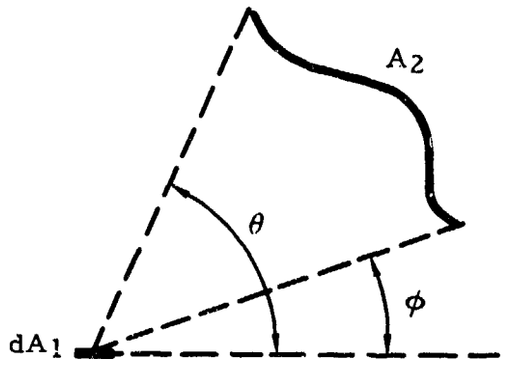

Figure 59. Diagram of Differential Area and Infinitely Long Surface

There is some error involved if A_2 is not infinitely long in one direction. However, if the length is greater than twice the distance from A_1 to A_2, the error is less than 10 percent. For small surfaces, the configuration factor can be found for two directions and averaged.

Equation 209 can be applied for several points along a finite surface A_1 and then averaged. This results in a fairly small error if sufficient points are taken.

Instead of calculating each point, it is simpler to draw the bodies to scale and use Figure 60, which is a graphical solution of Equation 209. The origin should be placed at several points on one shape to obtain an average configuration factor. Figure 61 also can be utilized in this way.

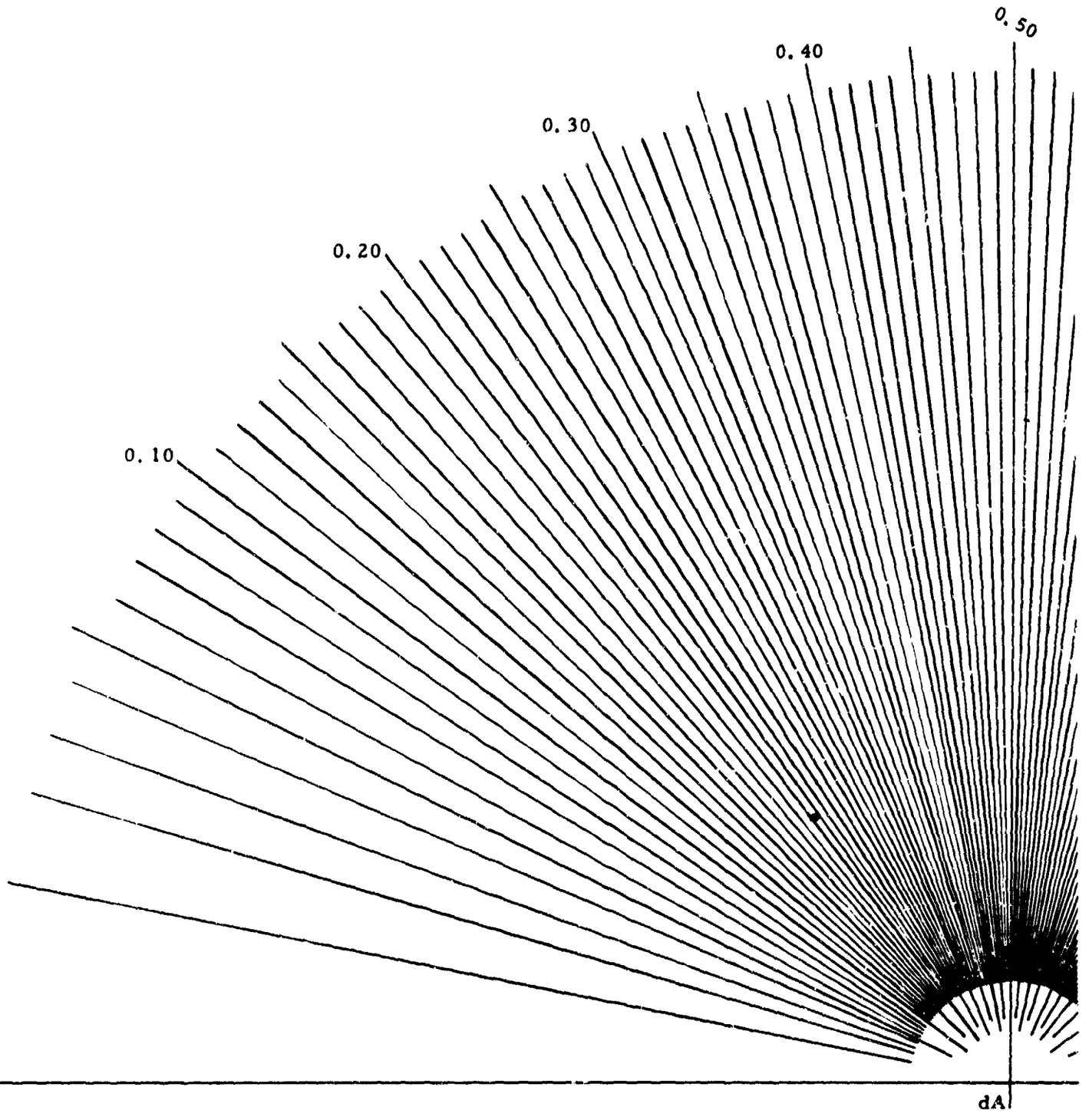
0.50
0.40
0.30
0.20
0.10
dA

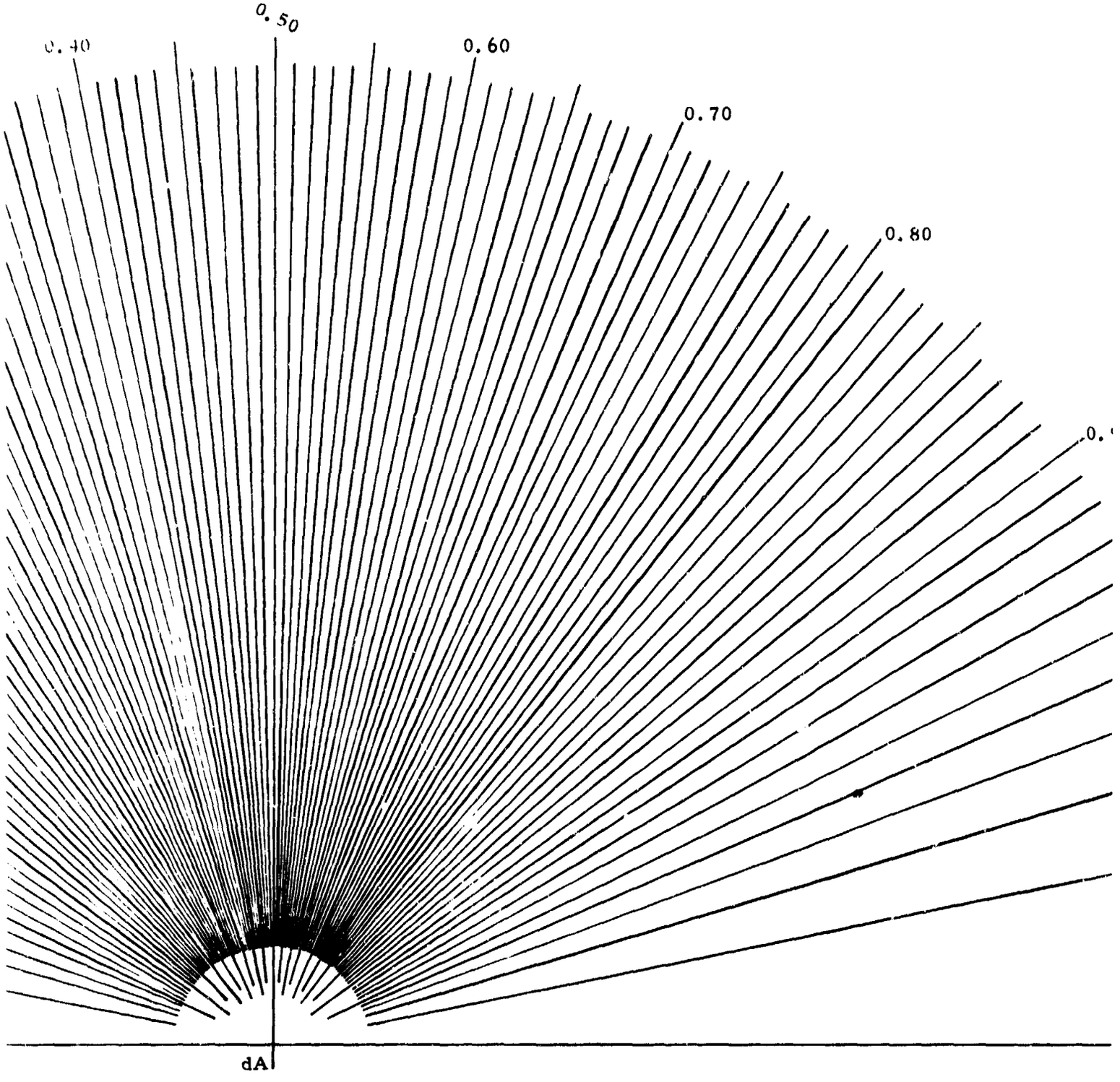

Figure 60. Differential Area Shape Factor for T

2

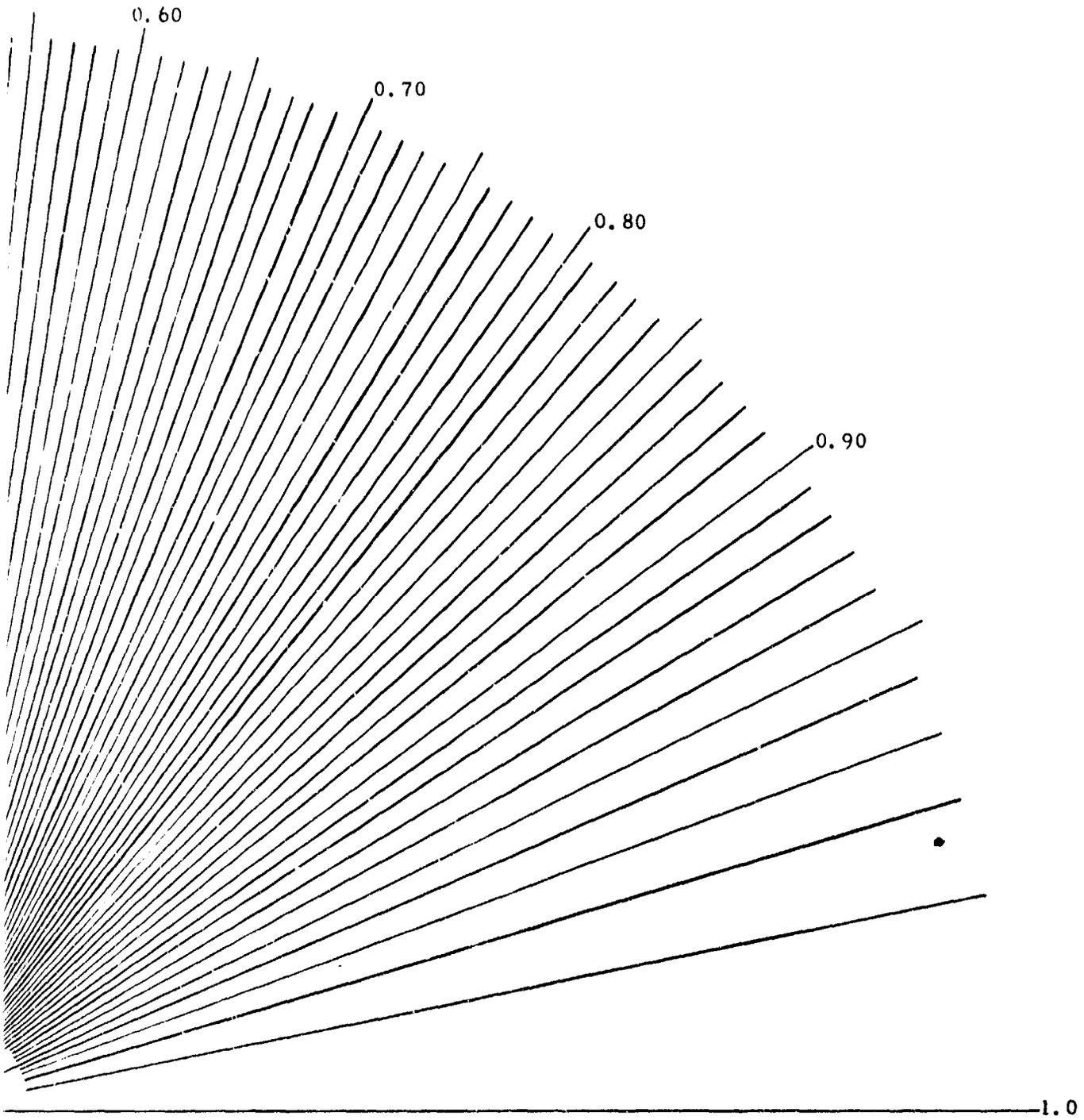

Figure 60. Differential Area Shape Factor for Two-Dimensional Case

3

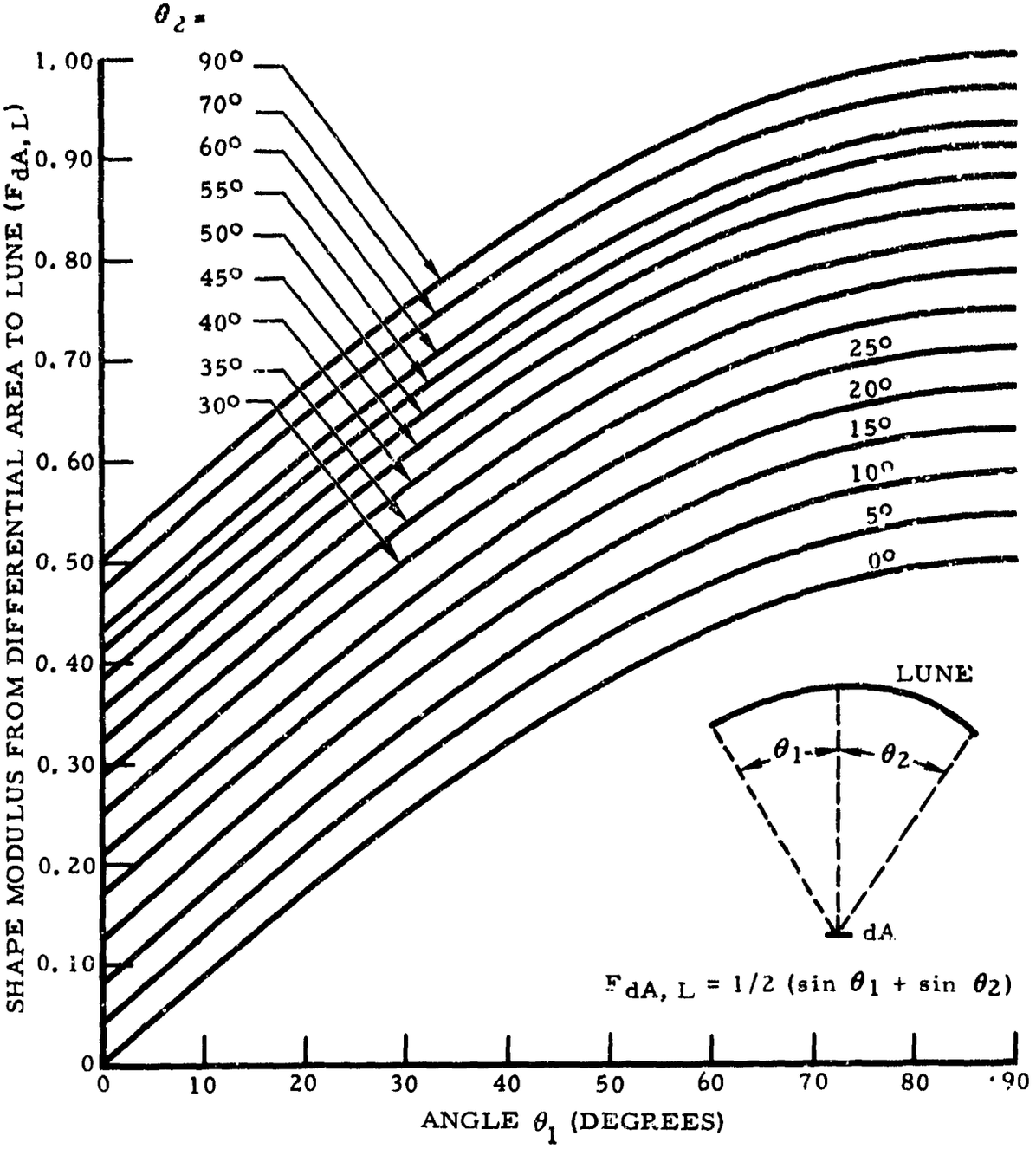

Figure 61. Shape Modulus From Differential Area to Lune

TABULATED DATA

DATA OF REPORT NACA TN 2836

One of the most widely used sources of tabulated configuration factor data is report NACA TN 2836, "Radiant - Interchange Configuration Factors," D. C. Hamilton and W. R. Morgan of Purdue University, December 1952 (Reference 22). This report includes configuration factor data for the following shapes:

1. A plane point source dA_1 and a plane rectangle A_2 parallel to the plane of dA_1
2. A plane point source dA_1 and a plane rectangle A_2, the planes of dA_1 and A_2 intersecting at an angle ϕ ($0° < \phi < 180°$)
3. A plane point source dA_1 and any surface A_2 generated by an infinitely long line moving parallel to itself and to the plane of dA_1
4. A plane point source dA_1 and any infinite plane A_2 with the planes of dA_1 and A_2 intersecting at an angle θ
5. A spherical point source dA_1 and a plane rectangle A_2
6. A plane point source dA_1 and a plane circular disk A_2
7. A plane point source dA_1 and a plane disk A_2, the planes of dA_1 and A_2 intersecting at an angle of 90 degrees
8. A plane point source dA_1 and a right circular cylinder A_2
9. Two concentric cylinders with a point source dA_1 on the inside of the large cylinder at one end
10. Same geometry as shape 2 with a triangular area added to the top of A_2
11. Same as shape 10 with the triangle reversed
12. An infinitely long cylinder A_1 and an infinite plane A_2, mutually parallel

13. A line source dA_1 and a plane rectangle A_2 parallel to the plane of dA_1 with dA_1 opposite one edge of A_2

14. A line source dA_1 and a plane rectangle A_2 which intersects the plane of dA_1 at an angle ϕ

15. A line source dA_1 and a right circular cylinder A_2 parallel to dA_1

16. Two concentric cylinders with a line source dA_1 on the inside of the large cylinder. The outside cylinder is A_1, the inside cylinder is A_2

17. Same geometry as shape 16, calculates configuration factor from dA_1 to the ends of the concentric cylinders

18. Identical, parallel, directly opposed rectangles

19. Two rectangles A_1 and A_2 with one common edge and an included angle ϕ between the two planes

20. Parallel, directly opposed, plane, circular disks

In addition to the graphical and tabular data presented in this report, the integrated equations of many of the shapes are given. Form factor algebra and basic theory are also presented.

DATA OF CONVAIR (FORT WORTH) STUDY

This discussion presents the results of a study conducted by the Fort Worth Division of Convair to determine the configuration factors for various shapes (Reference 23). No attempt has been made to present the derivation of the equations presented herein. A complete development of the equations can be found in Reference 23.

It should be noted that some of the integrations cannot be performed analytically and numerical methods are required.

Parallel Planes

For nodes 1 and 2, as defined in Figure 62, lying on parallel planes, the black body interchange factor is defined by the following equations.

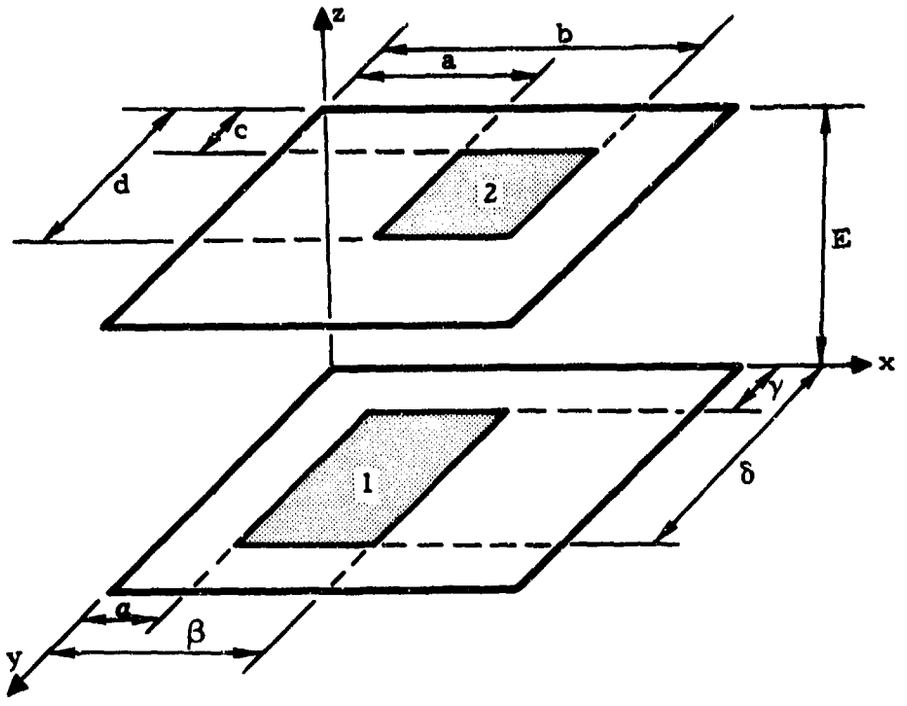

Figure 62. Nodes on Parallel Planes

$$F_{12} = \frac{1}{\pi A_1}\Big[f_1(\beta-b,\delta-c) - f_1(\beta-a,\delta-c) + f_1(\alpha-a,\delta-c) - f_1(\alpha-b,\delta-c)$$

$$+ f_1(\alpha-b,\gamma-c) - f_1(\alpha-a,\gamma-c) + f_1(\beta-a,\gamma-c)$$

$$- f_1(\beta-b,\gamma-c) + f_1(\beta-b,\gamma-d) - f_1(\beta-a,\gamma-d) + f_1(\alpha-a,\gamma-d)$$

$$- f_1(\alpha-b,\gamma-d) + f_1(\alpha-b,\delta-d) - f_1(\alpha-a,\delta-d) + f_1(\beta-a,\delta-d)$$

$$- f_1(\beta-b,\delta-d)\Big] \qquad (210)$$

where the function f_1 is defined by

$$f_1(\nu,\xi) = \frac{1}{2}\left(E\nu\tan^{-1}\frac{\nu}{E} - \xi\sqrt{E^2+\nu^2}\,\tan^{-1}\frac{\xi}{\sqrt{E^2+\nu^2}} \right. \qquad (211)$$

$$\left. - \nu\sqrt{E^2+\xi^2}\,\tan^{-1}\frac{\nu}{\sqrt{E^2+\xi^2}} + \frac{E^2}{2}\ln\frac{E^2+\nu^2+\xi^2}{E^2+\xi^2} \right)$$

For nodes 1 and 2, as defined in Figure 62 with $\gamma = c = 0$ and $\delta = d = \infty$, lying on parallel planes (i.e. infinite strips), the black body interchange factor is defined by

$$F_{12} = \frac{1}{2(\beta-\alpha)} \left(\sqrt{E^2 + (\beta-a)^2} - \sqrt{E^2 + (\beta-b)^2} + \sqrt{E^2 + (\alpha-b)^2} - \sqrt{E^2 + (\alpha-a)^2} \right) \quad (212)$$

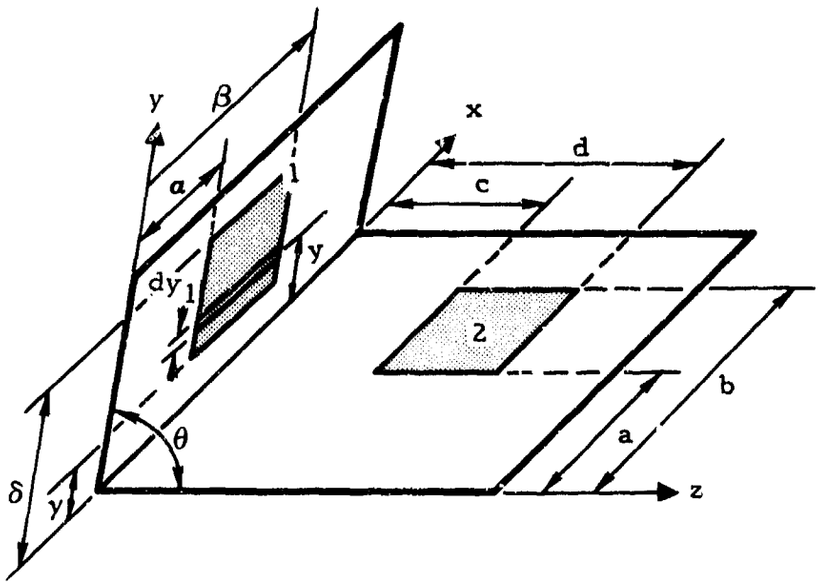

Figure 63. Nodes on Skewed Planes

Skewed Planes

For nodes 1 and 2, as defined in Figure 63, lying on nonparallel planes, the black body interchange factor is defined

$$F_{12} = \frac{1}{\pi A_1} \left(f_2(b-\alpha, d) - f_2(b-\alpha, c) + f_2(b-\beta, c) - f_2(b-\beta, d) + f_2(a-\beta, d) - f_2(a-\beta, c) + f_2(a-\alpha, c) - f_2(a-\alpha, d) \right) \quad (213)$$

where the function f_2 is defined by

$$f_2(\xi,\omega) = \frac{1}{2}\int_{\gamma}^{\delta}\left[\frac{1}{2}y_1 \sin^2\theta \log(\xi^2+\omega^2+y_1^2-2\omega y_1\cos\theta) + (\cos\theta)\sqrt{\xi^2+y_1^2\sin^2\theta}\ \tan^{-1}\frac{\omega-y_1\cos\theta}{\sqrt{\xi^2+y_1^2\sin^2\theta}}\right]dy_1$$

$$+ \frac{1}{2}\int_{\gamma}^{\delta}\left(y_1 \sin\theta\cos\theta\ \tan^{-1}\frac{y_1\cos\theta-\omega}{y_1\sin\theta} + \frac{\xi(\omega\cos\theta-y_1)}{\sqrt{\omega^2+y_1^2-2\omega y_1\cos\theta}}\tan^{-1}\frac{\xi}{\sqrt{\omega^2+y_1^2-2\omega y_1\cos\theta}}\right)dy_1 \quad (214)$$

For the case defined in Figure 63 when θ is 90 degrees, the black body interchange factor is defined by

$$F_{12} = \frac{1}{\pi A_1}\Big[f_3(b-\alpha, d^2+\gamma^2) - f_3(b-\alpha, d^2+\delta^2) + f_3(b-\alpha, c^2+\delta^2) - f_3(b-\alpha, c^2+\gamma^2) + f_3(b-\beta, c^2+\gamma^2) - f_3(b-\beta, c^2+\delta^2) + f_3(b-\beta, d^2+\delta^2) - f_3(b-\beta, d^2+\gamma^2) + f_3(a-\beta, d^2+\gamma^2) - f_3(a-\beta, d^2+\delta^2) + f_3(a-\beta, c^2+\delta^2) - f_3(a-\beta, c^2+\gamma^2) + f_3(a-\alpha, c^2+\gamma^2) - f_3(a-\alpha, c^2+\delta^2) + f_3(a-\alpha, d^2+\delta^2) - f_3(a-\alpha, d^2+\gamma^2)\Big] \quad (215)$$

where the function f_3 is

$$f_3(\xi,\nu) = \left[\frac{1}{2}\xi\sqrt{\nu}\tan^{-1}\frac{\xi}{\sqrt{\nu}} + \frac{1}{4}\xi^2 \ln(\xi^2+\nu) - \frac{1}{8}(\xi^2+\nu)\ln(\xi^2+\nu)\right] \quad (216)$$

For nodes 1 and 2, as defined in Figure 63 with $a = \alpha = 0$ and $b = \beta = \infty$, lying on nonparallel planes (i.e. infinite strips), the black body interchange factor is defined by

$$F_{12} = \frac{1}{2(\delta - \gamma)} \left(\sqrt{\delta^2 + c^2 - 2c\delta\cos\theta} - \sqrt{\delta^2 + d^2 - 2d\delta\cos\theta} + \sqrt{\gamma^2 + d^2 - 2d\gamma\cos\theta} - \sqrt{\gamma^2 + c^2 - 2c\gamma\cos\theta} \right) \quad (217)$$

Parallel Disks

The black body interchange factor between two disks, with radii of R_1 and R_2, respectively, whose centers lie on a line normal to both disks is given by

$$F_{12} = \frac{1}{2R_1^2} \left[E^2 + R_1^2 + R_2^2 - \sqrt{(E^2 + R_1^2 + R_2^2)^2 - (2R_1R_2)^2} \right] \quad (218)$$

where E is the distance between the disks.

Plane and Parallel Cylinder

For node 1 lying on the surface of a cylinder and node 2 lying on the surface of a plane (parallel to the cylinder) as defined in Figure 64, the black body interchange factor is defined by

$$\bar{\theta} = \cos^{-1} \frac{x_2}{\sqrt{x_2^2 + y_2^2}} \quad (219)$$

For $\theta_2 < \bar{\theta} < \theta_1$,

$$F_{12} = \frac{1}{2\pi A_1} \int_a^b \left\{ \left| f_4(\beta - c, \wedge_1) - f_4(\beta - c, \wedge_2) \right| - \left| f_4(\beta - d, \wedge_1) - f_4(\beta - d, \wedge_2) \right| + \left| f_4(\alpha - d, \wedge_1) - f_4(\alpha - d, \wedge_2) \right| - \left| f_4(\alpha - c, \wedge_1) - f_4(\alpha - c, \wedge_2) \right| \right\} dx_2 \quad (220)$$

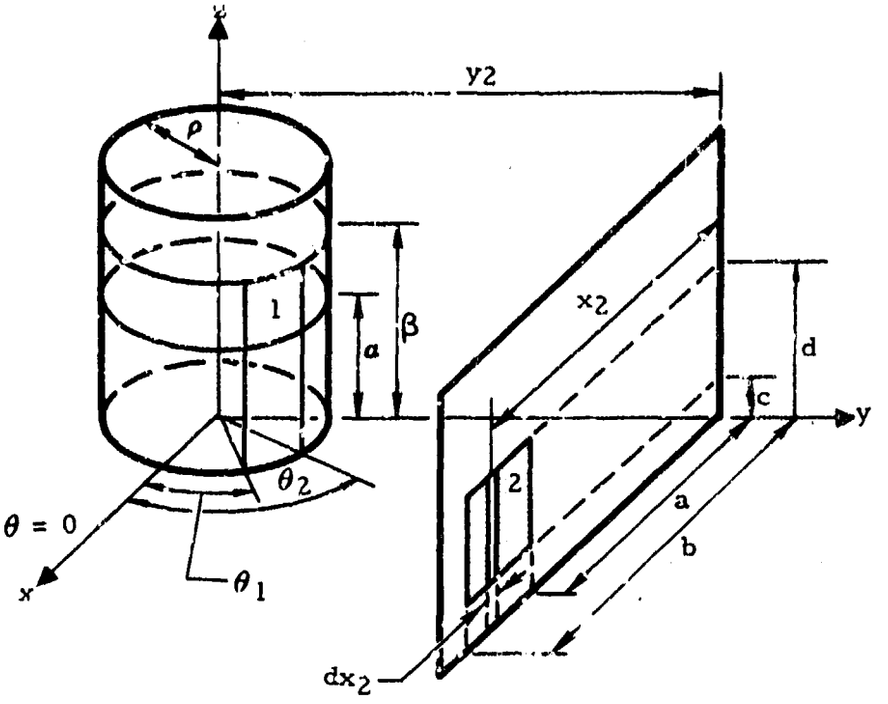

Figure 64. Nodes on Plane and Parallel Cylinder

For $\theta_1 < \bar{\theta} < \theta_2$,

$$F_{12} = \frac{1}{2\pi A_1}\int_a^b \Big\{ \Big| f_4(\beta\text{-}c, \wedge_1) + f_4(\beta\text{-}c, \wedge_2) - f_5(\beta\text{-}c) \Big| - \Big| f_4(\beta\text{-}d, \wedge_1) + f_4(\beta\text{-}d, \wedge_2) - f_5(\beta\text{-}d) \Big| + \Big| f_4(\alpha\text{-}d, \wedge_1) + f_4(\alpha\text{-}d, \wedge_2) - f_5(\alpha\text{-}d) \Big| - \Big| f_4(\alpha\text{-}c, \wedge_1) + f_4(\alpha\text{-}c, \wedge_2) - f_5(\alpha\text{-}c) \Big| \Big\} \, dx_2 \qquad (221)$$

where the functions f_4 and f_5 are defined as

$$f_4(\xi,\wedge) = \frac{\xi}{4(y_2^2 + x_2^2)}\left[\frac{2y_2\sqrt{\chi} + 2x_2(\epsilon+\wedge)}{\sqrt{\wedge}}\tan^{-1}\frac{\xi}{\sqrt{\wedge}}\right.$$

$$+ \xi x_2 \ln(\xi^2+\wedge) + \frac{\epsilon x_2}{\xi}\ln\frac{\wedge}{\xi^2+\wedge} \tag{222}$$

$$+ y_2\,\xi\sin^{-1}\frac{\eta-\wedge}{2\rho\sqrt{y_2^2+x_2^2}} - \frac{y_2\epsilon}{\xi}\sin^{-1}\frac{\wedge\eta-\epsilon^2}{2\rho\wedge\sqrt{y_2^2+x_2^1}}$$

$$\left.+ \frac{y_2}{\xi}\sqrt{\xi^4+2\xi^2\eta+\epsilon^2}\sin^{-1}\frac{\wedge(\eta+\xi^2)-\xi^2\eta-\epsilon^2}{2\rho(\wedge+\xi^2)\sqrt{y_2^2+x_2^2}}\right]$$

$$f_{5(\xi)} = \frac{\xi}{2(y_2^2+x_2^2)}\left[4x_2\sqrt{y_2^2+x_2^2}\tan^{-1}\frac{\xi}{\sqrt{y_2^2+x_2^2}-\rho}\right.$$

$$+ \xi x_2 \ln\left(\eta+\xi^2-2\rho\sqrt{y_2^2+x_2^2}\right) \tag{223}$$

$$+ \frac{\epsilon x_2}{\xi}\ln\frac{\eta-2\rho\sqrt{y_2^2+x_2^2}}{\eta+\xi^2-2\rho\sqrt{y_2^2+x_2^2}}$$

$$\left.+ \frac{\pi y_2}{2\xi}\left(\xi^2+\epsilon-\sqrt{\xi^4+2\eta\xi^2+\epsilon^2}\right)\right]$$

where

$$\eta = y_2^2 + x_2^2 + \rho^2$$

$$\epsilon = y_2^2 + x_2^2 - \rho^2$$

$$X = 4\rho^2(y_2^2 + x_2^2) - (\wedge - \eta)^2$$

$$\wedge_1 = \eta - 2\rho(x_2 \cos \theta_1 + y_2 \sin \theta_1)$$

$$\wedge_2 = \eta - 2\rho(x_2 \cos \theta_2 + y_2 \sin \theta_2)$$

Concentric Cylinders

For node 1 on the outside surface of the inner cylinder and node 2 on the inside of the outer cylinder, as defined in Figure 65, the black body interchange factor is defined by Equations 224 and 225. For $\theta'_1 > 90°$ or $\theta'_2 < 90°$,

$$F_{12} = \frac{\rho_o}{2\pi A_1} \int_{\psi_1}^{\psi_2} \Big\{ \Big| f_6(\beta\text{-}c, \wedge_1) - f_6(\beta\text{-}c, \wedge_2) \Big| - \Big| f_6(\beta\text{-}d, \wedge_1) - f_6(\beta\text{-}d, \wedge_2) \Big| + \Big| f_6(\alpha\text{-}d, \wedge_1) - f_6(\alpha\text{-}d, \wedge_2) \Big| - \Big| f_6(\alpha\text{-}c, \wedge_1) - f_6(\alpha\text{-}c, \wedge_2) \Big| \Big\} d\psi \quad (224)$$

For $\theta'_1 < 90° < \theta'_2$,

$$F_{12} = \frac{\rho_o}{2\pi A_1} \int_{\psi_1}^{\psi_2} \Big\{ \Big| f_6(\beta\text{-}c, \wedge_1) + f_6(\beta\text{-}c, \wedge_2) - f_7(\beta\text{-}c) \Big| - \Big| f_6(\beta\text{-}d, \wedge_1) + f_6(\beta\text{-}d, \wedge_2) - f_7(\beta\text{-}d) \Big| + \Big| f_6(\alpha\text{-}d, \wedge_1) + f_6(\alpha\text{-}d, \wedge_2) - f_7(\alpha\text{-}d) \Big| - \Big| f_6(\alpha\text{-}c, \wedge_1) + f_6(\alpha\text{-}c, \wedge_2) - f_7(\alpha\text{-}c) \Big| \Big\} d\psi \quad (225)$$

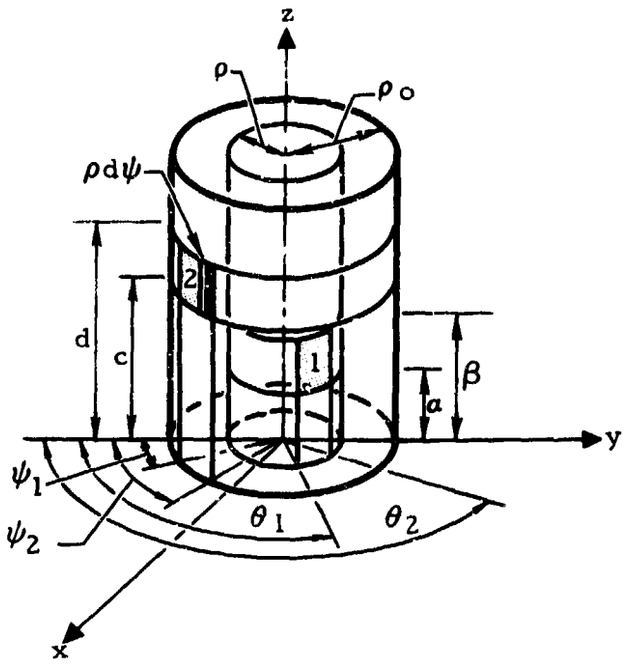

Figure 65. Nodes on Concentric Cylinders

where the functions f_6 and f_7 are defined as

$$f_6(\xi,\wedge) = \frac{\xi}{4\rho_0}\left\{\frac{2\sqrt{\chi}}{\sqrt{\wedge}}\tan^{-1}\frac{\xi}{\sqrt{\wedge}} + \xi\sin^{-1}\frac{\eta-\wedge}{2\rho\rho_0}\right.$$

$$- \frac{1}{\xi}\sqrt{\xi^4 + 2\eta\xi^2 + \epsilon^2}\,\sin^{-1}\frac{\wedge(\eta+\xi^2) - \eta\xi^2 - \epsilon^2}{2\rho\rho_0(\wedge+\xi^2)}$$

$$\left. - \frac{\epsilon}{\xi}\sin^{-1}\frac{\eta\wedge - \epsilon^2}{2\rho\rho_0\wedge}\right\} \qquad (226)$$

$$f_7(\xi) = \frac{\pi}{4\rho_0}\left\{\xi^2 + \epsilon - \sqrt{\xi^4 + 2\eta\xi^2 + \epsilon^2}\right\} \qquad (227)$$

where

$$\eta = \rho_o^2 + \rho^2$$

$$\epsilon = \rho_o^2 - \rho^2$$

$$X = 4\rho_o^2\rho^2 - (\wedge - \eta)^2$$

$$\wedge_1 = \eta - 2\rho_o\rho \sin \theta_1'$$

$$\wedge_2 = \eta - 2\rho_o\rho \sin \theta_2'$$

and θ' is related to θ and ψ as follows, when $0 < \theta$ (or ψ) $< 2\pi$,

For $0 < \psi < \pi$,

$$\theta' = \theta - \psi + \frac{\pi}{2} \quad \text{for } \theta < (\psi + \pi)$$

$$\theta' = \theta - \psi - \frac{\pi}{2} \quad \text{for } \theta > (\psi + \pi)$$

For $\pi < \psi < 2\pi$,

$$\theta' = \theta - \psi + \frac{5\pi}{2} \quad \text{for } \theta < (\psi - \pi)$$

$$\theta' = \theta - \psi + \frac{\pi}{2} \quad \text{for } \theta > (\psi - \pi)$$

Parallel Cylinders

For node 1 on the surface of the cylinder of radius ρ and node 2 on the surface of the cylinder of radius ρ_o as defined in Figure 66, the black body interchange factor is defined by Equations 228 and 229. For $\theta_1' > 90°$ or $\theta_2' < 90°$,

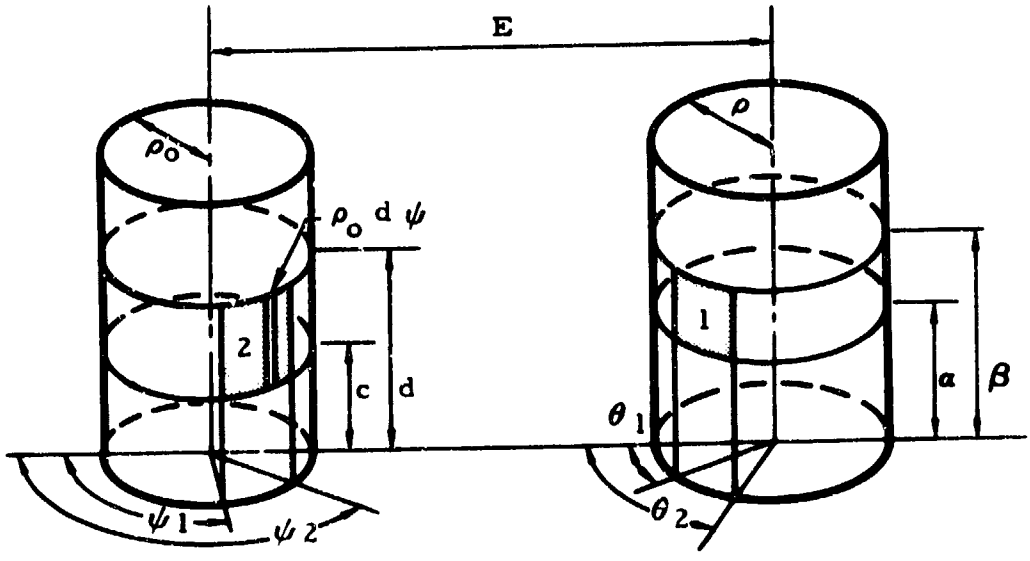

Figure 66. Nodes on Parallel Cylinders

$$F_{12} = \frac{\rho_o}{2\pi Z A_1} \int_{\psi_1}^{\psi_2} \left(E \left| \cos\psi \right| - \rho_o \right) \left[\left| f_8(\beta-c, \wedge_1) - f_8(\beta-c, \wedge_2) \right| \right.$$

$$- \left| f_8(\beta-d, \wedge_1) - f_8(\beta-d, \wedge_2) \right| + \left| f_8(\alpha-d, \wedge_1) - f_8(\alpha-d, \wedge_2) \right|$$

$$\left. - \left| f_8(\alpha-c, \wedge_1) - f_8(\alpha-c, \wedge_2) \right| \right] d\psi \qquad (228)$$

For $\theta_1' < 90° < \theta_2'$

$$F_{12} = \frac{\rho_o}{2\pi Z A_1} \int_{\psi_1}^{\psi_2} \left(E \left| \cos\psi \right| - \rho_o \right) \left[\left| f_8(\beta-c, \wedge_1) + f_8(\beta-c, \wedge_2) \right| \right.$$

$$- f_9(\beta-c) \Big| - \left| f_8(\beta-d, \wedge_1) + f_8(\beta-d, \wedge_2) - f_9(\beta-d) \right| \qquad (229)$$

$$+ \left| f_8(\alpha-d, \wedge_1) + f_8(\alpha-d, \wedge_2) - f_9(\alpha-d) \right| - \left| f_8(\alpha-c, \wedge_1) \right.$$

$$\left. + f_8(\alpha-c, \wedge_2) - f_9(\alpha-c) \right| \Big] d\psi$$

where the functions f_8 and f_9 are defined as

$$f_8(\xi,\wedge) = \frac{\xi}{4Z}\left(\frac{2\sqrt{X}}{\sqrt{\wedge}}\tan^{-1}\frac{\xi}{\sqrt{\wedge}} + \xi\sin^{-1}\frac{\eta-\wedge}{2\rho Z} - \frac{\epsilon}{\xi}\sin^{-1}\frac{\eta\wedge-\epsilon^2}{2\rho Z\wedge}\right.$$
$$\left. + \frac{1}{\xi}\sqrt{\xi^4+2\eta\xi^2+\epsilon^2}\sin^{-1}\frac{\wedge(\eta+\xi^2)-\eta\xi^2-\epsilon^2}{2\rho Z(\wedge+\xi^2)}\right) \qquad (230)$$

$$f_9(\xi) = \frac{\pi}{4Z}\left(\xi^2+\epsilon-\sqrt{\xi^4+2\eta\xi^2+\epsilon^2}\right) \qquad (231)$$

where

$$Z = \sqrt{E^2+\rho_o^2-2E\rho_o|\cos\psi|}$$

$$\eta = Z^2+\rho^2$$

$$\epsilon = Z^2-\rho^2$$

$$X = 4\rho^2Z^2-(\wedge-\eta)^2$$

$$\wedge_1 = \eta - 2\rho Z\sin\theta_1'$$

$$\wedge_2 = \eta - 2\rho Z\sin\theta_2'$$

when $0<\psi<2\pi$ and $-\pi<\theta<\pi$, θ' is related to θ and ψ as

$$\theta' = \theta + \frac{\pi}{2} - \tan^{-1}\frac{\rho_o\sin\psi}{E-\rho_o|\cos\psi|}$$

Cylinder and Skewed Plane

For nodes 1 and 2, as defined in Figure 67, lying on a cylinder and a plane (which is not parallel to the cylinder), respectively, the black body interchange factor is defined by

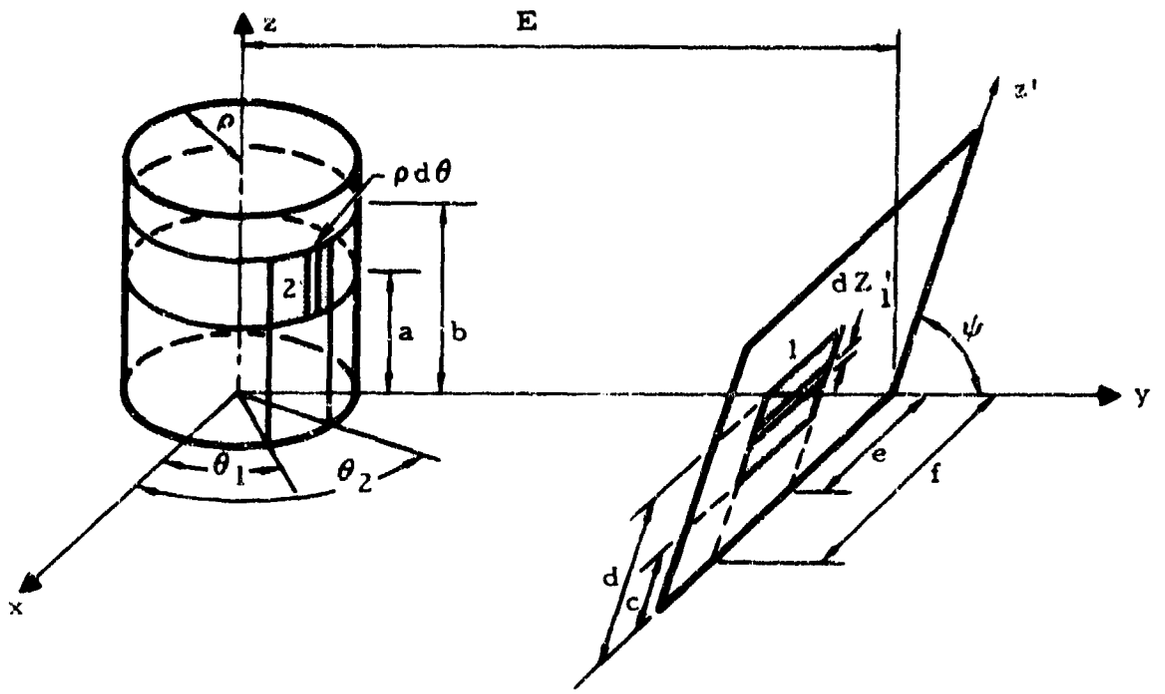

Figure 67, Nodes on Cylinder and Skewed Plane

$$F_{12} = \frac{\rho \sin\psi}{2\pi A_1} \int_c^d \int_{\theta_1}^{\theta_2} \left[f_{10}(b,f) - f_{10}(b,e) + f_{10}(a,e) - f_{10}(a,f) \right] d\theta dZ'_1 \qquad (232)$$

where the function f_{10} is given by

$$f_{10}(\xi,\wedge) = \frac{G_1}{2} \ln (\wedge^2 - 2\rho\wedge\cos\theta + \delta_2) - \frac{G_2}{2} \ln (\wedge^2 - 2\rho\wedge\cos\theta + \delta_1)$$

$$+ \frac{a_2(\wedge - \rho\cos\theta) + \sqrt{r}\cos\theta(\rho\wedge\cos\theta - \delta_1)}{(\delta_1 - \rho^2\cos^2\theta)\sqrt{\wedge^2 - 2\rho\wedge\cos\theta + \delta_1}} \tan^{-1}\frac{\xi - Z_1}{\sqrt{\wedge^2 - 2\rho\cos\theta + \delta_1}}$$

$$+ \frac{G_1\rho\cos\theta - G_3}{\sqrt{\delta_2 - \rho^2\cos^2\theta}} \tan^{-1}\frac{\wedge - \rho\cos\theta}{\sqrt{\delta_2 - \rho^2\cos^2\theta}} -$$

$$- \frac{G_2\rho\cos\theta - G_4}{\sqrt{\delta_1 - \rho^2\cos^2\theta}} \tan^{-1}\frac{\wedge - \rho\cos\theta}{\sqrt{\delta_1 - \rho^2\cos^2\theta}} \qquad (233)$$

where

$$G_1 = \frac{\beta_3 + 2\rho\cos\theta(a_3 + 2\rho\cos^2\theta\cot\psi) - \delta_2\cos\theta\cot\psi}{\delta_2 - \delta_1}$$

$$G_2 = \frac{\beta_3 + 2\rho\cos\theta(a_3 + 2\rho\cos^2\theta\cot\psi) - \delta_1\cos\theta\cot\psi}{\delta_2 - \delta_1}$$

$$G_3 = \frac{\delta_2(a_3 + 2\rho\cos^2\theta\cot\psi) - \gamma_3}{\delta_2 - \delta_1}$$

$$G_4 = \frac{\delta_1(a_3 + 2\rho\cos^2\theta\cot\psi) - \gamma_3}{\delta_2 - \delta_1}$$

$$r = (E - \rho\sin\theta + Z_1\cot\psi)^2$$

$$a_2 = \sqrt{r}\left[(E + Z_1\cot\psi)\sin\theta - \rho\right]$$

$$\delta_1 = (\rho\cos\theta)^2 + r$$

$$\delta_2 = \delta_1 + (Z_1 - \xi)^2$$

and

$$\beta_3 = \left(\frac{1}{\delta_1 - \rho^2 \cos^2\theta}\right) X$$

$$\left\{ (\xi - Z_1)(2\alpha_2 \rho\cos\theta + \rho^2 \cos^3\theta \sqrt{r} + \delta_1 \sqrt{r}\cos\theta) \right.$$

$$- (\delta_1 - \rho^2 \cos^2\theta) \cot\psi \cos\theta \left[\frac{(\xi - Z_1)(E - \rho\sin\theta)}{\cot\psi} - (\rho\cos\theta)^2 \right.$$

$$\left.\left. - r + Z_1(\xi - Z_1) + 2\rho(E + Z_1 \cot\psi)\sin\theta - 2\rho^2 \right] \right\}$$

$$\alpha_3 = \left\{ \frac{1}{\delta_1 - \rho^2 \cos^2\theta} \right\} \left\{ (Z_1 - \xi)(\alpha_2 + \rho\cos^2\theta\sqrt{r}) - \left[2\rho\cos^2\theta \right.\right.$$

$$\left.\left. - (E + Z_1 \cot\psi)\sin\theta + \rho \right] \left[(\delta_1 - \rho^2\cos^2\theta)\cot\psi\right] \right\}$$

$$\gamma_3 = \left\{ \frac{1}{\delta_1 - \rho^2 \cos^2\theta} \right\} \left\{ (Z_1 - \xi)(\rho\cos^2\theta)(\alpha_2 \rho + \delta_1 \sqrt{r}) \right.$$

$$- \left[(E + Z_1 \cot\psi)\sin\theta - \rho\right] \left[\frac{(E - \rho\sin\theta)(\xi - Z_1)}{\cot\psi} - \rho^2\cos^2\theta \right.$$

$$\left.\left. - r - Z_1(Z_1 - \xi) \right] \left[(\delta_1 - \rho^2\cos^2\theta)\cot\psi\right] \right\}$$

Cylinder (Internal)

For the case of two nodes lying on the inside of the same cylinder, as defined in Figure 68, the black body interchange factor is defined by

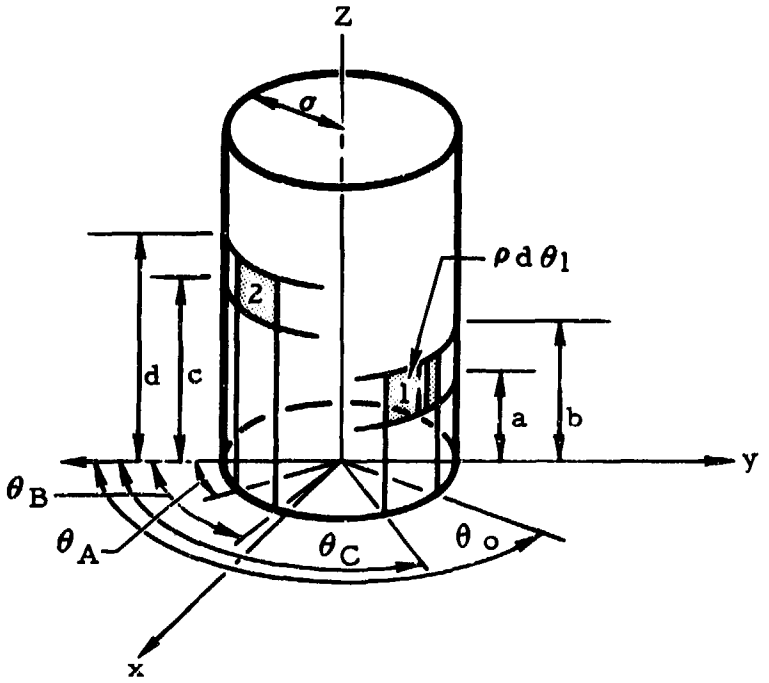

Figure 68. Nodes on Cylinder (Internal)

$$F_{12} = \frac{1}{\pi A_1}\int_{\theta_c}^{\theta_o} \Big\{ f_{11}(b\text{-}c, \theta B) - f_{11}(b\text{-}c, \theta A) + f_{11}(b\text{-}d, \theta A) - f_{11}(b\text{-}d, \theta B) + f_{11}(a\text{-}d, \theta B) - f_{11}(a\text{-}d, \theta A) + f_{11}(a\text{-}c, \theta A) - f_{11}(a\text{-}c, \theta B) \Big\} d\theta_1 \qquad (234)$$

where the function f_{11} is given by

$$f_{11}(\xi,\wedge) = \frac{\xi^2(\wedge - \theta_1)}{8} - \frac{\xi}{4}\sqrt{\xi^2 + 4\rho^2}\tan^{-1}\frac{\sqrt{\xi^2 + 4\rho^2}\tan\left(\frac{\wedge - \theta_1}{2}\right)}{\xi}$$

$$- \frac{\xi\rho}{2}\cos\left(\frac{\wedge - \theta_1}{2}\right)\tan^{-1}\frac{\xi}{2\rho\sin\left(\frac{\wedge - \theta_1}{2}\right)} \qquad (235)$$

Plane and Sphere

The black body interchange factor between node 1 on a plane and node 2 on a sphere, as defined in Figure 69 is given by

$$F_{12} = \frac{1}{\pi A_1}\int_c^d\int_a^b\int_{\psi_1}^{\psi_2}\int_{\theta_1}^{\theta_2}\frac{\rho^2\sin\psi(E - \rho\eta)(\epsilon - \rho)}{(X_1^2 + {}^2 + E^2 + (y_1')^2 - 2\rho\epsilon)^2}d\theta d\psi dx_1 dy_1 \qquad (236)$$

where

$$\eta = \sin\psi\sin\theta\sin\phi + \cos\psi\cos\phi$$

$$\epsilon = x\sin\psi\cos\theta + E\eta + y_1'(\sin\psi\sin\theta\sin\phi - \cos\psi\sin\phi)$$

Equation 236 is not integrated analytically because the resulting IBM compution routine is more complicated than the case wherein all four integrations are done numerically.

Internal Symmetrical Radiation

For the case where a node is defined as a ring around some symmetrical body, computation of the black body interchange factors is greatly simplified. The black body interchange factors between the various nodes of the sphere-cone-cylinder configuration of Figure 70 are given by the following equations.

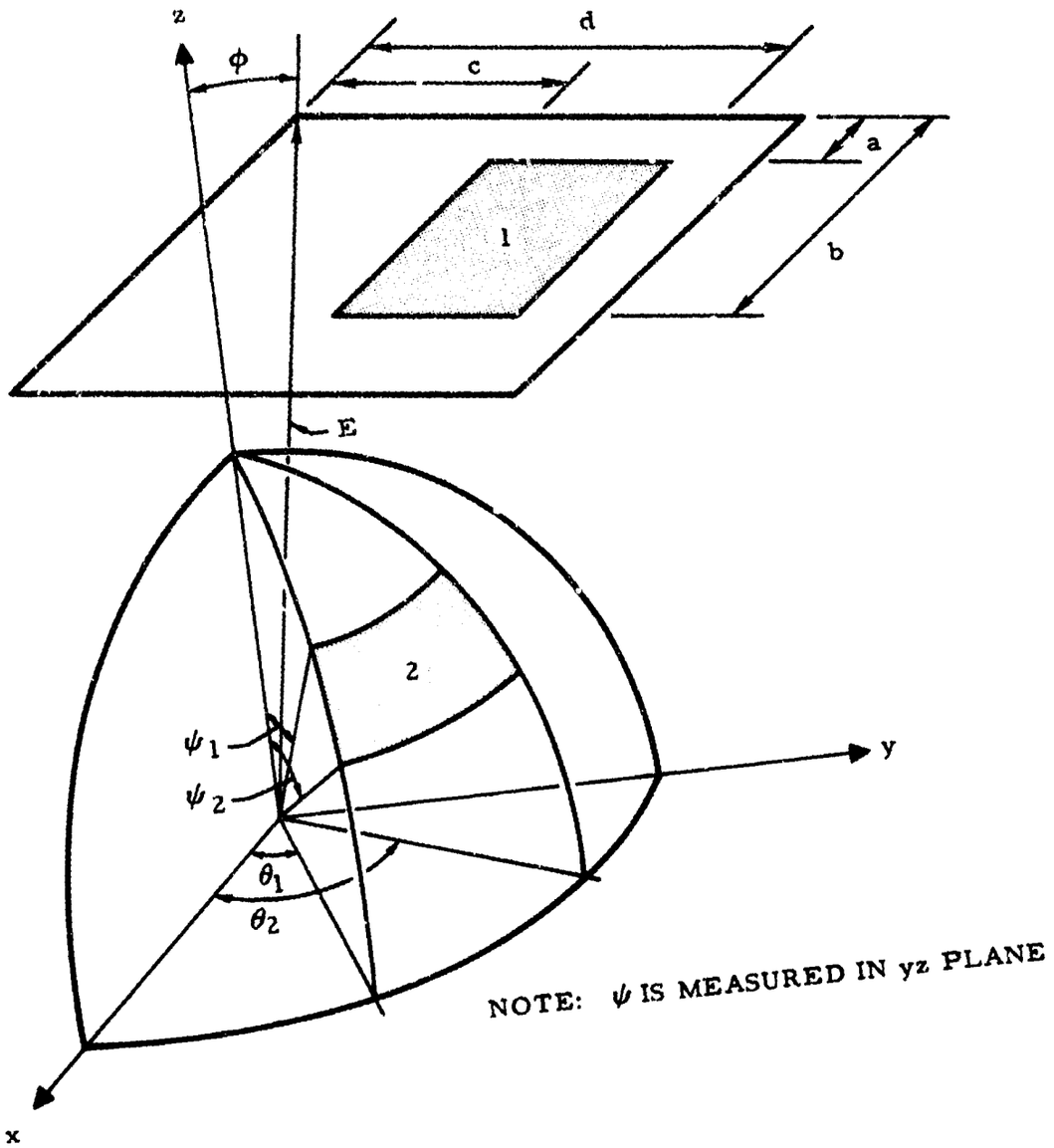

Figure 69. Nodes on Plane and Sphere

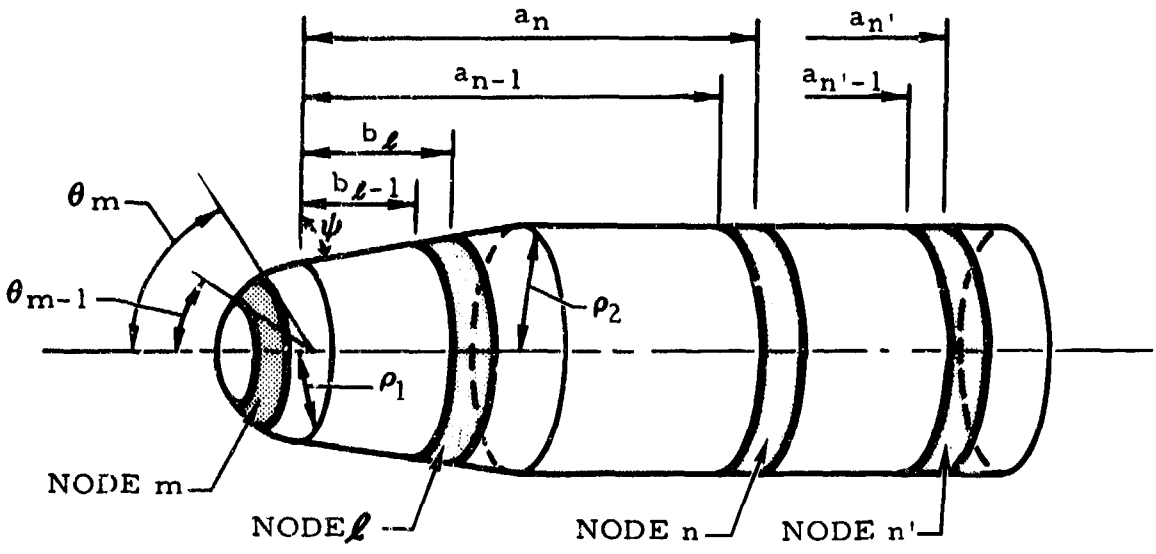

Figure 70. Sphere-Cone-Cylinder Configuration

For nodes on a cylinder,

$$F_{(n,n')} = \left\{ \frac{1}{4\rho_2 (a_n - a_{n-1})} \right\} \left\{ f_{12}(a_n - a_{n'-1}) - f_{12}(a_n - a_{n'}) + f_{12}(a_{n-1} - a_{n'}) - f_{12}(a_{n-1} - a_{n'-1}) \right\} \tag{237}$$

where

$$f_{12}(\xi) = \xi^2 - |\xi| \sqrt{\xi^2 + 4\rho^2} + 2\rho |\xi| \tag{238}$$

For nodes on a sphere,

$$F_{(m,m')} = \frac{1}{2}(\cos\theta_{m'-1} - \cos\theta_{m'}) \tag{239}$$

For nodes on a cone,

$$F(\ell, \ell') = \left[\frac{\frac{1}{2}\sin\psi}{2\rho_1 (b_\ell - b_{\ell-1}) + \frac{(b_\ell)^2 - (b_{\ell-1})^2}{\tan\psi}} \right] \Big[2 (b_\ell - b_{\ell-1})(b_{\ell'} - b_{\ell'-1})$$

$$+ f_{13}(b_\ell, b_{\ell'}) - f_{13}(b_{\ell-1}, b_{\ell'}) + f_{13}(b_{\ell-1}, b_{\ell'-1}) \qquad (240)$$

$$- f_{13}(b_\ell, b_{\ell'-1}) \Big]$$

where the function f_{13} is given by

$$f_{13}(\xi, \omega) = \left\{ \left[(\xi - \omega)^2 + \left(\rho_1 + \frac{\xi}{\tan\psi}\right)^2 + \left(\rho_1 + \frac{\omega}{\tan\psi}\right)^2 \right]^2 \right.$$

$$\left. - \left[2\left(\rho_1 + \frac{\xi}{\tan\psi}\right)\left(\rho_1 + \frac{\omega}{\tan\psi}\right) \right]^2 \right\}^{\frac{1}{2}} \qquad (241)$$

For a node on a sphere to a node on a cylinder,

$$F(m, n) = \left\{ \frac{1}{4\rho_0^2 (\cos\theta_{m-1} - \cos\theta_m)} \right\} \Big\{ 2\rho_c (a_n - a_{n-1})(\cos\theta_{m-1} - \cos\theta_m)$$

$$+ f_{14}(a_{n-1}, \theta_{m-1}) - f_{14}(a_{n-1}, \theta_m) \qquad (242)$$

$$+ f_{14}(a_n, \theta_m) - f_{14}(a_n, \theta_{m-1}) \Big\}$$

where

$$f_{14}(\xi, \omega) = \left\{ \left(\left[\xi + \rho_o (\cos \omega - \cos \psi) \right]^2 + \rho_2^2 + \rho_o^2 \sin^2 \omega \right)^2 - (2 \rho_o \rho_2 \sin \omega)^2 \right\}^{\frac{1}{2}} \tag{243}$$

and ρ_o (radius of sphere) is given by

$$\rho_o = \frac{\rho_1}{\sin \psi} \tag{244}$$

For a node on a sphere to a node on a cone,

$$F_{(m,\ell)} = \left\{ \frac{1}{4 \rho_o^2 (\cos \theta_{m-1} - \cos \theta_m)} \right\} \left\{ 2 \rho_o (b_\ell - b_{\ell-1})(\cos \theta_{m-1} - \cos \theta_m) + f_{15}(b_{\ell-1}, \theta_{m-1}) - f_{15}(b_{\ell-1}, \theta_m) + f_{15}(b_\ell, \theta_m) - f_{15}(b_\ell, \theta_{m-1}) \right\} \tag{245}$$

where ρ_o is defined by Equation 244 and

$$f_{15}(\xi, \omega) = \left[\left\{ \left(\xi + \rho_o (\cos \omega - \cos \psi) \right)^2 + \left(\rho_1 + \frac{\xi}{\tan \psi} \right)^2 + \rho_o^2 \sin^2 \omega \right\}^2 - \left\{ 2 \rho_o \sin \omega \left(\rho_1 + \frac{\xi}{\tan \psi} \right) \right\}^2 \right]^{\frac{1}{2}} \tag{246}$$

For a node on a cone to a node on a cylinder,

$$F_{(\ell, n)} = \left[\frac{\frac{1}{2}\sin\psi}{2\rho_1 (b_\ell - b_{\ell-1}) + \frac{(b_\ell)^2 - (b_{\ell-1})^2}{\tan\psi}}\right]\left[2(b_\ell - b_{\ell-1})(a_n - a_{n-1})\right.$$

$$+ f_{16}(a_{n-1},\ b_{\ell-1}) - f_{16}(a_{n-1},\ b_\ell) \qquad (247)$$

$$\left. + f_{16}(a_n,\ b_\ell) - f_{16}(a_n,\ b_{\ell-1})\right]$$

where f_{16} is defined by

$$f_{16}(\xi, \omega) = \left\{\left[(\xi - \omega)^2 + \rho_2^{\,2} + (\rho_1 + \frac{\omega}{\tan\psi})^2\right]^2 - \left[2\rho_2 (\rho_1 + \frac{\omega}{\tan\psi})\right]^2\right\}^{\frac{1}{2}} \qquad (248)$$

For the configuration of Figure 71, the black body interchange factor between two nodes (n and n') is given by

$$F_{(n, n')} = \left[\frac{1}{\pi(b+d)(a_n - a_{n-1})}\right]\left[f_{17}(a_n - a_{n'-1})\right.$$

$$- f_{17}(a_{n-1} - a_{n'-1}) + f_{17}(a_{n-1} - a_{n'}) \qquad (249)$$

$$\left. - f_{17}(a_n - a_{n'})\right]$$

where f_{17} is

$$f_{17}(\xi) = b\sqrt{\xi^2 + d^2}\,\tan^{-1}\frac{b}{\sqrt{\xi^2 + d^2}} - b\,\xi\,\tan^{-1}\frac{b}{\xi}$$

$$+ d\sqrt{\xi^2 + b^2}\,\tan^{-1}\frac{d}{\sqrt{\xi^2 + b^2}} - d\,\xi\,\tan^{-1}\frac{d}{\xi} \qquad (250)$$

$$+ \frac{\xi^2}{2}\ln\frac{(\xi^2 + b^2)(\xi^2 + d^2)}{\xi^2(\xi^2 + b^2 + d^2)}$$

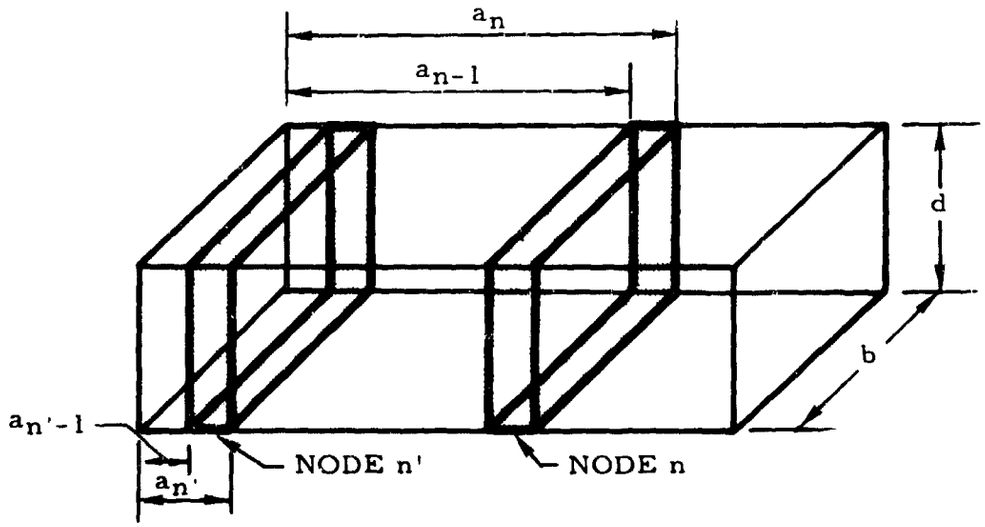

Figure 71. Rectangular Box Configuration

DATA OF ASME PAPER 56-A-144

The configuration factors for various cylindrical shapes presented here were published by H. Leuenberger and R. A. Person in Paper 56-A-144 of the American Society of Mechanical Engineers (Reference 24).

Directly Opposed Parallel Disks

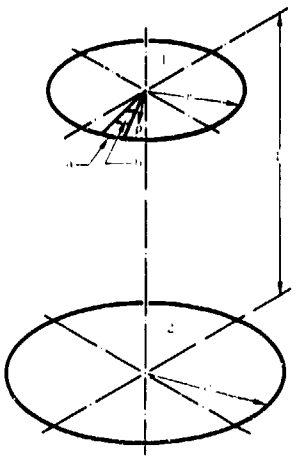

1	UPPER DISK
2	LOWER DISK
r	RADIUS OF UPPER DISK
R	RADIUS OF LOWER DISK
a	DIFFERENTIAL SECTOR OF 1
b	DIFFERENTIAL ELEMENT OF a
ρ	DISTANCE BETWEEN b & DISK AXIS
L	DISTANCE BETWEEN DISKS

$$F_{b,2} = \frac{1}{2}\left(1 - \frac{\rho^2 - R^2 + L^2}{\sqrt{(\rho^2 + R^2 + L^2)^2 - 4\rho^2 R^2}}\right) \tag{251}$$

$$F_{a,2} = F_{12} = \frac{1}{2}\left[1 + \frac{R^2 + L^2}{r^2} - \sqrt{\left(1 + \frac{R^2 + L^2}{r^2}\right)^2 - 4\frac{R^2}{r^2}}\right] \tag{252}$$

when R = r,

$$F_{12} = 1 - \frac{1}{2}\left(\frac{L}{R}\sqrt{4 + \frac{L^2}{R^2}} - \frac{L^2}{R^2}\right)$$

The limiting values are

$L \longrightarrow 0$	$F_{12} = 1$	$R \geq r$
	$F_{12} = R^2/r^2$	$R \leq r$
$L \longrightarrow \infty$	$F_{12} = 0$	
$R \longrightarrow 0$	$F_{12} = 0$	
$R \longrightarrow \infty$	$F_{12} = 1$	
$r \longrightarrow 0$	$F_{12} = R^2/(L^2 + R^2)$	
$r \longrightarrow \infty$	$F_{12} = 0$	

Cylinder

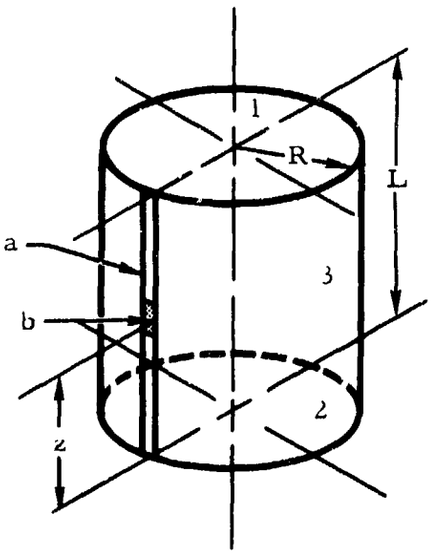

Cylinder

1	TOP OF CYLINDER
2	BOTTOM OF CYLINDER
3	CURVED SURFACE OF CYLINDER
R	RADIUS OF CYLINDER
L	HEIGHT OF CYLINDER
a	DIFFERENTIAL VERTICAL STRIP OF 3
b	DIFFERENTIAL ELEMENT OF a
z	DISTANCE BETWEEN b & 2

$$F_{b,2} = \frac{Z^2 + 2R^2}{2R\sqrt{Z^2 + 4R^2}} - \frac{Z}{2R} \tag{253}$$

$$F_{b,3} = 1 + \frac{L}{2R} - \frac{Z^2 + 2R^2}{2R\sqrt{Z^2 + 4R^2}} - \frac{(L - Z)^2 + 2R^2}{2R\sqrt{(L - Z)^2 + 4R^2}} \tag{254}$$

$$F_{13} = F_{23} = \frac{1}{2}\left(\frac{L}{R}\sqrt{4 + \frac{L^2}{R^2}} - \frac{L^2}{R^2}\right) \tag{255}$$

$$F_{a,2} = F_{32} \tag{256}$$

$$F_{a,3} = F_{33} = 1 - \frac{1}{2}\left(\sqrt{4 + \frac{L^2}{R^2}} - \frac{L}{R}\right) \tag{257}$$

The limiting values are

$L \longrightarrow \infty$ $\quad F_{13} = 1$ $\quad F_{33} = 1$

$L \longrightarrow 0$ $\quad F_{13} = 0$ $\quad F_{33} = 0$

$R \longrightarrow \infty$ $\quad F_{13} = 0$ $\quad F_{33} = 0$

$R \longrightarrow 0$ $\quad F_{13} = 1$ $\quad F_{33} = 1$

$Z \longrightarrow 0$ $\quad F_{b,2} = \frac{1}{2}$

$$F_{b,3} = \frac{1}{2} + \frac{L}{2R} - \frac{L^2 + 2R^2}{2R\sqrt{L^2 + 4R^2}}$$

Directly Opposed Parallel Annuli

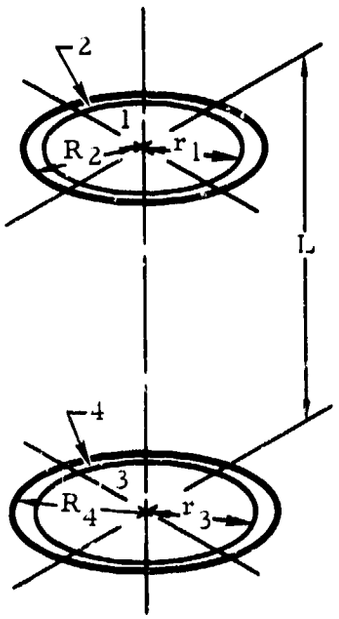

1 INNER DISK CONTAINED BY TOP ANNULUS
2 TOP ANNULUS
3 INNER DISK CONTAINED BY BOTTOM ANNULUS
4 BOTTOM ANNULUS
r INNER RADIUS OF ANNULUS
R OUTER RADIUS OF ANNULUS
L DISTANCE BETWEEN ANNULI
$R_2 > r_1$, $R_4 > r_3$

$$F_{14} = \frac{1}{2}\left[\frac{R_4^2 - r_3^2}{r_1^2} - \sqrt{\left(1 + \frac{R_4^2 + L^2}{r_1^2}\right)^2 - 4\frac{R_4^2}{r_1^2}} + \sqrt{\left(1 + \frac{r_3^2 + L^2}{r_1^2}\right)^2 - 4\frac{r_3^2}{r_1^2}}\right] \tag{258}$$

$$F_{24} = \frac{1}{2(R_2^2 - r_1^2)} \left[\sqrt{(R_2^2 + r_3^2 + L^2)^2 - (2r_3R_2)^2} \right.$$

$$- \sqrt{(R_2^2 + R_4^2 + L^2)^2 - (2R_2R_4)^2} + \sqrt{(r_1^2 + R_4^2 + L^2)^2 - (2r_1R_4)^2}$$

$$\left. - \sqrt{(r_1^2 + r_3^2 + L^2)^2 - (2r_1r_3)^2} \right] \qquad (259)$$

When $R_2 = R_4 = R$ and $r_1 = r_3 = r$,

$$F_{14} = \frac{1}{2} \left[\frac{R^2 - r^2}{r^2} - \sqrt{\left(1 + \frac{R^2 + L^2}{r^2}\right)^2 - 4\left(\frac{R}{r}\right)^2} + \frac{L}{R}\sqrt{4 + \frac{L^2}{R^2}} \right] \qquad (260)$$

$$F_{24} = \left(\frac{R^2}{R^2 - r^2}\right) \left[\sqrt{\left(1 + \frac{r^2 + L^2}{R^2}\right)^2 - 4\left(\frac{r}{R}\right)^2} - \frac{L}{2R}\left(\sqrt{4 + \frac{L^2}{R^2}} + \sqrt{4\frac{r^2}{R^2} + \frac{L^2}{R^2}}\right) \right] \qquad (261)$$

The limiting values are

$L \longrightarrow \infty \quad F_{14} = 0$

$L \longrightarrow \infty \quad F_{24} = 0$

$L \longrightarrow 0 \quad F_{14} = 0 \qquad r_3 > r_1$

$$= 1 - \frac{r_3^2}{r_1^2} \qquad R_4 > r_1 > r_3$$

$$= \frac{R_4^2 - r_3^2}{r_1^2} \qquad r_1 > R_4$$

$L \longrightarrow 0$ $\quad F_{24} = 0 \qquad r_3 > R_2$ or $r_1 > R_4$

$$= \frac{R_2^2 - r_3^2}{R_2^2 - r_1^2} \qquad R_4 > R_2 > r_3 > r_1$$

$$= 1 \qquad R_4 > R_2 \text{ and } r_1 > r_3$$

$$= \frac{R_4^2 - r_1^2}{R_2^2 - r_1^2} \qquad R_2 > R_4 \text{ and } r_1 > r_3$$

$R_2 \longrightarrow r_1$ $\quad F_{24} = \frac{1}{2}\left[\frac{r_1^2 - r_3^2 + L^2}{\sqrt{(r_1^2 + r_3^2 + L^2)^2 - (2r_3r_1)^2}}\right.$

$$\left. - \frac{r_1^2 - R_4^2 + L^2}{\sqrt{(r_1^2 + R_4^2 + L^2)^2 - (2R_4r_1)^2}}\right]$$

$r_1 \longrightarrow 0$ $\quad F_{14} = \frac{R_4^2}{L^2 + R_4^2} - \frac{r_3^2}{L^2 + r_3^2}$

Cylinder and Annulus Contained in Top

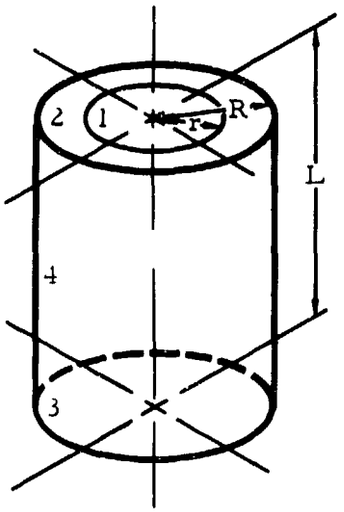

1	DISK CONTAINED IN CYLINDER TOP
2	ANNULUS IN CYLINDER TOP
3	BOTTOM OF CYLINDER
4	CURVED SURFACE OF CYLINDER
r	INNER RADIUS OF ANNULUS
R	RADIUS OF CYLINDER
L	HEIGHT OF CYLINDER

$$F_{24} = \frac{1}{2}\left[1 + \left(\frac{1}{R^2 - r^2}\right)\left(L\sqrt{4R^2 + L^2} - \sqrt{\left(r^2 + R^2 + L^2\right)^2 - (2Rr)^2}\right)\right] \tag{262}$$

$$F_{14} = \frac{1}{2}\left[1 - \frac{R^2 + L^2}{r^2} + \sqrt{\left(1 + \frac{R^2 + L^2}{r^2}\right)^2 - 4\frac{R^2}{r^2}}\right] \tag{263}$$

The limiting values are

$$r \longrightarrow R \qquad F_{24} = \frac{1}{2}\left(1 + \frac{L}{\sqrt{4R^2 + L^2}}\right)$$

Two Concentric Cylinders of Equal Radii (One Above Other)

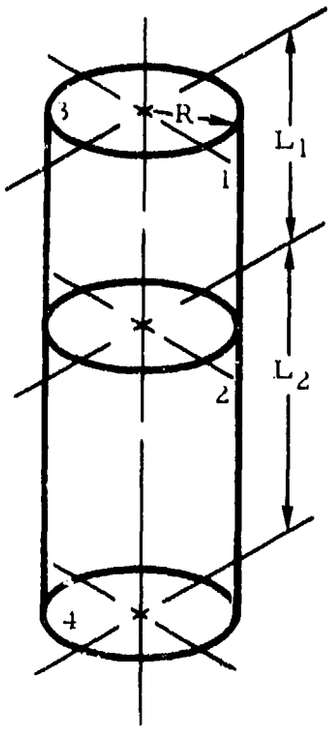

1 CURVED SURFACE OF TOP CYLINDER
2 CURVED SURFACE OF BOTTOM CYLINDER
3 TOP OF CYLINDER 1
4 BOTTOM OF CYLINDER 2
R RADIUS OF CYLINDERS
L_1 HEIGHT OF TOP CYLINDER
L_2 HEIGHT OF BOTTOM CYLINDER

$$F_{14} = \frac{1}{4}\left[\left(\frac{L_1 + L_2}{L_1}\right)\sqrt{4 + \left(\frac{L_1 + L_2}{R}\right)^2} - \frac{L_1 + 2L_2}{R} - \frac{L_2}{L_1}\sqrt{4 + \frac{L_2^2}{R^2}}\right] \quad (264)$$

$$F_{12} = \frac{L_2}{2R} + \frac{1}{4}\left[\sqrt{4 + \frac{L_1^2}{R^2}} + \frac{L_2}{L_1}\sqrt{4 + \frac{L_2^2}{R^2}} - \left(\frac{L_1 + L_2}{L_1}\right)\sqrt{4 + \left(\frac{L_1 + L_2}{R}\right)^2}\right] \quad (265)$$

when $L_1 = L_2 = L$,

$$F_{14} = \frac{1}{4}\left[4\sqrt{1 + \frac{L^2}{R^2}} - \frac{3L}{R} - \sqrt{4 + \frac{L^2}{R^2}}\right] \quad (266)$$

$$F_{12} = \frac{1}{2}\left[\frac{L}{R} + \sqrt{4 + \frac{L^2}{R^2}} - 2\sqrt{1 + \frac{L^2}{R^2}}\right] \quad (267)$$

The limiting values are

$$L_1 \longrightarrow 0 \qquad F_{14} = \frac{L_2^2 + 2R^2}{2R\sqrt{L_2^2 + 4R^2}} - \frac{L_2}{2R}$$

$$F_{12} = \frac{1}{2} + \frac{L_2}{2R} - \frac{L_2^2 + 2R^2}{2R\sqrt{L_2^2 + 4R^2}}$$

Two Concentric Cylinders of Equal Length (One Contained Within Other)

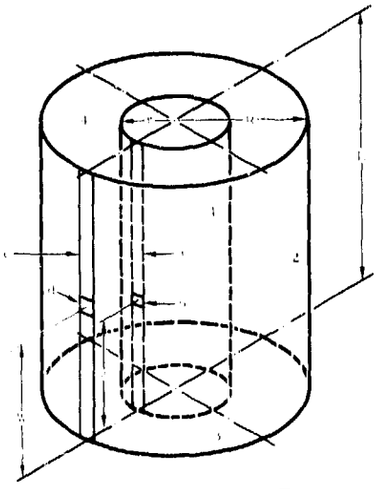

1	CURVED EXTERIOR SURFACE OF INNER CYLINDER
2	CURVED INTERIOR SURFACE OF OUTER CYLINDER
3	BOTTOM ANNULUS CONTAINED BETWEEN 1 & 2
4	TOP ANNULUS CONTAINED BETWEEN 1 & 2
R	RADIUS OF OUTER CYLINDER
r	RADIUS OF INNER CYLINDER
L	HEIGHT OF CYLINDERS
a	DIFFERENTIAL VERTICAL STRIP OF 1
b	DIFFERENTIAL ELEMENT OF a
c	DIFFERENTIAL VERTICAL STRIP OF 2
d	DIFFERENTIAL ELEMENT OF c
z	DISTANCE BETWEEN b & 3
W	DISTANCE BETWEEN d & 3

$$F_{d,1} = \frac{r}{R}\left[2 - \frac{1}{\pi}\left\{\cos^{-1}\frac{W^2 - R^2 + r^2}{W^2 + R^2 - r^2} + \cos^{-1}\frac{(L-W)^2 - R^2 + r^2}{(L-W)^2 + R^2 - r^2}\right.\right.$$

$$\left.\left. - \frac{W}{r}\left[\frac{W^2 + R^2 + r^2}{\sqrt{(W^2 + R^2 + r^2)^2 - 4r^2R^2}}\cos^{-1}\frac{r(W^2 - R^2 + r^2)}{R(W^2 + R^2 - r^2)}\right]\right\}\right]$$

$$- \frac{r}{R}\left[2 - \frac{1}{\pi}\left\{\left(\frac{L-W}{r}\right)\frac{(L-W)^2 + R^2 + r^2}{\sqrt{\left[(L-W)^2 + R^2 + r^2\right]^2 - 4r^2R^2}}\ \mathbf{X}\right.\right. \qquad (268)$$

$$\cos^{-1}\ \frac{r\left[(L-W)^2 - R^2 + r^2\right]}{R\left[(L-W)^2 + R^2 - r^2\right]}\Bigg\}\Bigg] + \frac{r}{R}\left[2 - \frac{1}{\pi}\left\{\frac{L}{r}\ \cos^{-1}\ \frac{r}{R}\right\}\right]$$

$$F_{d,2} = 2\left(1 - \frac{r}{R}\right) + \frac{L}{2R} - \frac{W^2 + 2R^2}{2R\sqrt{4R^2 + W^2}} - \frac{(L-W)^2 + 2R^2}{2R\sqrt{4R^2 + (L-W)^2}} \qquad (269)$$

$$+ \frac{1}{\pi}\Bigg[\frac{2r}{R}\left(\tan^{-1}\ \frac{2\sqrt{R^2 - r^2}}{W} + \tan^{-1}\ \frac{2\sqrt{R^2 - r^2}}{L-W}\right) + \frac{L}{R}\sin^{-1}\left(1 - \frac{2r^2}{R^2}\right)$$

$$- \frac{W^2 + 2R^2}{R\sqrt{4R^2 + W^2}}\ \sin^{-1}\ \frac{4(R^2 - r^2) + \frac{W^2}{R^2}(R^2 - 2r^2)}{W^2 + 4(R^2 - r^2)}$$

$$- \frac{(L-W)^2 + 2R^2}{R\sqrt{4R^2 + (L-W)^2}}\ \sin^{-1}\ \frac{4(R^2 - r^2) + \frac{(L-W)^2}{R^2}(R^2 - 2r^2)}{(L-W)^2 + 4(R^2 - r^2)}\Bigg]$$

$$F_{d,3} = \frac{1}{2} - (F^*_{d,1} + F^*_{d,2}) \qquad (270)$$

*Evaluated with L replaced by W

$$F_{b,3} = \frac{1}{2\pi}\Bigg\{\cos^{-1}\ \frac{Z^2 - R^2 + r^2}{Z^2 + R^2 - r^2} - \frac{Z}{r}\Bigg[\frac{Z^2 + R^2 + r^2}{\sqrt{(Z^2 + R^2 + r^2)^2 - 4R^2r^2}}\ X \qquad (271)$$

$$\cos^{-1}\ \frac{r(Z^2 - R^2 + r^2)}{R(Z^2 + R^2 - r^2)} - \cos^{-1}\ \frac{r}{R}\Bigg]\Bigg\}$$

$$F_{b,2} = 1 - (F_{b,3} + F_{b,4}) \qquad (272)$$

$$F_{21} = F_{c,1} = \frac{r}{R}\left[1 - \frac{1}{\pi}\left\{\cos^{-1}\frac{L^2 - R^2 + r^2}{L^2 + R^2 - r^2}\right.\right. \tag{273}$$

$$- \frac{1}{2rL}\left[\sqrt{(L^2 + R^2 + r^2)^2 - (2Rr)^2}\ \cos^{-1}\frac{r(L^2 - R^2 + r^2)}{R(L^2 + R^2 - r^2)}\right.$$

$$\left.\left.\left. + (L^2 - R^2 + r^2)\left(\sin^{-1}\frac{r}{R}\right) - \frac{\pi}{2}\ (L^2 + R^2 - r^2)\right]\right\}\right]$$

$$F_{22} = F_{c,2} = 1 - \frac{r}{R} + \frac{1}{\pi}\left\{\frac{2r}{R}\tan^{-1}\frac{2\sqrt{R^2 - r^2}}{L}\right. \tag{274}$$

$$- \frac{L}{2R}\left[\frac{\sqrt{4R^2 + L^2}}{L}\sin^{-1}\frac{4(R^2 - r^2) + \frac{L^2}{R^2}(R^2 - 2r^2)}{L^2 + 4(R^2 - r^2)}\right.$$

$$\left.\left. - \sin^{-1}\frac{R^2 - 2r^2}{R^2} + \frac{\pi}{2}\left(\frac{\sqrt{4R^2 + L^2}}{L} - 1\right)\right]\right\}$$

Values calculated from Equations 273 and 274 are in agreement with values obtained by approximate numerical methods by Hamilton and Morgan (Reference 22).

$$F_{23} = F_{c,3} = \frac{1}{2}(1 - F_{21} - F_{22}) \tag{275}$$

$$F_{34} = 1 - \left(\frac{L}{R^2 - r^2}\right)\left[r - R(F_{22} + 2F_{21} - 1)\right] \tag{276}$$

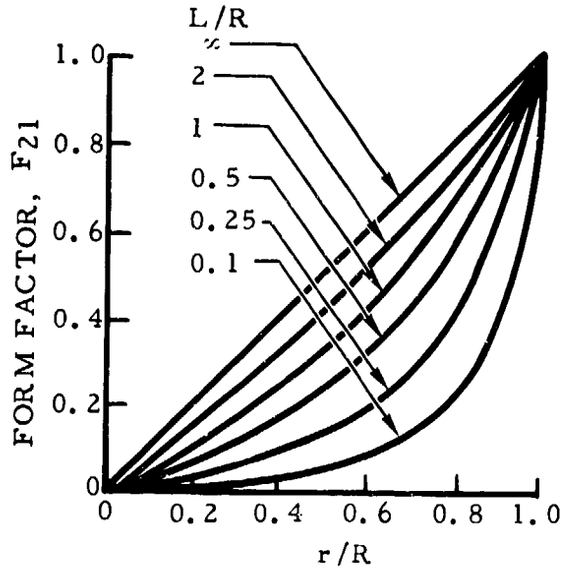

Figure 72. Form Factor From Outer Cylinder to Inner Cylinder

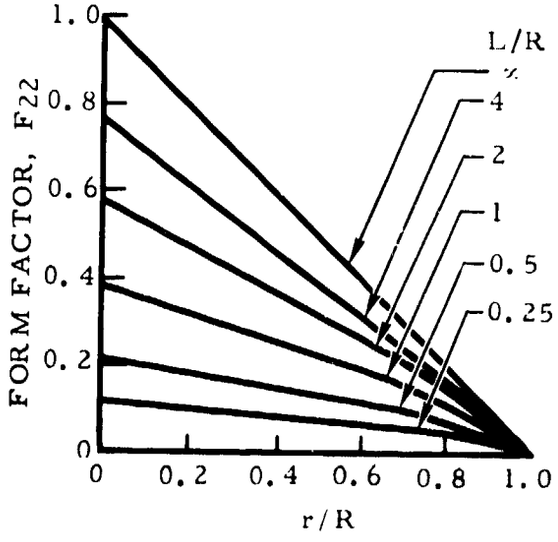

Figure 73. Form Factor From Outer Cylinder to Itself

The limiting values are

$L \longrightarrow 0$ $\quad F_{21} = 0$

$\quad F_{22} = 0$

$\quad F_{23} = 1/2$

$\quad F_{34} = 1$

$L \longrightarrow \infty$ $\quad F_{21} = r/R$

$\quad F_{22} = 1 - r/R$

$\quad F_{23} = 0$

$\quad F_{34} = 0$

$r \longrightarrow 0$ $\quad F_{21} = 0$

$$F_{22} = 1 - \frac{1}{2}\left(\sqrt{4 + \frac{L^2}{R^2}} - \frac{L}{R}\right)$$

$$F_{23} = \frac{1}{2}\left(\sqrt{4 + \frac{L^2}{R^2}} - \frac{L}{R}\right)$$

$$F_{34} = 1 - \frac{1}{2}\left(\frac{L}{R}\sqrt{4 + \frac{L^2}{R^2}} - \frac{L^2}{R^2}\right)$$

$r \longrightarrow R$ $\quad F_{21} = 1$

$\quad F_{22} = 0$

$\quad F_{23} = 0$

$\quad F_{34} = 0$

$W \longrightarrow L$ or $W \longrightarrow 0$

$$F_{d,1} = \frac{r}{R}\left[1 - \frac{1}{\pi}\left\{\cos^{-1}\frac{L^2 - R^2 + r^2}{L^2 + R^2 - r^2} - \frac{L}{r}\left[\frac{L^2 + R^2 + r^2}{\sqrt{(L^2 + R^2 + r^2)^2 - 4r^2R^2}} \times \cos^{-1}\frac{r(L^2 - R^2 + r^2)}{R(L^2 + R^2 - r^2)} - \cos^{-1}\frac{r}{R}\right]\right\}\right]$$

$$2 \longrightarrow L \text{ or } 2 \longrightarrow 0 \qquad F_{d,2} = 1 - \frac{r}{R} + \frac{L}{2R} - \frac{L^2 + 2R^2}{2R\sqrt{L^2 + 4R^2}}$$

$$+ \frac{1}{\pi}\left[\frac{2r}{R}\tan^{-1}\frac{2\sqrt{R^2 - r^2}}{L} + \frac{L}{R}\sin^{-1}\left(1 - \frac{2r^2}{R^2}\right)\right.$$

$$\left. - \frac{L^2 + 2R^2}{R\sqrt{L^2 + 4R^2}}\sin^{-1}\frac{4(R^2 - r^2) + \frac{L^2}{2}(R^2 - 2r^2)}{L^2 + 4(R^2 - r^2)}\right]$$

Cylinder and Plane of Equal Length Parallel to Cylinder Axis (Plane Outside Cylinder)

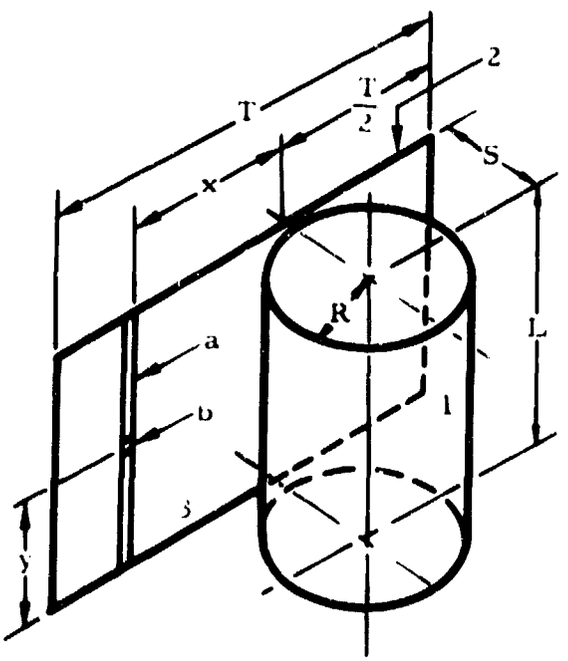

1	CURVED SURFACE OF CYLINDER
2	PLANE
3	ONE-HALF OF PLANE
R	RADIUS OF CYLINDER
L	HEIGHT OF CYLINDER & PLANE
S	DISTANCE FROM CYLINDER AXIS TO PLANE
T	LENGTH OF PLANE
a	VERTICAL DIFFERENTIAL STRIP OF 2
b	DIFFERENTIAL ELEMENT OF a
x	DISTANCE FROM a TO CENTER OF 2
y	DISTANCE FROM BOTTOM EDGE OF PLANE TO b
S	$\geq$ R

$$F_{b,1} = \frac{SR}{S^2+x^2}\left[2 - \frac{1}{\pi}\left\{\cos^{-1}\frac{y^2 - S^2 - x^2 + R^2}{y^2 + S^2 + x^2 - R^2}\right.\right.$$

$$+ \cos^{-1}\frac{(L-y)^2 - S^2 - x^2 + R^2}{(L-y)^2 + S^2 + x^2 - R^2} \qquad (277)$$

$$\left. - \frac{y}{R}\left[\frac{y^2 + S^2 + x^2 + R^2}{\sqrt{(y^2 + S^2 + x^2 - R^2)^2 + 4y^2R^2}}\right.\right. \times$$

$$\left.\left.\cos^{-1}\frac{R(y^2 - S^2 - x^2 + R^2)}{\left(\sqrt{S^2+x^2}\right)(y^2 + S^2 + x^2 - R^2)}\right]\right\}\Bigg]$$

$$- \frac{SR}{S^2+x^2}\left[2 - \frac{1}{\pi}\left\{\left(\frac{L-y}{R}\right)\frac{(L-y)^2 + S^2 + x^2 + R^2}{\sqrt{\left[(L-y)^2 + S^2 + x^2 - R^2\right]^2 + 4(L-y)^2R^2}}\right.\right. \times$$

$$\cos^{-1}\frac{R\left[(L-y)^2 - S^2 - x^2 + R^2\right]}{\sqrt{S^2+x^2}\left[(L-y)^2 + S^2 + x^2 - R^2\right]}$$

$$\left.\left. + \frac{L}{R}\cos^{-1}\frac{R}{\sqrt{S^2+x^2}}\right\}\right]$$

$$F_{a,1} = \frac{SR}{S^2+x^2}\left[1 - \frac{1}{\pi}\left\{\cos^{-1}\frac{L^2 - S^2 - x^2 + R^2}{L^2 + S^2 + x^2 - R^2}\right.\right.$$

$$- \frac{1}{2RL}\left[\sqrt{(L^2 + S^2 + x^2 + R^2)^2 + 4L^2R^2}\right. \times$$

$$\cos^{-1}\frac{R(L^2 - S^2 - x^2 + R^2)}{\sqrt{S^2+x^2}\,(L^2 + S^2 + x^2 - R^2)}$$

$$+ (L^2 - S^2 - x^2 + R^2)\sin^{-1}\frac{R}{\sqrt{S^2+x^2}}$$

$$\left.\left.\left. - \frac{\pi}{2}(L^2 + S^2 + x^2 - R^2)\right]\right\}\right] \qquad (278)$$

$$F_{21} = F_{31} = \frac{2}{T}\int_0^{T/2} F_{a,1}\, dx \qquad (279)$$

The limiting values are

$y \longrightarrow 0$ or $y \longrightarrow L$

$$F_{b,1} = \frac{SR}{S^2 + x^2}\left[1 - \frac{1}{\pi}\left\{\cos^{-1}\frac{L^2 - S^2 - x^2 + R^2}{L^2 + S^2 + x^2 - R^2} - \frac{L}{R}\left[\frac{L^2 + S^2 + x^2 + R^2}{\sqrt{(L^2 + S^2 + x^2 - R^2)^2 + 4L^2R^2}}\right.\right.\right.$$

$$\left.\left.\left. \times \cos^{-1}\frac{R(L^2 - S^2 - x^2 + R^2)}{\sqrt{S^2 + x^2}\,(L^2 + S^2 + x^2 - R^2)} - \cos^{-1}\frac{R}{\sqrt{S^2 + x^2}}\right]\right\}\right]$$

$L \longrightarrow \infty$

$$F_{b,1} = \frac{RS}{S^2 + x^2}$$

$$F_{a,1} = \frac{RS}{S^2 + x^2}$$

$$F_{21} = F_{31} = \frac{2R}{T}\tan^{-1}\frac{T}{2S}$$

$L \longrightarrow 0$

$$F_{b,1} = 0$$

$$F_{a,1} = 0$$

$$F_{21} = 0$$

$S \longrightarrow \infty$

$$F_{b,1} = 0$$

$$F_{a,1} = 0$$

$$F_{21} = 0$$

$R \longrightarrow 0$

$$F_{b,1} = 0$$

$$F_{a,1} = 0$$

$$F_{21} = 0$$

$T \longrightarrow 0$ $\quad F_{21} = F_{a,1}$ where $F_{a,1}$ is evaluated at $x = 0$

$$S \longrightarrow R \qquad F_{b,1} = \left(\frac{R^2}{R^2 + x^2}\right) \left[2 - \frac{1}{\pi} \left\{ \cos^{-1} \frac{y^2 - x^2}{y^2 + x^2} \right.\right.$$

$$+ \cos^{-1} \frac{(L - y)^2 - x^2}{(L - y)^2 + x^2} - \frac{y}{R} \left[\frac{y^2 + x^2 + 2R^2}{\sqrt{(y^2 + x^2)^2 - 4y^2R^2}} \times \right.$$

$$\left. \cos^{-1} \frac{R\,(y^2 - x^2)}{\sqrt{R^2 + x^2}\,(y^2 + x^2)} \right]$$

$$- \frac{L - y}{R} \left(\frac{(L - y)^2 + x^2 + 2R^2}{\sqrt{\left[(L - y)^2 + x^2\right]^2 - 4\,(L - y)^2\,R^2}} \times \right.$$

$$\left. \cos^{-1} \frac{R\,\left[(L - y)^2 - x^2\right]}{\sqrt{R^2 + x^2}\,\left[(L - y)^2 + x^2\right]} \right)$$

$$\left. \left. + \frac{L}{R} \cos^{-1} \frac{R}{\sqrt{R^2 + x^2}} \right\} \right]$$

$$S \longrightarrow R \qquad F_{a,1} = \frac{R^2}{R^2 + x^2} \left\{ 1 - \frac{1}{\pi} \left[\cos^{-1} \frac{L^2 - x^2}{L^2 + x^2} \right.\right.$$

$$- \frac{1}{2RL} \left\{ \sqrt{(L^2 + x^2)^2 + 4L^2R^2}\, \cos^{-1} \frac{R\,(L^2 - x^2)}{\sqrt{R^2 + x^2}\,(L^2 + x^2)} \right.$$

$$\left. \left. \left. + (L^2 - x^2)\, \sin^{-1} \frac{R}{\sqrt{R^2 + x^2}} - \frac{\pi}{2}\,(L^2 + x^2) \right\} \right] \right\}$$

Cylinder and Plane of Equal Length Parallel to Cylinder Axis (Plane Inside Cylinder)

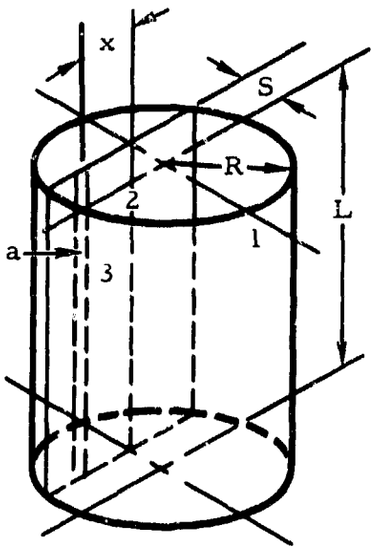

1	VERTICAL INNER SURFACE OF CYLINDER
2	SIDE OF PLANE FACING 1
3	ONE-HALF OF PLANE
R	RADIUS OF CYLINDER
L	HEIGHT OF CYLINDER & PLANE
S	DISTANCE FROM CYLINDER AXIS TO PLANE (TAKEN POSITIVE AS SHOWN)
a	VERTICAL DIFFERENTIAL STRIP OF 2
x	DISTANCE FROM a TO CENTER OF PLANE

$$F_{a,1} = 1 - \frac{1}{\pi}\Bigg[\tan^{-1}\frac{\sqrt{R^2-S^2}+x}{L} + \tan^{-1}\frac{\sqrt{R^2-S^2}-x}{L}$$

$$+ \frac{x\,(R^2-S^2-x^2)}{4L\,(x^2+S^2)}\ln\left[\left(\frac{\sqrt{R^2-S^2}+x}{\sqrt{R^2-S^2}-x}\right)^2\left(\frac{(\sqrt{R^2-S^2}-x)^2+L^2}{(\sqrt{R^2-S^2}+x)^2+L^2}\right)\right]$$

$$+ \frac{xL}{4\,(x^2+S^2)}\ln\frac{(\sqrt{R^2-S^2}-x)^2+L^2}{(\sqrt{R^2-S^2}+x)^2+L^2} + \left\{\frac{S}{4L\,(x^2+S^2)}\right\} X$$

$$\left\{L^2\left[\cos^{-1}\frac{S^2-x\sqrt{R^2-S^2}}{R\sqrt{S^2+x^2}} + \cos^{-1}\frac{S^2+x\sqrt{R^2-S^2}}{R\sqrt{S^2+x^2}} - 2\pi\right]\right.$$

$$\left. + \left[\sqrt{(L^2+R^2+S^2+x^2)^2 - 4R^2(x^2+S^2)}\right]\right\} X$$

$$\left[\cos^{-1}\frac{2R^2x^2+S^2(R^2-S^2-x^2-L^2)+x(R^2+S^2+x^2+L^2)\sqrt{R^2-S^2}}{R\sqrt{S^2+x^2}\left[(\sqrt{R^2-S^2}+x)^2+L^2\right]}\right]$$

(280)

$$+ \cos^{-1} \frac{2R^2x^2 + S^2(R^2 - S^2 - x^2 - L^2) - x(R^2 + S^2 + x^2 + L^2)\sqrt{R^2 - S^2}}{R\sqrt{S^2 + x^2}\left[\left(\sqrt{R^2 - S^2} - x\right)^2 + L^2\right]}\Bigg]$$

$$- (R^2 - S^2 - x^2)\left[\cos^{-1} \frac{S^2(R^2 - S^2 - x^2) + 2R^2x^2 - x(R^2 + S^2 + x^2)\sqrt{R^2 - S^2}}{R\sqrt{S^2 + x^2}\left(\sqrt{R^2 - S^2} - x\right)^2}\right.$$

$$\left.\left.\left. + \cos^{-1} \frac{S^2(R^2 - S^2 - x^2) + 2R^2x^2 + x(R^2 + S^2 + x^2)\sqrt{R^2 - S^2}}{R\sqrt{S^2 + x^2}\left(\sqrt{R^2 - S^2} + x\right)^2}\right]\right\}\Bigg]$$

$$F_{21} = F_{31} = \frac{1}{\sqrt{R^2 - S^2}} \int_0^{\sqrt{R^2 - S^2}} F_{a,1}\, dx \qquad (281)$$

The limiting values are

$$x \longrightarrow 0 \qquad F_{a,1} = 1 - \frac{2}{\pi}\left\{\tan^{-1}\frac{\sqrt{R^2 - S^2}}{L} + \frac{1}{4LS}\left[(L^2 - R^2 + S^2)\cos^{-1}\frac{S}{R}\right.\right.$$

$$\left.\left. - \pi L^2 + \sqrt{(L^2 + R^2 + S^2)^2 - 4R^2S^2}\,\cos^{-1}\frac{S(R^2 - S^2 - L^2)}{R(R^2 - S^2 + L^2)}\right]\right\}$$

$$S \longrightarrow 0 \qquad F_{a,1} = 1 - \frac{1}{\pi}\left\{\tan^{-1}\frac{R + x}{L} + \tan^{-1}\frac{R - x}{L}\right.$$

$$+ \frac{R^2 - x^2}{4LX}\ln\left[\left(\frac{R + x}{R - x}\right)^2\left(\frac{(R - x)^2 + L^2}{(R + x)^2 + L^2}\right)\right]$$

$$\left. + \frac{L}{4x}\ln\frac{(R - x)^2 + L^2}{(R + x)^2 + L^2}\right\}$$

$$x \longrightarrow 0 \quad \text{and } S \longrightarrow R \qquad F_{a,1} = \frac{1}{4}\left(\frac{\sqrt{L^2 + 4R^2}}{R} - \frac{L}{R}\right)$$

$$L \longrightarrow \infty \qquad F_{a,1} = 1$$

$$F_{21} = 1$$

Two Concentric Cylinders of Unequal Radii (One Atop Other)

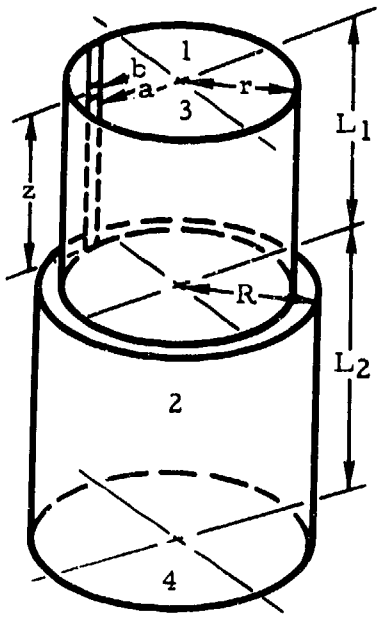

1	INNER CURVED SURFACE OF TOP CYLINDER
2	INNER CURVED SURFACE OF BOTTOM CYLINDER
3	TOP OF CYLINDER 1
4	BASE OF CYLINDER 2
R	RADIUS OF 2
r	RADIUS OF 1
L_1	HEIGHT OF 1
L_2	HEIGHT OF 2
a	DIFFERENTIAL VERTICAL ELEMENT OF 1
b	DIFFERENTIAL ELEMENT OF a
z	HEIGHT OF b FROM BASE OF 1
R	$\geqq$ r

For

$$\frac{L_2}{L_1} \leqq \frac{1}{2}\left(\frac{R}{r} - 1\right) \quad \text{(2 receives no direct radiation from 3)}$$

$$F_{12} = \frac{r}{4L_1}\left[1 - \frac{R^2 + L_2^2}{r^2} + \sqrt{\left(1 + \frac{R^2 + L_2^2}{r^2}\right)^2 - 4\frac{R^2}{r^2}}\right] \qquad (282)$$

$$F_{14} = \frac{1}{4}\left(\sqrt{4 + \frac{L_1^2}{r^2}} - \frac{L_1}{r}\right) - \frac{r}{4L_1}\left[1 - \frac{R^2 + L_2^2}{r^2} + \sqrt{\left(1 + \frac{R^2 + L_2^2}{r^2}\right)^2 - 4\frac{R^2}{r^2}}\right] \qquad (283)$$

For

$$\frac{L_2}{L_1} \geqq \frac{1}{2}\left(\frac{R}{r} - 1\right)$$

$$F_{b,4} = \frac{1}{\pi}\left[\frac{Z^2 + 2r^2}{r\sqrt{Z^2 + 4r^2}} \tan^{-1}\frac{\sqrt{Z^2 + 4r^2}\sqrt{R^2 - r^2}}{\sqrt{r^2(2L_2 + Z)^2 - R^2Z^2}}\right. \tag{284}$$

$$\left. - \frac{Z}{r}\sin^{-1}\frac{Z\sqrt{R^2 - r^2}}{2r\sqrt{L_2(L_2 + Z)}}\right] + \frac{1}{\pi}\left(\frac{Z + L_2}{2r}\right)\left\{\frac{R^2 + r^2 + (Z + L_2)^2}{\sqrt{\left[(Z + L_2)^2 + R^2 + r^2\right]^2 - 4R^2r^2}}\right. \text{X}$$

$$\cos^{-1}\frac{2r^2L_2\left[R^2 - r^2 - (Z + L_2)^2\right] + Z(R^2 - r^2)\left[R^2 - r^2 + (Z + L_2)^2\right]}{2Rr(Z + L_2)\left[L_2(Z + L_2) + R^2 - r^2\right]}$$

$$\left. - \cos^{-1}\frac{Z(R^2 - r^2) - 2L_2r^2}{2RrL_2}\right\}$$

$$F_{14} = F_{a,4} = \frac{\int_o^{L_1} F_{b,4}\,dZ}{L_1} \tag{285}$$

$$F_{12} = \frac{1}{4}\left[\sqrt{4 + \frac{L_1^2}{R^2}} - \frac{L_1}{R}\right] - F_{a,4} \tag{286}$$

The limiting values are

$$\cdot 0: \quad F_{b,4} = \frac{1}{\pi}\left\{\tan^{-1}\frac{\sqrt{R^2 - r^2}}{L_2} + \frac{L_2}{2r}\left[\left(\frac{R^2 + r^2 + L_2^2}{\sqrt{(L_2^2 + R^2 + r^2)^2 - 4R^2r^2}}\right) X\right.\right.$$

$$\left.\left.\left(\cos^{-1}\frac{r(R^2 - r^2 - L_2^2)}{R(L_2^2 + R^2 - r^2)}\right) - \cos^{-1}\left(-\frac{r}{R}\right)\right]\right\}$$

$$\begin{array}{l} Z \longrightarrow 0 \\ \text{and } r \longrightarrow R \end{array} \quad F_{b,4} = \frac{L_2^2 + 2R^2}{2R\sqrt{L_2^2 + 4R^2}} - \frac{L_2}{2R}$$

$$r \longrightarrow R \quad F_{14} = \frac{1}{4}\left[\left(\frac{L_1 + L_2}{L_1}\right)\sqrt{4 + \frac{(L_1 + L_2)^2}{R^2}} - \frac{L_1 + 2L_2}{R}\right.$$

$$\left. - \frac{L_2}{L_1}\sqrt{4 + \frac{L_2^2}{R^2}}\right]$$

Two Concentric Cylinders of Unequal Length (One Enclosed by Other)

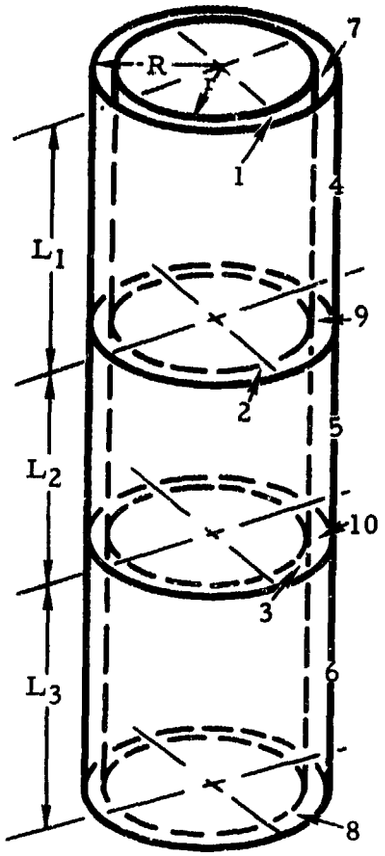

1	EXTERIOR SURFACE OF TOP INNER CYLINDER
2	EXTERIOR SURFACE OF MIDDLE INNER CYLINDER
3	EXTERIOR SURFACE OF BOTTOM INNER CYLINDER
4	INTERIOR SURFACE OF TOP OUTER CYLINDER
5	INTERIOR SURFACE OF MIDDLE OUTER CYLINDER
6	INTERIOR SURFACE OF BOTTOM OUTER CYLINDER
7	ANNULUS BETWEEN TOPS OF 1 & 4
8	ANNULUS BETWEEN BOTTOMS OF 3 & 6
9	ANNULUS BETWEEN BOTTOMS OF 1 & 4
10	ANNULUS BETWEEN BOTTOMS OF 2 & 5
R	RADIUS OF OUTER CYLINDERS
r	RADIUS OF INNER CYLINDERS
L_1	HEIGHT OF TOP CYLINDERS
L_2	HEIGHT OF MIDDLE CYLINDERS
L_3	HEIGHT OF BOTTOM CYLINDERS

9 & 10 ARE USED FOR CALCULATION PURPOSES ONLY & DO NOT SHIELD RADIATION BETWEEN CYLINDERS

$$F_{2,(4+5+6)} = 1 - \frac{R^2 - r^2}{2rL_2}\left[F_{7,(1+2)} + F_{8,(2+3)} - F_{71} - F_{83}\right] \tag{287}$$

$$F_{5,(1+2+3)} = F_{52} + \frac{1}{RL_2}\left[r(L_1F_{19} + L_3F_{3,10}) - \left(\frac{R^2 - r^2}{2}\right)(F_{10,(1+2)} - F_{9,(2+3)} - F_{10,2} - F_{92})\right] \tag{288}$$

The F's on the right-hand side of Equations 287 and 288 may be evaluated from data given for two concentric cylinders of equal length.

DISCUSSION

To permit full utilization of the foregoing tabulated data, a summary of configuration factor properties and a discussion of some useful techniques follows (from Reference 25).

Reciprocity

The reciprocity relationship for the configuration factor from A_1 to A_2 is

$$A_1 F_{12} = A_2 F_{21} \tag{289}$$

This relationship often allows a great simplification in the analysis of configuration factors; F_{21} can be obtained directly from F_{12} and the areas of the surfaces.

Sum Equals Unity

By definition, the sum of the configuration factors to all surfaces seen by a given surface is unity. This relationship is often written as

$$\sum_{n=2}^{n=m} F_{(1,n)} = 1.0 \tag{290}$$

where

m = Total number of surfaces

Yamauti Modified Reciprocity Relationship

A modified reciprocity relationship, given by Yamauti, is also useful. (A general proof of this relationship is given in Reference 26, p. 336-337). This relationship in terms of the areas of Figure 74 is

$$F_{14} A_1 = F_{32} A_3 = F_{23} A_2 = F_{41} A_4 \tag{291}$$

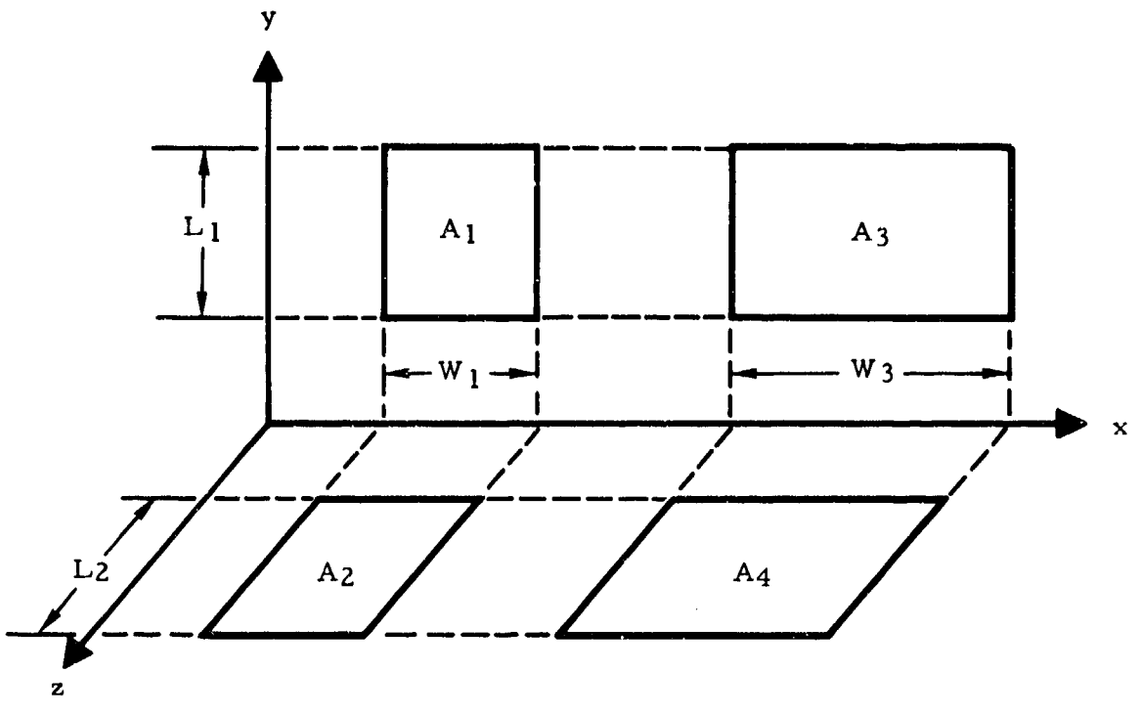

Figure 74. Geometry for Yamauti's Modified Reciprocity Relationship

The relations of Equation 291 assume perfectly diffusing surfaces of uniform radiant intensity located as shown in Figure 74. As indicated, areas A_1 and A_3 lie on one plane, and areas A_2 and A_4 lie on another plane. In addition, the width W_3 of A_3 and A_4 is the same as is the width W_1 of A_1 and A_2. As long as these geometrical conditions hold, the modified reciprocity relationship of Equation 291 is applicable and can be applied to planes at any other angle, including planes that are parallel. This relation is especially useful in dealing with rectangular areas.

Application of Configuration Factor Properties to Problem

Consider the infinitely long enclosure of Figure 75. Suppose that the configuration factor F_{32} is known and that the problem is to determine the remaining configuration factors in the enclosure. An obvious solution is to use the string method (page 156). However, for purposes of demonstration, the following solution will utilize several of the special properties described above.

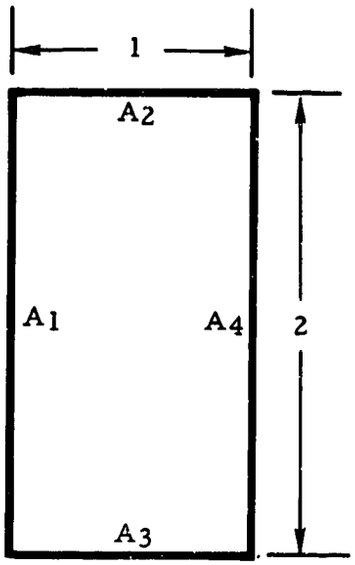

Figure 75. Diagram of Infinitely Long Enclosure

The enclosure of Figure 75 is symmetrical in that $A_1 = A_4$ and $A_2 = A_3$. Because of this symmetry, the following configuration factor relationship can be written as

$$F_{41} = F_{14}$$

$$F_{32} = F_{23} \tag{292}$$

$$F_{31} = F_{34} = F_{21} = F_{24}$$

Assuming that F_{34} is desired, apply Equation 290 to area A_3,

$$F_{32} + F_{31} + F_{34} = 1.0 \tag{293}$$

Using the relations of Equation 292 in Equation 293 yields an expression for F_{34} in terms of the known configuration factor F_{32}.

$$F_{34} = \frac{1 - F_{32}}{2} \tag{294}$$

Once F_{34} is known, the remaining configuration factors for Figure 75 can be determined by the reciprocity relationship. For example, the configuration factor F_{43} is given by

$$F_{43} = F_{34} \frac{A_3}{A_4} \tag{295}$$

Configuration Factor Algebra

In many instances it becomes necessary to determine configuration factors which cannot be found directly from the tabulated data. For example, consider the case of a surface A_3, which is perpendicular to a second surface A_2, and the two surfaces do not have a common edge as shown by diagram 2 of Figure 76. The configuration factor F_{32} for this configuration is desired. As is evident from the geometry of diagram 2 (Figure 76), F_{32} cannot be evaluated directly from the graphical data.

A convenient technique for evaluating F_{32} is to consider the flux transfer between a fictitious source consisting of surfaces A_3 and A_1 and the area A_2. Denote the flux received by area A_2 from $A_{(1+3)}$ as $\phi_{(1+3,2)}$. From this must be subtracted the flux ϕ_{12} due to the source A_1 yielding

$$\phi_{32} = \phi_{(1+3,2)} - \phi_{12} \tag{296}$$

The total flux leaving an area A_n which is incident on an area A_m is given by

$$\phi_{(n,m)} = J_n F_{(n,m)} A_n \tag{297}$$

where

J_n = Radiosity or total flux per unit area streaming away from surface n

Substituting Equation 297 into Equation 296 yields

$$J_3 F_{32} A_3 = J_{(1+3)} F_{(1+3,2)} A_{(1+3)} - J_1 F_{12} A_1 \tag{298}$$

Assuming that $J_3 = J_{(1+3)} = J_1 = 1.0$, Equation 298 becomes

$$F_{32} A_3 = F_{(1+3,2)} A_{(1+3)} - F_{12} A_1 \tag{299}$$

(1) 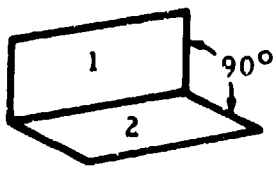

Basic perpendicular configuration (for F_{21} or F_{12} use configuration factor graphs)

$$A_3F_{32} = A_2F_{23}$$

(2) 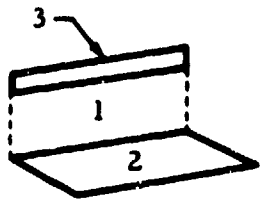

$$= A_{(1+3)}F_{(1+3,\,2)} - A_1F_{12}$$

$$A_1F_{14} = A_4F_{41}$$

(3) 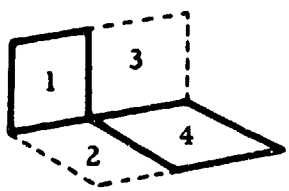

$$= 1/2\left[A_{(1+3)}F_{(1+3,\,2+4)} - A_1F_{12} - A_3F_{34}\right]$$

$$A_1F_{(1,\,2+4)} = A_{(2+4)}F_{(2+4,\,1)}$$

(4) 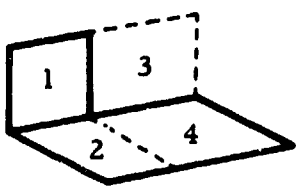

$$= 1/2\left[A_{(1+3)}F_{(1+3,\,2+4)} - A_3F_{34} + A_1F_{(12)}\right]$$

$$A_3F_{(3,\,2+4+6)} = A_{(2+4+6)}F_{(2+4+6,\,3)}$$

(5) 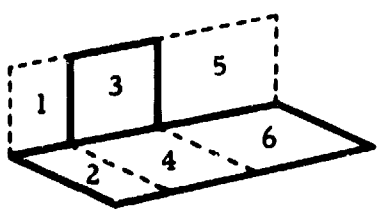

$$= 1/2\left[A_{(1+3)}F_{(1+3,\,2+4)} + A_{(3+5)}F_{(3+5,\,4+6)} - A_1F_{12} - A_5F_{5(}\right]$$

Figure 76. Diagrams of Configuration Factor Algebra (Sheet 1 of 2)

(6)

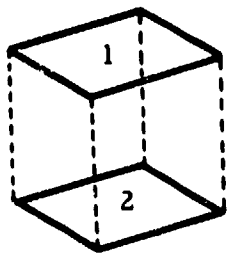

Basic parallel configuration ($A_1 = A_2$) (for F_{12} or F_{21} use configuration factor graphs)

$$A_1F_{(1,\,2+4)} = A_{(2+4)}F_{(2+4,\,1)}$$
$$= 1/2\left[A_{(1+3)}F_{(1+3,\,2+4)} + A_1F_{12} - A_3F_{34} \right]$$

(7)

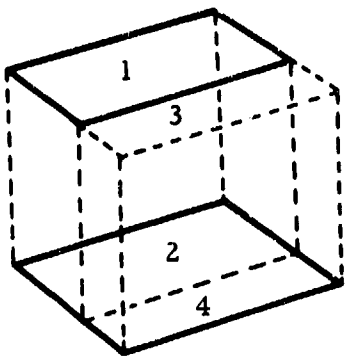

$$A_1F_{(1,\,x)} = A_xF_{(x,\,1)}$$
$$= A_{(1+3+5+7)}F_{(1+3+5+7,\,2+4+6+8)} + A_7F_{78} -$$
$$A_{(3+7)}F_{(3+7,\,4+8)} - A_{(5+7)}F_{(5+7,\,6+8)}$$

(8)

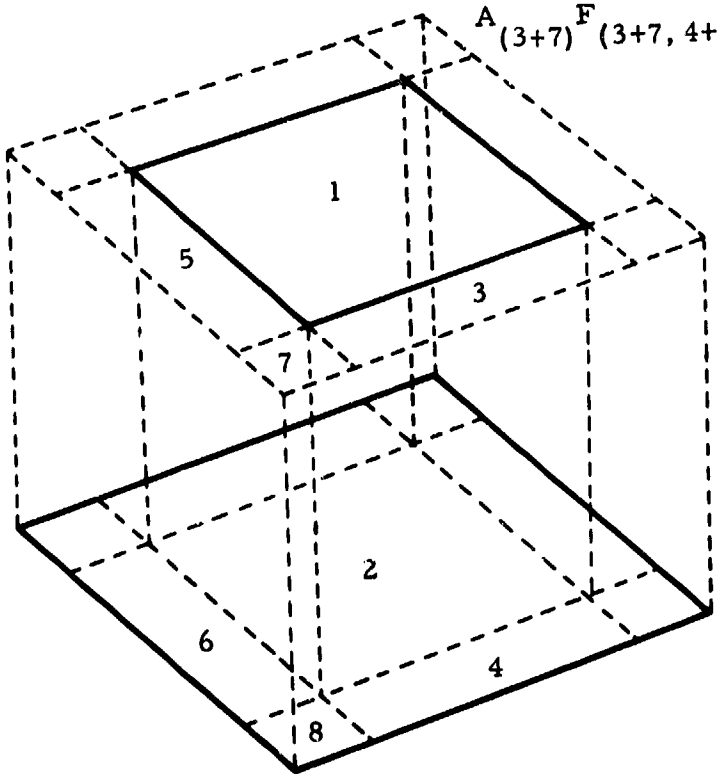

x is subscript for total lower surface

Figure 76. Diagrams of Configuration Factor Algebra (Sheet 2 of 2)

Solving for F_{32} from Equation 299 yields

$$F_{32} = \frac{1}{A_3}\left[F_{(1+3,\,2)}A_{(1+3)} - F_{12}A_1\right] \tag{300}$$

Equation 300 expresses the shape modulus F_{32} in terms of two shape moduli which can be obtained directly from graphical information available in NACA TN 2836 (Reference 22).

As a second example, consider finding F_{14} for diagram 3. Applying the same technique as for the first example yields

$$\phi_{14} = \phi_{(1+3,\;2+4)} - \phi_{12} - \phi_{34} - \phi_{32} \tag{301}$$

Now, if all surfaces have uniform emittance, Yamauti's modified reciprocity theorem can be applied, yielding

$$\phi_{14} = \phi_{32} = \phi_{23} = \phi_{41} \tag{302}$$

Substituting Equation 302 into Equation 301 and combining terms,

$$\phi_{14} = \frac{1}{2}\left[\phi_{(1+3,\;2+4)} - \phi_{12} - \phi_{34}\right] \tag{303}$$

Equation 297 is now substituted into Equation 303. The resulting equation is solved for F_{14}. This operation gives

$$F_{14} = \frac{1}{2}A_1\left[F_{(1+3,\;2+4)}A_{(1+3)} - F_{12}A_1 - F_{34}A_3\right] \tag{304}$$

Equation 304 is a relation for F_{14} in terms of configuration factors which can be evaluated graphically.

A similar procedure can be used to derive the configuration factor for almost any configuration in terms of configuration factors which can be evaluated directly. A number of the more common cases are summarized in Figure 76, which was obtained from Reference 26 (Table 38).

Finite Configuration Factor Conversion

An important technique for the evaluation of finite-finite configuration factors is called the area weighted method. Briefly, the finite-finite

configuration factor can be obtained from a knowledge of the differential-finite configuration factor at every point or, as in this method, at certain well chosen intervals.

Recalling the basic equation for a finite-finite configuration factor,

$$F_{12} = \frac{1}{\pi A_1} \int_{A_1} \int_{A_2} \frac{\cos \theta_1 \cos \theta_2}{S^2} dA_1 dA_2 \tag{305}$$

If A_1 is relatively small, the kernel $(\cos \theta_1 \cos \theta_2 / S^2)$ of this integral of the above equation is effectively independent of dA_1 or essentially constant and can be removed from the integral when integrating over A_1. Thus

$$F_{(\Delta A_1 - A_2)} = \left(\frac{\Delta A_1}{A_1}\right)\left(\frac{1}{\pi}\right) \int_{A_2} \frac{\cos \theta_1 \cos \theta_2}{S^2} dA_2 \tag{306}$$

which is the same as

$$F_{(\Delta A_1 - A_2)} = \frac{\Delta A_1}{A_1} F_{(dA_1 - A_2)} \tag{307}$$

The quantity ΔA_1 is a smaller finite area that forms some part of the larger area A_1. The configuration factor $F_{(dA_1 - A_2)}$ is taken from the center of ΔA_1, to the whole of A_2. By summing up terms such as given in Equation 307, the total shape modulus F_{12} is obtained.

$$F_{12} = \sum_{A_1} \left(\frac{\Delta A_1}{A_1}\right) F_{(dA_1 - A_2)} \tag{308}$$

IBM 7090 PROGRAM (GEOMETRIC CONFIGURATION FACTORS)

An IBM 7090 program (Reference 27) which calculates geometric configuration factors is now in final preparation. The program is limited to the calculation of the geometric configuration factor between two planes which must be parallelograms, including the special cases of squares, rectangles, and rhombi.

The method of calculation is a numerical approximation of the integral form of the configuration factor equation from a plane in space to any other plane. Under control of certain input data the two planes are divided into a number of incremental areas. The expression for the configuration factor from an incremental area in plane 1 to another in plane 2 is

$$F_{(dA_1-\Delta A_2)} = \frac{\cos\theta_1 \cos\theta_2 \Delta A_2}{\pi r^2} \tag{309}$$

where

θ = Angle between the normal to plane 1 and line connecting center points of two incremental areas

θ_2 = Same angle for plane 2

ΔA_2 = Incremental area in plane 2

r = Length of line connecting center points of two incremental areas

This calculation is repeated for all the incremental areas in plane 2, and the summation of these is the configuration factor from the incremental area ΔA_1 to the total second area. (Note that the calculated individual $F_{(dA_1-\Delta A_2)}$ takes the form of a differential area to finite area configuration factor. This is calculated from the midpoint of ΔA_1, and is assumed to be the average over ΔA_1.)

The foregoing process is then repeated for each incremental area in plane 1. An integrated average of the configuration factors from all the ΔA_1 to A_2 is equivalent to the configuration factor from plane 1 to plane 2.

UNIT SPHERE METHOD (DIFFERENTIAL-FINITE CONFIGURATION FACTOR)

An extremely useful method for the development of the differential-finite configuration factor is known as the unit sphere or solid angle projection method. This is discussed in some detail in Reference 26 (p 294-298).

Briefly, it can be stated that the configuration factor from dA_1 to A_2, in Figure 77 can be obtained as follows:

1. A hemisphere is drawn over dA_1 of radius R.

2. The area A_2' cut on the spherical surface by the solid angle from dA_1 to A_2 is obtained by central projection.

3. The projected area A_2' must then be projected once more by normal projection to the plane of the radiating surface dA_1. The area of the second projection is A_2'' in Figure 77.

4. The configuration factor $F_{(dA_1-A_2)}$ is given by the ratio of A_2'' to the area of the circle. Thus,

$$F_{(dA_1-A_2)} = \frac{A_2''}{\pi R^2} \tag{310}$$

It can be seen that A_2 need not be a plane surface as long as the perimeter of the surface is defined (i.e., A_2 could easily have been concave or convex and the same value of $F_{(dA_1-A_2)}$ would have been obtained).

To determine the configuration factor from a finite surface A_1 to a finite surface A_2, the surface A_1 must be divided into small areas of equal size and the unit sphere method must be used for the centers of every one of these areas. The average of these is the finite-finite configuration factor F_{12}.

The unit sphere method is often useful when the other methods of configuration factor analysis cannot be readily used. However, it is a somewhat tedious method. There are several ways in which to attack the problem:

1. Descriptive geometry. This is essentially a "brute force," hand calculation method, which employs ordinary descriptive geometry techniques.

2. Mechanical integrators. Several mechanical integrators have been built based on the unit sphere method (References 22 and 29 through 32). These usually require the use of models because they are employed by tracing the outline of the shape under consideration.

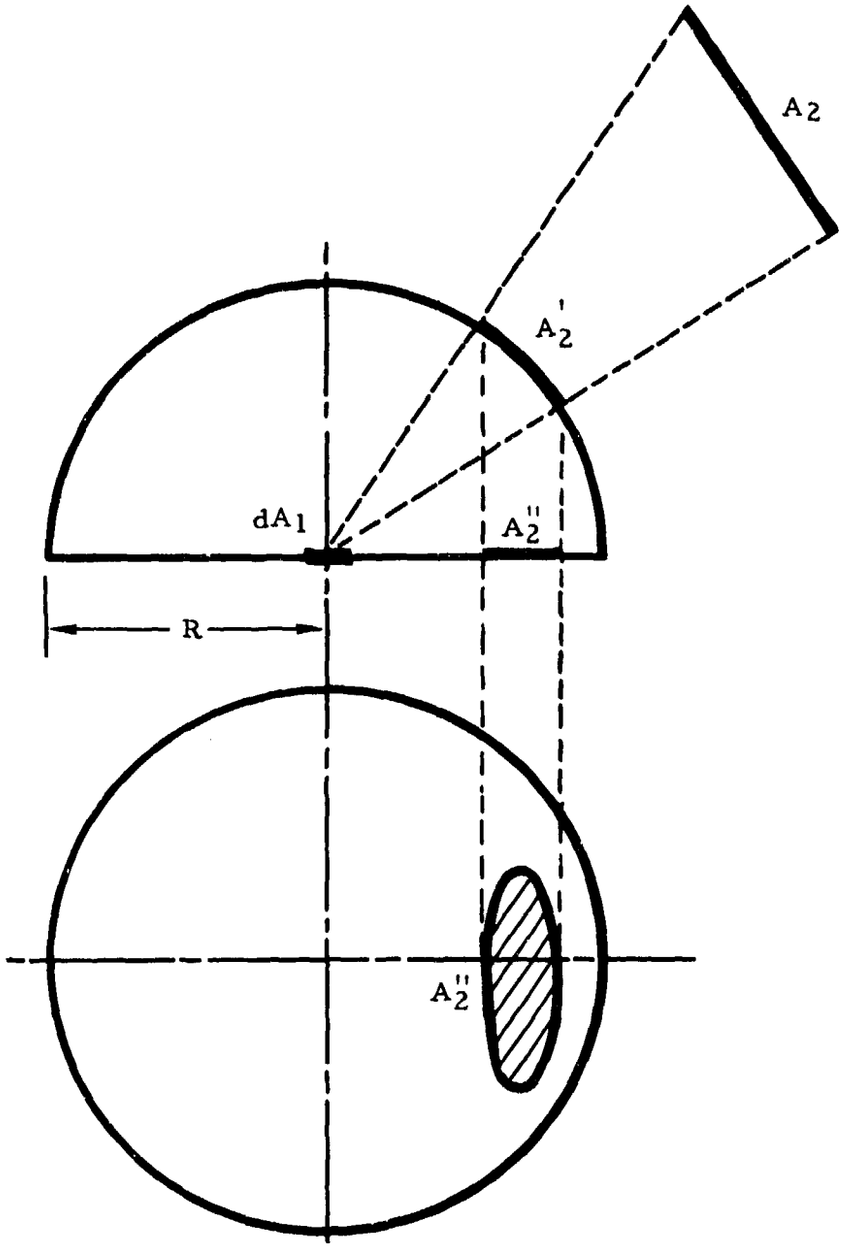

Figure 77. Diagram of Unit Sphere Method for Determining Configuration Factor

3. Photography. Considerable work has been done at the University of California at Los Angeles and elsewhere, based on a point source light being placed in the center of a milk-glass hemisphere. A model of the area A_2 is then placed inside the hemisphere in the proper position with respect to the point source dA_1. It is projected by the point source lamp as a shadow to the milk-glass hemisphere. When this hemisphere is photographed from a considerable distance, the ratio of the shadow of the model area to the area of the circle representing the glass sphere is the configuration factor (Reference 28, p 214-215).

DISCUSSION OF ASSUMPTIONS

When configuration factors are determined, the basic assumption is made that the thermal radiation involving these configuration factors exists in diffuse form. The complications produced by an attempted analysis of a partly diffuse, partly specular radiation problem are so great that a satisfactory method of analysis for this condition has not yet been devised.

Section VIII

EVALUATION STUDIES

This section of the report is concerned with the variables which influence satellite shell temperature and their effect on the cyclic temperature during each orbit revolution. Each parameter is independently varied by choosing various values within a realistic range of values. The evaluation studies point out the thermal problems associated with space vehicles and demonstrate the necessity for a large amount of analytical thermal prediction work required during design of a space vehicle.

These evaluation studies were completed through use of the IBM 7090 program, "Program for Determining Temperatures of Orbiting Space Vehicles" (Reference 33). This program is also discussed in Section V of this report.

NOMENCLATURE

a	Earth albedo
e	Eccentricity
h	Orbital height, mi
i	Inclination, deg
Q	Internal heat load, watt/sq ft of surface area
S	Solar constant, Btu/(hr)(sq ft)
α	Absorptivity
α/ϵ	Ratio of absorptivity to emissivity
ϵ	Emissivity
ω	Mass, lb/sq ft of surface area

VARIABLES SELECTED

The variables that were considered are those listed in Table 6. Simple configurations are used in evaluating the effects of the variables on the cyclic surface temperature and include a rotating sphere, an earth-oriented flat plate, an inertially oriented flat plate, and an eight-sided, earth-oriented prism.

Table 6. Study Variables for Rotating Sphere

Variable	Unit	Variation
Orbital height	Distance from planet, miles	150 to 2000
Orbital plane	Inclination from plane of ecliptic, degrees	0 to 80
Surface finish	Ratio of solar absorptivity to emissivity	0.1 to 20.0
Internal heat load	Watts per square foot of surface area	1.0 to 20.0
Mass	Pounds per square foot of surface area	0.25 to 10.0
Solar Constant	Near earth solar constant, Btu/(hour)(square foot)	433 to 453
Albedo	Earth's albedo	0.2 to 0.8

ROTATING SPHERE EVALUATION

Variation of Orbital Height

The cyclic variation in temperature for a rotating sphere is shown in Figure 78 as a function of orbital height. The orbital height in miles was varied from 150 to 2000 miles. The fixed parameters for the sphere were as follows:

Absorptivity α	0.7
Emissivity ϵ	0.5
Mass ω	1.5 lb/sq ft
Earth albedo a	0.35
Solar constant S	443 Btu/(hr)(sq ft)
Orbital inclination i	33.0 deg

The results point out the influence of increasing height on increasing percentage of time in sunlight and the influence of decreasing earth-emitted and solar-reflected energy with increasing height. The maximum temperatures for the 150- and 500-mile height are similar while the maximum temperature for the 250-mile orbit is higher, and the peak temperatures for the 1000- and 2000-mile orbits are lower. Due to the

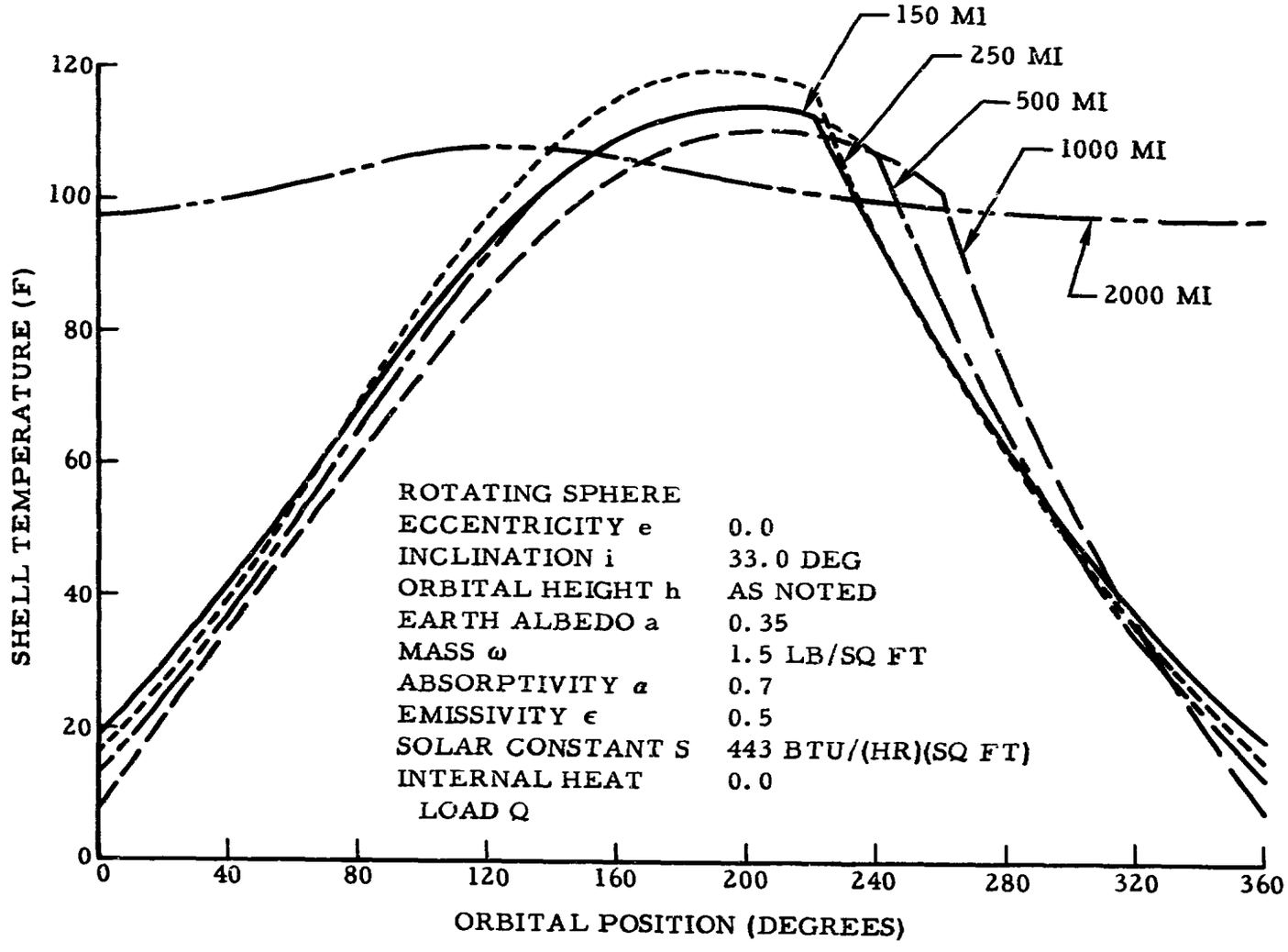

Figure 78. Variation of Orbital Height for Rotating Sphere

choice of fixed parameters, the time in direct sunlight is being opposed by the reduction in energy from the earth as the height increases.

The orbital period, percent of time in sunlight, and earth emitted form factor are listed in Table 7 for the various orbits.

Table 7. Variation of Orbital Height for Rotating Sphere

Orbital Height (mi)	Orbital Period (min)	Sun time (percent)	Earth-Emitted Form Factor
150	88.89	57	0.37
250	92.17	58	0.33
500	100.52	61	0.27
1000	117.92	72	0.199
2000	155.4	100	0.127

Variation of Orbital Plane

Using the same parameters as for the orbital height study and holding the orbital height at 250 miles, the effect of orbital plane on cyclic temperature variation was investigated. As shown in Figure 79 the inclination of the plane of the orbit to the plane of the ecliptic was varied from 0 to 80 degrees. Also, the year day from 1 January 1961 was chosen from the data in Figures 80 through 84 to give the maximum sun time for each orbit plane.

The results are as expected. The increase in sun time with increasing orbit plane raises the mean temperature and reaches a maximum when the vehicle is in the sun 100 percent of the time. The effect of launch day can be determined through comparison of the curve for 250 miles (Figure 78) compared with the curve for 33 degrees (Figure 79), because all parameters are the same except the year day.

Variation of Surface Finish

A primary consideration in any space vehicle temperature control system is the external surface finish. The amount of radiant energy received and the amount of heat radiated to space are direct functions of the external condition of the surface. For some space vehicles, where the internal heat loads are low and the equipment temperature tolerance fairly broad, complete control can be attained by the selection of the proper emissivity and solar absorptivity combination.

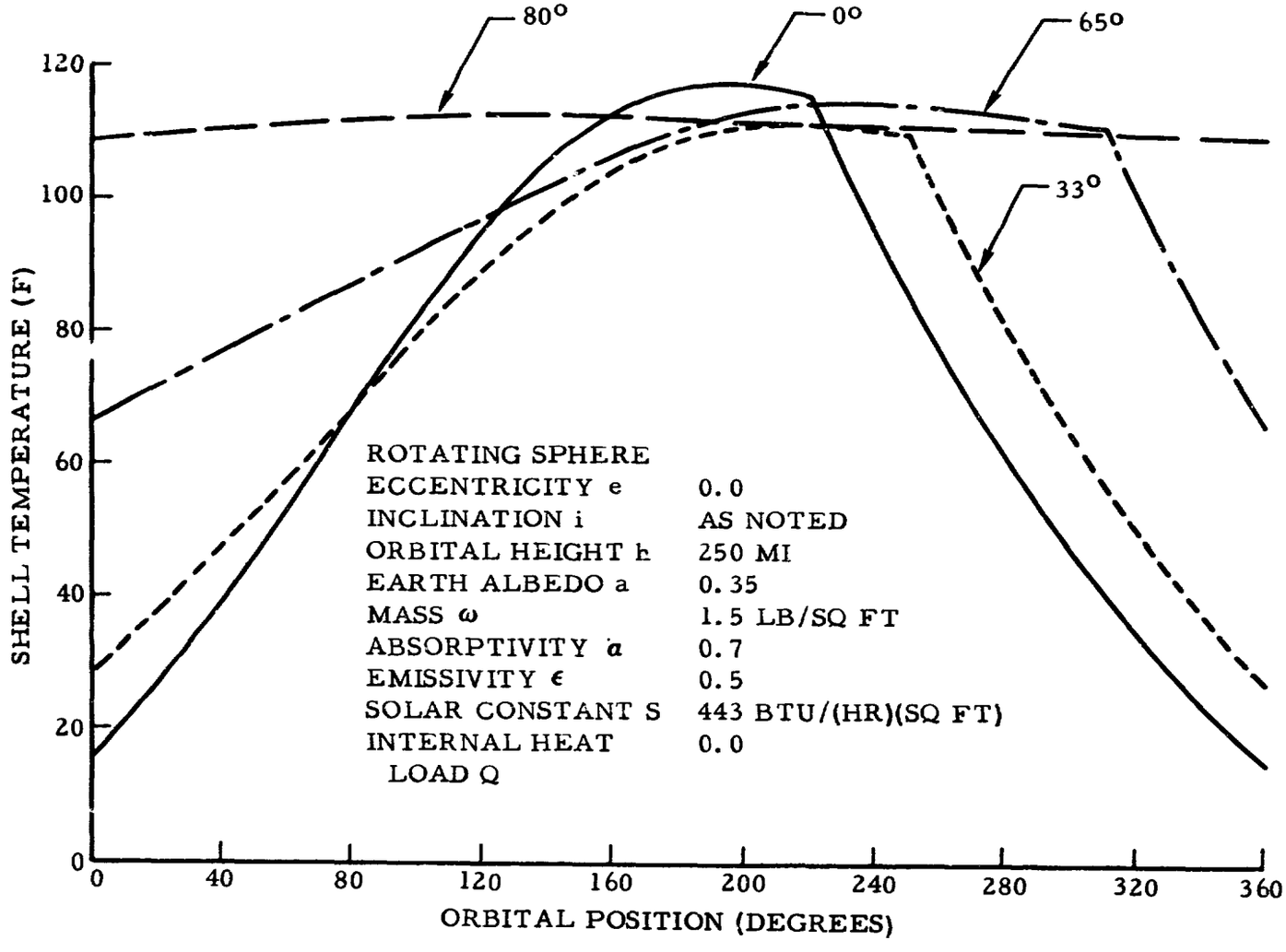

Figure 79. Variation of Orbital Inclination for Rotating Sphere

In the parametric study described here, the cyclic temperature variation was calculated for various combinations of absorptivity α and emissivity ϵ, with no association given to specific materials or coatings. (Unfortunately, although there are several coatings that have desirable thermal characteristics, these materials do not appear too practical for space application.) The same fixed parameters for the sphere were used.

The results of the study are shown in Figures 80 through 82. In each plot, solar absorptivity was held constant but emissivity varied over a wide range. To point out some of the trends, it is helpful to look at Table 8 where the α/ϵ ratio is tabulated along with the maximum and minimum temperatures.

Table 8. Variation of Surface Finish for Rotating Sphere

Solar Absorptivity	α/ϵ Ratio	Temperature (F)	
		Maximum	Minimum
0.1	0.1	-81	-96
0.1	0.125	-75	-91
0.1	0.20	-59	-75
0.1	0.33	-33	-50
0.3	0.375	-14	-60
0.5	0.5	13	-58
0.5	0.72	42	-32
0.1	1.0	53	36
0.5	1.0	74	-2
1.0	1.0	93	-38
1.0	1.11	104	-28
1.0	1.25	117	-15
0.7	1.40	120	18
1.0	1.43	133	-4
0.5	1.66	130	52
0.1	2.0	126	109
0.5	5.0	285	206
0.5	10.0	399	324
1.0	20.0	576	434

As the α/ϵ ratio increases, the mean temperature increases. Also, at a ratio of 1.0 for various values of solar absorptivity, the temperature spread (between maximum and minimum) decreases with decrease in solar absorptivity. This is due to the mass of the surface, where at low-energy transfer the storage term is more dominant than at high-energy transfer associated with high solar absorptivity. For the particular sphere used

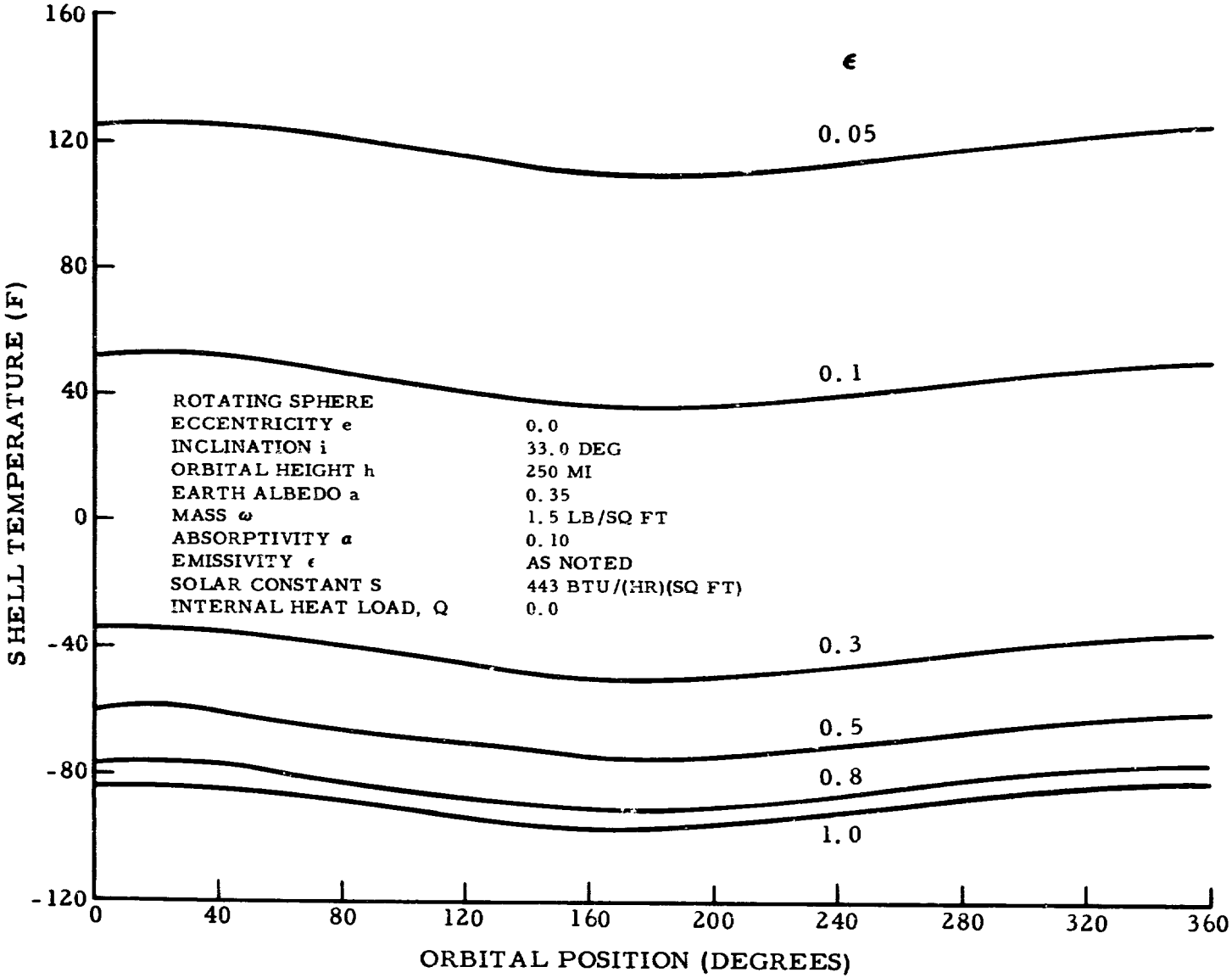

Figure 80. Variation of Emissivity for Rotating Sphere (Absorptivity 0.10)

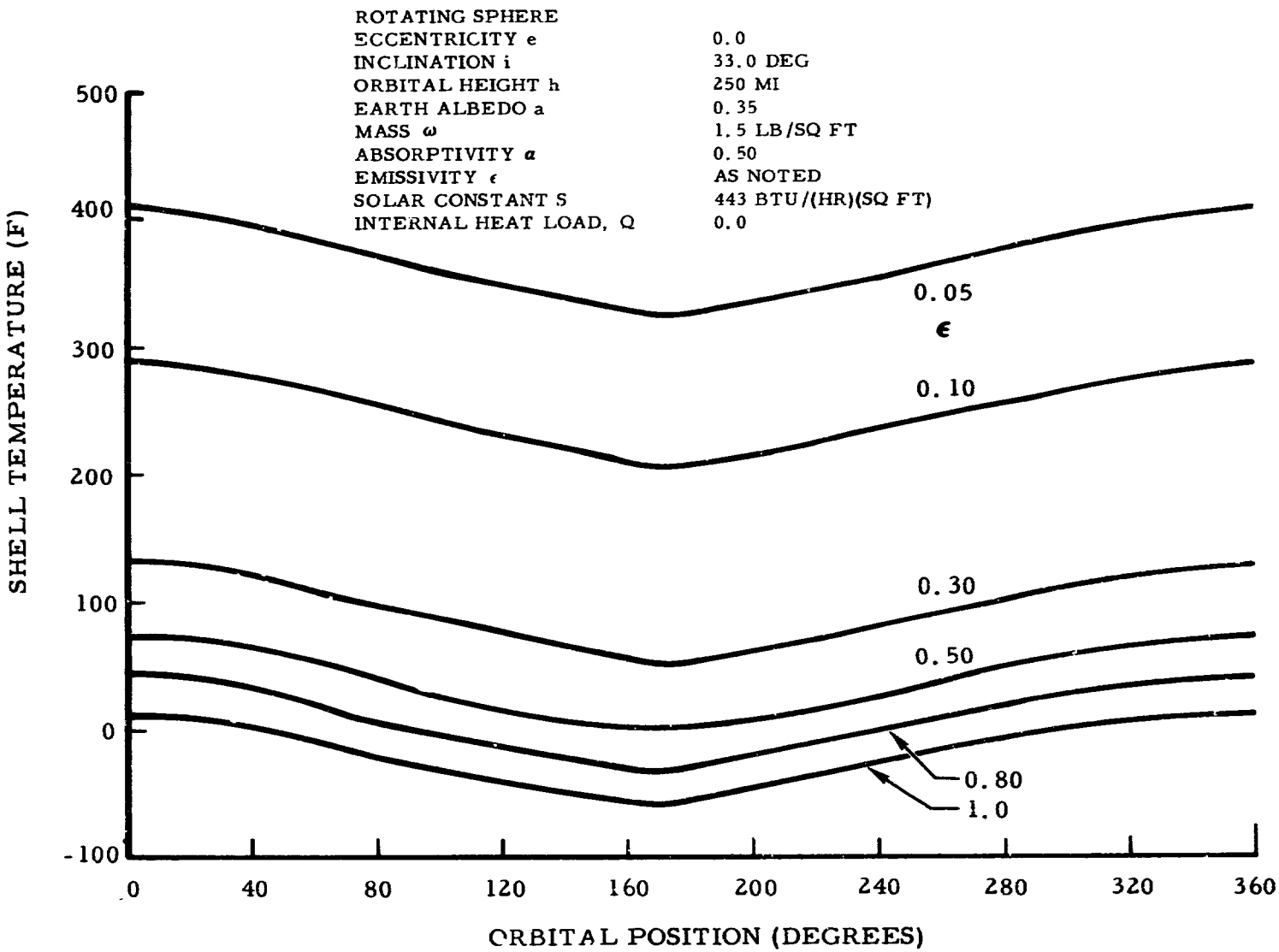

Figure 81. Variation of Emissivity for Rotating Sphere (Absorptivity 0.50)

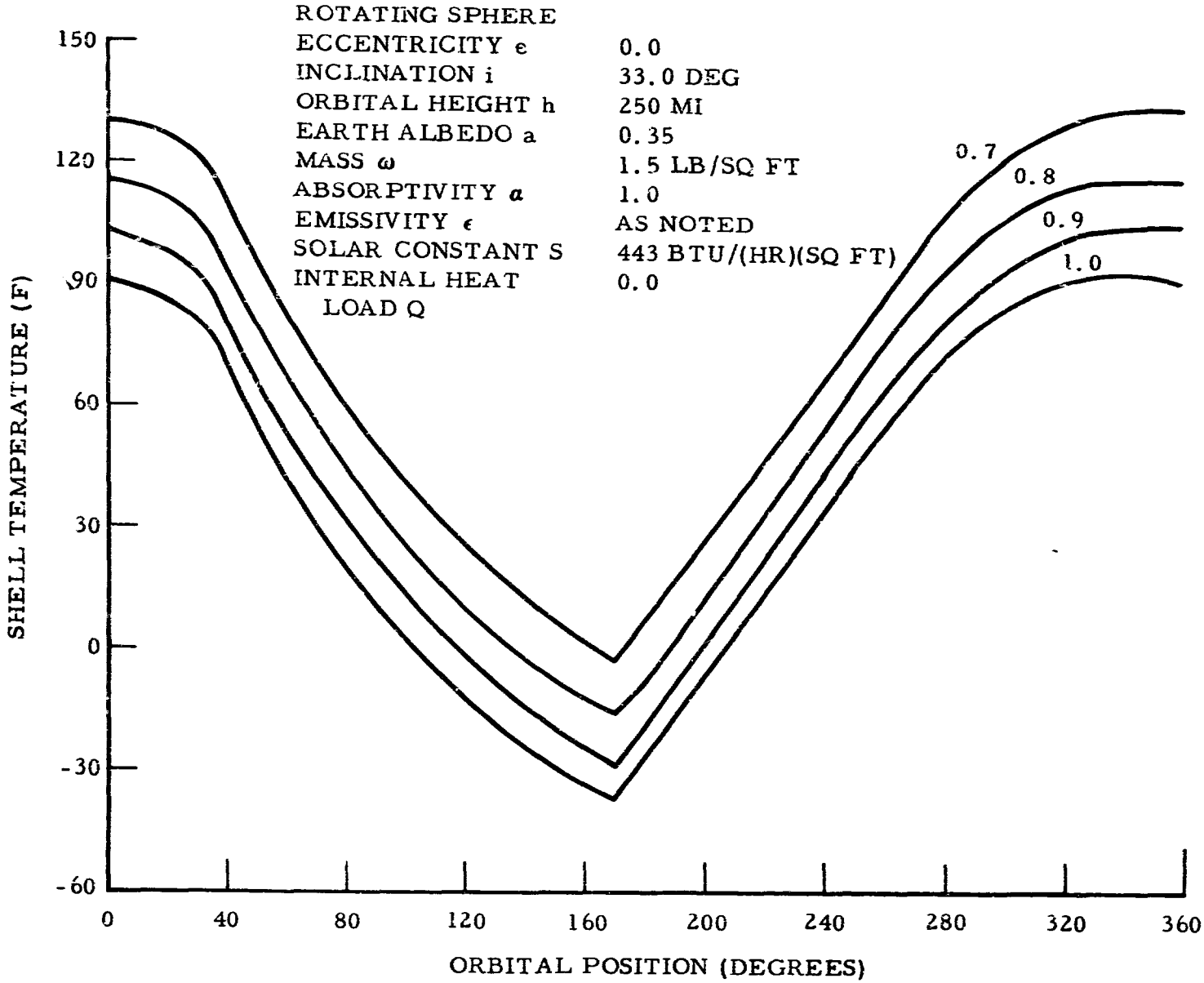

Figure 82. Variation of Emissivity for Rotating Sphere (Absorptivity 1.0)

in these studies with absorptivity of 0.7 and emissivity of 0.5, the maximum and minimum temperatures of 120 F and 18 F, respectively, would be quite tolerable for most equipment.

Variation of Mass

The cyclic temperature variation of a space vehicle surface is a function of the mass of that surface. As shown in Figure 83, the mass for the rotating sphere was varied from 0.25 to 10 pounds per square foot. The same fixed parameters were used.

The results point out, as expected, that as the mass of the surface increases the temperature excursion is decreased. Also, as the mass is increased, the calculated mean temperature increases to the limiting temperature, which for any mass is a function of the fourth root of the average of the temperature extremes to the fourth power. In Table 9, the calculated mean temperature and the maximum and minimum temperatures are tabulated.

Table 9. Variation of Mass for Rotating Sphere

Mass (lb/sq ft)	Temperature (F)			$\sqrt[4]{\frac{T_{max}^4 + T_{min}^4}{2}}$
	Mean	Maximum	Minimum	
0.25	44	154	-96	75°
0.75	62	139	-31	75°
1.5	67	118	14	75°
3.0	71	100	44	75°
10.0	72	84	67	75°

For any given orbit revolution, the energy input must equal the energy loss and, therefore, the total radiative power loss or input must be a constant, regardless of the mass of this particular vehicle. However, the mass regulates the thermal lag of the surface and determines the cyclic temperature excursion between the limits of equilibrium temperature with no mass and the limiting equilibrium temperature with a very large mass.

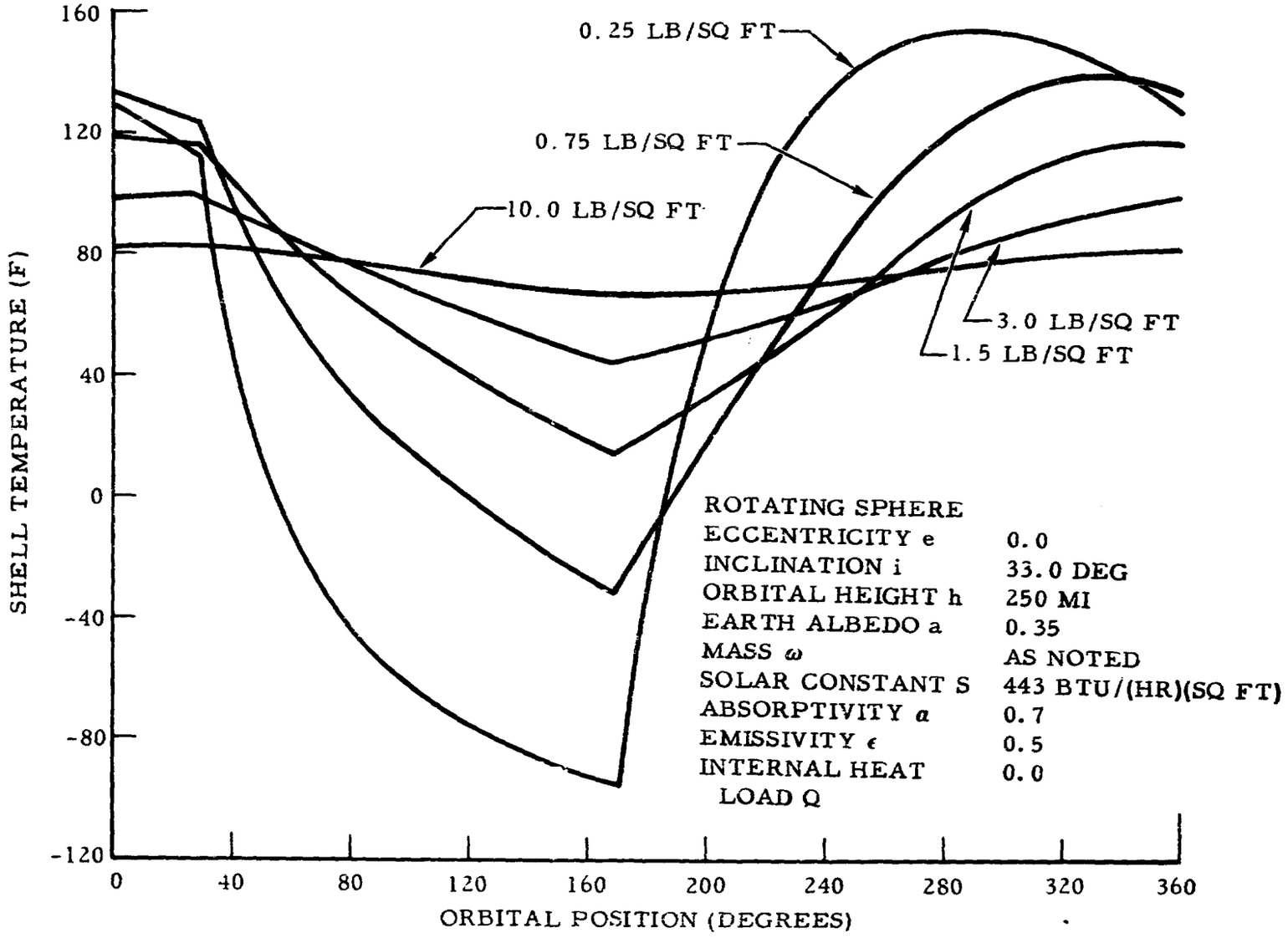

Figure 83. Variation of Mass for Rotating Sphere

Variation of Internal Heat Load

The cyclic variation in temperature for a rotating sphere is shown in Figure 84 as a function of internal heat load, with the same fixed parameters assumed. The internal heat load was varied from 1.0 to 20 watts per square foot. The results indicate, as expected, that the outer shell temperature increases as the internal heat load increases. The results at 1.0 watt per square foot show a maximum temperature of 125 F and a minimum temperature of 22 F. For the case with an internal heat load of 20 watts per square foot, the maximum temperature increases to 212 F and the minimum temperature is 121 F.

Variation of Earth Albedo

In the calculation of the cyclic temperature variation of a satellite in orbit, it is necessary to know the planet's albedo to properly account for the planet emission and reflected solar energy. As discussed in Section IV on the space thermal environment, the earth albedo varies because of the planet's surface, scattering by clouds and dust in the atmosphere, and molecular scattering by the atmospheric gases.

To determine the effect of various values of the earth's albedo on the cyclic temperature variation, an analysis was made on the rotating sphere. Four values of the earth albedo a were chosen: 0.2, 0.35, 0.5 and 0.8. For each value, various values of the α/ϵ ratio were chosen for each satellite.

The results of the analysis for earth albedos of 0.2, 0.5, and 0.8 are shown in Figures 85 through 87, with the same fixed parameters assumed.

A summary of the results is shown in Table 10, where the maximum and minimum temperatures are tabulated for the various ratios of α/ϵ. As the earth albedo is increased, the reflected solar energy from the earth that is incident on the vehicle is increased; however, the earth's emitted energy incident on the vehicle is decreased because the effective earth temperature is decreased. The maximum temperature is shown to increase, while the minimum temperature decreases for an increase in albedo. Also, the magnitude of the change increases with increase in α/ϵ ratio.

Variation of Solar Constant

To determine the effect on the cyclic temperature variation of changes in the solar constant, an analysis was made using 433, 443, and 453 Btu/(hour)(square foot) as values for the solar constant. For each value, various values of the α/ϵ ratio were chosen for each satellite. The same fixed parameters were used as in the previous runs.

Table 10. Variation of Earth Albedo for Rotating Sphere

Surface Characteristics			Temperature (F)							
			Albedo 0.2		Albedo 0.35		Albedo 0.5		Albedo 0.8	
α/ϵ	α	ϵ	Max	Min	Max	Min	Max	Min	Max	Min
0.5	0.5	1.0	13	-51	13	-58	13	-66	15	-82
1.0	0.5	0.5	70	0	74	-2	80	-4	90	-9
1.0	1.0	1.0	85	-32	93	-38	100	-44	118	-57
1.43	1.0	0.7	121	0	133	-4	144	-7	166	-15
1.67	0.5	0.3	122	51	130	52	140	53	156	55

Table 11. Variation of Solar Constant for Rotating Sphere

Surface Characteristics			Temperature (F)					
			Solar Constant 433 Btu/(Hr)(Sq Ft)		Solar Constant 443 Btu/(Hr)(Sq Ft)		Solar Constant 453 Btu/(Hr)(Sq Ft)	
α/ϵ	α	ϵ	Max	Min	Max	Min	Max	Min
0.5	0.5	1.0	11	-60	13	-58	17	-57
1.0	0.5	0.5	71	-4	74	-2	76	0
1.0	1.0	1.0	89	-40	93	-38	96	-36
1.43	1.0	0.7	130	-5	133	-4	138	-2
1.67	0.5	0.3	126	50	130	52	134	54

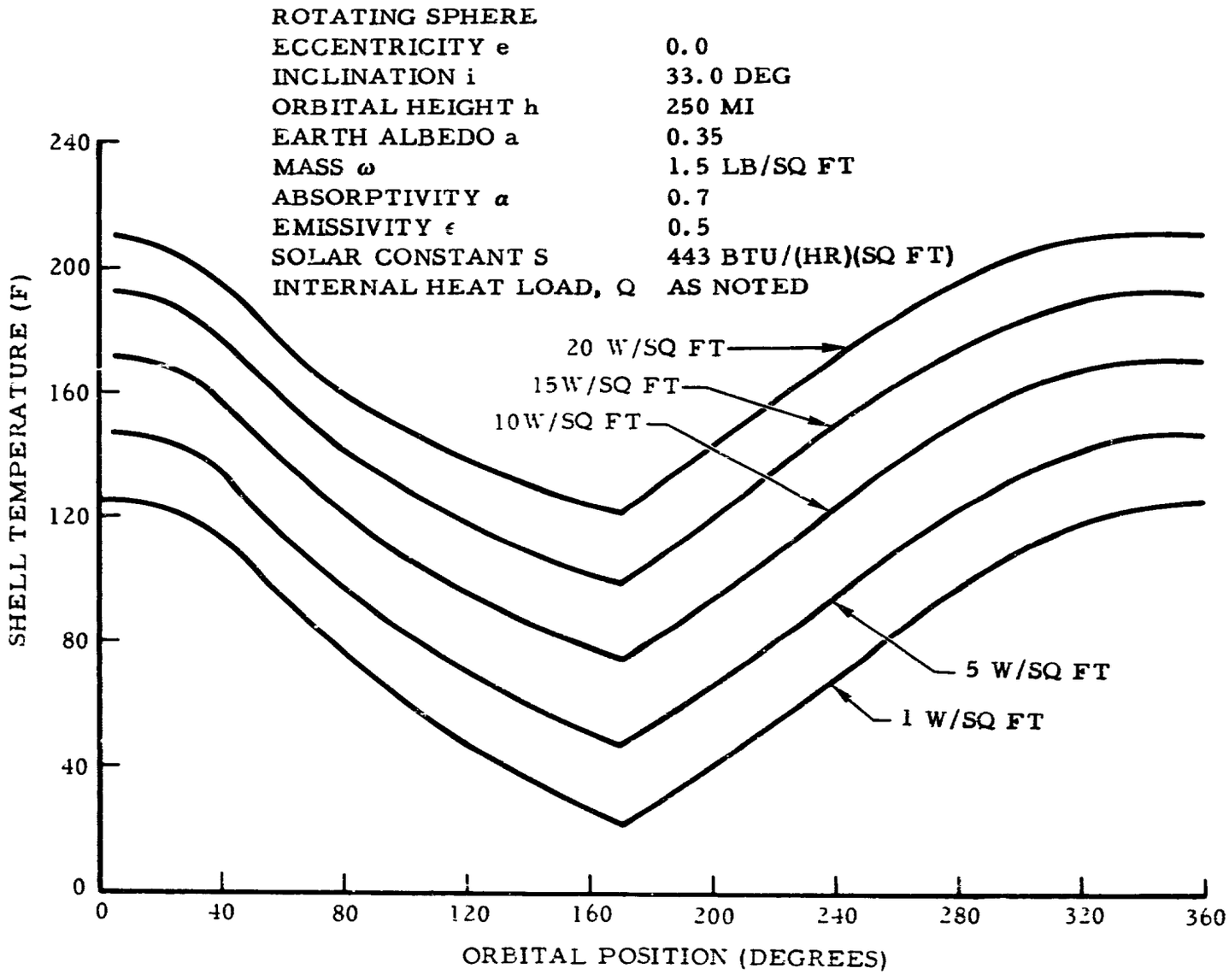

Figure 84. Variation of Internal Heat Load for Rotating Sphere

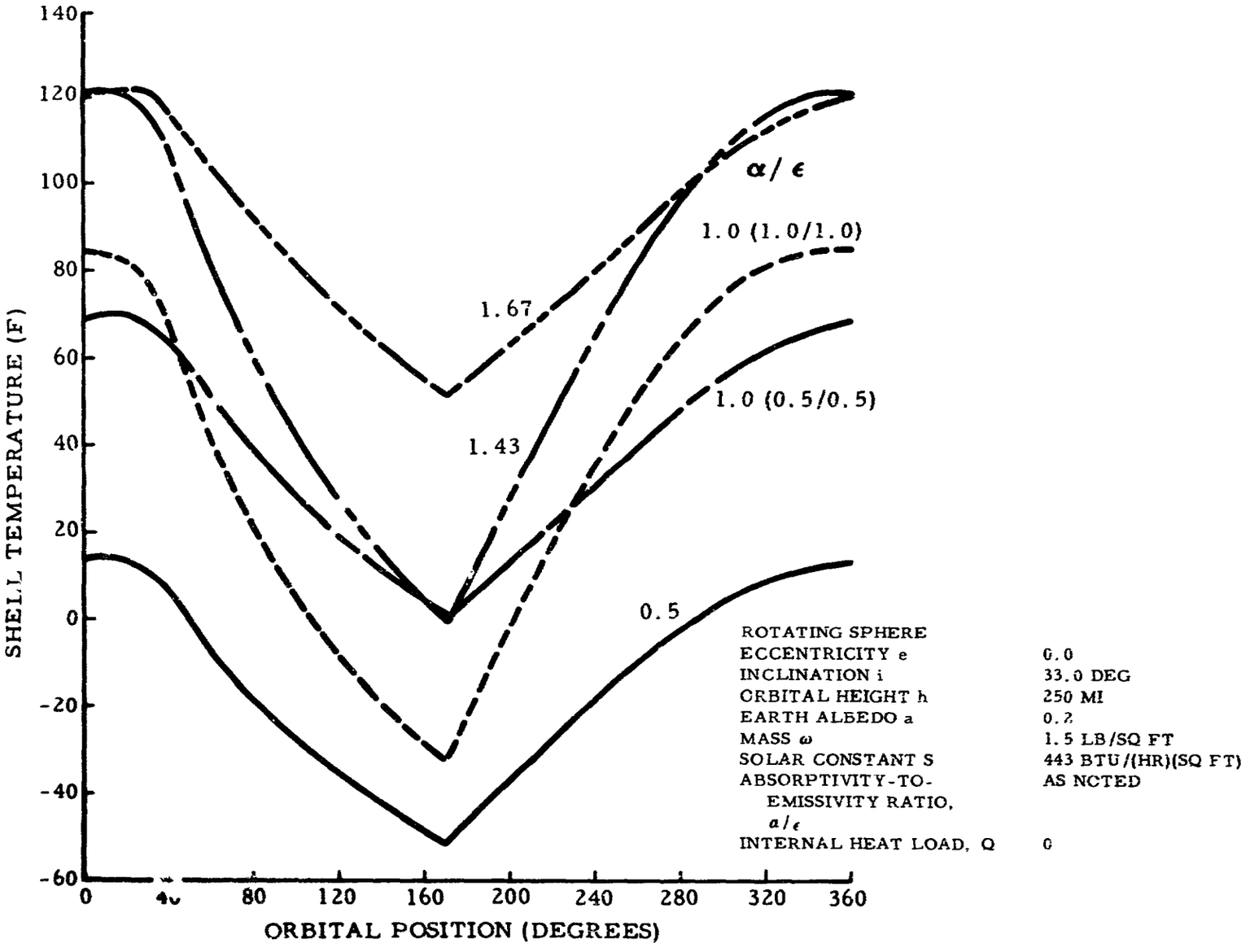

Figure 85. Variation of Absorptivity-to-Emissivity Ratio for Rotating Sphere (Earth Albedo 0.2)

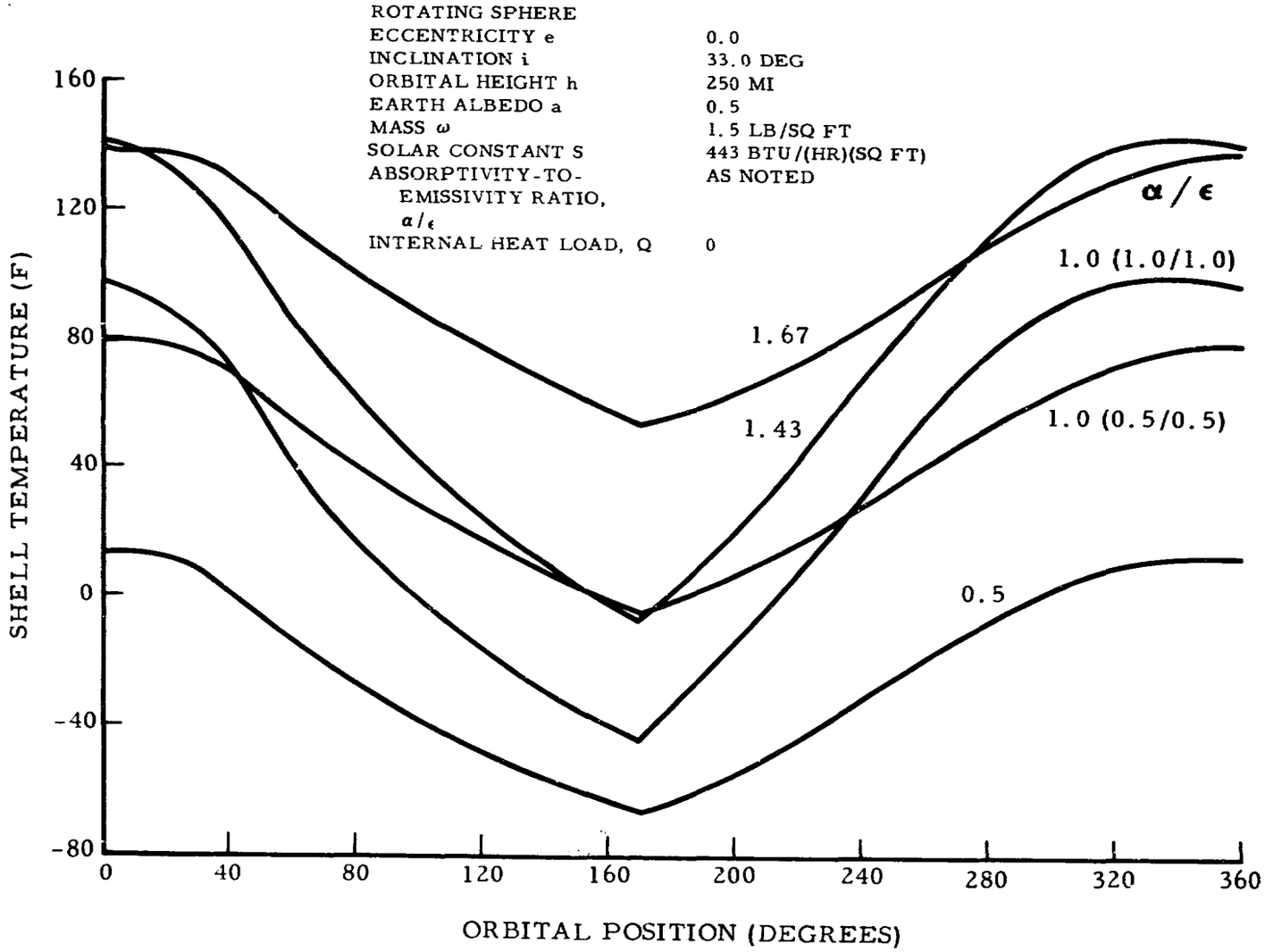

Figure 86. Variation of Absorptivity-to-Emissivity Ratio for Rotating Sphere (Earth Albedo 0.5)

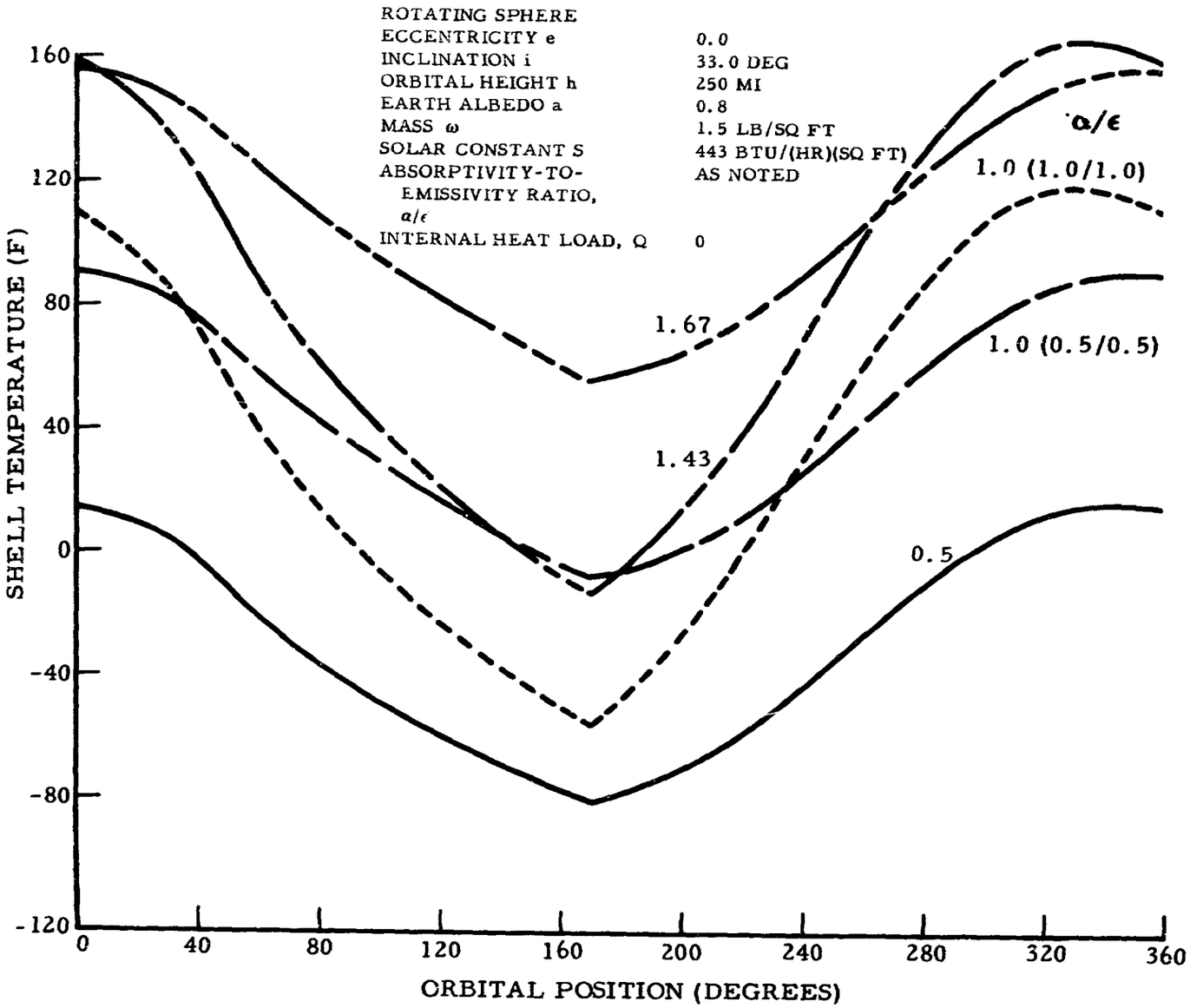

Figure 87. Variation of Absorptivity-to-Emissivity Ratio for Rotating Sphere (Earth Albedo 0.8)

The results of the analysis for 433 and 453 Btu/(hour)(square foot) are shown in Figures 88 and 89. A summary of the results is shown in Table 11, where the maximum and minimum temperatures are tabulated for the various ratios of α/ϵ. As expected, the cyclic temperature level is increased as the value of the solar constant is increased. The magnitude of the increase, for the set of conditions assumed for the sphere, appears to be approximately 0.4 to 0.9 percent in temperature level for a 2.0 percent change in solar constant.

COMPARISON OF ROTATING SPHERE AND FLAT PLATE

The cyclic variation in shell temperature for a rotating sphere was compared with inertially oriented and earth-oriented flat plates, as shown in Figure 90. The following parameters were used for the three surfaces:

Absorptivity α	0.7
Emissivity ϵ	0.5
Mass ω	1.7 lb/sq ft
Earth albedo a	0.35
Solar constant S	443 Btu/(hr)(sq ft)
Orbital inclination i	33.0 deg
Orbital height h	250 mi
Internal heat load Q	0

Also, the back faces of the flat plates were assumed to be perfectly insulated.

The earth-oriented flat plate shows a slight increase in temperature at 20 and 170 degrees. This is due to the plate's receiving direct solar energy for a short time, just after passing the terminator and before going into the earth's shadow, and again when leaving the earth's shadow just before passing over the terminator. The temperature level, in general, is higher than that of the inertially oriented plate because the geometric form factor for the earth-emitted energy is constant at approximately 0.88 for the earth-oriented plate. The form factor for the inertially oriented plate varies from 0 at 20 degrees to 0.88 at 185 degrees, where the surface is facing the earth and parallel to the orbit path, and then decreases to 0 again at 335 degrees.

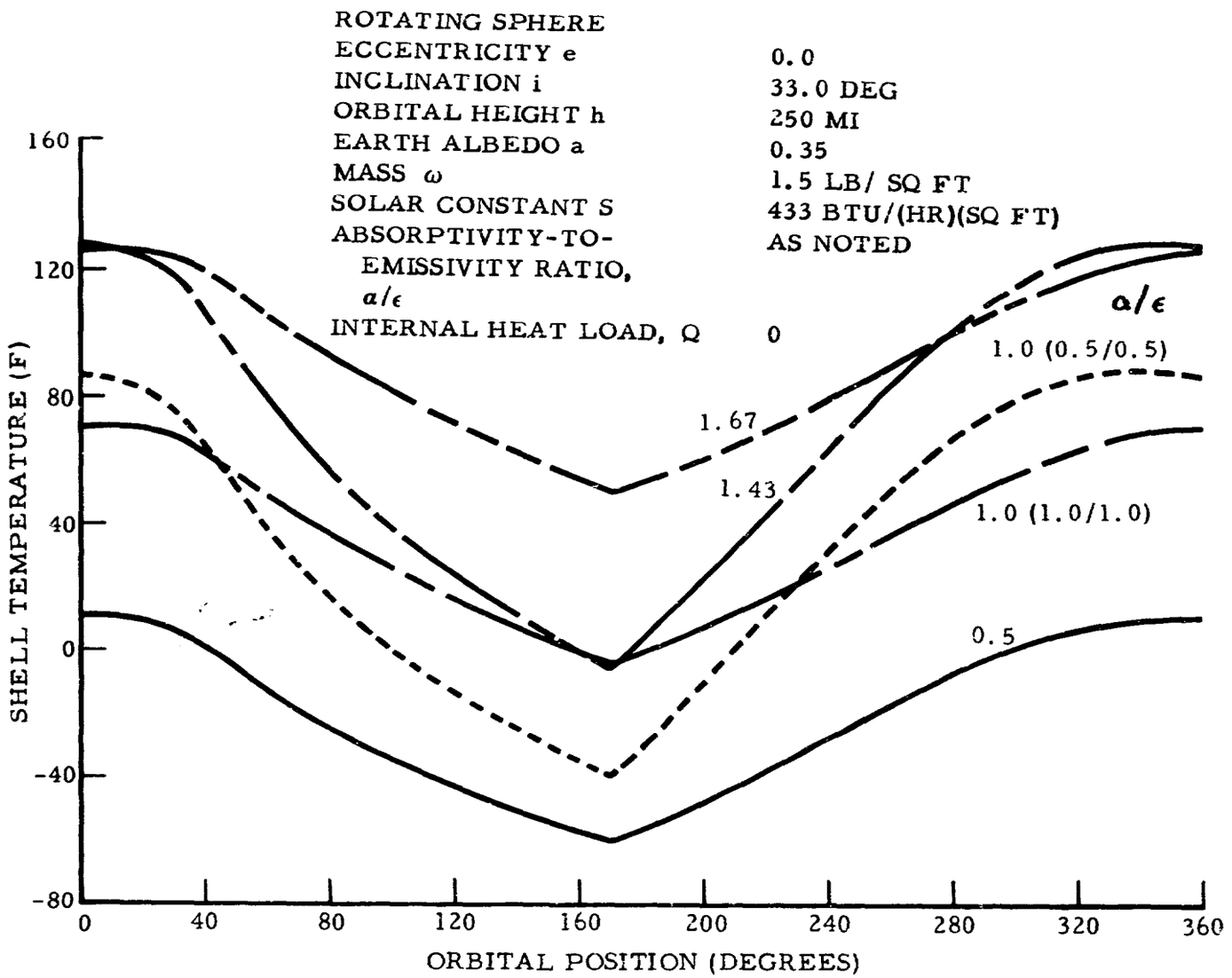

Figure 88. Variation of Absorptivity-to-Emissivity Ratio for Rotating Sphere [Solar Constant 433 Btu/(Hour)(Square Foot)]

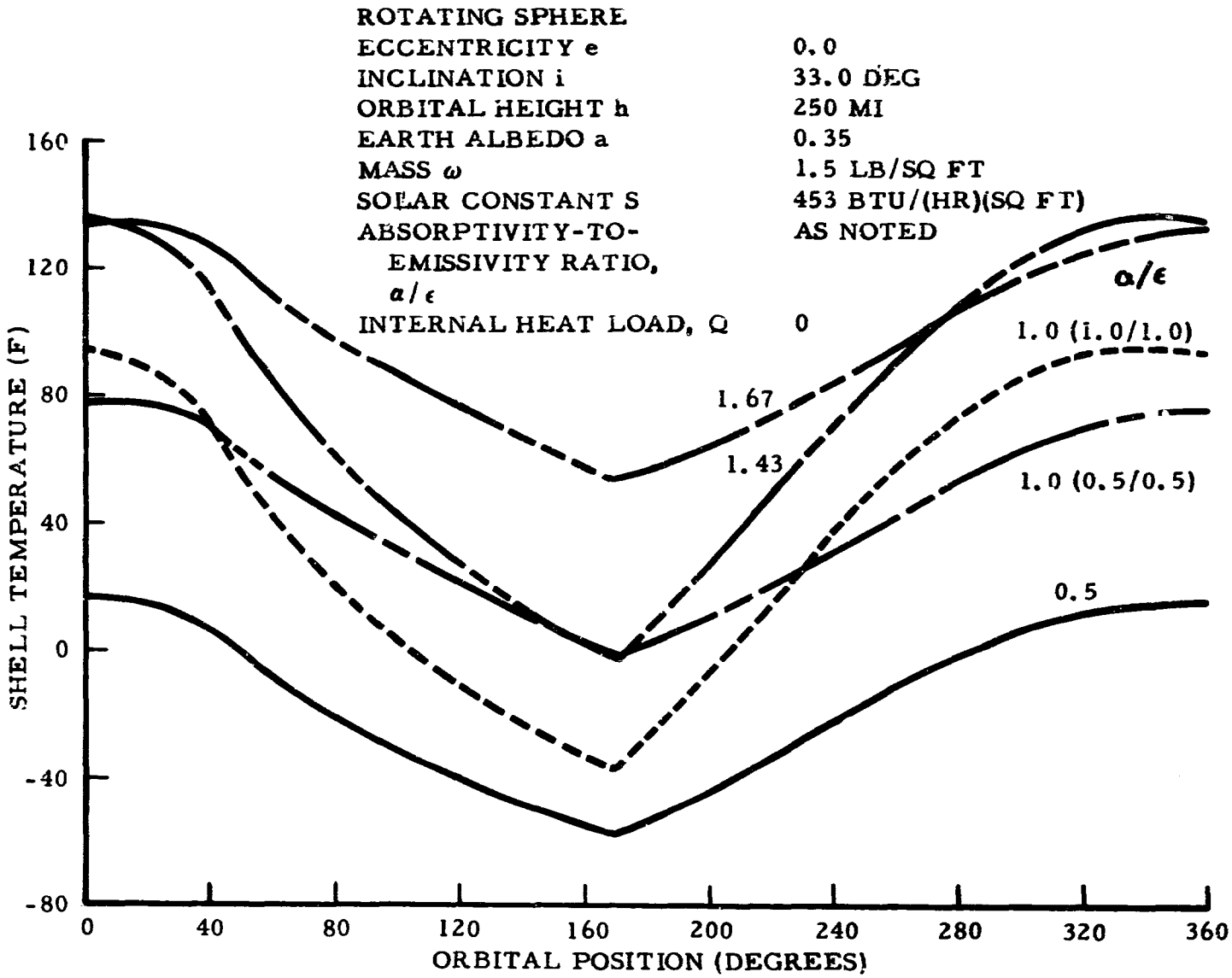

Figure 89. Variation of Absorptivity-to-Emissivity Ratio for Rotating Sphere [Solar Constant 453 Btu/(Hour)(Square Foot)]

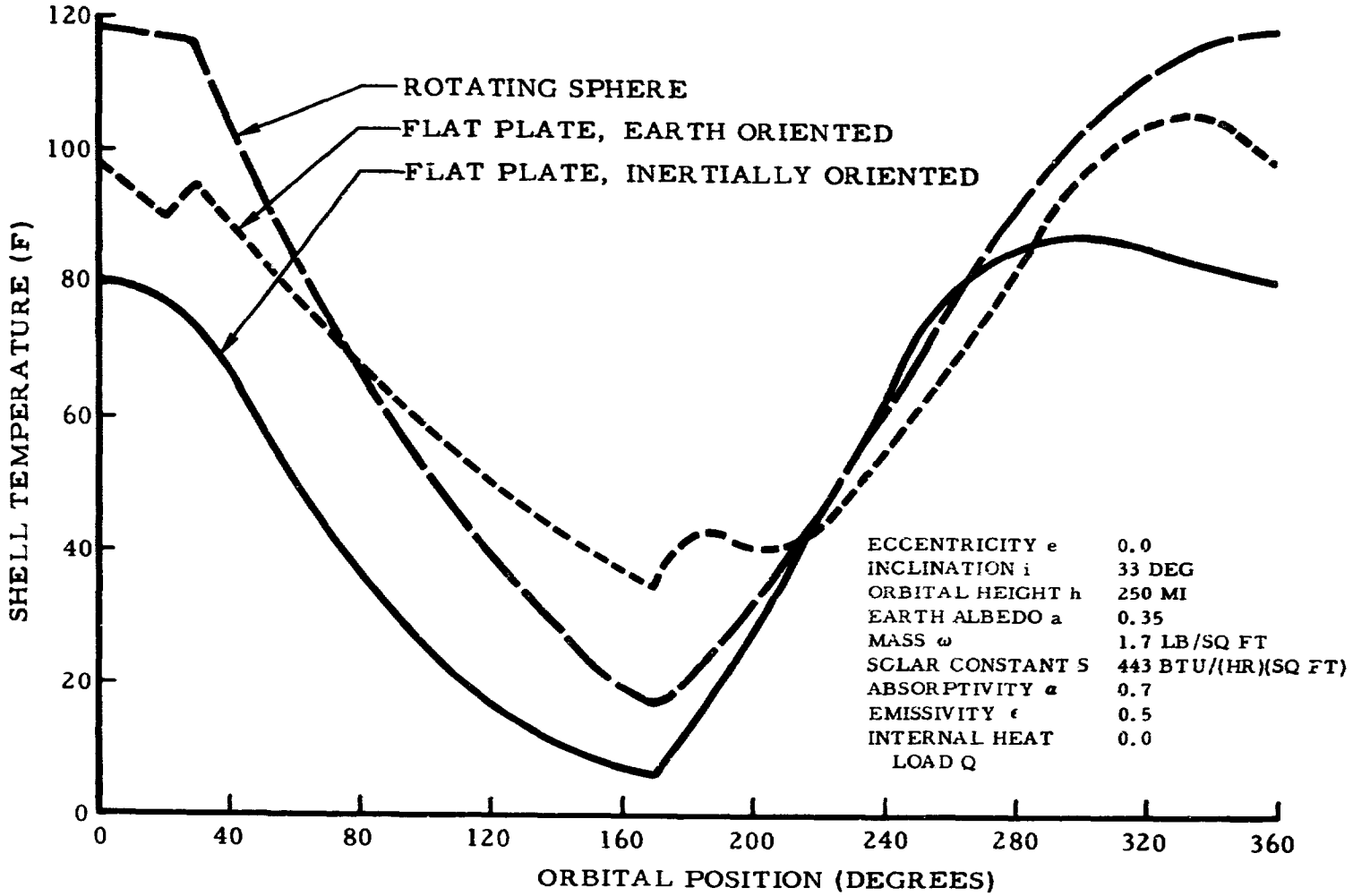

Figure 90. Comparison of Rotating Sphere and Flat Plate

CYCLIC TEMPERATURE VARIATION OF EIGHT-SIDED PRISM

A space vehicle configuration, consisting of an eight-sided prism with two ends, was considered in order to study the effects of cyclic temperature variation of the various sides. The vehicle was assumed to be earth-oriented so that the vehicle axis was on the orbital path. A retrograde orbit of 96.6-degree inclination was used in conjunction with an orbital height of 225 miles. The orientation of the vehicle surfaces in relationship to the earth and sun is shown in Figure 91. The bottom surfaces are 1, 4, and 10, and the top surfaces are 6, 2, and 8; the sides are 5 and 9, and the ends are 3 forward and 7 aft. The fixed parameters used for the prism were as follows:

Absorptivity α	0.7
Emissivity ϵ	0.5
Mass ω	0.5 lb/sq ft
Earth albedo a	0.35
Solar constant S	443 Btu/(hr)(sq ft)

The cyclic temperature variation for each surface is shown in Figure 92. To summarize the results and to point out the effects of changing the surface characteristics and increasing the mass of the individual surfaces, the maximum and minimum temperatures are tabulated in Table 12. The mass of the surfaces for the second case was 1.5 pounds per square foot.

Table 12. Maximum and Minimum Temperatures for Eight-Sided Prism

	Surface Finish		Temperature (F)		Surface Finish		Temperature (F)	
Surface	α	ϵ	Min	Max	α	ϵ	Min	Max
Bottom								
1	0.7	0.5	160	-17	0.4	0.3	101	37
4	0.7	0.5	116	-48	0.8	0.35	118	23
10	0.7	0.5	116	-48	0.8	0.35	119	25
Top								
2	0.7	0.5	315	-249	0.1	0.1	106	47
6	0.7	0.5	253	-227	0.1	0.075	96	52
8	0.7	0.5	258	-226	0.1	0.075	101	57
Sides								
5	0.7	0.5	8	-123	0.8	0.15	99	51
9	0.7	0.5	22	-123	0.8	0.20	89	34
Ends								
3	0.7	0.5	323	-123	0.1	0.1	89	39
7	0.7	0.5	323	-122	0.1	0.1	101	47

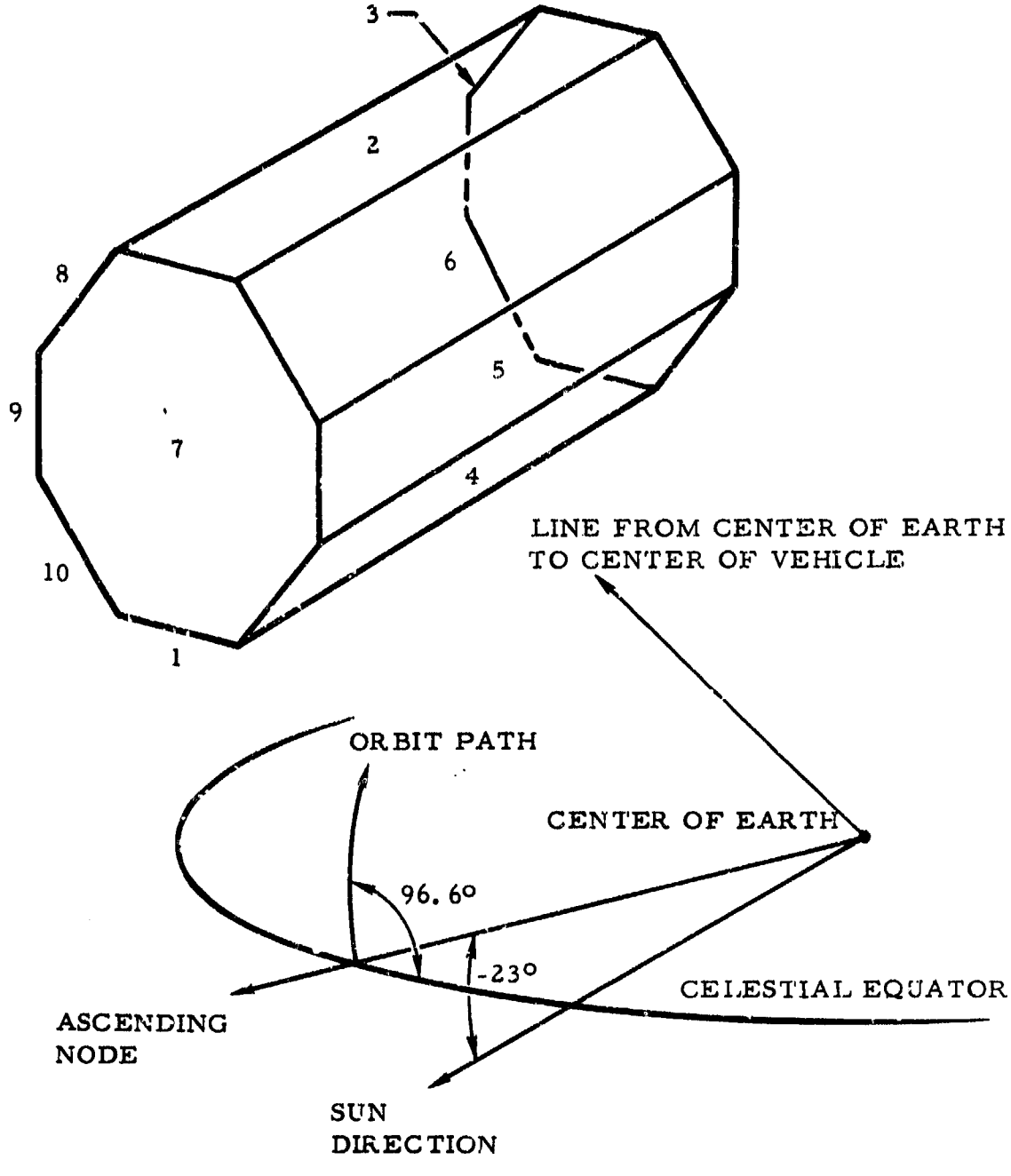

Figure 91. Diagram of Earth-Oriented Eight-Sided Prism

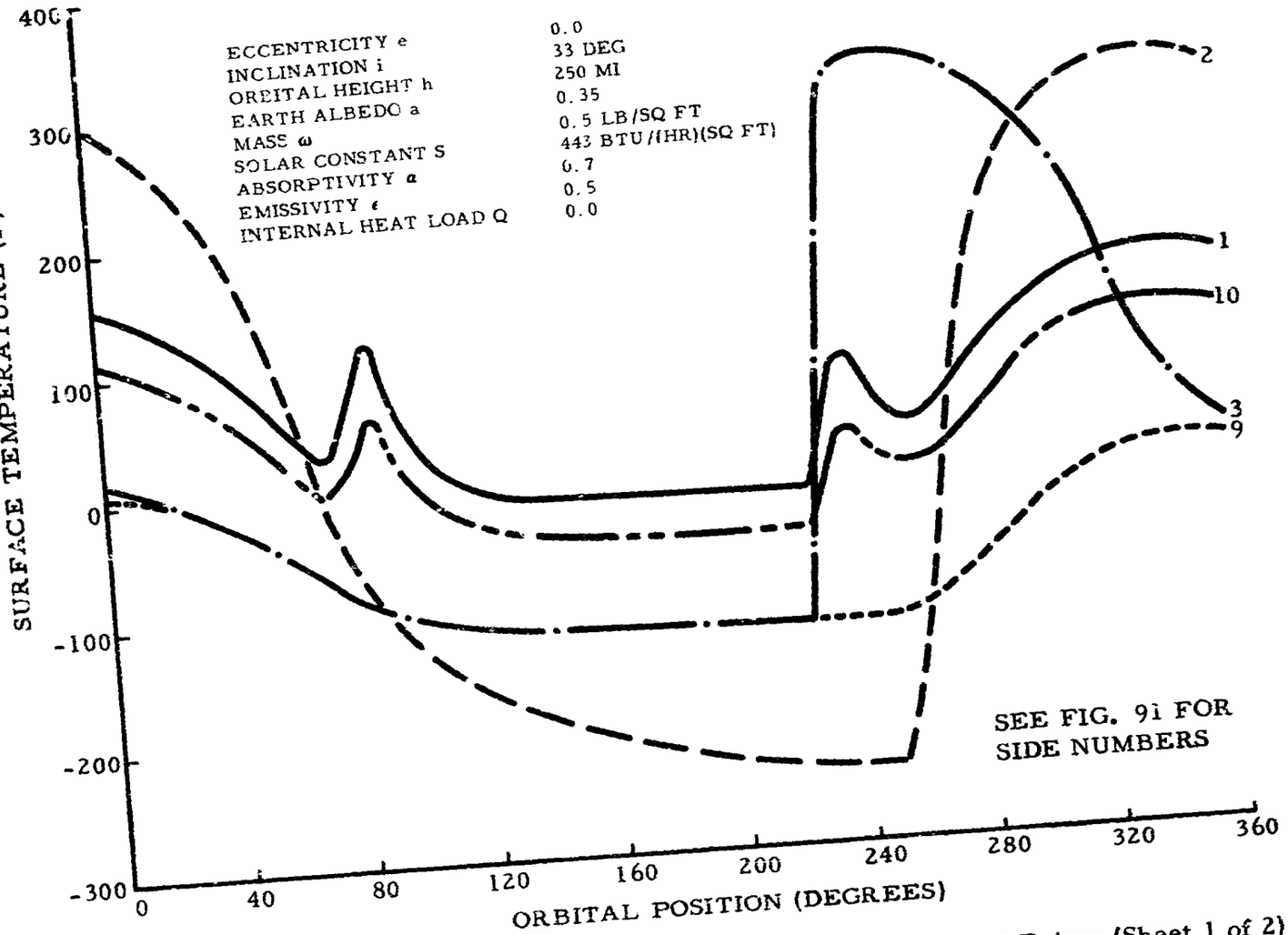

Figure 92. Cyclic Temperature Variation of Earth-Oriented Eight-Sided Prism (Sheet 1 of 2)

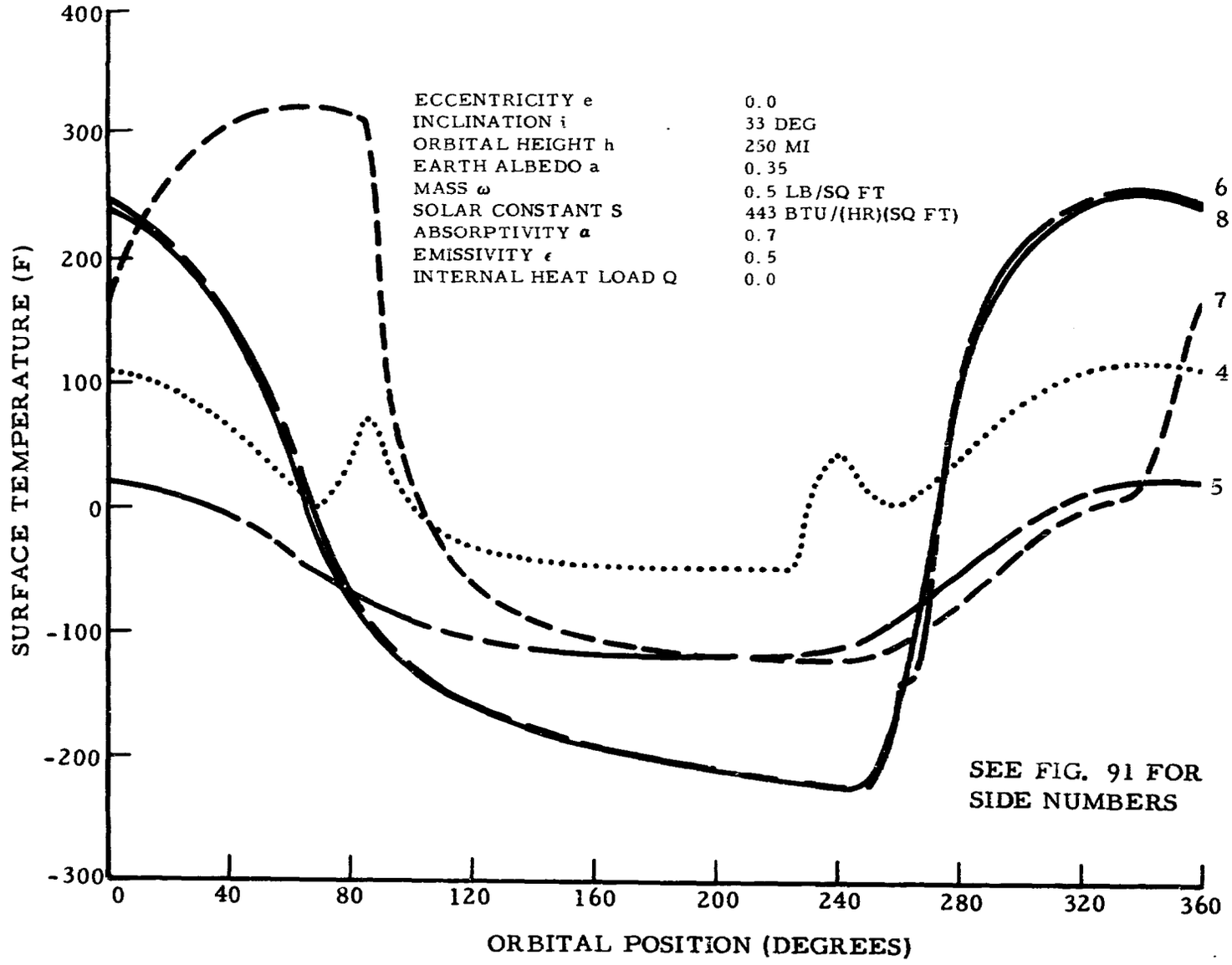

Figure 92. Cyclic Temperature Variation of Earth-Oriented Eight-Sided Prism (Sheet 2 of 2)

The effect of mass in reducing the temperature spread between maximum and minimum temperatures is shown by surface 1 (the bottom surface which always faces the earth) when compared with the earth-oriented flat plate in Figure 90. For the case with extremely small surface mass, surface 1 reaches the shadow side equilibrium temperature of -17 F. When the mass is increased to 1.5 pounds per square foot and absorptivity and emissivity are changed to 0.4 and 0.3, respectively, the maximum and minimum temperatures are 101 and 37 F. With the proper choice of surface finish and a reasonable structural mass, these particular vehicle surfaces can be maintained within reasonable temperature limits.

DISCUSSION OF ASSUMPTIONS

1. It is assumed in this analysis that the earth can be represented gravitationally by the zero-order and second-order spherical harmonics of its potential. The presence of harmonics in the earth's gravitational potential causes periodic and secular variations in several of the orbital elements. Only the secular perturbations which result in regression of the nodes and advance of the perigee position are considered in the analysis. Other periodic changes have negligible effect upon the shadow intersection problem.

2. A rigorous specification of the position at which the satellite enters and exits the earth's true shadow leads to needlessly complicated expressions. For this reason the following simplifications concerning shadow geometry are assumed:

   a. The earth is spherical with its radius equal to 3960 statute miles.
   b. The earth's shadow is cylindrical and umbral (sun at infinity).
   c. Penumbral effects are ignored.

   The error involved is extremely small even when large orbits are considered. For instance, a satellite in a circular orbit with an altitude of 10,000 miles has an orbit period of approximately 560 minutes, with perhaps 50 minutes spent in earth shadow (depending on orbit orientation). By assuming a cylindrical earth shadow and ignoring penumbral effects, the analysis uses an umbral shadow time that is about 50 seconds longer than the true umbral shadow time. This is a negligible error. For a 1000-mile-altitude circular orbit, the negligible error is approximately 18 seconds in an orbit period of 118 minutes. Additionally, it should be mentioned that the assumption of no penumbral effects tends to lessen the above errors introduced by the assumption of cylindrical umbral shadow, so that there is almost zero error from a thermal analysis standpoint.

3. It is assumed that all thermal radiation considered in the analysis, except solar radiation, is in diffuse form. Fortunately most thermal radiation is in diffuse form, which is relatively simple to analyze when compared with specular radiation.

4. It is assumed that direct solar radiation impinges upon the earth and upon the satellite with parallel rays, due to the great distance between the sun and its planets. Almost zero error is introduced into the analysis by the assumption.

5. In all cases, it is assumed that the earth emits as a black body and is in a state of thermal equilibrium (i. e., the planetary emitted energy is equal to the absorbed solar energy). It is also assumed that the earth emission is a constant at any point on its surface and does not vary from day to night. These are reasonable assumptions because little is known of the actual spectral and local variations in the planetary emitted radiation.

6. The earth reflected solar radiation is assumed to follow the cosine law (i. e., it is a maximum at the subsolar point and decreases to zero at the terminator). This assumption greatly simplifies the analysis and is quite accurate except in the region of the terminator, where a slight error is introduced.

7. In all cases, the planetary albedo σ is assumed to be constant over the surface of the planet, and the planet is assumed to be a diffuse reflector. This is done because of the complications of the problem and because local variations are almost impossible to define.

8. In all cases, conduction and convection between the satellite and its surroundings are neglected. This is reasonable because orbital heights are usually too far above the atmosphere for these types of thermal effects to appear.

9. It is assumed that the absorptivity of the vehicle surface to planetary thermal emission is equal to the emissivity of the vehicle surface. Since the effective temperature of the earth and the temperatures of most vehicle surfaces are nearly the same, this assumption is validated by Kirchhoff's law.

10. Any scattering effects of direct solar radiation upon the satellite due to the earth's atmosphere are ignored. It is felt that this will introduce a negligible error into the analysis.

11. The geometrical configuration factor from the spherical satellite to earth was calculated with the assumption that the satellite is a point source in space. The assumption is valid if the satellite is uniform in temperature, which it would be if spinning or if its shell had a very high thermal conductivity.

Section IX

CONCLUSIONS

ANALYSIS TECHNIQUES

This report has reviewed the basic principles of thermal radiation and has presented several available methods of radiation heat transfer analysis, with emphasis upon the situation encountered by a vehicle in space.

An IBM 7090 program has been written (Section V) with which it is possible to obtain space vehicle shell temperatures and the incident radiant energy impinging upon the vehicle from its space environment. The significance of this program is that it will accurately simulate any elliptical or circular orbit into which a satellite may be placed.

In the field of general radiation heat transfer analysis, a comparison has been made between various methods of analysis in which the accuracy and versatility of the radiosity analog network method is pointed out. It is hoped that a more widespread use of this relatively new technique will occur in industry.

One of the most difficult areas in the analysis of radiation heat transfer is the proper calculation of the geometric configuration factor. A considerable amount of tabulated data is presented in this report (Section VII), some of which has been heretofore unpublished. In conjunction with this report, an IBM 7090 program (Reference 27) has been written which will calculate the configuration factor between two plane areas in any orientation with respect to each other. While presently limited in scope, this program has promise of being developed into an extremely valuable tool for the heat transfer engineer.

PROBLEM AREAS

Thermal Analysis of Nondiffuse Radiation

A problem area which came to light in the preparation of this report and which needs further investigation concerns the thermal analysis of nondiffuse radiation. Presently used methods of analysis make the basic assumption that all radiant energy is diffuse, whereas, in actuality, radiant energy usually exists in partly diffuse, partly specular form. Data pertaining to directional emissive properties are very limited, almost not

available. Fortunately, the majority of radiant energy does exist in essentially diffuse form, so that presently available analytical methods are usually applicable. There are many occasions, however, when this is not true, and the engineer is forced to make questionable approximations.

Calculation of Geometric Configuration Factors

Another problem area concerns the calculation of geometric configuration factors, an essential part of radiation heat transfer analysis. This is probably the most tedious and time consuming job encountered in the analysis. Although much work has been done in this area, data are still limited. For other than simple shapes, numerical or mechanical integrators must be utilized, and this is a time consuming process. As mentioned, there is hope that an IBM program can be developed to aid in this area.

Measurement and Presentation of Data

The accurate thermal analysis of space vehicles depends heavily on the availability of accurate data on the thermal properties of materials, including solids, liquids, and gases. These properties include absorptivity, emissivity, conductivity, and specific heat, and they should be known for the entire temperature range of interest and as a function of wave length, angle, and pressure, as applicable. Much of the published data on thermal properties, however, are subject to serious question; handbook-type data generally represent only average values over a narrow range of conditions. The common practice of not differentiating between normal and hemispherical emissivity can lead to serious errors in temperature prediction.

The lack of accurate information on thermal properties jeopardizes the accuracy of thermal analyses and probably will lead to in-flight failures. With the multiplicity of data collecting and publishing agencies, the inconsistencies and contradictions between published data on the same materials creates increasing confusion. So it is concluded that standardized methods of measuring and presenting data on the thermal properties of materials are needed.

Effects of Space Environment on Space Vehicles

It is generally accepted that space vehicles will be subjected to deteriorating influences in a space environment. In some cases, the magnitude of these external influences is known. In almost every case, however, the effect of these influences on space vehicle materials is either incompletely known or totally unknown. The data from actual satellites are very meager and are being accumulated too slowly to support current needs.

Although the accumulation of data relative to the effects in materials of some of the components of the space environment is progressing on many fronts, the present lack of data casts doubt on the current designs of space vehicles. One factor that seems to be receiving little experimental attention is the effect of micrometeorite erosion on the absorptivity and emissivity of surface coatings. The short-term effects may reasonably be neglected; but for long durations, the deterioration may become quite pronounced. Comparative data on absorptivity and emissivity before and after a multiplicity of simulated micrometeorite impacts on representative coatings are needed as a guide for future vehicle designs.

The lack of accurate and complete information on the effects of the space environment on the absorptivity and emissivity of surface coatings makes the design of passive temperature control systems very questionable for long-duration vehicles. To compensate for unknown variations, it may be necessary to resort to semipassive or active temperature control systems.

The effect of the low-pressure environment encountered in space is known to cause a significant increase in thermal resistance across structural joints, whether they be bolted, riveted, or spot-welded. This thermal resistance is almost impossible to predict accurately, and it must be eliminated in conduction cooling paths and other thermally significant structures. At the present time, there is available a vacuum-resistant silicone type grease, often called "space grease," which seems to offer great promise in reducing contact resistance when applied to a structural joint. There are other materials, such as aluminum foil, that might also prove to be effective upon investigation. Although some work has been done in this area, further effort is needed.

Section X

ANNOTATED BIBLIOGRAPHY

This annotated bibliography was prepared as a result of a literature survey conducted by the reference staff of the Technical Information Center of S&ID.

PERIODICALS

Advances in Astronautical Sciences

Vol 3, 1958, p 22-1 - 22-11.
Temperature equilibrea in space vehicles. R. Cornog.

The equilibrium temperature reached within a space vehicle moving within the solar system is discussed. The effects of vehicle configuration, vehicle attitude, surface properties, and internal heat release are evaluated. Particular attention is given to methods of vehicle design whereby the range of equilibrium temperatures can be set at some desired value.

Aero/Space Engineering

Vol 19, March 1960, p 58-60, 64.
Evaluation of thermal problems at relatively low orbital altitudes.
L. D. Wing.

Presented here is a simple way to estimate the maximum and minimum heat inputs experienced anywhere on the outer skin face of an orbiting vehicle.

Vol 19, October 1960, p 16-19, 56, 58, 59, 62.
Surface effects on materials in near space. F. J. Clauss.

The problems associated with the behavior of materials in space, including passive temperature control are discussed.

Aero/Space Sciences, Journal of the

Vol 26, December 1959, p 772-774.
Space vehicle environment, thermal radiation. C. Gazley and others.

"The primary mode of heat exchange between, a space vehicle and its environment is radiation." A brief summary is presented of present knowledge of such heat exchange, as it depends on solar rationation, neighborhood of a planet, and space vehicle itself.

Vol 27, February 1960, p 146-147.
The minimum-weight straight fin of triangular profile radiating to space. E. N. Nilson and R. Curry.

A basic property of the nonlinear differential equation expressing the radiation of waste heat from a spacecraft yields a method of solution which is an extension of the solution of the problem of determining the triangular fin of optimum shape for discharging such heat by convection.

American Physical Society, Bulletin of the

Vol 3, 1958, p 303.
Temperature control problems of artificial satellites. G. B. Heller.

American Rocket Society, Journal of the

Vol 17, 1957, p 34-35.
Some remarks on the temperature problem in the interplanetary rocket. R. L. Sternberg.

Annals of the IGY (Vol 6, Manual on Rockets and Satellites)

Vol 4, 1958, p 304-310.
The IGY earth satellite program: satellite-temperature control (summary of paper by L. Drummeter and M. Schoch presented at IGY Rocket-Satellite Conference, Washington, D. C., 30 September - 5 October 1957.

ARS Journal

Vol 29, May 1959, p 358-361.
Thermostatic temperature control of satellites and space vehicles. R. A. Hanel.

The temperature of satellites and space vehicles varies considerably with orbital conditions. To achieve greater reliability and

efficiency in long-life instruments, an automatic temperature control is highly desirable; a radiation thermostat performing this function is discussed. The suggested method regulates temperature by adjusting the effective absorptivity and emissivity. Bimetallic strips automatically move a light shield which exposes surfaces with high and low absorptivity-to-emissivity ratios. No internal power source is needed. Calculations demonstrate the effectiveness of the radiation thermostat. The temperature of the satellite's instruments can be kept constant within a few degrees of the design value, regardless of orbital conditions, internally dissipated power, and some erosion of skin coatings.

Vol 30, April 1960, p 344-352.
Thermal control of the Explorer satellites. G. Heller.

Thermal control of the Explorer satellites is discussed. The theoretical studies that were made prior to the launching of these satellites are described, and examples of relationships are presented in graphs. The lower limit of the instrument temperature was 0 C (determined by the efficiency of the chemical batteries). The upper limit was specified as 65 C (based on long-time temperature limits of transistors in the electronic package). This paper relates some of the studies, describes the measuring results of telemetered temperatures, and evaluates expected and obtained data.

Vol 30, May 1960, p 479-484.
Solar heating of a rotating cylindrical space vehicle. A. Charnes and S. Raynor.

Solar heating in a space vehicle idealized as a thin-walled circular cylinder rotating with uniform velocity about its geometric axis is studied for a situation in which heat transfer by convection and heat exchange within the cylinder is negligible. The nonlinear problem is approximated through a perturbation analysis, and detailed estimates are made of the parameters of interest for various ranges of speed of rotation. An estimate of the error between the exact and perturbational approach is made in the case of an illustrative example which might be expected to entail an extreme deviation.

Astronautical Sciences, Journal of the

Vol 5, Autumn-Winter 1958, p 64.
Temperature equilibrea in space vehicles. R. A. Cornog.

The equilibrium temperature reached within a space vehicle moving within the solar system is discussed. The effects of vehicle configuration, vehicle attitude, surface properties and internal heat release are evaluated. Particular attention is given to methods of vehicle design whereby the range of equilibrium temperatures can be set at some desired value.

Astronautics

Vol 5, April 1960, p 40-41, 105-106.
Thermal protection of space vehicles. P. E. Glaser.

The near-steady heating conditions encountered in long-term space flight have sparked development of integrated systems designed to protect the vehicle while combining maximum insulating effectiveness and low weight.

Astronautics, Journal of

Vol 3, Spring 1956, p 4-8, 26.
Thermal control in a space vehicle. P. E. Sandroff and J. S. Prigge.

Astrophysical Journal

Vol 131, January 1960, p 68-74.
Use of the equation of hydrostatic equilibrium in determining the temperature distribution in the outer solar atmosphere. S. R. Pottasch.

The purpose of this paper is to use the observed variation of electron density between 3000 kilometers and 20 solar radii and, assuming hydrostatic equilibrium, to derive a distribution of electron temperature in this region. The plausibility of the temperatures derived in this way is discussed.

Vol 131, March 1960, p 459-469.
Radiometric observations of Mars. W. Sinton and J. Strong.

Aviation Age

Vol 30, August 1958, p 174-180.
How to find thermal equilibrium in space. R. E. Hess and A. E. Weller.

IRE Transactions on Military Electronics

Vol Mil-4, April-July 1960, p 98-112.
Problems concerning the thermal design of Explorer satellites.
G. B. Heller.

The thermal design of the Explorer VII satellite is described. A thermal testing program conducted in the vacuum chamber with a prototype of Explorer VII is described, and some preliminary results of temperature measurements of the Explorer VII are given.

Iron Age

Vol 182, 6 November 1958, p 105-107.
How metals help control satellite's temperature. P. M. Unterweiser.

Case histories are considered concerning two small Navy satellites. The problem of controlling the temperature of the satellite's magnesium shell, which was subjected to periodic variations, was solved by gold plating its surface and covering it with an evaporated layer of silicon monoxide. This coating was then overlaid with opaque film of evaporated aluminum for high reflectivity.

Izvestiya Akademii Nauk SSSR, Seriya Geofizicheskaya

Vol 4, April 1957, p 527-533.
Temperature regime of an artificial earth satellite. A. G. Karpenko and M. I. Lidov.

Jet Propulsion

Vol 27, October 1957, p 1079-1083.
Skin temperatures of a satellite. C. M. Schmidt and A. J. Hanawalt.

The need for a workable artificial earth satellite has been established both for reconnaissance and as a prerequisite for space travel. An attendant problem in the design of such a vehicle is the control, and therefore the prediction, of temperatures that will exist in flight. Previous papers on this topic have brought out many salient features of such predictions, but have not been entirely realistic. The present paper attempts to improve on these assumptions and gives numerical computations for a particular configuration considered feasible for a satellite design. The example investigated is a nonrotating cylindrical

shell with one end point earthward. The problem of analysis is largely one of geometry, involving spacewise as well as timewise variations in skin temperature. The skin temperatures that will exist are very dependent on the properties of the surface, particularly emissivity and absorptivity, large values producing the widest range in surface temperatures. By proper choice of these parameters, this range can be greatly controlled. In particular, the mean temperature of the satellite skin is primarily a function of ol/e. For the specific configuration considered herein, nominal limits on the skin temperatures are -200 and +400 F.

Optical Society of America, Journal of the

Vol 47, 1957, p 261-267.
Optical problems of the satellite. R. Tousey.

Vol 49, September 1959, p 918-924.
Temperature stabilization of highly reflecting spherical satellites. G. Hass, L. F. Drummeter, Jr., and M. Schoch.

Report of NRL Progress

May 1958, p 1-7.
Satellite temperature control. L. F. Drummeter, Jr., and M. Schoch.

Science

Vol 127, 11 April 1958, p 811-812.
Temperatures of a close earth satellite due to solar and terrestrial heating.

See Aero/Space Engineering, Vol 17, No. 10, October 1958, p 104.

SAE Journal

January 1959, p 54-55.
Water and ammonia evaporators show promise in cooling orbital space vehicles. J. S. Tupper.

See Aero/Space Engineering, Vol 18, No. 5, May 1959, p 102.

Vistas in Astronautics

Vol 1, p 157-158.
The temperature equilibrium of a space vehicle. J. E. Navgle.

The equilibrium temperature of a space vehicle is considered. In space, away from the earth, the vehicle will come into radiative equilibrium with the sun's radiation. The skin temperature of the vehicle will rise until the amount of energy radiated by the vehicle is equal to the sum of the energy absorbed from the sun and that produced in the vehicle itself. The absorbed solar energy is in the visible portion of the spectrum, whereas the emitted energy is in the far infrared. Equilibrium temperatures attainable with existing materials are too high; the basic problem is one of keeping the vehicle cool. The problem of interest is the effect of the environment on the surface of such vehicle. Additional research is needed both as to the nature of the environment to be encountered and as to the effect of this environment on the surface.

Western Machinery and Steel World

Vol 50, October 1959, p 72-74.
Coatings for space vehicles. J. L. Snell.

At Jet Propulsion Laboratory, California Institute of Technology, ordinary types 430 and 410 stainless steels, used to encase delicate instrument capsules, were made to have thermal characteristics not yet possible in metal alone. Discussed are the techniques for temperature control, fabrication of the final assembly, and application of special process coatings of Rokide A by Cooper Development Corporation, Monrovia.

REPORTS AND PAPERS

Air Force Cambridge Research Center

TN-58-633, March 1959.
The temperature of an object above the earth's atmosphere. M. H. Seavey. (AD-208, 863)

The equilibrium temperature of an object above the earth's atmosphere is calculated by considering the thermal radiation balance for the object.

American Rocket Society

Preprint 383-56, 1956.
Skin temperatures of a satellite. C. M. Schmidt and J. S. Prigge.

Army Ballistic Missile Agency

DV-TN-73-58, 1958.
Thermal problems of satellites. G. Heller.

California Institute of Technology

EP-481
Satellite temperature measurements for 1958 Alpha - Explorer I.

External Publication 514, 2 June 1958.
Scientific results from the Explorer satellites. A. R. Hibbs.

A brief history of Explorer satellite launchings is given, together with a description of payload instrumentation. Results of experiments made in the areas of temperatures of both case and internal instrumentation, micrometeorite activity, and cosmic ray intensity are summarized. The results of preliminary analyses of these various measurements as carried out by the responsible institutions are presented, and their implications for future measurements of this type are discussed.

External Publication 647, 7 May 1959.
Temperature control in the Explorer satellites and Pioneer space probes. E. P. Bulvalda and others.

The Jet Propulsion Laboratory participated in the Explorer and Juno II programs in the areas of payload design and method of achieving temperature control. This publication describes the basic theory for the passive temperature control of satellites and space probes and the application of this process to the Explorer and Pioneer III and IV vehicles. Some results of in-flight temperature measurements are also presented.

Memo 20-194, 15 February 1960.
Radiative properties of surfaces considered for use on the Explorer satellites and Pioneer space probes.

Spectral reflectance data in graphical form and tabular absorptance-emittance data are presented for surface materials considered for use on the Explorer satellites and Pioneer space probes. The surfaces ranged from bare aluminum, titanium, and stainless

steel to painted coatings, coatings of Rokide A, and anodized and plated coatings. A brief review of the temperature control problem is presented as background information.

Progress Report 20-294, 28 March 1956.
The temperature of an orbiting missile. A. R. Hibbs.

The successful operation of radio equipment carried in an orbiting missile requires fairly close control over the temperatures to which the equipment is subjected. This temperature is controlled by two factors. First, the temperature of the outer shell of the missile depends on radioactive transfer between the missile and its environment (sun, earth, and empty space). Secondly, the temperature of the equipment inside the missile depends on heat transfer from the shell (directly by radiation and through the structure by conduction). The analysis presented shows how the average temperature of the outer shell can be controlled (for a given missile shape, orientation, and trajectory) by a correct choice of surface coatings. It also indicates that the limits of temperature variation of the enclosed equipment can be held to within a few degrees of this average shell temperature by adequate insulation. Numerical calculations indicate the necessary characteristics of the coating and insulating materials.

Progress Report 20-319, 11 April 1957.
Evaluation of the absorptivities of surface materials to solar and terrestrial radiation, with plots of the reflectances (at wave-lengths of 0.4 to 25 m) for 10 sample materials including 2 types of fibrous-glass reinforced plastic. W. S. Shipley.

Progress Report 20-359, 3 September 1958.
Contributions of the Explorer to space technology. J. E. Froehlich and A. R. Hibbs.

The philosophy of the Explorer programs is presented and demonstrated in the description of missile design and flight operation of the Explorer vehicles. Scientific measurements of cosmic ray intensity, temperature environment, and micrometeorite densities are described, and the significance of these measurements is discussed.

General Electric Company, Aerosciences Laboratory

T. I. S. Report R60SD386, August 1960.
A method for calculating the thermal irradiance upon a space vehicle and determining its temperature. T. L. Altshuler.

A method is presented for determining the thermal irradiance upon a space vehicle as a result of direct radiation, planetary thermal radiation, and planetary albedo. From this information, the temperature of a space vehicle can be obtained. Calculations can be made for various space vehicle altitudes above a planet and for various solar angles with respect to both the planet and space vehicle. The planets and natural satellites considered are the earth, moon, Mars, and Venus.

Grumman Aircraft Engineering Corporation

Report Xp12. 20, May 1960.
Determination of thermal radiation incident upon the surfaces of an earth satellite in an elliptical orbit.

A procedure is presented for determining the radiation incident upon a satellite in an elliptical orbit. The satellite is treated as a set of plane areas, each area identified by the direction cosines of its outward normal with respect to a satellite coordinate system. This system is based on orbit orientation. Radiation emitted by and reflected by the parent body is computed by integrating over the spherical cap seen by the satellite. Solar radiation is considered constant. The method is applied to a hypothetical satellite in orbit. Comparisons of incident radiation have been made between rotating and nonrotating satellites in the same orbit. This type of comparison might be used to decide whether or not satellite rotation is desirable, and if so, to what extent. It is also possible to compare different orbits for the same satellite to optimize radiation to its surface.

IGY Satellite Report Series No. 3

Paper No. 4, 1 May 1958.
Satellite temperature measurements for 1958 Alpha - Explorer I.
E. P. Buwalda and A. R. Hibbs.

Internation Astronautical Federation

September 1956.
Studies of a minimum orbital unmanned satellite of the earth: part III. Radiation and equilibrium temperature, D. T. Goldman and S. F. Singer (Astronautica 0/86-733, Zeilen Garmond, Presented at 7th Congress of IAF).

National Academy of Sciences, National Research Council Materials Advisory Board

MAB-155-M, 20 October 1959.
Materials problems associated with the thermal control of space vehicles.

National Aeronautics and Space Administration

TND-357, June 1960.
Determination of the internal temperature in satellite 1959 Alpha (Vanguard II). V. R. Simar and others.

Satellite 1959 Alpha was equipped so that accurate measurement of the mini-track beacon frequency (with the doppler component removed) was sufficient to determine the satellite's internal temperature. To provide a precise measurement of this frequency, a sensitive receiving system, utilizing a highly stable but tunable first local oscillator and a noise-eliminating tracking filter, was developed. In addition to the temperature determination, other information such as roll rate and rocket performance was obtained from the observations.

North American Aviation, Los Angeles Division

NA-54-586, 2 July 1954.
A proposed research and development program directed toward reliable temperature prediction of aircraft structural components: part IV. radiation effects. M. R. Kinsler.

NA-56-68, 12 April 1957.
Performance specifications for a versatile spectrophotometer for thermal radiation measurements. E. L. Goodenow and M. W. Peterson.

NA-56-69, 12 April 1957.
Possible designs for a versatile spectrophotometer for thermal radiation measurements. E. L. Goodenow and M. W. Peterson.

NA-57-41, 12 April 1957.
Spectrophotometer for thermal radiation studies. P. E. Ohlsen and G. A. Ethemad.

NA-57-707, 28 June 1957.
Control of external skin temperatures by use of selective finishes.
G. C. Frey.

NA-57-330, 23 July 1957.
Spectral and total radiation data of various aircraft materials.
P. E. Ohlsen and G. A. Etemad.

NA-57-707-1, 5 February 1958.
Emissivity and reflectance of selected surface coatings. R. E. Klemm.

NA-58-525, March 1958. (Secret)
Thermo considerations for the design of satelloid vehicles.

NA-58-1599, 15 December 1958. (Secret)
Preliminary thermo analysis of extensive surfaces protection system requirements for B-70 air vehicle. P. Ohlsen and A. Nusenow.

NA-59-102, 11 August 1959. (Secret)
Preliminary thermodynamic analysis of I. R. seekers for B-70.

NA-59-53, 1959. (Secret)
Thermal radiation characteristics of B-70 weapon system.
R. Klemm and others.

NA-59-53-1, 31 July 1959. (Secret)
Thermal radiation characteristics of B-70 weapon system.
R. Klemm and others.

NA-59-1887. (Secret)
B-70 infra-red radiation and radar X-section. W. Kemp.

Office of Naval Research

IRIS Proceedings (Confidential), Vol 4, No. 1, 1959, p 115-27.
Temperature stabilization of Vanguard satellites, theory and practice.
L. F. Drummeter and G. H. Hass. (Chapter referenced is unclassified)

The temperature of an orbiting satellite depends on radiation balancing and on the parameters which control the radiation environment. The latter include orbital characteristics and the surface properties of the satellite skin. The surface properties are absorptance for extraterrestrial sunlight and hemispheric emittance, and the governing parameter is the ratio of these. Adjustment of the surface parameters permits a passive system of temperature stabilization and is used in the Vanguard program. For visibility reasons, the Vanguard

devices had to have specular reflecting surfaces with high visible reflection. For satisfactory temperatures, the infrared properties had to be modified to increase the surface emittance. The solution consisted of overcoating polished metal with a vacuum coating of partially oxidized SiO. This material is transparent in the visible but has infrared absorption between 8 and 12 microns. A film 0.54 micron thick has an emittance of 0.13 at 20 C; the emittance increases to 0.40 for a film 1.2 microns thick. Satellite coating is done in a 72-inch evaporator in a special rotating jig designed to provide relatively uniform thickness.

Oklahoma State University, Engineering Experiment Station

Publication 112, April 1960.
Radiation heat transfer and thermal control of spacecraft. F. Kreith.

The material in this report was presented as a lecture series. The basic principles of radiation are reviewed. The most important aspects of thermal control and solar power generation for spacecrafts and satellites are covered, as are methods for determining radiation properties with special emphasis on selective surfaces. Radiation processes in an enclosure (such as a cavity receiver of a solar powerplant or the interior of a space platform), important energy sources in the solar system (sun and planets), and the atmosphere of the earth are discussed. The fundamentals of solar powerplant design for spacecraft are given.

University of Wisconsin

1960.
The thermal radiation balance experiment on board Explorer VII.
V. E. Suomi.

The radiation energy budget of the earth is determined by the magnitude of three radiation currents: (1) the direct radiation from the sun, (2) the fraction of this that is diffusely reflected by the earth, the clouds, and the atmosphere, and (3) the fraction that is converted into heat and is ultimately reradiated back to space in the far infrared portion of the spectrum. On Explorer VII, three radiation currents are measured with simple bolometers in the form of hollow silver hemispheres. The hemispheres are thermally isolated from, but in close proximity to, specially aluminized mirrors. The image of the hemisphere, which appears in the mirror, makes the sensor look like a full sphere. Two of the hemispheres have a black coating which makes them respond about equally to solar and terrestrial

radiation. Another hemisphere, coated white, is more sensitive to terrestrial radiation than to solar radiation. A fourth has a gold metal surface which makes it more sensitive to solar than to terrestrial radiation. The information telemetered to the earth's surface is the sensor temperatures. The radiation currents are obtained by using these temperatures in heat-balance equations. Sample calculations are given and results are described.

Wright Aeronautical Development Division

WADD TR 54-42, 1954.
Total normal emissivities and solar absorptivities of materials. G.B. Wilkes.

BOOKS

Clauss, F.J., Editor

Surface effects on spacecraft materials. Wiley, 1960, p 3-54. Effect of surface thermal-radiation characteristics on the temperature-control problem in satellites. W.G. Camack and D.K. Edwards.

The satellite thermal problem is reviewed. Satellite temperatures are shown to depend upon exterior thermal radiation characteristics, external environment, orbit geometry, and internal power generation. A method is presented for estimating uncertainties in the predicted temperatures brought about by uncertainties in the determining variables. Graphs and formulas necessary for application of the method are included in appendixes. A survey is made of the origins of uncertainties in the determining variables. Uncertainties in radiation characteristics of surfaces are shown to arise from lack of precision in measurements, lack of control in manufacturing processes, and lack of surface finish stability. Numerical examples clearly illustrate the importance of the uncertainties in radiation characteristics. Methods of reducing uncertainties in internal satellite temperatures through careful selection of surface finishes are given, and active control systems are discussed.

Surface effects on spacecraft materials. Wiley, 1960. p 55-91. Temperature control of the Explorers and Pioneers. T.O. Thosten and others.

The Jet Propulsion Laboratory participated in the launching of the Explorer satellites and the Juno II space probes (Pioneers III and IV). This participation included payload design and the method of achieving temperature control. This paper describes the basic theory for the passive temperature control of satellites

and space probes and the application of this process to the Explorer and Pioneer III and IV vehicles. Some results of in-flight temperature measurements are also presented.

Surface effects on spacecraft materials. Wiley, 1960, p 92-116.
Coatings for space vehicles. J. C. Raymond.

Six general types of coatings and some of their properties of interest for spacecraft applications are discussed: organic coatings, electrodeposited coatings, phosphate-bonded ceramic coatings, porcelain enamels, high-temperature frit-refractory ceramic coatings, and flame-sprayed ceramic coatings. The four types of ceramic coatings are discussed in detail. A brief description of metal preparation, application and firing of coatings, and coating properties is included. Values for total hemispherical and normal spectral emittance are given where available.

Surface effects on spacecraft materials. Wiley, 1960, p 152-63.
Vanguard emittance studies at NRL. L. F. Drummeter, Jr., and E. Goldstein.

The general problem of passive control of temperature in the Vanguard devices involved many problem areas. This paper presents procedures and results associated with one phase of the thermal work—the studies of emittance. The total hemispheric emittances of several materials were measured by coating them on sample bodies, suspending the bodies in an evacuated chamber, and heating them. The emittances of Al_2O_3 and SiO coated on aluminum, gold, and silver surfaces, of polished tungsten carbide, and of silicon solar cells were measured.

Surface effects on spacecraft materials. Wiley, 1960, p 182-94.
Some methods used at the National Bureau of Standards for measuring thermal emittance at high temperatures. J. C. Richmond.

At the National Bureau of Standards, the Radiometry Section of the Atomic and Radiation Physics Division and the Enameled Metals Section of the Mineral Products Division are concerned with thermal emittance measurements. The investigations of the Radiometry Section include absorption of radiation and the interpretation of absorption spectra (including infrared absorption spectra), accurate evaluation of materials for use in wavelength calibration of spectrometers, and calibration of standards of spectral radiation and standards for total radiant energy. The Enameled Metals Section is engaged in developing instrumentation and procedures for determining total hemispherical emittance,

normal spectral emittance, and spectral reflectance of a wide variety of materials, including ceramics and ceramic-coated metal.

Hynek, J. A., Editor

Astrophysics, a topical symposium. 1951, p 259-301.
The sun and stellar radiation (chapter 6).

Radiation and stars from the sun are discussed, including the spectral energy curve of the sun and the solar constant. The various sources of heat in the photosphere are described. These include radiation from stars and planets, radiation from variable stars, and planetary heat. Radiation properties of the moon are also taken up.

Kuiper, G. P., Editor

The solar system: vol 2. The earth as a planet. University of Chicago Press, 1954, p 726-738.
Albedo, color and polarization of the earth. A. Dajon.

Malone, T. F., Editor

Compendium of meteorology. American Meteorological Society, 1951, p 25-28.
Solar radiant energy, its modification by the earth and its atmosphere. S. Fritz.

Van Allen, J., Editor

Scientific uses of earth satellites. University of Michigan Press, c1956, p 73-84.
Isolation of the upper atmosphere and of a satellite. P. R. Gast.

The temperature of a satellite is the resultant of the sum of radiations from three sources: directly from the sun, solar radiation returned from the atmosphere and the earth (both 6000 K radiation), and low-temperature (250 k) radiation from the earth. Assuming various characteristics for the model of the satellite (absorptivity of the surface, shape, mass, specific heat) and orbit trajectories (distance of perigee and apogee, duration of insolation, and duration in shadow of the earth), the ranges of maximum and minimum temperatures may be calculated. For one possible elliptical trajectory the mean temperatures for an 0.8-meter, 100-kilogram spherical satellite are not far from 0 C. As the satellite in its orbit passes from sunlight into the shadow

of the earth, the temporary maximum temperatures in the sunlight range from 13 to 3 C and the temporary minimum temperatures in the shadow range from -3 to 5 C. The highest maximum temperature is with the sun in line with the projected major axis and the illuminated satellite at a perigee of 300 miles, and the lowest minimum temperature with the sun in the same position and the satellite at an apogee of 1000 miles. Measurements of insolation freed from difficulties of atmospheric attenuation and measurements of the albedo of the earth will be possible from a satellite vehicle. To achieve the required accuracy, however, rather precise knowledge of the orientation of detectors is essential. Hazards which are unique to the environment may be encountered in attempting measurements from a satellite. These include the effects of the vacuum ultraviolet irradiation and of accumulation of micrometeorites on surfaces of detectors, windows, and satellite skin.

Scientific use of earth satellites. University of Michigan Press, c1956, p 133-136.

The radiative heat transfer of planet earth. J. J. F. King.

A method is developed for obtaining the vertical temperature distribution of a planetary atmosphere from the law of darkening of the planet's emission spectrum. The intensity of the radiation emerging from a planet is directly dependent on the vertical thermal structure of its atmosphere. For the monochromatic case, the emergent intensity is simply the Laplace transform of the Planck intensity considered as a function of optical depth. Now, for a given wavelength the Planck intensity is a single-valued function of temperature. Thus, in principle, a complete knowledge of the variation of the emergent intensity with zenith angle (law of darkening) suffices to determine the thermal structure of the accessible optical depth. In practice, to find the Planck intensity it is necessary to obtain the inverse Laplace transform, which is mathematically tantamount to solving a Fredholm integral equation of the first kind. An approximate solution to the problem is obtained using the Volterra method, which replaces the integral equation by a set of linear simultaneous equations with the Planck intensity expressed as a series of step functions. A sample calculation shows that as few as three values of the limb-darkening function yield quantitative information on the vertical temperature distribution. Alterations in the theory necessitated by considerations of band, rather than monochromatic, intensity measurements are indicated. A lightweight, rugged instrument which appears capable of such thermal measurements is discussed. This is the far infrared filter photometer currently being developed by Johns Hopkins University under Air Force contract AF 19(604)-949.

Scientific use of earth satellites. 2nd ed, c1958, p 69-72.
Experiments for measuring the temperature, meteor penetration and surface erosion of a satellite vehicle. H. E. LaGow.

White, C. S. and Benson, O. O., Editors

Physics and medicine of the upper atmosphere. University of New Mexico Press, 1952, p 88-89.
Thermal aspects of travel in the aeropause, problems of thermal radiation.

Section XI

REFERENCES

1. "Emissivity and Emittance, What Are They?," Defense Metals Information Center, Battelle Memorial Institute, OTS PB 161222 (DMIC Memorandum 72), 10 November 1960.

2. Giedt, W.H., "Principles of Engineering, Heat Transfer," D. Van Nostrand Company, Princeton, New Jersey, 1958.

3. Eckert, E.R.G., and Drake, R.M., Jr., "Heat and Mass Transfer," McGraw-Hill Book Company, New York, 1959.

4. "Elementary Heat Transfer," University of California Syllabus Series 317, University of California Press, Berkeley, California, June 1950.

5. Brown, A.I., and Marco, S.M., "Introduction to Heat Transfer," McGraw-Hill Book Company, New York, 1942.

6. Van Vliet, K.M., "Selective Coatings for Extraterrestrial Solar Energy Conversion, A Fundamental Analysis," Wright Air Development Division, WADD TR 60-773, 1960.

7. Johnson, F.S., "The Solar Constant," Journal of Meteorology, Vol II, No. 6, December 1954, p 413-439.

8. Eiwen, C.J., and Winer, D.E., "Criteria for Environmental Analysis of Weapon Systems," American Machine and Foundary Company, July 1960. (Preliminary Copy, WADD Technical Report)

9. "Handbook of Geophysics," 1st Ed, Geophysics Research Directorate, Air Force Cambridge Research Center.

10. Kuiper, G.P., "The Atmosphere of the Earth and Planets," 2nd Ed, Chicago Press, Chicago, Illinois, 1952.

11. Fritz, Sigmund, "The Albedo of the Planet Earth and of Clouds," Journal of Meteorology, 1949.

12. Altshuler, T.L., "A Method for Calculating the Thermal Irradiance Upon a Space Vehicle and Determining Its Temperature," General Electric Company, R60SD386, August 1960.

13. McCue, G.A., "Eclipse Characteristics of Close Earth Satellite Orbits," Space and Information Systems Division, North American Aviation, Inc., SID 61-50, February 1961.

14. Cunningham, L.E., "The Motion of a Nearby Satellite With Highly Inclined Orbit," Astronomical Journal, Vol 62, January 1957.

15. Ballinger, J., et al, "Thermal Environment of Space," Convair Astronautics Division, General Dynamics Corporation, ERR-AN-016, November 1960.

16. Oppenheim, A.K., "Radiation Analysis by the Network Method," Presented at Annual Meeting of American Society of Mechanical Engineers (New York), November 1954.

17. Brown, A.I., and Marco, S.M., "Introduction to Heat Transfer," McGraw-Hill Book Company, New York, 1942.

18. Obert, E.F., "Elements of Thermodynamics and Heat Transfer," McGraw-Hill Book Company, New York, 1949.

19. Peterson, M., "Radiation Effects," Los Angeles Division, North American Aviation, Inc., NA-56-399, 1956.

20. Giedt, W.H., "Principles of Engineering Heat Transfer," D. Van Nostrand Company, Princeton, New Jersey, 1958.

21. McAdams, W.H., "Heat Transmission," Third Edition, McGraw-Hill Book Company, New York, 1954.

22. Hamilton, D.C. and Morgan, W.R. "Radiant-Interchange Configuration Factors," National Advisory Committee for Aeronautics, NACA TN 2836, 1952.

23. Brock, O.K., "Thermal Radiation Interchange Between Black and Grey Surfaces," Convair Fort Worth, General Dynamics Corporation, PT-23, 3 June 1960.

24. Leuenberger, H., and Person, R.A., "Radiation Shape Factors for Cylindrical Assemblies", American Society of Mechanical Engineers, Paper 56-A-144.

25. "Thermal and Luminous Radiative Transfer", University of California at Los Angeles, Notes for Course X473GH, 1960. (P.F. O'Brien and J.A. Howard, Instructors)

26. Moon, P., "The Scientific Basis of Illuminating Engineering," McGraw-Hill Book Company, New York, 1936.

27. Nordwall, H. L., "Geometrical Configuration Factor Program," Space and Information Systems Division, North American Aviation, Inc., SID 61-90, 30 April 1960.

28. Eckert, E. R. G., "Introduction to the Transfer of Heat and Mass," McGraw-Hill Book Company, New York, 1950.

29. Townsend, H., "Journal of Scientific Instruments," Vol 8, 1931, p 177.

30. Hottel, H. C., "Radiant Heat Transmission," Mechanical Engineering, Vol 52, No 7, July 1930, p 699-704.

31. Boelter, L. M. K., et al, "A Mechanical Integrator for Determination of Illumination from Diffuse Surface Sources," Transactions of the Illuminating Engineering Society, Vol 34, No 9, November 1939, p 1085-1092.

32. Boelter, L. M. K., et al., "Engineering Airplane Cooling," College of Engineering, University of California at Los Angeles, January 1947.

33. McCue, G. A., "Program for Determining Temperatures of Orbiting Space Vehicles, "Space and Information Systems Division, North American Aviation, Inc., SID 61-105, 20 April 1961.

APPENDIX A

TABLES OF EMISSIVITY AND ABSORPTIVITY

This appendix was supplied by the AiResearch Manufacturing Division of the Garrett Corporation. The data presented are incomplete and will be expanded in the first revision of the basic report.

INTRODUCTION

Because radiative heat transfer is a surface phenomenon, it is usually desirable to coat the heat transfer surface to accomplish the desired radiative exchange. The properties of these surface coatings are of importance in the design of space heat rejection systems, because radiation is the only means of dissipating heat other than expelling large masses from the vehicle. The radiator may be exposed to radiation from the sun, nearby planets, and other parts of the vehicle.

Considerable work has been done in recent years in developing coatings, particularly those which are spectrally selective. Some of the applications and the desired types of coatings are listed in Table 1.

NOMENCLATURE

α	Total absorptivity
α_s	Total absorptivity to solar radiation
α_λ	Monochromatic absorptivity
ϵ	Total emissivity
ϵ_T	Total emissivity of radiator surface
ϵ_λ	Monochromatic emissivity
λ	Wavelength, microns
μ	Microns (1.0 micron = 10^{-4} centimeters)

Table 1. Coatings and Their Application

Application	Desired Coating	Result
Absorber for heat engine using solar energy	High solar absorptivity, low thermal emissivity	High-energy absorption, high temperature
Photovoltaic cell	High solar absorptivity for cell sensitivity range, high thermal emissivity	High-energy absorption, low temperature
Infrared detector window	High solar reflectivity, high thermal transmittance	Infrared detection, low temperature
Low-temperature radiator	Low solar absorptivity, high thermal emissivity	High heat rejection per unit area
High temperature	High thermal emissivity (low solar absorptivity desirable as long as ϵ_T is high)	High heat rejection per unit area
Solar concentrators	High solar reflectivity	High-efficiency concentrator
Passive temperature control system	Variable α_s/ϵ_T to accommodate solar flux and internal heat load changes	Constant internal temperature
Ultraviolet protective coating for organic materials	Reflective or absorbing	Reflection or conversion of ultraviolet into another form to protect organic materials

SELECTIVE ABSORPTION OR EMISSION

The use of spectrally selective coatings is often desirable to control energy flux. There are many materials whose total emissivity varies with temperature, and these can often be used to achieve the proper energy balance. Figure 1 shows, in general, how total emissivity varies with

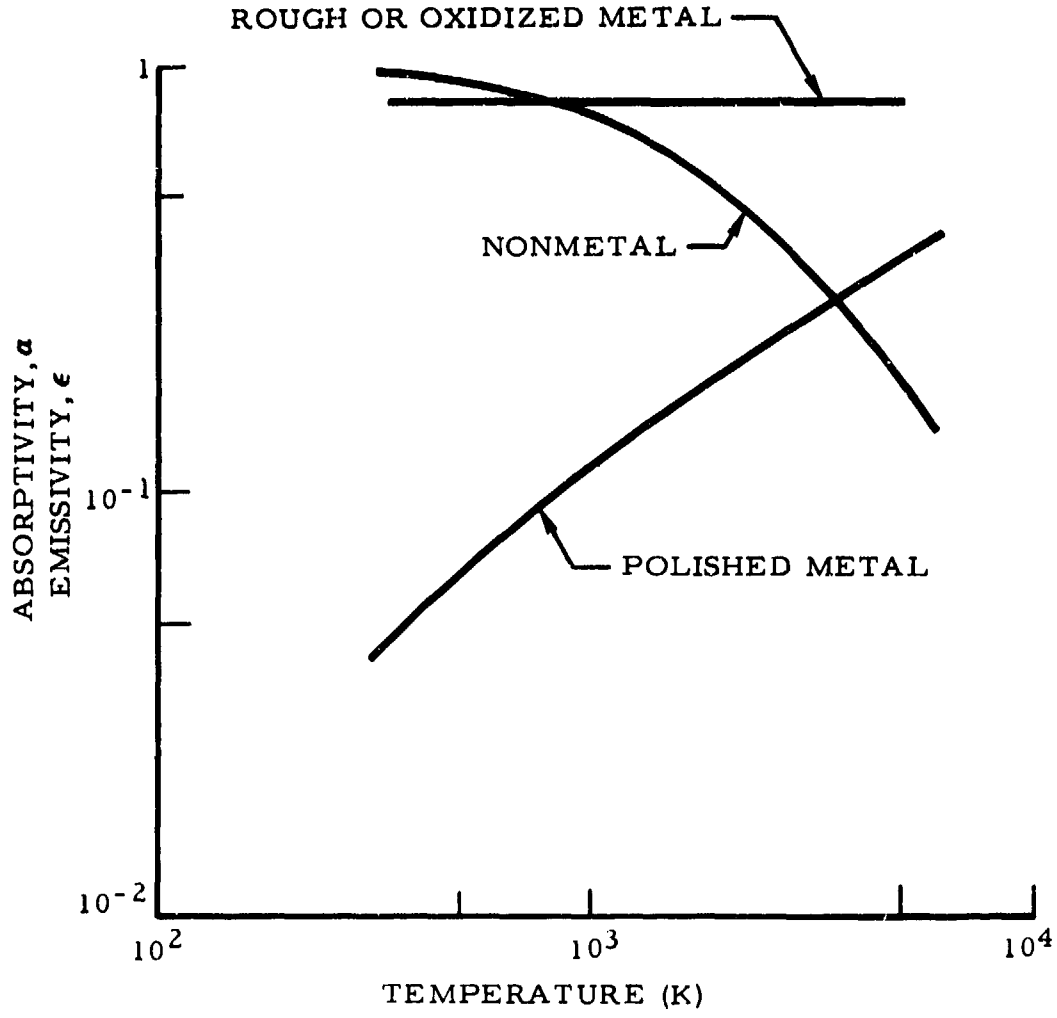

Figure 1. Typical Variation of Surface Absorptivity and Emissivity With Temperature

temperature for metals and nonmetals. For example, α_s/ϵ_T is shown to be greater than unity for polished metals and less than unity for nonmetals.

By use of the principles outlined in the body of this report, selective radiation surfaces can be fabricated by depositing multiple layers of coating material on the surface. Interference films, cavity absorption, absorbing undercoatings, Fresnel (or dielectric) films can be utilized.

For example, a gold smoke film evaporated from a tungsten filament in the presence of small amounts of nitrogen and oxygen has the property of being almost completely transparent to radiations above 2 microns. About 97 percent is transmitted, whereas only 20 percent of the visible spectrum is transmitted with 2 to 3 percent reflection, using a heat source of 120 F, Reference 1.

A polished copper surface may be assumed to be 75 percent reflective in the visible and 98 percent in the infrared range. Thus, if the gold smoke film were deposited on this copper surface, 92 percent of the radiation above 2 microns and only 5 percent of the visible radiation would be reflected due to the double absorption. However, at elevated temperatures the structure and optical properties of the film is affected and stability becomes a factor.

Because emissivity is strongly dependent on surface characteristics, it is necessary that the surface be maintained in a condition most closely approximating the operating environmental conditions during emissivity measurements. In the case of space radiators, high vacuum is most important. Grease, dust, impurities or absorbed gases can materially affect the expected response of a surface.

SPECTRAL CHARACTERISTICS OF COATINGS

The spectral characteristics of some coatings which may be applicable for space radiators are given here. The values for total emissivity are taken from several sources. These totals are only indicative of coating emissivity, because substrate preparation and method of deposition greatly influences the spectral characteristics.

The spectral characteristics of some enamels and pure oxides are shown in Figures 2 through 7 (Reference 2). These characteristics are presented as indicative of the type of information which can be found in the literature.

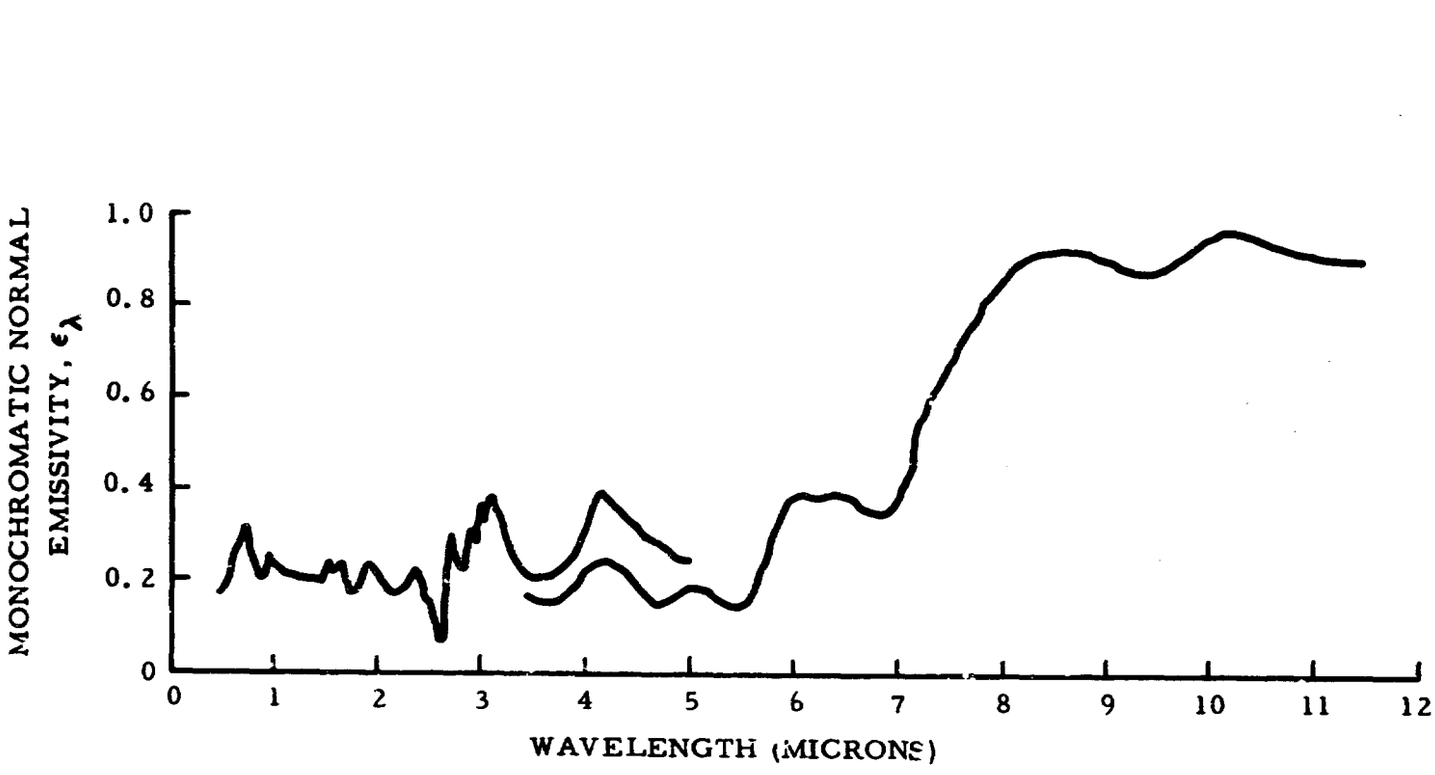

Figure 2. Monochromatic Normal Emissivity Versus Wavelength for Aluminum Oxide

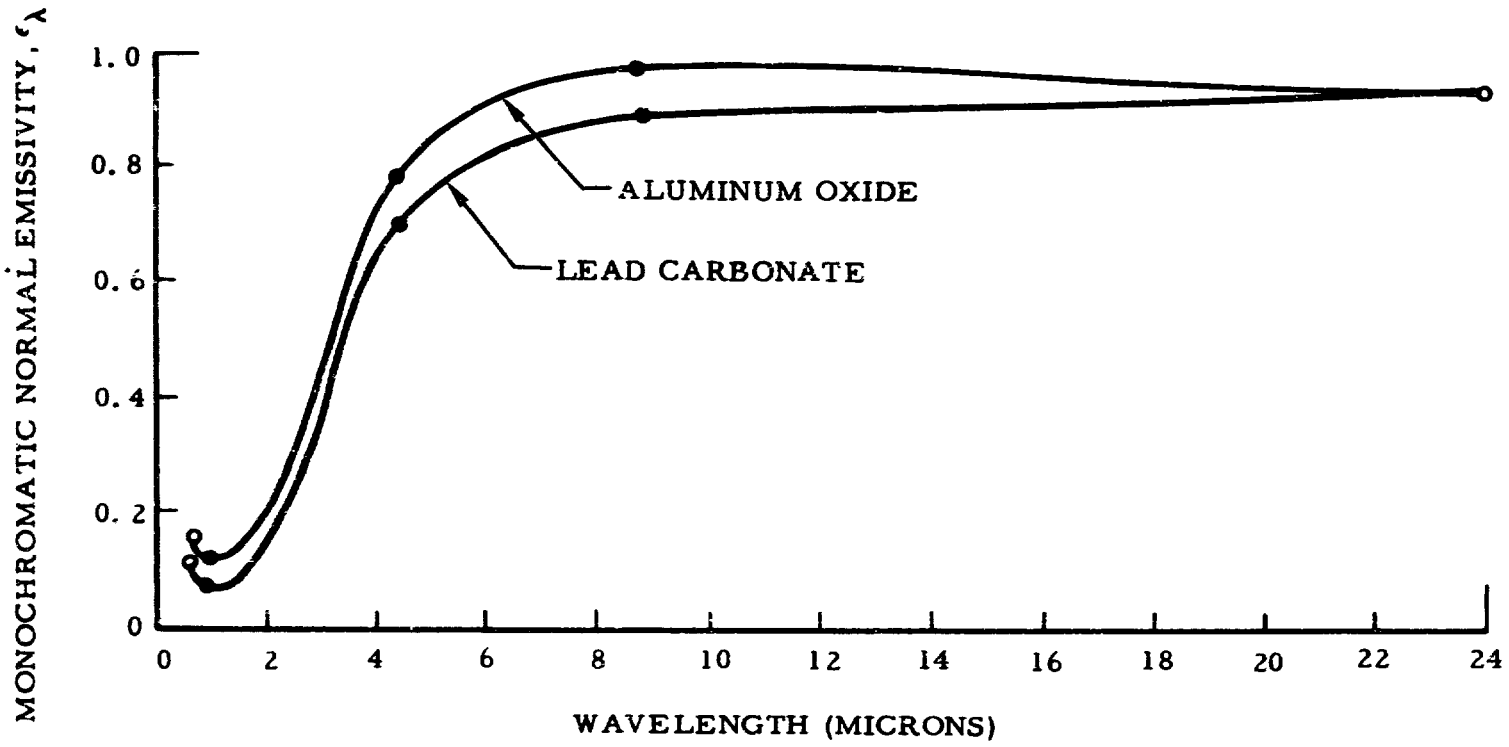

Figure 3. Monochromatic Normal Emissivity Versus Wavelength for Lead Carbonate and Aluminum Oxide

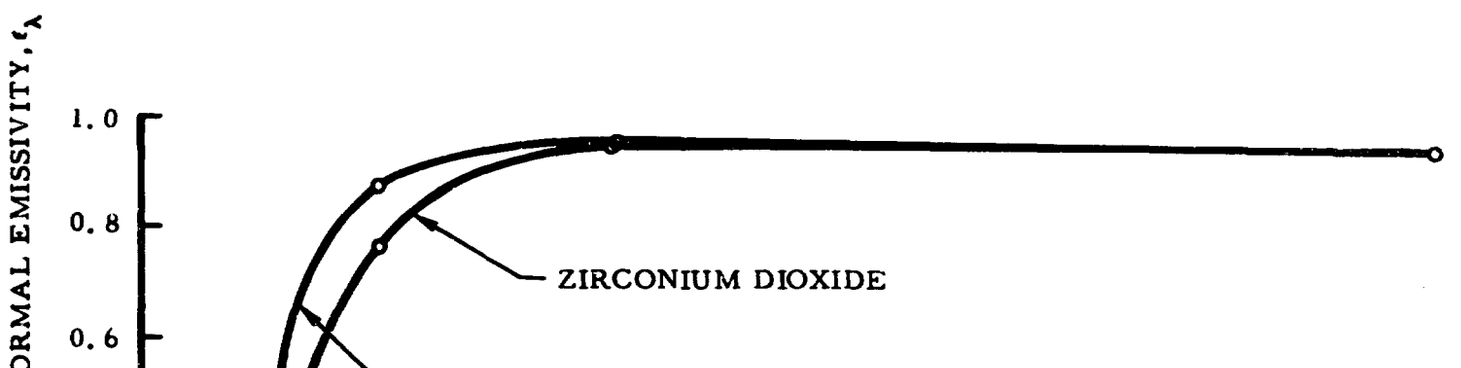

Figure 4. Monochromatic Normal Emissivity Versus Wavelength for Calcium Oxide and Zirconium Dioxide

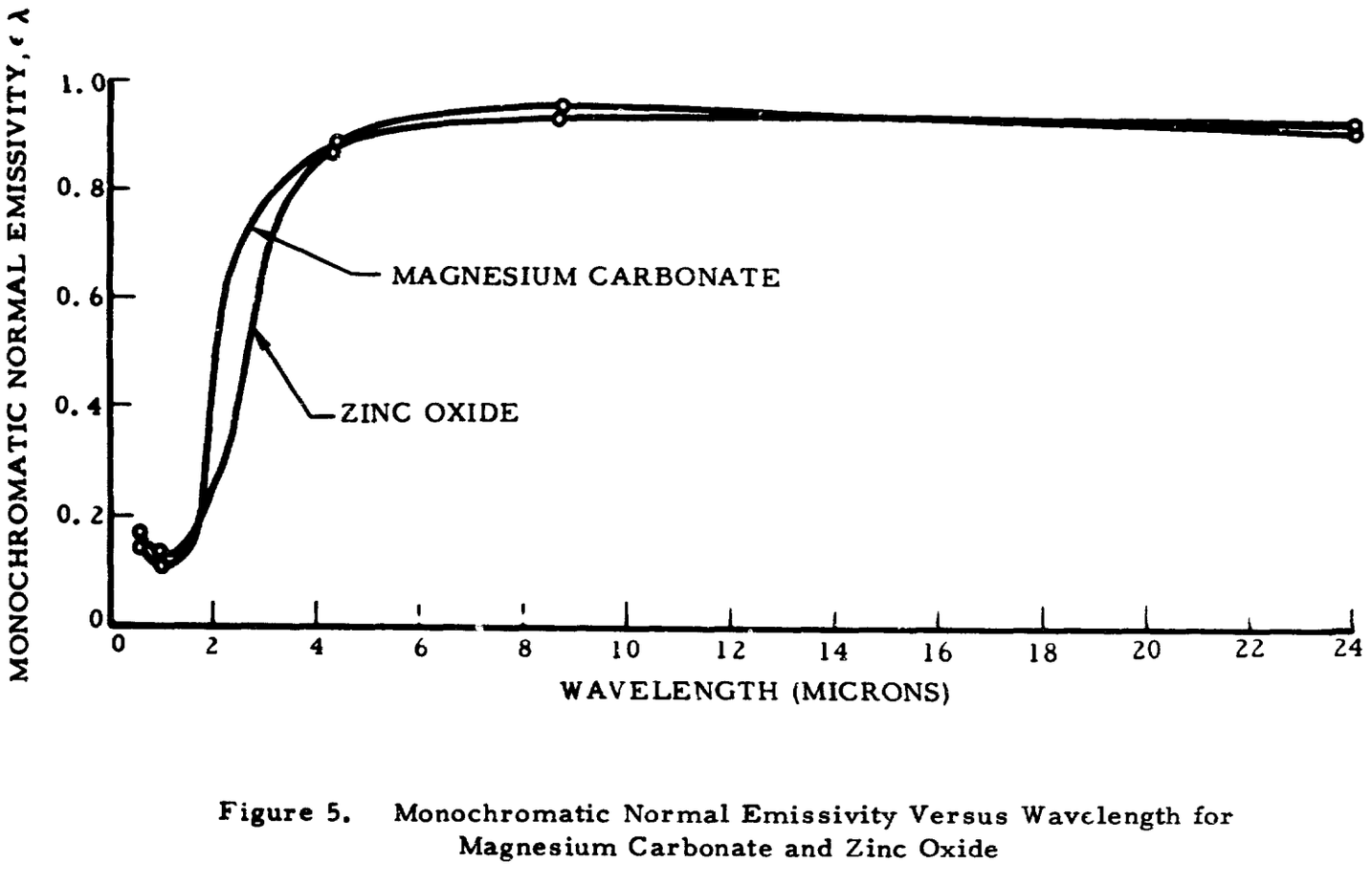

Figure 5. Monochromatic Normal Emissivity Versus Wavelength for Magnesium Carbonate and Zinc Oxide

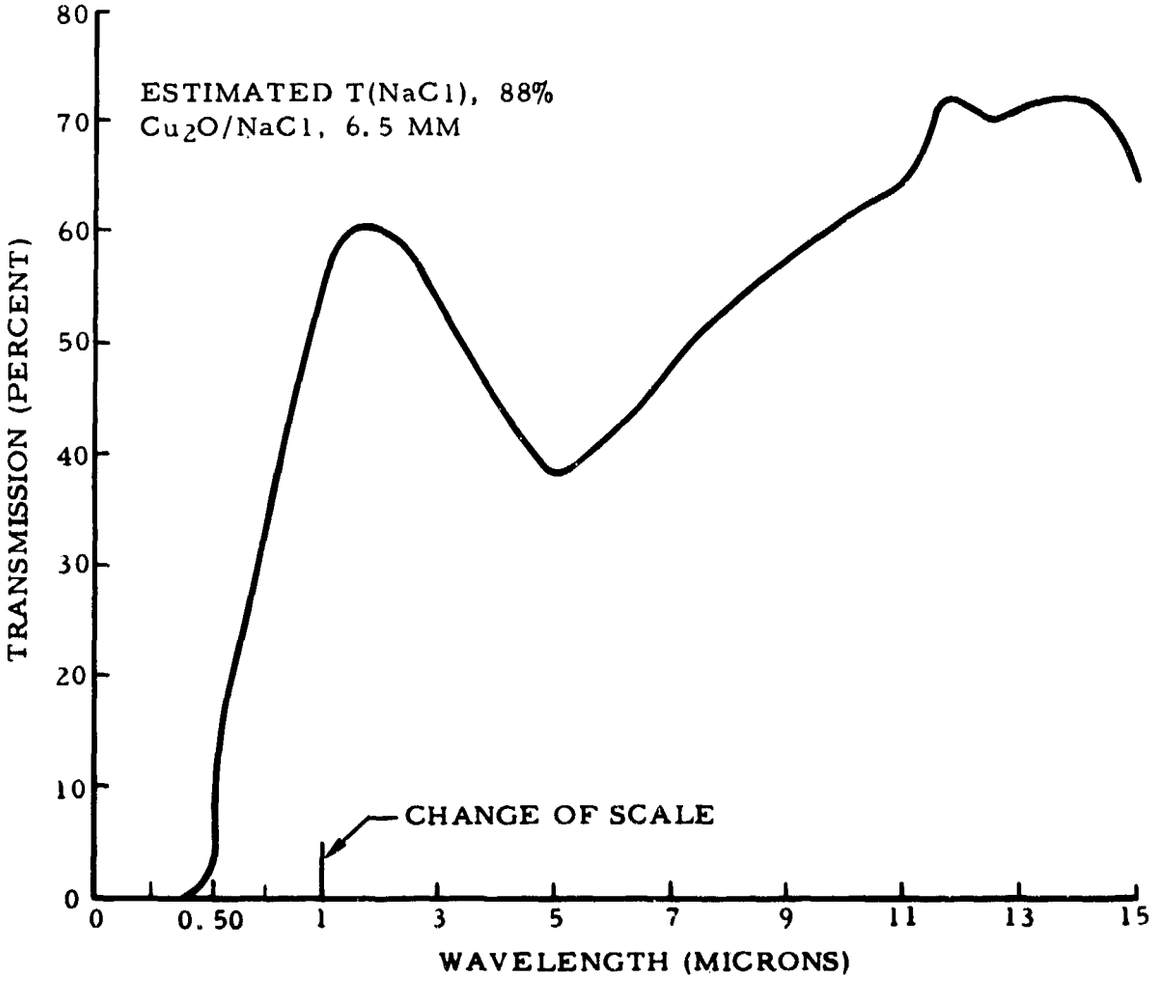

Figure 6. Cupric Oxide on Sodium Chloride

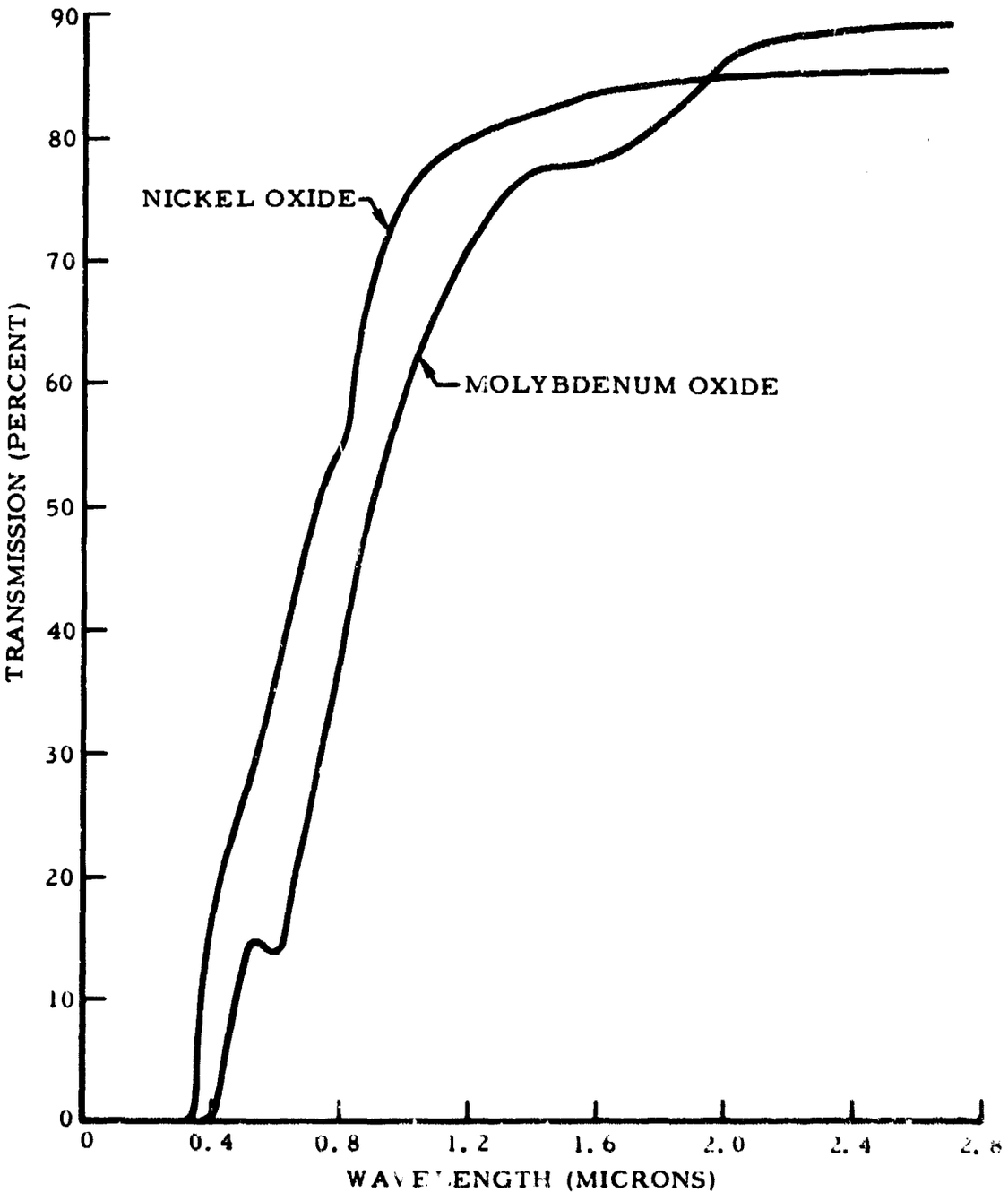

Figure 7. Transmission Versus Wavelength for Molybdenum Oxide and Nickel Oxide on Pyrex

ORGANIC COATINGS

Considerable effort is being directed toward development of organic coatings with high thermal emittance at relatively low temperature (from room temperature to 200 or 300 F). These coatings must be characterized by high resistance to ultraviolet and nuclear radiation, good thermal stability, and high molecular weight to minimize boiloff losses. Preliminary work indicates that organic coatings can be developed with a thermal emissivity greater than 0.95. At the present time, no organic coating can be recommended which will meet all the environmental requirements. Some work on protective ultraviolet absorbers is producing encouraging results, indicating that a high-emissivity coating which is sensitive to ultraviolet may be successfully protected. These organic protective coatings include 1, 1' ferrocane dicarboxylic acid, 2(2' hydroxy 5' methyl phenyl) benzotriazole, and 2 hydroxy 4 methoxy benzophenone.

INORGANIC COATINGS

Because pure metals are generally reflective at temperatures from 100 to 1200 F, they are not suitable for radiator coatings. However, there may be related components which require high thermal reflectance. Typical reflectivity values for vacuum-deposited gold on flat organic substrates are 0.95 for the near and far infrared regions. Aluminum, copper, and silver are also reflective from 0.90 to 0.95 for the same region (Reference 3). Care is required to prevent surface oxidation.

Metallic oxides have relatively high emissivities in the infrared region and low absorptivity for solar irradiation. The emissivities of some coatings as reported by various references are summarized in Table 2, which also lists some of the physical properties.

Information received from other sources and from tests conducted at AiResearch indicate that an emissivity of at least 0.85 at 100 to 200 F can easily be obtained for some of these oxides using flame spraying. The values of 0.93 to 0.97 at the low temperatures listed in Figure 1 can be obtained only under ideal conditions.

The dependence of emissivity on temperature for some other materials is given in Figure 8. Sheet 2 of Figure 8 shows that ϵ_T will be of the order of 0.8 and 0.9 while α_s should be in the range 0.1 to 0.2. If the coatings are roughened, ϵ_T and α_s should both increase.

The emittance of two ceramic coatings prepared by the National Bureau of Standards is shown in Figure 9. These coatings are barium silicate glass containing mixtures of quartz, aluminum oxide, chrome oxide, cerium oxide, and other oxides. They are sprayed on stainless steel

Table 2. Materials Having Desirable Radiation Characteristics for Space Radiators

Material		Specific Gravity	Melting Point (F)	Boiling Point (F)	Total Normal Emissivity			Application and Stability
					125 F	750 F	Solar	
Aluminum oxide	(Al_2O_3)	3.5 to 3.9	3700	4080	0.98	0.79	0.16	Good
Zirconium silicate	($ZrSiO_4$)	4.56	4600		0.92 (460 F)	0.80 (930 F)		Good
Zirconium oxide	(ZrO_2)	5.49	4900	7800	0.95	0.77	0.14	Good
Magnesium oxide	(MgO)	3.65 to 3.75	5080	6510	0.97	0.84	0.14	Fair, too soluble
Zinc oxide	(ZnO)	5.606	3270	subl 3270	0.97	0.91	0.18	Fair to bad, too soluble in water
Calcium oxide	(CaO)	3.40	4660	5180	0.96	0.78	0.15	Bad, decomposes in water
Thorium dioxide	(ThO_2)	9.69	5080	7980	0.93	0.53	0.14	Good
Anodized aluminum			3700	4080	0.77	0.49	0.15	Fair, not as easy to apply as Al_2O_3
Alumina		4.00	3700	4080				Fair, but not as good as pure Al_2O_3
White tile					0.96	0.85	0.18	Fair
Yttrium oxide	(Y_2O_3)	4.84 5.096	4380	7780	0.89	0.66	0.26	Fair
Ferrous oxide	(FeO), black, non-oxide	5.7	2580			0.90		Good
Nickel oxide	(NiO)	7.45	3795			0.95		Good

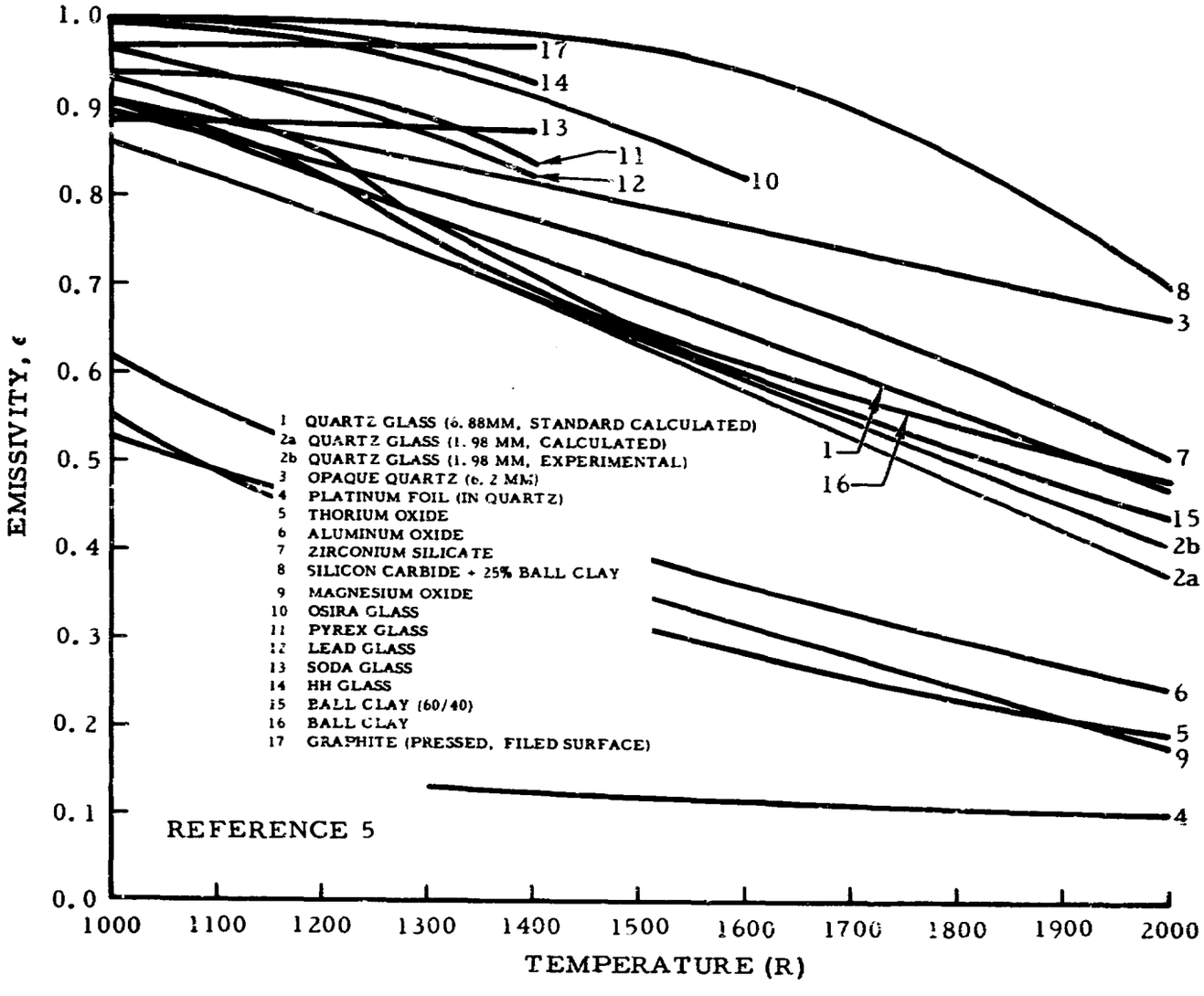

Figure 8. Emissivity Versus Temperature for Various Substances
(Sheet 1 of 2)

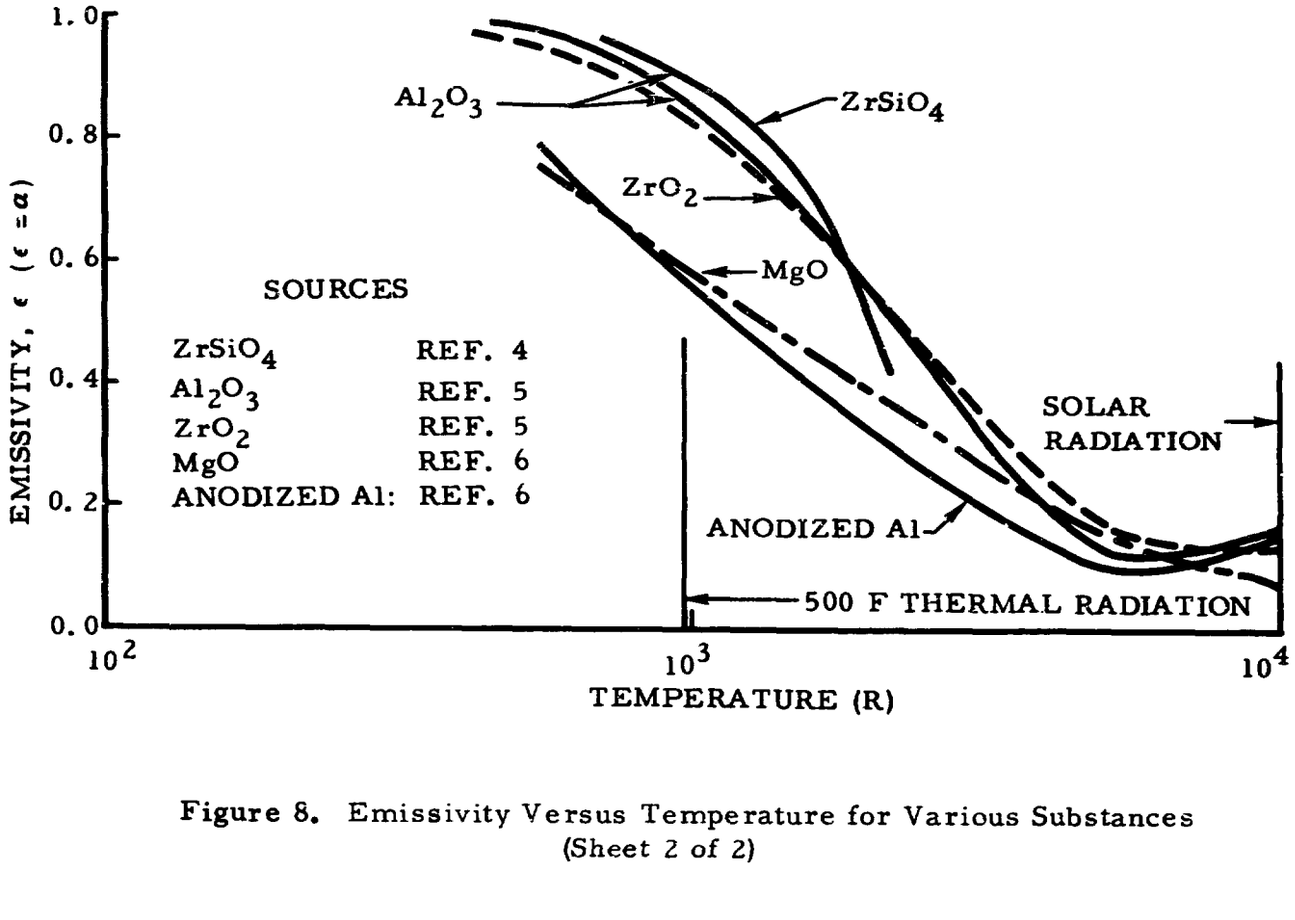

Figure 8. Emissivity Versus Temperature for Various Substances
(Sheet 2 of 2)

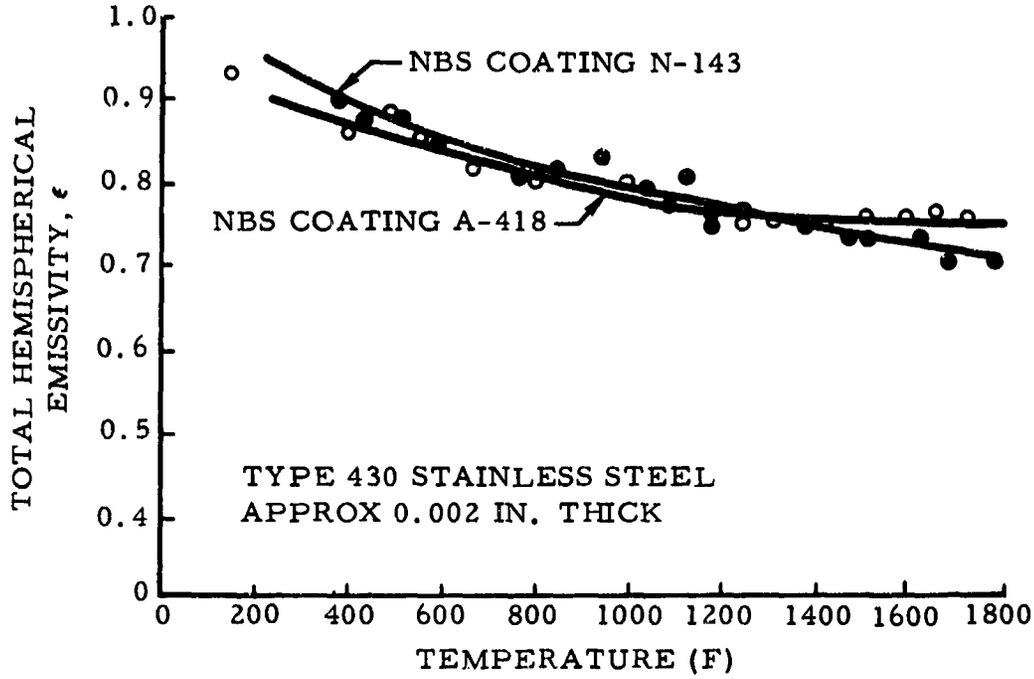

Figure 9. Total Hemispherical Emissivity Versus Wavelength for Type 430 Stainless Steel Coated With Two Ceramic Coatings

samples and then cured at elevated temperatures. Most of these coatings are spectrally selective with α_s / ϵ_T approximately 0.1 to 0.3. Conservative values of emissivities for low-temperature radiation are of the order of 0.85 to 0.90. Higher thermal emissivities are desirable, however, for high-temperature radiators such as required for space power systems. It is believed that for high temperature radiators, black iron oxide or nickel oxide coating (nickel penetrate) have emissivities near 0.95.

Total normal emissivity characteristics of various materials are shown in Figures 10 and 11.

COMPUTATION OF TOTAL EMISSIVITY OR ABSORPTIVITY

The methods used to predict radiation heat transfer require knowledge of the total emissivities of the surfaces involved as well as the total absorptivities. Much of the data published to date are in the form of monochromatic reflectivity or absorptivity as a function of wavelength. Thus, it is often necessary to calculate the total emissivity or absorptivity when only the spectral information is available. Basically, this is done by calculating the black body characteristics as given by Planck's Law. The actual power emitted or absorbed is then obtained by taking the product of the black body radiant power and the emissivity at each wavelength. The total emissivity is determined by integrating this product over all wavelengths and dividing by the black body energy over the same wavelengths.

To obtain the value of total emissivity or absorptivity, over all wavelengths ordinarily requires very tedious hand calculations and lengthy graphical integrations. Fortunately, there is available an IBM 7090 program which mechanizes the calculation and integration procedures such that accurate total emissivities and total absorptivities can be obtained very rapidly for any given temperature conditions and material properties. This program is titled "Total Emissivity and Absorptivity Program," and a complete description of the theory involved and usage of the program is available (Reference 7).

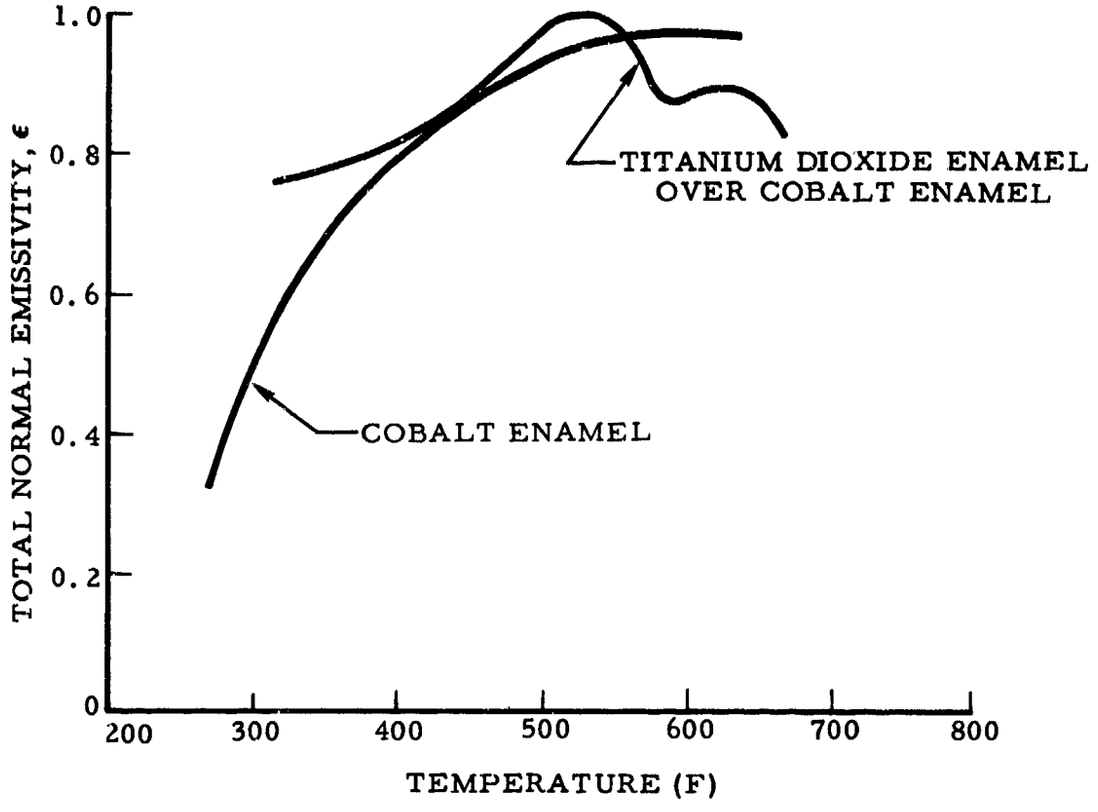

Figure 10. Total Normal Emissivity Versus Temperature for Titanium Dioxide and Cobalt Enamels

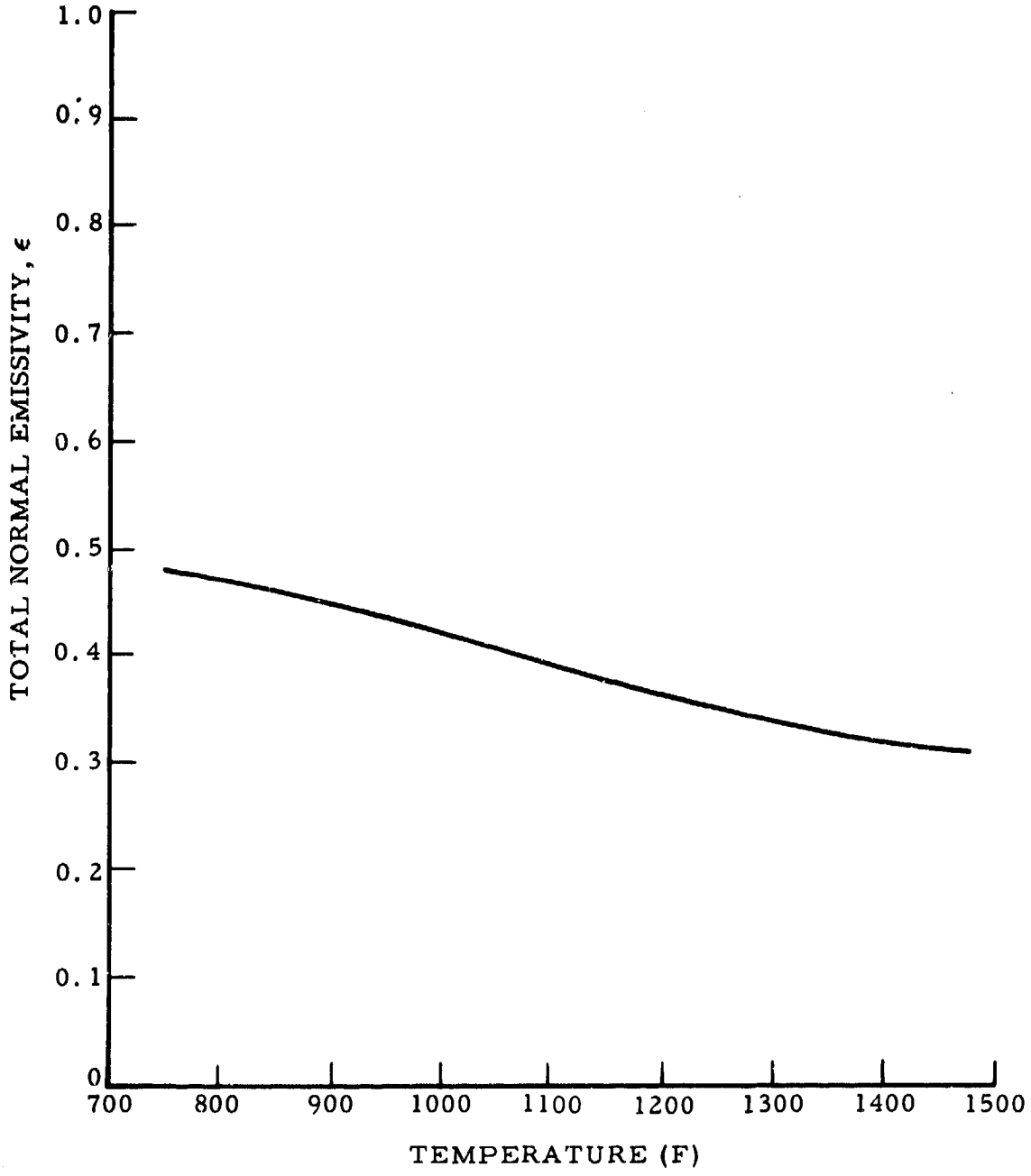

Figure 11. Total Normal Emissivity Versus Temperature for Aluminum Oxide

REFERENCES

1. Tabor, H., "Selective Radiation: I. Wavelength Discrimination," Transactions of Conference on Use of Solar Energy (Tucson, Arizona), Vol II, Part 1, Section A, October-November 1955.

2. "A Proposal for the Investigation of Space Heat Rejection Systems for Rankine Cycles," AiResearch Manufacturing Company and Electro-Optical Systems, Inc. (Joint Report), 22 January 1960.

3. Dunkle, R.V., "Spectral Reflectance Measurements," First Symposium on Surface Effects on Spacecraft (Palo Alto, California), 12-13 May 1959.

4. Pirani, M., Journal of Science Institute, Vol 16, 1939, p 12.

5. Coblentz, W.W., U. S. Bureau of Standards, No. 9, 1912, p 283-324. (Al_2O_3)

6. Sieber, W., Z, Tech. Physik, Vol 22, 1941, p 130-135. (MgO)

7. "Total Emissivity and Absorptivity Program," Space and Information Systems Division, North American Aviation, SID 61-3, February 1961.

APPENDIX B

PLANETARY THERMAL EMISSION AND PLANETARY REFLECTED SOLAR RADIATION INCIDENT TO SPACE VEHICLES

This appendix was supplied by the Astronautics Division of Convair (General Dynamics Corporation), San Diego, California.

DESCRIPTION AND DEFINITIONS

I PLANETARY THERMAL EMISSION

The planetary thermal radiation incident to a vehicle surface may be computed by the general equation

$$q = FAE_t \qquad (1)$$

where q = thermal radiation rate incident to the vehicle surface, BTU/hr.

A = characteristic area defining the surface, ft^2.

E_t = total energy rate emitted per planet unit area, $BTU/hr\text{-}ft^2$.

F = geometric factor for radiation from the planet to the vehicle surface, dimensionless

The value of E_t is tabulated for the planets in Table I. The geometric factors have been computed for standard vehicle surface geometries with respect to the earth and tabulated as a function of altitude from the earth. These geometric factors may also be used for vehicles in the vicinity of other planets or moons if the geometric factor is used which corresponds to the adjusted equivalent altitude determined by multiplying the altitude of the vehicle from the planet by the ratio of the radius of the earth to the radius of the planet. These radius ratios are tabulated for the planets in Table I.

(1) SPHERE:

Figure 1 describes the configuration for planetary thermal radiation to a sphere. The geometric factor is defined on the basis of the characteristic area $A = \pi r^2$,

where r is the radius of the sphere. Then

$$F = q / \pi r^2 E_t \qquad (2)$$

The geometric factor for a sphere with respect to the earth is tabulated in Table 2 as a function of altitude.

(2) CYLINDER

Figure 2 describes the configuration for planetary thermal radiation to the convex surface of a cylinder. Because of lack of three dimensional symmetry an attitude parameter, γ, is required and is the angle between the cylinder axis and the vertical to the vehicle. The geometric factor is defined on the basis of the characteristic area, A = DL, where D and L are the diameter and length, respectively, in feet for the cylinder. Then

$$F = q / DLE_t \qquad (3)$$

The geometric factor for a cylinder with respect to the earth is tabulated in table 3 as a function of altitude with the attitude angle, γ, as the parameter.

(3) HEMISPHERE

Figure 3 describes the configuration for planetary thermal radiation to the convex surface of a hemisphere. The geometric factor is defined on the basis of the characteristic area, $A = \pi r^2$, where r is the radius of the hemisphere. Then

$$F = q / \pi r^2 E_t \qquad (4)$$

The geometric factor for a hemisphere with respect to the earth is tabulated in Table 4 as a function of altitude with the attitude angle, γ, as parameter.

(4) FLAT PLATE

Figure 4 describes the configuration for plametary thermal radiation to one side of a flat plate. The angle, δ, between the normal to the plate and the vertical to the vehicle defines the attitude of the plate with respect to the planet. The geometric factor is defined on the basis of the characteristic area, A = P, the area of one side of the plate. Then

$$F = q/PE_t \qquad (5)$$

The geometric factor for a flat plate with respect to the earth is tabulated in Table 5 as a function of altitude with the attitude angle, δ, as parameter.

It should be noted that the flat plate thermal radiation solution may be used to approximate the thermal radiation incident to any generally convex vehicle surface by dividing the surface into a series of flat plate elements and summing the thermal radiation incident to each of these flat plates.

II PLANETARY REFLECTED SOLAR RADIATION

The planetary albedo incident to a vehicle surface may be computed from the general equation:

$$q = FASa \qquad (6)$$

where q = albedo heat flux rate incident to the vehicle surface, BTU/hr.
A = characteristic area defining the surface, ft^2
S = solar heat flux or "constant", BTU/hr.-ft^2
a = average reflectivity of the planet's surface, dimensionless
F = geometric factor which accounts for reflected energy distribution on the planetary surface and the geometry, dimensionless

The geometric factor for a sphere is independent of attitude due to

three dimensional symmetry. In the case of all surfaces the location of the vehicle with respect to the sun is defined by the zenith distance between the surface and sun, θ_s. The zenith distance is the angle between the earth-vehicle vector and the earth-sun vector. In the case of surfaces lacking spherical symmetry, the attitude of the surface is defined by two angles. One is the angle, γ , between the axis of the cylinder or hemisphere or normal to the flat plate and the vertical to the vehicle. The other is the angle, ϕ_c , of rotation of the axis or normal about the vertical to the vehicle from the planet. The datum $\phi_c = 0$ occurs when the axis or normal lies in the plane defined by the earth-vehicle vector and the earth-sun vector.

The value of S and a are tabulated for the planets in Table I. The geometric factors for albedo have been computed for standard vehicle surface geometries with respect to the earth and tabulated as a function of altitude from the earth. Again, as described for thermal radiation, these geometric factors may be applied to other planets by using the ratio of the radius of the earth to the radius of the planet tabulated in Table I.

(1) SPHERE

Figure 5 shows the configuration for albedo incident to a sphere. The geometric factor is defined on the basis of the characteristic area, $A = \pi r^2$, where r is the radius of the sphere, then

$$F = q \Big/ \pi r^2 Sa \qquad (7)$$

The geometric factor for albedo incident to a sphere from the earth is shown in Table 6 as a function of altitude in nautical miles with zenith distance, θ_s, as parameter.

(2) CYLINDER

Figure 6 shows the configuration for albedo to the convex surface of a cylinder. For a cylinder the geometric factor is defined on the basis

of the characteristic area, A = DL. Then

$$F = q/DLSa \qquad (8)$$

where D = diameter of cylinder, ft.

L = length of cylinder, ft.

The geometric factor for albedo incident to a cylinder from the earth is tabulated in Tables 7 through 28 as a function of altitude in nautical miles with θ_s, γ, and ϕ_c as parameters. Each table is for a constant γ and ϕ_c, i.e. particular attitude with respect to the earth.

(3) HEMISPHERE

Figure 7 shows the configuration for albedo to the convex surface of a hemisphere. For a hemisphere the geometric factor is computed on the basis of the characteristic area, $A = \pi r^2$. Then

$$F = q/\pi r^2 Sa \qquad (9)$$

where r = radius of hemisphere, ft.

The geometric factor for albedo incident to a hemisphere from the earth is tabulated in Tables 29 through 65, as a function of altitude in nautical miles with θ_s, γ, and ϕ_c as parameters. Each table is for a constant γ and ϕ_c, i.e., particular attitude.

(4) FLAT PLATE

Figure 8 shows the geometry for albedo to one side of a flat plate. For a flat plate the geometric factor is computed on the basis of the characteristic area, A = P. Then

$$F = q/PSa \qquad (10)$$

where P = area of one side of the flat plate, $ft.^2$

The geometric factor for albedo incident to one side of a flat plate from the earth is tabulated in Tables 66 through 101 as a function of altitude in nautical miles with θ_s, γ, and ϕ_c as parameters. Each table is for a constant γ and ϕ_c, i.e., particular attitude.

The flat plate albedo solution may also be used to approximate albedo heating of any generally convex satellite or satellite surface by dividing this surface into a series of flat plates and summing the albedo heating for each of these flat plates.

INDEX

INDEX (CONT.)

INDEX (CONT.)

INDEX (CONT.)

TABLE I PLANETARY DATA

Planet	Distance To The Sun (Astronomical Units)	Mean Radius (Naut Mi) (R)	Solar Heat Flux (Btu/Hr Ft^2) (S)	Albedo (a)	Planetary Thermal Radiation (Btu/Hr Ft^2) (E_t)	Altitude Correction Factor *	Umbra Cone Apex Altitude (Naut Mi)	Umbra Cone Angle (deg)
Mercury	0.387	1,308	2953.9	0.07	686.79	2.639	109,200	1.37
Venus	0.723	3,307	846.3	0.76	50.78	1.043	518,700	0.73
Earth	1.000	3,441	442.4	0.40	66.36	1.000	746,800	0.53
Mars	1.524	1,799	190.5	0.15	40.48	1.916	592,400	0.35
Jupiter	5.203	37,758	16.4	0.51	1.98	0.091	46,974,000	0.09
Saturn	9.539	31,067	4.9	0.50	0.61	0.111	69,477,000	0.05
Uranus	19.18	18,818	1.2	0.66	0.10	0.269	54,739,000	0.03
Neptune	30.06	11,645	0.5	0.62	0.05	0.296	77,686,000	0.02
Pluto	39.52	1,564	0.3	0.16	0.06	2.203	13,347,000	0.01
Moon	1.000	938	442.4	0.07	102.86	3.676	202,200	0.53

*To use the albedo and thermal radiation curves and tabular data for a planet other than the earth, an equivalent earth altitude for the planet must be found. This may be done by multiplying the planetary altitude under consideration by the altitude correction factor given in the above table. The abscissa of the curves should then be entered with this corrected altitude.

Example: Thermal radiation to a sphere 200 naut mi above the surface of Mars.

$200 \times 1.916 = 383.2$ naut mi

From Fig. 3, $q/\pi r^2 E_t = 1.12$

Using E_t for Mars gives $q/\pi r^2 = 45.3$ Btu/hr-ft^2

Figure 1. Geometry for Planetary Thermal Emission to a Sphere

$$\text{Geometric Factor, } F = \frac{q}{\pi r^2 E_t}$$

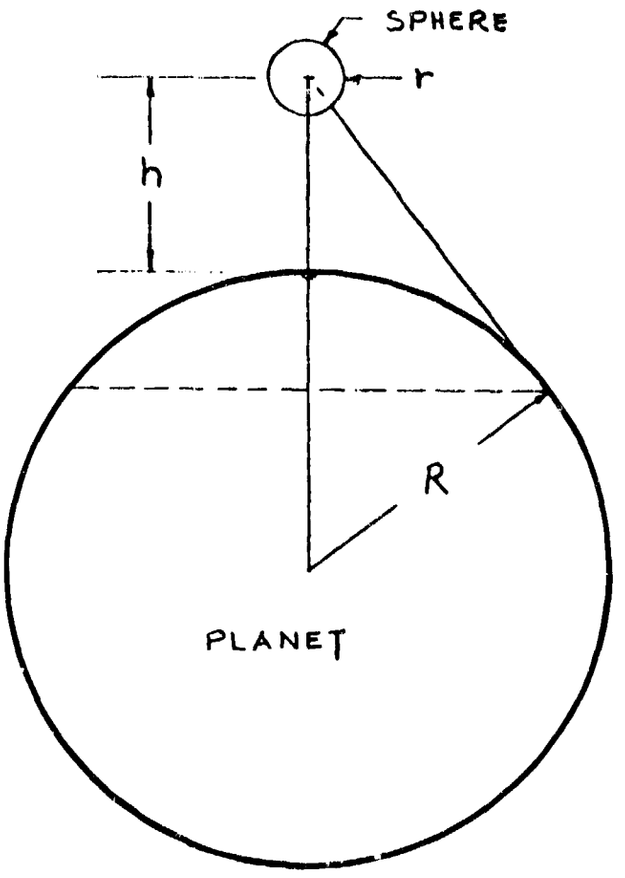

TABLE 2

Geometric Factor for Earth Thermal Radiation To a Sphere

Altitude n.m.	$F = (q/\pi r^2 E_t)$
10	1.8482
50	1.6626
100	1.5278
200	1.3464
400	1.1112
600	0.9512
800	0.8310
1,000	0.7358
2,000	0.4506
4,000	0.2266
6,000	0.1374
8,000	0.0926
10,000	0.0666
15,000	0.0352
20,000	0.0216

Figure 2. Geometry for Planetary Thermal Radiation to a Cylinder

Geometric Factor, $F = \frac{q}{DL\ E_t}$

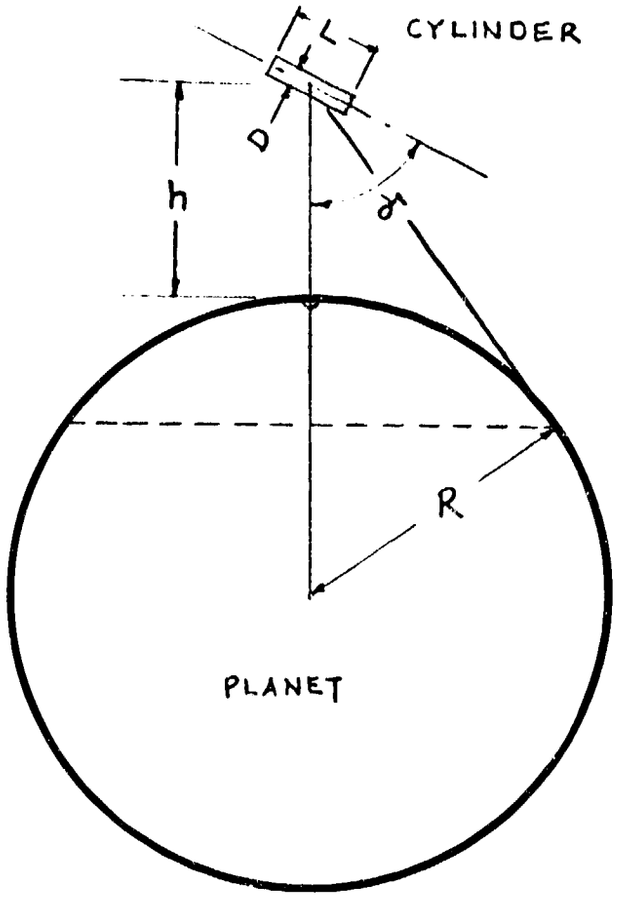

TABLE 3

Geometric Factor for Thermal Radiation to a Cylinder

Altitude (n. m)	Attitude Angle (γ) (degrees)	Geometric Factor	Altitude (n.m.)	Attitude Angle (γ) (degrees)	Geometric Factor
10	0	1.4171	600	0	0.5722
10	20	1.3957	600	20	0.5858
10	40	1.3982	600	40	0.6512
10	60	1.4194	600	60	0.7499
10	90	1.4533	600	90	0.8393
50	0	1.2350	800	0	0.4720
50	20	1.2278	800	20	0.4887
50	40	1.2448	800	40	0.5595
50	60	1.2833	800	60	0.6611
50	90	1.3495	800	90	0.7450
100	0	1.1032	1000	0	0.3964
100	20	1.1009	1000	20	0.4152
100	40	1.1289	1000	30	0.4461
100	60	1.1824	1000	40	0.4891
100	90	1.2610	1000	60	0.5899
200	0	0.9287	1000	90	0.6679
200	20	0.9281	2000	0	0.1947
200	40	0.9658	2000	20	0.2171
200	60	1.0348	2000	30	0.2491
200	90	1.1229	2000	40	0.2908
400	0	0.7121	2000	50	0.3337
400	20	0.7206	2000	60	0.3707
400	40	0.7768	2000	90	0.4248
400	60	0.8661			
400	90	0.9593			

TABLE 3 Continued

Geometric Factor for Thermal Radiation to a Cylinder (Cont'd)

Altitude (n. m.)	Altitude Angle (γ) (degrees)	Geometric Factor
4,000	0	.0707
4,000	10	.0750
4,000	20	.0914
4,000	30	.1170
4,000	40	.1447
4,000	50	.1697
4,000	60	.1905
4,000	90	.2199
6,000	0	.0336
6,000	10	.0376
6,000	20	.0512
6,000	30	.0697
6,000	40	.0877
6,000	50	.1036
6,000	60	.1167
6,000	90	.1349
8,000	0	.0186
8,000	10	.0222
8,000	20	.0333
8,000	40	.0590
8,000	60	.0790
8,000	90	.0913
10,000	0	.0114
10,000	10	.0146
10,000	20	.0235
10,000	30	.0333
10,000	40	.0425
10,000	50	.0505
10,000	60	.0570
10,000	90	.0660
20,000	0	.0021
20,000	10	.0040
20,000	20	.0074
20,000	30	.0108
20,000	40	.0138
20,000	50	.0165
20,000	60	.0186
20,000	90	.0216

Figure 3. Geometry for Planetary Thermal Emission to a Hemisphere

Geometric Factor, $F = \frac{q}{\pi r^2 E_t}$

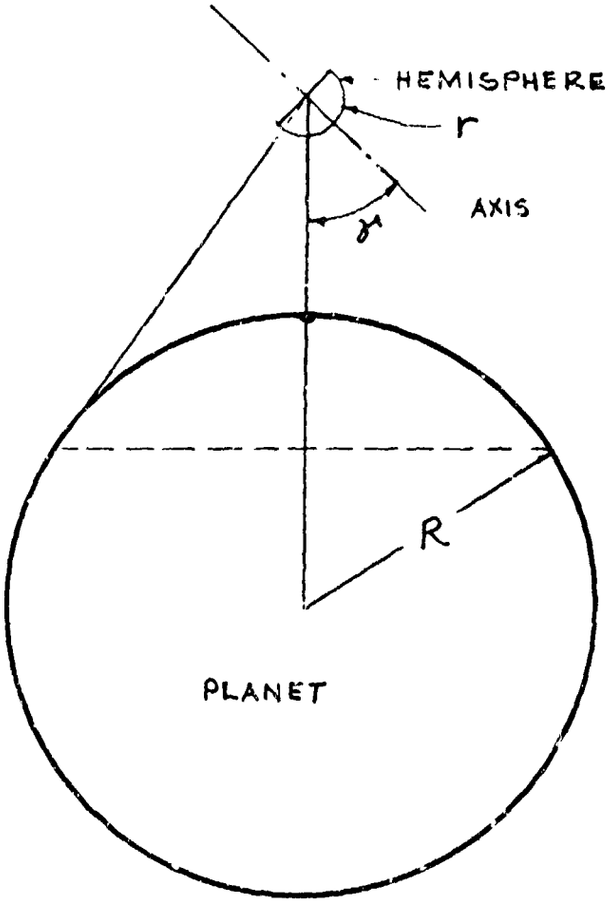

TABLE 4

Geometric Factor for Thermal Radiation to a Hemisphere

Altitude (n. m.)	Attitude Angle (δ) (degrees)	Geometric Factor	Altitude (n.m.)	Attitude Angle (δ) (degrees)	Geometric Factor
10	0	1.4103	100	120	0.5591
10	20	1.3931	100	140	0.4312
10	40	1.3193	100	160	0.3435
10	60	1.1978	100	180	0.3065
10	80	1.0432			
10	100	Q.8743	200	0	1.1127
10	120	Q.7114	200	20	1.0941
10	140	Q.5741	200	40	1.0248
10	160	Q.4790	200	60	0.9130
10	180	Q.4376	200	80	0.7725
			200	100	0.6197
50	0	1.3153	200	120	0.4734
50	20	1.2967	200	140	0.3513
50	40	1.2219	200	160	0.2680
50	60	1.1001	200	180	0.2335
50	80	0.9458			
50	100	0.7777	400	0	0.9536
50	120	0.6161	400	20	0.9357
50	140	0.4805	400	40	0.8720
50	160	0.3872	400	60	0.7701
50	180	0.3474	400	80	0.6423
			400	100	0.5041
100	0	1.2216	400	120	0.3721
100	20	1.2034	400	140	0.2623
100	40	1.1323	400	160	0.1878
100	60	1.0167	400	180	0.1577
100	80	0.8706			
100	100	0.7117			

TABLE 4 (Continued)

Geometric Factor for Thermal Radiation to a Hemisphere

Altitude (n. m.)	Attitude Angle (γ) (degrees)	Geometric Factor	Altitude (n. m.)	Attitude Angle (γ) (degrees)	Geometric Factor
600	0	0.8361	1000	100	0.3257
600	20	0.8192	1000	120	0.2269
600	40	0.7610	1000	140	0.1452
600	60	0.6683	1000	160	0.0903
600	80	0.5524	1000	180	0.0689
600	100	0.4272			
600	120	0.3079	2000	0	0.4248
600	140	0.2088	2000	20	0.4144
600	160	0.1419	2000	40	0.3813
600	180	0.1153	2000	60	0.3293
			2000	80	0.2648
800	0	0.7431	2000	100	0.1955
800	20	0.7273	2000	120	0.1299
800	40	0.6740	2000	140	0.0757
800	60	0.5895	2000	160	0.0396
800	80	0.4840	2000	180	0.0259
800	100	0.3702			
800	120	0.2619	4000	0	0.2200
800	140	0.1721	4000	20	0.2142
800	160	0.1117	4000	40	0.1962
800	180	0.0879	4000	60	0.1682
			4000	80	0.1336
1000	0	0.6668	4000	100	0.0966
1000	20	0.6521	4000	120	0.0615
1000	40	0.6032	4000	140	0.0328
1000	60	0.5259	4000	160	0.0137
1000	80	0.4295	4000	180	0.0067

TABLE 4 (Continued)

Geometric Factor for Thermal Radiation to a Hemisphere

Altitude (n. m.)	Attitude Angle (γ) (degrees)	Geometric Factor
6000	0	0.1351
6000	20	0.1314
6000	40	0.1201
6000	60	0.1027
6000	80	0.0811
6000	100	0.0581
6000	120	0.0364
6000	140	0.0186
6000	160	0.0058
6000	180	0.0025
8000	0	0.0914
8000	20	0.0889
8000	40	0.0812
8000	60	0.0693
8000	80	0.0546
8000	100	0.0389
8000	120	0.0241
8000	140	0.0120
8000	160	0.0040
8000	180	0.0012
15,000	0	0.0349
15,000	20	0.0339
15,000	40	0.0309
15,000	60	0.0263
15,000	80	0.0207
15,000	100	0.0146
15,000	120	0.0090
15,000	140	0.0043
15,000	160	0.0013
15,000	180	0.0002
20,000	0	0.0216
20,000	20	0.0210
20,000	40	0.0191
20,000	60	0.0162
20,000	80	0.0128
20,000	100	0.0090
20,000	120	0.0055
20,000	140	0.0026
20,000	160	0.0007
20,000	180	0.0001

Figure 4. Geometry for Planetary Thermal Radiation to a Flat Plate

Geometric Factor, $F = \frac{q}{P E_t}$

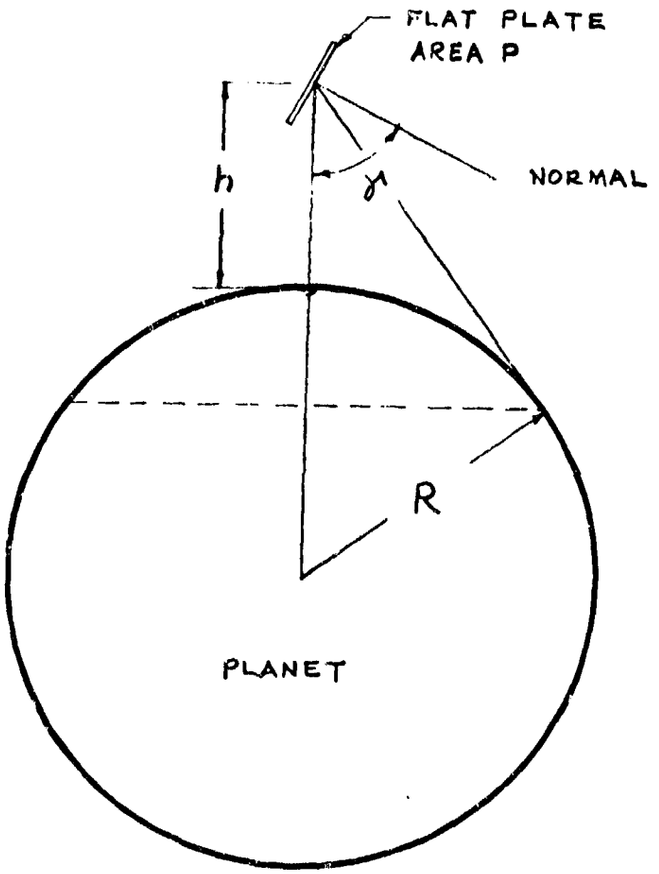

Table 5

Geometric Factor for Thermal Radiation to a Flat Plate

Altitude (n. m.)	Attitude Angle (δ) (degrees)	Geometric Factor	Altitude (n. m.)	Attitude Angle (δ) (degrees)	Geometric Factor
10	0	.9940	50	110	.2334
10	10	.9808	50	120	.1644
10	20	.9504	50	130	.1056
10	30	.9062	50	140	.0587
10	40	.8496	50	150	.0251
10	50	.7824	50	160	.0056
10	60	.7066	50	170	.0000
10	70	.6245			
10	80	.5386	100	0	.9440
10	90	.4516	100	10	.9300
10	100	.3660	100	20	.8890
10	110	.2845	100	30	.8323
10	120	.2095	100	40	.7647
10	130	.1433	100	50	.6887
10	140	.0880	100	60	.6068
10	150	.0452	100	70	.5215
10	160	.0162	100	80	.4353
10	170	.0017	100	90	.3512
			100	100	.2714
50	0	.9710	100	110	.1985
50	10	.9568	100	120	.1346
50	20	.9185	100	130	.0817
50	30	.8664	100	140	.0413
50	40	.8029	100	150	.0145
50	50	.7301	100	160	.0017
50	60	.6502			
50	70	.5657			
50	80	.4791			
50	90	.3932			
50	100	.3104			

Table 5 (Continued)

Geometric Factor for Thermal Radiation to a Flat Plate

Altitude (n. m.)	Attitude Angle (γ) (degrees)	Geometric Factor
200	0	.8930
200	10	.8800
200	20	.8393
200	30	.7787
200	40	.7072
200	50	.6285
200	60	.5452
200	70	.4603
200	80	.3762
200	90	.2957
200	100	.2211
200	110	.1548
200	120	.0987
200	130	.0543
200	140	.0230
200	150	.0052
200	160	.0000
400	0	.8020
400	10	.7890
400	20	.7530
400	30	.6954
400	40	.6225
400	50	.5432
400	60	.4611
400	70	.3792
400	80	.3003
400	90	.2267
400	100	.1609
400	110	.1047
400	120	.0598
400	130	.0273
400	140	.0077
400	150	.0003
600	0	.7290
600	10	.7170
600	20	.6850
600	30	.6310
600	40	.5577
600	50	.4804
600	60	.4012
600	70	.3233
600	80	.2495
600	90	.1822
600	100	.1236
600	110	.0753
600	120	.0386
600	130	.0143
600	140	.0022

Table 5 (Continued)

Geometric Factor for Thermal Radiation to a Flat Plate

Altitude (n. m.)	Attitude Angle (γ) (degrees)	Geometric Factor	Altitude (n. m.)	Attitude Angle (γ) (degrees)	Geometric Factor
800	0	.6610	2,000	0	.4010
800	10	.6510	2,000	10	.3942
800	20	.6210	2,000	20	.3760
800	30	.5720	2,000	30	.3470
800	40	.5047	2,000	40	.3065
800	50	.4306	2,000	50	.2575
800	60	.3548	2,000	60	.2021
800	70	.2810	2,000	70	.1489
800	80	.2120	2,000	80	.1014
800	90	.1503	2,000	90	.0620
800	100	.0977	2,000	100	.0320
800	110	.0558	2,000	110	.0121
800	120	.0256	2,000	120	.0021
800	130	.0074			
800	140	.0004	4,000	0	.2140
			4,000	10	.2110
1,000	0	.6000	4,000	20	.2010
1,000	10	.5910	4,000	30	.1855
1,000	20	.5645	4,000	40	.1640
1,000	30	.5200	4,000	50	.1376
1,000	40	.4599	4,000	60	.1070
1,000	50	.3896	4,000	70	.0742
1,000	60	.3174	4,000	80	.0450
1,000	70	.2476	4,000	90	.0225
1,000	80	.1831	4,000	100	.0079
1,000	90	.1262	4,000	110	.0010
1,000	100	.0789			
1,000	110	.0423			
1,000	120	.0172			
1,000	130	.0037			
1,000	140	.0000			

Table 5 (Continued)

Geometric Factor for Thermal Radiation to a Flat Plate

Altitude (n. m.)	Attitude Angle (δ) (degrees)	Geometric Factor	Altitude (n. m.)	Attitude Angle (δ) (degrees)	Geometric Factor
6,000	0	.1332	10,000	0	.0656
6,000	10	.1311	10,000	10	.0645
6,000	20	.1250	10,000	20	.0616
6,000	30	.1153	10,000	30	.0568
6,000	40	.1020	10,000	40	.0503
6,000	50	.0855	10,000	50	.0421
6,000	60	.0665	10,000	60	.0328
6,000	70	.0454	10,000	70	.0224
6,000	80	.0255	10,000	80	.0116
6,000	90	.0107	10,000	90	.0036
6,000	100	.0024	10,000	100	.0002
6,000	110	.0000			
			20,000	0	.0215
8,000	0	.0905	20,000	10	.0212
8,000	10	.0892	20,000	20	.0203
8,000	20	.0851	20,000	30	.0187
8,000	30	.0785	20,000	40	.0165
8,000	40	.0694	20,000	50	.0139
8,000	50	.0582	20,000	60	.0108
8,000	60	.0453	20,000	70	.0074
8,000	70	.0310	20,000	80	.0038
8,000	80	.0165	20,000	90	.0007
8,000	90	.0059			
8,000	100	.0008			

Figure 5. Geometry for Planetary Reflected Solar Radiation to a Sphere

$$\text{Geometric Factor, } F = \frac{q}{\pi r^2 S_a}$$

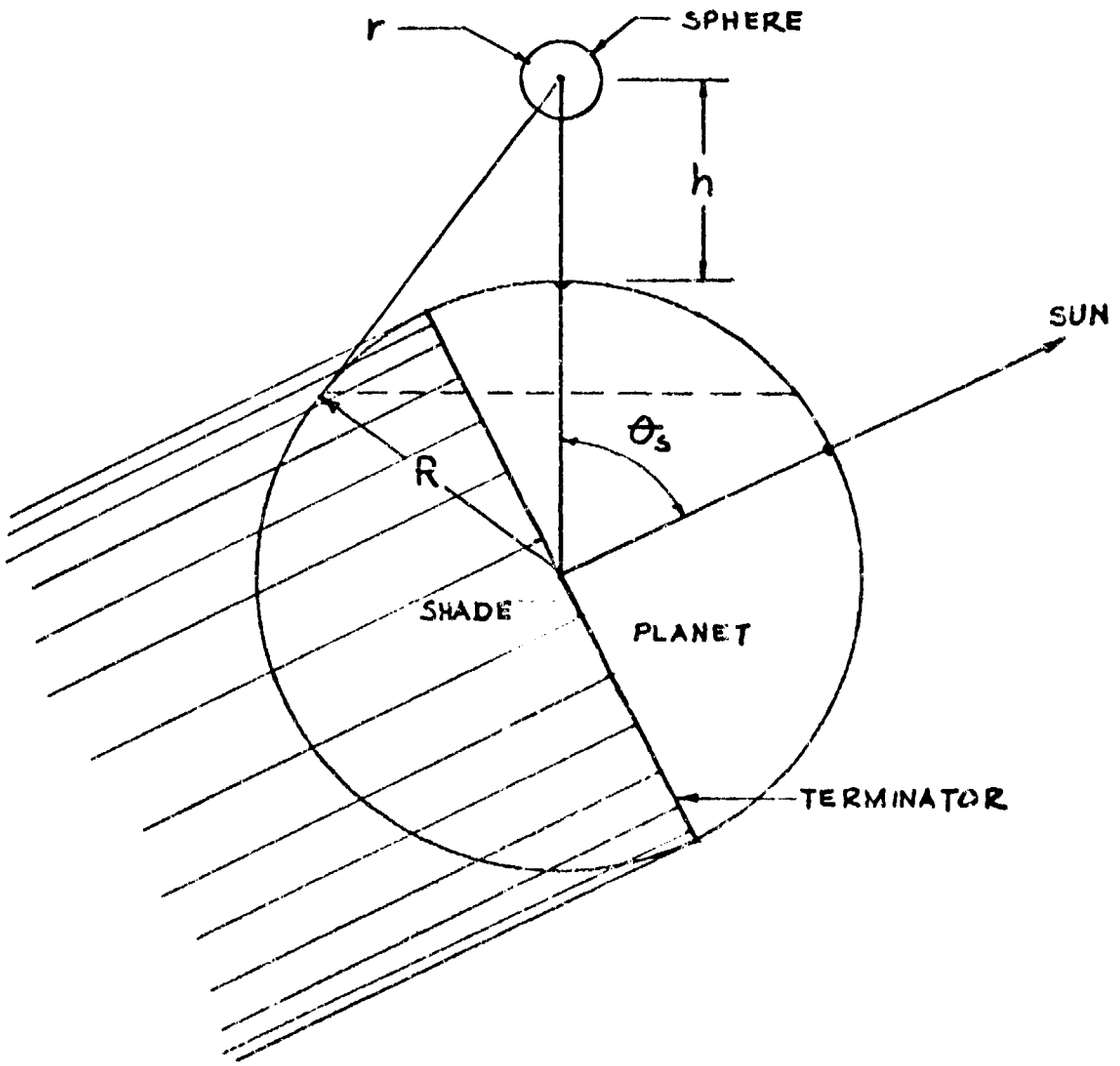

Table 6. Geometric Factor for Reflected Solar Radiation to a Sphere

Altitude n. m.	θ_s degrees	F
50	0	1.6661
50	10	1.6408
50	20	1.5656
50	30	1.4429
50	40	1.2763
50	50	1.0710
50	60	0.8331
50	70	0.5698
50	80	0.2893
50	85	0.1454
50	88	0.0609
50	90	0.0152
80	0	1.5757
80	10	1.5518
80	20	1.4807
80	30	1.3646
80	40	1.2071
80	50	1.0129
80	60	0.7879
80	70	0.5389
80	80	0.2736
80	85	0.1383
80	88	0.0609
80	90	0.0209
80	100	0. 0003
100	0	1.5259
100	10	1.5027
100	20	1.4339
100	30	1.3215
100	40	1.1689
100	50	0.9808
100	60	0.7630
100	70	0.5219
100	80	0.2650
100	85	0.1346
100	88	0.0613
100	90	0.0241
100	100	0. 0005
200	0	1.3393
200	10	1.3190
200	20	1.2585
200	30	1.1599
200	40	1.0260
200	50	0.8609
200	60	0.6697
200	70	0.4580
200	80	0.2334
200	85	0.1231
200	88	0.0649
200	90	0.0358
200	100	0.0017
500	0	1.0070
500	10	0.9917
500	20	0.9463
500	30	0.8721
500	40	0.7714
500	50	0.6473
500	60	0.5035
500	70	0.3448
500	80	0.1818
500	85	0.1080
500	88	0.0713
500	90	0.0516
500	100	0.0070
800	0	0.8053
800	10	0.7931
800	20	0.7568
800	30	0.6974
800	40	0.6169
800	50	0.5177
800	60	0.4027
800	70	0.2772
800	80	0.1527
800	85	0.0985
800	88	0.0714
800	90	0.0561
800	100	0.0129

Table 6. Geometric Factor for Reflected Solar Radiation to a Sphere (Cont)

Altitude n. m.	θ_s degrees	F	Altitude n. m.	θ_s degrees	F
7000	0	0.0910	10000	0	0.0523
7000	10	0.0896	10000	10	0.0515
7000	20	0.0855	10000	20	0.0491
7000	30	0.0788	10000	30	0.0453
7000	40	0.0700	10000	40	0.0404
7000	50	0.0597	10000	50	0.0347
7000	60	0.0486	10000	60	0.0286
7000	70	0.0375	10000	70	0.0225
7000	80	0.0273	10000	80	0.0168
7000	85	0.0226	10000	85	0.0142
7000	88	0.0201	10000	88	0.0127
7000	90	0.0184	10000	90	0,0118
7000	100	0.0119	10000	100	0.0078
8000	0	0.0743	12000	0	0.0387
8000	10	0.0732	12000	10	0.0381
8000	20	0.0698	12000	20	0.0364
8000	30	0.0644	12000	30	0.0336
8000	40	0.0573	12000	40	0.0300
8000	50	0.0489	12000	50	0.0258
8000	60	0.0400	12000	60	0.0214
8000	70	0.0311	12000	70	0.0169
8000	80	0.0228	12000	80	0.0128
8000	85	0.0191	12000	85	0.0109
8000	88	0.0170	12000	88	0.0098
8000	90	0.0157	12000	90	0.0091
8000	100	0.0102	12000	100	0.0061
9000	0	0.0618	15000	0	0.0264
9000	10	0.0609	15000	10	0.0260
9000	20	0.0581	15000	20	0.0249
9000	30	0.0536	15000	30	0.0230
9000	40	0.0477	15000	40	0.0206
9000	50	0.0409	15000	50	0.0178
9000	60	0.0336	15000	60	0.0148
9000	70	0.0263	15000	70	0.0118
9000	80	0.0195	15000	80	0.0090
9000	85	0.0164	15000	85	0.0078
9000	88	0.0146	15000	88	0.0070
9000	90	0.0135	15000	90	0.0065
9000	100	0.0089	15000	100	0.0045

Table 6. Geometric Factor for Reflected Solar Radiation to a Sphere (Cont)

Altitude n. m.	θ_s degree	F
18000	0	0.0192
18000	10	0.0189
18000	20	0.0181
18000	30	0.0167
18000	40	0.0150
18000	50	0.0130
18000	60	0.0109
18000	70	0.0088
18000	80	0.0068
18000	85	0.0058
18000	88	0.0053
18000	90	0.0049
18000	100	0.0034

Figure 6. Geometry for Planetary Reflected Solar Radiation to a Cylinder

Geometric Factor, $F = \frac{q}{DL\ S_a}$

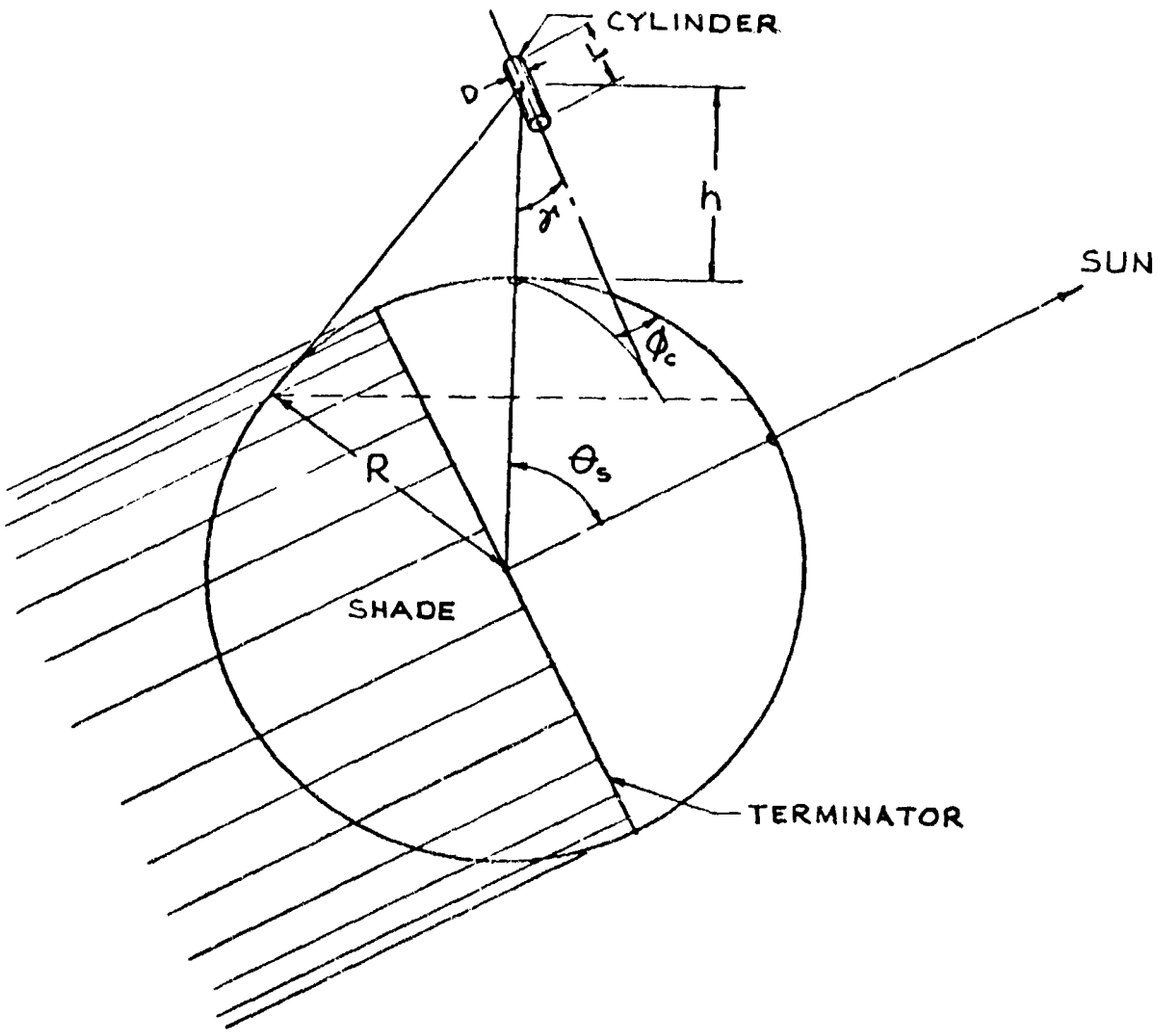

Table 7. Geometric Factor for Reflected Solar Radiation to a Cylinder

$\gamma' = 0°$ (vertical), $\phi_c = 0 - 360°$

Altitude n. m.	θ_s degrees	F	Altitude n. m.	θ_s degrees	F
100	0	1.1160	1000	70	0.1305
100	20	1.0487	1000	80	0.0766
100	30	0.9665	1000	85	0.0540
100	40	0.8549	1000	90	0.0354
100	50	0.7174	1000	95	0.0212
100	60	0.5580	3000	0	0.0951
100	70	0.3817	3000	20	0.0896
100	80	0.1910	3000	30	0.0827
100	85	0.0966	3000	40	0.0733
100	90	0.0206	3000	50	0.0619
100	95	0.0016	3000	60	0.0495
300	0	0.7974	3000	70	0.0371
300	20	0.7493	3000	80	0.0260
300	30	0.6905	3000	85	0.0211
300	40	0.6108	3000	90	0.0166
300	50	0.5125	3000	95	0.0127
300	60	0.3987	6000	0	0.0260
300	70	0.2719	6000	20	0.0245
300	80	0.1389	6000	30	0.0227
300	85	0.0787	6000	40	0.0202
300	90	0.0336	6000	50	0.0173
300	95	0.0100	6000	60	0.0143
600	0	0.5527	6000	70	0,0113
600	20	0.5199	6000	80	0.0085
600	30	0.4794	6000	85	0.0073
600	40	0.4244	6000	90	0.0061
600	50	0.3565	6000	95	0.0050
600	60	0.2772	10000	0	0.0082
600	70	0.1898	10000	20	0.0077
600	80	0.1037	10000	30	0.0071
600	85	0.0667	10000	40	0.0064
600	90	0.0378	10000	50	0.0056
600	95	0.0182	10000	60	0.0047
1000	0	0.3723	10000	70	0.0038
1000	20	0.3504	10000	80	0.0030
1000	30	0.3232	10000	85	0.0026
1000	40	0.2861	10000	90	0.0022
1000	50	0.2404	10000	95	0.0019
1000	60	0.1873			

Table 8. Geometric Factor for Reflected Solar Radiation to a Cylinder

$\gamma = 30°$, $\phi_c = 0°$

Altitude n. m.	θ_s degrees	F	Altitude n. m.	θ_s degrees	F
100	0	1.1311	1000	70	0.1251
100	20	1.0601	1000	80	0.0628
100	30	0.9755	1000	85	0.0386
100	40	0.8613	1000	90	0.0218
100	50	0.7208	1000	95	0.0116
100	60	0.5585	3000	0	0.1462
100	70	0.3792	3000	20	0.1312
100	80	0.1881	3000	30	0.1175
100	85	0.0914	3000	40	0.1003
100	90	0.0153	3000	50	0.0804
100	95	0.0012	3000	60	0.0595
300	0	0.8453	3000	70	0.0396
300	20	0.7882	3000	80	0.0230
300	30	0.7231	3000	85	0.0165
300	40	0.6360	3000	90	0.0114
300	50	0.5296	3000	95	0.0076
300	60	0.4072	6000	0	0.0578
300	70	0.2716	6000	20	0.0518
300	80	0.1300	6000	30	0.0464
300	85	0.0664	6000	40	0.0397
300	90	0.0232	6000	50	0.0324
300	95	0.0068	6000	60	0.0248
600	0	0.6052	6000	70	0.0178
600	20	0.5607	6000	80	0.0118
600	30	0.5125	6000	85	0.0093
600	40	0.4486	6000	90	0.0071
600	50	0.3712	6000	95	0.0054
600	60	0.2824	10000	0	0.0260
600	70	0.1853	10000	20	0.0235
600	80	0.0901	10000	30	0.0212
600	85	0.0510	10000	40	0.0184
600	90	0.0245	10000	50	0.0153
600	95	0.0109	10000	60	0.0122
1000	0	0.4325	10000	70	0.0092
1000	20	0.3973	10000	80	0.0065
1000	30	0.3613	10000	85	0.0054
1000	40	0.3143	10000	90	0.0044
1000	50	0.2577	10000	95	0.0035
1000	60	0.1930			

Table 9. Geometric Factor for Reflected Solar Radiation to a Cylinder

$\gamma = 30°$, $\phi_c = 30°$

Altitude n. m.	Θ_s degrees	F
100	0	1.1311
100	20	1.0605
100	30	0.9761
100	40	0.8620
100	50	0.7217
100	60	0.5595
100	70	0.3802
100	80	0.1892
100	85	0.0924
100	90	0.0161
100	95	0.0013
300	0	0.8453
300	20	0.7890
300	30	0.7243
300	40	0.6375
300	50	0.5314
300	60	0.4092
300	70	0.2738
300	80	0.1324
300	85	0.0687
300	90	0.0250
300	95	0.0074
600	0	0.6054
600	20	0.5621
600	30	0.5144
600	40	0.4510
600	50	0.3739
600	60	0.2855
600	70	0.1886
600	80	0.0934
600	85	0.0540
600	90	0.0269
600	95	0.0123
1000	0	0.4327
1000	20	0.3988
1000	30	0.3634
1000	40	0.3169
1000	50	0.2607
1000	60	0.1964
1000	70	0.1288
1000	80	0.0664
1000	85	0.0419
1000	90	0.0245
1000	95	0.0135
3000	0	0.1463
3000	20	0.1322
3000	30	0.1189
3000	40	0.1020
3000	50	0.0824
3000	60	0.0617
3000	70	0.0419
3000	80	0.0252
3000	85	0.0185
3000	90	0.0132
3000	95	0.0091
6000	0	0.0578
6000	20	0.0522
6000	30	0.0469
6000	40	0.0404
6000	50	0.0332
6000	60	0.0257
6000	70	0.0187
6000	80	0.0126
6000	85	0.0100
6000	90	0.0078
6000	95	0.0060
10000	0	0.0261
10000	20	0.0237
10000	30	0.0214
10000	40	0.0187
10000	50	0.0156
10000	60	0.0125
10000	70	0.0095
10000	80	0.0068
10000	85	0.0056
10000	90	0.0046
10000	95	0.0037

Table 10. Geometric Factor for Reflected Solar Radiation to a Cylinder

$\gamma = 30°$, $\phi_c = 60°$

Altitude n. m.	θ_s degrees	F
100	0	1.1311
100	20	1.0615
100	30	0.9776
100	40	0.8639
100	50	0.7240
100	60	0.5620
100	70	0.3830
100	80	0.1920
100	85	0.0953
100	90	0.0181
100	95	0.0014
300	0	0.8453
300	20	0.7912
300	30	0.7276
300	40	0.6418
300	50	0.5365
300	60	0.4149
300	70	0.2800
300	80	0.1387
300	85	0.0748
300	90	0.0294
300	95	0.0087
600	0	0.6062
600	20	0.5660
600	30	0.5197
600	40	0.4575
600	50	0.3815
600	60	0.2938
600	70	0.1975
600	80	0.1022
600	85	0.0621
600	90	0.0330
600	95	0.0156
1000	0	0.4333
1000	20	0.4030
1000	30	0.3691
1000	40	0.3240
1000	50	0.2690
1000	60	0.2057
1000	70	0.1386
1000	80	0.0759
1000	85	0.0505
1000	90	0.0314
1000	95	0.0182
3000	0	0.1466
3000	20	0.1348
3000	30	0.1226
3000	40	0.1067
3000	50	0.0880
3000	60	0.0678
3000	70	0.0480
3000	80	0.0309
3000	85	0.0237
3000	90	0.0178
3000	95	0.0129
6000	0	0.0579
6000	20	0.0532
6000	30	0.0484
6000	40	0.0423
6000	50	0.0353
6000	60	0.0280
6000	70	0,0210
6000	80	0.0147
6000	85	0.0120
6000	90	0.0098
6000	95	0.0075
10000	0	0.0261
10000	20	0.0241
10000	30	0.0220
10000	40	0.0194
10000	50	0.0164
10000	60	0.0133
10000	70	0.0103
10000	80	0.0076
10000	85	0.0063
10000	90	0.0052
10000	95	0.0042

Table 11. Geometric Factor for Reflected Solar Radiation to a Cylinder

$\gamma = 30$, $\phi_c = 90°$

Altitude n. m.	θ_s degrees	F	Altitude n. m.	θ_s degrees	F
100	0	1.1312	1000	70	0.1520
100	20	1.0629	1000	80	0.0884
100	30	0.9796	1000	85	0.0613
100	40	0.8665	1000	90	0.0394
100	50	0.7271	1000	95	0.0230
100	60	0.5656	3000	0	0.1469
100	70	0.3868	3000	20	0.1384
100	80	0.1959	3000	30	0.1277
100	85	0.0992	3000	40	0.1132
100	90	0.0205	3000	50	0.0955
100	95	0.0015	3000	60	0.0760
300	0	0.8453	3000	70	0.0562
300	20	0.7943	3000	80	0.0382
300	30	0.7320	3000	85	0.0302
300	40	0.6475	3000	90	0.0232
300	50	0.5433	3000	95	0.0172
300	60	0.4226	6000	0	0.0580
300	70	0.2884	6000	20	0.0547
300	80	0.1473	6000	30	0.0505
300	85	0.0828	6000	40	0.0449
300	90	0.0344	6000	50	0.0383
300	95	0.0101	6000	60	0.0311
600	0	0.6077	6000	70	0,0240
600	20	0.5716	6000	80	0.0174
600	30	0.5271	6000	85	0.0144
600	40	0.4666	6000	90	0.0117
600	50	0.3919	6000	95	0.0093
600	60	0.3053	10000	0	0.0261
600	70	0.2096	10000	20	0.0246
600	80	0.1140	10000	30	0.0228
600	85	0.0725	10000	40	0.0203
600	90	0.0401	10000	50	0.0175
600	95	0.0189	10000	60	0.0145
1000	0	0.4344	10000	70	0.0114
1000	20	0.4088	10000	80	0.0086
1000	30	0.3771	10000	85	0.0072
1000	40	0.3339	10000	90	0.0060
1000	50	0.2805	10000	95	0.0049
1000	60	0.2185			

Table 12. Geometric Factor for Reflected Solar Radiation to a Cylinder

γ = 30°, ϕ_c = 120°

Altitude n. m.	θ_s degrees	F
100	0	1.1312
100	20	1.0643
100	30	0.9816
100	40	0.8691
100	50	0.7302
100	60	0.5691
100	70	0.3907
100	80	0.1998
100	85	0.1030
100	90	0.0222
100	95	0.0016
300	0	0.8453
300	20	0.7974
300	30	0.7365
300	40	0.6533
300	50	0.5502
300	60	0.4304
300	70	0.2968
300	80	0.1557
300	85	0.0903
300	90	0.0383
300	95	0.0109
600	0	0.6099
600	20	0.5779
600	30	0.5352
600	40	0.4762
600	50	0.4028
600	60	0.3170
600	70	0.2219
600	80	0.1254
600	85	0.0819
600	90	0.0457
600	95	0.0213
1000	0	0.4360
1000	20	0.4151
1000	30	0.3854
1000	40	0.3440
1000	50	0.2922
1000	60	0.2314
1000	70	0.1653
1000	80	0.1001
1000	85	0.0709
1000	90	0.0457
1000	95	0.0266
3000	0	0.1475
3000	20	0.1422
3000	30	0.1330
3000	40	0.1197
3000	50	0.1031
3000	60	0.0840
3000	70	0.0640
3000	80	0.0446
3000	85	0.0356
3000	90	0.0275
3000	95	0.0205
6000	0	0.0582
6000	20	0.0561
6000	30	0.0525
6000	40	0.0474
6000	50	0.0412
6000	60	0.0341
6000	70	0.0268
6000	80	0.0198
6000	85	0.0165
6000	90	0.0135
6000	95	0.0108
10000	0	0.0262
10000	20	0.0252
10000	30	0.0236
10000	40	0.0213
10000	50	0.0186
10000	60	0.0156
10000	70	0.0125
10000	80	0.0095
10000	85	0.0081
10000	90	0.0068
10000	95	0.0056

Table 13. Geometric Factor for Reflected Solar Radiation to a Cylinder

$\gamma = 30°$, $\phi_c = 150°$

Altitude n. m.	θ_s degrees	F	Altitude n. m.	θ_s degrees	F
100	0	1.1312	1000	70	0.1749
100	20	1.0654	1000	80	0.1080
100	30	0.9831	1000	85	0.0768
100	40	0.8710	1000	90	0.0494
100	50	0.7325	1000	95	0.0285
100	60	0.5716	3000	0	0.1480
100	70	0.3934	3000	20	0.1451
100	80	0.2027	3000	30	0.1369
100	85	0.1058	3000	40	0.1246
100	90	0.0231	3000	50	0.1086
100	95	0.0016	3000	60	0.0897
300	0	0.8453	3000	70	0.0692
300	20	0.7996	3000	80	0.0486
300	30	0.7398	3000	85	0.0390
300	40	0.6575	3000	90	0.0301
300	50	0.5552	3000	95	0.0225
300	60	0.4360	6000	0	0.0583
300	70	0.3029	6000	20	0.0572
300	80	0.1618	6000	30	0.0541
300	85	0.0955	6000	40	0.0493
300	90	0.0405	6000	50	0.0432
300	95	0.0113	6000	60	0.0362
600	0	0.6124	6000	70	0,0288
600	20	0.5833	6000	80	0.0214
600	30	0.5418	6000	85	0.0179
600	40	0.4838	6000	90	0.0147
600	50	0.4111	6000	95	0.0117
600	60	0.3259	10000	0	0.0262
600	70	0.2310	10000	20	0.0256
600	80	0.1334	10000	30	0.0241
600	85	0.0879	10000	40	0.0220
600	90	0.0489	10000	50	0.0193
600	95	0.0225	10000	60	0.0163
1000	0	0.4379	10000	70	0.0132
1000	20	0.4202	10000	80	0.0101
1000	30	0.3920	10000	85	0.0086
1000	40	0.3519	10000	90	0.0072
1000	50	0.3011	10000	95	0.0060
1000	60	0.2410			

Table 14. Geometric Factor for Reflected Solar Radiation to a Cylinder

$\gamma = 30°$, $\phi_c = 180°$

Altitude n. m.	θ_s degrees	F
100	0	1.1312
100	20	1.0657
100	30	0.9837
100	40	0.8717
100	50	0.7333
100	60	0.5726
100	70	0.3945
100	80	0.2037
100	85	0.1068
100	90	0.0233
100	95	0.0016
300	0	0.8453
300	20	0.8004
300	30	0.7410
300	40	0.6590
300	50	0.5570
300	60	0.4381
300	70	0.3051
300	80	0.1640
300	85	0.0972
300	90	0.0411
300	95	0.0114
600	0	0.6135
600	20	0.5854
600	30	0.5443
600	40	0.4867
600	50	0.4143
600	60	0.3292
600	70	0.2343
600	80	0.1362
600	85	0.0899
600	90	0.0499
600	95	0.0229
1000	0	0.4389
1000	20	0.4224
1000	30	0.3947
1000	40	0.3550
1000	50	0.3045
1000	60	0.2446
1000	70	0.1785
1000	80	0.1107
1000	85	0.0787
1000	90	0.0505
1000	95	0.0291
3000	0	0.1484
3000	20	0.1462
3000	30	0.1384
3000	40	0.1264
3000	50	0.1106
3000	60	0.0917
3000	70	0.0710
3000	80	0.0499
3000	85	0.0401
3000	90	0.0310
3000	95	0.0231
6000	0	0.0584
6000	20	0.0576
6000	30	0.0546
6000	40	0.0500
6000	50	0.0440
6000	60	0.0370
6000	70	0,0294
6000	80	0.0219
6000	85	0.0184
6000	90	0.0151
6000	95	0.0121
10000	0	0.0262
10000	20	0.0258
10000	30	0.0243
10000	40	0.0222
10000	50	0.0196
10000	60	0.0166
10000	70	0.0134
10000	80	0.0103
10000	85	0.0088
10000	90	0.0074
10000	95	0.0061

Table 15. Geometric Factor for Reflected Solar Radiation to a Cylinder

$\gamma = 60°$, $\phi_c = 0°$

Altitude n. m.	θ_s degrees	F	Altitude n. m.	θ_s degrees	F
100	0	1.2133	1000	70	0.1762
100	20	1.1369	1000	80	0.0912
100	30	1.0460	1000	85	0.0564
100	40	0.9234	1000	90	0.0307
100	50	0.7727	1000	95	0.0149
100	60	0.5985	3000	0	0.2292
100	70	0.4061	3000	20	0.2117
100	80	0.2003	3000	30	0.1931
100	85	0.0963	3000	40	0.1686
100	90	0.0123	3000	50	0.1394
100	95	0.0006	3000	60	0.1076
300	0	0.9612	3000	70	0.0760
300	20	0.8966	3000	80	0.0480
300	30	0.8227	3000	85	0.0362
300	40	0.7238	3000	90	0.0264
300	50	0.6029	3000	95	0.0185
300	60	0.4637	6000	0	0.0962
300	70	0.3097	6000	20	0.0891
300	80	0.1483	6000	30	0.0814
300	85	0.0736	6000	40	0.0714
300	90	0.0211	6000	50	0.0599
300	95	0.0041	6000	60	0.0477
600	0	0.7441	6000	70	0,0358
600	20	0.6915	6000	80	0.0250
600	30	0.6331	6000	85	0.0203
600	40	0.5555	6000	90	0.0161
600	50	0.4610	6000	95	0.0125
600	60	0.3521	10000	0	0.0444
600	70	0.2325	10000	20	0.0412
600	80	0.1140	10000	30	0.0378
600	85	0.0631	10000	40	0.0334
600	90	0.0274	10000	50	0.0284
600	95	0.0090	10000	60	0.0232
1000	0	0.5712	10000	70	0.0180
1000	20	0.5291	10000	80	0.0132
1000	30	0.4835	10000	85	0.0111
1000	40	0.4232	10000	90	0.0091
1000	50	0.3500	10000	95	0.0074
1000	60	0.2658			

Table 16. Geometric Factor for Reflected Solar Radiation to a Cylinder

γ = 60°, ϕ_c = 30°

Altitude n. m.	θ_s degrees	F
100	0	1.2133
100	20	1.1373
100	30	1.0467
100	40	0.9243
100	50	0.7736
100	60	0.5996
100	70	0.4073
100	80	0.2015
100	85	0.0976
100	90	0.0137
100	95	0.0009
300	0	0.9613
300	20	0.8975
300	30	0.8240
300	40	0.7255
300	50	0.6049
300	60	0.4660
300	70	0.3121
300	80	0.1510
300	85	0.0764
300	90	0.0237
300	95	0.0054
600	0	0.7438
600	20	0.6924
600	30	0.6346
600	40	0.5575
600	50	0.4634
600	60	0.3549
600	70	0.2356
600	80	0.1174
600	85	0.0665
600	90	0.0304
600	95	0.0117
1000	0	0.5712
1000	20	0.5302
1000	30	0.4851
1000	40	0.4253
1000	50	0.3525
1000	60	0.2686
1000	70	0.1794
1000	80	0.0945
1000	85	0.0596
1000	90	0.0335
1000	95	0.0171
3000	0	0.2293
3000	20	0.2123
3000	30	0.1939
3000	40	0.1697
3000	50	0.1407
3000	60	0.1091
3000	70	0.0776
3000	80	0.0494
3000	85	0.0376
3000	90	0.0276
3000	95	0.0195
6000	0	0.0962
6000	20	0.0893
6000	30	0.0817
6000	40	0.0718
6000	50	0.0604
6000	60	0.0482
6000	70	0.0363
6000	80	0.0255
6000	85	0.0207
6000	90	0.0165
6000	95	0.0128
10000	0	0.0444
10000	20	0.0413
10000	30	0.0379
10000	40	0.0336
10000	50	0.0286
10000	60	0.0233
10000	70	0.0182
10000	80	0.0134
10000	85	0.0112
10000	90	0.0093
10000	95	0.0075

Table 17. Geometric Factor for Reflected Solar Radiation to a Cylinder

$\gamma = 60°$, $\phi_c = 60°$

Altitude n. m.	θ_s degrees	F
100	0	1.2133
100	20	1.1386
100	30	1.0484
100	40	0.9264
100	50	0.7763
100	60	0.6026
100	70	0.4105
100	80	0.2049
100	85	0.1012
100	90	0.0172
100	95	0.0013
300	0	0.9613
300	20	0.9000
300	30	0.8276
300	40	0.7301
300	50	0.6104
300	60	0.4722
300	70	0.3188
300	80	0.1580
300	85	0.0838
300	90	0.0300
300	95	0.0082
600	0	0.7439
600	20	0.6955
600	30	0.6391
600	40	0.5633
600	50	0.4704
600	60	0.3628
600	70	0.2442
600	80	0.1265
600	85	0.0754
600	90	0.0378
600	95	0.0165
1000	0	0.5713
1000	20	0.5334
1000	30	0.4898
1000	40	0.4312
1000	50	0.3595
1000	60	0.2765
1000	70	0.1880
1000	80	0.1032
1000	85	0.0678
1000	90	0.0405
1000	95	0.0222
3000	0	0.2294
3000	20	0.2139
3000	30	0.1963
3000	40	0.1727
3000	50	0.1443
3000	60	0.1130
3000	70	0.0816
3000	80	0.0532
3000	85	0.0410
3000	90	0.0306
3000	95	0.0221
6000	0	0.0962
6000	20	0.0899
6000	30	0.0826
6000	40	0.0730
6000	50	0.0617
6000	60	0.0496
6000	70	0.0377
6000	80	0.0267
6000	85	0.0219
6000	90	0.0176
6000	95	0.0138
10000	0	0.0444
10000	20	0.0416
10000	30	0.0383
10000	40	0.0340
10000	50	0.0291
10000	60	0.0238
10000	70	0.0187
10000	80	0.0138
10000	85	0.0116
10000	90	0.0096
10000	95	0.0078

Table 18. Geometric Factor for Reflected Solar Radiation to a Cylinder

$\gamma' = 60°$ $\phi_c = 90°$

Altitude n. m.	θ_s degrees	F
100	0	1.2134
100	20	1.1402
100	30	1.0508
100	40	0.9295
100	50	0.7799
100	60	0.6067
100	70	0.4150
100	80	0.2095
100	85	0.1058
100	90	0.0205
100	95	0.0015
300	0	0.9613
300	20	0.9034
300	30	0.8325
300	40	0.7364
300	50	0.6179
300	60	0.4806
300	70	0.3280
300	80	0.1674
300	85	0.0929
300	90	0.0364
300	95	0.0102
600	0	0.7448
600	20	0.7006
600	30	0.6461
600	40	0.5719
600	50	0.4803
600	60	0.3738
600	70	0.2560
600	80	0.1382
600	85	0.0860
600	90	0.0456
600	95	0.0206
1000	0	0.5721
1000	20	0.5383
1000	30	0.4965
1000	40	0.4398
1000	50	0.3694
1000	60	0.2875
1000	70	0.1995
1000	80	0.1142
1000	85	0.0775
1000	90	0.0480
1000	95	0.0271
3000	0	0.2297
3000	20	0.2163
3000	30	0.1996
3000	40	0.1768
3000	50	0.1491
3000	60	0.1183
3000	70	0.0869
3000	80	0.0579
3000	85	0.0452
3000	90	0.0342
3000	95	0.0249
6000	0	0.0963
6000	20	0.0908
6000	30	0.0838
6000	40	0.0745
6000	50	0.0634
6000	60	0.0515
6000	70	0,0395
6000	80	0.0283
6000	85	0.0234
6000	90	0.0188
6000	95	0.0148
10000	0	0.0444
10000	20	0.0419
10000	30	0.0387
10000	40	0.0346
10000	50	0.0297
10000	60	0.0245
10000	70	0.0193
10000	80	0.0144
10000	85	0.0122
10000	90	0.0101
10000	95	0.0083

Table 19. Geometric Factor for Reflected Solar Radiation to a Cylinder

$\gamma = 60°$, $\phi_c = 120°$

Altitude n. m.	θ_s degrees	F	Altitude n. m.	θ_s degrees	F
100	0	1.2134	1000	70	0.2108
100	20	1.1418	1000	80	0.1237
100	30	1.0532	1000	85	0.0849
100	40	0.9325	1000	90	0.0529
100	50	0.7835	1000	95	0.0298
100	60	0.6107	3000	0	0.2300
100	70	0.4194	3000	20	0.2187
100	80	0.2141	3000	30	0.2030
100	85	0.1102	3000	40	0.1810
100	90	0.0219	3000	50	0.1539
100	95	0.0015	3000	60	0.1234
300	0	0.9614	3000	70	0.0917
300	20	0.9067	3000	80	0.0619
300	30	0.8374	3000	85	0.0486
300	40	0.7427	3000	90	0.0369
300	50	0.6254	3000	95	0.0270
300	60	0.4891	6000	0	0.0964
300	70	0.3371	6000	20	0.0917
300	80	0.1765	6000	30	0.0850
300	85	0.1005	6000	40	0.0760
300	90	0.0398	6000	50	0.0652
300	95	0.0108	6000	60	0.0533
600	0	0.7470	6000	70	0,0412
600	20	0.7067	6000	80	0.0298
600	30	0.6539	6000	85	0.0246
600	40	0.5812	6000	90	0.0199
600	50	0.4909	6000	95	0.0158
600	60	0.3852	10000	0	0.0444
600	70	0.2679	10000	20	0.0422
600	80	0.1488	10000	30	0.0392
600	85	0.0942	10000	40	0.0351
600	90	0.0502	10000	50	0.0303
600	95	0.0224	10000	60	0.0252
1000	0	0.5736	10000	70	0.0199
1000	20	0.5438	10000	80	0.0149
1000	30	0.5038	10000	85	0.0127
1000	40	0.4484	10000	90	0.0105
1000	50	0.3794	10000	95	0.0086
1000	60	0.2985			

Table 20. Geometric Factor for Reflected Solar Radiation to a Cylinder

$\gamma = 60°$; $\phi_c = 150°$

Altitude n. m.	θ_s degrees	F	Altitude n. m.	θ_s degrees	F
100	0	1.2134	1000	70	0.2187
100	20	1.1430	1000	80	0.1294
100	30	1.0549	1000	85	0.0888
100	40	0.9347	1000	90	0.0549
100	50	0.7862	1000	95	0.0306
100	60	0.6137	3000	0	0.2304
100	70	0.4226	3000	20	0.2206
100	80	0.2175	3000	30	0.2055
100	85	0.1132	3000	40	0.1841
100	90	0.0219	3000	50	0.1575
100	95	0.0013	3000	60	0.1270
300	0	0.9614	3000	70	0.0950
300	20	0.9092	3000	80	0.0644
300	30	0.8410	3000	85	0.0507
300	40	0.7473	3000	90	0.0385
300	50	0.6309	3000	95	0.0282
300	60	0.4953	6000	0	0.0965
300	70	0.3438	6000	20	0.0923
300	80	0.1827	6000	30	0.0860
300	85	0.1048	6000	40	0.0771
300	90	0.0406	6000	50	0.0664
300	95	0.0105	6000	60	0.0545
600	0	0.7499	6000	70	0.0423
600	20	0.7123	6000	80	0.0307
600	30	0.6606	6000	85	0.0254
600	40	0.5888	6000	90	0.0206
600	50	0.4992	6000	95	0.0163
600	60	0.3940	10000	0	0.0445
600	70	0.2766	10000	20	0.0424
600	80	0.1555	10000	30	0.0395
600	85	0.0985	10000	40	0.0355
600	90	0.0518	10000	50	0.0308
600	95	0.0226	10000	60	0.0256
1000	0	0.5755	10000	70	0.0203
1000	20	0.5485	10000	80	0.0153
1000	30	0.5096	10000	85	0.0130
1000	40	0.4553	10000	90	0.0108
1000	50	0.3871	10000	95	0.0089
1000	60	0.3067			

Table 21. Geometric Factor for Reflected Solar Radiation to a Cylinder

$\gamma = 60°$, $\phi_c = 180°$

Altitude n. m.	θ_s degrees	F	Altitude n. m.	θ_s degrees	F
100	0	1.2134	1000	70	0.2215
100	20	1.1434	1000	80	0.1312
100	30	1.0555	1000	85	0.0900
100	40	0.9355	1000	90	0.0554
100	50	0.7871	1000	95	0.0307
100	60	0.6148	3000	0	0.2305
100	70	0.4238	3000	20	0.2213
100	80	0.2187	3000	30	0.2064
100	85	0.1142	3000	40	0.1853
100	90	0.0217	3000	50	0.1587
100	95	0.0012	3000	60	0.1283
300	0	0.9614	3000	70	0.0961
300	20	0.9100	3000	80	0.0652
300	30	0.8423	3000	85	0.0513
300	40	0.7490	3000	90	0.0390
300	50	0.6329	3000	95	0.0285
300	60	0.4975	6000	0	0.0965
300	70	0.3462	6000	20	0.0926
300	80	0.1848	6000	30	0.0863
300	85	0.1060	6000	40	0.0775
300	90	0.0406	6000	50	0.0669
300	95	0.0102	6000	60	0.0550
600	0	0.7515	6000	70	0,0427
600	20	0.7148	6000	80	0.0311
600	30	0.6634	6000	85	0.0257
600	40	0.5919	6000	90	0.0208
600	50	0.5024	6000	95	0.0165
600	60	0.3973	10000	0	0.0445
600	70	0.2797	10000	20	0.0425
600	80	0.1576	10000	30	0.0398
600	85	0.0997	10000	40	0.0357
600	90	0.0521	10000	50	0.0310
600	95	0.0225	10000	60	0.0258
1000	0	0.5763	10000	70	0.0205
1000	20	0.5502	10000	80	0,0154
1000	30	0.5118	10000	85	0.0131
1000	40	0.4578	10000	90	0.0109
1000	50	0.3899	10000	95	0.0089
1000	60	0.3087			

Table 22. Geometric Factor for Reflected Solar Radiation to a Cylinder

$\gamma = 90°$, $\phi_c = 0°$

Altitude n. m.	θ_s degrees	F	Altitude n. m.	θ_s degrees	F
100	0	1.2702	1000	70	0.2216
100	20	1.1936	1000	80	0.1238
100	30	1.1000	1000	85	0.0813
100	40	0.9730	1000	90	0.0478
100	50	0.8164	1000	95	0.0252
100	60	0.6351	3000	0	0.2620
100	70	0.4344	3000	20	0.2467
100	80	0.2193	3000	30	0.2277
100	85	0.1099	3000	40	0.2016
100	90	0.0164	3000	50	0.1699
100	95	0.0007	3000	60	0.1345
300	0	1.0357	3000	70	0.0982
300	20	0.9733	3000	80	0.0645
300	30	0.8970	3000	85	0.0499
300	40	0.7934	3000	90	0.0373
300	50	0.6657	3000	95	0.0268
300	60	0.5178	6000	0	0.1107
300	70	0.3534	6000	20	0.1043
300	80	0.1793	6000	30	0.0963
300	85	0.0960	6000	40	0.0856
300	90	0.0320	6000	50	0.0728
300	95	0.0070	6000	60	0.0590
600	0	0.8221	6000	70	0.0451
600	20	0.7731	6000	80	0.0322
600	30	0.7127	6000	85	0.0264
600	40	0.6308	6000	90	0.0212
600	50	0.5296	6000	95	0.0167
600	60	0.4120	10000	0	0.0512
600	70	0.2815	10000	20	0.0482
600	80	0.1490	10000	30	0.0446
600	85	0.0890	10000	40	0.0398
600	90	0.0431	10000	50	0.0342
600	95	0.0172	10000	60	0.0282
1000	0	0.6394	10000	70	0.0222
1000	20	0.6015	10000	80	0.0166
1000	30	0.5546	10000	85	0.0139
1000	40	0.4910	10000	90	0.0116
1000	50	0.4124	10000	95	0.0094
1000	60	0.3207			

Table 23. Geometric Factor for Reflected Solar Radiation to a Cylinder

$\gamma = 90°$, $\phi_c = 30°$

Altitude n. m.	θ_s degrees	F
100	0	1.2702
100	20	1.1936
100	30	1.1000
100	40	0.9730
100	50	0.8164
100	60	0.6351
100	70	0.4344
100	80	0.2193
100	85	0.1101
100	90	0.0174
100	95	0.0009
300	0	1.0357
300	20	0.9733
300	30	0.8970
300	40	0.7934
300	50	0.6657
300	60	0.5178
300	70	0.3534
300	80	0.1795
300	85	0.0969
300	90	0.0334
300	95	0.0073
600	0	0.8209
600	20	0.7721
600	30	0.7119
600	40	0.6300
600	50	0.5291
600	60	0.4116
600	70	0.2814
600	80	0.1496
600	85	0.0901
600	90	0.0444
600	95	0.0183
1000	0	0.6387
1000	20	0.6009
1000	30	0.5542
1000	40	0.4906
1000	50	0.4121
1000	60	0.3205
1000	70	0.2217
1000	80	0.1245
1000	85	0.0823
1000	90	0.0489
1000	95	0.0262
3000	0	0.2619
3000	20	0.2466
3000	30	0.2276
3000	40	0.2016
3000	50	0.1699
3000	60	0.1345
3000	70	0.0983
3000	80	0.0648
3000	85	0.0502
3000	90	0.0376
3000	95	0.0271
6000	0	0.1107
6000	20	0.1043
6000	30	0.0963
6000	40	0.0855
6000	50	0.0728
6000	60	0.0590
6000	70	0.0451
6000	80	0.0323
6000	85	0.0265
6000	90	0.0213
6000	95	0.0167
10000	0	0.0512
10000	20	0.0482
10000	30	0.0446
10000	40	0.0398
10000	50	0.0342
10000	60	0.0282
10000	70	0.0222
10000	80	0.0165
10000	85	0.0139
10000	90	0.0116
10000	95	0.0094

Table 24 Geometric Factor for Reflected Solar Radiation to a Cylinder

$\gamma = 90°$, $\rho_c = 60°$

Altitude n. m.	θ_s degrees	F
100	0	1.2792
100	20	1.1936
100	30	1.1000
100	40	0.9730
100	50	0.8164
100	60	0.6351
100	70	0.4344
100	80	0.2193
100	85	0.1105
100	90	0.0194
100	95	0.0013
300	0	1.0357
300	20	0.9733
300	30	0.8970
300	40	0.7934
300	50	0.6657
300	60	0.5178
300	70	0.3534
300	80	0.1801
300	85	0.0986
300	90	0.0363
300	95	0.0095
600	0	0.8196
600	20	0.7709
600	30	0.7108
600	40	0.6292
600	50	0.5285
600	60	0.4112
600	70	0.2814
600	80	0.1508
600	85	0.0923
600	90	0.0473
600	95	0.0205
1000	0	0.6379
1000	20	0.6002
1000	30	0.5536
1000	40	0.4901
1000	50	0.4118
1000	60	0.3204
1000	70	0.2220
1000	80	0.1259
1000	85	0.0843
1000	90	0.0511
1000	95	0.0282
3000	0	0.2618
3000	20	0.2465
3000	30	0.2275
3000	40	0.2016
3000	50	0.1699
3000	60	0.1347
3000	70	0.0986
3000	80	0.0653
3000	85	0.0508
3000	90	0.0382
3000	95	0.0277
6000	0	0.1106
6000	20	0.1043
6000	30	0.0963
6000	40	0.0856
6000	50	0.0728
6000	60	0.0591
6000	70	0.0452
6000	80	0.0324
6000	85	0.0267
6000	90	0.0215
6000	95	0.0169
10000	0	0.0512
10000	20	0.0482
10000	30	0.0446
10000	40	0.0398
10000	50	0.0342
10000	60	0.0282
10000	70	0.0222
10000	80	0.0166
10000	85	0.0140
10000	90	0.0116
10000	95	0.0095

Table 25. Geometric Factor for Reflected Solar Radiation to a Cylinder

$\gamma = 90°$, $\phi_c = 90°$

Altitude n. m.	θ_s degrees	F	Altitude n. m.	θ_s degrees	F
100	0	1.2702	1000	70	0.2222
100	20	1.1936	1000	80	0.1266
100	30	1.1000	1000	85	0.0853
100	40	0.9730	1000	90	0.0523
100	50	0.8164	1000	95	0.0292
100	60	0.6351	3000	0	0.2617
100	70	0.4344	3000	20	0.2465
100	80	0.2193	3000	30	0.2275
100	85	0.1107	3000	40	0.2015
100	90	0.0206	3000	50	0.1699
100	95	0.0015	3000	60	0.1347
300	0	1.0358	3000	70	0.0988
300	20	0.9733	3000	80	0.0656
300	30	0.8970	3000	85	0.0512
300	40	0.7934	3000	90	0.0386
300	50	0.6657	3000	95	0.0281
300	60	0.5178	6000	0	0.1106
300	70	0.3534	6000	20	0.1043
300	80	0.1803	6000	30	0.0963
300	85	0.0994	6000	40	0.0856
300	90	0.0379	6000	50	0.0729
300	95	0.0104	6000	60	0.0591
600	0	0.8192	6000	70	0.0453
600	20	0.7706	6000	80	0.0325
600	30	0.7106	6000	85	0.0267
600	40	0.6290	6000	90	0.0215
600	50	0.5283	6000	95	0.0170
600	60	0.4111	10000	0	0.0512
600	70	0.2814	10000	20	0.0482
600	80	0.1514	10000	30	0.0446
600	85	0.0934	10000	40	0.0398
600	90	0.0487	10000	50	0.0342
600	95	0.0216	10000	60	0.0282
1000	0	0.6377	10000	70	0.0222
1000	20	0.6001	10000	80	0.0166
1000	30	0.5535	10000	85	0.0140
1000	40	0.4900	10000	90	0.0116
1000	50	0.4117	10000	95	0.0095
1000	60	0.3204			

Table 26. Geometric Factor for Reflected Solar Radiation to a Cylinder

$\gamma = 90°$, $\psi_c = 120°$

Altitude n. m.	θ_s degrees	F
100	0	1.2702
100	20	1.1936
100	30	1.1000
100	40	0.9730
100	50	0.8164
100	60	0.6351
100	70	0.4344
100	80	0.2193
100	85	0.1105
100	90	0.0194
100	95	0.0013
300	0	1.0357
300	20	0.9733
300	30	0.8970
300	40	0.7934
300	50	0.6657
300	60	0.5178
300	70	0.3534
300	80	0.1801
300	85	0.0986
300	90	0.0363
300	95	0.0095
600	0	0.8201
600	20	0.7714
600	30	0.7113
600	40	0.6296
600	50	0.5287
600	60	0.4114
600	70	0.2815
600	80	0.1508
600	85	0.0923
600	90	0.0473
600	95	0.0205
1000	0	0.6383
1000	20	0.6005
1000	30	0.5538
1000	40	0.4903
1000	50	0.4119
1000	60	0.3205
1000	70	0.2220
1000	80	0.1259
1000	85	0.0843
1000	90	0.0511
1000	95	0.0282
3000	0	0.2618
3000	20	0.2466
3000	30	0.2276
3000	40	0.2016
3000	50	0.1699
3000	60	0.1347
3000	70	0.0987
3000	80	0.0654
3000	85	0.0508
3000	90	0.0382
3000	95	0.0277
6000	0	0.1106
6000	20	0.1043
6000	30	0.0963
6000	40	0.0856
6000	50	0.0728
6000	60	0.0591
6000	70	0,0452
6000	80	0.0324
6000	85	0.0267
6000	90	0.0215
6000	95	0.0169
10000	0	0.0512
10000	20	0.0482
10000	30	0.0446
10000	40	0.0398
10000	50	0.0342
10000	60	0.0282
10000	70	0.0222
10000	80	0.0166
10000	85	0.0140
10000	90	0.0116
10000	95	0.0095

Table 27. Geometric Factor for Reflected Solar Radiation to a Cylinder

$\gamma = 90°$, $\phi_c = 150°$

Altitude n. m.	θ_s degrees	F
100	0	1.2702
100	20	1.1936
100	30	1.1000
100	40	0.9731
100	50	0.8165
100	60	0.6351
100	70	0.4344
100	80	0.2193
100	85	0.1101
100	90	0.0174
100	95	0.0009
300	0	1.0357
300	20	0.9733
300	30	0.8970
300	40	0.7934
300	50	0.6657
300	60	0.5178
300	70	0.3534
300	80	0.1795
300	85	0.0969
300	90	0.0334
300	95	0.0078
600	0	0.8216
600	20	0.7727
600	30	0.7124
600	40	0.6305
600	50	0.5294
600	60	0.4118
600	70	0.2815
600	80	0.1496
600	85	0.0901
600	90	0.0444
600	95	0.0182
1000	0	0.6391
1000	20	0.6012
1000	30	0.5544
1000	40	0.4908
1000	50	0.4123
1000	60	0.3206
1000	70	0.2217
1000	80	0.1245
1000	85	0.0823
1000	90	0.0489
1000	95	0.0262
3000	0	0.2620
3000	20	0.2467
3000	30	0.2276
3000	40	0.2016
3000	50	0.1699
3000	60	0.1346
3000	70	0.0983
3000	80	0.0648
3000	85	0.0502
3000	90	0.0376
3000	95	0.0271
6000	0	0.1107
6000	20	0.1043
6000	30	0.0963
6000	40	0.0858
6000	50	0.0728
6000	60	0.0590
6000	70	0,0451
6000	80	0.0323
6000	85	0.0265
6000	90	0.0213
6000	95	0.0167
10000	0	0.0512
10000	20	0.0482
10000	30	0.0446
10000	40	0.0398
10000	50	0.0342
10000	60	0.0282
10000	70	0.0222
10000	80	0.0165
10000	85	0.0139
10000	90	0.0116
10000	95	0.0094

Table 28. Geometric Factor for Reflected Solar Radiation to a Cylinder

$\gamma = 90°$, $\phi_c = 180°$

Altitude n. m.	θ_s degrees	F
100	0	1.2702
100	20	1.1936
100	30	1.1000
100	40	0.9730
100	50	0.8164
100	60	0.6351
100	70	0.4344
100	80	0.2193
100	85	0.1099
100	90	0.0164
100	95	0.0007
300	0	1.0357
300	20	0.9733
300	30	0.8970
300	40	0.7934
300	50	0.6657
300	60	0.5178
300	70	0.3534
300	80	0.1793
300	85	0.0960
300	90	0.0320
300	95	0.0070
600	0	0.8221
600	20	0.7731
600	30	0.7127
600	40	0.6308
600	50	0.5296
600	60	0.4120
600	70	0.2815
600	80	0.1490
600	85	0.0890
600	90	0.0431
600	95	0.0172
1000	0	0.6394
1000	20	0.5546
1000	30	0.6015
1000	40	0.4910
1000	50	0.4124
1000	60	0.3207

Altitude n. m.	θ_s degrees	F
1000	70	0.2216
1000	80	0.1238
1000	85	0.0813
1000	90	0.0478
1000	95	0.0252
3000	0	0.2620
3000	20	0.2467
3000	30	0.2277
3000	40	0.2016
3000	50	0.1699
3000	60	0.1345
3000	70	0.0982
3000	80	0.0645
3000	85	0.0499
3000	90	0.0373
3000	95	0.0268
6000	0	0.1107
6000	20	0.1043
6000	30	0.0963
6000	40	0.0856
6000	50	0.0728
6000	60	0.0590
6000	70	0.0451
6000	80	0.0322
6000	85	0.0264
6000	90	0.0212
6000	95	0.0167
10000	0	0.0612
10000	20	0.0482
10000	30	0.0446
10000	40	0.0398
10000	50	0.0342
10000	60	0.0282
10000	70	0.0222
10000	80	0.0165
10000	85	0.0139
10000	90	0.0116
10000	95	0.0094

Figure 7. Geometry for Planetary Reflected Solar Radiation to a Hemisphere

$$\text{Geometric Factor, } F = \frac{q}{\pi r^2 S_a}$$

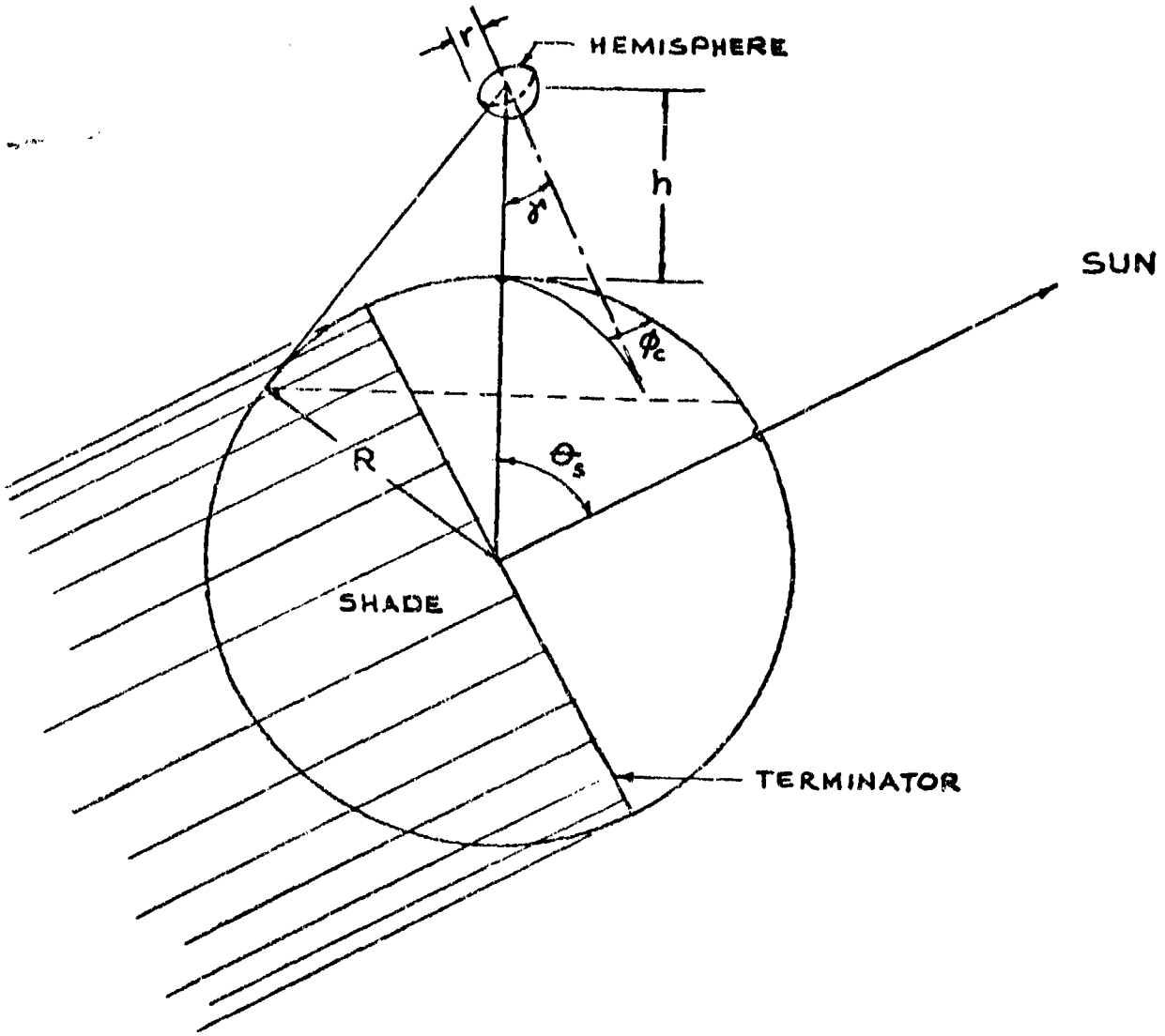

Table 29. Geometric Factor for Reflected Solar Radiation to a Hemisphere

$\gamma = 0°$, $\phi_c = 0 - 360°$

Altitude n. m.	θ_s degrees	F
100	0	1.2438
100	20	1.1688
100	30	1.0771
100	40	0.9528
100	50	0.7995
100	60	0.6219
100	70	0.4254
100	80	0.2147
100	85	0.1079
100	90	0.0177
100	95	0.0010
300	0	1.0237
300	20	0.9620
300	30	0.8866
300	40	0.7842
300	50	0.6580
300	60	0.5118
300	70	0.3493
300	80	0.1777
300	85	0.0964
300	90	0.0342
300	95	0.0084
600	0	0.8154
600	20	0.7669
600	30	0.7071
600	40	0.6259
600	50	0.5256
600	60	0.4089
600	70	0.2796
600	80	0.1492
600	85	0.0905
600	90	0.0454
600	95	0.0191
1000	0	0.6363
1000	20	0.5987
1000	30	0.5521
1000	40	0.4888
1000	50	0.4106
1000	60	0.3194
1000	70	0.2211
1000	80	0.1247
1000	85	0.0829
1000	90	0.0497
1000	95	0.0270
3000	0	0.2617
3000	20	0.2465
3000	30	0.2275
3000	40	0.2015
3000	50	0.1698
3000	60	0.1345
3000	70	0.0984
3000	80	0.0650
3000	85	0.0508
3000	90	0.0379
3000	95	0.0274
6000	0	0.1106
6000	20	0.1043
6000	30	0.0963
6000	40	0.0855
6000	50	0.0728
6000	60	0.0590
6000	70	0,0452
6000	80	0.0323
6000	85	0.0266
6000	90	0.0214
6000	95	0.0168
10000	0	0.0612
10000	20	0.0482
10000	30	0.0446
10000	40	0.0398
10000	50	0.0342
10000	60	0.0282
10000	70	0.0222
10000	80	0.0165
10000	85	0.0140
10000	90	0.0116
10000	95	0.0094

Table 30. Geometric Factor for Reflected Solar Radiation to a Hemisphere

$\gamma = 30°$, $\phi_c = 0°$

Altitude n. m.	θ_s degrees	F	Altitude n. m.	θ_s degrees	F
100	0	1.1799	1000	70	0.2205
100	20	1.1115	1000	80	0.1286
100	30	1.0259	1000	85	0.0875
100	40	0.9091	1000	90	0.0538
100	50	0.7648	1000	95	0.0299
100	60	0.5969	3000	0	0.2462
100	70	0.4111	3000	20	0.2331
100	80	0.2116	3000	30	0.2163
100	85	0.1100	3000	40	0.1928
100	90	0.0210	3000	50	0.1639
100	95	0.0013	3000	60	0.1313
300	0	0.9673	3000	70	0.0973
300	20	0.9135	3000	80	0.0654
300	30	0.8443	3000	85	0.0512
300	40	0.7495	3000	90	0.0387
300	50	0.6319	3000	95	0.0283
300	60	0.4951	6000	0	0.1034
300	70	0.3424	6000	20	0.0983
300	80	0.1802	6000	30	0.0912
300	85	0.1021	6000	40	0.0815
300	90	0.0391	6000	50	0.0698
300	95	0.0102	6000	60	0.0570
600	0	0.7699	6000	70	0.0440
600	20	0.7290	6000	80	0.0317
600	30	0.6749	6000	85	0.0262
600	40	0.6002	6000	90	0.0212
600	50	0.5073	6000	95	0.0167
600	60	0.3986	10000	0	0.0478
600	70	0.2775	10000	20	0.0454
600	80	0.1537	10000	30	0.0421
600	85	0.0963	10000	40	0.0377
600	90	0.0503	10000	50	0.0326
600	95	0.0220	10000	60	0.0270
1000	0	0.5991	10000	70	0.0213
1000	20	0.5883	10000	80	0.0160
1000	30	0.5266	10000	85	0.0135
1000	40	0.4690	10000	90	0.0113
1000	50	0.3970	10000	95	0.0092
1000	60	0.3125			

Table 31. Geometric Factor for Reflected Solar Radiation to a Hemisphere

$\gamma = 30°$, $\phi_c = 30°$

Altitude n. m.	θ_s degrees	F
100	0	1.1799
100	20	1.1112
100	30	1.0253
100	40	0.9084
100	50	0.7638
100	60	0.5960
100	70	0.4101
100	80	0.2105
100	85	0.1090
100	90	0.0204
100	95	0.0013
300	0	0.9673
300	20	0.9129
300	30	0.8434
300	40	0.7484
300	50	0.6305
300	60	0.4936
300	70	0.3407
300	80	0.1786
300	85	0.1006
300	90	0.0382
300	95	0.0099
600	0	0.7695
600	20	0.7280
600	30	0.6736
600	40	0.5987
600	50	0.5056
600	60	0.3968
600	70	0.2756
600	80	0.1519
600	85	0.0948
600	90	0.0493
600	95	0.0215
1000	0	0.5989
1000	20	0.5675
1000	30	0.5255
1000	40	0.4676
1000	50	0.3955
1000	60	0.3108
1000	70	0.2188
1000	80	0.1270
1000	85	0.0862
1000	90	0.0529
1000	95	0.0293
3000	0	0.2451
3000	20	0.2327
3000	30	0.2158
3000	40	0.1923
3000	50	0.1632
3000	60	0.1305
3000	70	0.0966
3000	80	0.0648
3000	85	0.0507
3000	90	0.0383
3000	95	0.0279
6000	0	0.1034
6000	20	0.0982
6000	30	0.0910
6000	40	0.0812
6000	50	0.0696
6000	60	0.0567
6000	70	0,0437
6000	80	0.0315
6000	85	0.0260
6000	90	0.0210
6000	95	0.0166
10000	0	0.0478
10000	20	0.0453
10000	30	0.0420
10000	40	0.0377
10000	50	0.0325
10000	60	0.0269
10000	70	0.0213
10000	80	0.0159
10000	85	0.0135
10000	90	0.0112
10000	95	0.0092

Table 32. Geometric Factor for Reflected Solar Radiation to a Hemisphere

γ = 30°, ϕ_c = 60°

Altitude n. m.	θ_s degrees	F	Altitude n. m.	θ_s degrees	F
100	0	1.1799	1000	70	0.2141
100	20	1.1101	1000	80	0.1229
100	30	1.0239	1000	85	0.0828
100	40	0.9065	1000	90	0.0503
100	50	0.7615	1000	95	0.0277
100	60	0.5934	3000	0	0.2450
100	70	0.4073	3000	20	0.2318
100	80	0.2078	3000	30	0.2145
100	85	0.1062	3000	40	0.1907
100	90	0.0189	3000	50	0.1614
100	95	0.0012	3000	60	0.1286
300	0	0.9673	3000	70	0.0947
300	20	0.9112	3000	80	0.0631
300	30	0.8410	3000	85	0.0492
300	40	0.7452	3000	90	0.0371
300	50	0.6268	3000	95	0.0270
300	60	0.4894	6000	0	0.1034
300	70	0.3362	6000	20	0.0978
300	80	0.1741	6000	30	0.0905
300	85	0.0966	6000	40	0.0807
300	90	0.0358	6000	50	0.0689
300	95	0.0091	6000	60	0.0561
600	0	0.7687	6000	70	0.0431
600	20	0.7255	6000	80	0.0310
600	30	0.6703	6000	85	0.0255
600	40	0.5947	6000	90	0.0206
600	50	0.5011	6000	95	0.0162
600	60	0.3918	10000	0	0.0478
600	70	0.2704	10000	20	0.0452
600	80	0.1471	10000	30	0.0419
600	85	0.0908	10000	40	0.0374
600	90	0.0466	10000	50	0.0323
600	95	0.0201	10000	60	0.0267
1000	0	0.5984	10000	70	0.0210
1000	20	0.5653	10000	80	0.0157
1000	30	0.5226	10000	85	0.0133
1000	40	0.4640	10000	90	0.0110
1000	50	0.3914	10000	95	0.0090
1000	60	0.3063			

Table 33. Geometric Factor for Reflected Solar Radiation to a Hemisphere

$\gamma = 30°$, $\phi_c = 90°$

Altitude n. m.	θ_s degrees	F	Altitude n. m.	θ_s degrees	F
100	0	1.1799	1000	70	0.2077
100	20	1.1088	1000	80	0.1172
100	30	1.0218	1000	85	0.0780
100	40	0.9039	1000	90	0.0468
100	50	0.7584	1000	95	0.0255
100	60	0.5899	3000	0	0.2448
100	70	0.4035	3000	20	0.2306
100	80	0.2037	3000	30	0.2128
100	85	0.1024	3000	40	0.1885
100	90	0.0169	3000	50	0.1589
100	95	0.0010	3000	60	0.1259
300	0	0.9673	3000	70	0.0921
300	20	0.9090	3000	80	0.0609
300	30	0.8377	3000	85	0.0473
300	40	0.7410	3000	90	0.0355
300	50	0.6218	3000	95	0.0257
300	60	0.4836	6000	0	0.1033
300	70	0.3300	6000	20	0.0974
300	80	0.1679	6000	30	0.0899
300	85	0.0912	6000	40	0.0799
300	90	0.0325	6000	50	0.0680
300	95	0.0080	6000	60	0.0551
600	0	0.7678	6000	70	0,0422
600	20	0.7221	6000	80	0.0302
600	30	0.6658	6000	85	0.0248
600	40	0.5893	6000	90	0.0200
600	50	0.4949	6000	95	0.0157
600	60	0.3851	10000	0	0.0478
600	70	0.2634	10000	20	0.0450
600	80	0.1406	10000	30	0.0416
600	85	0.0853	10000	40	0.0372
600	90	0.0429	10000	50	0.0319
600	95	0.0181	10000	60	0.0263
1000	0	0.5977	10000	70	0.0207
1000	20	0.5624	10000	80	0.0154
1000	30	0.5186	10000	85	0.0130
1000	40	0.4592	10000	90	0.0108
1000	50	0.3857	10000	95	0.0088
1000	60	0.3001			

Table 34. Geometric Factor for Reflected Solar Radiation to a Hemisphere

$\gamma = 30°$, $\phi_c = 120°$

Altitude n. m.	θ_s degrees	F	Altitude n. m.	θ_s degrees	F
100	0	1.1799	1000	70	0.2014
100	20	1.1074	1000	80	0.1116
100	30	1.0198	1000	85	0.0733
100	40	0.9013	1000	90	0.0433
100	50	0.7553	1000	95	0.0232
100	60	0.5864	3000	0	0.2447
100	70	0.3997	3000	20	0.2293
100	80	0.1998	3000	30	0.2110
100	85	0.0986	3000	40	0.1863
100	90	0.0149	3000	50	0.1564
100	95	0.0008	3000	60	0.1232
300	0	0.9673	3000	70	0.0895
300	20	0.9067	3000	80	0.0586
300	30	0.8344	3000	85	0.0453
300	40	0.7367	3000	90	0.0338
300	50	0.6167	3000	95	0.0244
300	60	0.4779	6000	0	0.1033
300	70	0.3239	6000	20	0.0969
300	80	0.1617	6000	30	0.0893
300	85	0.0857	6000	40	0.0791
300	90	0.0292	6000	50	0.0671
300	95	0.0069	6000	60	0.0542
600	0	0.7669	6000	70	0.0413
300	20	0.7188	6000	80	0.0294
600	30	0.6614	6000	85	0.0241
600	40	0.5840	6000	90	0.0194
600	50	0.4888	6000	95	0.0152
600	60	0.3784	10000	0	0.0477
600	70	0.2563	10000	20	0.0449
600	80	0.1340	10000	30	0.0414
600	85	0.0798	10000	40	0.0369
600	90	0.0392	10000	50	0.0316
800	95	0.0161	10000	60	0.0260
1000	0	0.5971	10000	70	0.0204
1000	20	0.5595	10000	80	0.0152
1000	30	0.5147	10000	85	0.0128
1000	40	0.4543	10000	90	0.0106
1000	50	0.3801	10000	95	0.0086
1000	60	0.2939			

Table 35. Geometric Factor for Reflected Solar Radiation to a Hemisphere

γ = 30°, ϕ_c = 150°

Altitude n. m.	θ_s degrees	F	Altitude n. m.	θ_s degrees	F
100	0	1.1799	1000	70	0.1967
100	20	1.1064	1000	80	0.1074
100	30	1.0183	1000	85	0.0698
100	40	0.8994	1000	90	0.0408
100	50	0.7531	1000	95	0.0216
100	60	0.5839	3000	0	0.2446
100	70	0.3969	3000	20	0.2284
100	80	0.1969	3000	30	0.2098
100	85	0.0958	3000	40	0.1847
100	90	0.0134	3000	50	0.1545
100	95	0.0007	3000	60	0.1212
300	0	0.9673	3000	70	0.0876
300	20	0.9050	3000	80	0.0570
300	30	0.8320	3000	85	0.0439
300	40	0.7336	3000	90	0.0326
300	50	0.6130	3000	95	0.0234
300	60	0.4737	6000	0	0.1033
300	70	0.3193	6000	20	0.0966
300	80	0.1572	6000	30	0.0888
300	85	0.0818	6000	40	0.0786
300	90	0.0268	6000	50	0.0665
300	95	0.0061	6000	60	0.0535
600	0	0.7663	6000	70	0.0407
600	20	0.7164	6000	80	0.0289
600	30	0.6582	6000	85	0.0236
600	40	0.5801	6000	90	0.0184
600	50	0.4843	6000	95	0.0148
600	60	0.3735	10000	0	0.0477
600	70	0.2511	10000	20	0.0447
600	80	0.1292	10000	30	0.0412
600	85	0.0758	10000	40	0.0367
600	90	0.0365	10000	50	0.0314
600	95	0.0147	10000	60	0.0258
1000	0	0.5967	10000	70	0.0202
1000	20	0.5574	10000	80	0.0150
1000	30	0.5119	10000	85	0.0126
1000	40	0.4508	10000	90	0.0104
1000	50	0.3761	10000	95	0.0085
1000	60	0.2894			

Table 36. Geometric Factor for Reflected Solar Radiation to a Hemisphere

$\gamma' = 30°$, $\phi_c = 180°$

Altitude n. m.	θ_s degrees	F	Altitude n. m.	θ_s degrees	F
100	0	1.1799	1000	70	0.1050
100	20	1.1060	1000	80	0.1059
100	30	1.0178	1000	85	0.0686
100	40	0.8087	1000	90	0.0399
100	50	0.7522	1000	95	0.0210
100	60	0.5829	3000	0	0.2445
100	70	0.3959	3000	20	0.2281
100	80	0.1958	3000	30	0.2093
100	85	0.0948	3000	40	0.1842
100	90	0.0129	3000	50	0.1539
100	95	0.0006	3000	60	0.1205
300	0	0.9673	3000	70	0.0869
300	20	0.9044	3000	80	0.0564
300	30	0.8311	3000	85	0.0433
300	40	0.7325	3000	90	0.0322
300	50	0.6116	3000	95	0.0231
300	60	0.4722	6000	0	0.1033
300	70	0.3177	6000	20	0.0965
300	80	0.1556	6000	30	0.0887
300	85	0.0803	6000	40	0.0783
300	90	0.0259	6000	50	0.0663
300	95	0.0058	6000	60	0.0533
600	0	0.7661	6000	70	0.0404
600	20	0.7156	6000	80	0.0287
600	30	0.6572	6000	85	0.0234
600	40	0.5787	6000	90	0.0188
600	50	0.4827	6000	95	0.0147
600	60	0.3717	10000	0	0.0477
600	70	0.2493	10000	20	0.0447
600	80	0.1275	10000	30	0.0412
600	85	0.0744	10000	40	0.0366
600	90	0.0355	10000	50	0.0313
600	95	0.0142	10000	60	0.0257
1000	0	0.5963	10000	70	0.0201
1000	20	0.5567	10000	80	0.0149
1000	30	0.5109	10000	85	0.0125
1000	40	0.4498	10000	90	0.0104
1000	50	0.3746	10000	95	0.0084
1000	60	0.2877			

Table 37. Geometric Factor for Reflected Solar Radiation to a Hemisphere

$\gamma = 60°$, $\phi_c = 0°$

Altitude n. m.	Θ_s degrees	F
100	0	1.0055
100	20	0.9496
100	30	0.8778
100	40	0.7792
100	50	0.6570
100	60	0.5149
100	70	0.3570
100	80	0.1872
100	85	0.1005
100	90	0.0219
100	95	0.0013
300	0	0.8132
300	20	0.7720
300	30	0.7157
300	40	0.6376
300	50	0.5402
300	60	0.4264
300	70	0.2988
300	80	0.1625
300	85	0.0958
300	90	0.0393
300	95	0.0109
600	0	0.6416
600	20	0.6120
600	30	0.5690
600	40	0.5086
600	50	0.4328
600	60	0.3436
600	70	0.2435
600	80	0.1397
600	85	0.0903
600	90	0.0490
600	95	0.0216
1000	0	0.4950
1000	20	0.4738
1000	30	0.4413
1000	40	0.3954
1000	50	0.3375
1000	60	0.2689
1000	70	0.1935
1000	80	0.1165
1000	85	0.0811
1000	90	0.0511
1000	95	0.0290
3000	0	0.1993
3000	20	0.1915
3000	30	0.1787
3000	40	0.1605
3000	50	0.1377
3000	60	0.1115
3000	70	0.0839
3000	80	0.0573
3000	85	0.0453
3000	90	0.0348
3000	95	0.0264
6000	0	0.0635
6000	20	0.0801
6000	30	0.0741
6000	40	0.0672
6000	50	0.0589
6000	60	0.0477
6000	70	0.0371
6000	80	0.0271
6000	85	0.0225
6000	90	0.0182
6000	95	0.0145
10000	0	0.0365
10000	20	0.0368
10000	30	0.0343
10000	40	0.0309
10000	50	0.0268
10000	60	0.0223
10000	70	0.0178
10000	80	0.0134
10000	85	0.0114
10000	90	0.0095
10000	95	0.0078

Table 38. Geometric Factor for Reflected Solar Radiation to a Hemisphere

$\gamma = 60°$, $\phi_c = 30°$

Altitude n. m.	Θ_s degrees	F	Altitude n. m.	Θ_s degrees	F
100	0	1.0035	1000	70	0.1905
100	20	0.9490	1000	80	0.1138
100	30	0.8768	1000	85	0.0789
100	40	0.7780	1000	90	0.0494
100	50	0.6558	1000	95	0.0280
100	60	0.5132	3000	0	0.1993
100	70	0.3553	3000	20	0.1909
100	80	0.1854	3000	30	0.1779
100	85	0.0987	3000	40	0.1595
100	90	0.0208	3000	50	0.1366
100	95	0.0015	3000	60	0.1103
300	0	0.8132	3000	70	0.0827
300	20	0.7709	3000	80	0.0582
300	30	0.7141	3000	85	0.0443
300	40	0.6357	3000	90	0.0338
300	50	0.5378	3000	95	0.0248
300	60	0.4237	6000	0	0.0835
300	70	0.2960	6000	20	0.0799
300	80	0.1597	6000	30	0.0744
300	85	0.0933	6000	40	0.0668
300	90	0.0378	6000	50	0.0576
300	95	0.0104	6000	60	0.0473
600	0	0.6410	6000	70	0.0367
600	20	0.6103	6000	80	0.0267
600	30	0.5667	6000	85	0.0221
600	40	0.5060	6000	90	0.0179
600	50	0.4298	6000	95	0.0142
600	60	0.3403	10000	0	0.0385
600	70	0.2402	10000	20	0.0367
600	80	0.1367	10000	30	0.0342
600	85	0.0878	10000	40	0.0308
600	90	0.0473	10000	50	0.0267
600	95	0.0213	10000	60	0.0222
1000	0	0.4946	10000	70	0.0176
1000	20	0.4723	10000	80	0.0133
1000	30	0.4394	10000	85	0.0113
1000	40	0.3931	10000	90	0.0094
1000	50	0.3348	10000	95	0.0077
1000	60	0.2660			

Table 39. Geometric Factor for Reflected Solar Radiation to a Hemisphere

γ = 60°, ϕ_c = 60°

Altitude n. m.	θ_s degrees	F	Altitude n. m.	θ_s degrees	F
100	0	1.0055	1000	70	0.1824
100	20	0.9472	1000	80	0.1067
100	30	0.8743	1000	85	0.0728
100	40	0.7747	1000	90	0.0450
100	50	0.6517	1000	95	0.0252
100	60	0.5088	3000	0	0.1990
100	70	0.3505	3000	20	0.1893
100	80	0.1804	3000	30	0.1757
100	85	0.0939	3000	40	0.1567
100	90	0.0184	3000	50	0.1333
100	95	0.0012	3000	60	0.1068
300	0	0.8132	3000	70	0.0793
300	20	0.7680	3000	80	0.0534
300	30	0.7099	3000	85	0.0419
300	40	0.6303	3000	90	0.0317
300	50	0.5315	3000	95	0.0232
300	60	0.4165	6000	0	0.0835
300	70	0.2881	6000	20	0.0794
300	80	0.1519	6000	30	0.0736
300	85	0.0864	6000	40	0.0658
300	90	0.0336	6000	50	0.0564
300	95	0.0090	6000	60	0.0461
600	0	0.6397	6000	70	0.0356
600	20	0.6059	6000	80	0.0257
600	30	0.5610	6000	85	0.0213
600	40	0.4991	6000	90	0.0172
600	50	0.4220	6000	95	0.0136
600	60	0.3317	10000	0	0.0385
600	70	0.2312	10000	20	0.0365
600	80	0.1284	10000	30	0.0339
600	85	0.0808	10000	40	0.0304
600	90	0.0426	10000	50	0.0263
600	95	0.0188	10000	60	0.0218
1000	0	0.4937	10000	70	0.0172
1000	20	0.4685	10000	80	0.0129
1000	30	0.4343	10000	85	0.0109
1000	40	0.3869	10000	90	0.0091
1000	50	0.3277	10000	95	0.0274
1000	60	0.2581			

Table 40. Geometric Factor for Reflected Solar Radiation to a Hemisphere

$\gamma = 60°$, $\phi_c = 90°$

Altitude n. m.	θ_s degrees	F	Altitude n. m.	θ_s degrees	F
100	0	1.0055	1000	70	0.1713
100	20	0.9448	1000	80	0.0969
100	30	0.8708	1000	85	0.0646
100	40	0.7702	1000	90	0.0390
100	50	0.6463	1000	95	0.0213
100	60	0.5027	3000	0	0.1987
100	70	0.3439	3000	20	0.1871
100	80	0.1736	3000	30	0.1727
100	85	0.0873	3000	40	0.1530
100	90	0.0149	3000	50	0.1290
100	95	0.0009	3000	60	0.1022
300	0	0.8132	3000	70	0.0748
300	20	0.7641	3000	80	0.0495
300	30	0.7042	3000	85	0.0385
300	40	0.6229	3000	90	0.0289
300	50	0.5227	3000	95	0.0209
300	60	0.4066	6000	0	0.0834
300	70	0.2774	6000	20	0.0786
300	80	0.1412	6000	30	0.0726
300	85	0.0770	6000	40	0.0645
300	90	0.0279	6000	50	0.0549
300	95	0.0070	6000	60	0.0445
600	0	0.6380	6000	70	0,0341
600	20	0.6001	6000	80	0.0244
600	30	0.5533	6000	85	0.0201
600	40	0.4897	6000	90	0.0161
600	50	0.4113	6000	95	0.0127
600	60	0.3201	10000	0	0.0384
600	70	0.2190	10000	20	0.0363
600	80	0.1171	10000	30	0.0335
600	85	0.0713	10000	40	0.0299
600	90	0.0361	10000	50	0.0257
600	95	0.0154	10000	60	0.0212
1000	0	0.4926	10000	70	0.0167
1000	20	0.4635	10000	80	0.0124
1000	30	0.4274	10000	85	0.0105
1000	40	0.3784	10000	90	0.0087
1000	50	0.3179	10000	95	0.0091
1000	60	0.2474			

Table 41. Geometric Factor for Reflected Solar Radiation to a Hemisphere

γ = 60°, ϕ_s = 120°

Altitude n. m.	θ_s degrees	F
100	0	1.0056
100	20	0.9428
100	30	0.8673
100	40	0.7657
100	50	0.6409
100	60	0.4967
100	70	0.3373
100	80	0.1667
100	85	0.0808
100	90	0.0114
100	95	0.0006
300	0	0.8132
300	20	0.7602
300	30	0.6985
300	40	0.6155
300	50	0.5139
300	60	0.3966
300	70	0.2667
300	80	0.1305
300	85	0.0675
300	90	0.0221
300	95	0.0051
600	0	0.6364
600	20	0.5943
600	30	0.5457
600	40	0.4808
600	50	0.4007
600	60	0.3084
600	70	0.2067
600	80	0.1057
600	85	0.0518
600	90	0.0297
600	95	0.0120
1000	0	0.4916
1000	20	0.4584
1000	30	0.4206
1000	40	0.3701
1000	50	0.3082
1000	60	0.2367
1000	70	0.1603
1000	80	0.0871
1000	85	0.0384
1000	90	0.0329
1000	95	0.0174
3000	0	0.1984
3000	20	0.1850
3000	30	0.1697
3000	40	0.1492
3000	50	0.1246
3000	60	0.0978
3000	70	0.0703
3000	80	0.0456
3000	85	0.0381
3000	90	0.0260
3000	95	0.0187
6000	0	0.0833
6000	20	0.0778
6000	30	0.0718
6000	40	0.0631
6000	50	0.0534
6000	60	0.0429
6000	70	0.0328
6000	80	0.0231
6000	85	0.0189
6000	90	0.0161
6000	95	0.0118
10000	0	0.0384
10000	20	0.0360
10000	30	0.0331
10000	40	0.0294
10000	50	0.0252
10000	60	0.0208
10000	70	0.0161
10000	80	0.0120
10000	85	0.0101
10000	90	0.0083
10000	95	0.0068

Table 42. Geometric Factor for Reflected Solar Radiation to a Hemisphere

$\gamma = 60°$ $\phi_c = 150°$

Altitude n. m.	θ_s degrees	F
100	0	1.0055
100	20	0.9407
100	30	0.8647
100	40	0.7624
100	50	0.6370
100	60	0.4922
100	70	0.3325
100	80	0.1617
100	85	0.0759
100	90	0.0088
100	95	0.0003
300	0	0.8132
300	20	0.7573
300	30	0.6943
300	40	0.6101
300	50	0.5075
300	60	0.3894
300	70	0.2589
300	80	0.1227
300	85	0.0606
300	90	0.0179
300	95	0.0037
600	0	0.6354
600	20	0.5902
600	30	0.5402
600	40	0.4738
600	50	0.3930
600	60	0.2999
600	70	0.1978
600	80	0.0974
600	85	0.0549
600	90	0.0250
600	95	0.0095
1000	0	0.4908
1000	20	0.4548
1000	30	0.4157
1000	40	0.3640
1000	50	0.3012
1000	60	0.2288
1000	70	0.1522
1000	80	0.0799
1000	85	0.0504
1000	90	0.0285
1000	95	0.0146
3000	0	0.1982
3000	20	0.1834
3000	30	0.1675
3000	40	0.1465
3000	50	0.1214
3000	60	0.0941
3000	70	0.0669
3000	80	0.0427
3000	85	0.0328
3000	90	0.0240
3000	95	0.0170
6000	0	0.0833
6000	20	0.0773
6000	30	0.0707
6000	40	0.0621
6000	50	0.0522
6000	60	0.0417
6000	70	0.0314
6000	80	0.0221
6000	85	0.0180
6000	90	0.0143
6000	95	0.0112
10000	0	0.0584
10000	20	0.0358
10000	30	0.0328
10000	40	0.0291
10000	50	0.0248
10000	60	0.0202
10000	70	0.0157
10000	80	0.0116
10000	85	0.0097
10000	90	0.0080
10000	95	0.0065

Table 43. Geometric Factor for Reflected Solar Radiation to a Hemisphere

γ - 60° ϕ_c - 180°

Altitude n. m.	θ_S degrees	F	Altitude n. m.	θ_S degrees	F
100	0	1.0055	1000	70	0.1492
100	20	0.9401	1000	80	0.0773
100	30	0.8638	1000	85	0.0482
100	40	0.7612	1000	90	0.0269
100	50	0.6356	1000	95	0.0136
100	60	0.4906	3000	0	0.1982
100	70	0.3307	3000	20	0.1829
100	80	0.1599	3000	30	0.1667
100	85	0.0742	3000	40	0.1455
100	90	0.0079	3000	50	0.1203
100	95	0.0093	3000	60	0.0929
300	0	0.8132	3000	70	0.0657
300	20	0.7563	3000	80	0.0417
300	30	0.6928	3000	85	0.0317
300	40	0.6082	3000	90	0.0232
300	50	0.5051	3000	95	0.0164
300	60	0.3867	6000	0	0.0833
300	70	0.2569	6000	20	0.0771
300	80	0.1199	6000	30	0.0704
300	85	0.0581	6000	40	0.0618
300	90	0.0164	6000	50	0.0518
300	95	0.0032	6000	60	0.0413
600	0	0.6352	6000	70	0.0310
600	20	0.5888	6000	80	0.0217
600	30	0.5383	6000	85	0.0177
600	40	0.4714	6000	90	0.0140
600	50	0.3902	6000	95	0.0109
600	60	0.2969	10000	0	0.0384
600	70	0.1946	10000	20	0.0357
600	80	0.0844	10000	30	0.0327
600	85	0.0523	10000	40	0.0289
600	90	0.0233	10000	50	0.0246
600	95	0.0086	10000	60	0.0201
1000	0	0.4907	10000	70	0.0156
1000	20	0.4536	10000	80	0.0115
1000	30	0.4140	10000	85	0.0096
1000	40	0.3618	10000	90	0.0079
1000	50	0.2986	10000	95	0.0064
1000	60	0.2260			

Table 44. Geometric Factor for Reflected Solar Radiation to a Hemisphere

$\gamma^* = 90°$, $\phi_c = 0°$

Altitude n. m.	θ_s degrees	F	Altitude n. m.	θ_s degrees	F
100	0	0.7672	1000	70	0.1471
100	20	0.7265	1000	80	0.0917
100	30	0.6725	1000	85	0.0563
100	40	0.5981	1000	90	0.0422
100	50	0.5055	1000	95	0.0246
100	60	0.3976	3000	0	0.1364
100	70	0.2776	3000	20	0.1328
100	80	0.1482	3000	30	0.1249
100	85	0.0819	3000	40	0.1132
100	90	0.0201	3000	50	0.0982
100	95	0.0015	3000	60	0.0808
300	0	0.6026	3000	70	0.0617
300	20	0.5753	3000	80	0.0429
300	30	0.5351	3000	85	0.0343
300	40	0.4786	3000	90	0.0264
300	50	0.4076	3000	95	0.0197
300	60	0.3242	6000	0	0.0563
300	70	0.2303	6000	20	0.0547
300	80	0.1293	6000	30	0.0514
300	85	0.0793	6000	40	0.0465
300	90	0.0348	6000	50	0.0405
300	95	0.0101	6000	60	0.0337
600	0	0.4651	6000	70	0.0265
600	20	0.4474	6000	80	0.0195
600	30	0.4178	6000	85	0.0163
600	40	0.3756	6000	90	0.0133
600	50	0.3220	6000	95	0.0106
600	60	0.2584	10000	0	0.0258
600	70	0.1867	10000	20	0.0249
600	80	0.1112	10000	30	0.0234
600	85	0.0741	10000	40	0.0212
600	90	0.0418	10000	50	0.0185
600	95	0.0196	10000	60	0.0155
1000	0	0.3519	10000	70	0.0124
1000	20	0.3404	10000	80	0.0094
1000	30	0.3189	10000	85	0.0080
1000	40	0.2878	10000	90	0.0067
1000	50	0.2479	10000	95	0.0055
1000	60	0.2002			

Table 45. Geometric Factor for Reflected Solar Radiation to a Hemisphere

$\gamma = 90°$, $\phi_c = 30°$

Altitude n. m.	θ_s degrees	F
100	0	0.7672
100	20	0.7257
100	30	0.6714
100	40	0.5967
100	50	0.5039
100	60	0.3957
100	70	0.2755
100	80	0.1461
100	85	0.0799
100	90	0.0191
100	95	0.0014
300	0	0.6026
300	20	0.5741
300	30	0.5333
300	40	0.4763
300	50	0.4049
300	60	0.3211
300	70	0.2270
300	80	0.1260
300	85	0.0764
300	90	0.0330
300	95	0.0095
600	0	0.4644
600	20	0.4453
600	30	0.4153
600	40	0.3726
600	50	0.3186
600	60	0.2547
600	70	0.1829
600	80	0.1076
600	85	0.0712
600	90	0.0398
600	95	0.0185
1000	0	0.3514
1000	20	0.3387
1000	30	0.3187
1000	40	0.2851
1000	50	0.2448
1000	60	0.1969
1000	70	(1437
1000	80	0.0886
1000	85	0.0628
1000	90	0.0403
1000	95	0.0234
3000	0	0.1383
3000	20	0.1322
3000	30	0.1240
3000	40	0.1120
3000	50	0.0968
3000	60	0.0792
3000	70	0.0602
3000	80	0.0417
3000	85	0.0332
3000	90	0.0256
3000	95	0.0189
6000	0	0.0563
6000	20	0.0545
6000	30	0.0510
6000	40	0.0461
6000	50	0.0400
6000	60	0.0332
6000	70	0,0260
6000	80	0.0191
6000	85	0.0159
6000	90	0.0130
6000	95	0.0103
10000	0	0.0258
10000	20	0.0248
10000	30	0.0232
10000	40	0.0210
10000	50	0.0183
10000	60	0.0153
10000	70	0.0123
10000	80	0.0093
10000	85	0.0079
10000	90	0.0066
10000	95	0.0054

Table 46. Geometric Factor for Reflected Solar Radiation to a Hemisphere

γ = 90°, ϕ_c = 60°

Altitude n. m.	Θ_s degrees	F	Altitude n. m.	Θ_s degrees	F
100	0	0.7672	1000	70	0.1343
100	20	0.7237	1000	80	0 0803
100	30	0.6685	1000	85	0.0558
100	40	0.5929	1000	90	0.0352
100	50	0.4993	1000	95	0.0201
100	60	0.3906	3000	0	0.1360
100	70	0.2700	3000	20	0.1303
100	80	0.1403	3000	30	0.1214
100	85	0.0744	3000	40	0.1088
100	90	0.0161	3000	50	0.0931
100	95	0.0012	3000	60	0.0752
300	0	0.6026	3000	70	0.0564
300	20	0.5708	3000	80	0.0384
300	30	0.5285	3000	85	0.0303
300	40	0.4701	3000	90	0.0232
300	50	0.3975	3000	95	0.0170
300	60	0.3127	6000	0	0.0562
300	70	0.2179	6000	20	0.0538
300	80	0.1170	6000	30	0.0501
300	85	0.0684	6000	40	0.0450
300	90	0.0281	6000	50	0.0387
300	95	0.0079	6000	60	0.0318
600	0	0.4628	6000	70	0,0247
600	20	0.4403	6000	80	0.0180
600	30	0.4086	6000	85	0.0149
600	40	0.3646	6000	90	0.0121
600	50	0.3095	6000	95	0.0096
600	60	0.2448	10000	0	0.0258
600	70	0.1725	10000	20	0.0246
600	80	0.0980	10000	30	0.0229
600	85	0.0631	10000	40	0.0206
600	90	0.0343	10000	50	0.0179
600	95	0.0156	10000	60	0.0149
1000	0	0.3504	10000	70	0.0118
1000	20	0.3343	10000	80	0.0089
1000	30	0.3109	10000	85	0.0075
1000	40	0.2779	10000	90	0.0063
1000	50	0.2366	10000	95	0.0051
1000	60	0.1878			

Table 47. Geometric Factor for Reflected Solar Radiation to a Hemisphere

$\gamma = 90°$, $\phi_c = 90°$

Altitude n. m.	θ_s degrees	F	Altitude n. m.	θ_s degrees	F
100	0	0.7672	1000	70	0.1216
100	20	0.7209	1000	80	0.0690
100	30	0.6644	1000	85	0.0463
100	40	0.5877	1000	90	0.0282
100	50	0.4931	1000	95	0.0156
100	60	0.3836	3000	0	0.1357
100	70	0.2624	3000	20	0.1278
100	80	0.1324	3000	30	0.1180
100	85	0.0663	3000	40	0.1045
100	90	0.0121	3000	50	0.0881
100	95	0.0008	3000	60	0.0698
300	0	0.6026	3000	70	0.0512
300	20	0.5662	3000	80	0.0339
300	30	0.5219	3000	85	0.0264
300	40	0.4616	3000	90	0.0199
300	50	0.3873	3000	95	0.0144
300	60	0.3013	6000	0	0.0561
300	70	0.2056	6000	20	0.0529
300	80	0.1047	6000	30	0.0489
300	85	0.0575	6000	40	0.0434
300	90	0.0215	6000	50	0.0370
300	95	0.0057	6000	60	0.0300
600	0	0.4609	6000	70	0.0230
600	20	0.4335	6000	80	0.0165
600	30	0.3997	6000	85	0.0135
600	40	0.3538	6000	90	0.0109
600	50	0.2972	6000	95	0.0086
600	60	0.2313	10000	0	0.0257
600	70	0.1584	10000	20	0.0243
600	80	0.0850	10000	30	0.0224
600	85	0.0522	10000	40	0.0200
600	90	0.0269	10000	50	0.0172
600	95	0.0117	10000	60	0.0142
1000	0	0.3491	10000	70	0.0112
1000	20	0.3285	10000	80	0.0083
1000	30	0.3029	10000	85	0.0070
1000	40	0.2682	10000	90	0.0058
1000	50	0.2253	10000	95	0.0047
1000	60	0.1754			

Table 48. Geometric Factor for Reflected Solar Radiation to a Hemisphere,

$\gamma = 90°$, $\phi_c = 120°$

Altitude n. m.	θ_s degrees	F	Altitude n. m.	θ_s degrees	F
100	0	0.7672	1000	70	0.1088
100	20	0.7182	1000	80	0.0577
100	30	0.6604	1000	85	0.0369
100	40	0.5825	1000	90	0.0212
100	50	0.4869	1000	95	0.0111
100	60	0.3766	3000	0	0.1354
100	70	0.2548	3000	20	0.1253
100	80	0.1245	3000	30	0.1145
100	85	0.0592	3000	40	0.1002
100	90	0.0080	3000	50	0.0831
100	95	0.0004	3000	60	0.0645
300	0	0.6026	3000	70	0.0459
300	20	0.5617	3000	80	0.0294
300	30	0.5152	3000	85	0.0225
300	40	0.4531	3000	90	0.0166
300	50	0.3772	3000	95	0.0118
300	60	0.2898	6000	0	0.0561
300	70	0.1932	6000	20	0.0520
300	80	0.0924	6000	30	0.0476
300	85	0.0466	6000	40	0.0419
300	90	0.0149	6000	50	0.0352
300	95	0.0035	6000	60	0.0281
600	0	0.4591	6000	70	0.0212
600	20	0.4269	6000	80	0.0149
600	30	0.3909	6000	85	0.0121
600	40	0.3431	6000	90	0.0097
600	50	0.2849	6000	95	0.0076
600	60	0.2178	10000	0	0.0257
600	70	0.1443	10000	20	0.0239
600	80	0.0719	10000	30	0.0220
600	85	0.0412	10000	40	0.0195
600	90	0.0195	10000	50	0.0166
600	95	0.0078	10000	60	0.0135
1000	0	0.3479	10000	70	0.0105
1000	20	0.3227	10000	80	0.0078
1000	30	0.2951	10000	85	0.0065
1000	40	0.2585	10000	90	0.0054
1000	50	0.2141	10000	95	0.0044
1000	60	0.1630			

Table 49. Geometric Factor for Reflected Solar Radiation to a Hemisphere

$\gamma = 90°$, $\phi_c = 150°$

Altitude n. m.	θ_s degrees	F
100	0	0.7872
100	20	0.7182
100	30	0.6574
100	40	0.5787
100	50	0.4824
100	60	0.3714
100	70	0.2492
100	80	0.1188
100	85	0.0536
100	90	0.0050
100	95	0.0001
300	0	0.6026
300	20	0.5584
300	30	0.5104
300	40	0.4469
300	50	0.3698
300	60	0.2814
300	70	0.1842
300	80	0.0834
300	85	0.0387
300	90	0.0101
300	95	0.0019
600	0	0.4579
600	20	0.4221
600	30	0.3846
600	40	0.3354
600	50	0.2760
600	60	0.2080
600	70	0.1339
600	80	0.0623
600	85	0.0332
600	90	0.0140
600	95	0.0050
1000	0	0.3471
1000	20	0.3185
1000	30	0.2894
1000	40	0.2515
1000	50	0.2060
1000	60	0.1540

Altitude n. m.	θ_s degrees	F
1000	70	0.0935
1000	80	0.0426
1000	85	0.0299
1000	90	0.0161
1000	95	0.0072
3000	0	0.1352
3000	20	0.1235
3000	30	0.1120
3000	40	0.0970
3000	50	0.0794
3000	60	0.0605
3000	70	0.0421
3000	80	0.0261
3000	85	0.0196
3000	90	0.0142
3000	95	0.0099
6000	0	0.0560
6000	20	0.0514
6000	30	0.0467
6000	40	0.0407
6000	50	0.0339
6000	60	0.0268
6000	70	0.0199
6000	80	0.0138
6000	85	0.0111
6000	90	0.0088
6000	95	0.0068
10000	0	0.0257
10000	20	0.0237
10000	30	0.0216
10000	40	0.0190
10000	50	0.0161
10000	60	0.0131
10000	70	0.0101
10000	80	0.0074
10000	85	0.0061
10000	90	0.0050
10000	95	0.0041

Table 50. Geometric Factor for Reflected Solar Radiation to a Hemisphere

$\gamma^* = 90°$, $\phi_c = 180°$

Altitude n. m.	θ_s degrees	F	Altitude n. m.	θ_s degrees	F
100	0	0.7672	1000	70	0.0961
100	20	0.7154	1000	80	0.0464
100	30	0.6563	1000	85	0.0274
100	40	0.5773	1000	90	0.0143
100	50	0.4807	1000	95	0.0067
100	60	0.3696	3000	0	0.1351
100	70	0.2472	3000	20	0.1229
100	80	0.1167	3000	30	0.1111
100	85	0.0516	3000	40	0.0958
100	90	0.0040	3000	50	0.0781
100	95	0.0001	3000	60	0.0591
300	0	0.6026	3000	70	0.0407
300	20	0.5572	3000	80	0.0249
300	30	0.5086	3000	85	0.0186
300	40	0.4446	3000	90	0.0133
300	50	0.3670	3000	95	0.0092
300	60	0.1809	6000	0	0.0560
300	70	0.2784	6000	20	0.0512
300	80	0.0801	6000	30	0.0464
300	85	0.0358	6000	40	0.0403
300	90	0.0083	6000	50	0.0334
300	95	0.0013	6000	60	0.0263
600	0	0.4576	6000	70	0,0194
600	20	0.4208	6000	80	0.0134
600	30	0.3824	6000	85	0.0108
600	40	0.3327	6000	90	0.0085
600	50	0.2728	6000	95	0.0065
600	60	0.2045	10000	0	0.0257
600	70	0.1302	10000	20	0.0236
600	80	0.0588	10000	30	0.0215
600	85	0.0303	10000	40	0.0189
600	90	0.0120	10000	50	0.0159
600	95	0.0039	10000	60	0.0129
1000	0	0.3469	10000	70	0.0099
1000	20	0.2874	10000	80	0.0072
1000	30	0.3171	10000	85	0.0060
1000	40	0.2490	10000	90	0.0049
1000	50	0.2030	10000	95	0.0040
1000	60	0,1507			

Table 51. Geometric Factor for Reflected Solar Radiation to a Hemisphere

$\gamma^* = 120°$ $\phi_c = 0°$

Altitude n. m.	θ_s degrees	F
100	0	0.5289
100	20	0.5018
100	30	0.4651
100	40	0.4142
100	50	0.3507
100	60	0.2766
100	70	0.1940
100	80	0.1050
100	85	0.0593
100	90	0.0163
100	95	0.0013
300	0	0.3920
300	20	0.3762
300	30	0.3510
300	40	0.3150
300	50	0.2695
300	60	0.2158
300	70	0.1551
300	80	0.0896
300	85	0.0570
300	90	0.0267
300	95	0.0032
600	0	0.2878
600	20	0.2790
600	30	0.2619
600	40	0.2369
600	50	0.2046
600	60	0.1660
600	70	0.1224
600	80	0.0756
600	85	0.0521
600	90	0.0306
600	95	0.0148
1000	0	0.2081
1000	20	0.2038
1000	30	0.1923
1000	40	0.1750
1000	50	0.1523
1000	60	0.1250
1000	70	0.0940
1000	80	0.0608
1000	85	0.0445
1000	90	0.0296
1000	95	0.0177
3000	0	0.0734
3000	20	0.0729
3000	30	0.0693
3000	40	0.0636
3000	50	0.0560
3000	60	0.0468
3000	70	0.0366
3000	80	0.0252
3000	85	0.0212
3000	90	0.0166
3000	95	0.0062
6000	0	0.0291
6000	20	0.0288
6000	30	0.0273
6000	40	0.0251
6000	50	0.0221
6000	60	0.0187
6000	70	0.0149
6000	80	0.0112
6000	85	0.0094
6000	90	0.0077
6000	95	0.0062
10000	0	0.0131
10000	20	0.0129
10000	30	0.0122
10000	40	0.0111
10000	50	0.0098
10000	60	0.0083
10000	70	0.0067
10000	80	0.0052
10000	85	0.0044
10000	90	0.0037
10000	95	0.0031

Table 52. Geometric Factor for Reflected Solar Radiation to a Hemisphere

$\gamma = 120°$ $\phi_c = 30°$

Altitude n. m.	θ_s degrees	F	Altitude n. m.	θ_s degrees	F
100	0	0.5289	1000	70	0.0910
100	20	0.5012	1000	80	0.0582
100	30	0.4641	1000	85	0.0423
100	40	0.4130	1000	90	0.0279
100	50	0.3493	1000	95	0.0166
100	60	0.2750	3000	0	0.0733
100	70	0.1923	3000	20	0.0723
100	80	0.1031	3000	30	0.0685
100	85	0.0576	3000	40	0.0626
100	90	0.0153	3000	50	0.0548
100	95	0.0012	3000	60	0.0456
300	0	0.3920	3000	70	0.0354
300	20	0.3752	3000	80	0.0251
300	30	0.3494	3000	85	0.0203
300	40	0.3131	3000	90	0.0158
300	50	0.2672	3000	95	0.0119
300	60	0.2132	6000	0	0.0291
300	70	0.1523	6000	20	0.0286
300	80	0.0867	6000	30	0.0270
300	85	0.0544	6000	40	0.0247
300	90	0.0251	6000	50	0.0217
300	95	0.0077	6000	60	0.0182
600	0	0.2869	6000	70	0,0145
600	20	0.2773	6000	80	0.0108
600	30	0.2597	6000	85	0.0091
600	40	0.2342	6000	90	0.0075
600	50	0.2016	6000	95	0.0060
600	60	0.1628	10000	0	0.0131
600	70	0.1190	10000	20	0.0128
600	80	0.0725	10000	30	0.0120
600	85	0.0495	10000	40	0.0110
600	90	0.0288	10000	50	0.0097
600	95	0.0139	10000	60	0.0082
1000	0	0.2077	10000	70	0.0066
1000	20	0.2024	10000	80	0.0051
1000	30	0.1904	10000	85	0.0043
1000	40	0.1727	10000	90	0.0036
1000	50	0.1497	10000	95	0.0030
1000	60	0.1221			

Table 53. Geometric Factor for Reflected Solar Radiation to a Hemisphere

γ - 120°, ϕ_c - 60°

Altitude n. m.	θ_s degrees	F
100	0	0.5289
100	20	0.4994
100	30	0.4616
100	40	0.4097
100	50	0.3453
100	60	0.2705
100	70	0.1875
100	80	0.0981
100	85	0.0528
100	90	0.0127
100	95	0.0010
300	0	0.3920
300	20	0.3723
300	30	0.3452
300	40	0.3077
300	50	0.2607
300	60	0.2059
300	70	0.1444
300	80	0.0789
300	85	0.0475
300	90	0.0209
300	95	0.0063
600	0	0.2856
600	20	0.2729
600	30	0.2540
600	40	0.2273
600	50	0.1938
600	60	0.1542
600	70	0.1101
600	80	0.0642
600	85	0.0425
600	90	0.0241
600	95	0.0115
1000	0	0.2068
1000	20	0.1986
1000	30	0.1853
1000	40	0.1665
1000	50	0.1425
1000	60	0.1142
1000	70	0.0829
1000	80	0.0510
1000	85	0.0363
1000	90	0.0235
1000	95	0.0138
3000	0	0.0730
3000	20	0.0707
3000	30	0.0662
3000	40	0.0598
3000	50	0.0516
3000	60	0.0422
3000	70	0.0321
3000	80	0.0223
3000	85	0.0178
3000	90	0.0137
3000	95	0.0102
6000	0	0.0290
6000	20	0.0280
6000	30	0.0263
6000	40	0.0237
6000	50	0.0206
6000	60	0.0171
6000	70	0,0134
6000	80	0.0099
6000	85	0.0082
6000	90	0.0067
6000	95	0.0053
10000	0	0.0131
10000	20	0.0126
10000	30	0.0118
10000	40	0.0106
10000	50	0.0093
10000	60	0.0078
10000	70	0.0062
10000	80	0.0047
10000	85	0.0040
10000	90	0.0033
10000	95	0.0027

Table 54. Geometric Factor for Reflected Solar Radiation to a Hemisphere

γ = 120° $\quad\quad$ ϕ_c = 90°

Altitude n. m.	θ_s degrees	F	Altitude n. m.	θ_s degrees	F
100	0	0.5289	1000	70	0.0718
100	20	0.4970	1000	80	0.0412
100	30	0.4581	1000	85	0.0281
100	40	0.4052	1000	90	0.0175
100	50	0.3400	1000	95	0.0099
100	60	0.2644	3000	0	0.0727
100	70	0.1809	3000	20	0.0685
100	80	0.0913	3000	30	0.0632
100	85	0.0462	3000	40	0.0560
100	90	0.0092	3000	50	0.0472
100	95	0.0007	3000	60	0.0375
300	0	0.3920	3000	70	0.0275
300	20	0.3684	3000	80	0.0184
300	30	0.3395	3000	85	0.0144
300	40	0.3003	3000	90	0.0109
300	50	0.2520	3000	95	0.0045
300	60	0.1960	6000	0	0.0289
300	70	0.1337	6000	20	0.0273
300	80	0.0682	6000	30	0.0252
300	85	0.0381	6000	40	0.0224
300	90	0.0152	6000	50	0.0191
300	95	0.0043	6000	60	0.0155
600	0	0.2839	6000	70	0.0119
600	20	0.2671	6000	80	0.0085
600	30	0.2463	6000	85	0.0070
600	40	0.2180	6000	90	0.0057
600	50	0.1831	6000	95	0.0045
600	60	0.1426	10000	0	0.0130
600	70	0.0978	10000	20	0.0123
600	80	0.0529	10000	30	0.0114
600	85	0.0330	10000	40	0.0101
600	90	0.0176	10000	50	0.0087
600	95	0.0081	10000	60	0.0072
1000	0	0.2056	10000	70	0.0057
1000	20	0.1935	10000	80	0.0042
1000	30	0.1785	10000	85	0.0036
1000	40	0.1580	10000	90	0.0029
1000	50	0.1328	10000	95	0.0024
1000	60	0.1035			

Table 55. Geometric Factor for Reflected Solar Radiation to a Hemisphere

$\gamma = 120°$, $\phi_c = 120°$

Altitude n. m.	θ_s degrees	F	Altitude n. m.	θ_s degrees	F
100	0	0.5289	1000	70	0.0608
100	20	0.4946	1000	80	0.0314
100	30	0.4546	1000	85	0.0198
100	40	0.4007	1000	90	0.0114
100	50	0.3346	1000	95	0.0060
100	60	0.2584	3000	0	0.0725
100	70	0.1743	3000	20	0.0664
100	80	0.0845	3000	30	0.0602
100	85	0.0396	3000	40	0.0523
100	90	0.0057	3000	50	0.0429
100	95	0.0004	3000	60	0.0328
300	0	0.3920	3000	70	0.0230
300	20	0.3645	3000	80	0.0145
300	30	0.3338	3000	85	0.0110
300	40	0.2929	3000	90	0.0080
300	50	0.2432	3000	95	0.0057
300	60	0.1861	6000	0	0.0288
300	70	0.1230	6000	20	0.0265
300	80	0.0576	6000	30	0.0241
300	85	0.0287	6000	40	0.0210
300	90	0.0095	6000	50	0.0175
300	95	0.0024	6000	60	0.0139
600	0	0.2823	6000	70	0.0103
600	20	0.2613	6000	80	0.0072
600	30	0.2387	6000	85	0.0058
600	40	0.2088	6000	90	0.0046
600	50	0.1725	6000	95	0.0036
600	60	0.1309	10000	0	0.0130
600	70	0.0856	10000	20	0.0120
600	80	0.0416	10000	30	0.0110
600	85	0.0235	10000	40	0.0096
600	90	0.0112	10000	50	0.0082
600	95	0.0047	10000	60	0.0066
1000	0	0.2046	10000	70	0.0051
1000	20	0.1885	10000	80	0.0037
1000	30	0.1717	10000	85	0.0031
1000	40	0.1497	10000	90	0.0026
1000	50	0.1231	10000	95	0.0021
1000	60	0.0927			

Table 56. Geometric Factor for Reflected Solar Radiation to a Hemisphere

γ = 120°, ϕ_c = 150°

Altitude n. m.	θ_s degrees	F	Altitude n. m.	θ_s degrees	F
100	0	0.5289	1000	70	0.0527
100	20	0.4929	1000	80	0.0243
100	30	0.4520	1000	85	0.0139
100	40	0.3974	1000	90	0.0070
100	50	0.3307	1000	95	0.0032
100	60	0.2539	3000	0	0.0723
100	70	0.1695	3000	20	0.0648
100	80	0.0794	3000	30	0.0581
100	85	0.0348	3000	40	0.0495
100	90	0.0032	3000	50	0.0397
100	95	0.0001	3000	60	0.0294
300	0	0.3920	3000	70	0.0197
300	20	0.3616	3000	80	0.0116
300	30	0.3296	3000	85	0.0085
300	40	0.2875	3000	90	0.0060
300	50	0.2368	3000	95	0.0041
300	60	0.1788	6000	0	0.0288
300	70	0.1152	6000	20	0.0258
300	80	0.0498	6000	30	0.0233
300	85	0.0218	6000	40	0.0200
300	90	0.0053	6000	50	0.0164
300	95	0.0010	6000	60	0.0127
600	0	0.2813	6000	70	0,0092
600	20	0.2572	6000	80	0.0062
600	30	0.2332	6000	85	0.0049
600	40	0.2020	6000	90	0.0038
600	50	0.1648	6000	95	0.0029
600	60	0.1224	10000	0	0.0130
600	70	0.0768	10000	20	0.0118
600	80	0.0333	10000	30	0.0107
600	85	0.0186	10000	40	0.0093
600	90	0.0065	10000	50	0.0078
600	95	0.0022	10000	60	0.0062
1000	0	0.2039	10000	70	0.0047
1000	20	0.1849	10000	80	0.0034
1000	30	0.1668	10000	85	0.0028
1000	40	0.1438	10000	90	0.0023
1000	50	0.1160	10000	95	0.0018
1000	60	0.0849			

Table 57. Geometric Factor for Reflected Solar Radiation to a Hemisphere

$\gamma = 120°$, $\phi_c = 180°$

Altitude n. m.	θ_s degrees	F
100	0	0.5289
100	20	0.4922
100	30	0.4611
100	40	0.3962
100	50	0.3292
100	60	0.2523
100	70	0.1677
100	80	0.0776
100	85	0.0330
100	90	0.0022
100	95	0.0000
300	0	0.3920
300	20	0.3605
300	30	0.3280
300	40	0.2856
300	50	0.2344
300	60	0.1761
300	70	0.1123
300	80	0.0469
300	85	0.0192
300	90	0.0037
300	95	0.0005
600	0	0.2811
600	20	0.2558
600	30	0.2313
600	40	0.1997
600	50	0.1620
600	60	0.1194
600	70	0.0734
600	80	0.0302
600	85	0.0141
600	90	0.0048
600	95	0.0013
1000	0	0.2037
1000	20	0.1837
1000	30	0.1650
1000	40	0.1414
1000	50	0.1135
1000	60	0.0821
1000	70	0.0497
1000	80	0.0216
1000	85	0.0117
1000	90	0.0054
1000	95	0.0022
3000	0	0.0723
3000	20	0.0643
3000	30	0.0573
3000	40	0.0485
3000	50	0.0386
3000	60	0.0282
3000	70	0.0185
3000	80	0.0106
3000	85	0.0076
3000	90	0.0052
3000	95	0.0035
6000	0	0.0288
6000	20	0.0257
6000	30	0.0230
6000	40	0.0197
6000	50	0.0160
6000	60	0.0123
6000	70	0.0088
6000	80	0.0058
6000	85	0.0046
6000	90	0.0036
6000	95	0.0027
10000	0	0.0130
10000	20	0.0117
10000	30	0.0106
10000	40	0.0092
10000	50	0.0076
10000	60	0.0060
10000	70	0.0046
10000	80	0.0032
10000	85	0.0027
10000	90	0.0022
10000	95	0.0017

Table 58. Geometric Factor for Reflected Solar Radiation to a Hemisphere

$\gamma = 150°$, $\phi_c = 0°$

Altitude n. m.	θ_s degrees	F	Altitude n. m.	θ_s degrees	F
100	0	0.3545	1000	70	0.0482
100	20	0.3359	1000	80	0.0322
100	30	0.3111	1000	85	0.0242
100	40	0.2768	1000	90	0.0166
100	50	0.2341	1000	95	0.0102
100	60	0.1842	3000	0	0.0270
100	70	0.1288	3000	20	0.0276
100	80	0.0691	3000	30	0.0267
100	85	0.0387	3000	40	0.0249
100	90	0.0112	3000	50	0.0224
100	95	0.0010	3000	60	0.0192
300	0	0.2379	3000	70	0.0155
300	20	0.2281	3000	80	0.0115
300	30	0.2126	3000	85	0.0095
300	40	0.1907	3000	90	0.0076
300	50	0.1630	3000	95	0.0058
300	60	0.1304	6000	0	0.0091
300	70	0.0935	6000	20	0.0094
300	80	0.0538	6000	30	0.0091
300	85	0.0348	6000	40	0.0085
300	90	0.0172	6000	50	0.0077
300	95	0.0056	6000	60	0.0067
600	0	0.1566	6000	70	0.0055
600	20	0.1522	6000	80	0.0042
600	30	0.1431	6000	85	0.0036
600	40	0.1295	6000	90	0.0030
600	50	0.1121	6000	95	0.0025
600	60	0.0912	10000	0	0.0038
600	70	0.0677	10000	20	0.0038
600	80	0.0425	10000	30	0.0037
600	85	0.0300	10000	40	0.0035
600	90	0.0183	10000	50	0.0031
600	95	0.0093	10000	60	0.0027
1000	0	0.1022	10000	70	0.0022
1000	20	0.1008	10000	80	0.0018
1000	30	0.0955	10000	85	0.0015
1000	40	0.0872	10000	90	0.0013
1000	50	0.0764	10000	95	0.0011
1000	60	0.0632			

Table 59. Geometric Factor for Reflected Solar Radiation to a Hemisphere

$\gamma^* = 150°$, $\phi_c = 30°$

Altitude n. m.	θ_s degrees	F	Altitude n. m.	θ_s degrees	F
100	0	0.3545	1000	70	0.0466
100	20	0.3355	1000	80	0.0306
100	30	0.3105	1000	85	0.0229
100	40	0.2761	1000	90	0.0157
100	50	0.2332	1000	95	0.0096
100	60	0.1833	3000	0	0.0270
100	70	0.1278	3000	20	0.0273
100	80	0.0680	3000	30	0.0262
100	85	0.0377	3000	40	0.0243
100	90	0.0107	3000	50	0.0217
100	95	0.0009	3000	60	0.0185
300	0	0.2379	3000	70	0.0148
300	20	0.2274	3000	80	0.0109
300	30	0.2117	3000	85	0.0090
300	40	0.1896	3000	90	0.0071
300	50	0.1617	3000	95	0.0055
300	60	0.1288	6000	0	0.0091
300	70	0.0918	6000	20	0.0092
300	80	0.0522	6000	30	0.0089
300	85	0.0333	6000	40	0.0083
300	90	0.0163	6000	50	0.0075
300	95	0.0053	6000	60	0.0064
600	0	0.1562	6000	70	0.0053
600	20	0.1512	6000	80	0.0040
600	30	0.1418	6000	85	0.0034
600	40	0.1280	6000	90	0.0029
600	50	0.1104	6000	95	0.0023
600	60	0.0893	10000	0	0.0038
600	70	0.0657	10000	20	0.0038
600	80	0.0407	10000	30	0.0036
600	85	0.0285	10000	40	0.0034
600	90	0.0173	10000	50	0.0030
600	95	0.0088	10000	60	0.0026
1000	0	0.1019	10000	70	0.0022
1000	20	0.0999	10000	80	0.0017
1000	30	0.0943	10000	85	0.0015
1000	40	0.0859	10000	90	0.0012
1000	50	0.0748	10000	95	0.0010
1000	60	0.0615			

Table 60. Geometric Factor for Reflected Solar Radiation to a Hemisphere

δ = 150, ϕ_c = 60°

Altitude n. m.	θ_s deg ees	F	Altitude n. m.	θ_s degrees	F
100	0	0.3545	1000	70	0.0418
100	20	0.3345	1000	80	0.0265
100	30	0.3090	1000	85	0.0194
100	40	0.2742	1000	90	0.0131
100	50	0.2310	1000	95	0.0080
100	60	0.1807	3000	0	0.0268
100	70	0.1250	3000	20	0.0264
100	80	0.0651	3000	30	0.0249
100	85	0.0349	3000	40	0.0227
100	90	0.0092	3000	50	0.0199
100	95	0.0008	3000	60	0.0165
300	0	0.2379	3000	70	0.0129
300	20	0.2258	3000	80	0.0093
300	30	0.2093	3000	85	0.0075
300	40	0.1865	3000	90	0.0059
300	50	0.1580	3000	95	0.0045
300	60	0.1246	6000	0	0.0090
300	70	0.0873	6000	20	0.0089
300	80	0.0477	6000	30	0.0085
300	85	0.0293	6000	40	0.0077
300	90	0.0139	6000	50	0.0068
300	95	0.0045	6000	60	0.0058
600	0	0.1554	6000	70	0.0046
600	20	0.1487	6000	80	0.0035
600	30	0.1385	6000	85	0.0029
600	40	0.1240	6000	90	0.0024
600	50	0.1058	6000	95	0.0020
600	60	0.0844	10000	0	0.0037
600	70	0.0606	10000	20	0.0037
600	80	0.0359	10000	30	0.0035
600	85	0.0245	10000	40	0.0032
600	90	0.0146	10000	50	0.0028
600	95	0.0073	10000	60	0.0024
1000	0	0.1014	10000	70	0.0019
1000	20	0.0977	10000	80	0.0015
1000	30	0.0914	10000	85	0.0013
1000	40	0.0823	10000	90	0.0011
1000	50	0.0707	10000	95	0.0009
1000	60	0.0570			

Table 61. Geometric Factor for Reflected Solar Radiation to a Hemisphere

$\gamma = 150°$, $\phi_c = 90°$

Altitude n. m.	θ_3 degrees	F
100	0	0.3545
100	20	0.3331
100	30	0.3070
100	40	0.2716
100	50	0.2279
100	60	0.1772
100	70	0.1212
100	80	0.0612
100	85	0.0311
100	90	0.0072
100	95	0.0006
300	0	0.2379
300	20	0.2235
300	30	0.2060
300	40	0.1822
300	50	0.1529
300	60	0.1189
300	70	0.0811
300	80	0.0415
300	85	0.0239
300	90	0.0106
300	95	0.0034
600	0	0.1545
600	20	0.1453
600	30	0.1340
600	40	0.1187
600	50	0.0997
600	60	0.0776
600	70	0.0535
600	80	0.0294
600	85	0.0190
600	90	0.0109
600	95	0.0054
1000	0	0.1007
1000	20	0.0948
1000	30	0.0875
1000	40	0.0774
1000	50	0.0651
1000	60	0.0508
1000	70	0.0354
1000	80	0.0208
1000	85	0.0147
1000	90	0.0096
1000	95	0.0058
3000	0	0.0267
3000	20	0.0251
3000	30	0.0232
3000	40	0.0206
3000	50	0.0138
3000	60	0.0173
3000	70	0.0103
3000	80	0.0079
3000	85	0.0056
3000	90	0.0043
3000	95	0.0032
6000	0	0.0090
6000	20	0.0085
6000	30	0.0078
6000	40	0.0070
6000	50	0.0059
6000	60	0.0048
6000	70	0.0037
6000	80	0.0027
6000	85	0.0022
6000	90	0.0018
6000	95	0.0014
10000	0	0.0037
10000	20	0.0035
10000	30	0.0032
10000	40	0.0029
10000	50	0.0025
10000	60	0.0021
10000	70	0.0015
10000	80	0.0012
10000	85	0.0010
10000	90	0.0008
10000	95	0.0007

Table 62. Geometric Factor for Reflected Solar Radiation to a Hemisphere

$\gamma = 150°$, $\phi_c = 120°$

Altitude n. m.	θ_s degrees	F	Altitude n. m.	θ_s degrees	F
100	0	0.3545	1000	70	0.0290
100	20	0.3317	1000	80	0.0152
100	30	0.3050	1000	85	0.0099
100	40	0.2690	1000	90	0.0061
100	50	0.2248	1000	95	0.0035
100	60	0.1737	3000	0	0.0265
100	70	0.1174	3000	20	0.0239
100	80	0.0572	3000	30	0.0215
100	85	0.0273	3000	40	0.0184
100	90	0.0052	3000	50	0.0148
100	95	0.0004	3000	60	0.0111
300	0	0.2379	3000	70	0.0076
300	20	0.2213	3000	80	0.0048
300	30	0.2027	3000	85	0.0036
300	40	0.1780	3000	90	0.0027
300	50	0.1478	3000	95	0.0019
300	60	0.1132	6000	0	0.0089
300	70	0.0740	6000	20	0.0080
300	80	0.0334	6000	30	0.0072
300	85	0.0184	6000	40	0.0062
300	90	0.0073	6000	50	0.0050
300	95	0.0022	6000	60	0.0039
600	0	0.1536	6000	70	0.0028
600	20	0.1420	6000	80	0.0019
600	30	0.1296	6000	85	0.0016
600	40	0.1133	6000	90	0.0012
600	50	0.0935	6000	95	0.0009
600	60	0.0709	10000	0	0.0037
600	70	0.0464	10000	20	0.0034
600	80	0.0229	10000	30	0.0030
600	85	0.0136	10000	40	0.0026
600	90	0.0072	10000	50	0.0022
600	95	0.0034	10000	60	0.0017
1000	0	0.1001	10000	70	0.0013
1000	20	0.0919	10000	80	0.0009
1000	30	0.0835	10000	85	0.0008
1000	40	0.0726	10000	90	0.0006
1000	50	0.0595	10000	95	0.0005
1000	60	0.0446			

Table 63. Geometric Factor for Reflected Solar Radiation to a Hemisphere

γ = 150°

Altitude n. m.	θ_s degrees	F
100	0	0.3545
100	20	0.3307
100	30	0.3035
100	40	0.2671
100	50	0.2225
100	60	0.1712
100	70	0.1146
100	80	0.0543
100	85	0.0245
100	90	0.0037
100	95	0.0003
300	0	0.2379
300	20	0.2196
300	30	0.2003
300	40	0.1748
300	50	0.1441
300	60	0.1090
300	70	0.0704
300	80	0.0309
300	85	0.0144
300	90	0.0048
300	95	0.0014
600	0	0.1530
600	20	0.1396
600	30	0.1265
600	40	0.1094
600	50	0.0891
600	60	0.0660
600	70	0.0412
600	80	0.0181
600	85	0.0095
600	90	0.0045
600	95	0.0020
1000	0	0.0997
1000	20	0.0898
1000	30	0.0807
1000	40	0.0691
1000	50	0.0554
1000	60	0.0401

ϕ_c = 150°

Altitude n. m.	θ_s degrees	F
1000	70	0.0244
1000	80	0.0111
1000	85	0.0065
1000	90	0.0038
1000	95	0.0019
3000	0	0.0264
3000	20	0.0230
3000	30	0.0202
3000	40	0.0168
3000	50	0.0130
3000	60	0.0092
3000	70	0.0057
3000	80	0.0031
3000	85	0.0022
3000	90	0.0015
3000	95	0.0010
6000	0	0.0089
6000	20	0.0077
6000	30	0.0067
6000	40	0.0056
6000	50	0.0044
6000	60	0.0032
6000	70	0.0022
6000	80	0.0014
6000	85	0.0010
6000	90	0.0008
6000	95	0.0006
10000	0	0.0037
10000	20	0.0032
10000	30	0.0029
10000	40	0.0024
10000	50	0.0019
10000	60	0.0015
10000	70	0.0011
10000	80	0.0007
10000	85	0.0006
10000	90	0.0005
10000	95	0.0003

Table 64. Geometric Factor for Reflected Solar Radiation to a Hemisphere

$\gamma = 150°$, $\phi_c = 180°$

Altitude n. m.	θ_s degrees	F
100	0	0.3545
100	20	0.3304
100	30	0.3030
100	40	0.2664
100	50	0.2217
100	60	0.1702
100	70	0.1136
100	80	0.0533
100	85	0.0235
100	90	0.0031
100	95	0.0002
300	0	0.2379
300	20	0.2190
300	30	0.1994
300	40	0.1737
300	50	0.1427
300	60	0.1075
300	70	0.0687
300	80	0.0292
300	85	0.0130
300	90	0.0039
300	95	0.0011
600	0	0.1528
600	20	0.1388
600	30	0.1254
600	40	0.1081
600	50	0.0875
600	60	0.0643
600	70	0.0394
600	80	0.0163
600	85	0.0081
600	90	0.0035
600	95	0.0015
1000	0	0.0996
1000	20	0.0891
1000	30	0.0797
1000	40	0.0678
1000	50	0.0539
1000	60	0.0385
1000	70	0.0227
1000	80	0.0095
1000	85	0.0052
1000	90	0.0026
1000	95	0.0013
3000	0	0.0264
3000	20	0.0227
3000	30	0.0197
3000	40	0.0162
3000	50	0.0123
3000	60	0.0084
3000	70	0.0050
3000	80	0.0025
3000	85	0.0017
3000	90	0.0010
3000	95	0.0006
6000	0	0.0089
6000	20	0.0076
6000	30	0.0066
6000	40	0.0054
6000	50	0.0042
6000	60	0.0030
6000	70	0.0020
6000	80	0.0012
6000	85	0.0009
6000	90	0.0006
6000	95	0.0004
10000	0	0.0037
10000	20	0.0032
10000	30	0.0028
10000	40	0.0023
10000	50	0.0019
10000	60	0.0014
10000	70	0.0010
10000	80	0.0006
10000	85	0.0005
10000	90	0.0004
10000	95	0.0003

Table 65. Geometric Factor for Reflected Solar Radiation to a Hemisphere

$\gamma = 180°$, $\phi_c = 0 - 360°$

Altitude n. m.	θ_s degrees	F
100	0	0.2907
100	20	0.2731
100	30	0.2517
100	40	0.2226
100	50	0.1868
100	60	0.1453
100	70	0.0994
100	80	0.0501
100	85	0.0256
100	90	0.0064
100	95	0.0006
300	0	0.1815
300	20	0.1705
300	30	0.1571
300	40	0.1390
300	50	0.1166
300	60	0.0907
300	70	0.0619
300	80	0.0318
300	85	0.0187
300	90	0.0089
300	95	0.0030
600	0	0.1073
600	20	0.1009
600	30	0.0931
600	40	0.0824
600	50	0.0692
600	60	0.0539
600	70	0.0373
600	80	0.0208
600	85	0.0139
600	90	0.0084
600	95	0.0044
1000	0	0.0625
1000	20	0.0588
1000	30	0.0542
1000	40	0.0480
1000	50	0.0403
1000	60	0.0316
1000	70	0.0221
1000	80	0.0134
1000	85	0.0098
1000	90	0.0067
1000	95	0.0042
3000	0	0.0098
3000	20	0.0093
3000	30	0.0085
3000	40	0.0076
3000	50	0.0064
3000	60	0.0052
3000	70	0.0039
3000	80	0.0028
3000	85	0.0024
3000	90	0.0019
3000	95	0.0015
6000	0	0.0017
6000	20	0.0016
6000	30	0.0015
6000	40	0.0013
6000	50	0.0011
6000	60	0.0009
6000	70	0.0008
6000	80	0.0006
6000	85	0.0005
6000	90	0.0004
6000	95	0.0003
10000	0	0.0003
10000	20	0.0003
10000	30	0.0003
10000	40	0.0002
10000	50	0.0002
10000	60	0.0002
10000	70	0.0001
10000	80	0.0001
10000	85	0.0001
10000	90	0.0001
10000	95	0.0001

Figure 8. Geometry for Planetary Reflected Solar Radiation to a Flat Plate

$$\text{Geometric Factor, } F = \frac{q}{P\,S_a}$$

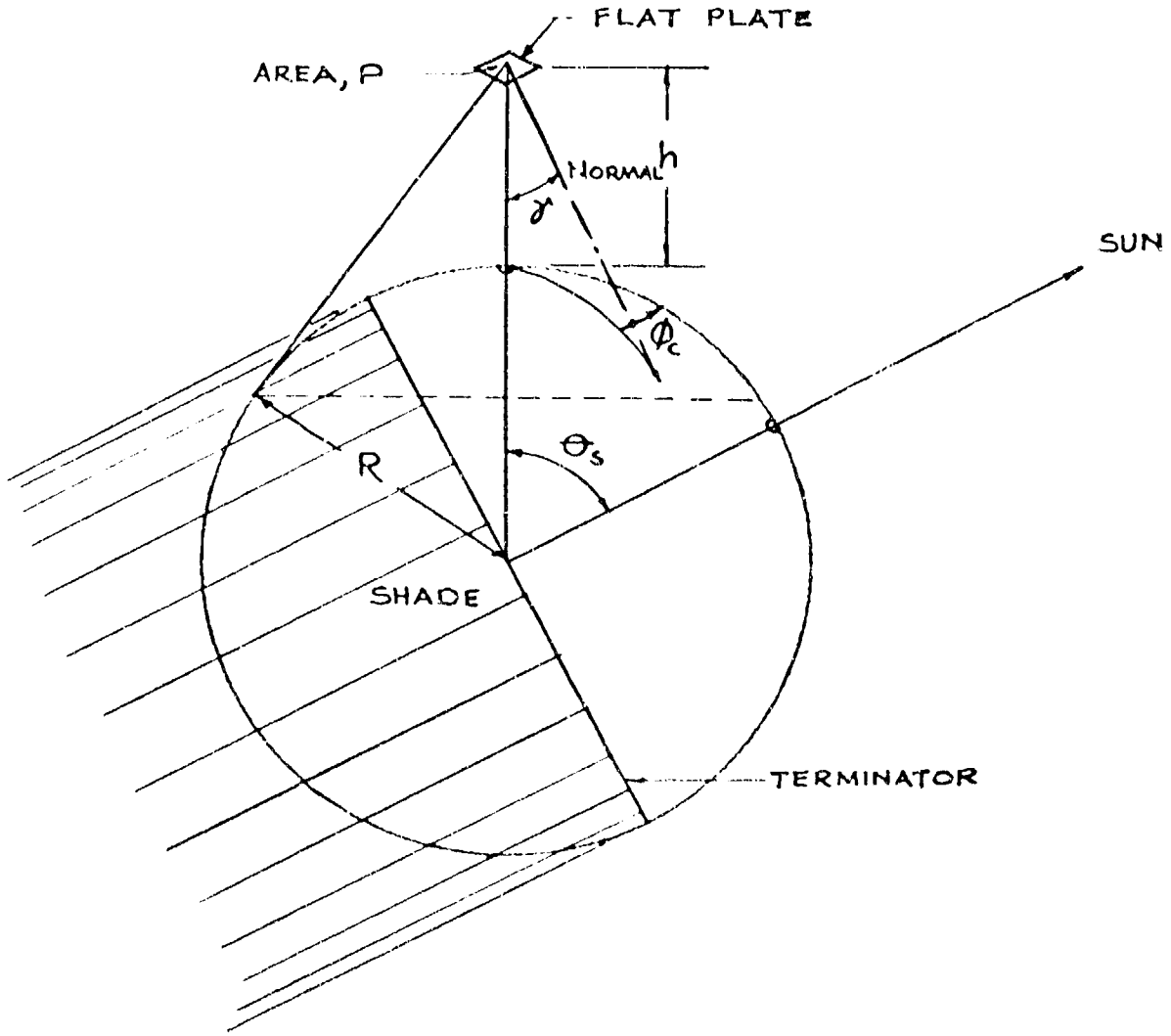

Table 66. Geometric Factor for Reflected Solar Radiation to a Flat Plate

$\gamma = 0°$ $\phi_c = 0°360°$

Altitude n. m.	θ_s degree	F	Altitude n. m.	θ_s degree	F
100	0	0.9531	3000	0	0.2549
100	20	0.8956	3000	20	0.2395
100	30	0.8254	3000	30	0.2207
100	40	0.7301	3000	40	0.1944
100	50	0.6126	3000	50	0.1625
100	60	0.4765	3000	60	0.1278
100	70	0.3259	3000	70	0.0934
100	80	0.1645	3000	80	0.0619
100	85	0.0823	3000	85	0.0480
100	90	0.0112	3000	90	0.0359
300	0	0.8422	6000	0	0.1102
300	20	0.7914	6000	20	0.1036
300	30	0.7294	6000	30	0.0950
300	40	0.6452	6000	40	0.0837
300	50	0.5414	6000	50	0.0708
300	60	0.4211	6000	60	0.0573
300	70	0.2874	6000	70	0.0440
300	80	0.1459	6000	80	0.0316
300	85	0.0777	6000	85	0.0260
300	90	0.0253	6000	90	0.0209
600	0	0.7121	10000	0	0.0514
600	20	0.6691	10000	20	0.0482
600	30	0.6167	10000	30	0.0442
600	40	0.5455	10000	40	0.0391
600	50	0.4577	10000	50	0.0335
600	60	0.3557	10000	60	0.0276
600	70	0.2423	10000	70	0.0218
600	80	0.1271	10000	80	0.0163
600	85	0.0760	10000	85	0.0138
600	90	0.0367	10000	90	0.0114
1000	0	0.5792	20000	0	0.0158
1000	20	0.5443	20000	20	0.0148
1000	30	0.5016	20000	30	0.0136
1000	40	0.4437	20000	40	0.0121
1000	50	0.3723	20000	50	0.0105
1000	60	0.2882	20000	60	0.0089
1000	70	0.1976	20000	70	0.0072
1000	80	0.1102	20000	80	0.0056
1000	85	0.0728	20000	85	0.0048
1000	90	0.0429	20000	90	0.0041

Table 67. Geometric Factor for Reflected Solar Radiation to a Flat Plate

γ - 30°

ϕ_c - c°

Altitude n. m.	θ_s degree	F	Altitude n. m.	θ_s degree	F
100	0	0.8243	3000	0	0.2207
100	20	0.7795	3000	20	0.2119
100	30	0.7211	3000	30	0.1977
100	40	0.6407	3000	40	0.1766
100	50	0.5409	3000	50	0.1503
100	60	0.4246	3000	60	0.1211
100	70	0.2955	3000	70	0.0912
100	80	0.1620	3000	80	0.0625
100	85	0.0970	3000	85	0.0494
100	90	0.0178	3000	90	0.0376
300	0	0.7241	6000	0	0.0954
300	20	0.6892	6000	20	0.0913
300	30	0.6399	6000	30	0.0846
300	40	0.5712	6000	40	0.0754
300	50	0.4851	6000	50	0.0647
300	60	0.3842	6000	60	0.0532
300	70	0.2750	6000	70	0.0416
300	80	0.1509	6000	80	0.0304
300	85	0.0890	6000	85	0.0252
300	90	0.0351	6000	90	0.0205
600	0	0.6167	10000	0	0.0445
600	20	0.5896	10000	20	0.0423
600	30	0.5489	10000	30	0.0391
600	40	0.4915	10000	40	0.0350
600	50	0.4192	10000	50	0.0302
600	60	0.3337	10000	60	0.0252
600	70	0.2370	10000	70	0.0202
600	80	0.1358	10000	80	0.0153
600	85	0.0876	10000	85	0.0129
600	90	0.0467	10000	90	0.0108
1000	0	0.5016	20000	0	0.0137
1000	20	0.4809	20000	20	0.0129
1000	30	0.4484	20000	30	0.0119
1000	40	0.4022	20000	40	0.0107
1000	50	0.3438	20000	50	0.0094
1000	60	0.2733	20000	60	0.0079
1000	70	0.1959	20000	70	0.0065
1000	80	0.1178	20000	80	0.0050
1000	85	0.0819	20000	85	0.0043
1000	90	0.0511	20000	90	0.0037

Table 68. Geometric Factor for Reflected Solar Radiation to a Flat Plate

γ = 30°			ϕ_c = 30°		
Altitude n. m.	θ_S degree	F	Altitude n. m.	θ_S degree	F
100	0	0.8243	3000	0	0.2207
100	20	0.7788	3000	20	0.2113
100	30	0.7201	3000	30	0.1968
100	40	0.6395	3000	40	0.1755
100	50	0.5394	3000	50	0.1490
100	60	0.4230	3000	60	0.1197
100	70	0.2937	3000	70	0.0898
100	80	0.1554	3000	80	0.0613
100	85	0.0841	3000	85	0.0483
100	90	0.0167	3000	90	0.0367
300	0	0.7241	6000	0	0.0954
300	20	0.6880	6000	20	0.0911
300	30	0.6382	6000	30	0.0843
300	40	0.5690	6000	40	0.0750
300	50	0.4824	6000	50	0.0642
300	60	0.3813	6000	60	0.0527
300	70	0.2680	6000	70	0.0411
300	80	0.1476	6000	80	0.0300
300	85	0.0861	6000	85	0.0249
300	90	0.0334	6000	90	0.0201
600	0	0.6167	10000	0	0.0446
600	20	0.5883	10000	20	0.0422
600	30	0.5469	10000	30	0.0390
600	40	0.4889	10000	40	0.0348
600	50	0.4161	10000	50	0.0301
600	60	0.3303	10000	60	0.0251
600	70	0.2334	10000	70	0.0200
600	80	0.1323	10000	80	0.0151
600	85	0.0847	10000	85	0.0128
600	90	0.0447	10000	90	0.0107
1000	0	0.5016	20000	0	0.0137
1000	20	0.4796	20000	20	0.0129
1000	30	0.4465	20000	30	0.0119
1000	40	0.3998	20000	40	0.0107
1000	50	0.3409	20000	50	0.0093
1000	60	0.2702	20000	60	0.0079
1000	70	0.1925	20000	70	0.0064
1000	80	0.1148	20000	80	0.0050
1000	85	0.0794	20000	85	0.0043
1000	90	0.0492	20000	90	0.0037

Table 69. Geometric Factor for Reflected Solar Radiation to a Flat Plate

γ = 30°			ϕ_c = 60°		
Altitude n. m.	θ_s degree	F	Altitude n. m.	θ_s degree	F
100	0	0.8243	3000	0	0.2207
100	20	0.7770	3000	20	0.2097
100	30	0.7178	3000	30	0.1944
100	40	0.6361	3000	40	0.1725
100	50	0.5354	3000	50	0.1455
100	60	0.4184	3000	60	0.1159
100	70	0.2887	3000	70	0.0860
100	80	0.1455	3000	80	0.0581
100	85	0.0790	3000	85	0.0455
100	90	0.0137	3000	90	0.0343
300	0	0.7241	6000	0	0.0954
300	20	0.6848	6000	20	0.0905
300	30	0.6335	6000	30	0.0834
300	40	0.5629	6000	40	0.0740
300	50	0.4752	6000	50	0.0630
300	60	0.3731	6000	60	0.0514
300	70	0.2595	6000	70	0.0398
300	80	0.1380	6000	80	0.0289
300	85	0.0778	6000	85	0.0239
300	90	0.0285	6000	90	0.0193
600	0	0.6167	10000	0	0.0445
600	20	0.5846	10000	20	0.0420
600	30	0.5415	10000	30	0.0387
600	40	0.4819	10000	40	0.0344
600	50	0.4078	10000	50	0.0296
600	60	0.3209	10000	60	0.0246
600	70	0.2234	10000	70	0.0195
600	80	0.1229	10000	80	0.0147
600	85	0.0767	10000	85	0.0124
600	90	0.0392	10000	90	0.0103
1000	0	0.5015	20000	0	0.0137
1000	20	0.4761	20000	20	0.0129
1000	30	0.4414	20000	30	0.0119
1000	40	0.3932	20000	40	0.0106
1000	50	0.3331	20000	50	0.0092
1000	60	0.2615	20000	60	0.0078
1000	70	0.1835	20000	70	0.0063
1000	80	0.1066	20000	80	0.0049
1000	85	0.0725	20000	85	0.0042
1000	90	0.0441	20000	90	0.0036

Table 70. Geometric Factor for Reflected Solar Radiation to a Flat Plate

$\gamma = 30°$

Altitude n. m.	θ_s degree	F
100	0	0.8243
100	20	0.7746
100	30	0.7138
100	40	0.6314
100	50	0.5298
100	60	0.4121
100	70	0.2819
100	80	0.1430
100	85	0.0721
100	90	0.0090
300	0	0.7241
300	20	0.6804
300	30	0.6271
300	40	0.5547
300	50	0.4654
300	60	0.3620
300	70	0.2475
300	80	0.1266
300	85	0.0671
300	90	0.0217
600	0	0.6167
600	20	0.5795
600	30	0.5340
600	40	0.4724
600	50	0.3964
600	60	0.3081
600	70	0.2098
600	80	0.1101
600	85	0.0658
600	90	0.0318
1000	0	0.5016
1000	20	0.4714
1000	30	0.4344
1000	40	0.3843
1000	50	0.3224
1000	60	0.2496
1000	70	0.1711
1000	80	0.0954
1000	85	0.0631
1000	90	0.0371

$\phi_c = 90°$

Altitude n. m.	θ_s degree	F
3000	0	0.2207
3000	20	0.2074
3000	30	0.1912
3000	40	0.1683
3000	50	0.1407
3000	60	0.1107
3000	70	0.0809
3000	80	0.0536
3000	85	0.0416
3000	90	0.0310
6000	0	0.0954
6000	20	0.0897
6000	30	0.0823
6000	40	0.0725
6000	50	0.0613
6000	60	0.0496
6000	70	0.0381
6000	80	0.0274
6000	85	0.0225
6000	90	0.0181
10000	0	0.0445
10000	20	0.0417
10000	30	0.0383
10000	40	0.0339
10000	50	0.0290
10000	60	0.0239
10000	70	0.0189
10000	80	0.0141
10000	85	0.0119
10000	90	0.0099
20000	0	0.0137
20000	20	0.0128
20000	30	0.0118
20000	40	0.0105
20000	50	0.0091
20000	60	0.0077
20000	70	0.0062
20000	80	0.0048
20000	85	0.0041
20000	90	0.0035

Table 71. Geometric Factor for Reflected Solar Radiation to a Flat Plate

γ = 30°			ϕ_c = 120°		
Altitude n. m.	θ_s degree	F	Altitude n. m.	θ_s degree	F
100	0	0.8243	3000	0	0.2207
100	20	0.7721	3000	20	0.2052
100	30	0.7102	3000	30	0.1879
100	40	0.6268	3000	40	0.1642
100	50	0.5243	3000	50	0.1359
100	60	0.4058	3000	60	0.1055
100	70	0.2751	3000	70	0.0757
100	80	0.1359	3000	80	0.0491
100	85	0.0652	3000	85	0.0376
100	90	0.0063	3000	90	0.0278
300	0	0.7241	6000	0	0.0954
300	20	0.6760	6000	20	0.0889
300	30	0.6207	6000	30	0.0811
300	40	0.5464	6000	40	0.0710
300	50	0.4556	6000	50	0.0596
300	60	0.3509	6000	60	0.0478
300	70	0.2355	6000	70	0.0363
300	80	0.1145	6000	80	0.0258
300	85	0.0565	6000	85	0.0211
300	90	0.0153	6000	90	0.0169
600	0	0.6167	10000	0	0.0445
600	20	0.5744	10000	20	0.0414
600	30	0.5266	10000	30	0.0378
600	40	0.4628	10000	40	0.0333
600	50	0.3850	10000	50	0.0284
600	60	0.2952	10000	60	0.0233
600	70	0.1962	10000	70	0.0183
600	80	0.0973	10000	80	0.0136
600	85	0.0549	10000	85	0.0114
600	90	0.0244	10000	90	0.0094
1000	0	0.5016	20000	0	0.0137
1000	20	0.4666	20000	20	0.0127
1000	30	0.4274	20000	30	0.0117
1000	40	0.3753	20000	40	0.0104
1000	50	0.3117	20000	50	0.0090
1000	60	0.2378	20000	60	0.0078
1000	70	0.1588	20000	70	0.0061
1000	80	0.0842	20000	80	0.0047
1000	85	0.0536	20000	85	0.0040
1000	90	0.0301	20000	90	0.0034

Table 72. Geometric Factor for Reflected Solar Radiation to a Flat Plate

γ = 30°

Altitude n. m.	θ_s degree	F
100	0	0.8243
100	20	0.7703
100	30	0.7076
100	40	0.6234
100	50	0.5202
100	60	0.4013
100	70	0.2701
100	80	0.1307
100	85	0.0603
100	90	0.0039
300	0	0.7241
300	20	0.6728
300	30	0.6160
300	40	0.5404
300	50	0.4484
300	60	0.3428
300	70	0.2267
300	80	0.1056
300	85	0.0488
300	90	0.0107
600	0	0.6167
600	20	0.5707
600	30	0.5212
600	40	0.4558
600	50	0.3766
600	60	0.2858
600	70	0.1863
600	80	0.0879
600	85	0.0470
600	90	0.0189
1000	0	0.5016
1000	20	0.4631
1000	30	0.4223
1000	40	0.3687
1000	50	0.3039
1000	60	0.2291
1000	70	0.1497
1000	80	0.0761
1000	85	0.0467
1000	90	0.0250

ϕ_c = 150°

Altitude n. m.	θ_s degree	F
3000	0	0.2207
3000	20	0.2036
3000	30	0.1855
3000	40	0.1612
3000	50	0.1324
3000	60	0.1016
3000	70	0.0719
3000	80	0.0458
3000	85	0.0348
3000	90	0.0254
6000	0	0.0954
6000	20	0.0883
6000	30	0.0802
6000	40	0.0699
6000	50	0.0583
6000	60	0.0465
6000	70	0.0350
6000	80	0.0247
6000	85	0.0201
6000	90	0.0160
10000	0	0.0445
10000	20	0.0412
10000	30	0.0375
10000	40	0.0329
10000	50	0.0279
10000	60	0.0228
10000	70	0.0178
10000	80	0.0132
10000	85	0.0111
10000	90	0.0091
20000	0	0.0137
20000	20	0.0127
20000	30	0.0116
20000	40	0.0103
20000	50	0.0089
20000	60	0.0075
20000	70	0.0060
20000	80	0.0046
20000	85	0.0040
20000	90	0.0034

Table 73. Geometric Factor for Reflected Solar Radiation to a Flat Plate

γ = 30°			ϕ_c = 180°		
Altitude n. m.	θ_s degree	F	Altitude n. m.	θ_s degree	F
100	0	0.8243	3000	0	0.2207
100	20	0.7696	3000	20	0.2030
100	30	0.7066	3000	30	0.1846
100	40	0.6221	3000	40	0.1601
100	50	0.5187	3000	50	0.1311
100	60	0.3996	3000	60	0.1003
100	70	0.2683	3000	70	0.0705
100	80	0.1288	3000	80	0.0446
100	85	0.0584	3000	85	0.0337
100	90	0.0030	3000	90	0.0245
300	0	0.7241	6000	0	0.0954
300	20	0.6717	6000	20	0.0880
300	30	0.6143	6000	30	0.0799
300	40	0.5382	6000	40	0.0695
300	50	0.4458	6000	50	0.0579
300	60	0.3398	6000	60	0.0460
300	70	0.2235	6000	70	0.0346
300	80	0.1024	6000	80	0.0243
300	85	0.0459	6000	85	0.0197
300	90	0.0090	6000	90	0.0157
600	0	0.6167	10000	0	0.0445
600	20	0.5693	10000	20	0.0411
600	30	0.5192	10000	30	0.0374
600	40	0.4533	10000	40	0.0328
600	50	0.3736	10000	50	0.0278
600	60	0.2824	10000	60	0.0226
600	70	0.1826	10000	70	0.0177
600	80	0.0844	10000	80	0.0130
600	85	0.0440	10000	85	0.0109
600	90	0.0169	10000	90	0.0090
1000	0	0.5016	20000	0	0.0137
1000	20	0.4618	20000	20	0.0127
1000	30	0.4205	20000	30	0.0116
1000	40	0.3663	20000	40	0.0103
1000	50	0.3010	20000	50	0.0089
1000	60	0.2259	20000	60	0.0074
1000	70	0.1464	20000	70	0.0060
1000	80	0.0731	20000	80	0.0046
1000	85	0.0442	20000	85	0.0039
1000	90	0.0232	20000	90	0.0033

Table 7-4. Geometric Factor for Reflected Solar Radiation to a Flat Plate

γ = 60° ϕ_c = 0°

Altitude n. m.	θ_s degree	F	Altitude n. m.	θ_s degree	F
100	0	0.6004	3000	0	0.1260
100	20	0.5708	3000	20	0.1259
100	30	0.5296	3000	30	0.1201
100	40	0.4723	3000	40	0.1116
100	50	0.4006	3000	50	0.0982
100	60	0.3168	3000	60	0.0820
100	70	0.2234	3000	70	0.0646
100	80	0.1220	3000	80	0.0464
100	85	0.0679	3000	85	0.0375
100	90	0.0196	3000	90	0.0292
300	0	0.4905	6000	0	0.0551
300	20	0.4727	6000	20	0.0546
300	30	0.4420	6000	30	0.0516
300	40	0.3979	6000	40	0.0470
300	50	0.3417	6000	50	0.0413
300	60	0.2751	6000	60	0.0349
300	70	0.3000	6000	70	0.0281
300	80	0.1170	6000	80	0.0211
300	85	0.0760	6000	85	0.0177
300	90	0.0355	6000	90	0.0146
600	0	0.3889	10000	0	0.0257
600	20	0.3798	10000	20	0.0251
600	30	0.3577	10000	30	0.0236
600	40	0.3248	10000	40	0.0214
600	50	0.2821	10000	50	0.0189
600	60	0.2334	10000	60	0.0160
600	70	0.1675	10000	70	0.0131
600	80	0.1050	10000	80	0.0101
600	85	0.0758	10000	85	0.0086
600	90	0.0441	10000	90	0.0072
1000	0	0.3017	20000	0	0.0079
1000	20	0.2979	20000	20	0.0076
1000	30	0.2823	20000	30	0.0071
1000	40	0.2582	20000	40	0.0064
1000	50	0.2262	20000	50	0.0057
1000	60	0.1885	20000	60	0.0048
1000	70	0.1390	20000	70	0.0040
1000	80	0.0938	20000	80	0.0032
1000	85	0.0691	20000	85	0.0027
1000	90	0.0456	20000	90	0.0023

Table 75. Geometric Factor for Reflected Solar Radiation to a Flat Plate

$\gamma = 60°$			$\phi_c = 30°$		
Altitude n. m.	θ_s degree	F	Altitude n. m.	θ_s degree	F
100	0	0.6004	3000	0	0.1260
100	20	0.5699	3000	20	0.1249
100	30	0.5283	3000	30	0.1186
100	40	0.4706	3000	40	0.1086
100	50	0.3986	3000	50	0.0955
100	60	0.3146	3000	60	0.0795
100	70	0.2209	3000	70	0.0622
100	80	0.1206	3000	80	0.0443
100	85	0.0686	3000	85	0.0357
100	90	0.0177	3000	90	0.0277
300	0	0.4905	6000	0	0.0551
300	20	0.4711	6000	20	0.0542
300	30	0.4397	6000	30	0.0510
300	40	0.3949	6000	40	0.0463
300	50	0.3381	6000	50	0.0405
300	60	0.2711	6000	60	0.0340
300	70	0.1962	6000	70	0.0272
300	80	0.1138	6000	80	0.0204
300	85	0.0721	6000	85	0.0171
300	90	0.0325	6000	90	0.0140
600	0	0.3889	10000	0	0.0267
600	20	0.3778	10000	20	0.0260
600	30	0.3549	10000	30	0.0234
600	40	0.3212	10000	40	0.0212
600	50	0.2778	10000	50	0.0186
600	60	0.2265	10000	60	0.0157
600	70	0.1664	10000	70	0.0128
600	80	0.1027	10000	80	0.0098
600	85	0.0707	10000	85	0.0084
600	90	0.0406	10000	90	0.0070
1000	0	0.3017	20000	0	0.0079
1000	20	0.2960	20000	20	0.0075
1000	30	0.2795	20000	30	0.0070
1000	40	0.2545	20000	40	0.0064
1000	50	0.2218	20000	50	0.0056
1000	60	0.1830	20000	60	0.0048
1000	70	0.1365	20000	70	0.0039
1000	80	0.0887	20000	80	0.0031
1000	85	0.0647	20000	85	0.0027
1000	90	0.0423	20000	90	0.0023

Table 76. Geometric Factor for Reflected Solar Radiation to a Flat Plate

γ = 60°			ϕ_c = 60°		
Altitude n. m.	θ_s degree	F	Altitude n. m.	θ_s degree	F
100	0	0.6004	3000	0	0.1260
100	20	0.5675	3000	20	0.1222
100	30	0.5248	3000	30	0.1146
100	40	0.4661	3000	40	0.1035
100	50	0.3933	3000	50	0.0895
100	60	0.3085	3000	60	0.0727
100	70	0.2143	3000	70	0.0556
100	80	0.1136	3000	80	0.0387
100	85	0.0616	3000	85	0.0307
100	90	0.0134	3000	90	0.0236
300	0	0.4905	6000	0	0.0551
300	20	0.4668	6000	20	0.0532
300	30	0.4334	6000	30	0.0495
300	40	0.3868	6000	40	0.0444
300	50	0.3285	6000	50	0.0383
300	60	0.2602	6000	60	0.0317
300	70	0.1837	6000	70	0.0250
300	80	0.1015	6000	80	0.0184
300	85	0.0606	6000	85	0.0153
300	90	0.0252	6000	90	0.0125
600	0	0.3889	10000	0	0.0257
600	20	0.3726	10000	20	0.0248
600	30	0.3472	10000	30	0.0228
600	40	0.3114	10000	40	0.0205
600	50	0.2660	10000	50	0.0178
600	60	0.2124	10000	60	0.0149
600	70	0.1518	10000	70	0.0120
600	80	0.0886	10000	80	0.0091
600	85	0.0580	10000	85	0.0077
600	90	0.0325	10000	90	0.0065
1000	0	0.3017	20000	0	0.0079
1000	20	0.2907	20000	20	0.0075
1000	30	0.2718	20000	30	0.0069
1000	40	0.2446	20000	40	0.0062
1000	50	0.2100	20000	50	0.0054
1000	60	0.1700	20000	60	0.0046
1000	70	0.1224	20000	70	0.0038
1000	80	0.0754	20000	80	0.0029
1000	85	0.0529	20000	85	0.0025
1000	90	0.0345	20000	90	0.0022

Table 77. Geometric Factor for Reflected Solar Radiation to a Flat Plate

δ = 60°			ϕ_c = 90°		
Altitude n. m.	θ_s degree	F	Altitude n. m.	θ_s degree	F
100	0	0.6004	3000	0	0.1260
100	20	0.5642	3000	20	0.1184
100	30	0.5200	3000	30	0.1091
100	40	0.4599	3000	40	0.0964
100	50	0.3869	3000	50	0.0812
100	60	0.3002	3000	60	0.0637
100	70	0.2053	3000	70	0.0434
100	80	0.1042	3000	80	0.0306
100	85	0.0525	3000	85	0.0235
100	90	0.0078	3000	90	0.0175
300	0	0.4905	6000	0	0.0551
300	20	0.4609	6000	20	0.0518
300	30	0.4248	6000	30	0.0475
300	40	0.3757	6000	40	0.0418
300	50	0.3153	6000	50	0.0354
300	60	0.2452	6000	60	0.0286
300	70	0.1675	6000	70	0.0220
300	80	0.0852	6000	80	0.0158
300	85	0.0469	6000	85	0.0130
300	90	0.0148	6000	90	0.0104
600	0	0.3889	10000	0	0.0257
600	20	0.3654	10000	20	0.0241
600	30	0.3368	10000	30	0.0221
600	40	0.2979	10000	40	0.0195
600	50	0.2499	10000	50	0.0167
600	60	0.1943	10000	60	0.0138
600	70	0.1325	10000	70	0.0109
600	80	0.0700	10000	80	0.0081
600	85	0.0420	10000	85	0.0069
600	90	0.0198	10000	90	0.0057
1000	0	0.3017	20000	0	0.0079
1000	20	0.2835	20000	20	0.0074
1000	30	0.2613	20000	30	0.0068
1000	40	0.2311	20000	40	0.0060
1000	50	0.1939	20000	50	0.0052
1000	60	0.1503	20000	60	0.0044
1000	70	0.1038	20000	70	0.0036
1000	80	0.0580	20000	80	0.0028
1000	85	0.0381	20000	85	0.0024
1000	90	0.0222	20000	90	0.0020

Table 78. Geometric Factor for Reflected Solar Radiation to a Flat Plate

$\gamma^{\wedge}$ = 60°			ϕ_c = 120°		
Altitude n. m.	θ_s degree	F	Altitude n. m.	θ_s degree	F
100	0	0.6004	3000	0	0.1263
100	20	0.5609	3000	20	0.1140
100	30	0.5152	3000	30	0.1036
100	40	0.4638	3000	40	0.0894
100	50	0.3786	3000	50	0.0729
100	60	0.2919	3000	60	0.0548
100	70	0.1963	3000	70	0.0378
100	80	0.0948	3000	80	0.0230
100	85	0.0435	3000	85	0.0170
100	90	0.0052	3000	90	0.0121
300	0	0.4905	6000	0	0.0551
300	20	0.4550	6000	20	0.0503
300	30	0.4162	6000	30	0.0454
300	40	0.3647	6000	40	0.0393
300	50	0.3021	6000	50	0.0324
300	60	0.2303	6000	60	0.0255
300	70	0.1514	6000	70	0.0189
300	80	0.0693	6000	80	0.0131
300	85	0.0320	6000	85	0.0106
300	90	0.0074	6000	90	0.0083
600	0	0.3889	10000	0	0.0257
600	20	0.3582	10000	20	0.0235
600	30	0.3263	10000	30	0.0213
600	40	0.2844	10000	40	0.0186
600	50	0.2339	10000	50	0.0157
600	60	0.1762	10000	60	0.0127
600	70	0.1132	10000	70	0.0098
600	80	0.0521	10000	80	0.0072
600	85	0.0271	10000	85	0.0060
600	90	0.0105	10000	90	0.0049
1000	0	0.3017	20000	0	0.0079
1000	20	0.2763	20000	20	0.0073
1000	30	0.2507	20000	30	0.0066
1000	40	0.2176	20000	40	0.0059
1000	50	0.1778	20000	50	0.0050
1000	60	0.1323	20000	60	0.0042
1000	70	0.0847	20000	70	0.0034
1000	80	0.0414	20000	80	0.0026
1000	85	0.0243	20000	85	0.0022
1000	90	0.0123	20000	90	0.0019

Table 79. Geometric Factor for Reflected Solar Radiation to a Flat Plate

$\gamma = 60°$

Altitude m. m.	θ_s degree	F
100	0	0.6004
100	20	0.5588
100	30	0.5116
100	40	0.4492
100	50	0.3732
100	60	0.2858
100	70	0.1897
100	80	0.0880
100	85	0.0370
100	90	0.0012
300	0	0.4905
300	20	0.4507
300	30	0.4099
300	40	0.3566
300	50	0.2924
300	60	0.2194
300	70	0.1396
300	80	0.0577
300	85	0.0222
300	90	0.0026
600	0	0.3889
600	20	0.3530
600	30	0.3186
600	40	0.2745
600	50	0.2221
600	60	0.1629
600	70	0.0992
600	80	0.0391
600	85	0.0166
600	90	0.0042
1000	0	0.3017
1000	20	0.2710
1000	30	0.2430
1000	40	0.2077
1000	50	0.1660
1000	60	0.1191
1000	70	0.0710
1000	80	0.0293
1000	85	0.0145
1000	90	0.0065

$\phi_c = 150°$

Altitude m. m.	θ_s degree	F
3000	0	0.1260
3000	20	0.1119
3000	30	0.0998
3000	40	0.0842
3000	50	0.0668
3000	60	0.0482
3000	70	0.0311
3000	80	0.0174
3000	85	0.0122
3000	90	0.0080
6000	0	0.0551
6000	20	0.0493
6000	30	0.0439
6000	40	0.0374
6000	50	0.0302
6000	60	0.0232
6000	70	0.0167
6000	80	0.0112
6000	85	0.0088
6000	90	0.0068
10000	0	0.0257
10000	20	0.0232
10000	30	0.0208
10000	40	0.0179
10000	50	0.0149
10000	60	0.0118
10000	70	0.0090
10000	80	0.0065
10000	85	0.0054
10000	90	0.0043
20000	0	0.0079
20000	20	0.0072
20000	30	0.0065
20000	40	0.0057
20000	50	0.0049
20000	60	0.0040
20000	70	0.0032
20000	80	0.0024
20000	85	0.0021
20000	90	0.0017

Table 80. Geometric Factor for Reflected Solar Radiation to a Flat Plate

$\gamma = 60°$ $\quad \phi_c = 180°$

Altitude n. m.	θ_s degree	F	Altitude n. m.	θ_s degree	F
100	0	0.6004	3000	0	0.1260
100	20	0.5576	3000	20	0.1108
100	30	0.5104	3000	30	0.0981
100	40	0.4476	3000	40	0.0823
100	50	0.3712	3000	50	0.0646
100	60	0.2836	3000	60	0.0458
100	70	0.1873	3000	70	0.0287
100	80	0.0855	3000	80	0.0154
100	85	0.0347	3000	85	0.0104
100	90	0.0003	3000	90	0.0066
300	0	0.4905	6000	0	0.0551
300	20	0.4491	6000	20	0.0489
300	30	0.4076	6000	30	0.0434
300	40	0.3536	6000	40	0.0367
300	50	0.2889	6000	50	0.0295
300	60	0.2154	6000	60	0.0223
300	70	0.1363	6000	70	0.0159
300	80	0.0534	6000	80	0.0105
300	85	0.0187	6000	85	0.0082
300	90	0.0010	6000	90	0.0062
600	0	0.3889	10000	0	0.0257
600	20	0.3511	10000	20	0.0230
600	30	0.3158	10000	30	0.0206
600	40	0.2709	10000	40	0.0177
600	50	0.2178	10000	50	0.0146
600	60	0.1581	10000	60	0.0115
600	70	0.0940	10000	70	0.0087
600	80	0.0344	10000	80	0.0062
600	85	0.0128	10000	85	0.0051
600	90	0.0020	10000	90	0.0041
1000	0	0.3017	20000	0	0.0079
1000	20	0.2691	20000	20	0.0072
1000	30	0.2402	20000	30	0.0065
1000	40	0.2040	20000	40	0.0057
1000	50	0.1617	20000	50	0.0048
1000	60	0.1143	20000	60	0.0040
1000	70	0.0660	20000	70	0.0031
1000	80	0.0249	20000	80	0.0024
1000	85	0.0109	20000	85	0.0020
1000	90	0.0032	20000	90	0.0017

Table 81. Geometric Factor for Reflected Solar Radiation to a Flat Plate

$\gamma = 90°$

Altitude n. m.	θ_s degree	F
100	0	0.3552
100	20	0.3393
100	30	0.3157
100	40	0.2825
100	50	0.2407
100	60	0.1916
100	70	0.1367
100	80	0.0890
100	85	0.0595
100	90	0.0161
300	0	0,2538
300	20	0.2475
300	30	0.2330
300	40	0.2114
300	50	0.1834
300	60	0.1498
300	70	0.1206
300	80	0.0779
300	85	0.0553
300	90	0.0264
600	0	0.1770
600	20	0.1765
600	30	0.1681
600	40	0.1547
600	50	0.1365
600	60	0.1204
600	70	0.0940
600	80	0.0644
600	85	0.0487
600	90	0.0297
1000	0	0.1198
1000	20	0.1221
1000	30	0.1177
1000	40	0.1097
1000	50	0.0983
1000	60	0.0864
1000	70	0.0696
1000	80	0.0507
1000	85	0.0406
1000	90	0.0278

$\phi_c = 0°$

Altitude n. m.	θ_s degree	F
3000	0	0.0306
3000	20	0.0332
3000	30	0.0330
3000	40	0.0324
3000	50	0.0304
3000	60	0.0274
3000	70	0.0236
3000	80	0.0200
3000	85	0.0164
3000	90	0.0130
6000	0	0.0084
6000	20	0.0095
6000	30	0.0098
6000	40	0.0100
6000	50	0.0098
6000	60	0.0095
6000	70	0.0086
6000	80	0.0076
6000	85	0.0065
6000	90	0.0048
10000	0	0.0026
10000	20	0.0031
10000	30	0.0032
10000	40	0.0032
10000	50	0.0031
10000	60	0.0029
10000	70	0.0025
10000	80	0.0022
10000	85	0.0020
10000	90	0.0017
20000	0	0.0004
20000	20	0.0005
20000	30	0.0005
20000	40	0.0005
20000	50	0.0005
20000	60	0.0005
20000	70	0.0004
20000	80	0.0004
20000	85	0.0003
20000	90	0.0003

Table 82. Geometric Factor for Reflected Solar Radiation to a Flat Plate

$\gamma = 90°$

Altitude n. m.	θ_s degree	F
100	0	0.3552
100	20	0.3385
100	30	0.3146
100	40	0.2811
100	50	0.2390
100	60	0.1897
100	70	0.1346
100	80	0.0777
100	85	0.0443
100	90	0.0142
300	0	0.2638
300	20	0.2463
300	30	0.2312
300	40	0.2091
300	50	0.1807
300	60	0.1467
300	70	0.1105
300	80	0.0663
300	85	0.0443
300	90	0.0233
600	0	0.1770
600	20	0.1751
600	30	0.1661
600	40	0.1521
600	50	0.1335
600	60	0.1126
600	70	0.0851
600	80	0.0553
600	85	0.0406
600	90	0.0232
1000	0	0.1198
1000	20	0.1208
1000	30	0.1153
1000	40	0.1073
1000	50	0.0955
1000	60	0.0816
1000	70	0.0633
1000	80	0.0438
1000	85	0.0343
1000	90	0.0248

$\phi_c = 30°$

Altitude n. m.	θ_s degree	F
3000	0	0.0306
3000	20	0.0326
3000	30	0.0322
3000	40	0.0310
3000	50	0.0284
3000	60	0.0255
3000	70	0.0206
3000	80	0.0163
3000	85	0.0140
3000	90	0.0144
6000	0	0.0084
6000	20	0.0093
6000	30	0,0092
6000	40	0.0090
6000	50	0.0084
6000	60	0.0076
6000	70	0.0065
6000	80	0.0055
6000	85	0.0049
6000	90	0.0042
10000	0	0.0026
10000	20	0.0030
10000	30	0.0032
10000	40	0.0030
10000	50	0.0028
10000	60	0.0025
10000	70	0.0023
10000	80	0.0019
10000	85	0.0017
10000	90	0.0015
20000	0	0.0004
20000	20	0.0005
20000	30	0.0005
20000	40	0.0005
20000	50	0.0005
20000	60	0.0004
20000	70	0.0004
20000	80	0.0003
20000	85	0.0003
20000	90	0.0003

Table 83. Geometric Factor for Reflected Solar Radiation to a Flat Plate

$\gamma = 90°$ $\quad \phi_c = 60°$

Altitude n. m.	θ_s degree	F	Altitude n. m.	θ_s degree	F
100	0	0.3552	3000	0	0.0306
100	20	0.3366	3000	20	0.0310
100	30	0.3116	3000	30	0.0298
100	40	0.2773	3000	40	0.0276
100	50	0.2345	3000	50	0.0243
100	60	0.1846	3000	60	0.0205
100	70	0.1290	3000	70	0.0165
100	80	0.0690	3000	80	0.0122
100	85	0.0382	3000	85	0.0100
100	90	0.0098	3000	90	0.0079
300	0	0.2538	6000	0	0.0084
300	20	0.2430	6000	20	0.0087
300	30	0.2264	6000	30	0.0084
300	40	0.2029	6000	40	0.0078
300	50	0.1732	6000	50	0.0070
300	60	0.1383	6000	60	0.0060
300	70	0.0992	6000	70	0.0051
300	80	0.0564	6000	80	0.0040
300	85	0.0352	6000	85	0.0034
300	90	0.0161	6000	90	0.0029
600	0	0.1770	10000	0	0.0026
600	20	0.1714	10000	20	0.0027
600	30	0.1607	10000	30	0.0027
600	40	0.1451	10000	40	0.0025
600	50	0.1251	10000	50	0.0023
600	60	0.1015	10000	60	0.0020
600	70	0.0738	10000	70	0.0017
600	80	0.0449	10000	80	0.0014
600	85	0.0310	10000	85	0.0012
600	90	0.0181	10000	90	0.0010
1000	0	0.1198	20000	0	0.0004
1000	20	0.1173	20000	20	0.0004
1000	30	0.1107	20000	30	0.0004
1000	40	0.1007	20000	40	0.0004
1000	50	0.0877	20000	50	0.0004
1000	60	0.0715	20000	60	0.0003
1000	70	0.0532	20000	70	0.0003
1000	80	0.0346	20000	80	0.0002
1000	85	0.0255	20000	85	0.0002
1000	90	0.0169	20000	90	0.0002

Table 84. Geometric Factor for Reflected Solar Radiation to a Flat Plate

Altitude n. m.	$\gamma = 90°$ θ_3 degree	F	Altitude n. m.	$\phi_c = 90°$ θ_3 degree	F
100	0	0.3552	3000	0	0.0306
100	20	0.3337	3000	20	0.0288
100	30	0.3076	3000	30	0.0265
100	40	0.2721	3000	40	0.0233
100	50	0.2283	3000	50	0.0194
100	60	0.1776	3000	60	0.0152
100	70	0.1214	3000	70	0.0111
100	80	0.0608	3000	80	0.0073
100	85	0.0305	3000	85	0.0056
100	90	0.0051	3000	90	0.0041
300	0	0.2538	6000	0	0.0084
300	20	0.2385	6000	20	0.0078
300	30	0.2198	6000	30	0.0072
300	40	0.1944	6000	40	0.0063
300	50	0.1631	6000	50	0.0053
300	60	0.1269	6000	60	0.0043
300	70	0.0865	6000	70	0.0033
300	80	0.0438	6000	80	0.0023
300	85	0.0238	6000	85	0.0019
300	90	0.0084	6000	90	0.0015
600	0	0.1770	10000	0	0.0026
600	20	0.1663	10000	20	0.0024
600	30	0.1532	10000	30	0.0022
600	40	0.1356	10000	40	0.0020
600	50	0.1137	10000	50	0.0017
600	60	0.0883	10000	60	0.0014
600	70	0.0599	10000	70	0.0011
600	80	0.0316	10000	80	0.0008
600	85	0.0191	10000	85	0.0006
600	90	0.0094	10000	90	0.0005
1000	0	0.1198	20000	0	0.0004
1000	20	0.1125	20000	20	0.0004
1000	30	0.1037	20000	30	0.0003
1000	40	0.0917	20000	40	0.0003
1000	50	0.0770	20000	50	0.0003
1000	60	0.0593	20000	60	0.0002
1000	70	0.0406	20000	70	0.0002
1000	80	0.0227	20000	80	0.0001
1000	85	0.0150	20000	85	0.0001
1000	90	0.0088	20000	90	0.0001

Table 85. Geometric Factor for Reflected Solar Radiation to a Flat Plate

γ = 90°			ϕ_c = 120°		
Altitude n. m.	θ_s degree	F	Altitude n. m.	θ_s degree	F
100	0	0.3552	3000	0	0.0306
100	20	0.3310	3000	20	0.0265
100	30	0.3035	3000	30	0.0232
100	40	0.2669	3000	40	0.0191
100	50	0.2221	3000	50	0.0146
100	60	0.1706	3000	60	0.0101
100	70	0.1138	3000	70	0.0062
100	80	0.0529	3000	80	0.0032
100	85	0.0230	3000	85	0.0022
100	90	0.0017	3000	90	0.0014
300	0	0.2538	6000	0	0.0084
300	20	0.2339	6000	20	0.0070
300	30	0.2132	6000	30	0.0060
300	40	0.1859	6000	40	0.0048
300	50	0.1530	6000	50	0.0036
300	60	0.1154	6000	60	0.0024
300	70	0.0742	6000	70	0.0016
300	80	0.0317	6000	80	0.0009
300	85	0.0135	6000	85	0.0007
300	90	0.0028	6000	90	0.0005
600	0	0.1770	10000	0	0.0026
600	20	0.1612	10000	20	0.0022
600	30	0.1458	10000	30	0.0018
600	40	0.1260	10000	40	0.0014
600	50	0.1023	10000	50	0.0011
600	60	0.0755	10000	60	0.0008
600	70	0.0464	10000	70	0.0005
600	80	0.0193	10000	80	0.0003
600	85	0.0092	10000	85	0.0002
600	90	0.0032	10000	90	0.0001
1000	0	0.1198	20000	0	0.0004
1000	20	0.1078	20000	20	0.0003
1000	30	0.0967	20000	30	0.0003
1000	40	0.0828	20000	40	0.0002
1000	50	0.0663	20000	50	0.0001
1000	60	0.0475	20000	60	0.0000
1000	70	0.0284	20000	70	0.0000
1000	80	0.0123	20000	80	0.0000
1000	85	0.0066	20000	85	0.0000
1000	90	0.0030	20000	90	0.0000

Table 86. Geometric Factor for Reflected Solar Radiation to a Flat Plate

$\gamma = 90°$			$\phi_c = 180°$		
Altitude n. m.	θ_s degree	F	Altitude n. m.	θ_s degree	F
100	0	0.3552	3000	0	0.0306
100	20	0.3290	3000	20	0.0249
100	30	0.3006	3000	30	0.0209
100	40	0.2631	3000	40	0.0161
100	50	0.2175	3000	50	0.0111
100	60	0.1654	3000	60	0.0065
100	70	0.1083	3000	70	0.0030
100	80	0.0471	3000	80	0.0009
100	85	0.0177	3000	85	0.0004
100	90	0.0002	3000	90	0.0001
300	0	0.2538	6000	0	0.0084
300	20	0.2306	6000	20	0.0064
300	30	0.2083	6000	30	0.0051
300	40	0.1797	6000	40	0.0037
300	50	0.1456	6000	50	0.0027
300	60	0.1070	6000	60	0.0016
300	70	0.0651	6000	70	0.0006
300	80	0.0231	6000	80	0.0002
300	85	0.0068	6000	85	0.0001
300	90	0.0003	6000	90	0.0000
600	0	0.1770	10000	0	0.0026
600	20	0.1575	10000	20	0.0019
600	30	0.1404	10000	30	0.0014
600	40	0.1190	10000	40	0.0010
600	50	0.0940	10000	50	0.0006
600	60	0.0661	10000	60	0.0002
600	70	0.0365	10000	70	0.0001
600	80	0.0109	10000	80	0.0000
600	85	0.0032	10000	85	0.0000
600	90	0.0004	10000	90	0.0000
1000	0	0.1198	20000	0	0.0004
1000	20	0.1043	20000	20	0.0003
1000	30	0.0918	20000	30	0.0002
1000	40	0.0762	20000	40	0.0001
1000	50	0.0585	20000	50	0.0000
1000	60	0.0389	20000	60	0.0000
1000	70	0.0197	20000	70	0.0000
1000	80	0.0055	20000	80	0.0000
1000	85	0.0018	20000	85	0.0000
1000	90	0.0004	20000	90	0.0000

Table 87. Geometric Factor for Reflected Solar Radiation to a Flat Plate

γ = 90°

Altitude n. m.	θ_s degree	F
100	0	0.3552
100	20	0.3282
100	30	0.2995
100	40	0.2617
100	50	0.2159
100	60	0.1635
100	70	0.1062
100	80	0.0450
100	85	0.0157
100	90	0.0000
300	0	0.2638
300	20	0.2294
300	30	0.2065
300	40	0.1774
300	50	0.1428
300	60	0.1039
300	70	0.0618
300	80	0.0199
300	85	0.0044
300	90	0.0000
600	0	0.1770
600	20	0.1561
600	30	0.1384
600	40	0.1164
600	50	0.0909
600	60	0.0627
600	70	0.0329
600	80	0.0079
600	85	0.0013
600	90	0.0000
1000	0	0.1198
1000	20	0.1030
1000	30	0.0898
1000	40	0.0738
1000	50	0.0556
1000	60	0.0367
1000	70	0.0185
1000	80	0.0031
1000	85	0.0004
1000	90	0.0000

ϕ_c = 180°

Altitude n. m.	θ_s degree	F
3000	0	0.0306
3000	20	0.0243
3000	30	0.0200
3000	40	0.0150
3000	50	0.0098
3000	60	0.0052
3000	70	0.0018
3000	80	0.0002
3000	85	0.0000
3000	90	0.0000
6000	0	0.0084
6000	20	0.0062
6000	30	0.0048
6000	40	0.0034
6000	50	0.0020
6000	60	0.0010
6000	70	0.0003
6000	80	0.0000
6000	85	0.0000
6000	90	0.0000
10000	0	0.0026
10000	20	0.0018
10000	30	0.0014
10000	40	0.0009
10000	50	0.0005
10000	60	0.0002
10000	70	0.0000
10000	80	0.0000
10000	85	0.0000
10000	90	0.0000
20000	0	0.0004
20000	20	0.0003
20000	30	0.0002
20000	40	0.0001
20000	50	0.0000
20000	60	0.0000
20000	70	0.0000
20000	80	0.0000
20000	85	0.0000
20000	90	0.0000

Table 88. Geometric Factor for Reflected Solar Radiation to a Flat Plate

$\gamma = 120°$ $\quad \phi_c = 0°$

Altitude n. m.	θ_s degree	F	Altitude n. m.	θ_s degree	F
100	0	0.1351	3000	0	
100	20	0.1299	3000	20	
100	30	0.1214	3000	30	
100	40	0.1091	3000	40	
100	50	0.0936	3000	50	
100	60	0.0752	3000	60	
100	70	0.0545	3000	70	
100	80	0.0321	3000	80	
100	85	0.0205	3000	85	
100	90	0.0088	3000	90	
300	0	0.0746	6000	0	
300	20	0.0740	6000	20	
300	30	0.0703	6000	30	
300	40	0.0645	6000	40	
300	50	0.0566	6000	50	
300	60	0.0471	6000	60	
300	70	0.0362	6000	70	
300	80	0.0241	6000	80	
300	85	0.0178	6000	85	
300	90	0.0113	6000	90	
600	0	0.0369	10000	0	
600	20	0.0379	10000	20	
600	30	0.0367	10000	30	
600	40	0.0343	10000	40	
600	50	0.0310	10000	50	
600	60	0.0266	10000	60	
600	70	0.0215	10000	70	
600	80	0.0157	10000	80	
600	85	0.0126	10000	85	
600	90	0.0094	10000	90	
1000	0	0.0157	20000	0	
1000	20	0.0165	20000	20	
1000	30	0.0166	20000	30	
1000	40	0.0159	20000	40	
1000	50	0.0147	20000	50	
1000	60	0.0130	20000	60	
1000	70	0.0110	20000	70	
1000	80	0.0086	20000	80	
1000	85	0.0073	20000	85	
1000	90	0.0059	20000	90	

Table 89. Geometric Factor for Reflected Solar Radiation to a Flat Plate

$\gamma^{\wedge} = 120°$

Altitude n. m.	θ_s degree	F
100	0	0.1351
100	20	0.1296
100	30	0.1208
100	40	0.1084
100	50	0.0927
100	60	0.0741
100	70	0.0534
100	80	0.0310
100	85	0.0210
100	90	0.0072
300	0	0.0746
300	20	0.0735
300	30	0.0695
300	40	0.0635
300	50	0.0555
300	60	0.0458
300	70	0.0347
300	80	0.0226
300	85	0.0165
300	90	0.0098
600	0	0.0369
600	20	0.0375
600	30	0.0361
600	40	0.0335
600	50	0.0300
600	60	0.0255
600	70	0.0203
600	80	0.0144
600	85	0.0117
600	90	0.0081
1000	0	0.0157
1000	20	0.0165
1000	30	0.0162
1000	40	0.0154
1000	50	0.0141
1000	60	0.0123
1000	70	0.0102
1000	80	0.0078
1000	85	0.0065
1000	90	0.0050

$\phi_c = 30°$

Altitude n. m.	θ_s degree	F
3000	0	
3000	20	
3000	30	
3000	40	
3000	50	
3000	60	
3000	70	
3000	80	
3000	85	
3000	90	
6000	0	
6000	20	
6000	30	
6000	40	
6000	50	
6000	60	
6000	70	
6000	80	
6000	85	
6000	90	
10000	0	
10000	20	
10000	30	
10000	40	
10000	50	
10000	60	
10000	70	
10000	80	
10000	85	
10000	90	
20000	0	
20000	20	
20000	30	
20000	40	
20000	50	
20000	60	
20000	70	
20000	80	
20000	85	
20000	90	

Table 90. Geometric Factor for Reflected Solar Radiation to a Flat Plate

γ = 120°			ϕ_c = 60°		
Altitude n. m.	θ_s degree	F	Altitude n. m.	θ_s degree	F
100	0	0.1361	3000	0	
100	20	0.1284	3000	20	
100	30	0.1192	3000	30	
100	40	0.1063	3000	40	
100	50	0.0902	3000	50	
100	60	0.0713	3000	60	
100	70	0.0503	3000	70	
100	80	0.0295	3000	80	
100	85	0.0188	3000	85	
100	90	0.0035	3000	90	
300	0	0.0746	6000	0	
300	20	0.0721	6000	20	
300	30	0.0675	6000	30	
300	40	0.0608	6000	40	
300	50	0.0523	6000	50	
300	60	0.0422	6000	60	
300	70	0.0308	6000	70	
300	80	0.0205	6000	80	
300	85	0.0148	6000	85	
300	90	0.0537	6000	90	
600	0	0.0369	10000	0	
600	20	0.0363	10000	20	
600	30	0.0343	10000	30	
600	40	0.0313	10000	40	
600	50	0.0273	10000	50	
600	60	0.0225	10000	60	
600	70	0.0180	10000	70	
600	80	0.0135	10000	80	
600	85	0.0105	10000	85	
600	90	0.0050	10000	90	
1000	0	0.0157	20000	0	
1000	20	0.0158	20000	20	
1000	30	0.0151	20000	30	
1000	40	0.0140	20000	40	
1000	50	0.0124	20000	50	
1000	60	0.0104	20000	60	
1000	70	0.0930	20000	70	
1000	80	0.0820	20000	80	
1000	85	0.0700	20000	85	
1000	90	0.0031	20000	90	

Table 91. Geometric Factor for Reflected Solar Radiation to a Flat Plate

γ = 120°			ϕ_c = 90°		
Altitude n. m.	θ_s degree	F	Altitude n. m.	θ_s degree	F
100	0	0.1351	3000	0	
100	20	0.1269	3000	20	
100	30	0.1170	3000	30	
100	40	0.1034	3000	40	
100	50	0.0868	3000	50	
100	60	0.0675	3000	60	
100	70	0.0462	3000	70	
100	80	0.0265	3000	80	
100	85	0.0160	3000	85	
100	90	0.0025	3000	90	
300	0	0.0746	6000	0	
300	20	0.0701	6000	20	
300	30	0.0646	6000	30	
300	40	0.0572	6000	40	
300	50	0.0479	6000	50	
300	60	0.0373	6000	60	
300	70	0.0280	6000	70	
300	80	0.0185	6000	80	
300	85	0.0128	6000	85	
300	90	0.0048	6000	90	
600	0	0.0369	10000	0	
600	20	0.0347	10000	20	
600	30	0.0320	10000	30	
600	40	0.0283	10000	40	
600	50	0.0237	10000	50	
600	60	0.0184	10000	60	
600	70	0.0145	10000	70	
600	80	0.0112	10000	80	
600	85	0.0092	10000	85	
600	90	0.0035	10000	90	
1000	0	0.0157	20000	0	
1000	20	0.0148	20000	20	
1000	30	0.0136	20000	30	
1000	40	0.0120	20000	40	
1000	50	0.0101	20000	50	
1000	60	0.0085	20000	60	
1000	70	0.0073	20000	70	
1000	80	0.0054	20000	80	
1000	85	0.0043	20000	85	
1000	90	0.0020	20000	90	

Table 92. Geometric Factor for Reflected Solar Radiation to a Flat Plate

ϕ_c = 120°			ϕ_c = 120°		
Altitude n. m.	θ_s degree	F	Altitude n. m.	θ_s degree	F
100	0	0.1351	3000	0	
100	20	0.1254	3000	20	
100	30	0.1147	3000	30	
100	40	0.1006	3000	40	
100	50	0.0834	3000	50	
100	60	0.0637	3000	60	
100	70	0.0420	3000	70	
100	80	0.0189	3000	80	
100	85	0.0076	3000	85	
100	90	0.0015	3000	90	
300	0	0.0746	6000	0	
300	20	0.0682	6000	20	
300	30	0.0618	6000	30	
300	40	0.0535	6000	40	
300	50	0.0436	6000	50	
300	60	0.0324	6000	60	
300	70	0.0220	6000	70	
300	80	0.0077	6000	80	
300	85	0.0030	6000	85	
300	90	0.0008	6000	90	
600	0	0.0369	10000	0	
600	20	0.0331	10000	20	
600	30	0.0296	10000	30	
600	40	0.0252	10000	40	
600	50	0.0201	10000	50	
600	60	0.0143	10000	60	
600	70	0.0081	10000	70	
600	80	0.0028	10000	80	
600	85	0.0011	10000	85	
600	90	0.0003	10000	90	
1000	0	0.0157	20000	0	
1000	20	0.0138	20000	20	
1000	30	0.0121	20000	30	
1000	40	0.0101	20000	40	
1000	50	0.0078	20000	50	
1000	60	0.0052	20000	60	
1000	70	0.0025	20000	70	
1000	80	0.0009	20000	80	
1000	85	0.0045	20000	85	
1000	90	0.0001	20000	90	

Table 93. Geometric Factor for Reflected Solar Radiation to a Flat Plate

γ = 120°			ϕ_c = 150°		
Altitude n. m.	θ_s degree	F	Altitude n. m.	θ_s degree	F
100	0	0.1351	3000	0	
100	20	0.1243	3000	20	
100	30	0.1131	3000	30	
100	40	0.0985	3000	40	
100	50	0.0809	3000	50	
100	60	0.0609	3000	60	
100	70	0.0390	3000	70	
100	80	0.0158	3000	80	
100	85	0.0049	3000	85	
100	90	0.0001	3000	90	
300	0	0.0746	6000	0	
300	20	0.0668	6000	20	
300	30	0.0597	6000	30	
300	40	0.0508	6000	40	
300	50	0.0404	6000	50	
300	60	0.0288	6000	60	
300	70	0.0160	6000	70	
300	80	0.0042	6000	80	
300	85	0.0007	6000	85	
300	90	0.0000	6000	90	
600	0	0.0369	10000	0	
600	20	0.0319	10000	20	
600	30	0.0279	10000	30	
600	40	0.0230	10000	40	
600	50	0.0174	10000	50	
600	60	0.0113	10000	60	
600	70	0.0051	10000	70	
600	80	0.0007	10000	80	
600	85	0.0001	10000	85	
600	90	0.0000	10000	90	
1000	0	0.0157	20000	0	
1000	20	0.0130	20000	20	
1000	30	0.0110	20000	30	
1000	40	0.0087	20000	40	
1000	50	0.0061	20000	50	
1000	60	0.0034	20000	60	
1000	70	0.0011	20000	70	
1000	80	0.0000	20000	80	
1000	85	0.0000	20000	85	
1000	90	0.0000	20000	90	

Table 94. Geometric Factor for Reflected Solar Radiation to a Flat Plate

γ = 120°

Altitude n. m.	θ_s degree	F
100	0	0.1351
100	20	0.1239
100	30	0.1125
100	40	0.0978
100	50	0.0800
100	60	0.0598
100	70	0.0378
100	80	0.0130
100	85	0.0024
100	90	0.0005
300	0	0.0746
300	20	0.0662
300	30	0.0589
300	40	0.0499
300	50	0.0393
300	60	0.0275
300	70	0.0145
300	80	0.0024
300	85	0.0005
300	90	0.0001
600	0	0.0369
600	20	0.0314
600	30	0.0272
600	40	0.0222
600	50	0.0164
600	60	0.0100
600	70	0.0040
600	80	0.0002
600	85	0.0000
600	90	0.0000
1000	0	0.0157
1000	20	0.0127
1000	30	0.0106
1000	40	0.0082
1000	50	0.0055
1000	60	0.0020
1000	70	0.0000
1000	80	0.0000
1000	85	0.0000
1000	90	0.0000

ϕ_c = 180°

Altitude n. m.	θ_s degree	F
3000	0	
3000	20	
3000	30	
3000	40	
3000	50	
3000	60	
3000	70	
3000	80	
3000	85	
3000	90	
6000	0	
6000	20	
6000	30	
6000	40	
6000	50	
6000	60	
6000	70	
6000	80	
6000	85	
6000	90	
10000	0	
10000	20	
10000	30	
10000	40	
10000	50	
10000	60	
10000	70	
10000	80	
10000	85	
10000	90	
20000	0	
20000	20	
20000	30	
20000	40	
20000	50	
20000	60	
20000	70	
20000	80	
20000	85	
20000	90	

Table 95. Geometric Factor for Reflected Solar Radiation to a Flat Plate

$\gamma = 150°$ $\quad \phi_c = 0°$

Altitude n. m.	θ_s degree	F	Altitude n. m.	θ_s degree	F
100	0	0.0144	3000	0	
100	20	0.0141	3000	20	
100	30	0.0132	3000	30	
100	40	0.0120	3000	40	
100	50	0.0104	3000	50	
100	60	0.0085	3000	60	
100	70	0.0064	3000	70	
100	80	0.0040	3000	80	
100	85	0.0028	3000	85	
100	90	0.0015	3000	90	
300	0	0.0015	6000	0	
300	20	0.0016	6000	20	
300	30	0.0015	6000	30	
300	40	0.0014	6000	40	
300	50	0.0013	6000	50	
300	60	0.0011	6000	60	
300	70	0.0009	6000	70	
300	80	0.0006	6000	80	
300	85	0.0005	6000	85	
300	90	0.0004	6000	90	
600	0		10000	0	
600	20		10000	20	
600	30		10000	30	
600	40		10000	40	
600	50		10000	50	
600	60		10000	60	
600	70		10000	70	
600	80		10000	80	
600	85		10000	85	
600	90		10000	90	
1000	0		20000	0	
1000	20		20000	20	
1000	30		20000	30	
1000	40		20000	40	
1000	50		20000	50	
1000	60		20000	60	
1000	70		20000	70	
1000	80		20000	80	
1000	85		20000	85	
1000	90		20000	90	

Table 96. Geometric Factor for Reflected Solar Radiation to a Flat Plate

γ = 150°

Altitude n. m.	θ_s degree	F
100	0	0.0144
100	20	0.0140
100	30	0.0131
100	40	0.0119
100	50	0.0103
100	60	0.0083
100	70	0.0062
100	80	0.0035
100	85	0.0025
100	90	0.0013
300	0	0.0015
300	20	0.0016
300	30	0.0015
300	40	0.0014
300	50	0.0012
300	60	0.0011
300	70	0.0008
300	80	0.0006
300	85	0.0005
300	90	0.0003
600	0	
600	20	
600	30	
600	40	
600	50	
600	60	
600	70	
600	80	
600	85	
600	90	
1000	0	
1000	20	
1000	30	
1000	40	
1000	50	
1000	60	
1000	70	
1000	80	
1000	85	
1000	90	

ϕ_c = 30°

Altitude n. m.	θ_s degree	F
3000	0	
3000	20	
3000	30	
3000	40	
3000	50	
3000	60	
3000	70	
3000	80	
3000	85	
3000	90	
6000	0	
6000	20	
6000	30	
6000	40	
6000	50	
6000	60	
6000	70	
6000	80	
6000	85	
6000	90	
10000	0	
10000	20	
10000	30	
10000	40	
10000	50	
10000	60	
10000	70	
10000	80	
10000	85	
10000	90	
20000	0	
20000	20	
20000	30	
20000	40	
20000	50	
20000	60	
20000	70	
20000	80	
20000	85	
20000	90	

Table 97. Geometric Factor for Reflected Solar Radiation to a Flat Plate

$\gamma = 150°$ $\qquad$ $\phi_c = 60°$

Altitude n. m.	θ_s degree	F	Altitude n. m.	θ_s degree	F
100	0	0.0144	3000	0	
100	20	0.0138	3000	20	
100	30	0.0129	3000	30	
100	40	0.0115	3000	40	
100	50	0.0098	3000	50	
100	60	0.0079	3000	60	
100	70	0.0056	3000	70	
100	80	0.0032	3000	80	
100	85	0.0015	3000	85	
100	90	0.0008	3000	90	
300	0	0.0015	6000	0	
300	20	0.0015	6000	20	
300	30	0.0014	6000	30	
300	40	0.0013	6000	40	
300	50	0.0011	6000	50	
300	60	0.0009	6000	60	
300	70	0.0007	6000	70	
300	80	0.0004	6000	80	
300	85	0.0003	6000	85	
300	90	0.0002	6000	90	
600	0		10000	0	
600	20		10000	20	
600	30		10000	30	
600	40		10000	40	
600	50		10000	50	
600	60		10000	60	
600	70		10000	70	
600	80		10000	80	
600	85		10000	85	
600	90		10000	90	
1000	0		20000	0	
1000	20		20000	20	
1000	30		20000	30	
1000	40		20000	40	
1000	50		20000	50	
1000	60		20000	60	
1000	70		20000	70	
1000	80		20000	80	
1000	85		20000	85	
1000	90		20000	90	

Table 98. Geometric Factor for Reflected Solar Radiation to a Flat Plate

γ = 150°

Altitude n. m.	θ_s degree	F
100	0	0.0144
100	20	0.0135
100	30	0.0125
100	40	0.0110
100	50	0.0092
100	60	0.0072
100	70	0.0049
100	80	0.0020
100	85	0.0007
100	90	0.0002
300	0	0.0015
300	20	0.0014
300	30	0.0013
300	40	0.0012
300	50	0.0010
300	60	0.0007
300	70	0.0005
300	80	0.0003
300	85	0.0001
300	90	0.0000
600	0	
600	20	
600	30	
600	40	
600	50	
600	60	
600	70	
600	80	
600	85	
600	90	
1000	0	
1000	20	
1000	30	
1000	40	
1000	50	
1000	60	
1000	70	
1000	80	
1000	85	
1000	90	

ϕ_c = 90°

Altitude n. m.	θ_s degree	F
3000	0	
3000	20	
3000	30	
3000	40	
3000	50	
3000	60	
3000	70	
3000	80	
3000	85	
3000	90	
6000	0	
6000	20	
6000	30	
6000	40	
6000	50	
6000	60	
6000	70	
6000	80	
6000	85	
6000	90	
10000	0	
10000	20	
10000	30	
10000	40	
10000	50	
10000	60	
10000	70	
10000	80	
10000	85	
10000	90	
20000	0	
20000	20	
20000	30	
20000	40	
20000	50	
20000	60	
20000	70	
20000	80	
20000	85	
20000	90	

Table 99. Geometric Factor for Reflected Solar Radiation to a Flat Plate

$\gamma = 150°$ $\qquad$ $\phi_c = 120°$

Altitude n. m.	θ_s degree	F	Altitude n. m.	θ_s degree	F
100	0	0.0144	3000	0	
100	20	0.0133	3000	20	
100	30	0.0121	3000	30	
100	40	0.0105	3000	40	
100	50	0.0086	3000	50	
100	60	0.0065	3000	60	
100	70	0.0042	3000	70	
100	80	0.0017	3000	80	
100	85	0.0004	3000	85	
100	90	0.0000	3000	90	
300	0	0.0015	6000	0	
300	20	0.0014	6000	20	
300	30	0.0012	6000	30	
300	40	0.0010	6000	40	
300	50	0.0008	6000	50	
300	60	0.0006	6000	60	
300	70	0.0004	6000	70	
300	80	0.0000	6000	80	
300	85	0.0000	6000	85	
300	90	0.0000	6000	90	
600	0		10000	0	
600	20		10000	20	
600	30		10000	30	
600	40		10000	40	
600	50		10000	50	
600	60		10000	60	
600	70		10000	70	
600	80		10000	80	
600	85		10000	85	
600	90		10000	90	
1000	0		20000	0	
1000	20		20000	20	
1000	30		20000	30	
1000	40		20000	40	
1000	50		20000	50	
1000	60		20000	60	
1000	70		20000	70	
1000	80		20000	80	
1000	85		20000	85	
1000	90		20000	90	

Table 100 Geometric Factor for Reflected Solar Radiation to a Flat Plate

γ = 150°			ϕ_c = 150°		
Altitude n. m.	θ_s degree	F	Altitude n. m.	θ_s degree	F
100	0	0.0144	3000	0	
100	20	0.0131	3000	20	
100	30	0.0118	3000	30	
100	40	0.0102	3000	40	
100	50	0.0082	3000	50	
100	60	0.0060	3000	60	
100	70	0.0036	3000	70	
100	80	0.0011	3000	80	
100	85	0.0001	3000	85	
100	90	0.0000	3000	90	
300	0	0.0015	6000	0	
300	20	0.0013	6000	20	
300	30	0.0011	6000	30	
300	40	0.0009	6000	40	
300	50	0.0007	6000	50	
300	60	0.0004	6000	60	
300	70	0.0002	6000	70	
300	80	0.0000	6000	80	
300	85	0.0000	6000	85	
300	90	0.0000	6000	90	
600	0		10000	0	
600	20		10000	20	
600	30		10000	30	
600	40		10000	40	
600	50		10000	50	
600	60		10000	60	
600	70		10000	70	
600	80		10000	80	
600	85		10000	85	
600	90		10000	90	
1000	0		20000	0	
1000	20		20000	20	
1000	30		20000	30	
1000	40		20000	40	
1000	50		20000	50	
1000	60		20000	60	
1000	70		20000	70	
1000	80		20000	80	
1000	85		20000	85	
1000	90		20000	90	

Table 101. Geometric Factor for Reflected Solar Radiation to a Flat Plate

$\gamma = 150°$			$\phi_c = 180°$		
Altitude n. m.	θ_s degree	F	Altitude n. m.	θ_s degree	F
100	0	0.0144	3000	0	
100	20	0.0130	3000	20	
100	30	0.0117	3000	30	
100	40	0.0100	3000	40	
100	50	0.0081	3000	50	
100	60	0.0058	3000	60	
100	70	0.0034	3000	70	
100	80	0.0007	3000	80	
100	85	0.0001	3000	85	
100	90	0.0000	3000	90	
300	0	0.0015	6000	0	
300	20	0.0013	6000	20	
300	30	0.0011	6000	30	
300	40	0.0009	6000	40	
300	50	0.0006	6000	50	
300	60	0.0004	6000	60	
300	70	0.0001	6000	70	
300	80	0.0000	6000	80	
300	85	0.0000	6000	85	
300	90	0.0000	6000	90	
600	0		10000	0	
600	20		10000	20	
600	30		10000	30	
600	40		10000	40	
600	50		10000	50	
600	60		10000	60	
600	70		10000	70	
600	80		10000	80	
600	85		10000	85	
600	90		10000	90	
1000	0		20000	0	
1000	20		20000	20	
1000	30		20000	30	
1000	40		20000	40	
1000	50		20000	50	
1000	60		20000	60	
1000	70		20000	70	
1000	80		20000	80	
1000	85		20000	85	
1000	90		20000	90	